

Advances

in Clinical and Experimental Medicine

MONTHLY ISSN 1899-5276 (PRINT) ISSN 2451-2680 (ONLINE)

advances.umw.edu.pl

2025, Vol. 34, No. 9 (September)

Impact Factor (IF) – 1.9
Ministry of Science and Higher Education – 70 pts
Index Copernicus (ICV) – 171.00 pts



WROCLAW
MEDICAL UNIVERSITY

Advances
in Clinical and Experimental
Medicine



Advances in Clinical and Experimental Medicine

ISSN 1899-5276 (PRINT)

ISSN 2451-2680 (ONLINE)

advances.umw.edu.pl

MONTHLY 2025
Vol. 34, No. 9
(September)

Advances in Clinical and Experimental Medicine (*Adv Clin Exp Med*) publishes high-quality original articles, research-in-progress, research letters and systematic reviews and meta-analyses of recognized scientists that deal with all clinical and experimental medicine.

Editorial Office

ul. Marcinkowskiego 2–6
50-368 Wrocław, Poland
Tel.: +48 71 784 12 05
E-mail: redakcja@umw.edu.pl

Editor-in-Chief

Prof. Donata Kurpas

Deputy Editor

Prof. Robert Śmigiel

Managing Editor

Marek Misiak, MA

Statistical Editors

Wojciech Bombała, MSc

Anna Kopszak, MSc

Dr. Krzysztof Kujawa

Jakub Wronowicz, MSc

Maciej Wuczyński, MSc

Manuscript editing

Marek Misiak, MA

Paulina Piątkowska, MA

Publisher

Wrocław Medical University
Wybrzeże L. Pasteura 1
50-367 Wrocław, Poland

Online edition is the original version
of the journal

Scientific Committee

Prof. Sabine Bährer-Kohler

Prof. Sandra Maria Barbalho

Prof. Antonio Cano

Prof. Chong Chen

Prof. Breno Diniz

Prof. Erwan Donal

Prof. Chris Fox

Prof. Yuko Hakamata

Prof. Carol Holland

Prof. Markku Kurkinen

Prof. Christopher S. Lee

Prof. Christos Lionis

Prof. Leszek Lisowski

Prof. Raimundo Mateos

Prof. Zbigniew W. Raś

Prof. Dorota Religa

Prof. Jerzy W. Rozenblit

Prof. Silvina Santana

Prof. Sajee Sattayut

Prof. Barbara Schneider

Prof. James Sharman

Prof. Jamil Shibli

Prof. Luca Testarelli

Prof. Michał J. Toborek

Prof. László Vécsei

Prof. Cristiana Vitale

Prof. Ming Yi

Prof. Hao Zhang

Section Editors

Basic Sciences

Prof. Iwona Bil-Lula
Prof. Dorota Danuta Diakowska
Prof. Bartosz Kempisty
Dr. Wiesława Kranc
Dr. Anna Lebedeva
Dr. Piotr Chmielewski
Dr. Phuc Van Pham
Dr. Sławomir Woźniak

Clinical Anatomy, Legal Medicine, Innovative Technologies

Prof. Rafael Boscolo-Berto

Dentistry

Prof. Marzena Dominiak
Prof. Tomasz Gedrange

Prof. Jamil Shibli

Prof. Luca Testarelli

Laser Dentistry

Prof. Kinga Grzech-Leśniak

Dermatology

Prof. Jacek Szepietowski

Assoc. Prof. Marek Konop

Emergency Medicine, Innovative Technologies

Prof. Jacek Smereka

Evidence-Based Healthcare

Assoc. Prof. Aleksandra Królikowska

Dr. Robert Prill

Gynecology and Obstetrics

Assoc. Prof. Tomasz Fuchs

Dr. Christopher Kobierzycki

Dr. Jakub Staniczek

Histology and Embryology

Dr. Mateusz Olbromski

Internal Medicine

Angiology

Dr. Angelika Chachaj

Cardiology

Dr. Daniel Morris

Assoc. Prof. Joanna Popiołek-Kalisz

Prof. Pierre François Sabouret

Endocrinology

Prof. Marek Bolanowski

Assoc. Prof. Agnieszka Zubkiewicz-Kucharska

Gastroenterology

Dr. Anna Kofla-Dłubacz

Assoc. Prof. Katarzyna Neubauer

Hematology

Prof. Andrzej Deptała

Prof. Dariusz Wołowicz

Nephrology and Transplantology

Prof. Mirosław Banasik
Prof. Krzysztof Letachowicz
Assoc. Prof. Tomasz Gołębiowski

Rheumatology

Assoc. Prof. Agata Sebastian
Dr. Sylwia Szafraniec-Buryło

Lifestyle Medicine, Nutrition and Health Promotion

Assoc. Prof. Michał Czapla
Prof. Raúl Juárez-Vela
Dr. Anthony Dissen

Microbiology

Dr. Malwina Brożyna
Assoc. Prof. Adam Junka

Molecular Biology

Dr. Monika Bielecka
Prof. Dorota Danuta Diakowska
Dr. Phuc Van Pham

Neurology

Assoc. Prof. Magdalena Koszewicz
Dr. Nasrollah Moradikor
Assoc. Prof. Anna Pokryszko-Dragan
Dr. Masaru Tanaka

Neuroscience

Dr. Simone Battaglia
Dr. Francesco Di Gregorio
Dr. Nasrollah Moradikor

Omics, Bioinformatics and Genetics

Assoc. Prof. Izabela Łaczmarska
Prof. Łukasz Łaczmarski
Prof. Mariusz Fleszar
Assoc. Prof. Paweł Andrzej Karpiński

Oncology

Prof. Andrzej Deptała
Prof. Adam Maciejczyk
Prof. Hao Zhang

Gynecological Oncology

Dr. Marcin Jędryka

Ophthalmology

Dr. Małgorzata Gajdzis
Prof. Marta Misiuk-Hojło

Orthopedics

Prof. Paweł Reichert

Otolaryngology

Prof. Tomasz Zatoński

Pediatrics

Pediatrics, Metabolic Pediatrics, Clinical Genetics, Neonatology, Rare Disorders

Dr. Anna Kofla-Dłubacz
Prof. Robert Śmigiel

Pediatric Nephrology

Prof. Katarzyna Kiliś-Pstrusińska

Pediatric Oncology and Hematology

Assoc. Prof. Marek Ussowicz

Pharmaceutical Sciences

Assoc. Prof. Marta Kepinska
Prof. Adam Matkowski

Pharmacoeconomics

Dr. Sylwia Szafraniec-Buryło

Psychiatry

Dr. Melike Küçükrapınar
Prof. Jerzy Leszek
Assoc. Prof. Bartłomiej Stańczykiewicz

Public Health

Prof. Monika Sawhney
Prof. Izabella Uchmanowicz

Pulmonology

Prof. Anna Brzecka

Qualitative Studies, Quality of Care

Prof. Ludmiła Marcinowicz
Assoc. Prof. Anna Rozensztrauch

Radiology

Prof. Paweł Gać

Rehabilitation

Assoc. Prof. Aleksandra Królikowska
Dr. Robert Prill

Surgery

Assoc. Prof. Mariusz Chabowski

Telemedicine, Geriatrics, Multimorbidity

Assoc. Prof. Maria Magdalena
Bujnowska-Fedak
Prof. Ferdinando Petrazzuoli

Editorial Policy

Advances in Clinical and Experimental Medicine (Adv Clin Exp Med) is an independent multidisciplinary forum for exchange of scientific and clinical information, publishing original research and news encompassing all aspects of medicine, including molecular biology, biochemistry, genetics, biotechnology and other areas. During the review process, the Editorial Board conforms to the "Uniform Requirements for Manuscripts Submitted to Biomedical Journals: Writing and Editing for Biomedical Publication" approved by the International Committee of Medical Journal Editors (www.ICMJE.org). The journal publishes (in English only) original papers and reviews. Short works considered original, novel and significant are given priority. Experimental studies must include a statement that the experimental protocol and informed consent procedure were in compliance with the Helsinki Convention and were approved by an ethics committee.

For all subscription-related queries please contact our Editorial Office: redakcja@umw.edu.pl

For more information visit the journal's website: advances.umw.edu.pl

Pursuant to the ordinance of the Rector of Wrocław Medical University No. 37/XVI R/2024, from March 1, 2024, authors are required to pay a fee for each manuscript accepted for publication in the journal Advances in Clinical and Experimental Medicine. The fee amounts to 1600 EUR for all types of papers.

Indexed in: MEDLINE, Science Citation Index Expanded, Journal Citation Reports/Science Edition, Scopus, EMBASE/Excerpta Medica, Ulrich'sTM International Periodicals Directory, Index Copernicus

Typographic design: Piotr Gil, Monika Kołęda

DTP: Wydawnictwo UMW

Cover: Monika Kołęda

Printing and binding: Drukarnia I-BiS Bierorący Sp.k.

Contents

Editorials

- 1419 Mahdi Esmaeilzadeh, Nasrollah Moradikor
Nutrition & exercise for brain health: Enhancing cognitive function and neuroplasticity
- 1425 Andrzej Marek Jaxa-Kwiatkowski, Anna Leszczyszyn, Hanna Gerber
ERAS protocols for oral cancer free tissue transfer reconstruction: Critical review and clinical checklist

Meta-analysis

- 1433 Xiaohua Sun, Zuwei Cao, Xin Li
Vestibular rehabilitation: Proven benefits in enhancing balance and reducing dizziness

Original papers

- 1451 Busra Korpe, Caner Kose, Kadriye Erdogan, Yaprak Engin-Ustun, Vakkas Korkmaz
Preoperative hemoglobin A1c as a predictor of lymph node metastasis in diabetic women with endometrial cancer
- 1459 Chao-Guang Ma, Ying-Nan Liu, Hua-Dong Wang
NLRP3 inflammasome in expressed prostatic secretions as a potential biomarker of chronic prostatitis/chronic pelvic pain syndrome
- 1467 Lanfen Zhan, Xinyao Xiang, Yu Zhang, Lingmin Zhou
Associations of propofol and midazolam with the 30-day mortality in patients with sepsis-associated encephalopathy: A study of the MIMIC database
- 1475 Yanjun Xu, Jing Yang, Zexing Jiang, Peng Liu, Xudong Wang
Association between stress-induced hyperglycemia ratio and sepsis risk in patients admitted to ICU
- 1485 Kacper K. KroczeK, Joanna Sebastian, Iwona Szymkuć-Bukowska, Małgorzata Pyskir, Przemysław Gałązka
Quality of life assessment after minimally invasive operative treatment in children with pectus excavatum: A single-center study and literature review
- 1493 Paweł Skorek, Magdalena M. Frączek-Jucha, Agnieszka Sarnecka, Maciej Skubera, Natasza Libiszewska, Lidia Tomkiewicz-Pająk
Experience with sodium glucose cotransporter-2 inhibitors in adult patients with Fontan circulation
- 1501 Sebastian Dominiak, Marzena Dominiak, Paweł Kubasiewicz-Ross, Tomasz Gedrange
Patient's characteristic included for treatment with individualized allogenic 3D bone block before or during/after orthodontic treatment: A 6-year observational study
- 1521 Marcin Kubeczko, Patrycja Tudrej, Tomasz Tyszkiewicz, Aleksandra Krzywón, Małgorzata Oczko-Wojciechowska, Michał Jarząb
MiRNA in archival serum samples derived from breast cancer patients treated with neoadjuvant chemotherapy vs freshly collected samples: Pilot study
- 1531 Sergii Sukhodolia, Olesia Kalmukova, Natalia Raksha, Anatoliy Sukhodolia, Olena Kuryk, Olexiy Savchuk
Peptide pool instability of precancerous lesions in rats with chronic pancreatitis model and/or without type 1 diabetes mellitus
- 1541 Ying Sun, Yingying Ma, Hailiang Wang
Chemopreventive role of β -caryophyllene in DMBA-induced skin cancer: Modulation of apoptotic pathways and PI3K/Akt signaling in Swiss albino mice

- 1553 Xuejiao Wang, Ke Wang, Hengfei Du
Anticancer potential of nerolidol on acute lymphoblastic leukemia cells through the interactions with the NF- κ B/STAT-3 and PI3K/Akt signaling pathways
- 1565 Michał Czapla, Bartłomiej Stańczykiewicz, Donata Kurpas, Izabella Uchmanowicz, Bartosz Uchmanowicz, Raúl Juárez-Vela, Piotr Karniej
Polish validation of the LGBTQ+ Healthcare Experiences Scale (LGBTQ+ HCES)

Reviews

- 1575 Paula Jabłonowska-Babij, Maciej Majcherek, Anna Kłopot, Agnieszka Szeremet, Tomasz Wróbel, Anna Czyż
The role of *p16* gene and P16INK4a protein in hematologic malignancies and therapeutic implications: A systematic review

Study protocol

- 1589 Ferdinando Petrazzuoli, Josep Vidal-Alaball, Joyce Kenkre, Thomas Kloppe, Sinah Evers, Hendrik Napierala, Jean-Pierre Jacquet, Wolfram J. Herrmann, Natasa Mrduljaš-Đujić, Andrea Neculau, Katerina Javorska, David Halata, Miriam Dolan, Joanne Robins, Patrick Ouvrard, Juan Manuel Mendive, Carmen López Fando, Jane Randall-Smith, Erwin Rebhandl, Sara Paternoster, Hans Thulesius, Sian Brand, Gindrovel Dumitra, Donata Kurpas
Best practice approaches to social prescribing in European Primary Care: A Delphi protocol focused on link workers

Nutrition & exercise for brain health: Enhancing cognitive function and neuroplasticity

Mahdi Esmailzadeh^{D,F}, Nasrollah Moradikor^{A,D–F}

International Center for Neuroscience Research, Tbilisi, Georgia

A – research concept and design; B – collection and/or assembly of data; C – data analysis and interpretation;
D – writing the article; E – critical revision of the article; F – final approval of the article

Advances in Clinical and Experimental Medicine, ISSN 1899–5276 (print), ISSN 2451–2680 (online)

Adv Clin Exp Med. 2025;34(9):1419–1423

Address for correspondence

Nasrollah Moradikor
E-mail: moradikor@neuroscience.edu.ge

Funding sources

None declared

Conflict of interest

None declared

Received on June 8, 2025
Reviewed on July 21, 2025
Accepted on July 23, 2025

Published online on September 4, 2025

Abstract

This editorial examines the relationship between nutrition, physical activity, and brain health, emphasizing their effects on cognitive function and mental well-being. Evidence supports a balanced diet – rich in antioxidants, omega-3 fatty acids, polyphenols, and patterned after the Mediterranean-DASH Intervention for Neurodegenerative Delay (MIND) diet – as crucial for sustaining neural structure, function, and plasticity. Similarly, regular exercise has been shown to enhance mood, attention, memory, and overall cognitive performance. However, despite these demonstrated benefits, the precise neurobiological mechanisms through which diet and exercise influence brain health remain unclear. This article explores both the efficacy of these interventions and the challenges involved in optimizing them for long-term cognitive resilience.

Key words: cognitive function, mental health, exercise, nutrition, brain health

Cite as

Esmailzadeh M, Moradikor N. Nutrition & exercise for brain health: Enhancing cognitive function and neuroplasticity. *Adv Clin Exp Med.* 2025;34(9):1419–1423. doi:10.17219/acem/208533

DOI

10.17219/acem/208533

Copyright

Copyright by Author(s)
This is an article distributed under the terms of the
Creative Commons Attribution 3.0 Unported (CC BY 3.0)
(<https://creativecommons.org/licenses/by/3.0/>)

Highlights

- Nutrition and exercise synergy enhances brain health and neuroplasticity: Combined diet and physical activity fortify brain structure, synaptic function, and learning capacity.
- Antioxidants, omega-3 fatty acids, polyphenols, and the MIND diet boost cognitive function: These key nutrients reduce oxidative stress and support memory, attention, and executive performance.
- Regular physical activity elevates mood, attention, memory, and overall cognitive performance: Aerobic and resistance training increase cerebral blood flow and neurotrophic factors for sharper thinking.
- Mechanistic insights still emerging on diet- and exercise-driven brain benefits: Ongoing research aims to unravel the molecular pathways linking nutritional compounds and exercise stimuli to neural health.

Introduction

In recent decades, a broad range of academic studies has shown interest in the mind–body relationship and published a number of empirical studies in this field.¹ The “mind–body connection” refers to the complex interplay between mental and physical well-being. Efficient bidirectional communication between the brain and body is vital for maintaining physiological homeostasis. The human organism comprises intricately connected systems that work in concert to regulate this balance and underpin both behavior and cognition.² This concept highlights on interaction of thoughts, emotions, and actions on our bodies and vice versa.³ Some factors such as psychological therapy, diet, exercise, and sleep significantly affect cognitive function and emotional stability, psychological status and physical health.⁴ For example, psychological therapy can improve quality of life and wellbeing.⁵ A healthy nutrition influences both mental and physical well-being and increases disease resistance.⁶

The capacity of neurons to modify the strength and structure of their synaptic connections in response to internal and external stimuli underlies the brain’s adaptive ability, a phenomenon known as neuroplasticity. A growing body of evidence indicates that physical activity (PA) enhances cognitive processes, such as memory and attention, in both children and adults.^{7,8} Studies have reported that brain capillaries improve and regulate these effects by supplying angiogenic growth factors such as the vascular endothelial growth factor (VEGF), brain-derived neurotrophic factor (BDNF), and the growth and differentiation factor 11 (GDF11), and induce genes responsible for neuroplasticity.^{9,10} Dietary regimens that emphasize caloric restriction may delay the onset of age-related diseases and slow the biological aging process.^{11,12}

Preventive policies and health promotion programs are crucial for healthy aging. As the elderly population grows, these strategies help support their well-being and decrease pressure on healthcare and pension systems. This change in population structure is linked to a higher disease burden and increased healthcare costs.^{13,14} Eating healthy foods with anti-aging properties is important for supporting healthy aging and reducing the risk of chronic diseases.¹⁵

This editorial explores the mind–body connection by examining how diet and exercise influence brain function. It synthesizes mounting evidence that lifestyle choices, specifically balanced nutrition and regular physical activity, are fundamental to cognitive health, emotional resilience, and overall quality of life. By reviewing the latest research, the letter advocates for lifestyle modifications that may slow biological aging and reduce the risk of age-related diseases, underscoring the critical interplay between mental and physical well-being.

Brain health

The cerebrum, the largest part of the brain, is responsible for higher cognitive functions such as memory, reasoning, and complex thought.¹⁶ The brainstem controls fundamental processes such as breathing, heartbeat, and digestion, while the cerebellum organizes movement and balance.¹⁷ The brain utilizes interconnected neuronal networks, linked by synapses, to transmit electrical impulses and facilitate communication both among its various regions and with the rest of the body. The brain can process sensory data, start movements, control emotions, and oversee all physiological processes that are required for survival.¹⁸ Despite its capabilities, the brain has several difficulties, especially as people age. Cognitive decline – a gradual deterioration of memory, learning, and reasoning abilities – is a common concern.¹⁹ Although aging is a primary contributor, lifestyle factors, genetic predisposition, and disease can accelerate this decline.²⁰ Mood disorders such as anxiety and depression can have a major effect on brain function. These disorders may also affect the structure and function of the brain, especially in areas such as the amygdala and prefrontal cortex.²¹ Neurodegenerative diseases – such as Alzheimer’s, Parkinson’s, and Huntington’s – pose significant threats to brain health. These conditions are characterized by progressive neuronal degeneration, resulting in declines in both motor function and cognitive abilities.²² For example, Alzheimer’s disease is characterized by the accumulation of aberrant proteins in the brain that disrupt neuronal communication, leading to memory

loss, disorientation, and other cognitive deficits.²³ Although aging is the primary risk factor, lifestyle choices, environmental exposures, and genetic predisposition also play significant roles in disease development.

The effects of nutrition on brain health

Nutrition has an important role for developing the brain and its functions. Diets containing sugar, unhealthy fats and/or too many calories can cause damages in brain function.²⁴ These types of diets increase stress in the brain and decrease its ability to adapt. An ideal nutrition is essential for brain function. It has been accepted that having breakfast helps children perform better in school.²⁵ Children who ate breakfast did better and made fewer mistakes than those who skipped it. As people age, cognitive abilities, such as memory and processing speed, naturally decline. Nutrition not only influences brain structure but also affects its function.²⁶ Antioxidants can positively influence cognitive performance and overall brain function.

In our study, we demonstrated that *Spirulina platensis*, a potent source of antioxidants, protects adolescent rats from oxidative stress.²⁷ Treatment with *S. platensis* increased expression of brain-derived neurotrophic factor (BDNF) and key antioxidant enzymes, thereby mitigating stress-induced damage.²⁷ Molecular factors like BDNF and VEGF can influence broader brain systems involved in thinking and emotional regulation, linking body activity to brain function.²⁸ Antioxidants can play protective roles during critical periods of adolescence. In our study, *Spirulina platensis* ameliorated scopolamine-induced memory deficits by attenuating oxidative stress, as evidenced by reduced malondialdehyde (MDA) levels.²⁹ Additional studies have examined how *S. platensis* modulates apolipoprotein E (APOE) and reticulon-4 (RTN4) protein expression in the rat prefrontal cortex.³⁰ Polyphenols are powerful antioxidants found in foods like fruits, tea, red wine, cocoa, and coffee.³¹ These nutrients may protect brain cells from damage caused by harmful toxins, reduce brain inflammation, and help improve memory, learning, and brain function.³² It has been shown that polyphenols decrease stress and inflammation in the brain, increase protective signals, and promote the production of proteins that help protect brain cells.³³ It was also reported that green tea extract and polyphenols increased brain activity in the prefrontal cortex in the human brain.³⁴ In a separate study, we demonstrated that quercetin nano-phytosomes significantly attenuated inflammation in rodent models of multiple sclerosis.³⁵ We also demonstrated that gingerol produces significant antidepressant-like effects through modulation of the serotonergic system.³⁶ Conversely, our group reported that high white and brown sugar consumption significantly decreased the concentration of brain-derived neurotrophic factor in animal models.³⁷ In our studies,

nutritional interventions, such as *S. platensis*, quercetin nano-phytosomes, and phenolic compounds, demonstrated neuroprotective effects by attenuating oxidative stress and inflammation and by supporting neurotransmitter function. These compounds increased BDNF levels and cognitive performance in animal models.^{27,29,35} In contrast, high intake of refined sugars adversely affected brain-derived neurotrophic factor levels.³⁷ In sum, our findings underscore the pivotal role of nutrition in modulating brain function, particularly during critical developmental and aging periods.

Adherence to the Mediterranean-DASH Intervention for Neurodegenerative Delay (MIND) diet has been associated with superior cognitive performance, independent of common neuropathological changes. The MIND diet can increase cognitive resilience in the elderly.³⁸ It was also reported that the MIND diet intervention could reverse the destructive effects of obesity on cognition and brain structure in healthy obese women.³⁹ A systematic review indicated that adherence to the MIND diet is linked to improved cognitive function in older adults, positioning it as a superior dietary strategy for preserving cognitive performance in this population.⁴⁰ A recent study found that greater adherence to the French version of the MIND diet is associated with a lower risk of dementia and preservation of white matter microstructure.²⁷ These studies suggest the MIND diet is a promising nutritional method for protecting brain health in aging populations.

The effects of exercise on brain health

Exercise has an important role in improving brain function. It has been reported that combining exercise and eating habits is the best way to support brain health.⁴ There are studies reporting the positive effects of physical activity on mental health.^{41,42} Physical activity improves mental health outcomes and helps to improve mood, self-esteem, stress, and cognitive function.⁴³ Exercise enhances mood, boosts self-esteem, and reduces stress. Exercise also stimulates the body's production of endogenous opioids and endocannabinoids.⁴⁴ Regular physical activity enhances cognitive function, lowers stress hormone levels, and helps regulate appetite-related hormones. In our study, voluntary exercise enhanced cognitive performance, elevated hippocampal BDNF levels, and promoted neuroanatomical remodeling in stressed female rats.⁴⁵ In a separate study, we demonstrated that voluntary exercise—administered alone or combined with *Spirulina platensis* microalgae supplementation—reduced oxidative stress and elevated BDNF expression in the adolescent rat brain.⁴⁵ Furthermore, voluntary exercise enhanced cognitive performance, increased hippocampal BDNF levels, and promoted neuroanatomical remodeling in the hippocampus of stressed female rats. These findings emphasize the synergistic

benefits of nutrition and physical activity on brain health. Physical exercise has been shown to accelerate reaction times in older adults and enhance executive functions mediated by the prefrontal cortex.⁴⁶ High-intensity exercise has been shown to impair cognitive performance and decrease oxygenation in the prefrontal cortex compared with moderate exercise or rest.⁴⁷ Although physical activity usually enhances executive function in older adults, excessively high intensity may have the opposite effect.

Challenges and future directions

Several studies have investigated the effects of exercise and diet on brain health, but several important questions remain unanswered. A major challenge is the complexity of the brain, as numerous factors affect its structure and function. This makes it difficult to identify the exact effects of specific foods or types of physical activity. In addition, individual differences in genetics, lifestyle, and environment make it hard to apply findings to everyone. Future research should aim to identify specific nutrition and exercise plans that support brain health. Another challenge is the need for extensive, long-term research to provide stronger evidence of the relation between exercise, diet, and brain health. Most current studies are observational data or short-term trials, which makes it difficult to determine a clear cause-and-effect relationship. Long-term randomized controlled trials examining the effects of nutrition and physical activity are needed to generate robust, reliable evidence. Although the mental health benefits of physical activity are well recognized, the specific types and amounts of exercise that best support brain function remain unclear. More research is needed to identify the most effective routines for different age groups and health conditions, especially in relation to cognitive decline and neurodegenerative diseases. However, the relationship between them requires deeper investigation.


Conclusions

This editorial emphasizes the important role that exercise and diet play in maintaining cognitive performance and brain health. Diet and regular physical activity can improve mood, memory, mental well-being, and overall brain function. This editorial highlights how nutrition, particularly antioxidant-rich diets such as the MIND regimen, and moderate exercise support brain health by reducing oxidative stress, elevating neurotrophic factors like BDNF, and enhancing cognitive function. Together, they offer a synergistic approach to preserving brain function throughout life. Although challenges persist, such as the need for personalized interventions and long-term clinical trials, the growing body of evidence underscores the value of healthy nutrition and regular exercise for

preserving cognitive function and mitigating age-related decline. Future research on these interactions will inform the development of targeted strategies to optimize brain health and enhance quality of life across the lifespan.

ORCID iDs

Nasrollah Moradikar  <https://orcid.org/0000-0001-9905-6845>

Mahdi Esmaeilzadeh  <https://orcid.org/0000-0002-2426-7637>

References

1. Greeson JM, McBride EE, Chin GR, Lee HH, Colangelo AP. Trait mindfulness and mind-body health in students: The role of gender, race, and ethnicity. *J Am Coll Health*. 2024;72(8):2844–2855. doi:10.1080/07448481.2022.2135374
2. Di Gregorio F, Battaglia S. The intricate brain–body interaction in psychiatric and neurological diseases. *Adv Clin Exp Med*. 2024;33(4):321–326. doi:10.17219/acem/185689
3. O'Toole C, Simovska V. Wellbeing and education: Connecting mind, body and world. In: *Transdisciplinary Perspectives in Educational Research*. Cham, Switzerland: Springer International Publishing; 2022: 21–33. doi:10.1007/978-3-030-95205-1_2
4. Zavitsanou A, Drigas A. Nutrition in mental and physical health. *Technium Soc Sci J*. 2021;23:67–77. doi:10.47577/tssj.v23i1.4126
5. Guo H, Yang Y. Assessing the efficacy of psychological interventions in enhancing the quality of life of patients diagnosed with cancer and psychiatric disorders: An umbrella analysis. *Adv Clin Exp Med*. 2025;34(6):871–884. doi:10.17219/acem/190503
6. Sandua D. *Mind-Body Connection: The Impact of Nutrition on Mental Health*. Oklahoma City, USA: Draft2Digital, LLC; 2023. ISBN:979-822 3434511.
7. Clemente-Suárez VJ, Rubio-Zarapuz A, Belinchón-deMiguel P, Beltrán-Velasco AI, Martín-Rodríguez A, Tornero-Aguilera JF. Impact of physical activity on cellular metabolism across both neurodegenerative and general neurological conditions: A narrative review. *Cells*. 2024;13(23):1940. doi:10.3390/cells13231940
8. Cefis M, Chaney R, Wirtz J, et al. Molecular mechanisms underlying physical exercise-induced brain BDNF overproduction. *Front Mol Neurosci*. 2023;16:1275924. doi:10.3389/fnmol.2023.1275924
9. Karakatsani A, Álvarez-Vergara MI, Ruiz De Almodóvar C. The vasculature of neurogenic niches: Properties and function. *Cell Dev*. 2023;174:203841. doi:10.1016/j.cdev.2023.203841
10. Shalabi S, Belayachi A, Larrivé B. Involvement of neuronal factors in tumor angiogenesis and the shaping of the cancer micro-environment. *Front Immunol*. 2024;15:1284629. doi:10.3389/fimmu.2024.1284629
11. Duque G, Al Saedi A, Rivas D, et al. Differential effects of long-term caloric restriction and dietary protein source on bone and marrow fat of the aging rat. Anderson R, ed. *J Gerontol A Biol Sci Med Sci*. 2020;75(11):2031–2036. doi:10.1093/gerona/glaa093
12. Velingkaar N, Mezhnina V, Poe A, Makwana K, Tulsian R, Kondratov RV. Reduced caloric intake and periodic fasting independently contribute to metabolic effects of caloric restriction. *Aging Cell*. 2020;19(4):e13138. doi:10.1111/acer.13138
13. Ros M, Carrascosa JM. Current nutritional and pharmacological anti-aging interventions. *Biochim Biophys Acta Mol Basis Dis*. 2020;1866(3):165612. doi:10.1016/j.bbdis.2019.165612
14. Oikawa SY, Brisbois TD, Van Loon LJC, Rollo I. Eat like an athlete: insights of sports nutrition science to support active aging in healthy older adults. *GeroScience*. 2021;43(5):2485–2495. doi:10.1007/s11357-021-00419-w
15. Rudnicka E, Napierała P, Podfigurna A, Męczekalski B, Smolarczyk R, Grymowicz M. The World Health Organization (WHO) approach to healthy ageing. *Maturitas*. 2020;139:6–11. doi:10.1016/j.maturitas.2020.05.018
16. Hermans F, Skeet J. *The Programmer's Brain: What Every Programmer Needs to Know About Cognition*. Shelter Island, USA: Manning; 2021. ISBN:978-1-61729-867-7.
17. Maldonado KA, Alsayouri K. Physiology: Brain. In: *StatPearls*. Treasure Island, USA: StatPearls Publishing; 2025:Bookshelf ID: NBK551718. <http://www.ncbi.nlm.nih.gov/books/NBK551718>. Accessed July 23, 2025.

18. Sultana OF, Bandaru M, Islam MA, Reddy PH. Unraveling the complexity of human brain: Structure, function in healthy and disease states. *Ageing Res Rev.* 2024;100:102414. doi:10.1016/j.arr.2024.102414
19. Yang Y, Wang D, Hou W, Li H. Cognitive decline associated with aging. *Adv Exp Med Biol.* 2023;1419:25–46. doi:10.1007/978-981-99-1627-6_3
20. Addo KM, Khan HTA. Factors affecting healthy aging and its interconnected pathways. *Turkish Journal of Healthy Aging Medicine.* 2024;1(1): 9–24. <https://dergipark.org.tr/en/download/article-file/3739220>.
21. Pizzagalli DA, Roberts AC. Prefrontal cortex and depression. *Neuropsychopharmacology.* 2022;47(1):225–246. doi:10.1038/s41386-021-01101-7
22. Górka E, Bogdan S, Gorodkiewicz E, Hermanowicz A. Neurodegenerations are diseases of the present and the future. *J Educ Health Sport.* 2022;12(11):23–32. doi:10.12775/jehs.2022.12.11.003
23. Gaur V, Bhatt A. Alzheimer's: A psycho-social concern. *Res Militaris.* 2023; 13(2):5819–5829. <https://resmilitaris.net/issue-content/alzheimer-s-a-psycho-social-concern-1975>.
24. Fuentes E, Venegas B, Muñoz-Arenas G, et al. High-carbohydrate and fat diet consumption causes metabolic deterioration, neuronal damage, and loss of recognition memory in rats. *J Chem Neuroanat.* 2023;129:102237. doi:10.1016/j.jchemneu.2023.102237
25. Kawabata M, Lee K, Choo HC, Burns SF. Breakfast and exercise improve academic and cognitive performance in adolescents. *Nutrients.* 2021; 13(4):1278. doi:10.3390/nu13041278
26. Ekstrand B, Scheers N, Rasmussen MK, Young JF, Ross AB, Landberg R. Brain foods: The role of diet in brain performance and health. *Nutr Rev.* 2021;79(6):693–708. doi:10.1093/nutrit/nuaa091
27. Moradikar N, Dadkhah M, Ghanbari A, et al. Protective effects of *Spirulina platensis*, voluntary exercise and environmental interventions against adolescent stress-induced anxiety and depressive-like symptoms, oxidative stress and alterations of BDNF and 5HT-3 receptors of the prefrontal cortex in female rats. *Neuropsychiatr Dis Treat.* 2020; 16:1777–1794. doi:10.2147/ndt.s247599
28. Nowacka M, Obuchowicz E. BDNF and VEGF in the pathogenesis of stress-induced affective diseases: An insight from experimental studies. *Pharmacol Rep.* 2013;65(3):535–546. doi:10.1016/s1734-1140(13)71031-4
29. Ghanbari A, Vafaei AA, Naghibi Nasab FS, Attarmoghaddam M, Bandegi AR, Moradikar N. *Spirulina microalgae* improves memory deficit induced by scopolamine in male pup rats: Role of oxidative stress. *S Afr J Botany.* 2019;127:220–225. doi:10.1016/j.sajb.2019.08.045
30. Haider S, Shahzad S, Batool Z, et al. *Spirulina platensis* reduces the schizophrenic-like symptoms in rat model by restoring altered APO-E and RTN-4 protein expression in prefrontal cortex. *Life Sci.* 2021;277:119417. doi:10.1016/j.lfs.2021.119417
31. Rana A, Samtiya M, Dhewa T, Mishra V, Aluko RE. Health benefits of polyphenols: A concise review. *J Food Biochem.* 2022;46(10):e14264. doi:10.1111/jfbc.14264
32. Winiarska-Mieczan A, Kwiecień M, Jachimowicz-Rogowska K, Donaldson J, Tomaszewska E, Baranowska-Wójcik E. Anti-inflammatory, antioxidant, and neuroprotective effects of polyphenols: Polyphenols as an element of diet therapy in depressive disorders. *Int J Mol Sci.* 2023;24(3):2258. doi:10.3390/ijms24032258
33. Rudrapal M, Khairnar SJ, Khan J, et al. Dietary polyphenols and their role in oxidative stress-induced human diseases: Insights into protective effects, antioxidant potentials and mechanism(s) of action. *Front Pharmacol.* 2022;13:806470. doi:10.3389/fphar.2022.806470
34. Gomez-Pinilla F, Nguyen TTJ. Natural mood foods: The actions of polyphenols against psychiatric and cognitive disorders. *Nutr Neurosci.* 2012;15(3):127–133. doi:10.1179/1476830511y.0000000035
35. Saadat M, Malekloo R, Davoodi M, et al. Beneficial effects of nano-phytosome of Quercetin on inflammatory parameters in mouse model of multiple sclerosis. *Eurasian Chem Commun.* 2022;4(5):432–440. doi:10.22034/ecc.2022.331138.1335
36. Sedighi S, Nasiri B, Alipoor R, Moradi-Kor N. Modulation of 6-gingerol antidepressant-like effects: An investigation of serotonergic system in mice model. *GMJ Med.* 2017;1(1):21–26. https://gmedicine.de/browse.php?a_id=253&slc_lang=en&sid=2&ftxt=1&html=1.
37. Shamsi-Goushki A, Mortazavi Z, Mirshekar MA, Behrasi F, Moradi-Kor N, Taghvaeifar R. Effects of high white and brown sugar consumption on serum level of brain-derived neurotrophic factor, insulin resistance, and body weight in albino rats. *J Obes Metab Syndr.* 2020;29(4):320–324. doi:10.7570/jomes20037
38. Dhana K, James BD, Agarwal P, et al. MIND diet, common brain pathologies, and cognition in community-dwelling older adults. *J Alzheimers Dis.* 2021;83(2):683–692. doi:10.3233/jad-210107
39. Arjmand G, Abbas-Zadeh M, Eftekhari MH. Effect of MIND diet intervention on cognitive performance and brain structure in healthy obese women: A randomized controlled trial. *Sci Rep.* 2022;12(1):2871. doi:10.1038/s41598-021-04258-9
40. Kheirouri S, Alizadeh M. MIND diet and cognitive performance in older adults: A systematic review. *Crit Rev Food Sci Nutr.* 2022;62(29): 8059–8077. doi:10.1080/10408398.2021.1925220
41. Schuch FB, Vancampfort D. Physical activity, exercise, and mental disorders: It is time to move on. *Trends Psychiatry Psychother.* 2021;43(3): 177–184. doi:10.47626/2237-6089-2021-0237
42. Ekkekakis P. *Routledge Handbook of Physical Activity and Mental Health.* London, UK: Routledge; 2023. doi:10.4324/9781003423430
43. Mahindru A, Patil P, Agrawal V. Role of physical activity on mental health and well-being: A review. *Cureus.* 2023;15(1):e33475. doi:10.7759/cureus.33475
44. White RL, Vella S, Biddle S, et al. Physical activity and mental health: A systematic review and best-evidence synthesis of mediation and moderation studies. *Int J Behav Nutr Phys Act.* 2024;21(1):134. doi:10.1186/s12966-024-01676-6
45. Moradikar N, Ghanbari A, Rashidipour H, Yousefi B, Bandegi AR, Rashidy-Pour A. Beneficial effects of *Spirulina platensis*, voluntary exercise and environmental enrichment against adolescent stress induced deficits in cognitive functions, hippocampal BDNF and morphological remodeling in adult female rats. *Horm Behav.* 2019;112:20–31. doi:10.1016/j.yhbeh.2019.03.004
46. Berchicci M, Lucci G, Di Russo F. Benefits of physical exercise on the aging brain: The role of the prefrontal cortex. *J Gerontol A Biol Sci Med Sci.* 2013;68(11):1337–1341. doi:10.1093/gerona/glt094
47. Chang H, Kim K, Jung YJ, Kato M. Effects of acute high-intensity resistance exercise on cognitive function and oxygenation in prefrontal cortex. *J Exerc Nutr Rehabil.* 2017;21(2):1–8. doi:10.20463/jenb.2017.0012

ERAS protocols for oral cancer free tissue transfer reconstruction: Critical review and clinical checklist

Andrzej Marek Jaxa-Kwiatkowski^{1,A–F}, Anna Leszczyszyn^{2,C–E}, Hanna Gerber^{1,A,E,F}

¹ Clinical Department of Maxillofacial Surgery, Faculty of Dentistry, Wrocław Medical University, Poland

² Oral Surgery Outpatient Clinic, 4th Military Hospital, Wrocław, Poland

A – research concept and design; B – collection and/or assembly of data; C – data analysis and interpretation; D – writing the article; E – critical revision of the article; F – final approval of the article

Advances in Clinical and Experimental Medicine, ISSN 1899–5276 (print), ISSN 2451–2680 (online)

Adv Clin Exp Med. 2025;34(9):1425–1431

Address for correspondence

Andrzej Marek Jaxa-Kwiatkowski
E-mail: andrzej.jaxa-kwiatkowski@umw.edu.pl

Funding sources

None declared

Conflict of interest

None declared

Received on May 31, 2025

Reviewed on June 23, 2025

Accepted on June 30, 2025

Published online on July 31, 2025

Abstract

The Enhanced Recovery After Surgery (ERAS) consensus offers a robust framework but must be tailored to the unique challenges of free-tissue transfer reconstructions in oral cancer. Factors such as clinical heterogeneity, institutional variability, inconsistent monitoring, and the absence of internal compliance audits can undermine postoperative recovery. By fostering multidisciplinary collaboration, ERAS can evolve from a theoretical guideline into a reproducible clinical pathway that enhances survival, functional outcomes and quality of life for oral cancer patients undergoing free-tissue reconstruction. Our proposed checklist merges evidence-based recommendations with practical adaptations to establish a more consistent, auditable and outcome-driven approach to perioperative care.

Key words: oral cancer, enhanced recovery after surgery (ERAS), perioperative care, clinical checklist

Cite as

Jaxa-Kwiatkowski AM, Leszczyszyn A, Gerber H.
ERAS protocols for oral cancer free tissue transfer
reconstruction: Critical review & clinical checklist.
Adv Clin Exp Med. 2025;34(9):1425–1431.
doi:10.17219/acem/207741

DOI

10.17219/acem/207741

Copyright

Copyright by Author(s)

This is an article distributed under the terms of the
Creative Commons Attribution 3.0 Unported (CC BY 3.0)
(<https://creativecommons.org/licenses/by/3.0/>)

Highlights

- Enhanced Recovery After Surgery (ERAS) provides a solid framework but requires adaptation for free-tissue transfer reconstructions in oral cancer patients.
- Challenges such as clinical heterogeneity, institutional variability, and lack of compliance audits can hinder postoperative recovery.
- Multidisciplinary collaboration is essential to transform ERAS from theoretical guidelines into reproducible clinical pathways.
- A proposed checklist integrates evidence-based recommendations with practical adaptations to ensure consistent, auditable, outcome-driven perioperative care.

Introduction

Enhanced Recovery After Surgery (ERAS) protocols have revolutionized perioperative care by substantially decreasing morbidity across numerous surgical disciplines. Dort et al. published a consensus on ERAS implementation in head and neck cancer surgery and free tissue transfer reconstruction (HNS-FTR).¹ However, when extrapolating to complex oncologic oral cavity reconstructions involving FTR, the ERAS framework begins to show signs of strain. That editorial addressed major controversial issues but left universal matters uncommented upon while stating that the general principles of early mobilization, multimodal analgesia, reduced perioperative fasting, and early urinary catheter removal remain universally beneficial. Nonetheless, several core elements of ERAS in this specific surgical context require critical adaptation or, in some cases, fundamental rethinking because even seemingly straightforward opioid-sparing analgesia requires improvements in monitoring. Kemp et al.² revealed inconsistencies in the implementation of the guidelines by showing that more than 64% of intensive care unit (ICU) patients did not receive a physician-documented pain assessment. This critical oversight highlights the urgent need for a structured checklist that includes ERAS recommendations for oral cancer FTR patients who may be tracheostomy-dependent and unable to self-report.

Preoperative nutritional optimization

The interval between diagnostic evaluation, definitive diagnosis and treatment initiation in oral cancer patients varies significantly depending on the institution and multiple individual patient factors.³ Given the significant delays before treatment reported by Rutkowska et al.,⁴ we believe that the time required for comprehensive diagnostics can be used to optimize the patient's nutritional status in every case where oral cancer is suspected, using validated tools such as Nutritional Risk Screening 2002 (NRS-2002)⁵ or the Malnutrition Universal Screening Tool (MUST).⁶

Early oral feeding vs prolonged nil by mouth

Institutions vary widely in their protocols for postoperative oral intake: Some enforce a strict nil-by-mouth (NBM) regimen for 7–10 days regardless of reconstruction type, based on the traditional belief that prolonged fasting reduces the risk of flap dehiscence, compromised healing and fistula formation. Both ERAS and European Society for Clinical Nutrition and Metabolism (ESPEN) support early oral feeding, though they underscore the limitation in robust data regarding oral cancer. When oral feeding is contraindicated, enteral nutrition should be initiated within 24 h of surgery, with careful monitoring and proactive management of refeeding syndrome.^{1,7,8} Kerawala et al. showed that early oral feeding did not increase the incidence of recipient site complications and was safe, even in patients with prior radiotherapy. Moreover, it significantly reduced the length of stay (LOS), supporting a shift from routine prolonged NBM practices.⁹ Brady and al. supported these findings and proposed a structured early feeding protocol that commences oral intake of a liquid diet on postoperative day 1, dietitian-supported nutritional planning, swallowing assessment by a speech and language therapist (SLT), and instrumental swallowing assessments when the clinical situation is unclear.¹⁰ In our experience, rigid fasting protocols often delay recovery and undermine nutritional goals that are critical in cancer care. It is time to abandon dogma in favor of a data-driven, patient-centered approach.

Airway management: Is tracheostomy still too routine?

Free tissue transfer reconstruction (FTR) involving the tongue base, floor of the mouth and extensive mandibular resections presents particular challenges in assessing the need for elective tracheostomy. According to Lederhof et al. and Le et al., elective tracheostomy should be reserved for patients with large lower oral cavity defects when the resection crosses the midline, involves the floor of the mouth, or requires bilateral neck dissections with FTR.^{11,12} Reconstructive flaps should be designed with

approx. 37% additional tissue to offset anticipated postoperative shrinkage and natural atrophy.¹³ In this context, postoperative edema can constrict the upper airway, posing a life-threatening risk if a tracheostomy is not performed. Although ERAS guidelines advocate for selective tracheostomy use and prompt decannulation once safe, they do not define explicit indications for elective tracheostomy, leaving this decision to the surgeon's clinical judgment and experience. Several validated scoring systems can aid in determining the need for elective tracheostomy in head and neck surgery. Cameron's original index evaluates factors such as surgical site, anticipated airway edema and comorbidities; Gupta's modification refines these criteria by incorporating intraoperative findings and patient risk profiles; and the TRACHY (Tracheostomy Risk Assessment Checklist in Head and Neck Surgery) protocol, developed by Mohamedbhai, combines preoperative, intraoperative and postoperative variables to generate a composite risk score that guides both tracheostomy placement and timing of decannulation.^{14–16} Table 1 presents a comparison of the 3 scoring systems.

Adhikari et al. defined decannulation timing as early (≤ 7 days) or delayed (≥ 7 days),¹⁷ whereas Patel et al. recommended that, in uncomplicated cases, decannulation can be safely performed between postoperative days 3 and 6

– provided there is adequate airway patency, an effective cough and no evidence of flap compromise.¹⁸

When tracheostomy is employed, the most widely accepted and safe protocols include tracheostomy tube cuff deflation on postoperative day 1 with subsequent early decannulation and surgical closure of the tracheostomy. These procedures lead to faster recovery and more effective respiratory and swallowing rehabilitation, though individualized assessments remain critical to avoid postoperative airway emergencies.^{1,19}

Tracheostomy should be a carefully considered intervention rather than a routine reflex. When it is required, protocols must emphasize structured weaning and early decannulation. This approach not only safeguards the airway but also accelerates recovery, minimizes complications and restores function at the earliest clinically appropriate time.

Postoperative ICU admission: Necessary or not?

Routine postoperative admission to the ICU is a case for ongoing discussion, and we believe it is time to question the reflexive ICU admission model. According to a systematic review and meta-analysis conducted by Mashrah

Table 1. Tracheostomy scoring systems focused on oral cancer surgery

Feature	Cameron et al. ¹⁴	CASST ¹⁵	TRACHY score ¹⁶
Study focus	Major head and neck surgery (including oral cancers)	Oral cavity and oropharyngeal cancers	Head and neck cancer with flap reconstruction, including oral sites
What about oral cancer?	Included oral sites like the anterior/posterior tongue, floor of mouth, and mandibular alveolus. Scoring emphasized tumor site proximity to the pharyngeal airway. High risk in tongue/floor of mouth resections	Exclusively focused on oral and oropharyngeal cancer surgeries. Identified tumor size, site, extent of resection, trismus, radiation, and flap bulk as major contributors to airway risk	Included oral cavity tumors as part of the overall H&N group. Oral cancers that needed bulky flaps or bilateral neck dissections scored higher
Study type	Retrospective review (148 procedures)	Retrospective analysis of 386 patients, prospective validation on 486 patients	Retrospective review (149 patients)
Tracheostomy criteria	Score based on tumor site, mandibulectomy, bilateral neck dissection, reconstruction	Score based on 6 major and 4 minor factors; surgical/anatomic risks and patient comorbidities	Score based on TRACHY (T-stage, reconstruction type, surgical site, ASA, treatment history, and neck dissection laterality)
Threshold for tracheostomy	Total score ≥ 5	Total score ≥ 7	Total score ≥ 4
Ease of use	Moderate – 4-factor model	Complex – 10 variables	Simple – 6 variables
Oral cancer suitability	Good general tool; flagged tongue and floor of mouth as high-risk	Best suited – built around oral cancer surgeries; robust data and validated, with the highest sensitivity (95.5%) and specificity (99.5%)	Applicable but not exclusive to oral cancers; strength in flap-specific risk
Key strengths	First structured scoring method; intuitive clinical categories	Highly predictive; prospectively validated in a large oral/oropharyngeal cancer cohort	Easy to apply; high-performing for flap-based reconstructions, including oral sites
Main limitation	Does not account for comorbidities; retrospective only	Many variables, less intuitive, and may be complex for routine use	Not yet externally validated; not exclusive to oral cancers

CASST – Clinical Assessment Scoring System for Tracheostomy; TRACHY – acronym based on 6 key factors: T-stage – tumor stage (based on TNM classification); reconstruction type – type of reconstruction (e.g., free flap, local flap); anatomic surgical site – surgical location (e.g., tongue, floor of mouth); ASA – American Society of Anesthesiologists physical status classification; history of treatment – prior therapies (e.g., radiation, surgery); Y/N neck dissection bilaterality – yes/no: Bilateral neck dissection performed; H&N – Head and Neck.

Table 2. Intensive care unit vs ward admission criteria for oral cancer free tissue transfer reconstruction

Parameter	ICU admission recommended	Ward/step-down admission safe	GoE	SoR
ASA physical status	ASA IV or unstable ASA III	ASA I–III, stable	III	A
Airway management	Anticipated airway difficulty without tracheostomy or unstable	Secured airway (tracheostomy or extubated safely in OR/PACU)	IV	A
Intraoperative hemodynamics	Vasopressor/inotrope use >1 h, persistent instability	Stable throughout the case, with low or no vasoactive support	II	A
Ventilation needs	Planned postoperative ventilation or $\text{FiO}_2 > 50\%$	Extubated, normal oxygen needs	III	B
Bleeding risk or coagulopathy	Active bleeding, platelet dysfunction, $\text{INR} > 1.5$	Controlled hemostasis, no known coagulopathy	III	A
Comorbidities	Decompensated CHF, ESRD, CAD with low EF, severe COPD	Controlled hypertension, DM, mild COPD	III	B
Free flap complexity	Bone flaps, previous radiation, bilateral neck, and long op (>12 h)	Soft tissue flap, unilateral neck, operative time <10–12 h	III	B
Postoperative pain/sedation plan	Requires i.v. PCA or deep sedation with hypoventilation risk	On multimodal PO analgesia or light sedation	II	B

GoE – grade of evidence; I – meta-analysis or more than 1 high-quality randomized controlled trial (RCT); II – prospective cohort study or lower-quality RCT; III – retrospective cohort, case-control study, or expert-informed institutional data; IV – case series or registry data; V – expert opinion or consensus without direct supporting studies; SoR – strength of recommendation; A – strong recommendation (clear benefit > risk; high-quality evidence); B – moderate recommendation (moderate-quality evidence or smaller benefit margin); C – weak recommendation (limited evidence or highly individualized decision); ASA – American Society of Anesthesiologists; CAD – coronary artery disease; CHF – congestive heart failure; COPD – chronic obstructive pulmonary disease; DM – diabetes mellitus; EF – ejection fraction; ERAS – enhanced recovery after surgery; ESRD – end-stage renal disease; FiO_2 – fraction of inspired oxygen; ICU – intensive care unit; INR – international normalized ratio; i.v. – intravenous; OR – operating room; PACU – post-anesthesia care unit; PCA – patient-controlled analgesia; PO – per os (by mouth); SCCM – Society of Critical Care Medicine.

et al., it does not improve outcomes in terms of flap survival or complication rates after HNS-FTR. Moreover, reducing ICU time or even limiting postoperative admissions can lower rates of pneumonia, sepsis, LOS, and healthcare costs.²⁰ Based on our experience and institutional setting, it is more efficient to monitor stable patients' when they remain in the same surgical ward rather than being transferred to the ICU, which also supports faster mobilization and improves continuity of care, but these findings require comprehensive research. Table 2 presents our institution's decision-support criteria for ICU compared to ward admission, which is grounded in recent literature and expert consensus. The presence of a single high-risk factor may be sufficient to warrant postoperative ICU admission.^{20–24}

Perioperative antibiotics: Tailored duration and choice

Prolonged antibiotic use remains common in oral cavity oncology and is usually connected to bone reconstruction, segmental mandibulectomy, preoperative radiation therapy, tracheotomy, longer operative time, and LOS.¹³ The Centers for Disease Control and Prevention (CDC) recommend antibiotic prophylaxis within 60 min before incision and discontinuation within 24 h postoperatively. Current guidelines emphasize pathogen-directed, short-term antibiotic regimens to optimize outcomes and reduce hospital-acquired infections.^{1,25,26} In contrast, a retrospective study by Daly et al. demonstrated that shortening the duration of antibiotic prophylaxis from a median of 9 days to 1 day, including the recommended cefazolin + metronidazole regimen, led to a significant increase in surgical site infection (SSI).²⁷

Recent evidence indicates that extending prophylactic antibiotic courses beyond 48–72 h offers no additional benefit; penicillins and cephalosporins remain the most effective agents for preventing surgical-site infections in head and neck/oral cancer surgery, whereas clindamycin performs poorly, especially in penicillin-allergic patients.^{26,28–30} Iocca et al. also highlighted that most reported penicillin allergies are not confirmed upon formal testing, suggesting that many patients may be unnecessarily excluded from receiving first-line prophylaxis.²⁶ Multidisciplinary research shows that the risk of cross-reactivity between penicillin and cefazolin is very low and supports its use in most surgical patients with a history of penicillin allergy, but current official clinical guidelines still do not fully align with these trends.^{31,32} Data on the optimal duration of postoperative antibiotic prophylaxis are limited – particularly in patients undergoing vascularized bone graft reconstruction or those who have received neoadjuvant therapy. Furthermore, no clear consensus has been established, underscoring the need for further research, ideally randomized controlled trials focused on these high-risk subgroups. Current perioperative antibiotic prophylaxis recommendations are summarized in Table 3.

Steroid use: Limited to single preoperative dose

Corticosteroid use in ERAS protocols for head and neck surgery (HNS) remains a subject of debate. Dort et al.¹ recommend a single preoperative dose of corticosteroids, primarily to reduce postoperative nausea and vomiting

Table 3. Recommended perioperative antibiotic therapy in oral cavity free flap reconstruction

Clinical scenario	Antibiotic regimen	Dosage and frequency	Duration	Notes/Alternatives	GoE	SoR
Standard case (clean-contaminated)	Ampicillin + sulbactam	3 g i.v. every 6 h	≤24 h	Preferred: discontinue unless high-risk*	II	A
Alternative (β-lactam allergy – non-anaphylaxis)	Cefazolin + metronidazole	Cefazolin 1–2 g i.v. q8h and metronidazole 500 mg i.v. q8h	≤24 h	Use only if allergy is mild (e.g., rash); avoid in-mediated reactions	II	B
Penicillin anaphylaxis (true allergy)	Clindamycin	Clindamycin 600 mg i.v. q8h	≤24 h	Limited Gram-negative coverage. Consider adding levofloxacin 500–750 mg i.v. q24h if Gram-negative risk is high. Monitor for <i>C. difficile</i>	III	B
High-risk	Ampicillin-sulbactam	As above	up to 72 h	For major contamination, ischemia, prior radiation, or immunocompromised hosts. De-escalate and consult ID if needed	II	B
Signs of infection or fistula	Tailored antibiotic therapy (based on cultures)	Per ID recommendation	Therapeutic course (7–14 days)	Start broad empiric coverage → de-escalate once cultures available. Cover oral flora, anaerobes, and skin flora	III	A

i.v. – intravenous; q8h – every 8 h; q12h – every 12 h; ID – infectious diseases specialist; *C. difficile* – *Clostridium difficile*; *High risk – bone reconstruction (e.g., fibula flap, segmental mandibulectomy), preoperative radiation therapy, tracheostomy or prolonged intubation, risk of salivary leak, operative time >8 h, reoperation or flap revision within 72 h; supporting sources for these recommendations include: Iocca et al. (Head Neck, 2022), Daly et al. (Open Forum Infect Dis, 2021), Khariwala et al. (Surg Infect, 2016), Haidar et al. (Head Neck, 2018), Balamohan et al. (Am J Otolaryngol, 2019), Sousa-Pinto et al. (JAMA Surg, 2021), Sexton & Kuruville (Antibiotics, 2024)^{26–32}

(PONV) after some types of surgery. However, the role of extended steroid administration is more controversial. In a randomized controlled trial, Kainulainen et al. examined the effects of a total of 60 mg dexamethasone intravenously (i.v.) for 3 days. The regimen did not reduce flap edema or shorten LOS and was associated with a higher rate of postoperative infections than placebo.³³

The ongoing PreSte-HN study³⁴ is the first multicenter, placebo-controlled, phase III trial specifically addressing whether a single, low-dose preoperative dexamethasone infusion can enhance recovery without increasing complications and establishing clearly defined ERAS guidelines for HNS-FTR. Once consensus is reached, the checklist should include a single preoperative dose of steroids; routine use of steroids beyond that single dose is not supported by the literature and may be harmful.

Venous thromboembolism prevention: Multimodal, risk-based strategy

Thromboprophylaxis following oral cancer FTR, where the balance between thrombosis and bleeding is particularly delicate, has led to wide variations in clinical practice; some centers initiate low-molecular-weight heparin (LMWH) within 6–12 h following the operation, while others delay pharmacologic prophylaxis, relying initially on mechanical methods.

Low-molecular-weight heparin and unfractionated heparin (UFH) are effective options for venous thromboembolism (VTE) prophylaxis, with LMWH offering practical

advantages such as predictable dosing and longer half-life, though no clear superiority has been proven. Aspirin alone is not recommended for VTE prophylaxis, and its role remains unclear since evidence indicates increased bleeding when combined with other anticoagulants.³⁵































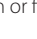


Current expert consensus supports a multimodal approach combining pharmacologic agents with mechanical prophylaxis, like intermittent pneumatic compression and early mobilization. Low-molecular-weight heparin should ideally commence within 12 h of surgery (following hemostasis) at prophylactic doses (40 mg daily) and continue for at least 7 days or extend to 28 days in high-risk scenarios (previous VTE, obesity, prolonged immobilization, and advanced cancer stage). It is also vital to assess patients' individualized thromboembolism risk factors preoperatively and adjust prophylaxis accordingly.

At present, the routine continuation of anticoagulant therapy to prevent metastatic spread is not standard practice, although preclinical studies indicate that anticoagulants may possess antitumor properties.³⁶

Conclusions

Perhaps the most glaring weakness in ERAS implementation for oral cavity reconstruction is the lack of monitoring systems. Protocols are frequently adopted in theory but inconsistently applied. Furthermore, elements such as early feeding, pain control, ambulation, and tracheostomy weaning are often left without documentation or audit.

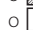
Table 4. Checklist for oral cancer free flap reconstruction (institutional adaptation of ERAS guidelines)

Phase	Component	Summary recommendation	Icon	Priority	(✓)
Pre-op	Nutritional screening	NRS-2002 or MUST at the first visit, at least ≥7 days pre-op; dietitian review			<input type="checkbox"/>
	Smoking/alcohol cessation	Counsel ≥2 weeks pre-op; document cessation		<input type="checkbox"/>	<input type="checkbox"/>
	Chlorhexidine rinse	Initiate 0.12% rinse 2–3 days before surgery		<input type="checkbox"/>	<input type="checkbox"/>
	Patient Education	Discuss surgery, feeding, airway, pain, and mobility			<input type="checkbox"/>
	Carb loading	400 mL iso-osmolar drink the night before (omit if diabetic)		<input type="checkbox"/>	<input type="checkbox"/>
Intra-op	Antibiotics	Administer ≤60 min pre-incision; limit to 24 h unless high-risk*			<input type="checkbox"/>
	Fluid management	Goal-directed/zero-balance fluids			<input type="checkbox"/>
	PONV prevention	Ondansetron + dexamethasone based on risk		<input type="checkbox"/>	<input type="checkbox"/>
	Tracheostomy	Selective only; avoid routine tracheostomy		<input type="checkbox"/>	<input type="checkbox"/>
Post-op	Analgesia	VAS-documented multimodal; minimize opioids			<input type="checkbox"/>
	Enteral nutrition	Start via NG/PEG <24 h; consider oral fluids POD 4–7			<input type="checkbox"/>
	Mobilization	Sit up ≥2 h POD 1; walk POD 2–3 with physio assist			<input type="checkbox"/>
	Laboratory tests	POD 1–3: Daily CBC, electrolytes, creatinine, CRP; q48 – 72 h LFTs, albumin, glucose POD ≥3: Patient-specific		<input type="checkbox"/>	<input type="checkbox"/>
	Tracheostomy decannulation	Cuff deflate POD 1, decannulation trial POD ≥3; criteria: Patent airway, effective cough, no leak, early stoma closure		<input type="checkbox"/>	<input type="checkbox"/>
	Foley catheter	Remove POD 1–2 if stable			<input type="checkbox"/>
	Flap monitoring	q1–2 h (POD 0–1), q2–4 h (POD 2–3), q6–12 h (POD ≥4 if stable ±Doppler)			<input type="checkbox"/>
	Swallowing evaluation	SLT assesses POD ≥5 or before oral intake		<input type="checkbox"/>	<input type="checkbox"/>
	VTE prophylaxis	LMWH + compression; extend to high-risk (Caprini ≥5)			<input type="checkbox"/>
	Nutrition	Define plan		<input type="checkbox"/>	<input type="checkbox"/>
Discharge	Tracheostomy care	Ensure closure or a follow-up		<input type="checkbox"/>	<input type="checkbox"/>
	Rehab follow-up	Ensure SLT and physiotherapy referral		<input type="checkbox"/>	<input type="checkbox"/>
	Audit & compliance	Track ERAS adherence, complications, LOS			<input type="checkbox"/>

POD – postoperative day; NRS-2002 – Nutritional Risk Screening 2002; MUST – Malnutrition Universal Screening Tool; NG – nasogastric; PEG – percutaneous endoscopic gastrostomy; PONV – postoperative nausea and vomiting; CBC – complete blood count; CRP – C-reactive protein; LFTs – liver function tests; PT/INR – prothrombin time/international normalized ratio; SLT – speech and language therapy; VTE – venous thromboembolism; LMWH – low-molecular-weight heparin; ERAS – enhanced recovery after surgery; LOS – length of stay; *high-risk – bone reconstruction (e.g., fibula flap, segmental mandibulectomy), preoperative radiation therapy, tracheostomy or prolonged intubation, risk of salivary leak, operative time >8 h, reoperation or flap revision within 72 h.

Priority flags:

 Essential for ERAS success and strongly evidence-based

 Recommended but may vary based on patient or institutional factors

Icons: Visual cues for quick reference by interdisciplinary teams

✓ Column: Use for bedside documentation, audits, or real-time team tracking


Given the increasing volume of microvascular procedures, there is a clear need for targeted research and consensus-building. ERAS should function as a living, actively implemented protocol – not a checklist gathering dust in a drawer. It should be a dynamic system, not a static guideline, that evolves with evidence, audits its own effectiveness, and adapts to institutional realities. Our proposed checklist (Table 4), a first step toward that vision, is a user-friendly protocol that centers not on what is easy but on what is necessary, a literature-based approach to optimal recovery.


Use of AI and AI-assisted technologies


Not applicable.

ORCID iDs

Andrzej Marek Jaxa-Kwiatkowski

 <https://orcid.org/0000-0001-8515-3978>

Anna Leszczyszyn  <https://orcid.org/0000-0001-7853-2814>

Hanna Gerber  <https://orcid.org/0000-0002-0954-3955>

References

1. Dort JC, Farwell DG, Findlay M, et al. Optimal perioperative care in major head and neck cancer surgery with free flap reconstruction: A consensus review and recommendations from the enhanced recovery after Surgery Society. *JAMA Otolaryngol Head Neck Surg.* 2017;143(3):292. doi:10.1001/jamaoto.2016.2981
2. Kemp HI, Bantel C, Gordon F, et al. Pain Assessment in INTensive care (PAINT): An observational study of physician-documented pain assessment in 45 intensive care units in the United Kingdom. *Anaesthesia.* 2017;72(6):737–748. doi:10.1111/anae.13786
3. Swaminathan D, George NA, Thomas S, Iype EM. Factors associated with delay in diagnosis of oral cancers. *Cancer Treat Res Commun.* 2024;40:100831. doi:10.1016/j.ctarc.2024.100831

4. Rutkowska M, Hnietka S, Nahajowski M, Dominiak M, Gerber H. Oral cancer: The first symptoms and reasons for delaying correct diagnosis and appropriate treatment. *Adv Clin Exp Med*. 2020;29(6):735–743. doi:10.17219/acem/116753
5. Kondrup J, Rasmussen HH, Hamberg O, Stanga Z; Ad Hoc ESPEN Working Group. Nutritional risk screening (NRS 2002): A new method based on an analysis of controlled clinical trials. *Clin Nutr*. 2003;22(3):321–336. doi:10.1016/s0261-5614(02)00214-5
6. Chao PC, Chuang HJ, Tsao LY, et al. The Malnutrition Universal Screening Tool (MUST) and a nutrition education program for high risk cancer patients: Strategies to improve dietary intake in cancer patients. *BioMed*. 2015;5(3):17. doi:10.7603/s40681-015-0017-6
7. Weimann A, Braga M, Carli F, et al. ESPEN practical guideline: Clinical nutrition in surgery. *Clin Nutr*. 2021;40(7):4745–4761. doi:10.1016/j.clnu.2021.03.031
8. Jaxa-Kwiatkowski A, Łysenko L, Gara-Rucińska M, Leszczyszyn A, Gerber H, Kubiak M. Potentially lethal but rarely considered: Risk of developing refeeding syndrome in primary oral squamous cell carcinoma. *J Stomatol Oral Maxillofac Surg*. 2024;125(5):101742. doi:10.1016/j.joms.2023.101742
9. Kerawala CJ, Riva F, Paleri V. The impact of early oral feeding following head and neck free flap reconstruction on complications and length of stay. *Oral Oncol*. 2021;113:105094. doi:10.1016/j.oraloncology.2020.105094
10. Brady G, Leigh-Doyle L, Riva F, Kerawala C, Roe J. Early post-operative feeding: An investigation of early functional outcomes for oral cancer patients treated with surgical resection and free flap reconstruction. *Dysphagia*. 2022;37(4):1008–1013. doi:10.1007/s00455-021-10363-8
11. Ledderhof NJ, Carlson ER, Heidel RE, Winstead ML, Fahmy MD, Johnston DT. Are tracheotomies required for patients undergoing composite mandibular resections for oral cancer? *J Oral Maxillofac Surg*. 2020;78(8):1427–1435. doi:10.1016/j.joms.2020.03.027
12. Le JM, Gigliotti J, Bourne GR, et al. Immediate extubation versus elective tracheostomy following free flap reconstruction of the oral cavity: A 7-year single institution retrospective study. *J Oral Maxillofac Surg*. 2023;81(9 Suppl):S57–S58. doi:10.1016/j.joms.2023.08.148
13. Schuderer JG, Hoferer F, Eichberger J, et al. Predictors for prolonged and escalated perioperative antibiotic therapy after microvascular head and neck reconstruction: A comprehensive analysis of 446 cases. *Head Face Med*. 2024;20(1):58. doi:10.1186/s13005-024-00463-9
14. Cameron M, Corner A, Diba A, Hankins M. Development of a tracheostomy scoring system to guide airway management after major head and neck surgery. *Int J Oral Maxillofac Surg*. 2009;38(8):846–849. doi:10.1016/j.ijom.2009.03.713
15. Gupta K, Mandlik D, Patel D, et al. Clinical assessment scoring system for tracheostomy (CASST) criterion: Objective criteria to predict pre-operatively the need for a tracheostomy in head and neck malignancies. *J Craniomaxillofac Surg*. 2016;44(9):1310–1313. doi:10.1016/j.jcms.2016.07.008
16. Mohamedbhai H, Ali S, Dimasi I, Kalavrezos N. TRACHY score: A simple and effective guide to management of the airway in head and neck cancer. *Br J Oral Maxillofac Surg*. 2018;56(8):709–714. doi:10.1016/j.bjoms.2018.07.015
17. Adhikari A, Noor A, Mair M, et al. Comparison of postoperative complications in early versus delayed tracheostomy decannulation in patients undergoing oral cancer surgery with microvascular reconstruction. *Br J Oral Maxillofac Surg*. 2023;61(1):101–106. doi:10.1016/j.bjoms.2022.11.285
18. Patel P, Patel P, Solanki K, Ahmed A, Visavadia B, Farook S. 42. Temporary tracheostomy in post-operative airway management of oral cavity surgery free flap patients: Is it necessary? *Br J Oral Maxillofac Surg*. 2022;60(10):e23. doi:10.1016/j.bjoms.2022.11.116
19. Bertazzoni G, Testa G, Tomasoni M, et al. The Enhanced Recovery After Surgery (ERAS) protocol in head and neck cancer: A matched-pair analysis. *Acta Otorhinolaryngol Ital*. 2022;42(4):325–333. doi:10.14639/0392-100X-N2072
20. Mashrah MA, Aldhohrah T, Abdelrehem A, et al. Postoperative care in ICU versus non-ICU after head and neck free-flap surgery: A systematic review and meta-analysis. *BMJ Open*. 2022;12(1):e053667. doi:10.1136/bmjopen-2021-053667
21. Nates JL, Nunnally M, Kleinpell R, et al. ICU admission, discharge, and triage guidelines: A framework to enhance clinical operations, development of institutional policies, and further research. *Crit Care Med*. 2016;44(8):1553–1602. doi:10.1097/CCM.0000000000001856
22. Chen WC, Hung KS, Chen SH, et al. Intensive care unit versus ward management after anterolateral thigh flap reconstruction after oral cancer ablation. *Ann Plast Surg*. 2018;80(2 Suppl):S11–S14. doi:10.1097/SAP.0000000000001301
23. Cervenka B, Olinde L, Gould E, et al. Use of a non-ICU specialty ward for immediate post-operative management of head and neck free flaps: A randomized controlled trial. *Oral Oncol*. 2019;99:104464. doi:10.1016/j.oraloncology.2019.104464
24. Van Valkinburgh D, Kerndt CC, Hashmi MF. Inotropes and vasopressors. In: *StatPearls*. Treasure Island, USA: StatPearls Publishing; 2025. <http://www.ncbi.nlm.nih.gov/books/NBK482411>. Accessed June 30, 2025.
25. Busch CJ, Knecht R, Münscher A, Matern J, Dalchow C, Lörincz BB. Postoperative antibiotic prophylaxis in clean-contaminated head and neck oncologic surgery: A retrospective cohort study. *Eur Arch Otorhinolaryngol*. 2016;273(9):2805–2811. doi:10.1007/s00405-015-3856-6
26. locca O, Copelli C, Ramieri G, Zocchi J, Savo M, Di Maio P. Antibiotic prophylaxis in head and neck cancer surgery: Systematic review and Bayesian network meta-analysis. *Head Neck*. 2022;44(1):254–261. doi:10.1002/hed.26908
27. Daly JF, Gearing PF, Tang NSJ, Ramakrishnan A, Singh KP. Antibiotic prophylaxis prescribing practice in head and neck tumor resection and free flap reconstruction. *Open Forum Infect Dis*. 2022;9(1):ofab590. doi:10.1093/ofid/ofab590
28. Khariwala SS, Le B, Pierce BHG, Isaksson Vogel R, Chipman JG. Antibiotic use after free tissue reconstruction of head and neck defects: Short course vs long course. *Surg Infect*. 2016;17(1):100–105. doi:10.1089/sur.2015.131
29. Haidar YM, Tripathi PB, Tjoa T, et al. Antibiotic prophylaxis in clean-contaminated head and neck cases with microvascular free flap reconstruction: A systematic review and meta-analysis. *Head Neck*. 2018;40(2):417–427. doi:10.1002/hed.24988
30. Balamohan SM, Sawhney R, Lang DM, et al. Prophylactic antibiotics in head and neck free flap surgery: A novel protocol put to the test. *Am J Otolaryngol*. 2019;40(6):102276. doi:10.1016/j.amjoto.2019.102276
31. Sousa-Pinto B, Blumenthal KG, Courtney L, Mancini CM, Jeffres MN. Assessment of the frequency of dual allergy to penicillins and cefazolin: A systematic review and meta-analysis. *JAMA Surg*. 2021;156(4):e210021. doi:10.1001/jamasurg.2021.0021
32. Sexton ME, Kuruvilla ME. Management of penicillin allergy in the perioperative setting. *Antibiotics (Basel)*. 2024;13(2):157. doi:10.3390/antibiotics13020157
33. Kainulainen S, Törnwall J, Koivusalo AM, Suominen AL, Lassus P. Dexamethasone in head and neck cancer patients with microvascular reconstruction: No benefit, more complications. *Oral Oncol*. 2017;65:45–50. doi:10.1016/j.oraloncology.2016.12.008
34. Shinozaki T, Imai T, Kobayashi K, et al. Preoperative steroid for enhancing patients' recovery after head and neck cancer surgery with free tissue transfer reconstruction: Protocol for a phase III, placebo-controlled, randomised, double-blind study (J-SUPPORT 2022, PreSte-HN Study). *BMJ Open*. 2023;13(5):e069303. doi:10.1136/bmjopen-2022-069303
35. Abraham M, Badhey A, Hu S, et al. Thromboprophylaxis in head and neck microvascular reconstruction. *Craniomaxillofac Trauma Reconstr*. 2018;11(2):85–95. doi:10.1055/s-0037-1607068
36. Ma SN, Mao ZX, Wu Y, et al. The anti-cancer properties of heparin and its derivatives: A review and prospect. *Cell Adh Migr*. 2020;14(1):118–128. doi:10.1080/19336918.2020.1767489

Vestibular rehabilitation: Proven benefits in enhancing balance and reducing dizziness

*Xiaohua Sun^{1,A,D,F}, *Zuwei Cao^{2,B,C,F}, Xin Li^{3,A,E,F}

¹ School of Sports Medicine and Rehabilitation, Beijing Sport University, China

² Department of Otolaryngology, Guizhou Branch of Shanghai Children's Medical Center, Shanghai Jiao Tong University School of Medicine, Guiyang, China

³ Beijing Tsinghua Changgung Hospital, School of Clinical Medicine, Tsinghua University, China

A – research concept and design; B – collection and/or assembly of data; C – data analysis and interpretation;

D – writing the article; E – critical revision of the article; F – final approval of the article

Advances in Clinical and Experimental Medicine, ISSN 1899–5276 (print), ISSN 2451–2680 (online)

Adv Clin Exp Med. 2025;34(9):1433–1449

Address for correspondence

Xin Li

E-mail: entlixintsinghua@sina.com

Funding sources

None declared

Conflict of interest

None declared

* Xiaohua Sun and Zuwei Cao contributed equally to this work.

Received on June 19, 2024

Reviewed on July 15, 2024

Accepted on September 12, 2024

Published online on June 5, 2025

Abstract

Background. Vestibular rehabilitation therapy (VRT) is widely utilized to enhance balance and mitigate dizziness in patients with vestibular disorders. However, its overall effectiveness remains to be comprehensively assessed, particularly in the context of variability among studies.

Objectives. This study aimed to address the current need for a systematic evaluation of VRT's efficacy.

Materials and methods. A meta-analysis was conducted using the “meta” and “dmetar” R packages to evaluate VRT's efficacy. The analysis included statistical tools, such as Begg's test, Egger's test, Baujat plots, Galbraith plots, and influence analysis. Additionally, heterogeneity and outliers were assessed using generalized scatterplot smoothing (GOSH) diagnostics and clustering methods, including K-means, density-based spatial clustering of applications with noise (DBSCAN) and Gaussian mixture model (GMM).

Results. The meta-analysis examined the impact of VRT on the dizziness handicap inventory (DHI) and Berg balance scale (BBS). For the DHI, VRT resulted in a significant mean improvement of 7.63 points, despite high heterogeneity ($I^2 = 88\%$). Similarly, the BBS exhibited significant improvement, with a mean difference (MD) of -2.31 points in the fixed effects model, while the random effects model also suggested improvement, though with greater variability ($I^2 = 92\%$). Subgroup analysis identified outliers significantly influencing the results.

Conclusions. We showed that VRT significantly enhanced patient outcomes as measured with both the DHI and BBS. These findings provide strong evidence supporting VRT's effectiveness, though the substantial heterogeneity underscores the need for further research to refine patient selection and intervention protocols. This study advances the understanding of VRT's role in managing vestibular disorders and highlights the importance of addressing variability in future studies.

Key words: meta-analysis, Berg Balance Scale, Dizziness Handicap Inventory, vestibular rehabilitation training

Cite as

Sun X, Cao Z, Li X. Vestibular rehabilitation: Proven benefits in enhancing balance and reducing dizziness.

Adv Clin Exp Med. 2025;34(9):1433–1449.

doi:10.17219/acem/193242

DOI

10.17219/acem/193242

Copyright

Copyright by Author(s)

This is an article distributed under the terms of the Creative Commons Attribution 3.0 Unported (CC BY 3.0) (<https://creativecommons.org/licenses/by/3.0/>)

Background

Vestibular rehabilitation therapy (VRT) is an essential intervention for individuals experiencing balance disorders and dizziness, particularly those recovering from conditions, such as stroke and multiple sclerosis (MS).^{1–3} Balance disturbances and dizziness are common complications for stroke survivors,^{4,5} and VRT has been shown to play a significant role in alleviating these symptoms.⁶ Sana et al.⁷ demonstrated that VRT effectively enhances balance, reduces dizziness and improves gait in patients with subacute stroke. Furthermore, Ekvall Hansson et al.⁸ provided evidence through a pilot study that VRT can also benefit stroke patients with concomitant dizziness. In a comprehensive review, Meng et al.⁹ confirmed the positive effects of VRT on post-stroke balance and gait through a systematic review and meta-analysis.

Understanding the underlying neuroscience of vestibular compensation is critical to understating how VRT contributes to recovery.^{10,11} Key neural structures, including the vestibular nuclei, cerebellum, thalamus, and cortical areas, play crucial roles in processing and compensating for vestibular deficits.^{12–14} The vestibular nuclei, located in the brainstem, are the primary centers for processing vestibular information and initiating the compensation process.^{15,16} The cerebellum further refines these signals, which is essential for adjusting motor responses and maintaining balance.¹⁷ The thalamus serves as a relay station, transmitting vestibular information to the cerebral cortex, where higher-order processing takes place, facilitating spatial orientation and movement perception.^{18,19} Neuroplasticity mechanisms involved in vestibular compensation include both peripheral and central changes. Peripheral adaptation refers to adjustments in the sensitivity of the hair cells in the inner ear, while central adaptation involves synaptic plasticity and reorganization within the vestibular nuclei and associated neural circuits.^{20,21} Evidence suggests that repeated vestibular stimuli can enhance synaptic efficacy and promote new neural connections, aiding in functional recovery.²²

Patients with MS also benefit from VRT. García-Muñoz et al.²³ demonstrated that vestibular therapy significantly improves balance and reduces dizziness in MS patients through a systematic review and meta-analysis. Additionally, García-Muñoz et al.²⁴ explored the combined use of immersive virtual reality and VRT, showing notable improvements in balance and dizziness rehabilitation for MS patients. Despite numerous studies on the effectiveness of VRT, including those conducted by Sulway and Whitney,²⁵ Bush and Dougherty²⁶ and Wang et al.,²⁷ there remains a need for a more comprehensive evaluation of the effectiveness of VRT in different patient populations. Studies carried out by Moore et al.,²⁸ Loftin et al.²⁹ and Smółka et al.³⁰ have reported promising results for VRT in treating persistent post-concussion symptoms and chronic unilateral vestibular dysfunction. However, there is still a lack of systematic assessment across diverse patient populations.

Objectives

The primary objective of this study was to address this gap by conducting a meta-analysis to systematically evaluate the effectiveness of VRT. This analysis aimed to consolidate findings from various studies, address heterogeneity and mitigate potential publication biases.

The aim was to identify relevant studies focusing on the Berg Balance Scale (BBS), Dizziness Handicap Inventory (DHI), and vestibular rehabilitation training, specifically within the context of randomized controlled trials (RCTs)

Methods

Search strategy

The search for this systematic review and meta-analysis was conducted over a period from January 2015 to May 2024. The primary databases searched included PubMed, Web of Science and Embase. The search terms used were a combination of key words and Medical Subject Headings (MeSH) terms to ensure comprehensive coverage. The key words included “Berg Balance Scale”, “Dizziness Handicap Inventory”, “vestibular rehabilitation training”, “randomized”, and “RCT”. Boolean operators such as AND and OR were employed to refine and expand the search results appropriately. In addition to the database searches, supplementary records were identified through other reputable sources including Cochrane Library, China National Knowledge Infrastructure (CNKI) and WanFang databases. This multi-database approach was designed to capture a broad range of studies, including those published in languages other than English and those that might not have been indexed in the primary databases. We conducted a systematic review and meta-analysis following the Preferred Reporting Items for Systematic reviews and Meta-analyses (PRISMA) guidelines to assess the efficacy of VRT. Studies were evaluated using the Grading of Recommendations Assessment, Development, and Evaluation (GRADE) approach to rate the certainty of evidence for key outcomes, including balance improvement and reduction in dizziness severity. The systematic review and meta-analysis were independently conducted by 2 authors, J.S. and A.M., who carried out the literature search. In the event of any conflict during the process, M.R. acted as a 3rd author to make the final decision, ensuring consistency and accuracy in study selection.

Inclusion criteria

Study design: Only RCTs were considered eligible, regardless of participants' gender, age, race, and country, as well as time of study. This broad inclusion ensured a diverse and comprehensive data analysis.

Intervention methods: Included studies had to use one of the following intervention methods:

- Balance and eye-movement exercises for persons with multiple sclerosis (BEEMS);
- Vestibulo-ocular reflex (VOR);
- Gaze and postural stability (GPS) retraining intervention;
- Dynamic motion instability system training (DMIST);
- Gaze stabilization exercises (GSEs);
- Turning-based treadmill training;
- Robot-assisted stair climbing training;
- Epley maneuver (canalith repositioning procedure);
- Gaze stability exercises combined with postural stability exercises;
- Outcome measures: The studies needed to report outcomes using either the DHI or the BBS, which are validated tools for assessing the effectiveness of vestibular rehabilitation training.

Exclusion criteria

- Non-RCTs: Any study that was not an RCT was excluded to maintain the rigor and reliability of the analysis.
- Small sample size: Studies with a patient number of 10 or less were excluded to ensure sufficient statistical power and the generalizability of the findings.
- Incomplete data: Studies where the full text was unavailable or the article data were incomplete were excluded from the analysis. This was done to ensure a comprehensive analysis.
- Non-English or Non-Chinese studies were not included.
- Similar intervention methods: Studies in which both interventions involved vestibular rehabilitation therapy were excluded to avoid redundancy and ensure the diversity of the interventions analyzed.

Data extraction

Data extraction was performed accurately and independently by J.S. and A.M., with M.R. resolving any discrepancies to ensure that the extraction process remained unbiased and valid, thereby reducing the potential for error.

Quality assessment

The quality of controlled intervention studies was evaluated using the Quality Assessment of Controlled Intervention Studies tool developed by the National Heart, Lung, and Blood Institute (NHLBI; National Institutes of Health (NIH), Bethesda, USA). This tool involves 14 criteria, including randomization, allocation concealment, blinding of participants, providers, outcome assessors, and baseline comparability between groups. It also helps evaluate drop-out rates, adherence to intervention protocols, consistency in applying other treatments, and the use of valid and reliable outcome measures. We used the tool to assess whether the studies clearly defined outcomes and subgroups at the time of study initiation, whether the sample

size was sufficiently powered to achieved at least 80% statistical power, whether the studies used intention-to-treat populations, and whether the target population was representative. To aid in determining the quality of these studies, each was evaluated and classified as good, fair or poor according to these criteria to prevent overreaching conclusions that are based on weak and possibly biased research.

The risk of bias plot was generated using the online tool available at robvis (<https://mcguinlu.shinyapps.io/robvis>) by selecting the Generic_example template and uploading the relevant data. The review was performed by 2 reviewers with the use of recommendations from Cochrane Handbook for Systematic Review of Interventions.³¹ Items assessed included: 1) random sequence generation (selection bias), 2) allocation concealment (selection bias), 3) blinding of participants and personnel (performance bias), 4) blinding of outcome assessment (detection bias), 5) incomplete outcome data (attrition bias), 6) selective reporting (reporting bias), and 7) other biases. The risk of bias of the included studies was noted as low, unclear or high. The question of risk bias suggested that most of the studies were at low risk in most categories, although there was an optional risk of performance bias due to lack of information on blinding of participants and personnel.

Statistical analyses

The meta-analysis was conducted using R software v. 4.3.2 (R Foundation for Statistical Computing, Vienna, Austria) with specific packages and statistical methods designed to handle meta-analytic data. The primary packages used were R tools “meta”³² and “dmetar”.³³

Begg’s test was employed to evaluate publication bias by examining the correlation between effect sizes and their variances.³⁴ Egger’s test was used to assess funnel plot asymmetry through linear regression of the intervention effect estimates on their standard errors (SEs).³⁵ It is important to note that Begg’s and Egger’s tests are typically recommended for use when the number of studies in a meta-analysis exceeds 10. This recommendation is based on the increased statistical power and reliability of these tests with larger sample sizes. In this study, these tests were used, but we recognized that with fewer studies, the results may have limited reliability and should be interpreted with caution.

Baujat plots were used to identify studies contributing most to the heterogeneity in the meta-analysis. Galbraith plots were utilized to detect outliers and influential studies by plotting standardized effect sizes against the inverse of their SEs.³⁶ To supplement the findings from Begg’s and Egger’s tests, qualitative assessments were also performed using funnel plots, Baujat plots and Galbraith plots. These additional methods helped to identify potential sources of heterogeneity and the impact of individual studies

on the overall results, providing a more comprehensive evaluation of potential biases.

Influence analysis was performed to determine the impact of each individual study on the overall meta-analysis results. This included leave-one-out analysis and various influence diagnostics such as *rstudent*, *dffits* and Cook's distance.

Generalized scatterplot smoothing (GOSH) diagnostics were used to explore the robustness of the meta-analytic findings by assessing the distribution of effect sizes and heterogeneity across a large number of potential meta-analytic models.³⁷

Clustering methods including K-means,³⁸ DBSCAN³⁹ and GMM⁴⁰ were applied to identify patterns and outliers within the dataset. For the clustering analysis, specific hyperparameters were selected for each method. In the K-means algorithm, the number of clusters was determined using the Elbow method and Silhouette score, with "k-means++" initialization and 10 initializations to avoid local minima. For DBSCAN, the epsilon (ϵ , *eps*) parameter was selected using the k-distance graph to find the "elbow" point, with a minimum sample parameter set to 5. In the GMM, the number of components was based on the Bayesian information criterion (BIC) and Akaike information criterion (AIC), and the covariance type was set to "full". These parameters were optimized using cross-validation and specific data characteristics. In case of the high heterogeneity in the outcomes, further analysis was conducted to explore potential sources of this variability. While the K-means algorithm indicated a different clustering pattern compared with DBSCAN and GMM, this discrepancy was attributed to K-means' assumption of spherical clusters with uniform sizes, which was not suitable for our dataset's characteristics. The final clustering interpretation prioritized the results from DBSCAN and GMM, which better accounted for clusters of varying densities and shapes. While GMM provided a probabilistic framework for cluster assignment, DBSCAN was particularly effective at identifying noise and outliers.

Notably, the meta-analysis utilized both fixed-effect and random-effects models. However, the final model was the random-effects model, aligning with the guidelines from the Cochrane Handbook for Systematic Reviews of Interventions.³¹ The decision to use the random-effects model was made a priori, based on the assumption that the included studies represented a random sample from a larger population, acknowledging the variability in effect sizes due to differences in study populations, interventions and other factors. This approach ensured that the meta-analytic findings were generalizable and robust. Meta-regression and subgroup analyses were employed to identify factors contributing to heterogeneity. Meta-regression was performed to assess the impact of study-level covariates, such as intervention type, follow-up time and patients' characteristics on effect sizes. Subgroup analysis was conducted based on intervention methods, geographical locations of studies and quality assessment ratings.

Sensitivity analysis

To assess the robustness of meta-analysis results and the potential impact of high-risk bias studies, sensitivity analysis was conducted. This involved excluding studies that were rated as having a high risk of bias in any of the key domains assessed. The risk of bias for each study was evaluated using the Cochrane Collaboration's tool, considering factors such as random sequence generation, allocation concealment, blinding, incomplete outcome data, and selective reporting. For the sensitivity analysis, we re-ran the meta-analysis excluding studies categorized with a high risk of bias in the domains of random sequence generation, allocation concealment, and blinding of participants and personnel. This approach aimed to determine whether the exclusion of these studies significantly altered the overall effect estimates and the conclusions drawn from the primary analysis.

Results

Selection and inclusion of studies

A comprehensive search strategy identified 629 records through database searches in PubMed, Web of Science and Embase. An additional 37 records were found through other sources, including Cochrane Library, CNKI and WanFang databases, leading to a total of 666 potential articles. After removing 20 duplicate records, 212 articles were considered for further examination. Title and abstract screening resulted in the exclusion of 89 articles for reasons such as irrelevance to the study, review articles, case reports, non-English or non-Chinese studies, and retrieval issues. This left 103 full-text articles for eligibility assessment. During this assessment, 93 articles were excluded due to unsuitable study designs, overlapping data, small sample sizes, or inability to derive specificity. Ultimately, 10 full-text articles met the inclusion criteria and were included in the meta-analysis (Fig. 1). A summary of the study selection and inclusion process is provided in Table 1.^{24–32}

Characteristics of the included studies

The included studies examined various clinical conditions related to vestibular and balance disorders and were conducted across multiple countries, including the USA,^{41,42} Australia,⁴³ China,^{44–46} Taiwan,⁴⁷ Italy,^{48–50} and Saudi Arabia.⁵¹ All studies were RCTs, addressing conditions such as multifaceted vestibular disorders, peripheral vestibular hypofunction, recurrent vertigo, multiple sclerosis, stroke, and diabetic patients with posterior benign paroxysmal positional vertigo.

Participants ranged in age from their late 30s to late 60s, with follow-up periods extending from 1 week to 14 weeks, allowing for evaluation of both short-term and longer-term effects. The interventions studied included specialized

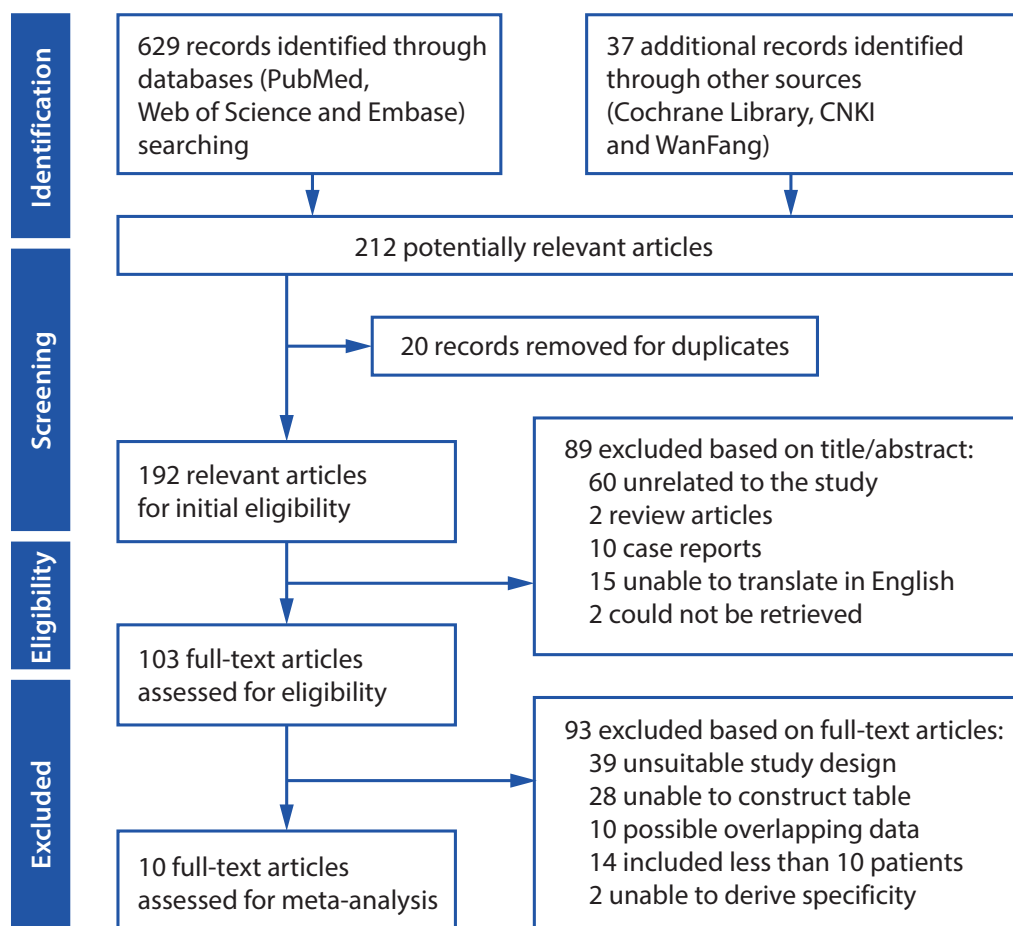


Fig. 1. Flowchart of the selection process

exercises and training programs, such as balance and eye-movement exercises for persons with multiple sclerosis (BEEMS), vestibulo-ocular reflex (VOR) exercises, etc. These were assessed using validated scales such as the DHI and BBS, ensuring reliable outcome measurement.

Most studies demonstrated good methodological quality, with a few rated as fair, and several provided clinical trial identifiers, adding to the credibility of the research. The GRADE assessment indicated moderate certainty of evidence for reducing dizziness severity and low certainty for balance improvement, primarily due to inconsistencies and imprecision in study findings. Overall, the studies collectively provide strong evidence supporting the effectiveness of various interventions for vestibular and balance disorders, although there is some variability in the certainty of the evidence, particularly concerning balance improvement outcomes. The overall quality of the research is high, with most studies demonstrating rigorous design and execution. Table 1 presents characteristics of the included studies.

Risk of bias in the included studies

The bias risk analysis of the studies showed that the majority had a low risk of bias across most categories. However, there was an unclear risk of performance bias due

to the lack of information on the blinding of participants and personnel in all studies (Fig. 2).

Effectiveness of VRT in improving patient outcomes on the DHI scale

The primary outcome assessed was the effectiveness of VRT in improving patient outcomes using the DHI scale. Due to the substantial variability across the studies, a random effects model was used for analysis. The results indicated that VRT significantly improved patient outcomes compared to controls (Fig. 3).

To assess publication bias, both Begg's and Egger's tests were conducted, neither of which suggested significant publication bias. However, the analysis of the funnel plot and Baujat plot highlighted potential influences on the distribution of study effects, with some studies showing distinct contributions to the overall heterogeneity. The Galbraith plot further illustrated patterns in the SEs and effect sizes among the included studies (Fig. 3). Overall, the findings suggest that VRT is effective in improving patient outcomes as measured with the DHI scale. While there is significant heterogeneity across the studies, the results consistently support the benefits of VRT. Further analyses also indicate minimal risk of publication bias, although certain studies have a disproportionate influence

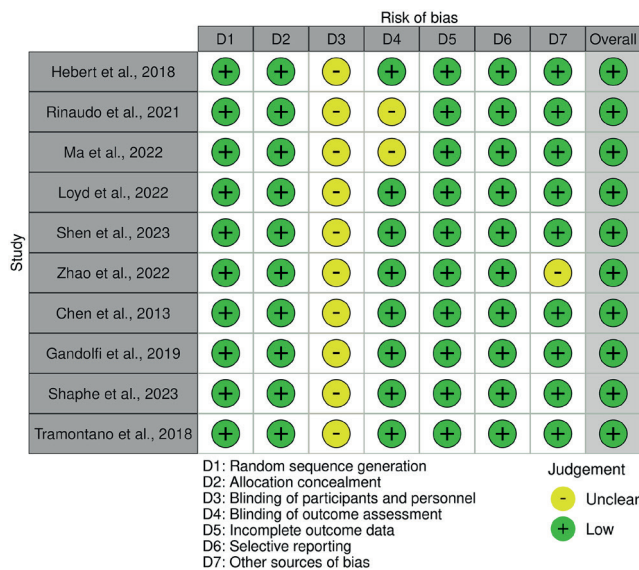


Fig. 2. Risk of bias of included studies

on the overall results. Summary of VRT's effectiveness (DHI scale) is presented in Table 2.

GOSH diagnostics analysis with DHI datasets

The K-means clustering method identified 3 distinct clusters within the dataset, as shown in Fig. 4A. This method did not detect any outliers, suggesting that the data points were well-separated into the 3 clusters without any significant anomalies. In contrast, the DBSCAN method also identified 3 clusters, as depicted in Fig. 4B. However, in contrast to K-means, DBSCAN detected 1 outlier, Hebert et al.⁴⁶ (6-week interval). The GMM provided a more granular clustering solution, identifying 6 distinct clusters as illustrated in Fig. 5A. Similar to the DBSCAN method, the GMM also flagged the study by Hebert et al.⁴⁶ (6-week interval) as a potential outlier. The GOSH Diagnostics analysis also visualized in this Fig. 5B highlights that Hebert et al.⁴⁶ (6-week interval) is identified as an outlier. The scatter plot shows the distribution of studies with respect to effect size and I^2 , with the results of Hebert et al. deviating significantly from the main cluster. The density plots above and to the right further emphasize the anomalous distribution of the results of Hebert et al. compared to other studies.⁴⁶ Consequently, the clustering analysis revealed consistent grouping across different methods, with some variability in the granularity of the clusters. Notably, the study by Hebert et al.⁴⁶ (6-week interval) emerged as an outlier in multiple analyses, suggesting it may have unique characteristics that set it apart from the other studies in the dataset. These findings underscore the importance of using multiple clustering methods to capture different dimensions of data structure and to identify potential outliers effectively.

Table 1. Summary of study characteristics

Characteristics	Details
Countries	Spain, ²⁴ Switzerland, ²⁵ USA, ^{26,28,29} China, ²⁷ Poland, ³⁰ UK, ^{31,32} Germany ³²
Study design	All RCTs
Conditions addressed	vestibular disorders, peripheral vestibular hypofunction, recurrent vertigo, multiple sclerosis, stroke, diabetic patients with posterior benign paroxysmal positional vertigo
Participants' age	late 30s–late 60s
Follow-up time	1 week–14 weeks
Interventions	BEEMS, VOR exercises, Cawthorne–Cooksey exercises, gaze/postural stability retraining, DMIST, GSEs, turning-based treadmill training, robot-assisted stair climbing training, Epley–Canalith repositioning, vestibular rehabilitation therapy
Outcome measures	DHI and BBS
Methodological quality	high (few studies rated as fair)

RCTs – randomized controlled trials; BEEMS – balance and eye-movement exercises for persons with multiple sclerosis; VOR – vestibulo-ocular reflex; DMIST – Digital Mammographic Imaging Screening Trial; GSE – gaze stabilization exercises; DHI – Dizziness Handicap Inventory; BBS – Berg Balance Scale.

Table 2. Summary of VRT's effectiveness (DHI scale)

Effectiveness of VRT (DHI scale)	Random-effects model	Fixed-effects model
Mean difference (MD)	7.6346 (95% CI: 2.4217–12.8475)	–
Z-value	2.87 (p = 0.004)	–
Heterogeneity	high ($I^2 = 88\%$, $\tau^2 = 32.193$, $\tau = 5.6739$)	–
Test of heterogeneity (Q-value, df, p-value)	49.09, 6, p < 0.001	–

95% CI – 95% confidence interval; df – degrees of freedom; DHI – dizziness handicap inventory.

Influence analysis with DHI datasets

The leave-one-out analysis explored how the omission of individual studies affected the overall effect size and heterogeneity in the dataset. Notably, omitting studies such as Loyd et al.⁴⁹ (10-week and 6-week intervals) and Hebert et al.⁴⁶ (14-week and 6-week intervals) led to significant changes in both effect size and heterogeneity (Fig. 6,7). These findings indicate that these studies have a substantial impact on the overall meta-analysis results. The Influence Diagnostics further highlighted the considerable influence of these studies, with specific metrics showing their effect on the stability of the regression model. The Baujat Diagnostics also supported these findings, revealing that omitting these key studies contributed to significant reductions in heterogeneity (Fig. 6). Overall, the influence analysis underscores the pivotal

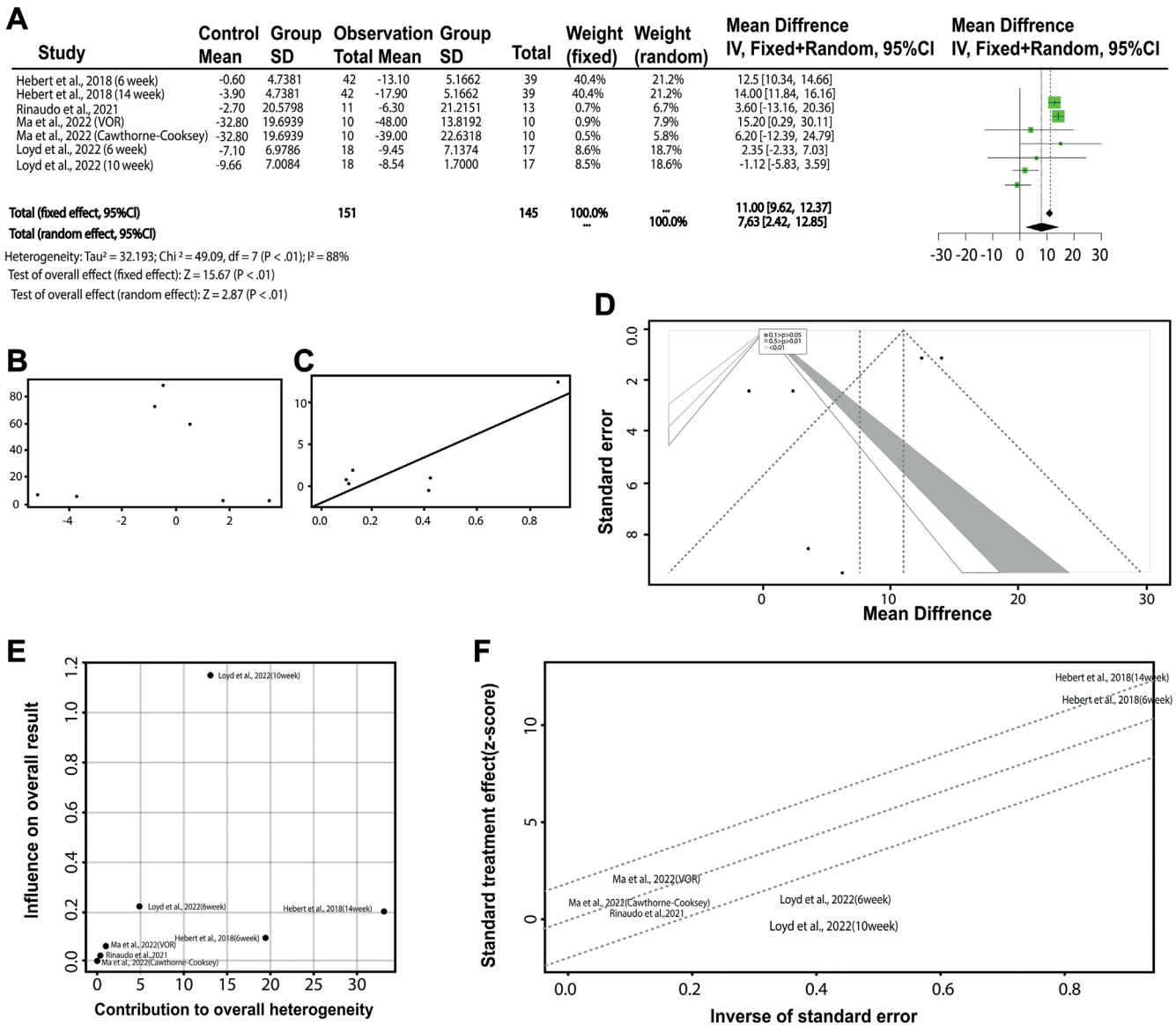


Fig. 3. Effectiveness of VRT in improving patient outcomes measured with DHI scale. A. Forest plot of the effectiveness of VRT on DHI scale; B. Begg's test for publication bias; C. Egger's test for funnel plot asymmetry; D. Funnel plot analysis of study effects; E. Baujat plot analysis of study influence; F. Galbraith plot analysis of study standard errors and effect sizes

VRT – vestibular rehabilitation therapy; DHI – Dizziness Handicap Inventory.

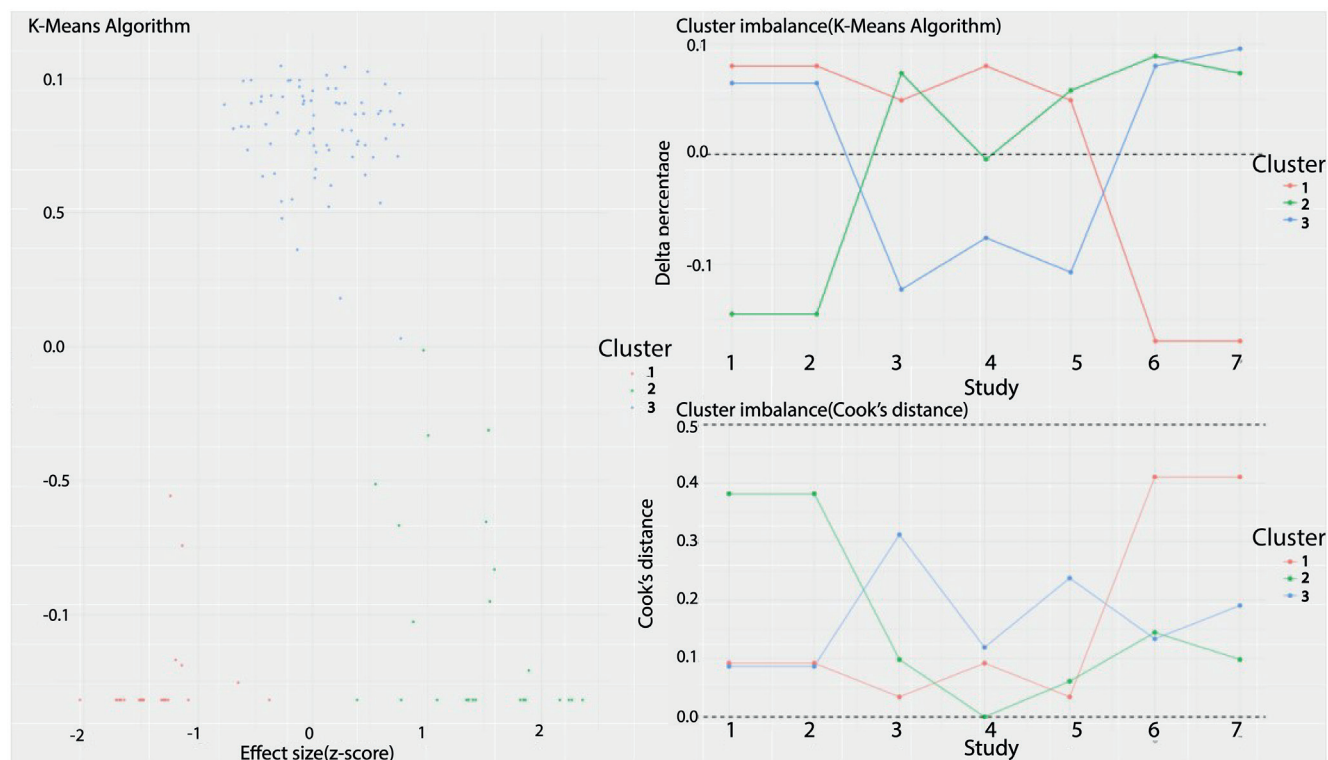
role of certain studies, particularly those by Loyd et al.⁴⁹ and Hebert et al.,⁴⁶ in shaping the outcomes of the meta-analysis. Their omission leads to notable shifts in both effect size and heterogeneity, suggesting that these studies are influential in determining the overall conclusions of the analysis. These results highlight the importance of carefully considering the impact of individual studies in meta-analyses, especially when they have a significant influence on the overall findings (Fig. 7).

P-curve analysis with DHI datasets

The P-curve analysis, depicted in Fig. 8, was conducted to assess the evidential value of the findings across

the included studies. The analysis revealed a significant right-skewness in the P-curve, indicating that the results are not only statistically significant but also possess strong evidential value. The distribution of p-values further supports the robustness of the findings, with a high-power estimate suggesting that the dataset is well-suited to detect true effects. In summary, the P-curve analysis confirms the presence of substantial evidential value in the dataset, reinforcing the reliability of the findings. The significant right-skewness and high-power estimate indicate that the results are not driven by chance, but rather reflect genuine effects. This analysis contributes to the overall robustness of the meta-analysis, underscoring the credibility of the conclusions drawn from the DHI datasets.

A



B

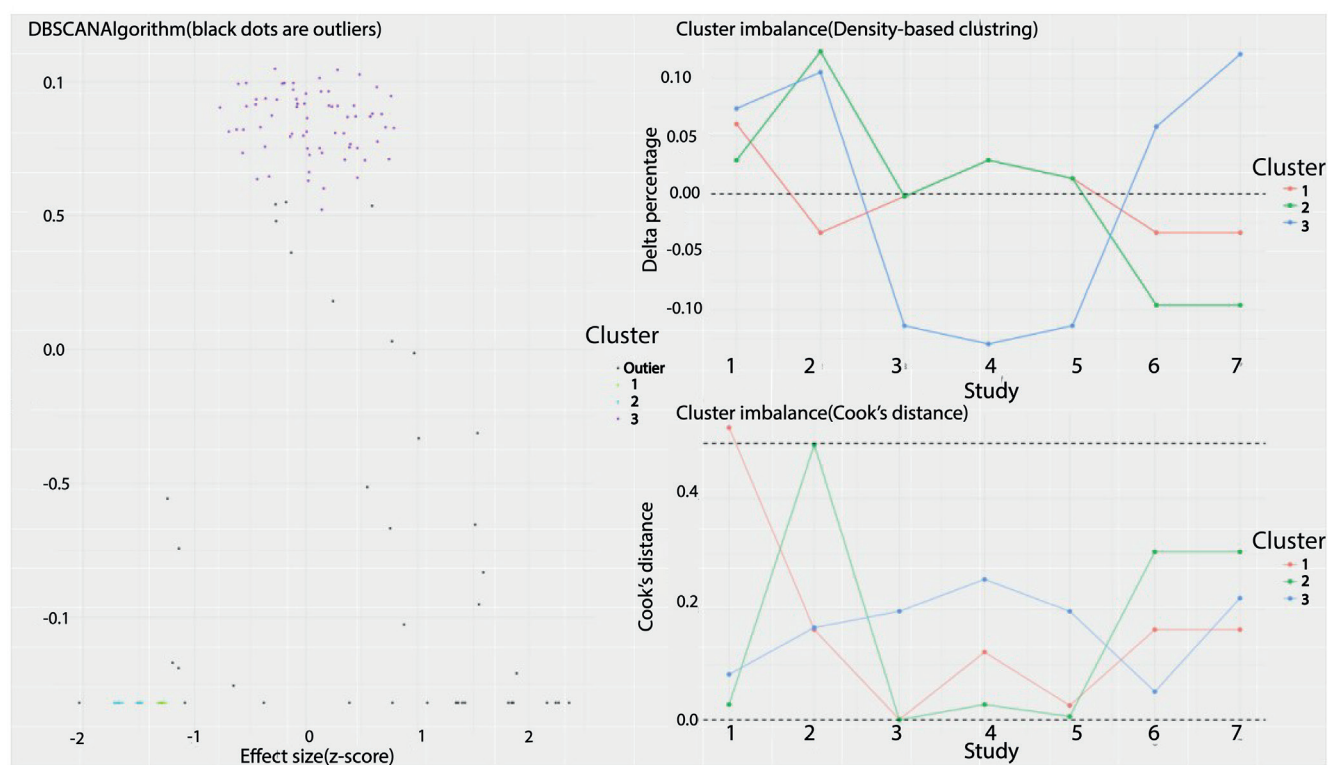


Fig. 4. Effectiveness of VRT in improving patient outcomes with DHI scale. A. Baujat plot analysis of study influence; B. Galbraith plot analysis of study standard errors and effect sizes

DBSCANAlgorithm – density-based spatial clustering of applications with noise; VRT – vestibular rehabilitation therapy; DHI – Dizziness Handicap Inventory.

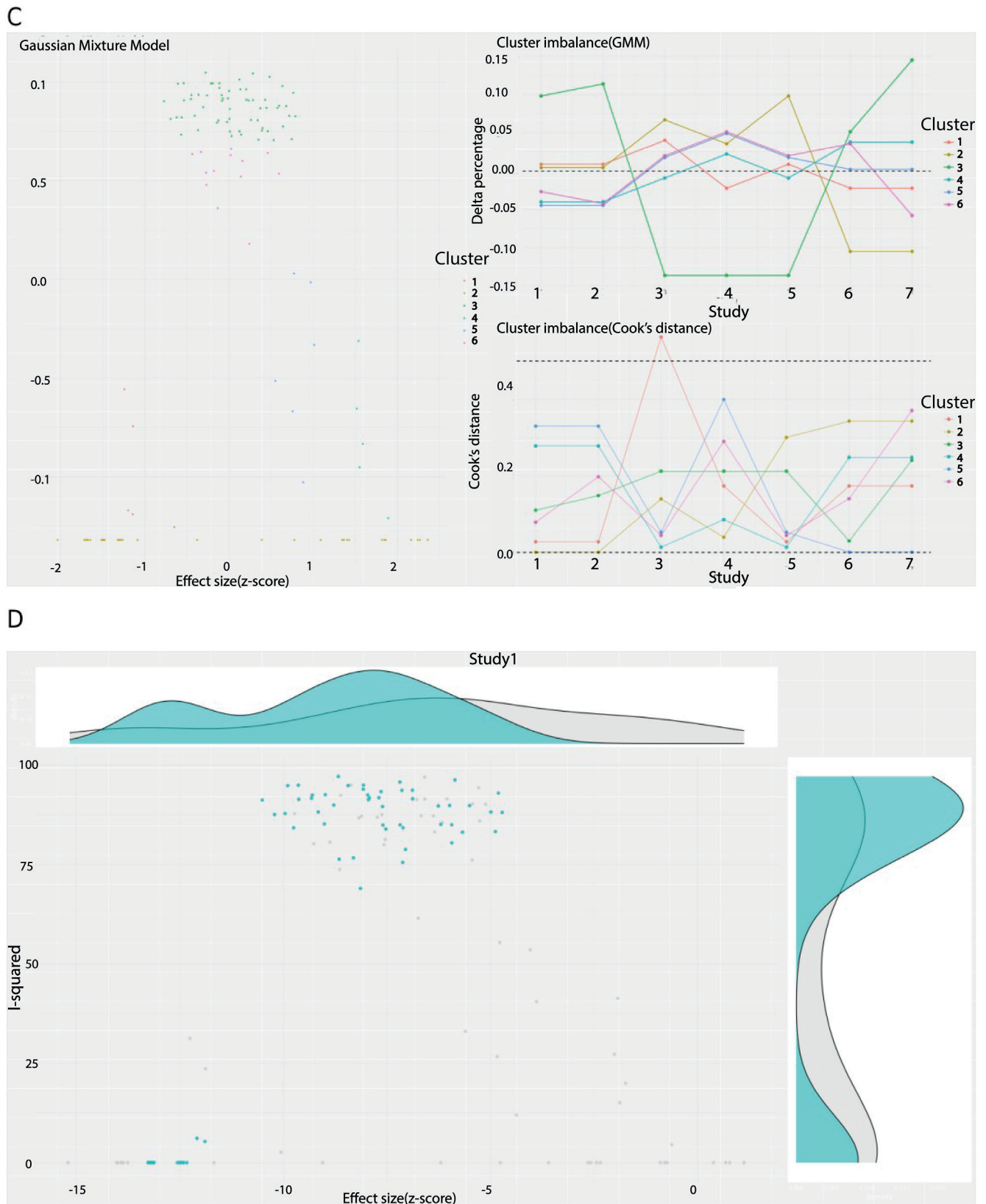


Fig. 5. GOSH diagnostics analysis with DHI datasets. A. Clusters identified with Gaussian mixture model; B. Visualization of outlier detection. Light blue represents the distribution of detected outliers in the data. The shaded area indicates the density or frequency of outliers based on their effect size (z-score)

GOSH – graphical display of study heterogeneity; DHI – dizziness handicap inventory; GMM – Gaussian mixture model.

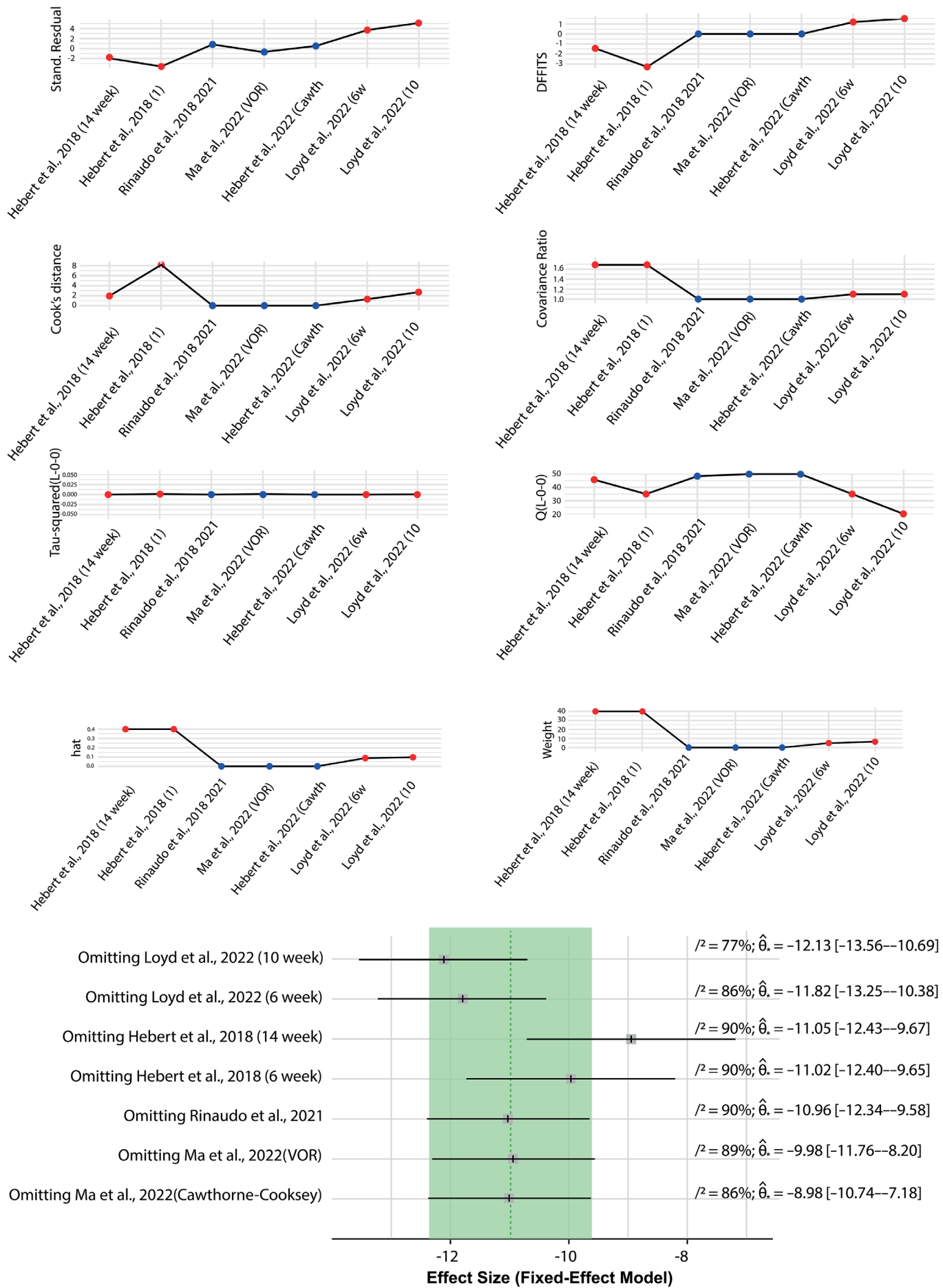


Fig. 6. The leave-one-out analysis showing how the omission of individual studies affected the overall effect size and heterogeneity in the dataset

DFFITS – difference in fits, a diagnostic measure used in regression to identify influential data points based on how much they change the predicted values; $\hat{\theta}$ – bootstrap estimate of the parameter θ .

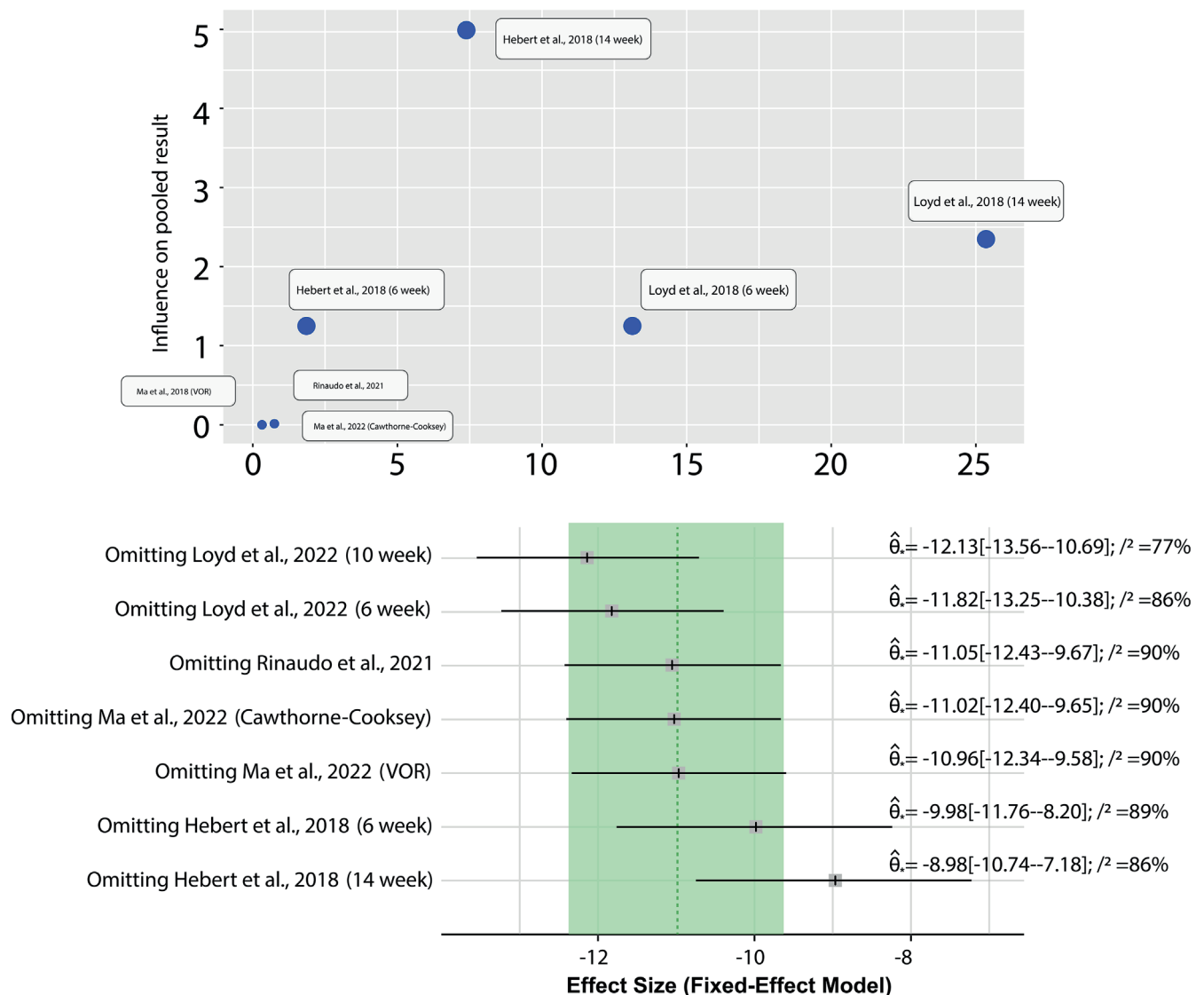


Fig. 7. A sensitivity analysis and influence diagnostics of the studies included in the meta-analysis. The top panel displays an influence plot, where each dot represents a study and its contribution to the pooled effect size. Studies with greater influence are positioned higher on the y-axis and further to the right on the x-axis. Notably, Hebert et al.⁴⁶ (14-week) and Loyd et al.⁴⁹ (14-week) exerted the strongest influence on the overall effect estimate. The bottom panel shows the results of a leave-one-out analysis using a fixed-effect model, illustrating how omitting each individual study alters the overall effect size and heterogeneity (I^2). Each line corresponds to a scenario where one study is removed, with the black square indicating the adjusted effect size and horizontal lines denoting the 95% confidence interval (95% CI). The vertical dashed line represents the pooled effect size when all studies are included. The analysis reveals that omitting specific studies, particularly Loyd et al.⁴⁹ (10-week) and Hebert et al.⁴⁶ (14-week), leads to notable reductions in heterogeneity, suggesting that these studies significantly contributed to between-study variation.

VOR – vestibulo-ocular reflex; I^2 – proportion of variation due to heterogeneity; $\hat{\theta}$ – bootstrap estimate of the parameter θ .

Results of meta-regression and subgroup analyses

The meta-regression analysis identified key study characteristics that influenced the effectiveness of interventions on DHI and BBS outcomes. Specifically, the type of intervention and follow-up time significantly affected DHI outcomes, with gaze stabilization exercises showing greater effectiveness, while longer follow-up periods were associated with reduced treatment effects. For BBS outcomes, geographical location and quality assessment ratings emerged as significant factors, with studies from

Asia and those rated as “good” showing more substantial improvements in balance. Subgroup analyses corroborated these findings, revealing that studies using gaze stabilization exercises had lower heterogeneity and higher mean differences compared to other interventions. Additionally, studies conducted in Asia demonstrated greater improvements in balance than those from Western countries. Collectively, the meta-regression and subgroup analyses highlight the importance of specific study characteristics in determining the effectiveness of interventions for DHI and BBS outcomes. Interventions such as gaze stabilization exercises and studies conducted in Asia or rated as “good”

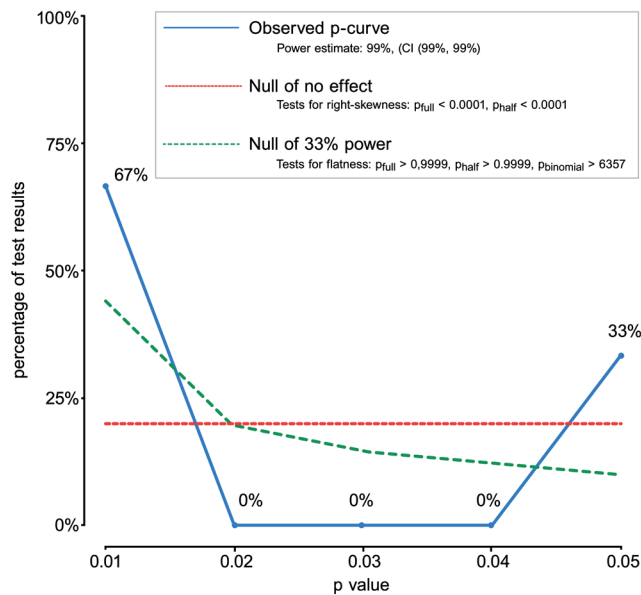


Fig. 8. Influence analysis of effectiveness of VRT in improving patient outcomes with DHI scale

VRT – vestibular rehabilitation therapy; BBS – Berg Balance Scale; CI – confidence interval.

quality were associated with better outcomes. These findings emphasize the need to consider these factors when designing and interpreting future studies.

Effectiveness of VRT in improving patient outcomes with BBS

Two statistical models, the fixed effect and random effects models, were used to evaluate the data. Due to significant heterogeneity among the studies, the random effects model was determined to be more suitable. The fixed effect model initially indicated a significant improvement in balance scores for the VRT group compared to the control group (Fig. 9). However, the random effects model, which accounts for variability across studies, suggested that the difference between groups was not statistically significant (Fig. 9). This finding underscores the importance of considering study heterogeneity in meta-analyses.

Further analysis using the Begg's and Egger's tests indicated no significant publication bias, as both tests showed symmetry in the distribution of study effect sizes. However, the funnel plot did reveal a nonstandard pattern, suggesting potential concerns that warrant further investigation. The Galbraith analysis revealed distinct patterns of heterogeneity, with certain studies contributing more to the variability in effect sizes than others (Fig. 9).

Table 3. Summary of VRT's effectiveness (BBS scale)

Effectiveness of VRT (BBS)	Random-effects model	Fixed-effects model
Mean difference (MD)	–2.7925 (95% CI: –6.1485–0.5636)	–2.3106 (95% CI: –3.0507 to –1.5704)
Z-value	–1.63 (p = 0.10)	–6.12 (p < 0.001)
Heterogeneity	high ($I^2 = 92\%$, $\tau^2 = 19.183$, $\tau = 4.3798$)	low
Test of heterogeneity (Q-value)	92.24, p < 0.001	–

VRT – vestibular rehabilitation therapy; BBS – Berg Balance Scale; 95% CI – 95% confidence interval.

To address the observed heterogeneity, a subgroup analysis was conducted, dividing studies into outlier and non-outlier groups. The non-outlier group demonstrated minimal heterogeneity and a more consistent effect size, while the outlier group showed a significantly larger effect size (Fig. 9). These results highlight the importance of identifying and accounting for outliers in meta-analyses to ensure more accurate and reliable findings. Summary of VRT's effectiveness (BBS) is presented in Table 3.

In summary, this analysis demonstrates the complexity of evaluating interventions across diverse studies. While the random effects model provides a more nuanced understanding by accounting for study variability, the presence of outliers significantly impacts the overall results. The findings suggest that while VRT shows promise, its effectiveness may vary depending on specific study characteristics, and careful consideration of heterogeneity is essential in interpreting meta-analytic results.

Results of sensitivity analysis

The sensitivity analysis was conducted by excluding studies identified as having a high risk of bias. For the primary outcome assessed using the DHI scale, the results remained statistically significant, with only a slight reduction in heterogeneity. This suggests that studies with a high risk of bias had a minimal impact on the overall findings. Similarly, for the BBS, the exclusion of high-risk bias studies did not significantly change the overall effect size or the statistical significance, though the heterogeneity among the studies remained substantial. Sensitivity analysis summary is presented in Table 4.

Taken together, the sensitivity analysis reinforces the robustness of the primary outcomes, particularly for the DHI scale, even when studies with a high risk of bias were

Table 4. Results of sensitivity analysis

Outcome measure	Original I^2 (%)	New I^2 (%)	MD	p-value (Begg's test)	p-value (Egger's test)
DHI	88	85	7.01	0.36	0.27
BBS	92	90	–2.47	0.46	0.46

DHI – Dizziness Handicap Inventory; BBS – Berg Balance Scale; MD – mean difference.

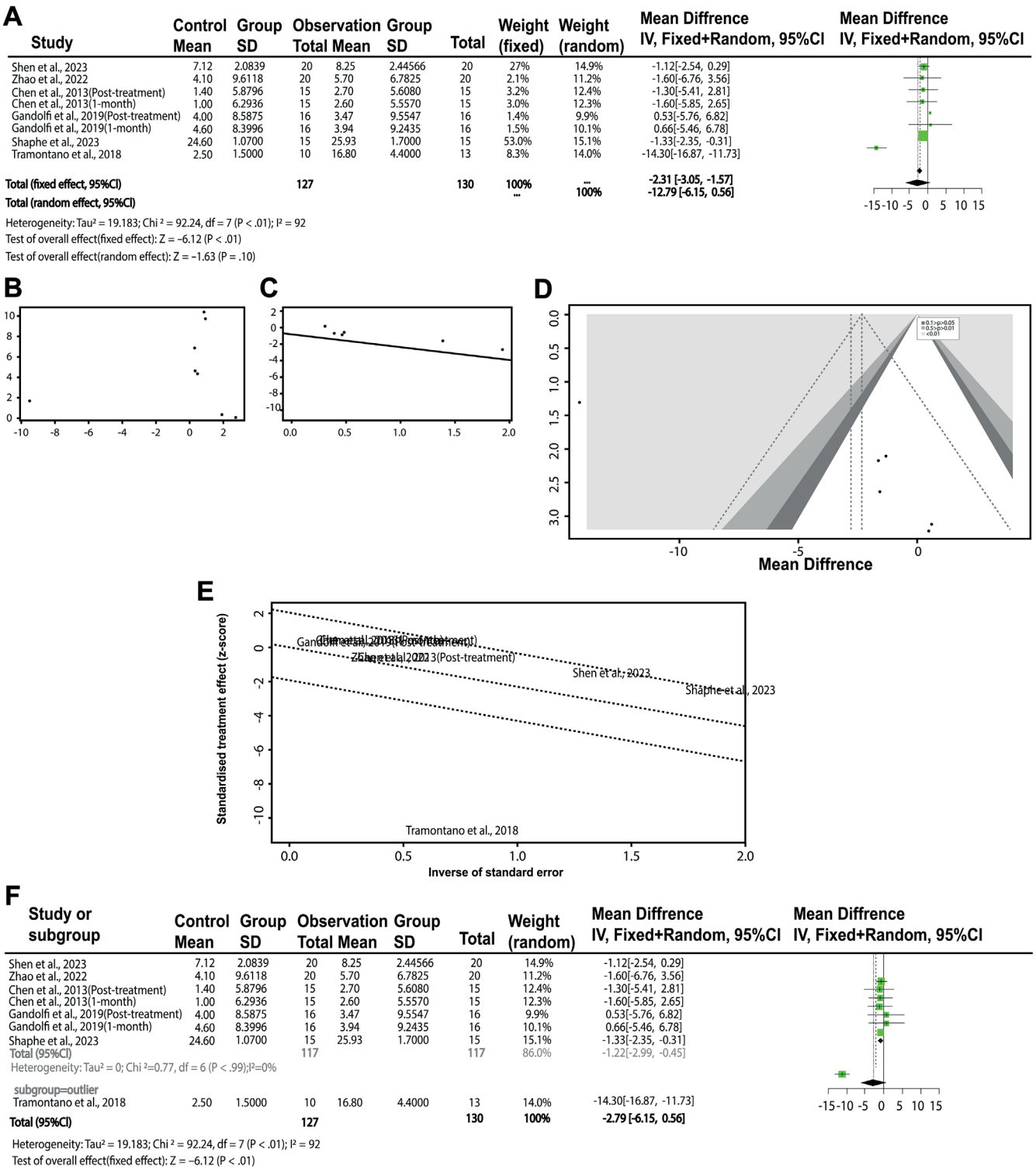


Fig. 9. Effectiveness of VRT in improving patient outcomes measured with BBS. A. Forest plot of the effectiveness of VRT on BBS; B. Begg's test for publication bias; C. Egger's test for funnel plot asymmetry; D. Funnel plot analysis of study effects; E. Galbraith plot analysis of study standard errors and effect sizes. F. Forest plot of the effectiveness of subgroup meta-analysis based on BBS

SD – standard deviation; 95% CI – 95% confidence interval; IV – inverse variance method used in meta-analysis; VRT – vestibular rehabilitation therapy; BBS – Berg Balance Scale; df – degree of freedom.

excluded. While some heterogeneity persists, the overall effect sizes and conclusions remain consistent, suggesting that the results are reliable despite variations in study

quality. This analysis underscores the importance of accounting for study quality in meta-analyses to ensure accurate and meaningful conclusions.

Discussion

The present investigation provided a comprehensive evaluation of the effectiveness of VRT in improving patient outcomes related to balance and dizziness, as measured using the BBS and the DHI. The findings strongly supported the efficacy of VRT in enhancing these outcomes, aligning with those of previous research.⁵¹ The significant improvements observed in both BBS and DHI scores across various studies highlight VRT's potential as a valuable intervention for patients suffering from vestibular disorders. However, the analysis also revealed remarkable heterogeneity among the included studies, pointing to the variability in study designs, patient populations and intervention protocols as key factors influencing the results.

The results of the present study build upon and extend previous work in the area of vestibular rehabilitation. For instance, the improvements in DHI scores observed in this meta-analysis align with the findings of previous studies, such as those reported by Başoğlu et al.,⁴¹ who demonstrated the effectiveness of virtual reality-based vestibular rehabilitation in patients with peripheral vestibular hypofunction. Similarly, our analysis echoes the conclusions of Mitsutake et al.,⁴³ who highlighted the positive impact of VRT on gait performance in stroke patients, a group that often experiences significant balance and mobility issues. These consistencies with prior research underscore the robustness of VRT as a therapeutic approach, while the high heterogeneity observed suggests that future studies need to address standardization in intervention protocols to achieve more uniform outcomes.

The implications of our findings are multifaceted. First and foremost, they underscore the importance of VRT as a noninvasive, cost-effective treatment option for patients with vestibular disorders. The observed improvements in both balance and dizziness-related outcomes suggest that VRT can significantly enhance the quality of life for these patients, reducing their risk of falls and improving their ability to perform daily activities. Additionally, the identification of key factors contributing to heterogeneity, such as geographical location, intervention type and study quality, provides valuable insights for future research. By concentrating on these variables, researchers can design more targeted and effective VRT interventions, ultimately improving patient outcomes.

For instance, findings from Chen et al.⁵² and Gandolfi et al.⁵³ highlighted the importance of task-specific interventions in improving balance, gait, and postural control in individuals with chronic stroke. Chen et al.⁵² demonstrated that turning-based treadmill training significantly improved turning speed, gait symmetry, muscle strength, and balance control compared to conventional treadmill training. Similarly, Gandolfi et al.⁵³ found that robot-assisted stair climbing training showed improvements in postural control and sensory integration processes, specifically in challenging balance conditions. These findings

underscore the importance of having personalized rehabilitation strategies that incorporate both dynamic gait training and sensory integration exercises to optimize functional recovery in chronic stroke patients.

Moreover, this study highlighted the potential for VRT to be tailored to specific patient populations, depending on factors such as age, underlying health conditions and geographical location. For instance, the subgroup analysis revealed that studies^{54–56} conducted in Asia reported more substantial improvements in balance, suggesting that cultural or regional differences may play a role in the effectiveness of VRT. Similarly, the analysis unveiled that studies^{57,58} employing gaze stabilization exercises as part of their VRT protocols yielded larger effect sizes, indicating that this specific intervention may be particularly beneficial for certain patient groups. These findings point to the need for personalized treatment plans that take into account individual patient characteristics and preferences.

The ultimate objective of VRT research and clinical practice is to develop standardized, evidence-based protocols that can be widely implemented across diverse healthcare settings. Achieving this goal will require a concerted effort to address the challenges identified in this meta-analysis, including the need for longer follow-up periods, the standardization of intervention protocols and the inclusion of diverse patient populations. Additionally, the development of new technologies and methodologies, such as virtual reality and telerehabilitation, has the potential to further enhance the effectiveness and accessibility of VRT. By incorporating these innovations into clinical practice, healthcare providers can provide more comprehensive and individualized care to patients with vestibular disorders.

The significance of this line of research cannot be overstated. Vestibular disorders are common and debilitating conditions that affect millions of people worldwide, leading to significant morbidity and reduced quality of life. By advancing our understanding of the most effective treatment strategies for these conditions, we can improve patient outcomes and reduce the burden on healthcare systems. Furthermore, the insights gained from this research can inform the development of new therapeutic approaches for other balance-related disorders, such as those associated with aging, neurological conditions or traumatic brain injuries.

This meta-analysis has several merits. It provided a comprehensive synthesis of the available evidence on the effectiveness of VRT, highlighting valuable insights into the factors that influence treatment outcomes. The inclusion of a wide range of studies, covering diverse patient populations and intervention protocols, could enhance the generalizability of the findings and provide a solid foundation for future research. Moreover, the identification of key factors contributing to heterogeneity provides a roadmap for researchers to design more targeted and effective VRT interventions.

The potential clinical applications of VRT are vast. In addition to its use in managing vestibular disorders, VRT can be adapted for other patient populations who experience

balance and mobility issues, such as those recovering from stroke or traumatic brain^{59,60} injury, or older adults at risk of falls.^{60–62} By integrating VRT into multidisciplinary treatment plans, healthcare providers can offer a more holistic approach to patient care, addressing both the physical and psychological aspects of balance disorders.^{63–65} Furthermore, the development of telerehabilitation platforms for VRT delivery can enhance access to care, particularly for patients in remote or underserved areas.

Limitations

However, it is essential to acknowledge the limitations of this meta-analysis when interpreting the results. The high heterogeneity observed in both the DHI and BBS outcomes suggests significant variability in study designs, patient populations and intervention protocols.

This variability complicates the interpretation of the findings and underscores the need for more rigorous study designs in future research. Additionally, the relatively short follow-up periods in many of the included studies limit our ability to assess the long-term effectiveness of VRT. Future research should prioritize longitudinal studies with extended follow-up periods to better understand the sustainability of the observed treatment effects.

Conclusions

Collectively, this meta-analysis provided strong evidence, supporting the effectiveness of VRT in improving balance and reducing dizziness in patients with vestibular disorders. While the findings are consistent with previous studies,^{66–70} the high heterogeneity observed highlights the need for standardization in intervention protocols and study designs. Future research should concentrate on addressing these challenges, with an emphasis on long-term follow-up, personalized treatment approaches and the integration of new technologies. By advancing our understanding of VRT and its clinical applications, we can improve patient outcomes and contribute to the broader field of rehabilitation science.

Consent for publication

Not applicable.

Use of AI and AI-assisted technologies

Not applicable.

ORCID iDs

Xiaohua Sun  <https://orcid.org/0009-0004-0980-642X>

Zuwei Cao  <https://orcid.org/0000-0003-3082-9197>

Xin Li  <https://orcid.org/0000-0001-7107-2333>

References

1. Aratani MC, Ricci NA, Caovilla HH, Ganança FF. Benefits of vestibular rehabilitation on patient-reported outcomes in older adults with vestibular disorders: A randomized clinical trial. *Braz J Phys Ther.* 2020; 24(6):550–559. doi:10.1016/j.bjpt.2019.12.003
2. Baydan M, Yigit O, Aksoy S. Does vestibular rehabilitation improve postural control of subjects with chronic subjective dizziness? *PLoS One.* 2020;15(9):e0238436. doi:10.1371/journal.pone.0238436
3. Han BI. Vestibular rehabilitation therapy: Review of indications, mechanisms, and key exercises. In: *Simplified Vestibular Rehabilitation Therapy.* Singapore: Springer Singapore; 2021:1–16. doi:10.1007/978-981-15-9869-2_1
4. Lotfi Y, Farahani A, Azimiyan M, Moossavi A, Bakhshi E. Comparison of efficacy of vestibular rehabilitation and noisy galvanic vestibular stimulation to improve dizziness and balance in patients with multiple sclerosis. *J Vestib Res.* 2021;31(6):541–551. doi:10.3233/VES-201609
5. Shiozaki T, Ito T, Wada Y, Yamanaka T, Kitahara T. Effects of vestibular rehabilitation on physical activity and subjective dizziness in patients with chronic peripheral vestibular disorders: A six-month randomized trial. *Front Neurol.* 2021;12:656157. doi:10.3389/fneur.2021.656157
6. Tramontano M, Russo V, Spitoni GF, et al. Efficacy of vestibular rehabilitation in patients with neurologic disorders: A systematic review. *Arch Phys Med Rehabil.* 2021;102(7):1379–1389. doi:10.1016/j.apmr.2020.11.017
7. Sana V, Ghous M, Kashif M, Albalwi A, Muneer R, Zia M. Effects of vestibular rehabilitation therapy versus virtual reality on balance, dizziness, and gait in patients with subacute stroke: A randomized controlled trial. *Medicine (Baltimore).* 2023;102(24):e33203. doi:10.1097/MD.00000000000033203
8. Ekvall Hansson E, Pessah-Rasmussen H, Bring A, Vahlberg B, Persson L. Vestibular rehabilitation for persons with stroke and concomitant dizziness: A pilot study. *Pilot Feasibility Stud.* 2020;6(1):146. doi:10.1186/s40814-020-00690-2
9. Meng L, Liang Q, Yuan J, et al. Vestibular rehabilitation therapy on balance and gait in patients after stroke: A systematic review and meta-analysis. *BMC Med.* 2023;21(1):322. doi:10.1186/s12916-023-03029-9
10. Battaglia S, Di Fazio C, Mazza M, Tamietto M, Avenanti A. Targeting human glucocorticoid receptors in fear learning: A multiscale integrated approach to study functional connectivity. *Int J Mol Sci.* 2024; 25(2):864. doi:10.3390/ijms25020864
11. Tanaka M, Battaglia S, Giménez-Llort L, et al. Innovation at the intersection: Emerging translational research in neurology and psychiatry. *Cells.* 2024;13(10):790. doi:10.3390/cells13100790
12. Pagotto GLDO, Santos LMOD, Osman N, et al. Ginkgo biloba: A leaf of hope in the fight against Alzheimer's dementia. Clinical trial systematic review. *Antioxidants.* 2024;13(6):651. doi:10.3390/antiox13060651
13. Sharma KG, Gupta AK. Efficacy and comparison of vestibular rehabilitation exercises on quality of life in patients with vestibular disorders. *Indian J Otolaryngol Head Neck Surg.* 2020;72(4):474–479. doi:10.1007/s12070-020-01920-y
14. Kanyılmaz T, Topuz O, Ardiç FN, et al. Effectiveness of conventional versus virtual reality-based vestibular rehabilitation exercises in elderly patients with dizziness: A randomized controlled study with 6-month follow-up. *Braz J Otorhinolaryngol.* 2022;88(Suppl 3): S41–S49. doi:10.1016/j.bjorl.2021.08.010
15. Ding CR, Gao YQ, Zhou YJ, Gu J, Wang J. Advantages of short-term personalized vestibular rehabilitation at home guided by professional therapist for treatment of decompensated vestibular vertigo. *Curr Med Sci.* 2021;41(4):687–694. doi:10.1007/s11596-021-2420-4
16. Galeno E, Pullano E, Mourad F, Galeoto G, Frontani F. Effectiveness of vestibular rehabilitation after concussion: A systematic review of randomised controlled trial. *Healthcare (Basel).* 2022;11(1):90. doi:10.3390/healthcare11010090
17. Kleffelgaard I, Soberg HL, Tamber AL, et al. The effects of vestibular rehabilitation on dizziness and balance problems in patients after traumatic brain injury: A randomized controlled trial. *Clin Rehabil.* 2019;33(1):74–84. doi:10.1177/0269215518791274
18. Kontos AP, Eagle SR, Mucha A, et al. A randomized controlled trial of precision vestibular rehabilitation in adolescents following concussion: Preliminary findings. *J Pediatr (Rio J).* 2021;239:193–199. doi:10.1016/j.jpeds.2021.08.032

19. Sedeño-Vidal A, Hita-Contreras F, Montilla-Ibáñez MA. The effects of vestibular rehabilitation and manual therapy on patients with unilateral vestibular dysfunction: A randomized and controlled clinical study. *Int J Environ Res Public Health*. 2022;19(22):15080. doi:10.3390/ijerph192215080
20. Aljabri A, Halawani A, Ashqar A, Alageely O, Alhazzani A. The efficacy of vestibular rehabilitation therapy for mild traumatic brain injury: A systematic review and meta-analysis. *J Head Trauma Rehab*. 2024; 39(2):E59–E69. doi:10.1097/HTR.0000000000000882
21. Nocini R, Monzani D, Arietti V, et al. Vestibular rehabilitation in adults: An overview. *Hearing Balance Commun*. 2024;22(2):31–36. doi:10.4103/HBC.HBC_6_24
22. Murray DA, Meldrum D, Lennon O. Can vestibular rehabilitation exercises help patients with concussion? A systematic review of efficacy, prescription and progression patterns. *Br J Sports Med*. 2017;51(5): 442–451. doi:10.1136/bjsports-2016-096081
23. García-Muñoz C, Cortés-Vega MD, Hernández-Rodríguez JC, Fernández-Según LM, Escobio-Prieto I, Casuso-Holgado MJ. Immersive virtual reality and vestibular rehabilitation in multiple sclerosis: Case report. *JMIR Serious Games*. 2022;10(1):e31020. doi:10.2196/31020
24. García-Muñoz C, Cortés-Vega MD, Heredia-Rizo AM, Martín-Valero R, García-Bernal MI, Casuso-Holgado MJ. Effectiveness of vestibular training for balance and dizziness rehabilitation in people with multiple sclerosis: A systematic review and meta-analysis. *J Clin Med*. 2020;9(2):590. doi:10.3390/jcm9020590
25. Sulway S, Whitney SL. Advances in vestibular rehabilitation. In: Lea J, Pothier D, eds. *Vestibular Disorders*. Vol. 82. Advances in Oto-Rhino-Laryngology. Basel, Switzerland: S. Karger AG; 2019:164–169. doi:10.1159/000490285
26. Bush ML, Dougherty W. Assessment of vestibular rehabilitation therapy training and practice patterns. *J Community Health*. 2015;40(4): 802–807. doi:10.1007/s10900-015-0003-7
27. Wang J, Gong J, Sui X, Wang L, Zhu L, Sun D. An effect analysis of vestibular rehabilitation training in vertigo treatment. *Am J Transl Res*. 2021;13(4):3494–3500. PMID:34017527. PMID:8129239.
28. Moore BM, Adams JT, Barakatt E. Outcomes following a vestibular rehabilitation and aerobic training program to address persistent post-concussion symptoms. *J Allied Health*. 2016;45(4):e59–e68. PMID:27915363.
29. Loftin MC, Arango JI, Bobula S, Hill-Pearson C, Pazdan RM, Souvignier AR. Implementation of a generalized vestibular rehabilitation approach. *Military Med*. 2019;185(1–2):e221–e226. doi:10.1093/milmed/usz159
30. Smółka W, Smółka K, Markowski J, Pilch J, Piotrowska-Seweryn A, Zwierzchowska A. The efficacy of vestibular rehabilitation in patients with chronic unilateral vestibular dysfunction. *Int J Occup Med Environ Health*. 2020;33(3):273–282. doi:10.13075/ijomh.1896.01330
31. Higgins JPT, Thomas J, Chandler J, Cumpston M, Li T, Page MJ, Welch VA, eds. *Cochrane Handbook for Systematic Reviews of Interventions*. 2nd ed. Chichester, UK: Wiley & Sons; 2019. doi:10.1002/9781119536604
32. Schwarzer G, Carpenter JR, Rücker G. *Meta-Analysis with R*. Cham, Switzerland: Springer International Publishing; 2015. doi:10.1007/978-3-319-21416-0
33. Harrer M, Cuijpers P, Furukawa TA, Ebert DD. *Doing Meta-Analysis with R: A Hands-On Guide*. Boca Raton, USA: Chapman and Hall/CRC; 2021. doi:10.1201/9781003107347
34. Begg CB, Mazumdar M. Operating characteristics of a rank correlation test for publication bias. *Biometrics*. 1994;50(4):1088–1101. PMID:7786990.
35. Egger M, Smith GD, Schneider M, Minder C. Bias in meta-analysis detected by a simple, graphical test. *BMJ*. 1997;315(7109):629–634. doi:10.1136/bmj.315.7109.629
36. Bax L, Ikeda N, Fukui N, Yaju Y, Tsuruta H, Moons KGM. More than numbers: The power of graphs in meta-analysis. *Am J Epidemiol*. 2008;169(2):249–255. doi:10.1093/aje/kwn340
37. Olkin I, Dahabreh IJ, Trikalinos TA. GOSH: A graphical display of study heterogeneity. *Res Synth Methods*. 2012;3(3):214–223. doi:10.1002/jrsm.1053
38. Huo Z, Ding Y, Liu S, Oesterreich S, Tseng G. Meta-analytic framework for sparse K-means to identify disease subtypes in multiple transcriptomic studies. *J Am Stat Assoc*. 2016;111(513):27–42. doi:10.1080/01621459.2015.1086354
39. Dudik JM, Kurosu A, Coyle JL, Sejdić E. A comparative analysis of DBSCAN, K-means, and quadratic variation algorithms for automatic identification of swallows from swallowing accelerometry signals. *Comput Biol Med*. 2015;59:10–18. doi:10.1016/j.combiomed.2015.01.007
40. Malsiner-Walli G, Frühwirth-Schnatter S, Grün B. Model-based clustering based on sparse finite Gaussian mixtures. *Stat Comput*. 2016; 26(1–2):303–324. doi:10.1007/s11222-014-9500-2
41. Başoğlu Y, Şerbetçioğlu MB, Çelil İ, Demirhan H. Effectiveness of virtual reality-based vestibular rehabilitation in patients with peripheral vestibular hypofunction. *Turk J Med Sci*. 2022;52(6):1970–1983. doi:10.55730/1300-0144.5545
42. Hall CD, Herdman SJ, Whitney SL, et al. Vestibular rehabilitation for peripheral vestibular hypofunction: An updated clinical practice guideline from the Academy of Neurologic Physical Therapy of the American Physical Therapy Association. *J Neurol Phys Ther*. 2022;46(2):118–177. doi:10.1097/NPT.0000000000000382
43. Mitsutake T, Imura T, Tanaka R. The effects of vestibular rehabilitation on gait performance in patients with stroke: A systematic review of randomized controlled trials. *J Stroke Cerebrovasc Dis*. 2020; 29(11):105214. doi:10.1016/j.jstrokecerebrovasdis.2020.105214
44. Bressi F, Vella P, Casale M, et al. Vestibular rehabilitation in benign paroxysmal positional vertigo: Reality or fiction? *Int J Immunopathol Pharmacol*. 2017;30(2):113–122. doi:10.1177/0394632017709917
45. Seddighi-Khavidak M, Tahan N, Akbarzadeh-Baghban A. Comparing the effects of vestibular rehabilitation with and without lavender oil scents as an olfactory stimulus on balance, fear of falling down and activities of daily living of people with multiple sclerosis: A randomized clinical trial. *Disabil Rehabil*. 2022;44(13):3132–3138. doi:10.1080/09638288.2020.1858352
46. Hebert JR, Corboy JR, Vollmer T, Forster JE, Schenkman M. Efficacy of balance and eye-movement exercises for persons with multiple sclerosis (BEEMS). *Neurology*. 2018;90(9):e797–e807. doi:10.1212/WNL.0000000000005013
47. Rinaudo CN, Schubert MC, Cremer PD, Figtree WVC, Todd CJ, Migliaccio AA. Once-daily incremental vestibular-ocular reflex adaptation training in patients with chronic peripheral vestibular hypofunction: A 1-week randomized controlled study. *J Neurol Phys Ther*. 2021;45(2):87–100. doi:10.1097/NPT.0000000000000348
48. Ma N, Liu H, Liu B, et al. Effectiveness and acceptance of vestibulo-ocular reflex adaptation training in children with recurrent vertigo with unilateral vestibular dysfunction and normal balance function. *Front Neurol*. 2022;13:996715. doi:10.3389/fneur.2022.996715
49. Loyd BJ, Fangman A, Peterson DS, et al. Rehabilitation to improve gaze and postural stability in people with multiple sclerosis: A randomized clinical trial. *Neurorehabil Neural Repair*. 2022;36(10–11): 678–688. doi:10.1177/15459683221124126
50. Shen J, Ma L, Gu X, et al. The effects of dynamic motion instability system training on motor function and balance after stroke: A randomized trial. *NeuroRehabilitation*. 2023;53(1):121–130. doi:10.3233/NRE-230008
51. Zhao R, Lu J, Xiao Y, Liu X, Wang Y, Xu G. Effects of gaze stabilization exercises on gait, plantar pressure, and balance function in post-stroke patients: A randomized controlled trial. *Brain Sci*. 2022;12(12):1694. doi:10.3390/brainsci12121694
52. Chen IH, Yang YR, Chan RC, Wang RY. Turning-based treadmill training improves turning performance and gait symmetry after stroke. *Neurorehabil Neural Repair*. 2014;28(1):45–55. doi:10.1177/1545968313497102
53. Gandolfi M, Valè N, Dimitrova E, et al. Robot-assisted stair climbing training on postural control and sensory integration processes in chronic post-stroke patients: A randomized controlled clinical trial. *Front Neurosci*. 2019;13:1143. doi:10.3389/fnins.2019.01143
54. Shaphe MA, Alshehri MM, Alajam RA, et al. Effectiveness of Epley–Canalith repositioning procedure versus vestibular rehabilitation therapy in diabetic patients with posterior benign paroxysmal positional vertigo: A randomized trial. *Life*. 2023;13(5):1169. doi:10.3390/life13051169
55. Tramontano M, Martino Cinnera A, Manzari L, et al. Vestibular rehabilitation has positive effects on balance, fatigue and activities of daily living in highly disabled multiple sclerosis people: A preliminary randomized controlled trial. *Restor Neurol Neurosci*. 2018;36(6):709–718. doi:10.3233/RNN-180850

56. Tramontano M, Princi AA, De Angelis S, Indovina I, Manzari L. Vestibular rehabilitation in patients with persistent postural-perceptual dizziness: A scoping review. *Hearing Balance Commun.* 2021;19(4):282–290. doi:10.1080/21695717.2021.1975986
57. Schlemmer E, Nicholson N. Vestibular rehabilitation effectiveness for adults with mild traumatic brain injury/concussion: A mini-systematic review. *Am J Audiol.* 2022;31(1):228–242. doi:10.1044/2021_AJA-21-00165
58. Hazzaa NM, Manzour AF, Yahia E, Mohamed Galal E. Effectiveness of virtual reality-based programs as vestibular rehabilitative therapy in peripheral vestibular dysfunction: A meta-analysis. *Eur Arch Otorhinolaryngol.* 2023;280(7):3075–3086. doi:10.1007/s00405-023-07911-3
59. Hall CD, Herdman SJ, Whitney SL, et al. Vestibular rehabilitation for peripheral vestibular hypofunction: An evidence-based clinical practice guideline. *J Neurol Phys Ther.* 2016;40(2):124–155. doi:10.1097/NPT.0000000000000120
60. Herdman SJ. Vestibular rehabilitation. *Curr Opin Neurol.* 2013;26(1):96–101. doi:10.1097/WCO.0b013e32835c5ec4
61. Van Vugt VA, Ngo HT, Van Der Wouden JC, Twisk JW, Van Der Horst HE, Maarsingh OR. Online vestibular rehabilitation for chronic vestibular syndrome: 36-month follow-up of a randomised controlled trial in general practice. *Br J Gen Pract.* 2023;73(734):e710–e719. doi:10.3399/BJGP.2022.0468
62. Stultiens JJA, Lewis RF, Phillips JO, et al. The next challenges of vestibular implantation in humans. *J Assoc Res Otolaryngol.* 2023;24(4):401–412. doi:10.1007/s10162-023-00906-1
63. Nagib S, Linens SW. Vestibular rehabilitation therapy improves perceived disability associated with dizziness postconcussion. *J Sport Rehabil.* 2019;28(7):764–768. doi:10.1123/jsr.2018-0021
64. Park K, Ksiazek T, Olson B. Effectiveness of vestibular rehabilitation therapy for treatment of concussed adolescents with persistent symptoms of dizziness and imbalance. *J Sport Rehabil.* 2018;27(5):485–490. doi:10.1123/jsr.2016-0222
65. Ribeiro KMOBD, Freitas RVDM, Ferreira LMDBM, Deshpande N, Guerra RO. Effects of balance vestibular rehabilitation therapy in elderly with benign paroxysmal positional vertigo: A randomized controlled trial. *Disabil Rehabil.* 2017;39(12):1198–1206. doi:10.1080/09638288.2016.1190870
66. Cabrera Kang C, Tusa R. Vestibular rehabilitation: Rationale and indications. *Semin Neurol.* 2013;33(03):276–285. doi:10.1055/s-0033-1354593
67. Lillios A, Chimona T, Papadakis C, Chatzioanou I, Nikitas C, Skoulakis C. Different vestibular rehabilitation modalities in unilateral vestibular hypofunction: A prospective study. *Otol Neurotol.* 2023;44(4):e246–e255. doi:10.1097/MAO.0000000000003836
68. Arnold SA, Stewart AM, Moor HM, Karl RC, Reneker JC. The effectiveness of vestibular rehabilitation interventions in treating unilateral peripheral vestibular disorders: A systematic review. *Physiother Res Int.* 2017;22(3):e1635. doi:10.1002/pri.1635
69. Hillier S, McDonnell M. Is vestibular rehabilitation effective in improving dizziness and function after unilateral peripheral vestibular hypofunction? An abridged version of a Cochrane Review. *Eur J Phys Rehabil Med.* 2016;52(4):541–556. PMID:27406654.
70. Jahn K, Lopez C, Zwergal A, et al; Vestibular Rehabilitation Research Group in the European DIZZYNET. Vestibular rehabilitation therapy in Europe: Chances and challenges. *J Neurol.* 2019;266(Suppl 1):9–10. doi:10.1007/s00415-019-09368-z

Preoperative hemoglobin A1c as a predictor of lymph node metastasis in diabetic women with endometrial cancer

Busra Korpe^{1,A–D,F}, Caner Kose^{1,A,B,D,F}, Kadriye Erdogan^{1,E,F}, Yaprak Engin-Ustun^{2,E,F}, Vakkas Korkmaz^{1,A,E,F}

¹ Department of Gynecology and Obstetrics, Ankara Etlik City Hospital, Turkey

² Department of Gynecology and Obstetrics, Ankara Etlik Zübeyde Hanim Women's Health and Research Hospital, Turkey

A – research concept and design; B – collection and/or assembly of data; C – data analysis and interpretation;

D – writing the article; E – critical revision of the article; F – final approval of the article

Advances in Clinical and Experimental Medicine, ISSN 1899–5276 (print), ISSN 2451–2680 (online)

Adv Clin Exp Med. 2025;34(9):1451–1457

Address for correspondence

Caner Kose

E-mail: dr.canerkose@gmail.com

Funding sources

None declared

Conflict of interest

None declared

Received on June 4, 2024

Reviewed on November 26, 2024

Accepted on December 17, 2024

Published online on March 11, 2025

Abstract

Background. Glycated hemoglobin A1c (HbA1c) is a well-established marker for glycemic control; recent studies suggest its potential role in cancer prognosis. Understanding the relationship between preoperative HbA1c levels and lymph node metastasis (LNM) in diabetic women with endometrial cancer (EC) can enhance prognostic assessments and treatment strategies.

Objectives. This study aimed to evaluate the predictive value of preoperative HbA1c levels for LNM in diabetic women with EC.

Materials and methods. A retrospective analysis was conducted on 233 diabetic women who underwent surgery for endometrioid-type EC at a tertiary referral hospital between 2010 and 2021. Data collected included demographic information, fasting plasma glucose, HbA1c levels, ultrasound findings, and tumor characteristics. Receiver operating characteristic (ROC) analysis was used to assess the predictive power of HbA1c levels for LNM. Univariate and multivariate regression analyses were performed to identify independent risk factors for LNM.

Results. The mean preoperative HbA1c level was $7.03 \pm 1.37\%$. A cutoff HbA1c level $\geq 7.26\%$ demonstrated a sensitivity of 73.7%, a specificity of 72.3% and an area under the curve (AUC) of 0.781 for predicting LNM ($p < 0.001$). Significant correlations were found between HbA1c levels and endometrial thickness ($r = 0.231$, $p < 0.001$), primary tumor diameter (PTD) ($r = 0.173$, $p = 0.008$) and duration of diabetes ($r = 0.203$, $p = 0.002$). Multivariate analysis identified HbA1c level (odds ratio (OR) = 2.621, 95% confidence interval (95% CI): 1.722–3.987, $p < 0.001$), lymphovascular space involvement (LVSI) (OR = 19.193, 95% CI: 5.805–63.458, $p < 0.001$), body mass index (BMI) (OR = 1.095, 95% CI: 1.010–1.188, $p = 0.029$), and duration of diabetes (OR = 1.019, 95% CI: 1.001–1.301, $p = 0.039$) as independent risk factors for LNM.

Conclusions. Preoperative HbA1c levels serve as a significant predictor for LNM in diabetic women with EC. A cutoff HbA1c level $\geq 7.26\%$ indicates higher risk of LNM. These findings underscore the importance of glycemic control in reducing cancer progression risks and improving the prognosis of diabetic patients with EC. Integrating HbA1c monitoring into preoperative assessments can help tailor personalized treatment strategies for better outcomes.

Key words: endometrial neoplasms, diabetes mellitus, glycated hemoglobin

Cite as

Korpe B, Kose C, Erdogan K, Engin-Ustun Y, Korkmaz V. Preoperative hemoglobin A1c as a predictor of lymph node metastasis in diabetic women with endometrial cancer. *Adv Clin Exp Med.* 2025;34(9):1451–1457. doi:10.17219/acem/198152

DOI

10.17219/acem/198152

Copyright

Copyright by Author(s)

This is an article distributed under the terms of the Creative Commons Attribution 3.0 Unported (CC BY 3.0) (<https://creativecommons.org/licenses/by/3.0/>)

Highlights

- Preoperative HbA1c levels were evaluated as a predictor of lymph node metastasis in diabetic women with endometrial carcinoma.
- Higher HbA1c levels were associated with an increased risk of lymph node metastasis.
- The study highlights the potential role of glycemic control in endometrial cancer progression.
- HbA1c may serve as a useful biomarker for risk stratification in diabetic women with endometrial carcinoma.
- Findings suggest integrating HbA1c assessment into preoperative evaluations for better clinical decision-making.

Background

Diabetes mellitus is a significant global health problem, closely linked to the development and progression of various cancers.¹ Among these, endometrial cancer (EC) stands out as the most common gynecological malignancy in industrialized countries.² Epidemiological studies consistently report an increased risk of developing EC in diabetic women.³ The interplay between diabetes and cancer is complex, with hyperinsulinemia, hyperglycemia and chronic inflammation believed to be common pathways that may contribute to both conditions.^{4–8} Hyperinsulinemia, in particular, is thought to promote tumor growth through increased insulin-like growth factor (IGF) signaling, which can enhance cell proliferation and inhibit apoptosis.^{9,10} Additionally, elevated blood glucose levels may lead to the formation of advanced glycation end-products (AGEs), which can trigger inflammatory pathways that promote carcinogenesis.¹¹

Glycated hemoglobin A1c (HbA1c) is a well-established marker used to assess long-term glycemic control.¹² Beyond its role in diabetes management, elevated HbA1c levels have gained attention in the context of cancer prognosis. Recent studies suggest that high HbA1c levels are associated with poorer outcomes in a variety of cancers, including breast, colorectal and pancreatic cancers.^{13–16} In EC, studies have shown that elevated HbA1c levels may be associated with an increased risk of lymphovascular space invasion (LVSI) and a more advanced cancer stage at the time of diagnosis.^{5,17–19} Additionally, HbA1c levels can be used in patients with endometrial intraepithelial neoplasia (EIN) to help diagnose concurrent EC, as higher HbA1c may indicate the presence of malignancy or a higher likelihood of progression to invasive cancer.²⁰

Due to the shared pathophysiological mechanisms between diabetes and EC, it is crucial to explore how HbA1c levels might influence cancer prognosis. Higher HbA1c levels could be indicative of more aggressive disease and a higher likelihood of lymph node metastasis (LNM), a critical factor in determining disease stage and guiding treatment decisions.^{10,12–14}

Objectives

This study aimed to investigate the potential role of preoperative HbA1c levels as a predictor of LNM in diabetic women with EC. Given the established link between diabetes and the increased risk of EC, understanding how HbA1c levels correlate with tumor progression and metastasis could provide valuable insights into patient prognosis.

Clinically, this research aims to enhance risk assessment and treatment planning for diabetic women with EC. By identifying elevated HbA1c as a predictive marker for more aggressive disease and a higher likelihood of LNM, clinicians could better stratify patients, allowing for tailored treatment approaches. This could lead to more intensive monitoring and earlier interventions, ultimately improving survival rates and reducing the risk of recurrence.

Materials and methods

Study design

A retrospective analysis was conducted on 1,163 EC patients who received primary treatment at the Gynecologic Oncology Clinic of Ankara Etlik City Hospital, Turkey, between March 2011 and August 2023.

Participants

From this cohort, 233 patients were selected based on specific criteria, focusing on diabetic individuals with endometrioid-type EC according to final pathological results who had their HbA1c levels measured within 3 months before surgery. Patients with non-diabetic, non-endometrioid histology, irregular follow-up or incomplete data were excluded from the study.

Setting

Diabetes was diagnosed according to the American Diabetes Association (ADA) criteria: fasting plasma glucose level ≥ 126 mg/dL, HbA1c level $\geq 6.5\%$ or a plasma glucose level ≥ 200 mg/dL 2 h post-glucose load.²¹

Cancer staging was classified based on the 2009 FIGO (Fédération Internationale de Gynécologie et d'Obstétrique) staging system.²² Surgical procedures for early-stage EC included: hysterectomy, bilateral salpingo-oophorectomy (adjusted for patient age), infracolic omental biopsy, and peritoneal washings tailored to specific histological subtypes. During the study period, lymphadenectomy cases in our clinic were determined using a frozen-section-based approach, and no sentinel lymph node procedures were performed on any EC cases. The decision to perform lymph node dissection was guided by the criteria described by Mariani et al.²³ Specifically, patients with a greatest surface dimension ≤ 2 cm, myometrial invasion $\leq 50\%$ and no intraoperative evidence of macroscopic disease were classified as low risk and treated with hysterectomy only, without lymph node dissection. For cases that did not meet these criteria, lymph node dissection was performed. All operations were performed by gynecologic oncologists.

All EC patients underwent intraoperative frozen section evaluation to assess histopathologic type, grade and depth of myometrial invasion. Surgical specimens were examined by gynecologic pathologists. Lymphovascular space invasion was characterized by the presence of tumor cells or clusters within the vessel walls, as identified through hematoxylin and eosin (H&E) staining.²⁴

Adjuvant treatment followed the guidelines of the European Society for Medical Oncology (ESMO), the European Society of Gynecological Oncology (ESGO) and the European Society for Radiotherapy and Oncology (ESTRO).²⁵ Disease-free survival (DFS) was calculated from the start of treatment to recurrence or last follow-up for non-recurrent cases, or to the date of death. Overall survival (OS) was measured from the time of diagnosis until either death or the most recent hospital admission.

Data sources

Patient follow-up records included: age, body mass index (BMI), menopausal status, fasting plasma glucose and HbA1c levels, ultrasound findings, surgery dates, LVSI status (based on postoperative pathology), cancer stage and grade, myometrial invasion, risk group classification, lymph node involvement, adjuvant therapy details, recurrence (location and timing), and deaths during follow-up.

Patients were monitored every 3 months during the 1st year and every 6 months during the 2nd year. Each visit included a physical examination, ultrasonography and review of laboratory parameters. Data were extracted from medical records.

Statistical analyses

All statistical analyses were conducted using IBM SPSS v. 23.0 (IBM Corp., Armonk, USA). Normality of the data was assessed using histograms and the skewness and kurtosis values (see Supplementary data). Normally

distributed quantitative data presented as mean \pm standard deviation (\pm SD) and qualitative data as frequency (percentage). Given the relatively large sample size of our study, we proceeded with t-tests for group comparisons. The use of t-tests was further justified by the central limit theorem (CLT), which supports the robustness of parametric tests under these conditions even with minor deviations from normality. To ensure reliability, we conducted sensitivity analyses to evaluate the potential impact of non-normality, confirming the appropriateness of the approach. Pearson's χ^2 test of independence was used for comparing categorical variables. Pearson correlation analysis was employed to examine relationships between normally distributed variables with linear relationships. Receiver operating characteristic (ROC) analysis was performed to assess the predictivity of HbA1c levels for LNM, calculating sensitivity, specificity and cutoff values. According to the literature, increased age, BMI, lymphovascular space involvement, myometrial invasion, and primary tumor diameter (PTD) are recognized risk factors for lymph node metastasis in EC patients. Based on this, we included these variables, along with HbA1c, in our multivariate logistic regression analysis. This selection aimed to address potential confounding factors and enhance the explanatory strength of the model. All data were analyzed with 95% confidence intervals (95% CIs), and statistical significance was assumed at $p < 0.05$.

Results

The median age at diagnosis was 57 years (range: 26–80 years), with a majority of women being postmenopausal (68.2%). Among these women, 195 (83.6%) exhibited high fasting glucose levels, while 213 (93.5%) were classified as overweight and obese based on their BMI. Table 1 provides a comprehensive summary of demographic characteristics, laboratory results and clinical outcomes of the study population. Additionally, the overview of tumor characteristics is presented in Table 1. Figure 1 shows the comparison of HbA1c levels according to LNM.

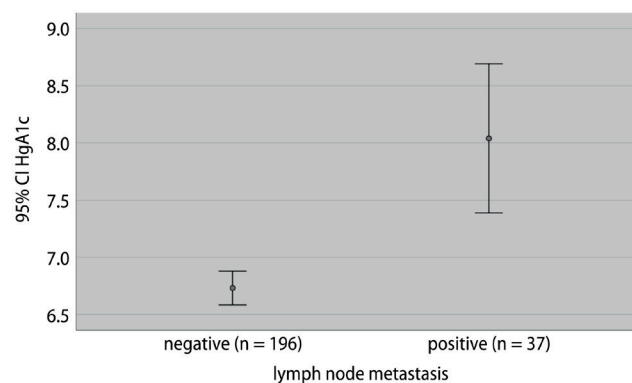


Fig. 1. Comparison of glycated hemoglobin A1c (HbA1c) levels according to lymph node metastasis

Table 1. Baseline demographic and clinical characteristics of endometrial cancer patients

Variables		Mean \pm SD
Age [years], mean \pm SD		57.33 \pm 8.85
BMI [kg/m ²], mean \pm SD		33.84 \pm 6.18
Fasting glucose [mg/dL], mean \pm SD		157.68 \pm 57.44
HbA1c [%], mean \pm SD		7.03 \pm 1.37
Endometrial thickness [mm], mean \pm SD		13.59 \pm 8.98
Tumor diameter [mm], mean \pm SD		31.67 \pm 23.06
Menopause, n (%)		159 (68.2)
Stage, n (%)	IA	131 (56.2)
	IB	35 (15)
	II	28 (12.1)
	IIIC1	24 (10.3)
	IIIC2	13 (5.5)
Grade, n (%)	1	143 (61.4)
	2	62 (28)
	3	28 (12)
LVSI, n (%)	(+)	51 (21.9)
	(-)	182 (78.1)
MMI, n (%)	<50%	157 (67.4)
	\geq 50%	76 (32.6)
LNM, n (%)	(+)	37 (15.9)
	(-)	196 (84.1)
Recurrence, n (%)		10 (4.3)
DFS [months], n (%)		64 (6–118)

HbA1c – glycated hemoglobin A1c; BMI – body mass index; LVSI – lymphovascular space involvement; MMI – myometrial invasion; LNM – lymph node metastasis; DFS – disease free survival; SD – standard deviation.

Table 2 compares patients based on preoperative HbA1c levels. Two groups were created according to ADA diabetes criteria of HbA1c ($\geq 6.5\%$). There were no significant differences in age, BMI and fasting glucose values between the groups ($p > 0.05$). However, the group with HbA1c $\geq 6.5\%$ showed a higher prevalence of LVSI and MMI $\geq 50\%$ (44 vs 7, 57 vs 19; $p < 0.001$, $p = 0.004$, respectively) (Table 2). Notably, all patients with lymph node involvement and recurrence were in the HbA1c $\geq 6.5\%$ group.

To evaluate the predictive value of preoperative HbA1c levels for LNM, a ROC analysis was performed. It revealed

Table 2. Comparison of patient characteristics based on HbA1c levels according to American Diabetes Association (ADA) criteria (HbA1c $\geq 6.5\%$)

Variables		HbA1c <6.5 % (n = 90)	HbA1c ≥ 6.5 % (n = 143)	p-value
Age [years]*, mean \pm SD		56.07 \pm 8.88	58.13 \pm 8.76	0.068
BMI [kg/m ²]*, mean \pm SD		34.19 \pm 6.46	33.62 \pm 6	0.471
Fasting glucose [mg/dL]*, mean \pm SD		150.71 \pm 55.75	162.06 \pm 58.25	0.142
LVSI**, n (%)	(+)	7 (7.8)	44 (30.8)	<0.001
	(-)	83 (92.2)	99 (69.2)	
MMI**, n (%)	<50%	71 (78.9)	86 (60.1)	0.004
	$\geq 50\%$	19 (21.1)	57 (39.9)	
LNM**, n (%)	(+)	0	38 (25.9)	<0.001
	(-)	90 (100)	105 (74.1)	
Recurrence**, n (%)	(+)	0	10 (7)	0.008
	(-)	90 (100)	133 (93)	
Stage**, n (%)	I	75 (83.3)	91 (63.6)	0.001
	\geq II	15 (16.7)	52 (36.4)	
Grade**, n (%)	1	67 (74.4)	76 (53.1)	<0.001
	2	19 (21.1)	43 (30.1)	
	3	4 (4.4)	24 (16.8)	

SD – standard deviation; HbA1c – glycated hemoglobin A1c; BMI – body mass index; LVSI – lymphovascular space involvement; MMI – myometrial invasion; LNM – lymph node metastasis; *Student's t-test was used for the comparisons. **Pearson χ^2 test was used for the comparisons. Values in bold are statistically significant.

a sensitivity of 73.7% and a specificity of 72.3% at an optimal cutoff HbA1c value of 7.26%. The area under the curve (AUC) was 0.781 ($p < 0.001$), indicating good discriminatory power. These results suggest that preoperative HbA1c levels can reliably differentiate between patients with and without LNM (Fig. 2).

Table 3 illustrates the correlation between HbA1c levels and various variables. Significant positive correlations were observed between HbA1c and endometrial thickness, PTD, tumor stage and grade, number of pelvic and para-aortic lymph nodes, and duration of diabetes (Table 3).

In multivariate logistic regression analysis, variables including age, BMI, PTD, HbA1c level, LVSI, and myometrial invasion were assessed as potential risk factors for LNM. The findings of the study indicated that HbA1c level, LVSI, and BMI were independent risk factors for LNM (odds ratio (OR) = 2.215, 95% CI: 1.657–3.539, $p < 0.001$;

Table 3. Correlations between HbA1c and clinical variables in endometrial cancer patients

Variable	Glucose [mg/dL] (n = 233)	BMI [kg/m ²] (n = 233)	Duration of diabetes [years] (n = 233)	PTD [mm] (n = 233)	Endometrial thickness [mm] (n = 233)	Stage of tumor	Grade of tumor
HbA1c (%)	$r = 0.067$	$r = -0.007$	$r = 0.203^{**}$	$r = 0.173^{**}$	$r = 0.231^{**}$	$r = 0.350^{**}$	$r = 0.367^{**}$
	$p = 0.308$	$p = 0.920$	$p < 0.002$	$p = 0.008$	$p < 0.001$	$p < 0.001$	$p < 0.001$

**Correlation is significant at the 0.01 level (2-tailed); HbA1c – glycated hemoglobin A1c; BMI – body mass index; PTD – primary tumor diameter; r – Pearson's correlation coefficient.

Table 4. Multivariate logistic regression analysis of predictors for lymph node metastasis in endometrial cancer

Variable	B	β	Lower 95% CI	Upper 95% CI	p-value
Age [years]	−0.018	0.982	.926	1.041	0.537
BMI [kg/m ²]	0.082	1.085	1.006	1.171	0.036
HbA1c	0.884	2.215	1.657	3.539	<0.001
LVSI	2.964	19.373	5.892	63.699	<0.001
Myometrial invasion	0.295	1.343	0.413	4.364	0.624
Primary tumor diameter [mm]	−0.102	0.903	0.724	1.127	0.367

95% CI – 95% confidence interval; HbA1c – glycated hemoglobin A1c; BMI – body mass index; LVSI – lymphovascular space invasion; B – unstandardized regression coefficient; β – standardized regression coefficient. Values in bold are statistically significant.

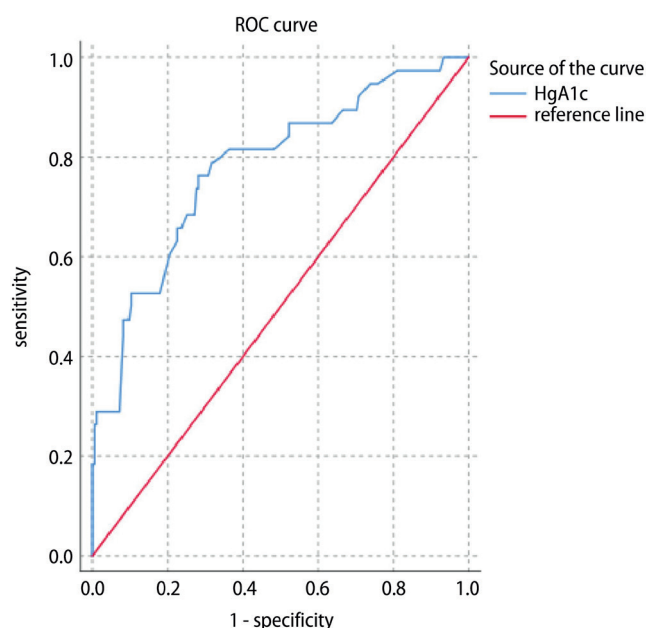


Fig. 2. Receiver operating characteristic (ROC) analysis of glycated hemoglobin A1c (HbA1c) in predicting lymph node metastasis (area under the curve (AUC): 78.1, $p < 0.001$, 95% confidence interval (95% CI): 0.696–0.866, cutoff: 7.26, sensitivity: 73.7%, specificity: 72.3%)

$\chi^2 = 19.373$, 95% CI: 5.892–63.699, $p < 0.001$; $\chi^2 = 1.085$, 95% CI: 1.006–1.171, $p = 0.036$; respectively). The results are summarized in Table 4.

Discussion

Our analysis of 233 cases of endometrioid EC revealed a significant association between elevated preoperative HbA1c levels and the risk of LNM, as well as between LVSI and the risk of LNM. Although the relationship between LVSI and LNM has been emphasized in numerous previous studies,^{23,25–28} our study suggests that diabetic EC patients with poor glycemic control, as reflected by higher preoperative HbA1c levels, are at an increased risk for LNM.

Several studies have shown that elevated HbA1c levels may increase the risk of various cancers, including EC.^{18,29–31} A study by Senkaya et al. analyzed HbA1c levels and fasting glucose in 138 diabetic EC patients and found a significant

association between HbA1c and LVSI, but no correlation with endometrial thickness. However, a low positive correlation between fasting glucose and endometrial thickness was noted.³² In contrast, our study identified significant correlations between HbA1c and several clinical parameters, including endometrial thickness, PTD, tumor stage and grade, lymph node involvement, and duration of diabetes, further supporting the role of glycemic control in influencing the invasive potential of EC.

Other studies have examined the impact of elevated HbA1c levels on the prognosis of various cancers. For instance, Cheon et al. demonstrated that elevated HbA1c levels were associated with worse survival in patients with advanced pancreatic cancer and diabetes.³³ Similarly, HbA1c has been identified as a potential preoperative predictor of aggressive tumor profiles in diabetic patients with clinically localized prostate cancer.³⁴ Siddiqi et al. found that elevated HbA1c is an independent predictor of aggressive colorectal cancer patterns.¹⁸ In contrast, Nief et al. found that in diabetic patients with endometrioid EC, glycemic control markers such as HbA1c, BMI and antihyperglycemic medications did not correlate with progression-free survival (PFS), while diabetic neuropathy was associated with an increased risk of recurrence.³⁵ In a review of 55,475 EC patients, diabetes was linked to worse cancer-specific and OS, reinforcing the notion that poor glycemic control may influence EC prognosis.³⁶ However, discrepancies in findings, such as those observed by Nief et al., highlight the need for further exploration of the role of HbA1c in cancer progression, particularly in EC.

Despite these findings, the relationship between HbA1c and cancer stage, grade and histological type in diabetic patients remains underexplored. Karaman et al. reported significantly higher HbA1c levels in EC patients compared to controls, but no significant correlation with tumor stage, grade or histological type.¹⁹ Similarly, Stevens et al. observed a trend of more advanced stages in patients with elevated HbA1c; however, HbA1c was not a strong predictor of EC prognosis.⁵ Folsom et al. showed that diabetes mellitus is associated with worse survival after EC, independent of tumor stage and grade.³⁷ However, their study did not examine HbA1c or glucose levels. In contrast, our study identified a clear correlation between elevated preoperative HbA1c levels and both tumor stage and grade, as well as lymph node

involvement, suggesting that HbA1c may serve as a valuable prognostic biomarker in diabetic EC patients.

The potential mechanisms linking diabetes, poor glycemic control and cancer progression are multifactorial.³ Hyperglycemia has been shown to create a favorable microenvironment for tumor growth by inducing oxidative stress, inflammation and angiogenesis.^{4–8} Glycolysis enhances glucose metabolism in cancer cells, supplying substrates essential for rapid proliferation.¹¹ Han et al. suggested that glucose stimulates cell proliferation through several complex signaling pathways, supporting the hypothesis that elevated glucose levels may increase cancer risk.⁸ Furthermore, chronic hyperglycemia can elevate pro-inflammatory cytokine levels, facilitating tumor cell invasion and metastasis.^{6–9} Hyperinsulinemia and insulin resistance, both hallmarks of diabetes, may also play pivotal roles by activating the insulin/IGF-1 pathway, which promotes cell growth and survival.^{9,10} These mechanisms have been implicated in other malignancies, including breast, genitourinary and gastrointestinal cancers, and may also contribute to the aggressive behavior of EC in diabetic patients.³⁸ Mitsuhashi et al. reported common impaired glucose metabolism and insulin resistance (IR) in patients with endometrial intraepithelial neoplasia (EIN) and EC.³⁹

Limitations

The retrospective design and reliance on medical records for data collection are the main limitations of our study. As a result, the assessment of preoperative HbA1c's impact on long-term survival was not feasible. Additionally, the follow-up of patients has not been completed yet, preventing the evaluation of HbA1c's prognostic significance on survival. Future investigations are planned to address these limitations and provide a more comprehensive understanding of the relationship between preoperative HbA1c levels and long-term outcomes in diabetic EC patients.

Conclusions

The findings indicate that inadequate glycemic control, as demonstrated by elevated HbA1c levels, could be a significant prognostic factor, impacting tumor behavior and metastasis. This highlights the potential clinical application of HbA1c as a biomarker to guide treatment decisions, such as identifying patients at higher risk for aggressive disease who may benefit from more intensive surgical or adjuvant therapies. Additionally, the study contributes to the growing body of literature on the role of diabetes and glycemic control in cancer prognosis.

Declarations

Ethical approval was obtained from the relevant institutional review board (approval No. 26.07.2022-09/25),

and informed consent was waived due to the retrospective nature of the study and the use of anonymized data. The study adhered to the principles outlined in the Declaration of Helsinki.

Supplementary data

The Supplementary materials are available at <https://doi.org/10.6084/m9.figshare.28382411>. The package includes the following files:

Supplementary Fig. 1. Histogram analysis of the age.

Supplementary Fig. 2. Histogram analysis of the BMI.

Supplementary Fig. 3. Histogram analysis of the glucose level.

Supplementary Fig. 4. Histogram analysis of the HbA1c.

Supplementary Fig. 5. Histogram analysis of the endometrial thickness.

Supplementary Fig. 6. Histogram analysis of the tumor diameter.

Supplementary File 1. T-test with variance homogeneity.

Supplementary File 2. Correlations and multicollinearity.

Supplementary File 3. Normality test results.

Data availability

The datasets generated and/or analyzed during the current study are available from the corresponding author on reasonable request.


Consent for publication

Not applicable.


Use of AI and AI-assisted technologies

ChatGPT was solely used to improve the language and readability of the text. After utilizing this tool, the authors thoroughly reviewed and edited the content as needed and take full responsibility for the content of the publication.


ORCID iDs

Busra Korpe  <https://orcid.org/0000-0002-4315-5518>

Caner Kose  <https://orcid.org/0000-0002-3044-4804>

Kadriye Erdogan  <https://orcid.org/0000-0002-8789-1875>

Yaprak Engin-Ustun  <https://orcid.org/0000-0002-1011-3848>

Vakkas Korkmaz  <https://orcid.org/0000-0001-8895-6864>

References

1. Cho NH, Shaw JE, Karuranga S, et al. IDF Diabetes Atlas: Global estimates of diabetes prevalence for 2017 and projections for 2045. *Diabetes Res Clin Pract.* 2018;138:271–281. doi:10.1016/j.diabres.2018.02.023
2. Sung H, Ferlay J, Siegel RL, et al. Global Cancer Statistics 2020: GLOBOCAN estimates of incidence and mortality worldwide for 36 cancers in 185 countries. *CA Cancer J Clin.* 2021;71(3):209–249. doi:10.3322/caac.21660
3. Wang M, Yang Y, Liao Z. Diabetes and cancer: Epidemiological and biological links. *World J Diabetes.* 2020;11(6):227–238. doi:10.4239/wjcd.v11.i6.227

4. Shikata K, Ninomiya T, Kiyohara Y. Diabetes mellitus and cancer risk: Review of the epidemiological evidence. *Cancer Sci*. 2013;104(1):9–14. doi:10.1111/cas.12043
5. Stevens EE, Yu S, Van Sise M, et al. Hemoglobin A1c and the relationship to stage and grade of endometrial cancer. *Arch Gynecol Obstet*. 2012;286(6):1507–1512. doi:10.1007/s00404-012-2455-7
6. Giovannucci E, Harlan DM, Archer MC, et al. Diabetes and cancer. *Diabetes Care*. 2010;33(7):1674–1685. doi:10.2337/dc10-0666
7. Sanz-Chávez TLN, Vilar-Compte D, de Nicola-Delfin L, Meneses-García A. Overweight, obesity, diabetes, and hypertension in endometrial cancer [in Spanish]. *Rev Med Inst Mex Seguro Soc*. 2013;51(3):326–329. PMID:23883464.
8. Han J, Zhang L, Guo H, et al. Glucose promotes cell proliferation, glucose uptake and invasion in endometrial cancer cells via AMPK/mTOR/S6 and MAPK signaling. *Gynecol Oncol*. 2015;138(3):668–675. doi:10.1016/j.ygyno.2015.06.036
9. Gallagher EJ, LeRoith D. The proliferating role of insulin and insulin-like growth factors in cancer. *Trends Endocrinol Metab*. 2010;21(10):610–618. doi:10.1016/j.tem.2010.06.007
10. Zhang AMY, Wellberg EA, Kopp JL, Johnson JD. Hyperinsulinemia in obesity, inflammation, and cancer. *Diabetes Metab J*. 2021;45(3):285–311. doi:10.4093/dmj.2020.0250
11. Shen CY, Lu CH, Cheng CF, et al. Advanced glycation end-products acting as immunomodulators for chronic inflammation, inflammaging and carcinogenesis in patients with diabetes and immune-related diseases. *Biomedicines*. 2024;12(8):1699. doi:10.3390/biomedicines12081699
12. Gilstrap LG, Chernew ME, Nguyen CA, et al. Association between clinical practice group adherence to quality measures and adverse outcomes among adult patients with diabetes. *JAMA Netw Open*. 2019;2(8):e199139. doi:10.1001/jamanetworkopen.2019.9139
13. Natalicchio A, Marrano N, Montagnani M, et al. Glycemic control and cancer outcomes in oncologic patients with diabetes: An Italian Association of Medical Oncology (AIOM), Italian Association of Medical Diabetologists (AMD), Italian Society of Diabetology (SID), Italian Society of Endocrinology (SIE), Italian Society of Pharmacology (SIF) multidisciplinary critical view. *J Endocrinol Invest*. 2024;47(12):2915–2928. doi:10.1007/s40618-024-02417-z
14. Dankner R, Boker LK, Boffetta P, et al. A historical cohort study on glycemic-control and cancer-risk among patients with diabetes. *Cancer Epidemiol*. 2018;57:104–109. doi:10.1016/j.canep.2018.10.010
15. Shimada S, Kamiyama T, Orimo T, Nagatsu A, Kamachi H, Taketomi A. High HbA1c is a risk factor for complications after hepatectomy and influences for hepatocellular carcinoma without HBV and HCV infection. *Hepatobiliary Surg Nutr*. 2021;10(4):454–463. doi:10.21037/hbsn.2020.01.03
16. Jousheghany F, Phelps J, Crook T, Hakkak R. Relationship between level of HbA1C and breast cancer. *BBA Clin*. 2016;6:45–48. doi:10.1016/j.bbacli.2016.04.005
17. Byrne FL, Martin AR, Kosasih M, Caruana BT, Farrell R. The role of hyperglycemia in endometrial cancer pathogenesis. *Cancers (Basel)*. 2020;12(5):1191. doi:10.3390/cancers12051191
18. Siddiqui AA, Spechler SJ, Huerta S, Dredar S, Little BB, Cryer B. Elevated HbA1c is an independent predictor of aggressive clinical behavior in patients with colorectal cancer: A case-control study. *Dig Dis Sci*. 2008;53(9):2486–2494. doi:10.1007/s10620-008-0264-4
19. Karaman E, Karaman Y, Numanoglu C, Ark HC. Evaluation of hemoglobin A1c levels in endometrial cancer patients: A retrospective study in Turkey. *Asian Pac J Cancer Prev*. 2015;16(5):1817–1820. doi:10.7314/APJCP.2015.16.5.1817
20. Kose C, Korpe B, Korkmaz V, Engin-Ustun Y. Is hemoglobin A1c valuable for predicting concurrent endometrial cancer in diabetic women with endometrial intraepithelial neoplasia? *Gynecol Oncol*. 2022;38(11):1003–1007. doi:10.1080/09513590.2022.2129611
21. Poltavskiy E, Kim DJ, Bang H. Comparison of screening scores for diabetes and prediabetes. *Diabetes Res Clin Pract*. 2016;118:146–153. doi:10.1016/j.diabres.2016.06.022
22. Lewin SN. Revised FIGO Staging System for Endometrial Cancer. *Clin Obstet Gynecol*. 2011;54(2):215–218. doi:10.1097/GRF.0b013e3182185baa
23. Mariani A, Webb MJ, Keeney GL, Haddock MG, Calori G, Podratz KC. Low-risk corpus cancer: Is lymphadenectomy or radiotherapy necessary? *Am J Obstet Gynecol*. 2000;182(6):1506–1519. doi:10.1067/mob.2000.107335
24. Köse C, Meydanli MM. Prognostic importance of lymph-vascular space involvement in stage I endometrioid type endometrial cancer. *Bezmialem Sci*. 2023;11(3):254–259. doi:10.14235/bas.galenos.2023.18189
25. Kalampokas E, Giannis G, Kalampokas T, et al. Current approaches to the management of patients with endometrial cancer. *Cancers (Basel)*. 2022;14(18):4500. doi:10.3390/cancers14184500
26. Hahn H, Lee I, Kim T, et al. Lymphovascular space invasion is highly associated with lymph node metastasis and recurrence in endometrial cancer. *Aust N Z J Obstet Gynaecol*. 2013;53(3):293–297. doi:10.1111/ajo.12089
27. Yarandi F, Shirali E, Akhavan S, Nili F, Ramhormozian S. The impact of lymphovascular space invasion on survival in early stage low-grade endometrioid endometrial cancer. *Eur J Med Res*. 2023;28(1):118. doi:10.1186/s40001-023-01084-9
28. Kim SI, Yoon JH, Lee SJ, et al. Prediction of lymphovascular space invasion in patients with endometrial cancer. *Int J Med Sci*. 2021;18(13):2828–2834. doi:10.7150/ijms.60718
29. Rinaldi S, Rohrmann S, Jenab M, et al. Glycosylated hemoglobin and risk of colorectal cancer in men and women: The European prospective investigation into cancer and nutrition. *Cancer Epidemiol Biomarkers Prev*. 2008;17(11):3108–3115. doi:10.1158/1055-9965.EPI-08-0495
30. Pliszka M, Szablewski L. Associations between diabetes mellitus and selected cancers. *Int J Mol Sci*. 2024;25(13):7476. doi:10.3390/ijms25137476
31. Chen HF, Liu MD, Chen P, et al. Risks of breast and endometrial cancer in women with diabetes: A population-based cohort study. *PLoS One*. 2013;8(6):e67420. doi:10.1371/journal.pone.0067420
32. Senkaya AR, Kantarci S, Yildirim Karaca S, Sancı M. Hemoglobin A1c level is associated with lymphovascular space invasion in diabetic endometrial cancer patients. *Gynecol Obstet Reprod Med*. 2024;30(1):50–54. doi:10.21613/GORM.2023.1386
33. Cheon YK, Koo JK, Lee YS, Lee TY, Shim CS. Elevated hemoglobin A1c levels are associated with worse survival in advanced pancreatic cancer patients with diabetes. *Gut Liver*. 2014;8(2):205–214. doi:10.5009/gnl.2014.8.2.205
34. Hong SK, Lee ST, Kim SS, et al. Significance of preoperative HbA1c level in patients with diabetes mellitus and clinically localized prostate cancer. *Prostate*. 2009;69(8):820–826. doi:10.1002/pros.20932
35. Nief CA, Long SE, McCleary TL, Kidd E, Litkouhi B, Howitt BE. Diabetes mellitus complications associated with recurrence of stage I endometrioid endometrial cancer: A single-center retrospective study. *Gynecol Oncol*. 2024;190:298–306. doi:10.1016/j.ygyno.2024.09.007
36. McVicker L, Cardwell CR, Edge L, et al. Survival outcomes in endometrial cancer patients according to diabetes: A systematic review and meta-analysis. *BMC Cancer*. 2022;22(1):427. doi:10.1186/s12885-022-09510-7
37. Folsom AR, Anderson KE, Sweeney C, Jacobs DR. Diabetes as a risk factor for death following endometrial cancer. *Gynecol Oncol*. 2004;94(3):740–745. doi:10.1016/j.ygyno.2004.06.027
38. Zabuliene L, Kaceniene A, Steponaviciene L, et al. Risk of endometrial cancer in women with diabetes: A population-based retrospective cohort study. *J Clin Med*. 2021;10(16):3453. doi:10.3390/jcm10163453
39. Mitsuhashi A, Uehara T, Hanawa S, Shozu M. Prospective evaluation of abnormal glucose metabolism and insulin resistance in patients with atypical endometrial hyperplasia and endometrial cancer. *Support Care Cancer*. 2017;25(5):1495–1501. doi:10.1007/s00520-016-3554-y

NLRP3 inflammasome in expressed prostatic secretions as a potential biomarker of chronic prostatitis/chronic pelvic pain syndrome

Chao-Guang Ma^{A,B,D}, Ying-Nan Liu^{A,B,E}, Hua-Dong Wang^{A–F}

Department of Urology, Tianjin Medical University Baodi Hospital, China

A – research concept and design; B – collection and/or assembly of data; C – data analysis and interpretation;

D – writing the article; E – critical revision of the article; F – final approval of the article

Advances in Clinical and Experimental Medicine, ISSN 1899–5276 (print), ISSN 2451–2680 (online)

Adv Clin Exp Med. 2025;34(9):1459–1466

Address for correspondence

Hua-Dong Wang

E-mail: baodiywhd@163.com

Funding sources

None declared

Conflict of interest

None declared

Received on April 13, 2024

Reviewed on July 7, 2024

Accepted on August 22, 2024

Published online on December 4, 2024

Abstract

Background. Pyroptosis has been implicated in the progression of chronic prostatitis (CP)/chronic pelvic pain syndrome (CPPS).

Objectives. The present study was performed to explore the diagnostic value of the levels of the pyroptosis-related protein nucleotide-binding oligomerization domain, leucine-rich repeat and pyrin domain-containing 3 (NLRP3) inflammasome in the expressed prostatic secretions (EPS) of patients with CP.

Materials and methods. A total of 167 CP patients, including 85 National Institutes of Health (NIH)-IIIA CP patients and 82 NIH-IIIB CP patients, as well as 80 benign prostatic hyperplasia (BPH) patients and 80 healthy controls, were enrolled. The levels of NLRP3, interleukin 1 beta (IL-1 β), and interleukin 18 (IL-18) in EPS were detected using an enzyme-linked immunosorbent assay (ELISA). Disease severity was assessed using the Bergman CP scale. Differences in EPS NLRP3 inflammasome levels between the groups were analyzed, and receiver operating characteristic (ROC) curves were used to investigate the clinical value of the NLRP3 inflammasome in the diagnosis of CP. The numerical rating scale (NRS), the National Institutes of Health Chronic Prostatitis Symptom Index (NIH-CPSI) and the Danish Prostatic Symptom Score (DAN-PSS-1) were applied to evaluate symptom severity. The cutoff value of NLRP3 expression was calculated using R language.

Results. NLRP3 inflammasome levels in EPS were significantly higher in CP patients of NIH-IIIA and NIH-IIIB compared to the BPH patients and controls. NLRP3 levels in EPS were positively associated with Bergman grade. In addition, NRS levels were in a positive relationship with NIH-CPSI and DAN-PSS-1. The ROC curve analysis demonstrated that NLRP3 in EPS may act as a decent indicator for the diagnosis of CP/CPPS. The cutoff value of EPS NLRP3 expression was ≥ 55.25 ng/mL.

Conclusions. NLRP3 levels in EPS were significantly higher in NIH-IIIA and NIH-IIIB patients compared to BPH patients and healthy controls. NLRP3 inflammasome levels in EPS may be valuable as diagnostic indicators, and targeting chemokines may present a promising approach to treatment for those suffering from CPPS.

Key words: chronic prostatitis, chronic pelvic pain syndrome, NLRP3 inflammasome, pyroptosis

Cite as

Ma C-G, Liu Y-N, Wang H-D. NLRP3 inflammasome in expressed prostatic secretions as a potential biomarker of chronic prostatitis/chronic pelvic pain syndrome.

Adv Clin Exp Med. 2025;34(9):1459–1466.

doi:10.17219/acem/192548

DOI

10.17219/acem/192548

Copyright

Copyright by Author(s)

This is an article distributed under the terms of the Creative Commons Attribution 3.0 Unported (CC BY 3.0) (<https://creativecommons.org/licenses/by/3.0/>)

Background

Chronic prostatitis (CP) has a prevalence of nearly 5–10% among young and middle-aged individuals, significantly affecting their daily lives.¹ Chronic prostatitis is categorized into 3 types by National Institutes of Health (NIH): NIH-II (chronic bacterial prostatitis), NIH-III (chronic prostatitis/chronic pelvic pain syndrome (CPPS)) and NIH-IV (asymptomatic prostatitis).² Chronic prostatitis can manifest with a variety of symptoms that significantly impact quality of life, such as pelvic pain, lower urinary tract symptoms, psychological distress, and sexual dysfunction.³

The NIH-III, also referred to as CP/CPPS, is characterized by pelvic pain without any detectable bacterial infection. It is further classified into 2 subcategories: category IIIA, which is the inflammatory type, indicated by the presence of white blood cells in the expressed prostatic secretion (EPS), and category IIIB, the non-inflammatory type, where leukocytes are not present in the EPS or seminal fluid.⁴ Chronic prostatitis/CPPS, falling under NIH category III, is frequently encountered in clinical settings, with its prevalence in the general population estimated to be between 5% and 14.2%.⁵ Therefore, CP/CPPS accounts for approx. 60–80% of all prostatitis cases.

Cytokines and chemokines, which are inflammatory mediators, have been linked to the development of CPPS.⁶ Cytokines are signaling proteins that are secreted by different types of cells to facilitate intercellular communication and regulate immune responses.

In recent years, pyroptosis has been implicated in the progression of CP/CPPS.⁷ The NLRP3 inflammasome, a multi-component protein complex, is composed of the NOD-like receptor family, pyrin domain containing 3 (NLRP3), the adaptor protein ASC, and the precursor enzyme pro-caspase-1.⁸ The NLRP3 protein is composed of 3 homologous domains: The C-terminal features a leucine-rich repeat, the central region houses a nucleotide-binding oligomerization domain, and the N-terminal is characterized by a pyrin domain.⁹ Intracellular NLRP3 levels are markedly low under resting conditions. Upon activation, NLRP3 inflammasomes serve as scaffolds that initiate the activation of caspase-1, promote the secretion of cytokines and lead to the induction of pyroptosis.¹⁰

The initiation of pyroptosis, a form of cell death, is primarily driven by the activation of the NLRP3 inflammasome. Research by Lu et al. on a rat model with hormone imbalance-induced chronic non-bacterial prostatitis revealed that the activation of the NLRP3 inflammasome sets off a cascade of inflammatory reactions within the prostate glands of these rats.¹¹ Another study indicated that the regulation of cell autophagy in central neuropathic pain (CNP) might be governed by the NLRP3 inflammasome, which exerts its effects through the IL-6/STAT3 signaling pathway.¹²

Objectives

The collective findings from the aforementioned research suggest that pyroptosis, mediated by the NLRP3 inflammasome, could play a significant role in the development of CP/CPPS. However, no studies have investigated the presence of the NLRP3 inflammasome and its correlation with CP severity. Therefore, this research is the initial investigation into the expression of the NLRP3 inflammasome within the EPS of patients categorized under both CPPS IIIA and IIIB.

Methods

Study participants

From May 2022 to February 2024, we selected 167 patients with NIH-III CP, who exhibited pronounced symptoms of CP syndrome and fulfilled the NIH criteria for CP diagnosis, as participants.¹³ Based on the NIH classification system,¹³ 85 cases were NIH-IIIA while the other 82 cases were NIH-IIIB. In addition, 80 benign prostatic hyperplasia (BPH) patients were also enrolled, and 80 healthy men receiving physical examinations without any clinical symptoms served as the control group. Within the healthy control group, no abnormalities were found during physical examinations, nor were any irregularities detected in the examination of EPS, urine routine tests, or in the bacterial cultures of urine samples taken before and after prostatic massage.

Each patient submitted a comprehensive medical profile that encompassed their history of medication use and aspects of their sexual health. Individuals with conditions similar to the presenting symptoms, such as diabetes, urethritis, epididymitis, varicocele, and diseases of the rectum and perianal area, were excluded from the study.

This study was approved by the ethical committee of Tianjin Medical University Baodi Hospital (Tianjin, China; approval No. 20220015). All patients signed written consent forms.

Sample collection and ELISA

Participants were instructed to refrain from sexual activity for a period of 3 to 5 days and to thoroughly cleanse and disinfect the glans penis and external urethral area prior to sample collection. Urine samples were collected both before and after prostate massage to conduct standard urinalysis and to assess urinary bacterial cultures.

The EPS was extracted by massaging the prostate gland through digital rectal examination. The patient adopted a knee-chest position and a bent position. The doctor wore gloves and applied paraffin oil, then slowly extended his fingers into the anus, touched the prostate, and then gently massaged the prostate. When EPS was secreted into the urethral opening, sterile slides were used to collect prostate fluid. The sample was placed into a cryovial and

initially stored at -20°C for about 2 h. Subsequently, it was moved to a -70°C environment for long-term preservation until it was time to thaw it for examination.

Double-blinded quantitative measurements of EPS NLRP3 levels were assessed using a commercial enzyme-linked immunosorbent assay (ELISA) kit (cat. No. ab274401; Abcam, Cambridge, UK). Following the manufacturer's protocol, standard samples of recombinant human NOD-like receptor family, pyrin domain containing 3 (NLRP3) were pipetted into each well of a microplate that had been precoated with an antibody specific to NLRP3. The wells were left to incubate at room temperature for 2 h before being washed 3 times with the washing reagent. Following this, each well received a pipetted amount of NLRP3 conjugate and was then incubated for an additional 2 h at room temperature. Following 3 wash cycles, the substrate solution was dispensed into every well. The microplate was subsequently incubated for 20 min at room temperature and shielded from light. To halt the reactions, stop solution was added, and the optical density (OD) of the contents was measured at 450 nm using a microplate reader (Infinite M200 PRO; Tecan, Männedorf, Switzerland).

The coefficient of variation (CV) within the assay for NLRP3 was 2.5%, while the variation between assays was less than 5.1%. The sensitivity of the ELISA kit for detecting NLRP3 is 1.63 ng/mL. Additionally, the detection range for the kit is between 4.38 ng/mL and 280 ng/mL. An optical density–concentration standard curve was created to ascertain the value of NLRP3. Expressed prostatic secretions interleukin (IL)-1 β (cat. No. DLB50; R&D Systems, Minneapolis, USA) and IL-18 (cat. No. DL180; R&D Systems) concentrations were also examined. The CV within the assay was 5.5% for IL-1 β and 5.9% for IL-18, while the CV between assays was 7.5% for IL-1 β and 8.8% for IL-18.

Evaluation of disease severity

The disease severity of CP was evaluated using the Bergman scale as follows¹⁴: grade 0: No symptoms, normal sexual function; grade 1: Occasional lower abdominal pain, frequent urination at night or when feeling cold, frequent ejaculation after waking up or defecating, relief of symptoms after ejaculation, and normal sexual desire; grade 2: Persistent bloating in the lower abdomen, accompanied by abnormal urination and decreased libido, can induce ejaculation due to sexual intercourse, and symptoms may worsen after ejaculation; grade 3: Severe urination disorder, even acute urinary retention, accompanied by obvious decline in sexual desire, unable to conduct normal sexual behavior. Only patients with grade 1 or above were included in the study.

Evaluation of symptom severity

NLRP3 inflammasome levels were linked to clinical severity, as measured using 3 different scales: The numerical rating scale (NRS), the National Institutes of Health

Chronic Prostatitis Symptom Index (NIH-CPSI) and the Danish Prostatic Symptom Score (DAN-PSS-1).

The NRS is a numerical rating standard. It is a common method of using numbers to represent pain intensity that is used in pain assessment and clinical research. The NRS typically ranges from 0 to 10, with 0 indicating the absence of pain and 10 signifying the most intense pain imaginable.¹⁵ When using the NRS, patients are usually asked to select a number to reflect their current level of pain. This can be achieved by verbally asking the patient or asking them to choose a number on their own. Typically, the definition of pain score may be as follows: 0: no pain; 1–3: mild pain; 4–6: moderate pain; 7–10: severe pain.

The NIH-CPSI is a dependable and user-friendly self-reporting tool extensively utilized in both scientific research and clinical trials. It evaluates pain symptoms (sum of items 1–4), urinary symptoms (sum of items 5 and 6) and impact on quality of life (QOL) (sum of items 7–9).¹⁶

The DAN-PSS-1 is derived from the patient's self-reported data regarding the existence and intensity of 12 symptoms associated with the functions of bladder storage and emptying, known as the symptom score. In addition, the extent to which these symptoms are troublesome to the patient is also documented. The degree of bother and severity of each symptom are rated on a scale ranging from 0 to 3. A weighted score is derived by taking the product of the symptom score and bother score, resulting in an overall score for each symptom that could vary between 0 and 9. Therefore, a symptom is considered irrelevant if it does not cause the patient any distress. This occurs when the patient rates a symptom with a score of 0 (absent) or assigns a bother score of 0 (not bothersome).¹⁷

Statistical analyses

Data were expressed as mean \pm standard deviation (SD) for normally distributed variables and as median with interquartile range (IQR) for variables not normally distributed. Variance homogeneity was examined using the F-test. The distribution data were tested using the Kolmogorov–Smirnov test. Student's t-test or the Mann–Whitney U test was carried out between 2 groups, where appropriate. One-way analysis of variance (ANOVA) or the Kruskal–Wallis test was applied to statistically test the differences among ≥ 3 groups. Spearman's correlation analysis was used to examine the association between NLRP3 expression and Bergman grade, NRS, NIH-CPSI, and DAN-PSS-1 scores, as well as IL-1 β and IL-18 levels. Receiver operating characteristic (ROC) curve analysis was conducted to test the potential diagnostic value of NLRP3 expression with regard to Bergman grade. All statistical evaluations were carried out using GraphPad Prism v. 9.0 (GraphPad Software, San Diego, USA). The cutoff value of NLRP3 expression was calculated using the R language (R Foundation for Statistical Computing, Vienna, Austria). A p-value < 0.05 was regarded to be statistically significant.

Results

Demographic statistics

Table 1 displays the demographic data for the study cohorts. The distribution of age and body mass index (BMI) and showed no significant differences between the CP group and the controls. However, NLRP3 levels were significantly elevated in the CP subgroup (NIH-III A: 52.1 ± 7.1 ng/mL; NIH-III B: 51.7 ± 8.0 ng/mL) when compared to both the control group (15.4 ± 2.9 ng/mL) and the BPH group (15.7 ± 2.8 ng/mL) (one-way ANOVA, $F = 69.35$, degrees of freedom (df) = 326, $p < 0.001$ vs control, $p < 0.001$ vs BPH), as shown in Table 1 and Fig. 1.

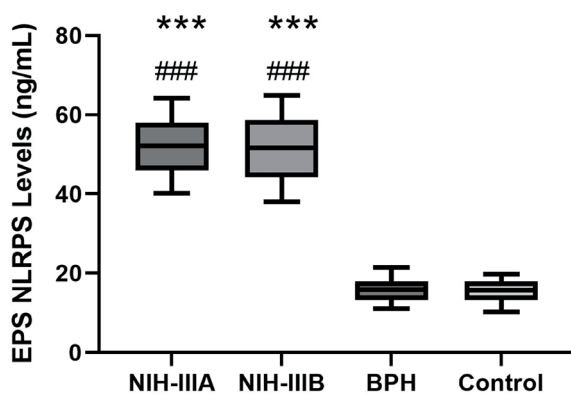


Fig. 1. Comparison of EPS NLRP3 levels among CP National Institutes of Health (NIH)-III A (n = 85), CP NIH-III B (n = 82), control (n = 80), and BPH (n = 80). One-way analysis of variance (ANOVA) was applied to statistically test the differences

EPS – expressed prostatic secretions; NLRP3 – nucleotide-binding oligomerization domain, leucine-rich repeat and pyrin domain-containing 3; CP – chronic prostatitis; BPH – benign prostatic hyperplasia.

EPS NLRP3 levels with disease severity

The EPS NLRP3 levels of the 167 NIH-III CP patients with different Bergman grades are shown in Table 1. NIH-III CP patients were divided into 3 groups based

on Bergman grade. NIH-III CP patients included 56 patients with Bergman grade 1, 60 with Bergman grade 2 and 51 with Bergman grade 3. NIH-III CP patients with Bergman grade 3 showed significantly higher EPS NLRP3 concentrations compared to those with Bergman grade 2 (55.8 ± 6.5 ng/mL vs 53.0 ± 7.3 ng/mL, Mann–Whitney U test, $U = 827.5$, $df = 109$, $p = 0.033$) (Fig. 2A). NIH-III CP patients with Bergman grade 2 demonstrated significantly higher EPS NLRP3 levels compared with Bergman grade 1 (53.0 ± 7.3 ng/mL vs 46.8 ± 5.9 ng/mL, Mann–Whitney U test, $U = 1,168$, $df = 114$, $p < 0.001$) (Fig. 2A). The analysis using Spearman's correlation revealed a positive relationship between NLRP3 levels in EPS and Bergman grade, with a correlation coefficient of 0.485, indicating a statistically significant association (Spearman's correlation, $r = 0.485$, $T(N-2) = 165$, $p < 0.001$) (Fig. 2B).

ROC curve analysis

The ROC curve analysis was conducted to evaluate the diagnostic potential of NLRP3 in EPS as a possible biomarker for CP/CPPS. As shown in Fig. 3, elevated NLRP3 levels showed a significant AUC in discriminating between Bergman grade 1 and Bergman grade 2 ($AUC = 0.753$, $p \leq 0.001$) (Fig. 3A) as well as Bergman grade 2 compared to Bergman grade 3 ($AUC = 0.619$, $p = 0.032$) (Fig. 3B). These findings suggest that elevated EPS NLRP3 level may serve as a potential diagnostic marker to evaluate disease severity in CP/CPPS. The cutoff value of EPS NLRP3 expression was ≥ 55.25 ng/mL.

NLRP3 levels with symptom severity

The association between NLRP3 levels in EPS and clinical outcomes was examined, as measured with NRS, NIH-CPSI and DAN-PSS-1 scores. We found EPS NLRP3 levels were positively associated with NRS scores (Spearman's correlation, $r = 0.513$, $T(N-2) = 165$, $p < 0.001$) (Fig. 4A), NIH-CPSI scores (Spearman's correlation, $r = 0.443$, $T(N-2) = 65$, $p < 0.001$) (Fig. 4B) and DAN-PSS-1 scores

Table 1. Demographic data for CP and BPH patients and healthy controls

Items	NIH-III A CP patients (n = 85)	NIH-III B CP patients (n = 82)	BPH patients (n = 80)	Healthy controls (n = 80)	p-value
Age [years]	36.3 ± 7.9	38.1 ± 8.1	37.4 ± 7.4	37.9 ± 7.8	0.318
BMI [kg/m^2]	23.2 ± 2.1	23.3 ± 2.0	22.9 ± 2.3	23.0 ± 2.2	0.411
NRS scores	4.6 ± 1.5		–	–	–
NIH-CPSI	20.7 ± 4.8		–	–	–
DAN-PSS-1	5.5 ± 2.2		–	–	–
Bergman grade (1/2/3)	56/60/51				
EPS	51.9 ± 7.1	51.6 ± 8.0	15.7 ± 2.8	15.4 ± 2.9	<0.001

All data are given as mean value \pm SD or median. One-way analysis of variance (ANOVA) was applied. NRS scores, NIH-CPSI, DAN-PSS-1, and Bergman grade (1/2/3) are designated scores for CP patients; CP – chronic prostatitis; BPH – benign prostatic hyperplasia; NIH – National Institutes of Health; BMI – body mass index; NRS – numerical rating scale; NIH-CPSI – National Institutes of Health Chronic Prostatitis Symptom Index; DAN-PSS-1 – Danish Prostatic Symptom Score; EPS – expressed prostatic secretions; SD – standard deviation.

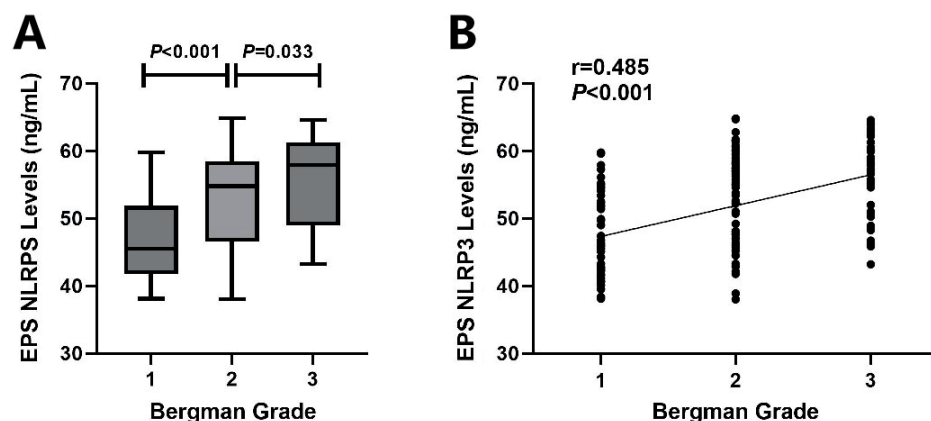


Fig. 2. A. Comparison of EPS NLRP3 levels among different Bergman grades; B. Correlation of EPS NLRP3 levels with Bergman grade. The Mann–Whitney U test was used to compare NLRP3 expression between Bergman grade 1 ($n = 56$) compared to grade 2 ($n = 60$), as well as Bergman grade 2 ($n = 60$) compared to grade 3 ($n = 51$)

EPS – expressed prostatic secretions; NLRP3 – nucleotide-binding oligomerization domain, leucine-rich repeat and pyrin domain-containing 3.

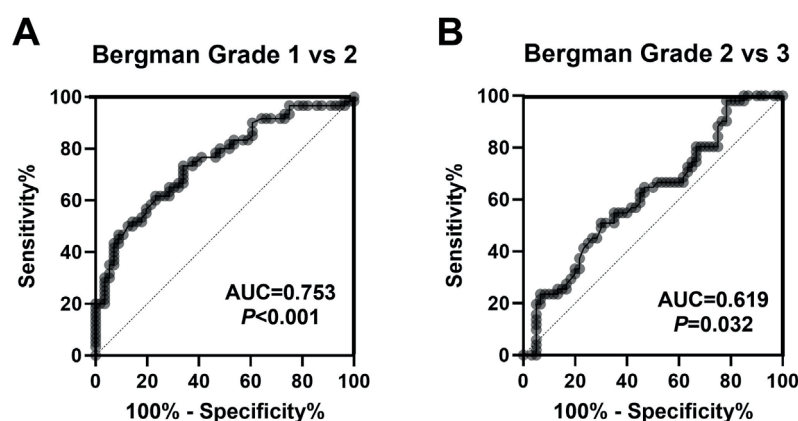


Fig. 3. A. ROC curve analysis of NLRP3 levels between Bergman grade 1 ($n = 56$) vs Bergman grade 2 ($n = 60$). B. ROC curve analysis of NLRP3 levels between Bergman grade 2 ($n = 60$) vs Bergman grade 3 ($n = 51$)

ROC – receiver operating characteristic; NLRP3 – nucleotide-binding oligomerization domain, leucine-rich repeat and pyrin domain-containing 3.

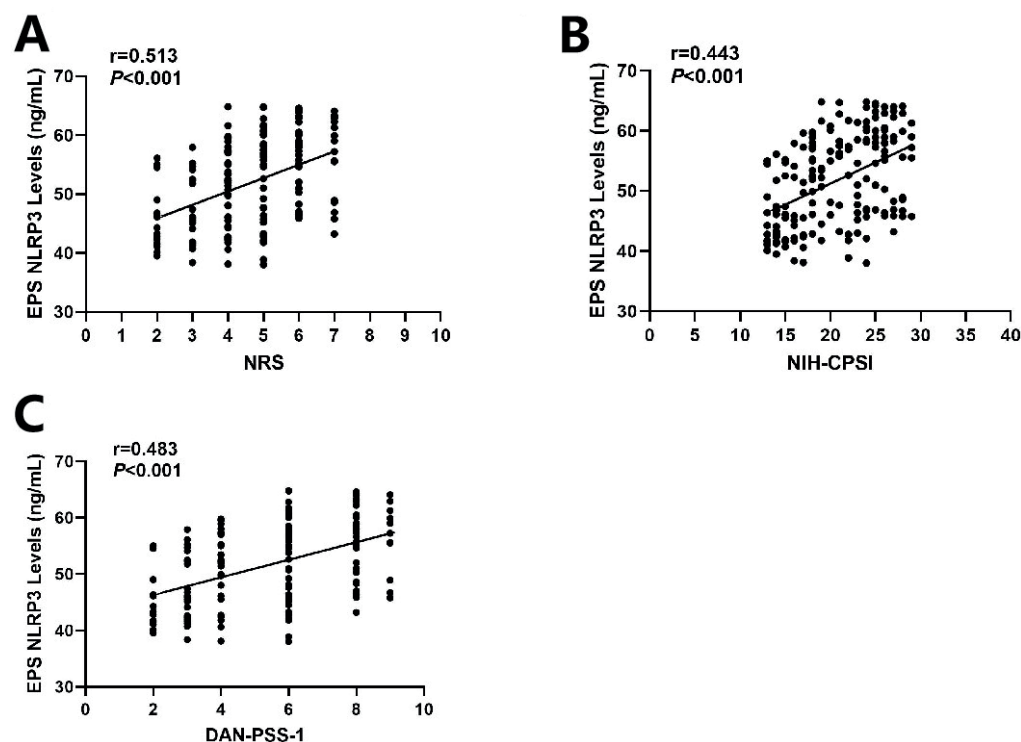


Fig. 4. A. Spearman's correlation analysis of EPS NLRP3 levels with the NRS in CP/CPPS patients ($n = 168$); B. Spearman's correlation analysis of EPS NLRP3 levels with the NIH-CPSI in CP/CPPS patients ($n = 168$); C. Spearman's correlation analysis of EPS NLRP3 levels with the DAN-PSS-1 in CP/CPPS patients ($n = 168$)

EPS – expressed prostatic secretions; NLRP3 – nucleotide-binding oligomerization domain, leucine-rich repeat and pyrin domain-containing 3; NRS – numerical rating scale; NIH-CPSI – National Institutes of Health Chronic Prostatitis Symptom Index; CP – chronic prostatitis; CPPS – chronic pelvic pain syndrome; DAN-PSS-1 – Danish Prostatic Symptom Score.

(Spearman's correlation, $r = 0.483$, $T(N-2) = 165$, $p < 0.001$) (Fig. 4C). These findings imply that CP/CPPS patients with higher EPS NLRP3 levels may suffer more severe clinical symptoms.

Interleukin 1 beta and IL-18 have been shown to be important markers in CP/CPPS. Interleukin 1 beta¹⁸ and IL-18¹⁹ have been implicated as potential triggers of CP progression. In this study, EPS NLRP3 levels were positively

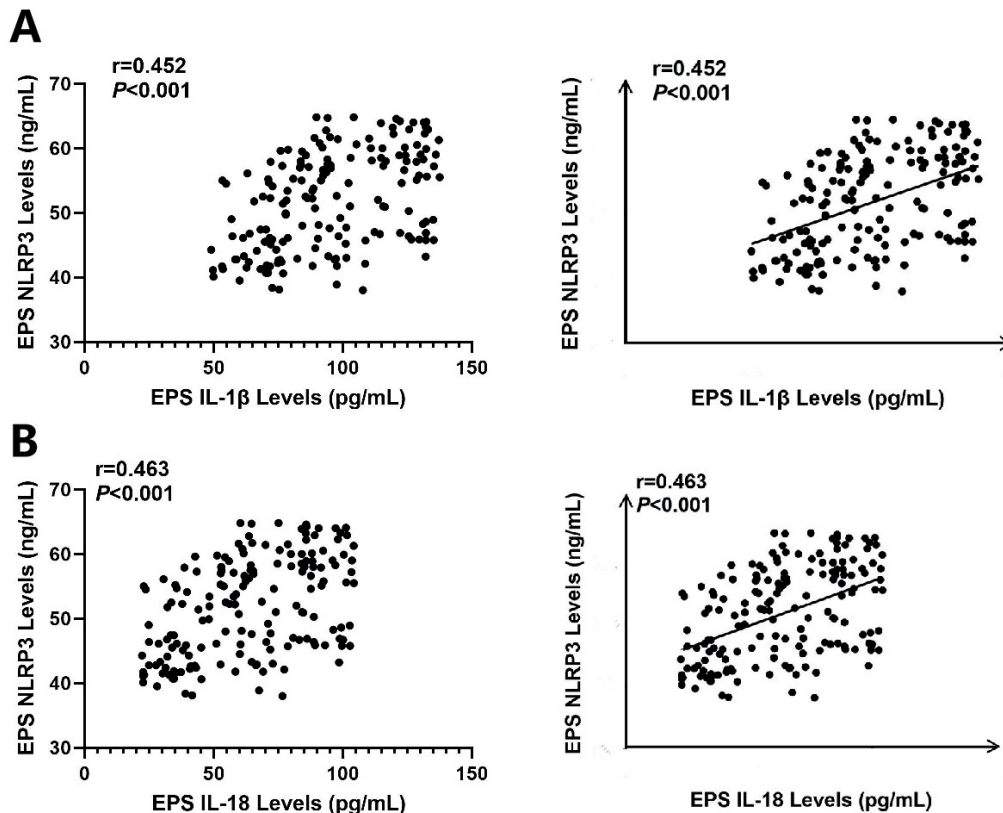


Fig. 5. A. Spearman's correlation analysis of EPS NLRP3 levels with EPS IL-1 β levels in CP/CPPS patients (n = 168); B. Spearman's correlation analysis of EPS NLRP3 levels with EPS IL-18 levels in CP/CPPS patients (n = 168)

EPS – expressed prostatic secretions; NLRP3 – nucleotide-binding oligomerization domain, leucine-rich repeat and pyrin domain-containing 3; IL-1 β – interleukin-1 beta; CP – chronic prostatitis; CPPS – chronic pelvic pain syndrome; IL-18 – interleukin 18.

correlated with EPS IL-1 β levels (Spearman's correlation, $r = 0.345$, $T(N-2) = 165$, $p < 0.001$) (Fig. 5A) and IL-18 levels (Spearman's correlation, $r = 0.326$, $T(N-2) = 165$, $p < 0.001$) (Fig. 5B).

Discussion

Our research examined the correlation between the expression of NLRP3 in EPS and the severity of CP/CPPS. For the first time, we have shown that NLRP3 levels in EPS are markedly higher in patients with CP/CPPS than in those with BPH or in healthy individuals. In addition, elevated NLRP3 levels in EPS exhibited a positive correlation with Bergman grade. The ROC curve analysis showed that an elevated EPS NLRP3 level may act as a potential indicator of CP/CPPS disease severity. In addition, EPS NLRP3 concentrations were positively correlated with NRS, NIH-CPSI and DAN-PSS-1. Finally, we found a positive association between the concentrations of NLRP3 in EPS and the levels of IL-1 β and IL-18 in EPS. These results suggest that an increase in NLRP3 levels in EPS could indicate the severity of CP/CPPS.

Prostatitis is the 3rd most common disease of the prostate gland after BPH and prostate cancer.²⁰ Though not a direct threat to life, prostatitis manifests through symptoms like erectile dysfunction, issues with the lower urinary tract and localized discomfort in the perineal or testicular regions, all of which can greatly influence a patient's quality of life.²¹

The primary methods for diagnosing prostatitis include evaluating clinical signs, performing a thorough physical examination, assessing the white blood cell count (WBC), and conducting bacterial cultures of expressed prostatic secretions.²² However, the value of routinely analyzing leukocytes is a matter of debate, chiefly due to the lack of correlation between leukocyte count and symptom severity. Consequently, there is a pressing need to pinpoint specific biomarkers for the diagnosis of CP/CPPS.

Research in clinical settings has revealed that factors that modulate inflammation play a role in numerous pathological processes.²³ Chronic inflammation typically correlates with intensified symptoms of the lower urinary tract in cases of prostate pathology.²⁴

The NLRP3 inflammasome has been recognized as a crucial mediator of pathogenic inflammation across a range of inflammatory disorders and is linked to persistent inflammatory responses. Imbalances in the NLRP3 inflammasome have been implicated in an array of illnesses, such as multiple sclerosis,²⁵ diabetes,²⁶ atherosclerosis,²⁷ Alzheimer's disease,²⁸ inflammatory bowel disease,²⁹ and numerous other autoimmune conditions.³⁰ In this study, we found that EPS NLRP3 levels were significantly up-regulated in CP/CPPS patients, indicating that NLRP3 may participate in CP progression.

Pain is the main symptom of CP/CPPS. An increasing amount of evidence indicates that dysregulation of the NLRP3 inflammasome is associated with chronic pain conditions and plays a role in the development of chronic pain.³¹ Previous studies have demonstrated

the involvement of the NLRP3 inflammasome in various pain conditions, such as complex regional pain syndrome type-I,³² CNP,³³ inflammatory pain,³⁴ cancer-related pain,³⁵ and muscle pain,³⁶ among others. Our findings also reveal a positive correlation between EPS NLRP3 levels and the severity of pain and dysfunction in CP/CPPS patients, indicating that higher EPS NLRP3 levels may be associated with more severe symptoms.

Mature IL-1 β acts as a strong proinflammatory agent in various immune responses, playing a key role in attracting innate immune cells to infection sites and adjusting the activity of adaptive immune cells. On the other hand, mature IL-18 is crucial for stimulating interferon gamma (IFN- γ) production and enhancing the cell-killing functions of natural killer cells and T cells.³⁷ The NLRP3 inflammasome is recognized as a vital element of the innate immune system, responsible for the maturation process of IL-1 β and IL-18.³⁸ Additionally, we observed a correlation between NLRP3 levels in EPS and the concentrations of IL-1 β and IL-18 in the EPS of patients with CP/CPPS.

Limitations

There are some limitations that should be taken into account. First, this study was conducted at a single center and involved a relatively small cohort of patients, all of whom were of Han Chinese ethnicity. Therefore, multicenter studies with larger samples are needed in further research. Furthermore, the cross-sectional design of the study prevented the longitudinal tracking of NLRP3 inflammasome levels in correlation with disease progression, and as a result, the potential causal link between NLRP3 inflammasome activity and the severity of CP could not be comprehensively demonstrated. In addition, we evaluated only the NLRP3 inflammasome (pyroptosis classical pathway) in this study; investigation of other pyroptosis-related proteins involved in CP/CPPS may reveal more valuable information. Additionally, we did not investigate the potential mechanism that the NLRP3 inflammasome plays in CP/CPPS; other proteins that interact with the NLRP3 inflammasome may provide additional insight for understanding the pathogenesis of CP/CPPS.

Conclusions

The study represented a pioneering effort in demonstrating that levels of the NLRP3 inflammasome in EPS were significantly elevated in patients with CP/CPPS when compared to those with BPH and healthy controls. Moreover, the presence of NLRP3 in EPS showed a positive correlation with the onset of CP/CPPS. There was also a direct correlation between the concentration of NLRP3 and the intensity of symptoms, as well as with the levels of the inflammatory cytokines IL-1 β and IL-18 in EPS. These findings support the hypothesis that elevated levels of NLRP3 could

indicate the progression of CP/CPPS and suggest the potential of NLRP3 to serve as a biomarker for diagnosing this condition. However, further research is needed to elucidate the underlying mechanisms of NLRP3-mediated pyroptosis.

Supplementary data

The Supplementary materials are available at <https://doi.org/10.5281/zenodo.13911503>. The package includes the following files:

Supplementary Fig. 1. Cutoff value calculation of NLRP3 process using R.

Supplementary File 1. Normality check and variance homogeneity check.

Data availability


The datasets generated and/or analyzed during the current study are available from the corresponding author on reasonable request.

Consent for publication

Not applicable.

ORCID iDs

Chao-Guang Ma  <https://orcid.org/0009-0001-5801-7951>

Ying-Nan Liu  <https://orcid.org/0009-0009-8507-7907>

Hua-Dong Wang  <https://orcid.org/0009-0009-9318-5166>

References

1. Krieger JN, Lee SWH, Jeon J, Cheah PY, Liong ML, Riley DE. Epidemiology of prostatitis. *Int J Antimicrob Agents*. 2008;31:85–90. doi:10.1016/j.ijantimicag.2007.08.028
2. McNaughton Collins M, Pontari MA, O'Leary MP, et al; The Chronic Prostatitis Collaborative Research Network. Quality of life is impaired in men with chronic prostatitis: The chronic prostatitis collaborative research network. *J Gen Intern Med*. 2001;16(10):656–662. doi:10.1111/j.1525-1497.2001.01223.x
3. Nickel JC, Nyberg LM, Hennenfent M. Research guidelines for chronic prostatitis: Consensus report from the First National Institutes of Health International Prostatitis Collaborative Network. *Urology*. 1999;54(2):229–233. doi:10.1016/S0090-4295(99)00205-8
4. Shakur A, Hames K, O'Shea A, Harisinghani MG. Prostatitis: Imaging appearances and diagnostic considerations. *Clin Radiol*. 2021;76(6):416–426. doi:10.1016/j.crad.2021.01.007
5. Wagenlehner FME, Van Till JWO, Magri V, et al. National Institutes of Health Chronic Prostatitis Symptom Index (NIH-CPSI) symptom evaluation in multinational cohorts of patients with chronic prostatitis/chronic pelvic pain syndrome. *Eur Urol*. 2013;63(5):953–959. doi:10.1016/j.eururo.2012.10.042
6. Huang TR, Li W, Peng B. Correlation of inflammatory mediators in prostatic secretion with chronic prostatitis and chronic pelvic pain syndrome. *Andrologia*. 2018;50(2):e12860. doi:10.1111/and.12860
7. Zhao M, Guo J, Gao QH, et al. Relationship between pyroptosis-mediated inflammation and the pathogenesis of prostate disease. *Front Med (Lausanne)*. 2023;10:1084129. doi:10.3389/fmed.2023.1084129
8. Fu J, Wu H. Structural mechanisms of NLRP3 inflammasome assembly and activation. *Annu Rev Immunol*. 2023;41(1):301–316. doi:10.1146/annurev-immunol-081022-021207
9. Zheng M, Kanneganti T. The regulation of the ZBP1-NLRP3 inflammasome and its implications in pyroptosis, apoptosis, and necroptosis (PANoptosis). *Immunol Rev*. 2020;297(1):26–38. doi:10.1111/imr.12909

10. Huang Y, Xu W, Zhou R. NLRP3 inflammasome activation and cell death. *Cell Mol Immunol.* 2021;18(9):2114–2127. doi:10.1038/s41423-021-00740-6
11. Lu J, Su Y, Chen X, et al. Rapamycin-induced autophagy attenuates hormone-imbalance-induced chronic non-bacterial prostatitis in rats via the inhibition of NLRP3 inflammasome-mediated inflammation. *Mol Med Rep.* 2018;19(1):221–230. doi:10.3892/mmr.2018.9683
12. Chen L, Wang H, Ge S, Tai S. IL-6/STAT3 pathway is involved in the regulation of autophagy in chronic non-bacterial prostatitis cells, and may be affected by the NLRP3 inflammasome. *Ultrastruct Pathol.* 2021;45(4–5):297–306. doi:10.1080/01913123.2021.1966149
13. Dun RL, Tsai J, Hu XH, et al. A systematic review of cross-cultural adaptation of the National Institutes of Health Chronic Prostatitis Symptom Index. *Health Qual Life Outcomes.* 2021;19(1):159. doi:10.1186/s12955-021-01796-8
14. Bergman J, Zeitlin SI. Prostatitis and chronic prostatitis/chronic pelvic pain syndrome. *Exp Rev Neurother.* 2007;7(3):301–307. doi:10.1586/14737175.7.3.301
15. Thong ISK, Jensen MP, Miró J, Tan G. The validity of pain intensity measures: What do the NRS, VAS, VRS, and FPS-R measure? *Scand J Pain.* 2018;18(1):99–107. doi:10.1515/sjpain-2018-0012
16. Nickel JC, Downey J, Hunter D, Clark J. Prevalence of prostatitis-like symptoms in a population based study using the National Institutes of Health Chronic Prostatitis Symptom Index. *J Urol.* 2001;165(3):842–845. PMID:11176483.
17. Tibaek S, Jensen R, Klarskov P, Iversen HK, Gard G. The Danish Prostatic Symptom Score (DAN-PSS-1) questionnaire is reliable in stroke patients. *Neurol Urol Dyn.* 2006;25(4):319–323. doi:10.1002/nau.20223
18. Nadler RB, Koch AE, Calhoun EA, et al. IL-1 β and TNF- α in prostatic secretions are indicators in the evaluation of men with chronic prostatitis. *J Urol.* 2000;164(1):214–218. doi:10.1016/S0022-5347(05)67497-6
19. Han CL, Deng YX, Hu P, et al. Comparison of cytokine levels in prostatic secretion between the IIIa and IIIb subtypes of prostatitis. *Asia J Androl.* 2024;26(1):77–84. doi:10.4103/aja202336
20. Lam JC, Stokes W. Acute and chronic prostatitis. *Am Fam Physician.* 2024;110(1):45–51. PMID:39028781.
21. Yebes A, Toribio-Vazquez C, Martinez-Perez S, et al. Prostatitis: A review. *Curr Urol Rep.* 2023;24(5):241–251. doi:10.1007/s11934-023-01150-z
22. Khan FU, Ihsan AU, Khan HU, et al. Comprehensive overview of prostatitis. *Biomed Pharmacother.* 2017;94:1064–1076. doi:10.1016/j.biopha.2017.08.016
23. Paulis G. Inflammatory mechanisms and oxidative stress in prostatitis: The possible role of antioxidant therapy. *Res Rep Urol.* 2018;10:75–87. doi:10.2147/RRU.S170400
24. Alkan I, Yüksel M, Özveri H, et al. Semen reactive oxygen species levels are correlated with erectile function among chronic prostatitis/chronic pelvic pain syndrome patients. *Int J Impot Res.* 2018;30(6):335–341. doi:10.1038/s41443-018-0047-1
25. Olcum M, Tastan B, Kiser C, Genc S, Genc K. Microglial NLRP3 inflammasome activation in multiple sclerosis. *Adv Protein Chem Struct Biol.* 2020;119:247–308. doi:10.1016/bs.apcsb.2019.08.007
26. Rovira-Llopis S, Apostolova N, Bañuls C, Muntané J, Rocha M, Victor VM. Mitochondria, the NLRP3 inflammasome, and sirtuins in type 2 diabetes: New therapeutic targets. *Antioxid Redox Signal.* 2018;29(8):749–791. doi:10.1089/ars.2017.7313
27. Grebe A, Hoss F, Latz E. NLRP3 inflammasome and the IL-1 pathway in atherosclerosis. *Circ Res.* 2018;122(12):1722–1740. doi:10.1161/CIRCRESAHA.118.311362
28. Heneka MT, Kummer MP, Stutz A, et al. NLRP3 is activated in Alzheimer's disease and contributes to pathology in APP/PS1 mice. *Nature.* 2013;493(7434):674–678. doi:10.1038/nature11729
29. Zhen Y, Zhang H. NLRP3 inflammasome and inflammatory bowel disease. *Front Immunol.* 2019;10:276. doi:10.3389/fimmu.2019.00276
30. Li Z, Guo J, Bi L. Role of the NLRP3 inflammasome in autoimmune diseases. *Biomed Pharmacother.* 2020;130:110542. doi:10.1016/j.biopha.2020.110542
31. Chen R, Yin C, Fang J, Liu B. The NLRP3 inflammasome: An emerging therapeutic target for chronic pain. *J Neuroinflammation.* 2021;18(1):84. doi:10.1186/s12974-021-02131-0
32. Chen R, Yin C, Hu Q, et al. Expression profiling of spinal cord dorsal horn in a rat model of complex regional pain syndrome type-I uncovers potential mechanisms mediating pain and neuroinflammation responses. *J Neuroinflammation.* 2020;17(1):162. doi:10.1186/s12974-020-01834-0
33. Youm YH, Nguyen KY, Grant RW, et al. The ketone metabolite β -hydroxybutyrate blocks NLRP3 inflammasome-mediated inflammatory disease. *Nat Med.* 2015;21(3):263–269. doi:10.1038/nm.3804
34. Hua T, Wang H, Fan X, et al. BRD4 inhibition attenuates inflammatory pain by ameliorating NLRP3 inflammasome-induced pyroptosis. *Front Immunol.* 2022;13:837977. doi:10.3389/fimmu.2022.837977
35. Chen SP, Zhou YQ, Wang XM, et al. Pharmacological inhibition of the NLRP3 inflammasome as a potential target for cancer-induced bone pain. *Pharmacol Res.* 2019;147:104339. doi:10.1016/j.phrs.2019.104339
36. Yoshida S, Hagiwara Y, Tsuchiya M, et al. Involvement of inflammasome activation via elevation of uric acid level in nociception in a mouse model of muscle pain. *Mol Pain.* 2019;15:174480691985879. doi:10.1177/1744806919858797
37. He Y, Hara H, Núñez G. Mechanism and regulation of NLRP3 inflammasome activation. *Trends Biochem Sci.* 2016;41(12):1012–1021. doi:10.1016/j.tibs.2016.09.002
38. Fujimura K, Karasawa T, Komada T, et al. NLRP3 inflammasome-driven IL-1 β and IL-18 contribute to lipopolysaccharide-induced septic cardiomyopathy. *J Mol Cell Cardiol.* 2023;180:58–68. doi:10.1016/j.jmcc.2023.05.003

Associations of propofol and midazolam with the 30-day mortality in patients with sepsis-associated encephalopathy: A study of the MIMIC database

Lanfen Zhan^{1,A,D–F}, Xinyao Xiang^{2,B,C,F}, Yu Zhang^{2,B,C,F}, Lingmin Zhou^{2,A,E,F}

¹ Department of Clinical Pharmacy, Taizhou First People's Hospital, China

² Department of Critical Care Medicine, Taizhou First People's Hospital, China

A – research concept and design; B – collection and/or assembly of data; C – data analysis and interpretation;

D – writing the article; E – critical revision of the article; F – final approval of the article

Advances in Clinical and Experimental Medicine, ISSN 1899–5276 (print), ISSN 2451–2680 (online)

Adv Clin Exp Med. 2025;34(9):1467–1474

Address for correspondence

Lingmin Zhou

E-mail: zhoulingmintfph@outlook.com

Funding sources

None declared

Conflict of interest

None declared

Received on March 15, 2024

Reviewed on July 5, 2024

Accepted on November 18, 2024

Published online on April 24, 2025

Cite as

Zhan L, Xiang X, Zhang Y, Zhou L. Associations of propofol and midazolam with the 30-day mortality in patients with sepsis-associated encephalopathy: A study of the MIMIC database.

Adv Clin Exp Med. 2025;34(9):1467–1474.

doi:10.17219/acem/196102

DOI

10.17219/acem/196102

Copyright

Copyright by Author(s)

This is an article distributed under the terms of the

Creative Commons Attribution 3.0 Unported (CC BY 3.0)

(https://creativecommons.org/licenses/by/3.0/)

Abstract

Background. Propofol and midazolam have been widely used in patients with sepsis. However, the effectiveness of these drugs in reducing the duration of mechanical ventilation and the risk of mortality remains controversial.

Objectives. To investigate and compare effects of propofol and midazolam on 30-day mortality in patients with sepsis-associated encephalopathy (SAE).

Materials and methods. A retrospective cohort study was conducted on data from 952 adult patients with SAE extracted from the Medical Information Mart for Intensive Care IV (MIMIC-IV) database. Univariable and multivariable Cox proportional hazard models were utilized to investigate the associations of propofol and midazolam with 30-day mortality; and univariable and multivariable logistic regression analyses were used to explore the relationships of propofol and midazolam with ventilation duration. The outcome measures were hazard ratios (HRs), odds ratios (ORs), and 95% confidence intervals (95% CIs). In addition, subgroup analyses of age, simplified acute physiological score (SAPS)-II, Charlson Comorbidity Index (CCI), and ventilation duration were also performed to further assess the associations of propofol and midazolam with 30-day mortality.

Results. Among eligible patients, 265 (27.84%) died within 30 days. After adjusting for covariates, treatment with propofol was associated with both lower risk of 30-day mortality (HR = 0.67, 95% CI: 0.51–0.88) and lower odds of prolonged ventilation duration (OR = 0.71, 95% CI: 0.53–0.96) compared to treatment with midazolam. Moreover, the negative association between treatment with propofol and 30-day mortality was also significant in subgroups of age ≥ 65 years, SAPS-II score ≥ 47 , CCI score ≥ 3 , and ventilation duration ≥ 5 days (all $p < 0.05$).

Conclusions. Among patients with SAE, treatment with propofol was relatively more effective than treatment with midazolam in reducing the risk of 30-day mortality and the duration of mechanical ventilation. However, the causal relationships of propofol and midazolam with prognosis in patients with SAE need further clarification.

Key words: propofol, midazolam, 30-day mortality, SAE, ventilation duration

Background

Sepsis-associated encephalopathy (SAE) is a severe neurologic syndrome, namely the brain dysfunction occurring during the course of sepsis.¹ Sepsis-associated encephalopathy significantly increased the length of hospital stay as well as the risk of short-term mortality in patients.² Evidence has suggested that even mild changes in consciousness can result in a significant increase in mortality risk in patients with sepsis.³ Hence, it is important to explore factors influencing the short-term mortality risk in patients with SAE, which may help improve SAE prognoses.

Propofol and midazolam are commonly used sedatives in the intensive care units (ICUs),⁴ and they have been also widely used among sepsis patients.^{5–7} A meta-analysis showed that compared to midazolam, propofol reduced the length of ICU stay, mechanical ventilation time and extubation time among the ICU patients.⁴ Also, treatment with propofol has a significant advantage in the incidence of short-term postoperative cognitive dysfunction,⁸ e.g., patients treated with propofol had lower rates of delirium compared to those treated with midazolam.⁹ In addition, a recent study in children indicated that the application of midazolam could increase the risk of SAE.¹⁰ However, whether propofol or midazolam is more suitable for patients with sepsis remains controversial, especially in the presence of SAE. To date, no studies have been conducted to directly compare the effects of propofol and midazolam on the prognosis of SAE.

Objectives

This study was designed to investigate associations of propofol and midazolam with 30-day mortality in patients with SAE, comparing effects of these 2 sedatives on short-term prognosis in patients with SAE, and to provide some references for choice of sedatives for patients with SAE in clinical practice.

Methods

Study participants

This is a retrospective cohort study. Data of participants were obtained from the Medical Information Mart for Intensive Care (MIMIC)-IV database in 2008–2019. The MIMIC database is jointly published by the computational physiology laboratory of the Massachusetts Institute of Technology (MIT; Cambridge, USA), Beth Israel Deaconess Medical Center (BIDMC; Boston, USA) and Philips Medical (Amsterdam, the Netherlands) since 2001, which collects and sorts out information on clinical diagnosis and treatment of more than 40,000 ICU

patients. More details about the MIMIC database can be found elsewhere: <https://mimic.mit.edu/docs/iv>.

For participants screening, the inclusion criteria were: 1) age ≥ 18 years, 2) diagnosed with SAE at the ICU admission and 3) treated with midazolam or propofol exclusively as sedative. The exclusion criteria were: 1) not using mechanical ventilation, 2) having traumatic brain injury (TBI),^{11,12} ischemic/hemorrhagic stroke, intracranial infection or epilepsy, 3) chronic alcohol or drug abuse, 4) pre-existing liver or kidney diseases affecting consciousness,¹³ and 5) missing information on survival. Finally, 952 patients met the necessary criteria for inclusion in the study. The MIMIC database has obtained ethical approval from the relevant Institutional Review Boards (IRBs) (<https://mimic.mit.edu>). Since the database is publicly available, ethical approval has been waived by our hospital's IRB. Informed consent was not required due to the retrospective nature of the study.

Diagnosis of SAE

According to a previous study, SAE was defined as sepsis accompanied by a Glasgow Coma Scale (GCS) ≤ 14 in the first 24 h of ICU admission or delirium based on the International Classification of Diseases v. 9. (ICD-9) code (2930, 2931) and ICD-10 code (F05).¹⁴

Assessment of propofol and midazolam use

Records of the use of propofol or midazolam in patients with SAE were extracted from the MIMIC input event tables, with item ID 222168 for propofol and 221668 for midazolam.

Variables selection

We also extracted variables as potential confounding factors from the database, including race, age, gender, congestive heart failure (CHF), peripheral vascular disease (PVD), chronic obstructive pulmonary disease (COPD), renal failure (RF), liver disease, hypertension, diabetes mellitus (DM), heart rate (HR), weight, systolic blood pressure (SBP), diastolic blood pressure (DBP), temperature, respiratory rate (RR), oxygen saturation (SpO_2), inspiratory oxygen concentration (FIO_2), simplified acute physiological score (SAPS)-II, GCS, Charlson Comorbidity Index (CCI), red cell distribution width (RDW), white blood cell (WBC) count, platelet count, hemoglobin (HB), hematocrit, creatinine (Cr), blood urea nitrogen (BUN), glucose, lactate, sodium (Na), bicarbonate, potassium (K), pH, chloride, international normalized ratio (INR), ventilation duration, prothrombin time (PT), vasopressors use, opiates use, norepinephrine use, and antibiotics use. In addition, only information on these variables was extracted from patients when they were first admitted to the ICU.

Study outcomes

Primary study outcome was 30-day mortality, and the secondary study outcome was ventilation duration. The ventilation duration was divided into 2 categories according to the median value, including <5 days and ≥5 days. The MIMIC followed up through information recorded in electronic medical charts and hospital department, or contacting with the patients (including family members, attending healthcare workers and family physicians) via phone calls. In our study, the follow-up ended when patients died or 30 days after the ICU admission.

Statistical analyses

Non-normal data were described in median and quartiles (Me (Q₁, Q₃)), and Wilcoxon ran-sum tests were used for inter-group comparisons. The enumeration data were described in terms of number of cases and composition ratio (n (%)). The χ^2 test was used for comparison between groups.

The covariates screening process included 2 steps. First, variables significantly associated with 30-day mortality in patients with SAE were selected via univariable Cox proportional hazard model. Then, the selected variables were test using the best subset method, and those with the lowest Bayesian information criterion (BIC) values were chosen as the final covariates. Finally, the selected covariates were further included in the adjustment of multivariate models.

The screening of covariates associated with ventilation duration was similar to that associated with 30-day mortality except using the univariable logistic regression.

Univariate and multivariate Cox proportional hazard models were established to explore the associations of propofol and midazolam with 30-day mortality, with hazard ratios (HRs) and 95% confidence intervals (95% CIs). Model 1 was unadjusted. Model 2 was adjusted for the selected covariates, including age, race, RR, temperature, SpO₂, SAPS-II score, CCI score, RDW, WBC, BUN, lactate, chloride, INR, PT, vasopressor use, opiates use, and nor-epinephrine use. Additionally, subgroup analysis of age, SAPS-II score, CCI score and ventilation duration were also performed to further assess these associations.

Univariate and multivariate logistic regression analyses were used to investigate the associations of propofol and midazolam with duration of ventilation in patients with SAE, with odds ratios (ORs) and 95% CIs as assessment indices. Model 1 was unadjusted. Model 2 was adjusted for selected covariates, including SpO₂, SAPS-II, vasopressor use, norepinephrine use, and antibiotics use.

Two-sided $p < 0.05$ was considered statistically significant. Variables with missing values were removed if the proportion was >20%; otherwise, they were interpolated using a random forest interpolation method (Supplementary Table 1).¹⁵ Sensitivity analyses of patients'

characteristics before and after interpolation of missing data are shown in Supplementary Table 2. The associations of midazolam and propofol with 30-day mortality (Supplementary Table 3) and duration of mechanical ventilation (Supplementary Table 4) in patients with SAE were also assessed using the original unimplemented data. Statistical analyses were performed using Python 3.9.12 (Python Software Foundation, Wilmington, USA) and R v. 4.3.1 (2023-06-16 ucrt; R Foundation for Statistical Computing, Vienna, Austria).

Results

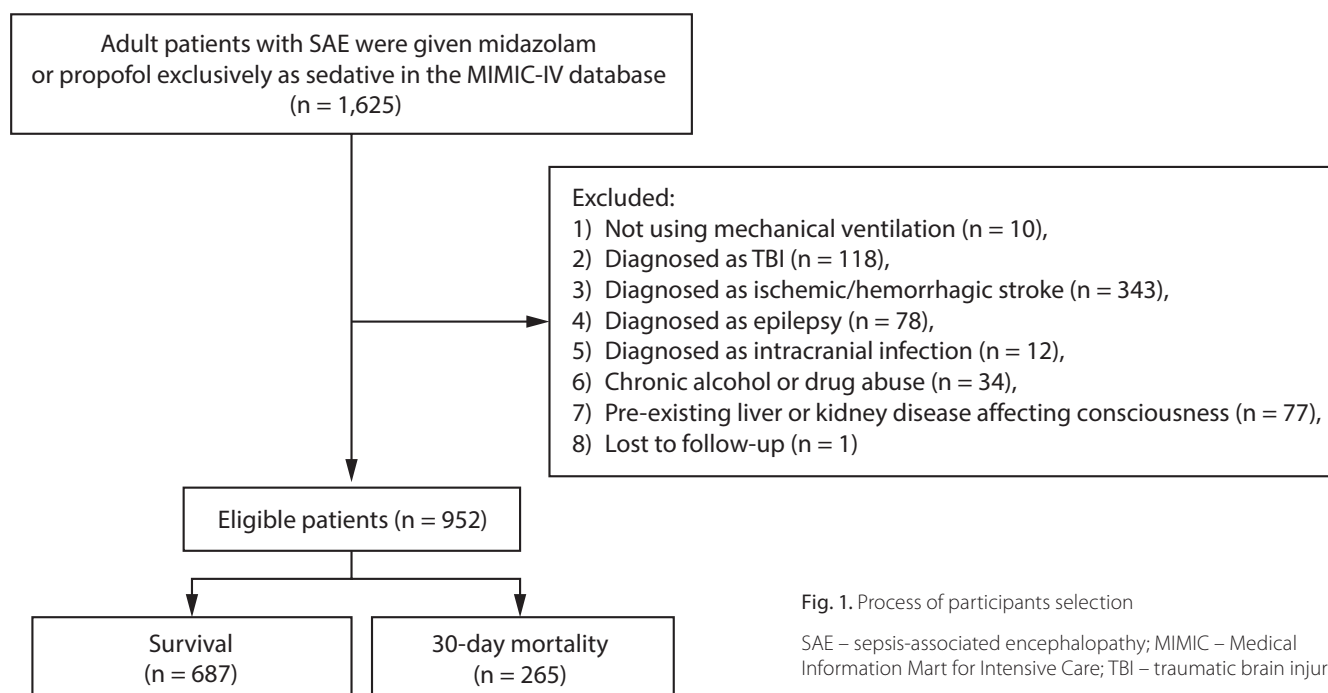
Characteristics of participants

Figure 1 shows inclusion and exclusion of research subjects. There were 1,625 adult SAE patients who received treatment with propofol or midazolam in the database. Those who without mechanical ventilation use ($n = 10$), diagnosed as TBI ($n = 118$), ischemic/hemorrhagic stroke ($n = 343$), epilepsy ($n = 78$), or intracranial infection ($n = 12$), with chronic alcohol or drug abuse ($n = 34$), with pre-existing liver/kidney disease affecting consciousness ($n = 77$), or lost to the follow-up ($n = 1$) were excluded. Finally, 952 were eligible.

Among the eligible participants, 265 (27.84%) died within 30 days. The median age of total population was 70 years, and 546 (57.35%) were male. We compared the characteristics of patients between the midazolam ($n = 259$) and propofol group ($n = 693$) (Table 1). Disease conditions (CHF and COPD), clinical indexes (HR, SBP, RR, SAPS-II, GCS, platelet, HB, hematocrit, Cr, BUN, glucose, pH, and PT) and treatments (ventilation duration, opiates use and nor-epinephrine use) were all significantly different between the 2 groups (all $p < 0.05$).

Associations of midazolam and propofol with 30-day mortality

Before investigating relationships between different sedatives and 30-day mortality in patients with SAE, covariates have been screened (Supplementary Table 3). As shown in Table 2, treatment with propofol was linked to lower 30-day mortality risk (HR = 0.67, 95% CI: 0.51–0.88), compared to treatment with midazolam after covariates adjustment. Moreover, we assessed this relationship in subgroups of age, SAPS-II score, CCI, and ventilation duration (Fig. 2). The results showed that in aged ≥65 years (HR = 0.61, 95% CI: 0.45–0.84), SAPS-II score ≥47 (HR = 0.55, 95% CI: 0.40–0.75), CCI score ≥3 (HR = 0.63, 95% CI: 0.46–0.87) and ventilation duration ≥5 (HR = 0.58, 95% CI: 0.41–0.84) subgroups, treatment with propofol was also significantly linked to lower 30-day mortality risk comparing to treatment with midazolam.

**Table 1.** Characteristics of patients with SAE

Variables		Total (n = 952)	Midazolam (n = 259)	Propofol (n = 693)	Statistics	p-value
Age [years], M (Q ₁ , Q ₃)		70 (58, 79)	71 (57, 80)	69 (58, 78)	W = 94,683.5	0.191
Gender, n (%)	female	406 (42.65)	120 (46.33)	286 (41.27)	$\chi^2 = 1.774$	0.183
	male	546 (57.35)	139 (53.67)	407 (58.73)		
Race, n (%)	white	89 (9.35)	30 (11.58)	59 (8.51)	$\chi^2 = 4.116$	0.249
	black	110 (11.55)	27 (10.42)	83 (11.98)		
	others	119 (12.5)	26 (10.04)	93 (13.42)		
	unknown	634 (66.6)	176 (67.95)	458 (66.09)		
CHF, n (%)	no	514 (53.99)	107 (41.31)	407 (58.73)	$\chi^2 = 22.329$	<0.001
	yes	438 (46.01)	152 (58.69)	286 (41.27)		
Peripheral vascular disease, n (%)	no	788 (82.77)	220 (84.94)	568 (81.96)	$\chi^2 = 0.974$	0.324
	yes	164 (17.23)	39 (15.06)	125 (18.04)		
COPD, n (%)	no	626 (65.76)	152 (58.69)	474 (68.4)	$\chi^2 = 7.471$	0.006
	yes	326 (34.24)	107 (41.31)	219 (31.6)		
RF, n (%)	no	883 (92.75)	233 (89.96)	650 (93.8)	$\chi^2 = 3.571$	0.059
	yes	69 (7.25)	26 (10.04)	43 (6.2)		
Liver disease, n (%)	no	775 (81.41)	213 (82.24)	562 (81.1)	$\chi^2 = 0.096$	0.757
	yes	177 (18.59)	46 (17.76)	131 (18.9)		
Hypertension, n (%)	no	438 (46.01)	108 (41.7)	330 (47.62)	$\chi^2 = 2.427$	0.119
	yes	514 (53.99)	151 (58.3)	363 (52.38)		
DM, n (%)	no	607 (63.76)	163 (62.93)	444 (64.07)	$\chi^2 = 0.062$	0.804
	yes	345 (36.24)	96 (37.07)	249 (35.93)		
Weight [kg], M (Q ₁ , Q ₃)		81.51 (69.85, 95.8)	81 (67.86, 94.8)	81.9 (70.51, 96.34)	W = 86,539.5	0.396
HR [bpm], M (Q ₁ , Q ₃)		92.5 (80, 109)	97 (83, 113)	90 (79, 107)	W = 104,280.5	<0.001
SBP [mm Hg], M (Q ₁ , Q ₃)		117.5 (102, 135)	115 (99.5, 132)	118 (103, 137)	W = 82,825.5	0.067
DBP [mm Hg], M (Q ₁ , Q ₃)		63 (52, 77)	63 (51, 77)	63 (52, 77)	W = 86,520.5	0.393
RR [bpm], M (Q ₁ , Q ₃)		20 (16, 24)	21 (18, 25.5)	19 (16, 24)	W = 10,431.1	<0.001
Temperature [°C], M (Q ₁ , Q ₃)		36.72 (36.39, 37.11)	36.83 (36.33, 37.28)	36.7 (36.39, 37.06)	W = 95,551.5	0.124

Table 1. Characteristics of patients with SAE – cont.

Variables		Total (n = 952)	Midazolam (n = 259)	Propofol (n = 693)	Statistics	p-value
SpO ₂ [%] M (Q ₁ , Q ₃)		97 (94, 100)	97 (94.99, 100)	98 (94, 100)	W = 88,773	0.794
FIO ₂ [%], M (Q ₁ , Q ₃)		70 (50, 100)	70 (50, 100)	70 (50, 100)	W = 88,510.5	0.737
SAPS-II score, M (Q ₁ , Q ₃)		47 (37, 58)	51 (39.5, 67)	46 (36, 55)	W = 107,765	<0.001
GCS score, M (Q ₁ , Q ₃)		13 (9, 14)	13 (7, 14)	14 (10, 14)	W = 74,421.5	<0.001
CCI score, M (Q ₁ , Q ₃)		3 (2, 5)	3 (2, 5)	3 (2, 5)	W = 92,261	0.501
RDW [%], M (Q ₁ , Q ₃)		15.2 (14, 17)	15.3 (14, 17.1)	15.2 (14, 17)	W = 89,004.5	0.845
Platelets [K/μL], M (Q ₁ , Q ₃)		189 (127, 260.25)	217 (140, 286)	176 (124, 247)	W = 106,038.5	<0.001
WBC [K/μL], M (Q ₁ , Q ₃)		12.9 (8.78, 18.4)	13.4 (9, 20)	12.7 (8.7, 17.4)	W = 96,670	0.067
HB [g/dL], M (Q ₁ , Q ₃)		10 (8.4, 11.7)	10.2 (8.9, 11.9)	9.8 (8.2, 11.6)	W = 100,815	0.003
Hematocrit [%], M (Q ₁ , Q ₃)		30.7 (26, 35.92)	31.9 (27.55, 36.9)	30.1 (25.3, 35.6)	W = 101,052.5	0.003
Cr [mg/dL], M (Q ₁ , Q ₃)		1.2 (0.8, 1.9)	1.4 (0.9, 2.3)	1.2 (0.8, 1.8)	W = 102,517	0.001
BUN [mg/dL], M (Q ₁ , Q ₃)		27 (17–43)	32 (19.5–50)	24 (16–41)	W = 105,882	<0.001
Glucose [mg/dL], M (Q ₁ , Q ₃)		138 (108–174)	146 (109.5–194.5)	136 (108–170)	W = 99,292	0.011
Lactate [mmol/L], M (Q ₁ , Q ₃)		1.85 (1.4–3)	1.8 (1.32–2.89)	1.85 (1.4–3)	W = 88,494.5	0.741
Bicarbonate [Eq/L], M (Q ₁ , Q ₃)		22 (19–26)	22 (18–26)	22 (19–25)	W = 86,390	0.374
Na [mEq/L], M (Q ₁ , Q ₃)		138 (134–141)	138 (134–141)	138 (134–141)	W = 90,778.5	0.784
K [mEq/L], M (Q ₁ , Q ₃)		4.2 (3.7–4.8)	4.1 (3.6–4.8)	4.2 (3.8–4.8)	W = 84,399.5	0.157
Chloride [mEq/L], M (Q ₁ , Q ₃)		103 (99–108)	104 (98–108.5)	103 (99–107)	W = 93,618	0.304
pH, M (Q ₁ , Q ₃)		7.36 (7.29–7.42)	7.35 (7.26–7.41)	7.37 (7.29–7.42)	W = 79,401	0.006
INR, M (Q ₁ , Q ₃)		1.4 (1.2–1.8)	1.4 (1.2–1.9)	1.4 (1.2–1.7)	W = 93,049	0.380
Pt [s], M (Q ₁ , Q ₃)		15.4 (13.67–19.22)	15.52 (14.1–20.4)	15.34 (13.5–18.8)	W = 98,135.5	0.026
Ventilation duration, n (%)	<5	468 (49.16)	110 (42.47)	358 (51.66)	$\chi^2 = 6.006$	0.014
	≥5	484 (50.84)	149 (57.53)	335 (48.34)		
Vasopressor use, n (%)	no	215 (22.58)	57 (22.01)	158 (22.8)	$\chi^2 = 0.030$	0.863
	yes	737 (77.42)	202 (77.99)	535 (77.2)		
Opiates use, n (%)	no	95 (9.98)	8 (3.09)	87 (12.55)	$\chi^2 = 17.764$	<0.001
	yes	857 (90.02)	251 (96.91)	606 (87.45)		
Norepinephrine use, n (%)	no	393 (41.28)	84 (32.43)	309 (44.59)	$\chi^2 = 10.998$	0.001
	yes	559 (58.72)	175 (67.57)	384 (55.41)		
Antibiotics use, n (%)	no	15 (1.58)	4 (1.54)	11 (1.59)	–	1.000
	yes	937 (98.42)	255 (98.46)	682 (98.41)		
Length of ICU stay [days], M (Q ₁ , Q ₃)		9.25 (6.37–13.7)	9.26 (6.07–12.89)	9.25 (6.45–13.92)	W = 87,244	0.508
Follow-up duration [days], M (Q ₁ , Q ₃)		30 (22.51–30)	30 (14.55–30)	30 (30–30)	W = 78,102	<0.001
30-day survival status, n (%)	survival	687 (72.16)	164 (63.32)	523 (75.47)	$\chi^2 = 13.254$	<0.001
	death	265 (27.84)	95 (36.68)	170 (24.53)		

W – Wilcoxon rank sum test; Me – median; Q₁ – 1st quartile; Q₃ – 3rd quartile; SAE – sepsis-associated encephalopathy; SD – standard deviation; CHF – congestive heart failure; COPD – chronic obstructive pulmonary disease; RF – renal failure; DM – diabetes mellitus; HR – heart rate; SBP – systolic blood pressure; DBP – diastolic blood pressure; RR – respiratory rate; SAPS-II – Simplified Acute Physiological Score II; GCS – Glasgow Coma Scale; CCI – Charlson Comorbidity Index; RDW – red cell distribution width; WBC – white blood cell; HB – hemoglobin; Cr – creatinine; BUN – blood urea nitrogen; Na – sodium; K – potassium; INR – international normalized ratio; PT – prothrombin time; ICU – intensive care unit. SpO₂ – oxygen saturation; FIO₂ – inspiratory oxygen concentration.

Relationship between different sedatives and ventilation duration in SAE patients

In addition, we explored the associations of midazolam and propofol with ventilation duration in patients with SAE. The process of covariates screening was shown

in Supplementary Table 4. We found that treatment with propofol was associated with lower odds of long ventilation duration comparing to that with midazolam (OR = 0.71, 95% CI: 0.53–0.96), indicating that treatment with propofol may be more effective than that with midazolam in improving excessive ventilation duration among SAE patients (Table 3).

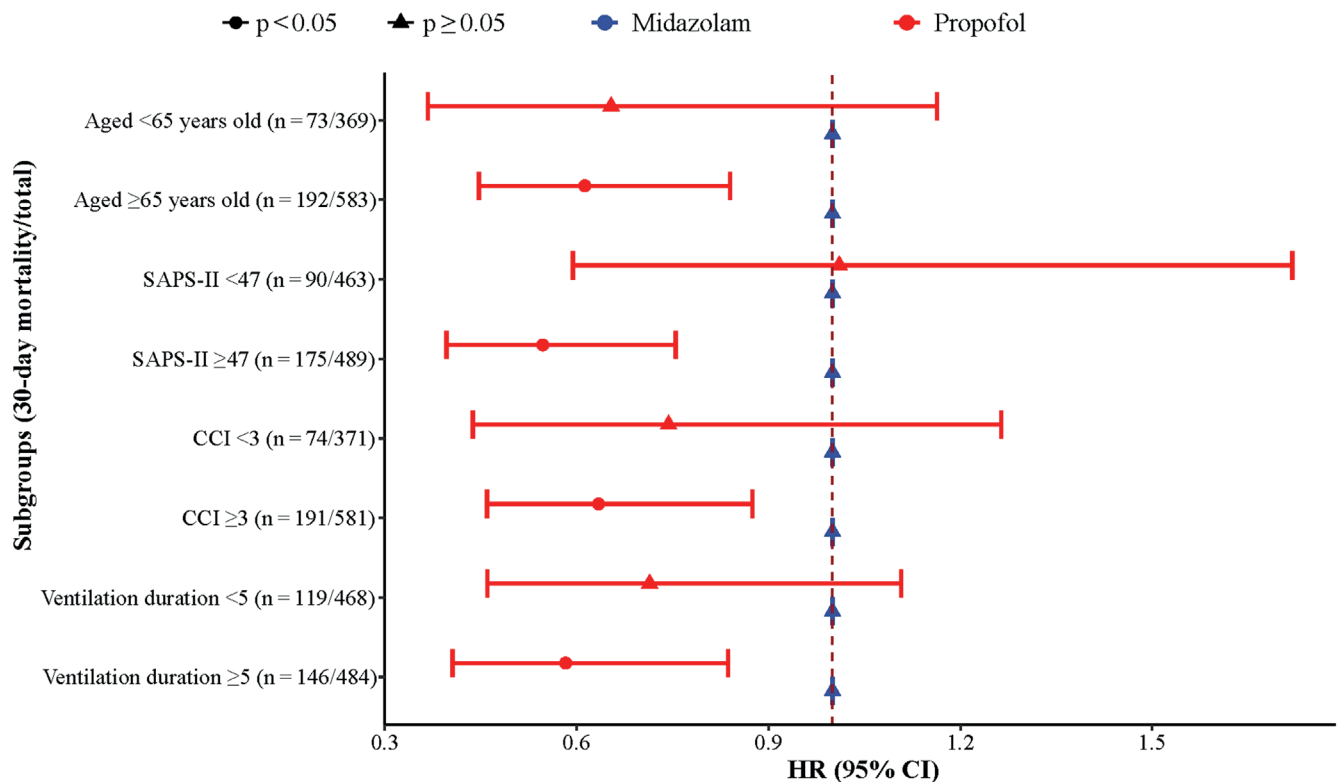


Fig. 2. Association of midazolam and propofol with 30-day mortality in age, SAPS-II, CCI, and ventilation duration subgroups

SAPS -II – Simplified Acute Physiological Score II; CCI – Charlson Comorbidity Index; HR – hazard ratio; 95% CI – 95% confidence interval.

Table 2. Associations of midazolam and propofol with 30-day mortality in SAE patients

Sedatives	Model 1		Model 2	
	HR (95% CI)	p-value	HR (95% CI)	p-value
Midazolam	Ref	–	Ref	–
Propofol	0.61 (0.47–0.78)	<0.001	0.67 (0.51–0.88)	0.004

SAE – sepsis-associated encephalopathy; HR – hazard ratio; 95% CI – 95% confidence interval; Ref – reference; Model 1 – crude model; The bold p-values are statistically significant. Model 2 – adjusted for age, race, respiratory rate, temperature, oxygen saturation, Simplified Acute Physiological Score II, Charlson Comorbidity Index, red cell distribution width, white blood cell, blood urea nitrogen, lactate, chloride, international normalized ratio, prothrombin time, vasopressor use, opiates use, and norepinephrine use.

Table 3. Associations of midazolam and propofol with ventilation duration in SAE patients

Sedatives	Model 1		Model 2	
	OR (95% CI)	p-value	OR (95% CI)	p-value
Midazolam	Ref	–	Ref	–
Propofol	0.69 (0.52–0.92)	0.012	0.71 (0.53–0.96)	0.028

SAE – sepsis-associated encephalopathy; OR – odds ratio; 95% CI – 95% confidence interval; Ref – reference; Model 1 – crude model; The bold p-values are statistically significant. Model 2 – adjusted for oxygen saturation, Simplified Acute Physiological Score II, vasopressor use, norepinephrine use, and antibiotics use.

Discussion

The current study explored the associations of propofol and midazolam with 30-day mortality in patients with SAE. The results suggested that patients with SAE treated with propofol had a lower risk of 30-day mortality compared to those treated with midazolam. This association was also significant in the subgroups of adults aged ≥65 years, SAPS-II score ≥47, CCI score ≥3, and ventilation duration ≥5. In addition, treatment with propofol was significantly associated with lower odds of long duration of ventilation in patients with SAE compared to patients treated with midazolam.

We believe our study is the first to explore and compare associations of propofol and midazolam with short-term

mortality and ventilation duration in patients with SAE. Previous studies have discussed the effects of propofol and midazolam on outcomes in ICU patients. For instance, a post hoc analysis of the DESIRE trial conducted by Miyagawa et al.¹⁶ found that patients with sepsis required mechanical ventilation during the acute phase. That study also found that sedation with midazolam was associated with an increased risk of coma and delirium compared to propofol. Another study in adult ICU patients showed that propofol was associated with improved clinical outcomes compared to midazolam sedation, reducing extubation time and mechanical ventilation time in acute surgical patients and extubation time in critically ill patients.⁴ Yet another observational, propensity-matched study suggested

that, compared with midazolam, sedation with propofol reduced mortality and bleeding rates in patients with cardiogenic shock.¹⁷ However, the associations of propofol and midazolam with short-term mortality in SAE have not been clarified. By observing negative associations of propofol treatment with 30-day mortality risk and prolonged duration of mechanical ventilation, our findings relatively filled a gap in the literature on patients with SAE. However, further research is needed on the causal associations of midazolam and propofol with ICU outcomes in this population.

The acute phase of SAE is characterized primarily by delirium symptoms,¹⁸ which are associated with worse outcomes.³ In ICU patients, maintaining light sedation was linked to increased survival and decreased delirium.¹⁹ Researches suggested that midazolam could prolong the time to light sedation in comparison with propofol.^{20,21} Also, in the study by Miyagawa et al., midazolam produced significantly deeper and more inappropriate sedation than propofol in the acute phase (day 3 of hospitalization), despite the use of light sedation protocols.¹⁶ Similarly, in our study population, the GCS score of patients in the midazolam group was significantly lower than that in the propofol group (10.61 vs 11.62). In fact, it has been reported that even mild alterations of the mental status (GCS of 13–14) have prognostic potential towards a worse outcome in sepsis.³ Nevertheless, in the present study, we could not clarify the mechanism of the potential superior effect of propofol to that of midazolam on short-term mortality in SAE, and whether it was related to the mental status or delirium of the patients. In addition, neuroinflammation induced by microglial activation is closely linked to the development of SAE.²² Guan et al.²³ suggested that propofol attenuated the inflammatory response by inhibiting metabolic reprogramming via down-regulation of the ROS/PI3K/Akt/mTOR/HIF-1 α signaling pathway. On the contrary, higher doses of midazolam may be an independent risk factor for sepsis-associated delirium among mechanically ventilated patients with sepsis.²⁴ Additionally, Sasabuchi et al.²⁵ retrospectively analyzed 30-day mortality and intubation duration in children ventilated for ≥ 3 days and sedated with midazolam or propofol and showed that weaning from mechanical ventilation was slower in children sedated with midazolam than in those sedated with propofol. Further investigation is necessary to determine the specific mechanism that led to the selection of propofol sedation as the preferred option for patients with SAE over midazolam sedation.

Results of subgroup analysis showed that among patients with SAE aged ≥ 65 years, SAPS-II score ≥ 47 , CCI score ≥ 3 , or with ventilation duration ≥ 5 , the association of propofol with lower 30-day mortality risk was also significant. In fact, age (≥ 75 years) and SAPS-II score (≥ 23) were common risk factors for SAE.²⁶ The progression of SAE and neurological deficits resulted from age-related reconstruction of the brain tissue with senescence of astroglia.²⁷ In patients admitted to the ICU for sepsis, SAPS-II also showed good performance in predicting mortality. Our

results suggest that in patients with SAE with older age or higher SAPS-II score, treatment with propofol may be a better choice to reduce short-term mortality than that with midazolam. The CCI seemed to be helpful for early identification of septic shock patients with poorer outcomes.²⁸ In our research, although the CCI score had no significant difference between the midazolam group and the propofol group (3.65 vs 3.56), it seemed that clinicians should consider propofol as the first choice of sedative. Mechanical ventilation is a cornerstone of sepsis treatment, and prolonged mechanical ventilation (exceeding 21 days) is associated with increased mortality rates of both in-hospital and post-discharge.²⁹ In the present study, 57.53% of patients in the midazolam group had a ventilation duration ≥ 5 days, whereas the proportion in the propofol group was 48.34%. Duration of ventilation was not found to be significantly associated with 30-day mortality, but in the subgroup with duration of ventilation ≥ 5 , the association between propofol and lower 30-day mortality risk was significant, suggesting that this potentially high-risk population should receive more attention.

Limitations

The current study was the first to explore effects of treatment with 2 different sedatives on short-term mortality risk in patients with SAE. In statistical analyses, we have considered and evaluated important variables associated with sedation in SAE, including scores reflecting severity and prognosis of patients, comorbidities and multiple laboratory indicators. However, there were still some limitations. As a retrospective cohort study, it is difficult to avoid the inherent bias of this study design. Data in the MIMIC database were collected from a single medical center, which may limit the representativeness of the study sample, and therefore, large-scale multi-center studies are needed to further verify our findings. Besides, due to limitations of the MIMIC database, we could not obtain the detailed sedation information, such as different drug dosages, treatment duration and daily sedation level data, which could cause some bias.

Conclusions

Sedation with propofol was a potentially better choice than midazolam for patients with SAE in clinical practice, which may reduce the risk of short-term mortality and prolonged duration of ventilation. However, the causal associations of propofol and midazolam with prognosis in SAE patients need to be further clarified.

Supplementary data

The supplementary materials are available at <https://doi.org/10.5281/zenodo.15061951>. The package includes the following files:

Supplementary Table 1. Variables with missing data and processing.

Supplementary Table 2. Sensitivity analysis of characteristics of patients before and after interpolation of missing data.

Supplementary Table 3. Covariates associated with 30-day mortality in SAE patients.

Supplementary Table 4. Covariates associated with ventilation duration in SAE patients.

Data availability

The datasets generated and/or analyzed during the current study are available from the corresponding author on reasonable request.

Consent for publication

Not applicable.

Use of AI and AI-assisted technologies


Not applicable.

ORCID iDs

Langfen Zhan  <https://orcid.org/0009-0005-5304-3658>

Xinyao Xiang  <https://orcid.org/0009-0001-7605-3729>

Yu Zhang  <https://orcid.org/0009-0002-9648-1605>

Lingmin Zhou  <https://orcid.org/0009-0000-7616-8553>

References

1. Sonnevile R, Benganham S, Jeantin L, et al. The spectrum of sepsis-associated encephalopathy: A clinical perspective. *Crit Care*. 2023; 27(1):386. doi:10.1186/s13054-023-04655-8
2. Gofton TE, Young GB. Sepsis-associated encephalopathy. *Nat Rev Neurol*. 2012;8(10):557–566. doi:10.1038/nrneurol.2012.183
3. Sonnevile R, De Montmollin E, Poujade J, et al. Potentially modifiable factors contributing to sepsis-associated encephalopathy. *Intensive Care Med*. 2017;43(8):1075–1084. doi:10.1007/s00134-017-4807-z
4. Garcia R, Salluh JIF, Andrade TR, et al. A systematic review and meta-analysis of propofol versus midazolam sedation in adult intensive care (ICU) patients. *J Crit Care*. 2021;64:91–99. doi:10.1016/j.jccr.2021.04.001
5. Marler J, Mohrien K, Kimmons LA, et al. Effects of propofol on vasopressor use in patients with sepsis and severe sepsis: A pilot study. *J Crit Care*. 2016;35:155–160. doi:10.1016/j.jccr.2016.05.015
6. Tekwani KL, Watts HF, Sweis RT, Rzechula KH, Kulstad EB. A comparison of the effects of etomidate and midazolam on hospital length of stay in patients with suspected sepsis: A prospective, randomized study. *Ann Emerg Med*. 2010;56(5):481–489. doi:10.1016/j.annemergmed.2010.05.034
7. Ding J, Chen Y, Gao Y. Effect of propofol, midazolam and dexmedetomidine on ICU patients with sepsis and on arterial blood gas. *Exp Ther Med*. 2019;18(6):4340–4346. doi:10.3892/etm.2019.8091
8. Li WX, Luo RY, Chen C, et al. Effects of propofol, dexmedetomidine, and midazolam on postoperative cognitive dysfunction in elderly patients: A randomized controlled preliminary trial. *Chin Med J (Engl)*. 2019;132(4):437–445. doi:10.1097/CM9.0000000000000098
9. Casault C, Soo A, Lee CH, et al. Sedation strategy and ICU delirium: A multicentre, population-based propensity score-matched cohort study. *BMJ Open*. 2021;11(7):e045087. doi:10.1136/bmjopen-2020-045087
10. Chen Y, Hu Y, Li X, et al. Clinical features and factors associated with sepsis-associated encephalopathy in children: Retrospective single-center clinical study. *Front Neurol*. 2022;13:838746. doi:10.3389/fneur.2022.838746
11. Mao B, Feng L, Lin D, et al. The predictive role of systemic inflammation response index in the prognosis of traumatic brain injury: A propensity score matching study. *Front Neurol*. 2022;13:995925. doi:10.3389/fneur.2022.995925
12. Wang R, Cai L, Zhang J, He M, Xu J. Prediction of acute respiratory distress syndrome in traumatic brain injury patients based on machine learning algorithms. *Medicina (Kaunas)*. 2023;59(1):171. doi:10.3390/medicina59010171
13. Zhao L, Wang Y, Ge Z, Zhu H, Li Y. Mechanical learning for prediction of sepsis-associated encephalopathy. *Front Comput Neurosci*. 2021;15:739265. doi:10.3389/fncom.2021.739265
14. Yang Y, Liang S, Geng J, et al. Development of a nomogram to predict 30-day mortality of patients with sepsis-associated encephalopathy: A retrospective cohort study. *J Intensive Care*. 2020;8(1):45. doi:10.1186/s40560-020-00459-y
15. Hu J, Szymczak S. A review on longitudinal data analysis with random forest. *Brief Bioinform*. 2023;24(2):bbad002. doi:10.1093/bib/bbad002
16. Miyagawa N, Kawazoe Y, Sato T, et al. Comparison between midazolam and propofol in acute phase for ventilated patients with sepsis: A post-hoc analysis of the DESIRE trial. *Acute Med Surg*. 2022;9(1):e746. doi:10.1002/ams2.746
17. Scherer C, Kleeberger J, Kellnar A, et al. Propofol versus midazolam sedation in patients with cardiogenic shock: An observational propensity-matched study. *J Crit Care*. 2022;71:154051. doi:10.1016/j.jccr.2022.154051
18. Chung HY, Wickel J, Brunkhorst FM, Geis C. Sepsis-associated encephalopathy: From delirium to dementia? *J Clin Med*. 2020;9(3):703. doi:10.3390/jcm9030703
19. Shehaby Y, Bellomo R, Kadiman S, et al. Sedation intensity in the first 48 hours of mechanical ventilation and 180-day mortality: A multinational prospective longitudinal cohort study. *Crit Care Med*. 2018; 46(6):850–859. doi:10.1097/CCM.0000000000003071
20. Carrasco G, Molina R, Costa J, Soler JM, Cabré L. Propofol vs midazolam in short-, medium- and long-term sedation of critically ill patients. *Chest*. 1993;103(2):557–564. doi:10.1378/chest.103.2.557
21. Chamorro C, De Latorre FJ, Montero A, et al. Comparative study of propofol versus midazolam in the sedation of critically ill patients: Results of a prospective, randomized, multicenter trial. *Crit Care Med*. 1996; 24(6):932–939. doi:10.1097/00003246-199606000-00010
22. Ren C, Yao RQ, Zhang H, Feng YW, Yao YM. Sepsis-associated encephalopathy: A vicious cycle of immunosuppression. *J Neuroinflammation*. 2020;17(1):14. doi:10.1186/s12974-020-1701-3
23. Guan S, Sun L, Wang X, Huang X, Luo T. Propofol inhibits neuroinflammation and metabolic reprogramming in microglia in vitro and in vivo. *Front Pharmacol*. 2023;14:1161810. doi:10.3389/fphar.2023.1161810
24. Yamamoto T, Mizobata Y, Kawazoe Y, et al. Incidence, risk factors, and outcomes for sepsis-associated delirium in patients with mechanical ventilation: A sub-analysis of a multicenter randomized controlled trial. *J Crit Care*. 2020;56:140–144. doi:10.1016/j.jccr.2019.12.018
25. Sasabuchi Y, Yasunaga H, Matsui H, Lefor AK, Fushimi K. Prolonged propofol infusion for mechanically ventilated children. *Anaesthesia*. 2016;71(4):424–428. doi:10.1111/anae.13401
26. Lu X, Kang H, Zhou D, Li Q. Prediction and risk assessment of sepsis-associated encephalopathy in ICU based on interpretable machine learning. *Sci Rep*. 2022;12(1):22621. doi:10.1038/s41598-022-27134-6
27. Shulyatnikova T, Verkhatsky A. Astroglia in sepsis associated encephalopathy. *Neurochem Res*. 2020;45(1):83–99. doi:10.1007/s11064-019-02743-2
28. Jouffroy R, Parfait PA, Gilbert B, et al. Relationship between prehospital modified Charlson Comorbidity Index and septic shock 30-day mortality. *Am J Emerg Med*. 2022;60:128–133. doi:10.1016/j.ajem.2022.08.003
29. Klein M, Israeli A, Hassan L, et al. Can the duration of in-hospital ventilation in patients with sepsis help predict long-term survival? *J Clin Med*. 2022;11(20):5995. doi:10.3390/jcm11205995

Association between stress-induced hyperglycemia ratio and sepsis risk in patients admitted to ICU

YanJun Xu^{1,A,D–F}, Jing Yang^{1,B,C,F}, Zexing Jiang^{1,B,C,F}, Peng Liu^{1,B,C,F}, Xudong Wang^{2,3,A,E,F}

¹ Department of Critical Care Medicine, Xuzhou Renci Hospital, China

² Department of Critical Care Medicine, the Affiliated Xuzhou Municipal Hospital of Xuzhou Medical University, China

³ Department of Critical Care Medicine, Xuzhou First People's Hospital, China

A – research concept and design; B – collection and/or assembly of data; C – data analysis and interpretation;

D – writing the article; E – critical revision of the article; F – final approval of the article

Advances in Clinical and Experimental Medicine, ISSN 1899–5276 (print), ISSN 2451–2680 (online)

Adv Clin Exp Med. 2025;34(9):1475–1483

Address for correspondence

Xudong Wang

E-mail: xdwangicu@hotmail.com

Funding sources

None declared

Conflict of interest

None declared

Received on March 18, 2024

Reviewed on September 19, 2024

Accepted on October 11, 2024

Published online on January 10, 2025

Abstract

Background. Sepsis is a life-threatening condition characterized by a dysregulated host immune response to infection. Currently, stress hyperglycemia is frequently associated with an unfavorable prognosis in cardiovascular and cerebrovascular disease. During sepsis, the progression of the immune response and inflammation often leads to aberrant metabolic indicators. However, the association between the stress-induced hyperglycemia ratio (SHR) and sepsis in patients admitted to the intensive care unit (ICU) remains uncertain.

Objectives. This study aimed to explore the potential correlation between SHR and sepsis.

Materials and methods. In this retrospective cohort study, data were obtained from the Medical Information Mart for Intensive Care-IV (MIMIC-IV) database. Patients with recorded glucose and glycosylated HbA1c levels within 24-h ICU admission were identified. The endpoints of the follow-up period were the occurrence of sepsis during ICU stay or ICU discharge. After adjustment for factors including demographics, vital signs and biochemical indicators, the univariate and multivariate logistic regression model was employed to examine the relationship between SHR, baseline blood glucose levels and the risk of sepsis. The associations were further explored in subgroups based on age, gender and presence/absence of type 2 diabetes.

Results. Of the total 2,161 patients, with the average age of 64.96 ± 16.84 years, 205 (9.49%) had sepsis. After adjustment for confounders, high SHR levels were associated with the risk of sepsis odds ratio (OR) = 1.53, 95% confidence interval (95% CI): 1.07–2.17. Similar results were found in patients aged ≥ 65 years (OR = 1.91, 95% CI: 1.16–3.17), in men (OR = 1.64, 95% CI: 1.02–2.63) and patients without type 2 diabetes history (OR = 1.58, 95% CI: 1.01–2.48). The baseline blood glucose level did not exhibit a significant association with the risk of sepsis.

Conclusions. Elevated SHR levels were correlated with sepsis. Bedside monitoring of SHR may be a valuable tool for clinicians to identify patients at high risk of sepsis, and be beneficial to promptly implement clinical interventions.

Key words: sepsis, intensive care unit, glucose, stress-induced hyperglycemia ratio

Cite as

Xu Y, Yang J, Jiang Z, Liu P, Wang X. Association between stress-induced hyperglycemia ratio and sepsis risk in patients admitted to ICU. *Adv Clin Exp Med.* 2025;34(9):1475–1483. doi:10.17219/acem/194503

DOI

10.17219/acem/194503

Copyright

Copyright by Author(s)

This is an article distributed under the terms of the Creative Commons Attribution 3.0 Unported (CC BY 3.0) (<https://creativecommons.org/licenses/by/3.0/>)

Background

Sepsis is a life-threatening condition characterized by a dysregulated host immune response to infection, leading to systemic inflammatory response syndrome (SIRS), septic shock and multi-organ dysfunction.¹ The manifestation of acute respiratory and kidney failure, as well as multiple organ dysfunction syndrome resulting from sepsis, impose a substantial burden on patients in the intensive care unit (ICU).^{2,3} The estimated incidence of sepsis in ICU settings is approx. 58 cases per 100,000 person-years, with a pre-discharge mortality rate of 41.9%.⁴ Globally, the annual incidence of hospital-treated sepsis cases is estimated to exceed 30 million, with 5.3 million patients succumbing to sepsis.⁵ Conversely, sepsis may also serve as a predisposing factor for secondary atrial fibrillation and cardiogenic stroke.⁶ The early identification of high-risk patients prone to sepsis development is of paramount importance for sepsis prevention and reducing disease burden.

Previous reports indicate that patients with hyperglycemia or diabetes are susceptible to infection and even sepsis, which may be attributed to chronic suboptimal glycemic control.^{7,8} The presence of inflammation and neurohormonal disorders during the disease can lead to a relative increase in glucose levels, resulting in stress hyperglycemia.⁹ This condition significantly impacts prognosis by inducing mechanisms like endothelial dysfunction and oxidative stress.⁹ However, the blood glucose levels only reflect the patient's blood glucose status at a specific moment and do not indicate glycemic control.¹⁰ To minimize the potential misinterpretation of stress-induced hyperglycemia prevalence, the stress-induced hyperglycemia ratio (SHR) has been proposed as a strategy to assess the influence of chronic glycemic factors on stress-induced glucose levels, incorporating admission blood glucose and glycosylated hemoglobin A1c (HbA1c) measurements.¹¹ The SHR is widely recognized as a more accurate indicator of long-term glycemic control compared to glucose and HbA1c, as it considers chronic hyperglycemia levels.¹² The pathophysiological mechanisms of stress-induced hyperglycemia involve hormonal and metabolic responses to stress. During acute stress, the hypothalamic–pituitary–adrenal axis becomes active, releasing stress hormones like cortisol, epinephrine and glucagon.¹³ These hormones exert counter-regulatory effects on insulin action, stimulating hepatic gluconeogenesis and glycogenolysis, while concurrently inhibiting peripheral glucose uptake.¹⁴ Additionally, the stress-induced activation of the sympathetic nervous system and inflammatory mediators further exacerbates insulin resistance and hyperglycemia.¹⁴ Cumulatively, these pathophysiological changes disrupt glucose homeostasis, resulting in sustained hyperglycemia in critically ill patients. Studies indicated that stress-induced hyperglycemia significantly increase the risk of postoperative infection among non-diabetic orthopedic trauma patients in the ICU.^{15,16} Studies also reported an association of elevated SHR with higher

mortality rates in ICU patients, regardless of their diabetes status.^{17–19} Moreover, it has been observed that high SHR significantly enhances the predictive value of the Global Registry of Acute Coronary Events (GRACE) score for mortality prediction.²⁰ Currently, stress hyperglycemia is commonly associated with an adverse prognosis in cardiovascular and cerebrovascular diseases.^{21,22} During sepsis, the progression of immune response and inflammation often leads to abnormal metabolic indicators. However, the relationship between SHR and sepsis in patients admitted to the ICU remains unexplored.

Objectives

This study aimed to investigate the association between SHR, baseline blood glucose levels and sepsis risk in patients admitted to the ICU. Additionally, subgroup analysis was performed among individuals aged ≥ 65 years, in men and in patients without type 2 diabetes.

Methods

Study design

The data for this retrospective cohort study were extracted from the Medical Information Mart for Intensive Care-IV (MIMIC-IV) database, a comprehensive longitudinal database encompassing data collected between 2008 and 2019.²³ The protocol of National Health and Nutrition Examination Survey (NHANES) was approved by the National Center for Health Statistics ethics review board and all participants signed informed consent forms. In this study, data of the participants were de-identified and there is no need for approval from the hospital ethics committee.

Patients with recorded glucose and HbA1c levels within 24 h after admission to ICU were identified from the MIMIC-IV database. The SHR was determined using the following formula: $\text{SHR} = [\text{admission glucose (mg/dL)}] / [28.7 \times \text{HbA1c (\%)} - 46.7]$.^{11,18} The blood glucose levels measured within 24 h of admission to the ICU were considered as the baseline blood glucose. Both SHR and baseline glucose were classified according to the tertiles.

The inclusion criteria were patients with glucose and HbA1c examinations within 24 h after admission to ICU. The exclusion criteria were as follows: patients who 1) were under 18 years of age, 2) had a duration of ICU stay shorter than 24 h, 3) were diagnosed with sepsis upon ICU admission, and 4) for whom requisite information for sepsis assessment was lacking.

Covariates

Demographic information was extracted, including age, gender and race. Additionally, quick sequential organ failure assessment (qSOFA), Charlson comorbidity index (CCI),

SIRS scores, white blood cell (WBC) count, red blood cell distribution width (RDW), creatinine, prothrombin time (PT), blood urea nitrogen (BUN), calcium and sodium levels, as well as information on mechanical ventilation within 24-h ICU admission were extracted for use as covariates in our study. The SIRS measurements were: 1) tachycardia (heart rate >90 bpm), 2) tachypnea or hyperventilation (respiratory rate >20 breaths/min or partial pressure of carbon dioxide (PaCO₂) <32 mm Hg), 3) fever or hypothermia (temperature >38 or <36°C) and 4) leukocytosis, leukopenia or bandemia (WBC >12×10⁹/L, <4×10⁹/L or bandemia ≥10%). The SIRS status was determined with the criteria (from 0 (best) to 4 (worst)).^{23,24}

Outcome and follow-up

Sepsis was the outcome of this study. The median follow-up duration was 2.1 (1.6, 3.4) days. Sepsis was diagnosed based on the Sepsis-3 criteria.² In brief, patients with confirmed or suspected infection and a sudden increase in total qSOFA score of ≥2 points were classified as having sepsis. The identification of infection was determined using the International Classification of Diseases (ICD) code.

Statistical analyses

The data cleaning, imputation of missing values, covariate screening, logistic regression analysis, and subgroup analysis were conducted using R v. 4.2.3 (The R Foundation for Statistical Computing, Vienna, Austria).

The variables with a missing rate ≤20% underwent multiple imputations. Subsequently, a sensitivity analysis was conducted to compare the variables before and after imputation. Assuming that the data is Missing Completely at Random (MCAR), missing values can be predicted and interpolated from observed values. The measurement data with a normal distribution were presented as the mean ± standard deviation (mean ±SD). The normality of continuous variables was tested by skewness and kurtosis, while homogeneity was detected using the Levene test. For data with homogeneity of variance, a t-test was employed to compare between 2 groups, while for data with non-homogeneity of variance, Satterthwaite's t-test was utilized. Measurement data that did not conform to a normal distribution were described using the median (Me) and quartile, and differences between any 2 groups were compared using the Wilcoxon rank sum tests. Count data were described as the number of cases and constituent ratio, and group differences were assessed using the χ^2 test. The confounding factors were screened using univariate logistic regression models. After adjusting for confounders including age, gender, race, qSOFA score, CCI, SIRS, calcium levels, sodium levels, and mechanical ventilation status, the multivariate logistic regression model was employed to examine the relationship between SHR, baseline blood glucose levels and the risk of sepsis. Model 1

represents a univariate logistic regression model. Model 2 incorporates adjustments for qSOFA, CCI, SIRS, calcium, sodium, and mechanical ventilation. Model 3 further adjusts for age, gender, race, qSOFA, CCI, SIRS, calcium, sodium, and mechanical ventilation. The present study adopted the Box–Tidwell test to verify whether the predictors and the logit of the response variable were linear. The line test results show a linear relationship between all continuous predictor variables and sepsis. The generalized variance inflation factor (gVIF) test was adopted to detect multicollinearity among the explanatory variables, with all gVIFs < 10 indicating that no multicollinearity was observed. Cook's distances were conducted to detect the presence of extreme outliers. Subgroup analyses were conducted based on age, gender, and presence or absence of history of type 2 diabetes. A p-value of 0.05 was considered significant.

Results

Clinical characteristics of ICU patients

The data extraction and screening process were conducted following the workflow depicted in Fig. 1. No significant difference was observed before and after data interpolation (Supplementary Tables 1 and 2).

A total of 4,004 patients with documented blood glucose and HbA1c levels within 24 h of admission to the ICU were included in this study. After excluding 1,105 patients diagnosed with sepsis upon ICU admission and 738 patients who stayed in the ICU for less than 24 h, the final cohort consisted of 2,161 patients, of which 205 (9.49%)

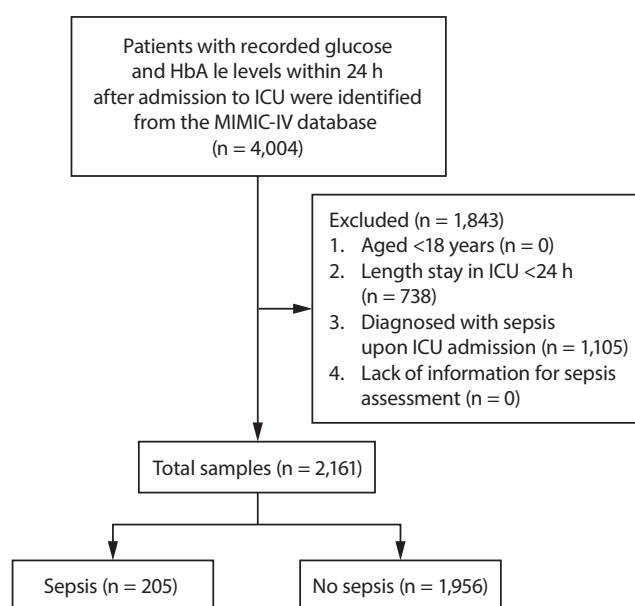


Fig. 1. The screening process of patients included

ICU – intensive care unit; HbA – hemoglobin A; MIMIC-IV – Medical Information Mart for Intensive Care-IV.

Table 1. Characteristics of ICU patients

Variables		Total (n = 2,161)	Non-sepsis (n = 1,956)	Sepsis (n = 205)	Statistics	p-value
Age [years], n (%)	<65	996 (46.09)	907 (46.37)	89 (43.41)	$\chi^2 = 0.539$	0.463
	≥65	1,165 (53.91)	1,049 (53.63)	116 (56.59)		
Gender, n (%)	female	939 (43.45)	855 (43.71)	84 (40.98)	$\chi^2 = 0.459$	0.498
	male	1,222 (56.55)	1,101 (56.29)	121 (59.02)		
Insurance status, n (%)	Medicaid/Medicare	1,025 (47.43)	923 (47.19)	102 (49.76)	$\chi^2 = 0.393$	0.531
	others	1,136 (52.57)	1,033 (52.81)	103 (50.24)		
24-h urine output [mL], mean ±SD		1,962.07 ±1,244.88	1,969.39 ±1250.42	1,892.19 ±1,191.42	t = 0.845	0.398
Type 2 diabetes, n (%)	no	1,484 (68.67)	1,348 (68.92)	136 (66.34)	$\chi^2 = 0.458$	0.498
	yes	677 (31.33)	608 (31.08)	69 (33.66)		
Trauma/injury, n (%)	no	2,018 (93.38)	1,830 (93.56)	188 (91.71)	$\chi^2 = 0.751$	0.386
	yes	143 (6.62)	126 (6.44)	17 (8.29)		
SAPS-II score, mean ±SD		28.53 ±10.60	28.07 ±10.47	32.98 ±10.84	t = -6.371	<0.001
SOFA score, mean ±SD		2.87 ±2.28	2.62 ±2.10	5.18 ±2.66	t' = -13.339	<0.001
qSOFA score, mean ±SD		1.72 ±0.76	1.67 ±0.75	2.22 ±0.69	t' = -10.895	<0.001
qSOFA score, n (%)	≤2	1,859 (86.02)	1,729 (88.39)	130 (63.41)	$\chi^2 = 94.245$	<0.001
	>2	302 (13.98)	227 (11.61)	75 (36.59)		
GCS score, mean ±SD		13.66 ±2.23	13.70 ±2.18	13.28 ±2.65	t' = 2.196	0.029
CCI score, mean ±SD		3.04 ±2.06	2.96 ±2.03	3.85 ±2.13	t = -5.957	<0.001
SIRS score, mean ±SD		0.96 ±0.94	0.94 ±0.93	1.20 ±1.00	t = -3.753	<0.001
Heart rate [bpm], mean ±SD		82.70 ±18.22	82.45 ±18.09	85.07 ±19.24	t = -1.960	0.050
SBP [mm Hg], mean ±SD		138.14 ±24.43	138.40 ±24.28	135.65 ±25.71	t = 1.531	0.126
DBP [mm Hg], mean ±SD		77.61 ±17.33	77.71 ±17.33	76.63 ±17.36	t = 0.844	0.399
Respiratory rate [insp/min], mean ±SD		18.66 ±5.19	18.63 ±5.20	18.98 ±5.12	t = -0.919	0.358
Temperature [°C], Me (Q ₁ , Q ₃)		36.72 (36.50–37.00)	36.72 (36.50–37.00)	36.83 (36.56–37.11)	W = 172,865	0.001
WBC [K/μL], Me (Q ₁ , Q ₃)		9.60 (7.50–12.50)	9.50 (7.40–12.20)	11.00 (8.60–14.50)	W = 157,985	<0.001
Platelet count [K/μL], mean ±SD		224.11 ±78.51	224.13 ±77.86	223.91 ±84.66	t' = 0.036	0.971
Hemoglobin [g/dL], mean ±SD		12.33 ±2.00	12.35 ±1.98	12.08 ±2.18	t' = 1.717	0.087
RDW-CV [%], mean ±SD		13.99 ±1.66	13.95 ±1.61	14.33 ±2.04	t' = -2.578	0.011
Hematocrit [%], mean ±SD		37.05 ±5.61	37.09 ±5.56	36.64 ±6.13	t' = 1.011	0.313
Creatinine [mg/dL], Me (Q ₁ , Q ₃)		0.90 (0.70–1.10)	0.90 (0.70–1.10)	1.00 (0.80–1.20)	W = 181,827.5	0.027
PT [s], Me (Q ₁ , Q ₃)		12.40 (11.50–13.80)	12.40 (11.50–13.70)	12.60 (11.60–14.40)	W = 182,827	0.038
PTT [s], Me (Q ₁ , Q ₃)		29.30 (26.30–34.60)	29.30 (26.30–34.40)	29.40 (26.30–37.10)	W = 197,235	0.702
BUN [mg/dL], Me (Q ₁ , Q ₃)		16.00 (12.00–22.00)	16.00 (12.00–22.00)	18.00 (13.00–25.00)	W = 179,846	0.015
Calcium [mg/dL], Me (Q ₁ , Q ₃)		8.70 (8.30–9.10)	8.70 (8.30–9.10)	8.60 (8.00–9.00)	W = 222,882	0.008
Sodium [mEq/L], mean ±SD		138.85 ±4.04	138.79 ±4.06	139.40 ±3.76	t = -2.057	0.040
Chloride [mEq/L], mean ±SD		103.57 ±4.91	103.52 ±4.94	104.05 ±4.58	t = -1.477	0.140
Bicarbonate [mEq/L], mean ±SD		23.04 ±4.40	23.08 ±4.45	22.60 ±3.86	t = 1.479	0.139
Mechanical ventilation, n (%)	no	1,077 (49.84)	1,015 (51.89)	62 (30.24)	$\chi^2 = 33.922$	<0.001
	yes	1,084 (50.16)	941 (48.11)	143 (69.76)		
Antibiotics, n (%)	no	1,965 (90.93)	1,787 (91.36)	178 (86.83)	$\chi^2 = 4.085$	0.043
	yes	196 (9.07)	169 (8.64)	27 (13.17)		
Insulin, n (%)	no	1,589 (73.53)	1,442 (73.72)	147 (71.71)	$\chi^2 = 0.290$	0.590
	yes	572 (26.47)	514 (26.28)	58 (28.29)		
HbA1c [%], mean ±SD		6.66 ±2.16	6.70 ±2.21	6.28 ±1.50	t' = 3.566	<0.001
Blood glucose [mg/dL], n* (%)	<110	714 (33.04)	659 (33.69)	55 (26.83)	$\chi^2 = 3.645$	0.056
	≥110	1,447 (66.96)	1,297 (66.31)	150 (73.17)		
SHR, n (%)	<0.9	736 (34.06)	684 (34.97)	52 (25.37)	$\chi^2 = 7.198$	0.007
	≥0.9	1,425 (65.94)	1,272 (65.03)	153 (74.63)		

SD – standard deviation; Me – median; Q₁ – 1st quartile; Q₃ – 3rd quartile; t – Student's t-test; t' – Satterthwaite t-test; W – Wilcoxon rank sum test; χ^2 – χ^2 test. The classification of both SHR and baseline blood glucose was performed based on 1/3 subsites. ICU – intensive care unit; SAPS-II score – Simplified Acute Physiology Score-II score; SOFA – Sequential Organ Failure Assessment; qSOFA – quick Sequential Organ Failure Assessment; GCS – Glasgow Coma Scale; CCI – Charlson Comorbidity Index; SIRS – systemic inflammatory response syndrome; SBP – systolic blood pressure; DBP – diastolic blood pressure; WBC – white blood cell; RDW-CV – red blood cell distribution width-coefficient of variation; PT – prothrombin time; PTT – partial thromboplastin time; BUN – blood urea nitrogen; HbA1c – hemoglobin A1c; SHR – stress-induced hyperglycemia ratio. *Blood glucose level was categorized as <110 mg/dL and ≥110 mg/dL groups. The number of patients in these 2 groups is presented here separately.

patients had sepsis during the ICU stay. The average age of all patients was 64.96 ± 16.84 years, with men accounting for 56%. The characteristics of the included patients were presented in Table 1. In comparison to the non-sepsis group, the sepsis group exhibited higher levels of temperature ($p = 0.001$). Additionally, the sepsis group exhibited elevated SAPS-II score ($p < 0.001$), SOFA score ($p < 0.001$), qSOFA score ($p < 0.001$), GCS score ($p = 0.029$), CCI score ($p < 0.001$), and SIRS score ($p < 0.001$). Moreover, compared to the non-sepsis group, the sepsis group showed significantly higher levels of WBC count ($p < 0.001$), red blood cell distribution width-coefficient of variation (RDW-CV) ($p = 0.011$), creatinine ($p = 0.027$), PT ($p = 0.038$), BUN ($p = 0.015$), and sodium ($p = 0.040$) concentration; whereas calcium ($p = 0.008$) and HbA1c levels ($p < 0.001$) were significantly lower in this group. The proportion of mechanical ventilation and antibiotic usage was higher among patients with sepsis. Additionally, the distribution of elevated glucose levels (≥ 110 , $p < 0.001$) and SHR (≥ 0.9 , $p = 0.007$) were significantly higher in the sepsis group.

Association of SHR and baseline glucose levels with sepsis

Ultimately, the qSOFA score, CCI score, SIRS score, calcium, and sodium were identified as confounding factors. Additionally, demographic factors such as age, gender and race were included in model 3 as covariates to account for their potential influence (Supplementary Table 3).

After adjustment for confounders (Table 2), SHR ≥ 0.9 (odds ratio (OR): = 1.53, 95% confidence interval (95% CI): 1.07–2.17, $p = 0.020$) was also associated with the risk of sepsis (model 3). Conversely, glucose levels ≥ 110 did not exhibit any significant association with the risk of sepsis ($p = 0.588$).

Association between SHR and sepsis in subgroups of ages, gender and type 2 diabetes

In patients aged ≥ 65 years (OR: 1.91, 95% CI: 1.16–3.17, $p = 0.011$), among men (OR: 1.64, 95% CI: 1.02–2.63, $p = 0.040$)

Table 2. Associations of SHR and blood glucose levels with sepsis

Variables		Model 1		Model 2		Model 3	
		OR (95% CI)	p-value	OR (95% CI)	p-value	OR (95% CI)	p-value
SHR	<0.9	Ref	–	Ref	–	Ref	–
	≥ 0.9	1.58 (1.14–2.20)	0.006	1.48 (1.04–2.10)	0.028	1.53 (1.07–2.17)	0.019
Blood glucose	<110 mmol/L	Ref	–	Ref	–	Ref	–
	≥ 110 mmol/L	1.39 (1.00–1.91)	0.048	1.12 (0.79–1.59)	0.519	1.10 (0.78–1.57)	0.588

Ref – reference; OR – odds ratio; 95% CI – 95% confidence interval; Model 1 – no adjusted; Model 2 – adjusted for qSOFA, CCI, SIRS, calcium, sodium, and mechanical ventilation; Model 3 – adjusted for age, gender, race, qSOFA, CCI, SIRS, calcium, sodium, and mechanical ventilation. SHR – stress-induced hyperglycemia ratio; qSOFA – quick Sequential Organ Failure Assessment; CCI – Charlson Comorbidity Index; SIRS – systemic inflammatory response syndrome. Blood glucose level was categorized as <110 mg/dL and ≥ 110 mg/dL groups. The number of patients in these 2 groups is presented here separately.

Table 3. Associations between glucose levels and sepsis in subgroups of age, gender and type 2 diabetes

Variables (sepsis/total)		Glucose (sepsis/total)		OR (95% CI)	p-value
Age	<65 years (89/996)	<110 mmol/L (27/320)		Ref	–
		≥ 110 mmol/L (62/676)		0.98 (0.58–1.67)	0.940
	≥ 65 years (116/1165)	<110 mmol/L (28/394)		Ref	–
		≥ 110 mmol/L (88/771)		1.25 (0.78–2.03)	0.355
Gender	female (84/939)	<110 mmol/L (28/333)		Ref	–
		≥ 110 mmol/L (56/606)		0.72 (0.42–1.22)	0.225
	male (121/1222)	<110 mmol/L (27/381)		Ref	–
		≥ 110 mmol/L (94/841)		1.49 (0.92–2.43)	0.109
Type 2 diabetes	no (136/1484)	<110 mmol/L (45/632)		Ref	–
		≥ 110 mmol/L (91/852)		1.22 (0.81–1.84)	0.346
	yes (69/677)	<110 mmol/L (10/82)		Ref	–
		≥ 110 mmol/L (59/595)		0.73 (0.34–1.58)	0.425

Age subgroup – adjusting gender, race, qSOFA, CCI, SIRS, calcium, sodium, and mechanical ventilation; Gender subgroup – adjusted for age, race, qSOFA, CCI, SIRS, calcium, sodium, and mechanical ventilation; Type 2 diabetes subgroup – adjusted for age, gender, race, qSOFA, CCI, SIRS, calcium, sodium, and mechanical ventilation. OR – odds ratio; 95% CI – 95% confidence interval; Ref – reference; qSOFA – quick Sequential Organ Failure Assessment; CCI – Charlson Comorbidity Index; SIRS – systemic inflammatory response syndrome. Blood glucose level was categorized as <110 mg/dL and ≥ 110 mg/dL groups. The number of patients in these 2 groups is presented here separately.

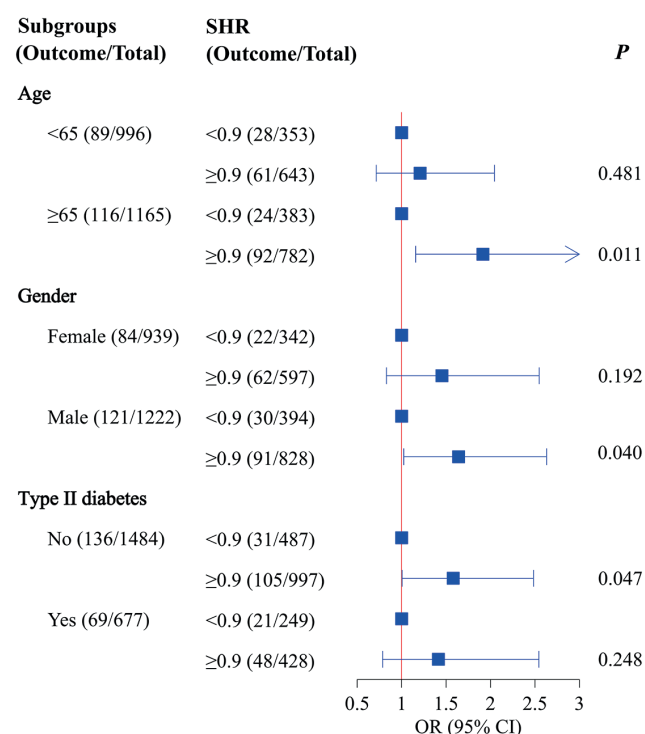


Fig. 2. Association between SHR and sepsis risk in subgroups of age, gender, and type 2 diabetes. The arrow indicates that an interval beyond the range. Age subgroup: adjusted for gender, race, qSOFA, CCI, SIRS, calcium, sodium, and mechanical ventilation. Gender subgroup: adjusted for age, race, qSOFA, CCI, SIRS, calcium, sodium, and mechanical ventilation. Type 2 diabetes subgroup: adjusted for age, sex, race, qSOFA, CCI, SIRS, calcium, sodium, and mechanical ventilation.

OR – odds ratio; 95% CI – 95% confidence interval; SHR – stress-induced hyperglycemia ratio; qSOFA – quick Sequential Organ Failure Assessment; CCI – Charlson Comorbidity Index; SIRS – systemic inflammatory response syndrome.

and in patients without history of type 2 diabetes (OR: 1.58, 95% CI: 1.01–2.48, $p = 0.047$), elevated levels of SHR were associated with higher odds of sepsis (Fig. 2). The baseline blood glucose level did not exhibit a significant association with the risk of sepsis in these patients ($p > 0.05$) (Table 3).

Discussion

Our study aimed to explore the association between baseline blood glucose levels, SHR and the risk of sepsis in ICU patients. We found that elevated SHR levels were related to higher odds of sepsis. Moreover, our findings showed that elevated SHR levels were associated with sepsis among patients aged ≥ 65 years, who were men and in patients without a history of type 2 diabetes. The baseline blood glucose level did not exhibit a significant association with sepsis risk.

Sepsis represents a significant global health challenge and is associated with substantial mortality rates.¹ The incidence of sepsis varies considerably across different regions worldwide, ranging from 14% to 39%.²⁵ Patients requiring intensive care demonstrate an elevated

susceptibility to sepsis development compared to those admitted to general wards.²⁶ Currently reported factors associated with sepsis occurrence include bone mineral density,²⁷ qSOFA,²⁸ PCT,²⁸ and emergency surgery.²⁹ However, in a study investigating risk factors for sepsis following geriatric surgery,²⁹ blood glucose was found to be associated with sepsis in patients. In contrast to our findings, we did not observe the association between glucose levels and sepsis risk, which may be attributed to differences in the study population. Generally, blood glucose fluctuations are controlled during early hospitalization in elderly surgical patients, reflecting the patient's long-term blood glucose status with some degree of stability. Given the high incidence of diabetes in the ICU, evaluating chronic hyperglycemia based solely on absolute glucose concentration is deemed ineffective.¹⁰ The measurement of HbA1c serves as an indicator of chronic hyperglycemia in patients with both overt and recessive diabetes. Conversely, the admission glucose concentration in critically ill patients indicates the severity of acute hyperglycemia.³⁰ Similarly, elevated glucose levels (≥ 110 mmol/L) and SHR (≥ 0.9) were more prevalent in the sepsis group in our study.

The calculation of SHR considers admission glucose and HbA1c concentrations, estimating stress-induced hyperglycemia while accounting for chronic hyperglycemia in patients with or without diabetes.¹¹ Previous research suggests that SHR may be associated with more severe adverse outcomes compared to chronic hyperglycemia, particularly in severe conditions such as acute myocardial infarction, trauma and acute ischemic stroke.^{18,22,31} Similarly, we also observed the relationship between SHR and sepsis in ICU patients.

Stress-induced hyperglycemia is characterized by increased blood glucose levels due to the activation of stress hormones such as cortisol and catecholamines.¹⁴ This hyperglycemic state can lead to immune dysfunction through several interconnected pathways. First, hyperglycemia has been shown to impair various components of the immune response, including neutrophil function, macrophage activity and lymphocyte proliferation.³² Neutrophils, key mediators of the innate immune response, exhibit reduced chemotaxis and phagocytic activity in hyperglycemic conditions, compromising their ability to effectively clear pathogens.³³ Additionally, hyperglycemia impairs the function of macrophages, inhibiting antigen presentation and cytokine production essential for coordinating the immune response.³⁴ Second, hyperglycemia promotes a pro-inflammatory state characterized by increased production of inflammatory cytokines such as interleukin 6 (IL-6) and tumor necrosis factor alpha (TNF- α).³⁵ These cytokines not only contribute to tissue damage but also disrupt the delicate balance between pro-inflammatory and anti-inflammatory responses, potentially exacerbating the systemic inflammatory response associated with sepsis. Furthermore, hyperglycemia-induced oxidative stress may play a role in immune dysregulation and tissue

damage. Elevated glucose levels promote the production of reactive oxygen species (ROS) and reactive nitrogen species (RNS), leading to oxidative damage to cells and tissues.³⁶ Oxidative stress not only impairs immune cell function but also exacerbates endothelial dysfunction and microvascular damage, contributing to organ dysfunction commonly seen in sepsis.³⁶

In the subgroup of individuals aged ≥ 65 years, among men and in individuals without type 2 diabetes, elevated levels of SHR were associated with sepsis in our study. The association can be ascribed to the diminished immune function observed in elderly patients compared to their younger counterparts, rendering them more susceptible to infections.³⁷ Additionally, the delayed clearance of pathogens at local infection sites further exacerbates the likelihood of sepsis development among elderly individuals.³⁸ Elevated SHR levels indicate an imminent surge in blood glucose levels, which can inflict additional harm on the immune system and escalate the progression of localized infections into septic conditions.¹⁷ Furthermore, it is worth noting that male patients demonstrate a higher propensity for sepsis development compared to women in similar circumstances. Numerous studies have substantiated this observation by demonstrating that men display heightened susceptibility to bacterial, fungal and viral infections, and other diseases owing to their robust physiological constitution and infrequent occurrence of regular illnesses or systematic immune clearance processes.^{39,40} Consequently, they tend to accumulate prolonged immunological debt which amplifies their vulnerability to sepsis. In patients with elevated SHR levels but without a diagnosis of type 2 diabetes, stress-induced hyperglycemia manifests as a consequence of traumatic events, infections and other acute precipitating factors.⁴¹ The elevated blood glucose levels exert varying degrees of deleterious effects on the nervous, cardiovascular and immune systems.⁹ The sudden increase in blood glucose levels compromises the immune system rapidly, allowing insufficient time for adaptation and resulting in exacerbation of pre-existing infections or direct progression to severe infection followed by sepsis.⁸ In the subgroup analysis investigating the relationship between baseline glucose levels and sepsis, we did not observe a statistically significant correlation. This may be attributed to several confounding factors that can influence patients' glucose levels within 24 h of admission to the ICU, such as concurrent administration of therapeutic medications, impaired renal function and hepatic failure.¹⁶ It appears that immediate glucose levels have limited prognostic relevance for patients.

The present study represents the potential effort to investigate the correlation between SHR and sepsis risk in ICU, aiming to offer valuable insights for prognostic marker screening and identification of high-risk patients, as well as potential applications of SHR through subgroup analysis. The association between SHR and sepsis suggests

that timely and regular monitoring of SHR in ICU patients by clinicians can readily identify high-risk groups for sepsis and enable promptly implementing clinical interventions to enhance patient prognosis.

Limitations

First, due to the retrospective design and single-center setting, there is an inherent selection bias. Moreover, the limited exposure to HbA1c further exacerbates this bias. Additionally, as it was an observational study, we can only establish associations rather than determine a causal relationship between SHR and sepsis risk in ICU patients. Future prospective studies are warranted to validate our findings.

Conclusions

The elevated level of SHR was identified to be significantly correlated with sepsis. Bedside monitoring of SHR is a valuable tool for clinicians to identify patients at high risk of sepsis and promptly implement clinical interventions, thereby improving patient outcomes.

Supplementary data

The Supplementary materials are available at <https://doi.org/10.5281/zenodo.13901764>. The package includes the following files:

Supplementary Table 1. The distribution of missing values.

Supplementary Table 2. Sensitivity analysis before and after interpolation of missing values.

Supplementary Table 3. Covariates screening in regression analysis.

Supplementary Table 4. Box–Tidwell tests between variables and sepsis (model 2).

Supplementary Table 5. Box–Tidwell tests between variables and sepsis (model 3).

Supplementary Table 6. The gVIF among variables.

Supplementary Table 7. The tests of normality and homogeneity assumptions.

Supplementary Table 8. The confusion matrix.

Supplementary Table 9. The accuracy, precision and recall values of the study.

Supplementary Fig. 1. Cook's distance plot of 3 models.

Supplementary Fig. 2. Receiver operating characteristic (ROC) curve of the study.

Data availability

The datasets generated and/or analyzed during the current study are available from the corresponding author on reasonable request.

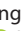
Consent for publication

Not applicable.


ORCID iDs

Yanjun Xu  <https://orcid.org/0009-0005-2881-8749>

Jing Yang  <https://orcid.org/0009-0005-6141-6979>

Zexing Jiang  <https://orcid.org/0009-0004-7758-6262>

Peng Liu  <https://orcid.org/0009-0004-6932-2996>

Xudong Wang  <https://orcid.org/0009-0001-0708-6607>

References

- Drăgoescu AN, Pădureanu V, Stănculescu AD, et al. Presepsin as a potential prognostic marker for sepsis according to actual practice guidelines. *J Pers Med*. 2020;11(1):2. doi:10.3390/jpm11010002
- Singer M, Deutschman CS, Seymour CW, et al. The Third International Consensus Definitions for Sepsis and Septic Shock (Sepsis-3). *JAMA*. 2016;315(8):801. doi:10.1001/jama.2016.0287
- Markwart R, Saito H, Harder T, et al. Epidemiology and burden of sepsis acquired in hospitals and intensive care units: A systematic review and meta-analysis. *Intensive Care Med*. 2020;46(8):1536–1551. doi:10.1007/s00134-020-06106-2
- Fleischmann-Struzek C, Mellhammar L, Rose N, et al. Incidence and mortality of hospital- and ICU-treated sepsis: Results from an updated and expanded systematic review and meta-analysis. *Intensive Care Med*. 2020;46(8):1552–1562. doi:10.1007/s00134-020-06151-x
- Fleischmann C, Scherag A, Adhikari NKJ, et al. Assessment of global incidence and mortality of hospital-treated sepsis: Current estimates and limitations. *Am J Respir Crit Care Med*. 2016;193(3):259–272. doi:10.1164/rccm.201504-0781OC
- Leng Y, Li Y, Wang J, et al. Sepsis as an independent risk factor in atrial fibrillation and cardioembolic stroke. *Front Endocrinol (Lausanne)*. 2023;14:1056274. doi:10.3389/fendo.2023.1056274
- Koh GCKW, Peacock SJ, Van Der Poll T, Wiersinga WJ. The impact of diabetes on the pathogenesis of sepsis. *Eur J Clin Microbiol Infect Dis*. 2012;31(4):379–388. doi:10.1007/s10096-011-1337-4
- Shaked I, Foo C, Mächler P, et al. A lone spike in blood glucose can enhance the thrombo-inflammatory response in cortical venules. *J Cereb Blood Flow Metab*. 2023;44(2):252–271. doi:10.1177/0271678X231203023
- Dungan KM, Braithwaite SS, Preiser JC. Stress hyperglycaemia. *Lancet*. 2009;373(9677):1798–1807. doi:10.1016/S0140-6736(09)60553-5
- Wang YL, Leng XY, Dong Y, et al. Fasting glucose and HbA1c levels as risk factors for the presence of intracranial atherosclerotic stenosis. *Ann Transl Med*. 2019;7(24):804. doi:10.21037/atm.2019.12.56
- Roberts GW, Quinn SJ, Valentine N, et al. Relative hyperglycemia, a marker of critical illness: Introducing the stress hyperglycemia ratio. *J Clin Endocrinol Metab*. 2015;100(12):4490–4497. doi:10.1210/jc.2015-2660
- Chu H, Huang C, Tang Y, Dong Q, Guo Q. The stress hyperglycemia ratio predicts early hematoma expansion and poor outcomes in patients with spontaneous intracerebral hemorrhage. *Ther Adv Neurol Disord*. 2022;15:17562864211070681. doi:10.1177/17562864211070681
- Wong YN, Cassano JR, Jr, D'Mello AP. Acute-stress-induced facilitation of the hypothalamic-pituitary-adrenal axis. *Neuroendocrinology*. 2000;71(6):354–365. doi:10.1159/000054556
- Marik PE, Bellomo R. Stress hyperglycemia: An essential survival response! *Crit Care*. 2013;17(2):305. doi:10.1186/cc12514
- Richards JE, Kauffmann RM, Obrebsky WT, May AK. Stress-induced hyperglycemia as a risk factor for surgical-site infection in nondiabetic orthopedic trauma patients admitted to the intensive care unit. *J Orthop Trauma*. 2013;27(1):16–21. doi:10.1097/BOT.0b013e31825d60e5
- Pan J, Zou J, Bao Y, et al. Use of glycated albumin to distinguish occult diabetes mellitus from stress-induced hyperglycemia in Chinese orthopedic trauma patients. *J Trauma Acute Care Surg*. 2012;72(5):1369–1374. doi:10.1097/TA.0b013e3182464ba4
- Henrique LR, Crispim D, Vieceli T, et al. Copeptin and stress-induced hyperglycemia in critically ill patients: A prospective study. *PLoS One*. 2021;16(4):e0250035. doi:10.1371/journal.pone.0250035
- Zhang C, Shen HC, Liang WR, et al. Relationship between stress hyperglycemia ratio and all-cause mortality in critically ill patients: Results from the MIMIC-IV database. *Front Endocrinol (Lausanne)*. 2023;14:1111026. doi:10.3389/fendo.2023.1111026
- Li L, Ding L, Zheng L, et al. U-shaped association between stress hyperglycemia ratio and risk of all-cause mortality in cardiac ICU. *Diabetes Metab Syndr*. 2024;18(1):102932. doi:10.1016/j.dsx.2023.102932
- Chen Q, Su H, Yu X, et al. The stress hyperglycemia ratio improves the predictive ability of the GRACE score for in-hospital mortality in patients with acute myocardial infarction. *Hellenic J Cardiol*. 2023;70:36–45. doi:10.1016/j.hjc.2022.12.012
- Duan H, Yun HJ, Rajah GB, et al. Large vessel occlusion stroke outcomes in diabetic vs. non-diabetic patients with acute stress hyperglycemia. *Front Neurosci*. 2023;17:1073924. doi:10.3389/fnins.2023.1073924
- Mi D, Li Z, Gu H, et al. Stress hyperglycemia is associated with in-hospital mortality in patients with diabetes and acute ischemic stroke. *CNS Neurosci Ther*. 2022;28(3):372–381. doi:10.1111/cns.13764
- Yao SL, Chen XW, Liu J, Chen XR, Zhou Y. Effect of mean heart rate on 30-day mortality in ischemic stroke with atrial fibrillation: Data from the MIMIC-IV database. *Front Neurol*. 2022;13:1017849. doi:10.3389/fneur.2022.1017849
- Bone RC, Balk RA, Cerra FB, et al. Definitions for sepsis and organ failure and guidelines for the use of innovative therapies in sepsis. *Chest*. 1992;101(6):1644–1655. doi:10.1378/chest.101.6.1644
- Beniwal A, Singh O, Juneja D, et al. Clinical course and outcomes of cancer patients admitted in medical ICU with sepsis. *J Intensive Care Soc*. 2023;24(4):351–355. doi:10.1177/17511437221136831
- Lei W, Ren Z, Su J, et al. Immunological risk factors for sepsis-associated delirium and mortality in ICU patients. *Front Immunol*. 2022;13:940779. doi:10.3389/fimmu.2022.940779
- Zhang X, Man KW, Li GHY, Tan KC, Kung AWC, Cheung CL. Osteoporosis is a novel risk factor of infections and sepsis: A cohort study. *eClinicalMedicine*. 2022;49:101488. doi:10.1016/j.eclinm.2022.101488
- Ling H, Chen M, Dai J, Zhong H, Chen R, Shi F. Evaluation of qSOFA combined with inflammatory mediators for diagnosing sepsis and predicting mortality among emergency department. *Clin Chim Acta*. 2023;544:117352. doi:10.1016/j.cca.2023.117352
- Peng X, Chen C, Chen J, et al. Tree-based, two-stage risk factor analysis for postoperative sepsis based on Sepsis-3 criteria in elderly patients: A retrospective cohort study. *Front Public Health*. 2022;10:1006955. doi:10.3389/fpubh.2022.1006955
- Lin S, He W, Zeng M. Association of diabetes and admission blood glucose levels with short-term outcomes in patients with critical illnesses. *J Inflamm Res*. 2020;13:1151–1166. doi:10.2147/JIR.S287510
- Krinsley JS, Rule P, Pappy L, et al. The interaction of acute and chronic glycemia on the relationship of hyperglycemia, hypoglycemia, and glucose variability to mortality in the critically ill. *Crit Care Med*. 2020;48(12):1744–1751. doi:10.1097/CCM.0000000000004599
- Xia Z, Gu T, Zhao Z, et al. The stress hyperglycemia ratio, a novel index of relative hyperglycemia, predicts short-term mortality in critically ill patients after esophagectomy. *J Gastrointest Oncol*. 2022;13(1):56–66. doi:10.21037/jgo-22-11
- Rau CS, Kuo SCH, Tsai CH, et al. Elevation of white blood cell subtypes in adult trauma patients with stress-induced hyperglycemia. *Diagnostics (Basel)*. 2023;13(22):3451. doi:10.3390/diagnostics13223451
- Manriquez-Núñez J, Mora O, Villarroja F, Reynoso-Camacho R, Pérez-Ramírez IF, Ramos-Gómez M. Macrophage activity under hyperglycemia: A study of the effect of resveratrol and 3H-1,2-dithiole-3-thione on potential polarization. *Molecules*. 2023;28(16):5998. doi:10.3390/molecules28165998
- McCowan KC, Malhotra A, Bistrian BR. Stress-induced hyperglycemia. *Crit Care Clin*. 2001;17(1):107–124. doi:10.1016/S0749-0704(05)70154-8
- Tan Y, Cheong MS, Cheang WS. Roles of reactive oxygen species in vascular complications of diabetes: Therapeutic properties of medicinal plants and food. *Oxygen*. 2022;2(3):246–268. doi:10.3390/oxygen2030018
- Frydrych LM, Fattahi F, He K, Ward PA, Delano MJ. Diabetes and sepsis: Risk, recurrence, and ruination. *Front Endocrinol (Lausanne)*. 2017;8:271. doi:10.3389/fendo.2017.00271

38. Parks OB, Eddens T, Sojati J, et al. Terminally exhausted CD8⁺ T cells contribute to age-dependent severity of respiratory virus infection. *Immun Ageing*. 2023;20(1):40. doi:10.1186/s12979-023-00365-5
39. Al Abbasi B, Torres P, Ramos-Tuarez F, et al. Implementation of the surviving sepsis campaign in patients with heart failure: Gender-specific outcomes. *Cureus*. 2020;12(7):e9140. doi:10.7759/cureus.9140
40. Mewes C, Runzheimer J, Böhnke C, et al. Association of sex differences with mortality and organ dysfunction in patients with sepsis and septic shock. *J Pers Med*. 2023;13(5):836. doi:10.3390/jpm13050836
41. Akinosoglou K, Kapsokosta G, Mouktaroudi M, et al. Diabetes on sepsis outcomes in non-ICU patients: A cohort study and review of the literature. *J Diabetes Complications*. 2021;35(1):107765. doi:10.1016/j.jdiacomp.2020.107765

Quality of life assessment after minimally invasive operative treatment in children with pectus excavatum: A single-center study and literature review

Kacper K. Krocze^{1,A–F}, Joanna Sebastian^{2,A,B}, Iwona Szymkuć-Bukowska^{2,A}, Małgorzata Pyskir^{2,A,C,E}, Przemysław Gałązka^{1,A,C,E,F}

¹ Department of Pediatric Surgery, Antoni Jurasz University Hospital No. 1, Faculty of Medicine, Ludwik Rydygier Medical College in Bydgoszcz, Nicolaus Copernicus University in Toruń, Poland

² Department of Clinical Rehabilitation, Ludwik Rydygier Collegium Medicum in Bydgoszcz, Poland

A – research concept and design; B – collection and/or assembly of data; C – data analysis and interpretation; D – writing the article; E – critical revision of the article; F – final approval of the article

Advances in Clinical and Experimental Medicine, ISSN 1899–5276 (print), ISSN 2451–2680 (online)

Adv Clin Exp Med. 2025;34(9):1485–1492

Address for correspondence

Kacper K. Krocze

E-mail: kacper.krocze@gmail.com

Funding sources

None declared

Conflict of interest

None declared

Received on March 25, 2024

Reviewed on May 30, 2024

Accepted on October 10, 2024

Published online on January 16, 2025

Cite as

Krocze K, Sebastian J, Szymkuć-Bukowska I, Pyskir M, Gałązka P. Quality of life assessment after minimally invasive operative treatment in children with pectus excavatum: A single-center study and literature review.

Adv Clin Exp Med. 2025;34(9):1485–1492.

doi:10.17219/acem/194483

DOI

10.17219/acem/194483

Copyright

Copyright by Author(s)

This is an article distributed under the terms of the Creative Commons Attribution 3.0 Unported (CC BY 3.0) (<https://creativecommons.org/licenses/by/3.0/>)

Abstract

Background. Most patients with chest wall deformities have a negative body image, which affects their self-esteem and quality of life (QoL).

Objectives. The aim of this study was to evaluate changes in patients' QoL after minimally invasive repair of pectus excavatum (MIRPE).

Materials and methods. A prospective, single-center study was conducted between 2019 and 2023. We included 20 pediatric patients at a median age of 15 years and 9 months who underwent MIRPE. Two QoL questionnaires were used: the KIDSCREEN-52 and the EQ-5D-Y. The data were statistically analyzed with the Wilcoxon and Mann–Whitney tests. All patients and their parents were asked to complete questionnaires preoperatively and 12 months after surgical treatment.

Results. All patients were followed up during the 12-month study period. The study group was comprised of 65% male patients. The median Haller index was 5.0 standard deviation (SD) = 1.58). The assessment of general health condition was higher among the boys (with postoperative improvement), though this finding was not statistically significant. Routine daily activities were easier for all patients after MIRPE ($p = 0.048$). The patients showed improved physical activity ($p = 0.038$) and psychological wellbeing ($p = 0.013$) after elevation of the anterior chest wall. There was no impact on relations with parents, free time or school environment, but we found better patient contact with peers in the postoperative period. A high correlation was confirmed between the parents' and the patients' responses in each questionnaire.

Conclusions. Chest wall deformities can have a strong impact on the patient's wellbeing, which is a very important part of psychological development in adolescents. Our study showed that improved QoL should be always considered as an indication for surgical treatment of chest wall deformities in children.

Key words: quality of life, pectus excavatum, thoracic wall, adolescent health, health-related quality of life

Background

Pectus excavatum (PE) is a congenital chest wall anomaly characterized by an anterior depression of the sternum and ribs with an incidence of 1:1,000 in children.¹ Pectus excavatum can present at an early age, but commonly occurs during the rapid physiological growth associated with puberty.²

A negative body image is found in most patients with chest wall deformities, which affects their self-esteem and quality of life (QoL).³ Many patients reduce their daily activities to avoid the embarrassment and fear of feeling abnormal compared to their peers. Cosmetic complaints are still the main indication for surgical treatment.⁴

The main goal of PE correction is to improve the patient's self-esteem, body image and physical difficulties.^{5,6} Currently, the "gold standard" surgical treatment for PE is the Nuss procedure. The aim of this surgery was to elevate the anterior chest wall and stabilize the sternum in a neutral position. This method uses the elasticity of the chest wall in adolescents, allowing for successful remodeling over time.⁷ Patient satisfaction and good long-term outcomes have been reported following minimally invasive repairs of PE (MIRPE) in children and adults.

Objectives

The aim of this study was to investigate whether MIRPE improves QoL and overall satisfaction in adolescents.

Material and methods

Study design

We conducted a prospective study between October 2019 and August 2023. All patients were children and underwent MIRPE with titanium bars and titanium stabilizers (ChM Sp. z o.o., Lewickie, Poland). All patients over the age of 16 years gave informed consent, as did their parents. In total, 20 patients were included in the study. The mean age was 15 years and 9 months (range: 13–17.8; SD = 1.48), with 65% of them being male. All patients underwent a Nuss procedure for PE.

The responses to the EQ-5D-Y questionnaire were compared between the male (n = 13) and female (n = 7) groups. Each patient and their parents completed the questionnaire before surgery and 12 months afterwards. Each dimension in the questionnaire was analyzed.

The study was approved by the Institutional Bioethics Board of Collegium Medicum UMK in Bydgoszcz, Poland (approval No. KB 710/2019). This study applied the Strengthening the Reporting of Observational Studies in Epidemiology (STROBE) statement.

Clinical information

The minimal age for inclusion was 12 years. Patients with coexisting chest wall anomalies, congenital heart disease, pulmonary disease, or a history of cardiac/thoracic surgery were excluded from the study.

All operations were performed by the same pediatric surgeon. The operative technique was similar in every patient. All MIRPE procedures were performed under general anesthesia. A bilateral oblique skin incision was made in an anterior axillary line on both sides of the chest wall after the points of deepest deformity were identified. Subcutaneous tunnels were created bilaterally. A 5-mm trocar was introduced into the right pleural cavity and the procedure was performed under thoracoscopic visualization. A dedicated dissector was inserted from the right side of the chest, going across the anterior mediastinum to the left side. A titanium bar was fixed to the tip of the dissector and inserted when the dissector was removed from the chest. Next, the bar was rotated 180 degrees and short stabilizers were implanted at each tip of each bar. Additional bars were placed in a similar approach as needed to ensure appropriate correction. The pneumothorax was evacuated with tube connected to the thoracoscopic port under a water seal. Lung expansion and bar position were always confirmed for about 6 h postoperatively. The bar removal was scheduled for 3 years after the Nuss procedure. Postoperative pain management was based on a local analgesia protocol. Each patient was discharged with a well-controlled oral pain medication.

Quality of life assessment

The patients were examined with 2 standardized QoL protocols – preoperatively and 1 year postoperatively. The 1st instrument was the EQ-5D-Y questionnaire, which is a tool for measuring health-related QoL in the context of cost-effectiveness. It is designed to be completed by children and adolescents. The EQ-5D-Y descriptive system consists of 5 dimensions: "mobility", "looking after myself", "doing usual activities", "having pain or discomfort", and "feeling worried, sad or unhappy". Each dimension has 3 levels: "no problem", "some problems" and "a lot of problems".^{8,9}

The 2nd QoL assessment tool was the KIDSCREEN-52 questionnaire. This instrument is intended to provide a multidimensional analysis of health-related QoL in children. It is divided into 10 main domains: "physical well-being", "psychological well-being", "mood and emotions", "self-perception", "autonomy", "parental relations and home life", "financial resources", "peers and social support", "school environment", and "bullying". We used 2 types of the KIDSCREEN-52 questionnaire designed for patients between 8 and 18 years old and for parents.¹⁰

Statistical analyses

Statistical analysis was carried out using SPSS for Windows v. 12.0 (SPSS Inc., Chicago, USA). The Wilcoxon test was used to assess the significance of differences between preoperative and postoperative results and between parents' and patients' responses. The Mann–Whitney test was used to compare preoperative and postoperative results between the male and female groups. The distribution of the data was assessed using the Shapiro–Wilk test. Due to the non-normal distribution, the analysis was performed using nonparametric tests. A p -value <0.05 was considered a significant result.

Results

The patients' general characteristics are presented in Table 1.

Preoperative and postoperative evaluation using EQ-5D-Y was completed by parents and patients, divided into a male and a female group. The results of this analysis are presented in Table 2.

No male patients declared problems with mobility in either the preoperative or postoperative evaluation.

Table 1. Patient characteristics

Feature	Mean	SD
Age [years]	15.76	1.48
Weight [kg]	56.79	7.90
Height [cm]	173.72	8.28
BMI	18.82	2.17
Haller index	5.0	1.58
Length of stay [days]	6.6	1.35

SD – standard deviation; BMI – body mass index.

Table 2. Mann–Whitney test (comparing male and female groups in preoperative and postoperative evaluation) and multiple correction comparison

EQ-5DY Dimension	Z	p-value	Benjamini–Hochberg
EQ-5DY Mobility I	–1.980	0.048	0.192
EQ-5DY Mobility II	–1.363	0.173	0.336
EQ-5DY “Looking after myself” I	–1.216	0.224	0.336
EQ-5DY “Looking after myself” II	0.000	1.000	1
EQ-5DY Daily activities I	–1.828	0.068	0.204
EQ-5DY Daily activities II	–1.980	0.048	0.192
EQ-5DY Pain and discomfort I	–1.287	0.198	0.336
EQ-5DY Pain and discomfort II	–1.699	0.089	0.213
EQ-5DY Feeling sad I	–0.715	0.474	0.632
EQ-5DY Feeling sad II	–1.977	0.048	0.192
EQ-5DY General health condition I	–0.476	0.634	0.760
EQ-5DY General health condition II	–0.243	0.808	0.881

Statistically significant results are in bold.

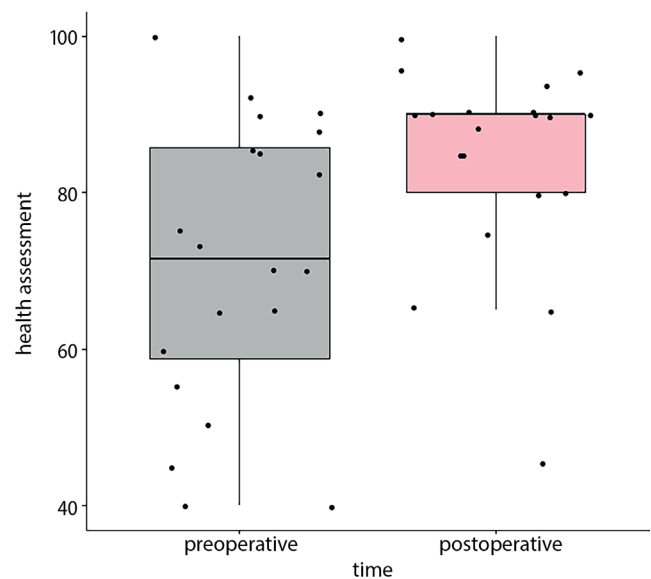


Fig. 1. EQ-5-DY health assessment (time)

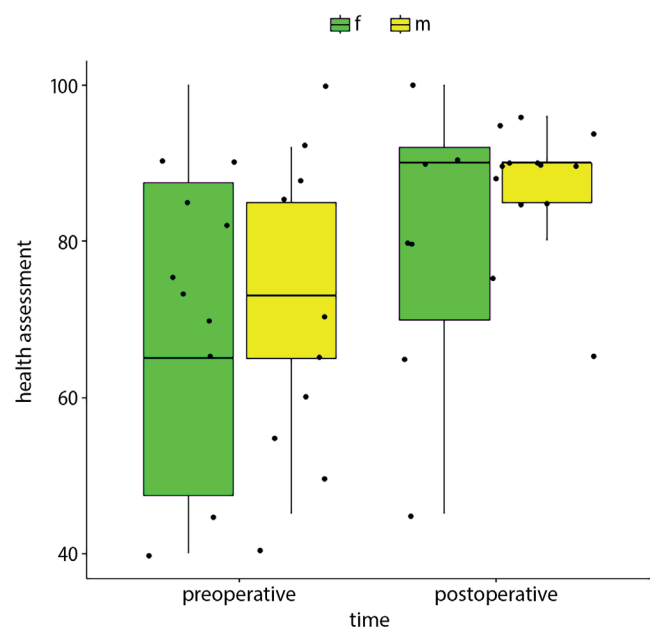


Fig. 2. EQ-5-DY Health assessment (sex)

Preoperative problems with mobility were more pronounced in girls than boys ($p = 0.048$), with no differences after surgical treatment. Daily routine activities were easier for patients postoperatively, mainly among the boys (mean = 1.0 vs 1.29; $p = 0.048$). There were no differences in the dimension of anxiety and “feeling sad” among the girls, but this indicator was higher in the postoperative period than in the group of “boys” (mean = 1.71 vs 1.15; $p = 0.048$). We did not reveal any important differences in postoperative mobility, perioperative “looking after myself” or “feeling pain and discomfort”, and daily activities. The boys’ assessments of their general health condition were higher (with postoperative improvement), though this finding was not statistically significant (Fig. 1,2).

Table 3. Results of Wilcoxon tests with multiple comparison correction

KIDSCREEN-52 Dimension	Z	p-value	Benjamini–Hochberg
KIDSCREEN-52 PHYSICAL ACTIVITY II – KIDSCREEN-52 PHYSICAL ACTIVITY I	–2.073	0.038	0.095
KIDSCREEN-52 WELL-BEING II – KIDSCREEN-52 WELL-BEING I	–2.470	0.013	0.077
KIDSCREEN-52 GENERAL MOOD II – KIDSCREEN-52 GENERAL MOOD I	–2.279	0.023	0.077
KIDSCREEN-52 SELF-PERCEPTION II – KIDSCREEN-52 SELF-PERCEPTION I	–1.483	0.138	0.173
KIDSCREEN-52 FREE TIME II – KIDSCREEN-52 FREE TIME I	–1.626	0.104	0.173
KIDSCREEN-52 PARENTAL RELATIONS AND HOME LIFE II – KIDSCREEN-52 PARENTAL RELATIONS AND HOME LIFE I	–1.257	0.209	0.232
KIDSCREEN-52 FINANCIAL PROBLEMS II – KIDSCREEN-52 FINANCIAL PROBLEMS I	–1.940	0.052	0.104
KIDSCREEN-52 CONTACT WITH PEERS II – KIDSCREEN-52 CONTACT WITH PEERS I	–2.333	0.020	0.077
KIDSCREEN-52 SCHOOL ENVIRONMENT II – KIDSCREEN-52 SCHOOL ENVIRONMENT I	–1.529	0.126	0.173
KIDSCREEN-52 BULLYING II – KIDSCREEN-52 BULLYING I	–0.574	0.566	0.566

Descriptive statistics (I – preoperative, II – postoperative). Statistically significant results are in bold.

Table 4. Patients descriptive statistic results

KIDSCREEN-52 Dimension	n	Mean	Median	IQR	Lower quartile	Upper quartile
KIDSCREEN-52 PHYSICAL ACTIVITY I	20	16.50	17	4.5	14.5	19
KIDSCREEN-52 PHYSICAL ACTIVITY II	20	18.65	19	3	17	20
KIDSCREEN-52 WELL-BEING I	20	21.05	21	3.25	19.75	23
KIDSCREEN-52 WELL-BEING II	20	23.75	25	5	21	26
KIDSCREEN-52 GENERAL MOOD I	20	13.65	14	5.25	10.75	16
KIDSCREEN-52 GENERAL MOOD II	20	11.00	9.5	3.25	9	12.25
KIDSCREEN-52 SELF-PERCEPTION I	20	15.00	16	2	14	16
KIDSCREEN-52 SELF-PERCEPTION II	20	13.90	14	1.25	13	14.25
KIDSCREEN-52 FREE TIME I	20	18.55	19	3	17	20
KIDSCREEN-52 FREE TIME II	20	19.50	20	5	17	22
KIDSCREEN-52 PARENTAL RELATIONS AND HOME LIFE I	20	22.90	22	5.25	20	25.25
KIDSCREEN-52 PARENTAL RELATIONS AND HOME LIFE II	20	24.15	24	4.5	22	26.5
KIDSCREEN-52 FINANCIAL PROBLEMS I	20	11.85	11.5	5	10	15
KIDSCREEN-52 FINANCIAL PROBLEMS II	20	12.75	12	4	11	15
KIDSCREEN-52 CONTACT WITH PEERS I	20	19.20	20.5	7.5	15.5	23
KIDSCREEN-52 CONTACT WITH PEERS II	20	22.15	24	7	18	25
KIDSCREEN-52 SCHOOL ENVIRONMENT I	20	19.25	20.5	2.5	18.75	21.25
KIDSCREEN-52 SCHOOL ENVIRONMENT II	20	21.10	22	5.25	19	24.25
KIDSCREEN-52 BULLYING I	20	3.7	3	1.25	3	4.25
KIDSCREEN-52 BULLYING II	20	3.70	3	1.25	3	4.25

Descriptive statistics (I – preoperative, II – postoperative). IQR – interquartile range.

A comparative analysis of preoperative and postoperative results in patients with PE using the KIDSCREEN-52 questionnaire was performed. We also analyzed the postoperative responses of children and parents. The results are presented in Table 3,4.

Following the MIRPE procedure, patients exhibited increased levels of physical activity (Fig. 3) (18.65 vs 16.50; $p = 0.038$). Improvement in psychological wellbeing was also reported in the postoperative period (23.75 vs 21.05; $p = 0.013$). There were no differences in self-perception, free time, parental relations and home life, or financial problems.

Also, there was no impact on school environment or bullying, but the patients reported better contact with peers after the operation (22.15 vs 19.20; $p = 0.02$) (Fig. 4). Our study found worse general mood after correction of PE than before the operation (11.0 vs 13.65; $p = 0.023$). In the authors' opinion, this was probably caused by typical mood variability in adolescents, especially since the improvement in general psychological wellbeing during the postoperative period was revealed to be statistically significant ($p = 0.013$).

An increase in total points for the postoperative assessment was observed for physical activity, patient wellbeing,

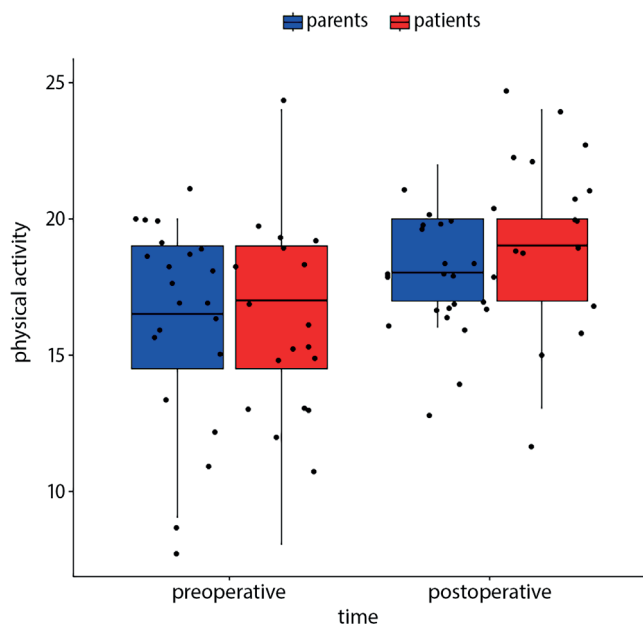


Fig. 3. Physical activity results

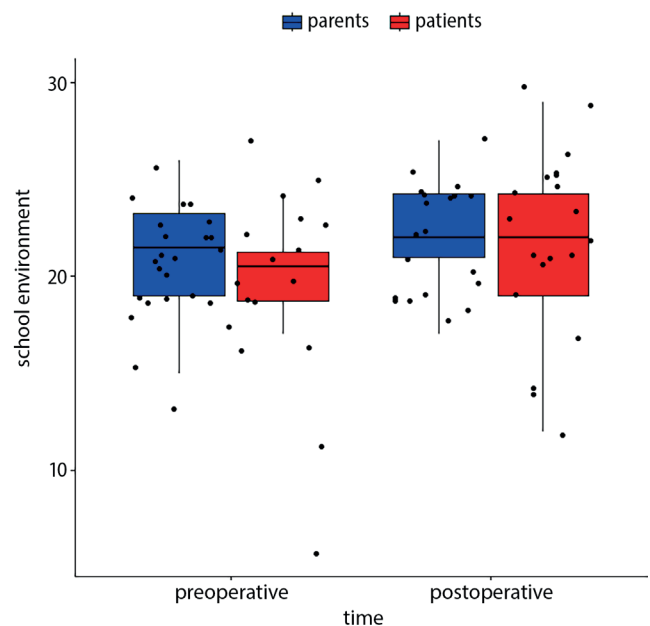


Fig. 5. School environment results

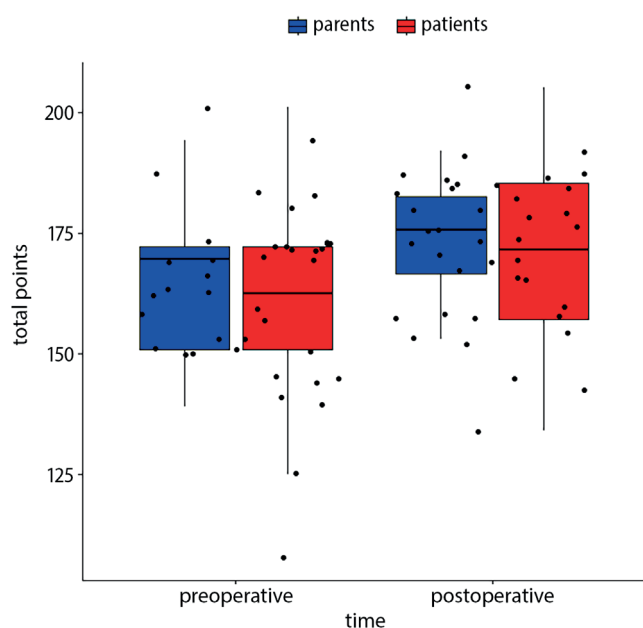


Fig. 4. Total points results

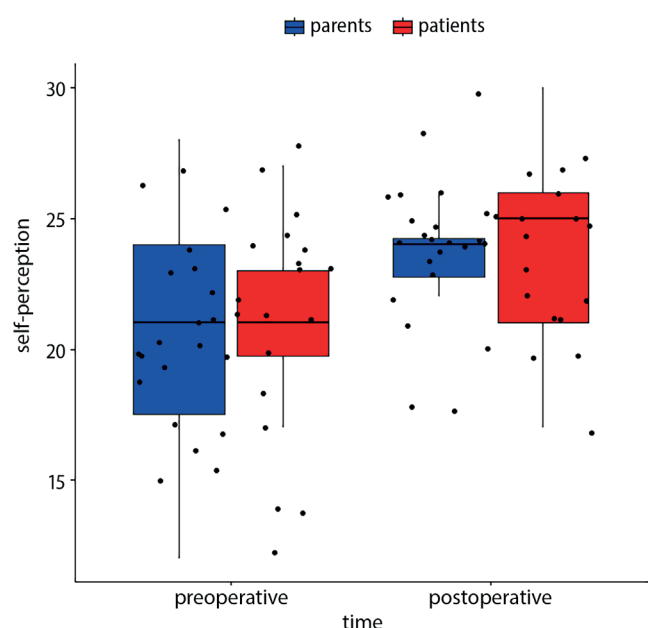


Fig. 6. Self-perception results

contact with peers, and school environment (box-whisker plots in Fig. 3–7).

We found a high correlation between the patients' and their parents' responses in each dimension of the KID-SCREEN-52 questionnaire. No statistically significant differences were identified between these groups (Table 5,6).

Discussion

Quality of life was defined by the World Health Organization in 1994 as “an individual's perception of their position in life in the context of the culture and value systems

in which they live and in relation to their goals, expectations, standards, and concerns.”¹¹ Adolescence is a period of life where many physical, social and emotional changes take place. During this time, physical appearance is an important subject because of changes in the body during puberty.¹²

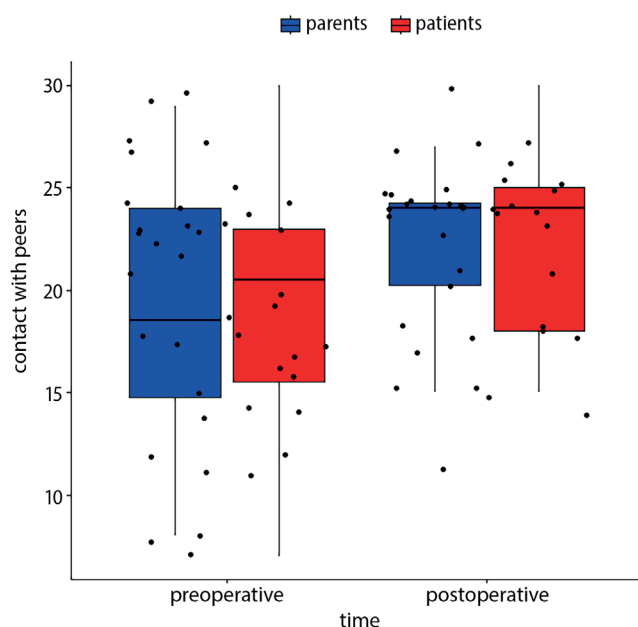
Frieson and Frieson and de Castro et al. described this transitional period as a strong impact point on an adult patient's life. One important area is self-esteem, a personal evaluation of oneself that influences one's behavior. It is well known that people with positive self-esteem are more capable of coping with life.^{13,14}

The main factor for the importance of body appearance during adolescence was first reported by Elkind in 1967

Table 5. Results of Wilcoxon tests with multiple comparison correction – comparison of postoperative results between parents and children

KIDSCREEN-52 Dimension	Z	p-value	Benjamini–Hochberg
KIDSCREEN-52 (parents) PHYSICAL ACTIVITY II – KIDSCREEN-52 PHYSICAL ACTIVITY II	0.328	0.743	0.826
KIDSCREEN-52 (parents) WELL-BEING II – KIDSCREEN-52 WELL-BEING II	0.641	0.520	0.826
KIDSCREEN-52 (parents) GENERAL MOOD II – KIDSCREEN-52 GENERAL MOOD II	0.574	0.566	0.826
KIDSCREEN-52 (parents) ABOUT YOUR CHILD II – KIDSCREEN-52 SELF-PERCEPTION II	0.345	0.730	0.826
KIDSCREEN-52 (parents) FREE TIME II – KIDSCREEN-52 FREE TIME II	0.654	0.512	0.826
KIDSCREEN-52 (parents) PARENTAL RELATIONS AND HOME LIFE II – KIDSCREEN-52 PARENTAL RELATIONS AND HOME LIFE II	0.995	0.320	0.826
KIDSCREEN-52 (parents) FINANCIAL PROBLEMS II – KIDSCREEN-52 FINANCIAL PROBLEMS II	0.854	0.393	0.826
KIDSCREEN-52 (parents) CONTACT WITH CHILD PEERS II – KIDSCREEN-52 CONTACT WITH PEERS II	0.027	0.978	0.978
KIDSCREEN-52 (parents) SCHOOL ENVIRONMENT II – KIDSCREEN-52 SCHOOL ENVIRONMENT II	0.939	0.347	0.826
KIDSCREEN-52 (parents) BULLYING II – KIDSCREEN-52 BULLYING II	0.407	0.684	0.826

Descriptive statistics (I – preoperative, II – postoperative).

**Fig. 7.** Contact with peers results

as “adolescent egocentrism.” It is a result of a typical social cognitive development process. Adolescents are unable to discriminate between other people’s thought and their own mental preoccupations. They are apprehensive about other people’s opinions, especially about body image and actions.^{15,16}

Pectus excavatum is a deformity with a physiological and psychological impact on patients, decreasing their QoL. Patients with this condition can experience a disturbed body image and lower self-esteem. Chest wall congenital anomaly can cause embarrassment, which in turn may negatively affect social interactions.^{3,17} In 2008, Kelly et al. reported that PE has a significant impact on patients’ and their parents’ wellbeing. The main goal of surgical treatment is to improve body image, self-esteem and QoL.¹⁸ The Nuss procedure (MIRPE) has become the gold

standard surgical treatment of pectus excavatum in the pediatric population.

We compared QoL of our patients prior to the operation and 12 months afterwards. We found remarkable differences in the patients’ perception of specific dimensions of their life. These findings are similar to other reported results. Lawson et al. and Roberts et al. revealed that the Nuss procedure has a positive impact on physical and psychological wellbeing of children and their perception of QoL.^{19,20}

Chest deformation decreases children’s daily activities in over 70% of cases (reported generally for PE and carinatum). Usually, patients withdraw from social activities like swimming or sunbathing because of fear of being judged by their peers. A higher incidence of depression was reported in the PE patient group.¹

Walsh et al. state that the perception of congenital chest wall deformity is individual; for many patients, a mild defect is tolerated, but for some, it is a source of severe psychological distress. It usually occurs during adolescence – the time of social development and interaction with peers.

We found better contact with peers after treatment in the study group. Patients who withdrew from social activities because of PE had reduced health-related QoL.²¹

In our study group, the patients’ assessment of their general health condition was better postoperatively. This confirms lower health-related QoL in the pediatric population with chest wall deformities.

Many authors have assessed QoL using health-related generic questionnaires. In 2016, Lomholt et al. studied a group of 107 patients evaluated with the Child Health Questionnaire and compared to 183 controls. The patients and their parents revealed improved self-esteem, emotional wellbeing and social activities when comparing preoperative and postoperative periods.²²

An interesting fact of our study was that we did not find any important differences in the perioperative “looking after myself” dimension. This probably is an effect

Table 6. Patients and parents descriptive statistic results

KIDSCREEN-52 Dimension	n	Mean	Median	IQR	Lower quartile	Upper quartile
KIDSCREEN-52 PHYSICAL ACTIVITY II	20	18.65	19	3	17	20
KIDSCREEN-52 (parents) PHYSICAL ACTIVITY II	20	18.65	19	3	17	20
KIDSCREEN-52 WELL-BEING II	20	23.75	25	5	21	26
KIDSCREEN-52 (parents) WELL-BEING II	20	23.75	25	5	21	26
KIDSCREEN-52 GENERAL MOOD II	20	11.00	9.5	3.25	9	12.25
KIDSCREEN-52 (parents) GENERAL MOOD II	20	11.00	9.5	3.25	9	12.25
KIDSCREEN-52 SELF-PERCEPTION II	20	13.90	14	1.25	13	14.25
KIDSCREEN-52 (parents) ABOUT YOUR CHILD II	20	13.90	14	1.25	13	14.25
KIDSCREEN-52 FREE TIME II	20	19.50	20	5	17	22
KIDSCREEN-52 (parents) FREE TIME II	20	19.50	20	5	17	22
KIDSCREEN-52 PARENTAL RELATIONS AND HOME LIFE II	20	24.15	24	4.5	22	26.5
KIDSCREEN-52 (parents) PARENTAL RELATIONS AND HOME LIFE II	20	24.15	24	4.5	22	26.5
KIDSCREEN-52 FINANCIAL PROBLEMS II	20	12.75	12	4	11	15
KIDSCREEN-52 (parents) FINANCIAL PROBLEMS II	20	12.75	12	4	11	15
KIDSCREEN-52 CONTACT WITH PEERS II	20	22.15	24	7	18	25
KIDSCREEN-52 (parents) CONTACT WITH CHILD PEERS II	20	22.15	24	7	18	25
KIDSCREEN-52 SCHOOL ENVIRONMENT II	20	21.10	22	5.25	19	24.25
KIDSCREEN-52 (parents) SCHOOL ENVIRONMENT II	20	21.10	22	5.25	19	24.25
KIDSCREEN-52 BULLYING II	20	3.70	3	1.25	3	4.25
KIDSCREEN-52 (parents) BULLYING II	20	3.70	3	1.25	3	4.25

Descriptive statistics (I – preoperative, II – postoperative). IQR – interquartile range.

of the small sample size and their individual perception of their body image.

Kelly et al. reported a multicenter study on 264 children and 291 parents. They used the Pectus Excavatum Evaluation Questionnaire (PEEQ). The children noted a significant improvement in body image and physical difficulties after surgery. The parents also noted an improvement in their children's emotions, self-consciousness and physical problems.¹⁸

The patients in our study had no problems with mobility before or after operative treatment. This is probably due to good compliance: each of them was obliged to perform a set of exercises in the preoperative and postoperative periods. We assume that preoperative problems with mobility and daily activities were higher in the group of girls because of their lower motivation to engage in physical activities during adolescence.

It was also demonstrated that disease severity and symptoms varied and were patient-specific. Every case should be individualized because there is no correlation between the degree of anterior chest wall depression and the patient's problems.¹⁸ The PEEQ has been used as a disease-specific tool in many studies. The PEEQ is centered on aspects strongly including questions about typical patients' problems with chest wall deformity. In our study, we evaluated children after MIRPE to detect changes in general areas of patient life, not only treatment-related changes.

Our results are similar to those of Lawson et al., who found that patients' assessment of QoL after a Nuss procedure correlates to their parents' assessment.¹⁹

Limitations

Our study has several limitations, such as the small study group and the lack of long-term follow-up (e.g., after removal of the titanium bar). The statistical analysis methods used in this research (Mann–Whitney and Wilcoxon tests) are only one-dimensional, so they give a simplified picture of the relationships between variables. More detailed statistical analyses, such as a multifactorial model, could be used in larger groups of patients. Multi-center studies including all children who underwent MIRPE could evaluate multifactorial aspects which have an impact on general QoL (differences between culture, environment, family, preschool problems, etc.). Such a survey would be significantly more valuable.

Conclusions

This study shows that PE correction with the Nuss procedure has a good effect on patients' wellbeing. Future studies should include multi-center studies using standardized questionnaires designed for children with chest wall deformities.

In conclusion, the Nuss procedure for correcting PE in children has a positive impact on QoL. This fact should be always considered during the qualification process for operative treatment of congenital chest deformities.

Data availability

The datasets generated and/or analyzed during the current study are available from the corresponding author on reasonable request.

Consent for publication

Not applicable.

ORCID iDs

Kacper K. Krocze  <https://orcid.org/0000-0002-1765-943X>
 Małgorzata Pyskir  <https://orcid.org/0000-0002-4305-7950>
 Przemysław Gałązka  <https://orcid.org/0000-0002-8227-8350>

References

- Steinmann C, Krille S, Mueller A, Weber P, Reingruber B, Martin A. Pectus excavatum and pectus carinatum patients suffer from lower quality of life and impaired body image: A control group comparison of psychological characteristics prior to surgical correction. *Eur J Cardiothorac Surg*. 2011;40(5):1138–1145. doi:10.1016/j.ejcts.2011.02.019
- Kelly RE, Martinez-Ferro M. Chest wall deformities. In: Holcomb GW, Murphy JP, St Peter SD, Gatti JM, Ashcraft KW, eds. *Holcomb and Ashcraft's Pediatric Surgery*. 7th ed. Edinburgh, UK-New York, USA: Elsevier; 2020:302–331.
- Krille S, Müller A, Steinmann C, Reingruber B, Weber P, Martin A. Self- and social perception of physical appearance in chest wall deformity. *Body Image*. 2012;9(2):246–252. doi:10.1016/j.bodyim.2012.01.005
- Krasopoulos G, Goldstraw P. Minimally invasive repair of pectus excavatum deformity. *Eur J Cardiothorac Surg*. 2011;39(2):149–158. doi:10.1016/j.ejcts.2010.07.019
- Lawson ML, Mellins RB, Paulson JF, et al. Increasing severity of pectus excavatum is associated with reduced pulmonary function. *J Pediatr*. 2011;159(2):256–261.e2. doi:10.1016/j.jpeds.2011.01.065
- Kelly RE, Mellins RB, Shamberger RC, et al. Multicenter study of pectus excavatum, final report: Complications, static/exercise pulmonary function, and anatomic outcomes. *J Am Coll Surg*. 2013;217(6):1080–1089. doi:10.1016/j.jamcollsurg.2013.06.019
- Nuss D, Kelly RE. Indications and technique of Nuss procedure for pectus excavatum. *Thorac Surg Clin*. 2010;20(4):583–597. doi:10.1016/j.thorsurg.2010.07.002
- Kelly RE, Goretsky MJ, Obermeyer R, et al. Twenty-one years of experience with minimally invasive repair of pectus excavatum by the Nuss procedure in 1215 patients. *Ann Surg*. 2010;252(6):1072–1081. doi:10.1097/SLA.0b013e3181effdce
- Wille N, Badia X, Bonsel G, et al. Development of the EQ-5D-Y: A child-friendly version of the EQ-5D. *Qual Life Res*. 2010;19(6):875–886. doi:10.1007/s11136-010-9648-y
- Bethell CD, Read D, Stein REK, Blumberg SJ, Wells N, Newacheck PW. Identifying children with special health care needs: Development and evaluation of a short screening instrument. *Ambul Pediatr*. 2002;2(1):38–48. doi:10.1367/1539-4409(2002)002<0038:ICWSHC>2.0.CO;2
- The WHOQOL Group. Development of the World Health Organization WHOQOL-BREF Quality of Life Assessment. *Psychol Med*. 1998;28(3):551–558. doi:10.1017/S0033291798006667
- Rumsey N, Harcourt D. Body image and disfigurement: Issues and interventions. *Body Image*. 2004;1(1):83–97. doi:10.1016/S1740-1445(03)00005-6
- Frieson T, Frieson C. Relationship between hope and self-esteem in renal transplant recipients. *J Transpl Coord*. 1996;6(1):20–23. doi:10.7182/prtr.1.6.1.q52347756145h374
- De Castro EK, Moreno-Jiménez B, Rodríguez-Carvajal R. Psychological well-being in adults transplanted in childhood. *Pediatr Transplant*. 2007;11(3):272–278. doi:10.1111/j.1399-3046.2006.00648.x
- Elkind D. Egocentrism in adolescence. *Child Dev*. 1967;38(4):1025–1034. doi:10.2307/1127100
- Choudhury S, Blakemore SJ, Charman T. Social cognitive development during adolescence. *Soc Cogn Affect Neurosci*. 2006;1(3):165–174. doi:10.1093/scan/nsl024
- Davison TE, McCabe MP. Adolescent body image and psychosocial functioning. *J Soc Psychol*. 2006;146(1):15–30. doi:10.3200/SOCP.146.1.15-30
- Kelly RE, Cash TF, Shamberger RC, et al. Surgical repair of pectus excavatum markedly improves body image and perceived ability for physical activity: Multicenter study. *Pediatrics*. 2008;122(6):1218–1222. doi:10.1542/peds.2007-2723
- Lawson ML, Cash TF, Akers R, et al. A pilot study of the impact of surgical repair on disease-specific quality of life among patients with pectus excavatum. *J Pediatr Surg*. 2003;38(6):916–918. doi:10.1016/S0022-3468(03)00123-4
- Roberts J, Hayashi A, Anderson JO, Martin JM, Maxwell LL. Quality of life of patients who have undergone the Nuss procedure for pectus excavatum: Preliminary findings. *J Pediatr Surg*. 2003;38(5):779–783. doi:10.1016/j.jpeds.2003.50166
- Walsh J, Walsh R, Redmond K. Systematic review of physiological and psychological outcomes of surgery for pectus excavatum supporting commissioning of service in the UK. *BMJ Open Res*. 2023;10(1):e001665. doi:10.1136/bmjresp-2023-001665
- Lomholt JJ, Jacobsen EB, Thastum M, Pilegaard H. A prospective study on quality of life in youths after pectus excavatum correction. *Ann Cardiothorac Surg*. 2016;5(5):456–465. doi:10.21037/acs.2016.08.02

Experience with sodium glucose cotransporter-2 inhibitors in adult patients with Fontan circulation

Paweł Skorek^{1,A–D,F}, Magdalena M. Frączek-Jucha^{2,3,A,D–F}, Agnieszka Sarnecka^{2,C–F},
Maciej Skubera^{2,B,E,F}, Natasza Libiszewska^{2,B,D,F}, Lidia Tomkiewicz-Pająk^{4,2,A,C,E,F}

¹ Doctoral School of Medical and Health Sciences, Jagiellonian University Medical College, Cracow, Poland

² Institute of Cardiology, Jagiellonian University Medical College, Cracow, Poland

³ Department of Disaster and Emergency Medicine, Jagiellonian University Medical College, Cracow, Poland

⁴ St. John Paul II Hospital, The Adult Congenital Heart Disease Centre, Jagiellonian University Medical College, Cracow, Poland

A – research concept and design; B – collection and/or assembly of data; C – data analysis and interpretation;

D – writing the article; E – critical revision of the article; F – final approval of the article

Advances in Clinical and Experimental Medicine, ISSN 1899–5276 (print), ISSN 2451–2680 (online)

Adv Clin Exp Med. 2025;34(9):1493–1499

Address for correspondence

Paweł Skorek

E-mail: pawel.skorek23@gmail.com

Funding sources

None declared

Conflict of interest

None declared

Acknowledgements

This article was supported by the Science Fund of St. John Paul II Hospital, Cracow, Poland (grant No. FN/11/2024 to L.T.P.) and the Jagiellonian University Medical College (grant No. N41/DBS/001106).

Received on June 5, 2024

Reviewed on August 24, 2024

Accepted on October 14, 2024

Published online on January 14, 2025

Cite as

Skorek P, Frączek-Jucha M, Sarnecka A, Skubera M, Libiszewska N, Tomkiewicz-Pająk L. Experience with sodium glucose cotransporter-2 inhibitors in adult patients with Fontan circulation. *Adv Clin Exp Med.* 2025;34(9):1493–1499. doi:10.17219/acem/194617

DOI

10.17219/acem/194617

Copyright

Copyright by Author(s)

This is an article distributed under the terms of the Creative Commons Attribution 3.0 Unported (CC BY 3.0) (<https://creativecommons.org/licenses/by/3.0/>)

Abstract

Background. We still know little about the effective pharmacological treatment of heart failure (HF) associated with the Fontan circulation. One of the new options may be sodium glucose cotransporter-2 inhibitors (SGLT2i), which have been proven effective in classic forms of left ventricular HF.

Objectives. To evaluate the effect and safety of SGLT2i inclusion in adults with Fontan circulation. To this end, we conducted observation and complex diagnostics of adult Fontan patients in whom we started treatment with flozins.

Materials and methods. The study population consisted of 17 adult Fontan patients with average age 30.5 (9.7) years, 59% in II New York Heart Association (NYHA) class, among whom 53% received dapagliflozin and rest empagliflozin.

Results. The average observation time was 11.0 (3.7) months. None of the patients have reported side effects or complications related to treatment. We observed a significant increase (20.1 mL/kg/min vs 24.2 mL/kg/min, $p = 0.008$) in the median of maximum oxygen uptake ($\dot{V}O_2$ max) among participants (9) who completed at least 2 reliable cardiopulmonary exercise tests. We did not notice any significant differences in N-terminal prohormone of brain natriuretic peptide concentration (641.35 (923.7) vs 741.47 (1,139.02), $p = 0.12$) after the inclusion. Interestingly, we observed a significant increase in erythrocytes (+6%, $p = 0.003$), hemoglobin (+7%, $p = 0.03$) and hematocrit (+7%, $p = 0.02$).

Conclusions. To the best of our knowledge, this is the first study to demonstrate that the implementation of SGLT2i may have a positive effect on exercise capacity among adults with Fontan circulation. Our experience confirms the high safety of using these drugs in Fontan adults.

Key words: heart failure, congenital heart disease, Fontan circulation, flozins

Background

The increasing number of adult patients with Fontan circulation (FC) is one of the greatest successes and at the same time challenges of modern cardiology of congenital heart disease (CHD). Recent studies indicate that in 2020, among 11 analyzed countries, the number of people after Fontan procedure was 47,881, of which 55% were adults, and in 2030 it will increase to 59,777 (64% adults).¹

Unfortunately, the number of multi-organ complications increases during follow-up, with heart failure (HF) being one of the most significant problems. In a single-center cohort study, clinical symptoms of HF were observed in 40% of FC patients over an average follow-up of 15.7 years.² Fontan circulation pathophysiology is not only complex but also poorly understood and includes, i.a., systolic and/or diastolic dysfunction of systemic ventricle, fibrosis and increased pulmonary resistance. The presence of HF symptoms in Fontan patients is associated with a very poor prognosis and reduced quality of life, and is the leading cause of death.³

Despite significant advances in care, there is still a lack of effective and guideline-directed options for managing FC failure, especially pharmacological ones.³ Previous attempts have largely been adapted from the recommendations dedicated strictly to the classic forms of HF,^{4,5} but these have generally yielded unsatisfactory results. Nevertheless, there are also promising reports of attempts to introduce new drugs, such as sacubitril/valsartan (ARNI) or sodium glucose cotransporter-2 inhibitors (SGLT2i), into the population of CHD. Fusco et al. in their study showed that the implementation of ARNI was associated with significant clinical improvement, including New York Heart Association (NYHA) class change and/or increased 6-minute walking distance after 1 year of follow-up among 50 adult patients with systemic right ventricle.⁶ There are also the first reports on the use of SGLT2i (commonly flozins) in the population with CHD. Despite the fact that SGLT2i are one of the newest additions to medical therapy in HF, their position is already well-established in HF guidelines and their update.^{4,5} According to these documents, SGLT2i (dapagliflozin or empagliflozin) are recommended for patients with HF with preserved ejection fraction, mildly reduced ejection fraction and with reduced ejection fraction to decrease the risk of HF hospitalization and/or death.^{4,5} These recommendations are based on the reduction of the primary composite endpoint used, e.g., in DAPA-HF, EMPEROR-Reduced, EMPEROR-Preserved and DELIVER trials.^{7–10} The above “universality” is even more important because patients with a single-ventricle heart after the Fontan procedure present a very heterogeneous picture of HF, with diastolic dysfunction dominating.^{1–3}

Objectives

Although SGLT2i are a cornerstone of HF pharmacotherapy, the literature on the use of flozins in the treatment of FC failure is still very limited.¹¹ This encouraged us to share our experience with the use of SGLT2i in the treatment of adult patients after Fontan surgery. The aim of this study was to evaluate the effect and safety of SGLT2i inclusion in adults with Fontan circulation.

Materials and methods

Study design and participants

The study was prepared in accordance with the appropriate Strengthening the Reporting of Observational Studies in Epidemiology (STROBE) checklist.¹² It was conducted from June 2022 to February 2024. The investigation included adult patients with symptoms of Fontan failure, defined as at least NYHA class II and/or chronic organ complications related to FC without any other objective cause (liver stiffness assessed with elastography to at least Metavir F3 score or proteinlosing enteropathy), hospitalized in our center and receiving SGLT2i in addition to their previous treatment. Each participant underwent detailed diagnostics to exclude potentially reversible or treatable causes of Fontan failure, including: tunnel stenosis, the presence of significant vascular anastomoses/malformations, pulmonary artery stenosis, and significant coarctation of the aorta, prior to initiation of SGLT2i. The exclusion criteria were: inability to give informed consent, cancer, pregnancy, current urinary tract infection, or a history of severe urinary tract infection in the last 12 months.

The investigation conforms with the principles outlined in the Declaration of Helsinki. The Ethics Committee at the Jagiellonian University (Cracow, Poland) approved the study (approval No. 118.6120.57.2023), and each participant provided written informed consent.

The following variables were collected from medical records: patient demographics, exact anatomy of CHD, medical therapy, past interventions and clinical complications, and hemodynamic data from the last invasive diagnostics. Before and after the initiation of SGLT2i treatment, each patient underwent a comprehensive diagnostic procedure used in our center for patients with FC.

The study was not blinded. Follow-up examinations were performed according to the clinical indications of the attending physician, but at intervals of at least 12 months.

Each patient was instructed in detail about the mechanism of action of SGLT2i, possible side effects, complications, and ways to reduce the risk of their occurrence. The above information was provided verbally and in writing in the discharge documentation.

Data sources and measurements

Venous blood was drawn from an antecubital vein with minimal stasis after an overnight fast. Laboratory tests such as the N-terminal prohormone of brain natriuretic peptide (NT-proBNP), blood cell count, total protein, creatinine, and aspartate aminotransferase (AST) levels were assayed using routine laboratory techniques.

The exercise tolerance was evaluated by the cardiopulmonary exercise testing (CPET) on a treadmill in the modified Bruce protocol (Reynolds Medical System, ZAN-600; Lode BV, Groningen, the Netherlands). Maximum oxygen uptake (VO_2 max) was defined as the highest value at peak workload in mL/kg/min and percentage of predicted value. The ventilatory equivalent for carbon dioxide (VE/VCO_2) was defined as the amount of ventilation needed for elimination of a given amount of CO_2 . The respiratory exchange ratio (RER) was calculated by dividing the VO_2 by VCO_2 . The test was considered reliable if the RER was at least 1.0. However, if the patient was unable to perform 2 reliable tests (initial and follow-up), their data were not included in the analysis of changes in exercise tolerance. Most of these cases involved musculoskeletal problems, both chronic and acute. Less frequently, the inability to perform this test was related to neurological disorders, fear of performing the test and, in only 1 case, poor clinical condition.

The NYHA functional class was estimated by an experienced adult CHD specialist based on the patient's self-reported symptoms and exercise tolerance. Abdominal ultrasound examination with elastography was conducted on all participants by a highly experienced researcher using Philips iU22 XMatrix Ultrasound System (Koninklijke Philips N.V., Amsterdam, the Netherlands). The transthoracic echocardiographic was performed (Philips CVx EPIQ model; Koninklijke Philips N.V.) by the same echocardiographer according to a uniform scheme. The following parameters were analyzed: ventricle morphology, peak velocity of blood flow through the dominant atrioventricular valve from left ventricular relaxation in early diastole (E) to peak flow velocity in late diastole due to atrial contraction (A), E/A ratio, velocity of annulus tissue of the dominant atrioventricular valve in early diastole (E'), E/E', annular plane systolic excursion of dominant atrioventricular valve (TAPSE/MAPSE), and, in a similar way, also Doppler tissue imaging-derived annular systolic velocity (S'). In patients with FC, it is difficult to assess the ejection fraction using echocardiography precisely and in accordance with classical terminology. However, various techniques were used to estimate systemic ventricular systolic function (primarily visual assessment by an experienced investigator), trying to replicate the classic ejection fraction (as preserved $\geq 50\%$, mildly reduced 41–49% and reduced $\leq 40\%$).

Statistical analyses

IBM SPSS Statistics v. 29.0 (IBM Corp., Armonk, USA) software was used for statistical analysis. Values of continuous

data were presented as mean \pm standard deviation (\pm SD) or median [interquartile range (IQR)], while the qualitative data were shown as the number and percentages. Continuous variables were first checked for normal distribution using the Shapiro–Wilk test. For repeated-measures analysis, a dedicated two-sided t-test for dependent groups or the Wilcoxon test was used. For all tests, p-value less than 0.05 was considered significant. Subgroup analysis was adjusted with Bonferroni's method. Study power was estimated at 0.93 for VO_2 max.

Results

To date, our study cohort includes 17 patients, whose clinical data are summarized in Table 1. The mean age of the group and time since the Fontan procedure were 30.5 ± 9.7 years and 24.8 ± 9.8 years, respectively. In a slight majority of cases, the systemic ventricle had the structure of the right ventricle 9 (53%). The average height was 171.2 ± 8.9 cm and the average body weight was 62.6 ± 9.5 kg. Initially, most patients were in class II of the NYHA classification of HF symptoms (10 patients, 59%). The pharmacological treatment used before and during SGLT2i therapy is presented in Table 2.

Of the total number of participants, 9 (53%) received dapagliflozin, while the remaining participants were administered empagliflozin. The mean time from the start of treatment to the last follow-up visit was 11.0 ± 3.7 months. None of the patients reported any treatment-related adverse events or complications.

In the analysis of the entire study group, we did not observe any significant differences in NT-proBNP concentration before and after the inclusion of SGLT2i (Table 3, Fig. 1). The quantitatively analyzed echocardiographic parameters indirectly indicating systolic function, such as S' (7.7 ± 2.5 vs 7.5 ± 2.1 cm/s, $p = 0.78$) and TAPSE/MAPSE 13.6 ± 3.3 vs 14.3 ± 5.7 mm, $p = 0.64$), did not change significantly during the observation. Importantly, the E/A ($1.6 [1.1–1.8]$ vs $1.5 [1.1–1.8]$, $p = 0.55$) and E/E' ($8.3 [5.7–10.2]$ vs $8.2 [5.9–11]$ ratios, which are parameters of diastolic function, also remained similar. At the same time, we did not note any significant changes in the function of kidneys, liver or other analyzed laboratory tests (Table 3). The clinical condition of almost the entire group generally remained stable during follow-up. The analysis also showed no significant changes in the NYHA class ($p = 0.96$).

Initial and follow-up ergospirometry was performed in only 9 cases, for the reasons mentioned above. Interestingly, we observed a significant increase ($20.1 [18.6–23.7]$ vs $24.2 [22.5–25.9]$ mL/kg/min, $p = 0.008$) in VO_2 max among those who underwent the test (Fig. 2). However, we did not observe any significant difference ($42.4 [37.8–50.8]$ vs $40.9 [35.6–44.1]$, $p = 0.51$) in VE/VCO_2 . In additional analysis of this subgroup, there was also no significant difference in NT-proBNP levels before and after treatment (452.8 ± 353.9 vs 467.4 ± 389.4 pg/mL, $p = 0.70$).

Table 1. Baseline characteristics of study population.

Patient ID	Sex	Age	FO type	Years from FO	SV	NYHA	Liver stiffness	SpO ₂ [%]	PE/ Ascites	PLE	Fontan Mp [mm Hg]	EDP in SV [mm Hg]	Cath time [months]
1	F	41	LT + Fen	26	R	III	F2/3	88	++	–	15	11	+6
2	M	38	LT + Fen	32	L	III	F4	85	+++	–	DA	DA	DA
3	M	32	LT + Fen	23	R	III	F4	92	+++	+	15	13	–45
4	F	20	LT	18	R	II	F2/3	94	–	–	12	6	0
5	F	40	LT	35	R	II	F3/4	83	–	–	15	9	–15
6	F	32	LT + Fen	29	L	II/III	F2/3	85	+	–	9	7	14
7	M	20	TCPC + Fen	19	R	II	F2	80	–	–	12	10	–3
8	M	19	LT + Fen	6	L	III/IV	F2/3	81	+	+	15	8	+15
9	M	37	APC*	35	R	II	F2	93	–	–	8	5	+1
10	M	25	LT	19	R	II	F2/3	84	–	–	12	10	0
11	M	27	LT + Fen	25	L	II	F2/3	95	–	–	12	5	–76
12	M	33	LT	33	L	II	F2	90	–	+	10	6	–68
13	M	42	LT	40	L	I/II	F3/4	90	–	+	DA	DA	DA
14	F	51	APC**	37	L	II	F2	97	–	+	10	6	+14
15	M	19	LT + Fen	14	L	II	F2	89	–	+	14	13	+2
16	F	22	TCPC	12	R	II	F2/3	94	–	–	13	9	–26
17	M	23	LT + Fen	21	R	I/II	F3/4	91	–	–	12	9	–26

* – qualified for TCPC, the above observation was completed at the time of surgery due to the early perioperative period; ** – lack of patient consent to the proposed conversion to TCPC; APC – atriopulmonary connection; cath time – cardiac catheterization time in relation to the inclusion of flozins; DA – does not agree to invasive diagnostic; EDP in SV – end diastolic pressure in systemic ventricle; F – female; Fen – fenestration; Fontan Mp – Fontan connection mean pressure; FO – Fontan operation; FU – follow-up; L – left ventricle; LT – lateral tunnel; M – male; NYHA – New York Heart Association class; PE – peripheral edema; PLE – protein-losing enteropathy; R – right ventricle; SpO₂ – oxygen saturation; SV – systemic ventricle; TCPC – total cavopulmonary connection.

Table 2. The pharmacological treatment

Patient ID	Systolic function of SV*	Care time before SGLT2 [years]	FU time after add SGLT2 [months]	SGLT2i Type	ACEI/ ARB	ARNI	MRA	Loop diuretics	BB	Sildenafil	ASA	VKA	NOAC
1	R	11	17.6	DAPA	0	1	1	1	1	0	0	1	0
2	P	17	9.8	DAPA	0	0	1	1	0	0	0	1	0
3	P	5	19.2	DAPA	0	0	1	1	1	1	0	1	0
4	P	0	12.6	DAPA	0	0	0	0	0	0	1	0	0
5	M	4	10.5	EMPA	0	0	1	1	1	1	0	0	1
6	P	12	12.7	DAPA	0	0	0	0	0	1	0	0	1
7	M	0	11.5	EMPA	0	0	1	0	1	0	1	0	0
8	P	0	8	DAPA	0	0	1	1	0	0	0	0	1
9	M	12	3.2	DAPA	0	0	0	0	1	1	0	1	0
10	P	0	13.6	EMPA	0	1	1	0	0	1	1	0	0
11	P	7	10.5	DAPA	0	0	1	0	0	0	0	0	1
12	P	14	12.7	EMPA	1	0	1	0	1	0	1	0	0
13	P	12	8.8	EMPA	0	0	1	0	1	0	0	1	0
14	P	10	10.6	EMPA	0	1	0	1	0	1	0	0	1
15	P	0	9.5	EMPA	1	0	1	1	0	0	0	1	0
16	P	2	11.7	EMPA	1	0	1	0	1	0	1	0	0
17	P	4	11.7	DAPA	0	0	1	0	1	0	0	0	1
Overall		6.5 ±5.8	11.0 ±3.7	9 DAPA 8 EMPA	3 (18%)	3 (18%)	13 (76%)	7 (41%)	9 (53%)	6 (35%)	5 (29%)	6 (35%)	6 (35%)

* – Estimated using various techniques, trying to replicate the classic ejection fraction (as preserved ≥50%, mildly reduced for 41–49% and reduced ≤40%); ACEI – angiotensin-converting-enzyme inhibitors; ARB – angiotensin receptor blockers; ARNI – angiotensin receptor-neprilysin inhibitors; ASA – acetylsalicylic acid; BB – beta-blockers; DAPA – dapagliflozin; EMPA – empagliflozin; FU – follow-up; M – mildly-reduced systolic function; MRA – mineralocorticoid receptor antagonists; NOAC – non-VKA oral anticoagulants; P – preserved systolic function; R – reduced systolic function; SGLT2i – sodium glucose cotransporter-2 inhibitors; SV – single ventricle; VKA – vitamin K antagonists.

Table 3. Laboratory data

Factor	Initial	Last FU	p-value
SBP [mm Hg]	116 ±11	115 ±13	0.79
DBP [mm Hg]	67 [58–74]	62 [58–82]	0.78
SpO ₂ [%]	90 [84–93]	90 [86–93]	0.73
NT-proBNP [pg/mL]	641.35 ±923.7	741.47 ±1139.02	0.12
Hemoglobin [g/dL]	16.51 ±1.7	17.61 ±1.9	0.03
Hematocrit [%]	48.61 ±4.6	51.82 ±5.4	0.02
RBC [g/dL]	5.72 ±0.5	6.06 ±0.72	0.003
MCH [pg]	29.7 [27.75–31.15]	29.9 [28.25–31.3]	0.33
MCHC [g/dL]	34.1 [33.15–35.0]	34.2 [33.7–35.05]	0.96
MCV [fL]	85.8 [82.25–89.3]	87.7 [82.3–90.2]	0.48
RDW [%]	14.76 ±2.1	15.13 ±3.0	0.56
WBC [10 ³ /μL]	5.65 ±1.3	5.27 ±1.3	0.29
PLT [10 ³ /μL]	139.0 [98–170]	132.0 [94–168]	0.54
Creatinine [μmol/L]	84.06 ±13.5	82.0 ±14.9	0.40
eGFR-CKD-EPI creatinine [mL/min/1.73 m ²]	99.53 ±21.1	100.65 ±21.7	0.71
Cystatin C [mg/L]	1.15 ±0.2	1.14 ±0.2	0.92
eGFR-CKD-EPI cystatin [mL/min/1.73 m ²]	74.88 ±16.2	74.41 ±15.9	0.83
ALT [U/L]	27.59 ±13.9	29.41 ±12.7	0.39
AST [U/L]	29.29 ±8.2	29.11 ±7.4	0.10
GGT [U/L]	91.71 ±59.9	91.71 ±49.8	1.0
Glucose [mmol/L]	4.9 [4.4–5.25]	4.7 [4.3–5.5]	0.51
Total protein [g/L]	74.67 ±10.9	75.19 ±8.6	0.81
Albumin [g/L]	43.09 ±6.7	42.95 ±7.1	0.9

ALT – alanine aminotransferase; AST – aspartate aminotransferase; CKD-EPI – Chronic Kidney Disease Epidemiology Collaboration equation; DBP – diastolic blood pressure; eGFR – estimated glomerular filtration rate; FU – follow-up; GGT – γ-glutamyltransferase; HCT – hematocrit; MCH – mean corpuscular hemoglobin; MCHC – mean corpuscular hemoglobin concentration; MCV – mean corpuscular volume; NT-proBNP – N-terminal prohormone of brain natriuretic peptide; PLT – platelets; RBC – red blood cells; RDW – red cell distribution width; SBP – systolic blood pressure; SpO₂ – peripheral oxygen saturation; WBC – white blood cells. Values are presented as mean ± standard deviation or median [interquartile range].

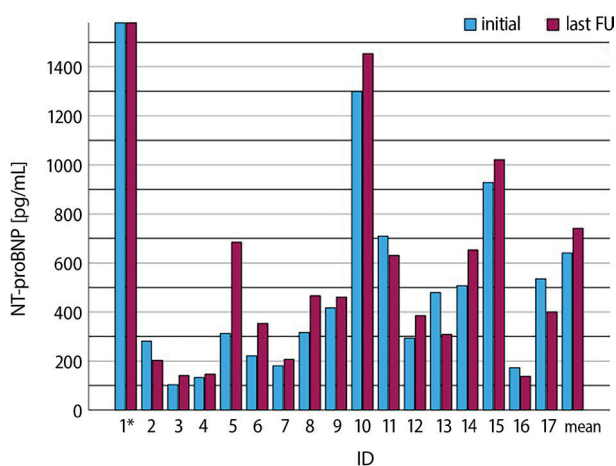


Fig. 1. Comparison of mean N-terminal prohormone of brain natriuretic peptide (NT-proBNP) values before treatment initiation and at the last follow-up. *NTproBNP levels in the observation number 1 (initial 4,018 pg/mL, in the last follow-up 4,955 pg/mL)

Interestingly, we observed a significant increase in red blood cell count (+6%, $p = 0.003$), hemoglobin level (+7%, $p = 0.03$) and hematocrit (+7%, $p = 0.02$) compared to baseline values in the entire cohort (Table 3). At the same time, the other

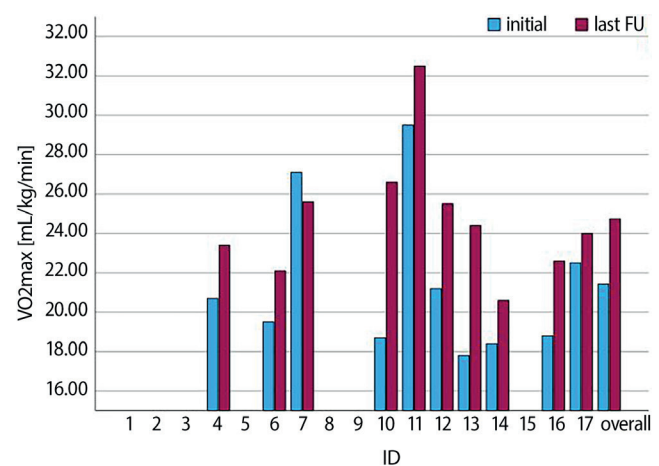


Fig. 2. Changes in the median values of maximum oxygen uptake (VO₂ max) during follow up in ergospirometry. The “overall” bar presents the median value for the entire analyzed group

analyzed erythrocytes parameters as well as the number of leukocytes and platelets did not differ significantly.

Additional subgroup analyzed in terms of systemic ventricular morphology (left vs right) showed no significant

differences in initial values of NT-proBNP (479.0 [257–608] vs 181.0 [152–917], $p = 0.54$) and VO_2 max (19.5 [18.1–25.4] vs 20.7 [18.8–24.8], $p = 0.66$). The subgroups did not differ in the final values of the above parameters (respectively, 385.0 [331–642] vs 207.0 [142–927], $p = 0.74$; 24.4 [20.6–29.0] vs 24.0 [23.0–26.1], $p = 0.84$).

Discussion

This is one of the first reports on the use of SGLT2i in the treatment of adult patients with a single-ventricle heart after the Fontan procedure.¹¹ Our experience confirms the high safety profile of using these drugs. We hope that our efforts to educate patients about the mechanism of action of SGLT2i have contributed to the lack of complications. However, our preliminary study also revealed interesting and important effects of flozins in patients with FC.

First of all, the average VO_2 max increased significantly during the observation period. This seems to be an important finding, whereas improvement in functional capacity is a component (besides improvement in clinical status and quality of life) of the 3 major goals of treatment of patients with HF. Our observations are similar to those from a large randomized controlled trial (RCT) in heart failure with reduced ejection fraction (HFrEF) patients, where VO_2 max significantly improved in the empagliflozin-treated group compared to placebo-treated patients.¹³

Like in many other studies, we used ergospirometry to assess the effectiveness of the therapeutic intervention.^{14–19} As we mentioned earlier, many of the previous attempts to apply recommendations from classic forms of HF to Fontan population have unfortunately not brought the expected results. Therefore, in trials using enalapril or carvedilol, as typical groups of drugs in HF, no improvement in exercise capacity was observed in the Fontan population.^{14–16} The effect of treatment with pulmonary vasodilators on changes in VO_2 max among Fontan patients remains unclear and controversial.¹⁷ Thus, this encourages further research on SGLT2i, especially considering the recently published positive results of using this drug group in adult patients with systemic right ventricle.¹⁸

The 2nd important finding from our study is a significant increase in erythrocytes, hemoglobin and hematocrit during follow-up. These changes are consistent with theories explaining many positive pleiotropic effects of flozins, not only due to reduced plasma volume secondary to increased diuresis.^{19–21} The organ primarily responsible for erythropoietin synthesis in adults is the kidney. The most basic hypotheses suggest a beneficial effect of SGLT2i on renal hemodynamics (with rejuvenation and protection of erythropoietin-producing cells) and on local hypoxia triggered by increased tubular workload.^{19–21} However, the above theories also have limitations, preventing a full explanation of this phenomenon.¹⁹ Packer suggests that SGLT2i may increase the role of the liver in erythropoietin regulation. Hepatocytes are the main

source of erythropoietin during fetal life, but they retain a latency to synthesize it also in adulthood. SGLT2i may influence inflammatory and cellular stress pathways, as well as erythropoietin gene transcription, especially in the liver.¹⁹ This is particularly interesting in Fontan population, as liver damage is an inherent part of long-term complications.^{22,23} However, frequent central cyanosis and the presence of additional vascular collaterals complicate the interpretation of these findings related to the red blood cell system in FC patients. The importance of the above processes in the cardioprotective effect remains unclear. Additionally, other pleiotropic effects associated with SGLT2i that may benefit FC and warrant further investigation.²⁴

In our study, we did not find significant changes in analyzed echocardiographic parameters. Patients with a single-ventricular heart after Fontan surgery constitute a very heterogeneous group of complex CHD. Echocardiographic examinations are very demanding, and the high risk of measurement error makes analysis of these parameters particularly challenging. However, there are reports in patients with normal cardiac anatomy where empagliflozin significantly improved left ventricular filling pressure.^{25,26}

In our study, we did not observe a significant decrease NT-proBNP levels after treatment, as in study by Neijenhuis et al.¹⁸ It should be emphasized that our study group reflects a real-life population of Fontan patients. Patients with various complications related to Fontan physiology and comorbidities were taken into consideration. For example, the impact of protein-losing enteropathy on the SGLT2i effect is unknown.² It was very common in our study population and may significantly interfere with absorption and metabolic processes.^{2,3} The very complex impact of protein-losing enteropathy on the body deserves to be taken into account in further studies of SGLT2i in patients with Fontan circulation. However, we did not notice that the inclusion of SGLT2i led to an intensification of symptoms, including protein-losing enteropathy. It is worth considering whether not only improvement but also the absence of deterioration is satisfactory, especially in such a demanding form of HF. So far, we have not analyzed the impact on the number of hospitalizations and HF exacerbations, which was the main focus of one of the largest studies on SGLT2i.^{4,5,7–10} However, the observation of our patients will be continued and flozins will be introduced in subsequent participants.

Limitations

There are several limitations to this study. First, this is only an observational study in a small group of patients. Large, high-quality studies are needed to confirm our findings. Second, there was no control group in our study. However, the high heterogeneity of patients with FC and their clinical condition makes it very difficult to select a suitable control group, and we decided that it would be best to observe the fate of specific patients. Third, the interpretation of the VO_2 max increase should be done with caution,

while not all patients were able to perform this test. Finally, our cohort of Fontan patients is heterogeneous in terms of the medications used, but represents real patients.

Conclusions

This study showed for the first time that the use of SGLT2i can improve VO₂ max in adult Fontan patients. We also observed significant changes that may support the hypothesis of a significant effect of SGLT2i on erythropoiesis. Finally, our experience shows that the use of SGLT2i in adult patients with FC is safe. Multicenter collaborations and large, high-quality trials are needed to more reliably assess the clinical effects of flosins in the adult FC population.

Data availability

The datasets generated and/or analyzed during the current study are available from the corresponding author on reasonable request.

Consent for publication

Not applicable.

ORCID iDs

Paweł Skorek  <https://orcid.org/0000-0002-4589-3696>
 Magdalena M. Frączek-Jucha  <https://orcid.org/0000-0003-3935-6250>
 Agnieszka Sarnecka  <https://orcid.org/0000-0002-8664-4717>
 Maciej Skubera  <https://orcid.org/0000-0001-6680-5504>
 Natasza Libiszewska  <https://orcid.org/0000-0001-8592-439X>
 Lidia Tomkiewicz-Pająk  <https://orcid.org/0000-0003-1564-7539>

References

- Plappert L, Edwards S, Senatore A, De Martini A. The epidemiology of persons living with Fontan in 2020 and projections for 2030: Development of an epidemiology model providing multinational estimates. *Adv Ther.* 2022;39(2):1004–1015. doi:10.1007/s12325-021-02002-3
- Piran S, Veldtman G, Siu S, Webb GD, Liu PP. Heart failure and ventricular dysfunction in patients with single or systemic right ventricles. *Circulation.* 2002;105(10):1189–1194. doi:10.1161/hc1002.105182
- Baumgartner H, De Backer J, Babu-Narayan SV, et al. 2020 ESC Guidelines for the management of adult congenital heart disease. *Eur Heart J.* 2021;42(6):563–645. doi:10.1093/eurheartj/ehaa554
- McDonagh TA, Metra M, Adamo M, et al; ESC Scientific Document Group. 2021 ESC Guidelines for the diagnosis and treatment of acute and chronic heart failure: Developed by the Task Force for the diagnosis and treatment of acute and chronic heart failure of the European Society of Cardiology (ESC). With the special contribution of the Heart Failure Association (HFA) of the ESC. *Eur J Heart Fail.* 2022;24(1):4–131. doi:10.1002/ehfj.2333
- McDonagh TA, Metra M, Adamo M, et al. 2023 Focused Update of the 2021 ESC Guidelines for the diagnosis and treatment of acute and chronic heart failure. *Eur Heart J.* 2023;44(37):3627–3639. doi:10.1093/eurheartj/ehad195
- Fusco F, Scognamiglio G, Merola A, et al. Safety and efficacy of sacubitril/valsartan in patients with a failing systemic right ventricle: A prospective single-center study. *Circ Heart Fail.* 2023;16(2):e009848. doi:10.1161/CIRCHEARTFAILURE.122.009848
- McMurray JJV, Solomon SD, Inzucchi SE, et al. Dapagliflozin in patients with heart failure and reduced ejection fraction. *N Engl J Med.* 2019;381(21):1995–2008. doi:10.1056/NEJMoa1911303
- Packer M, Anker SD, Butler J, et al. Cardiovascular and renal outcomes with empagliflozin in heart failure. *N Engl J Med.* 2020;383(15):1413–1424. doi:10.1056/NEJMoa2022190
- Anker SD, Butler J, Filippatos G, et al. Empagliflozin in heart failure with a preserved ejection fraction. *N Engl J Med.* 2021;385(16):1451–1461. doi:10.1056/NEJMoa2107038
- Solomon SD, De Boer RA, DeMets D, et al. Dapagliflozin in heart failure with preserved and mildly reduced ejection fraction: Rationale and design of the DELIVER trial. *Eur J Heart Fail.* 2021;23(7):1217–1225. doi:10.1002/ehfj.2249
- Muneuchi J, Sugitani Y, Kobayashi M, Ezaki H, Yamada H, Watanabe M. Feasibility and safety of sodium glucose cotransporter-2 inhibitors in adults with heart failure after the Fontan procedure. *Case Rep Cardiol.* 2022;2022:5243594. doi:10.1155/2022/5243594
- von Elm E, Altman DG, Egger M, et al. The Strengthening of Reporting of Observational Studies in Epidemiology (STROBE) statement: Guidelines for reporting observational studies. *Ann Intern Med.* 2007;147(8):573–577. doi:10.7326/0003-4819-147-8-200710160-00010
- Santos-Gallego CG, Vargas-Delgado AP, Requena-Ibanez JA, et al. Randomized trial of empagliflozin in nondiabetic patients with heart failure and reduced ejection fraction. *J Am Coll Cardiol.* 2021;77(3):243–255. doi:10.1016/j.jacc.2020.11.008
- Kouatli AA, Garcia JA, Zellers TM, Weinstein EM, Mahony L. Enalapril does not enhance exercise capacity in patients after Fontan procedure. *Circulation.* 1997;96(5):1507–1512. doi:10.1161/01.CIR.96.5.1507
- Hartevelde LM, Blom NA, Terol Espinosa De Los Monteros C, et al. 3-month enalapril treatment in pediatric Fontan patients with moderate to good systolic ventricular function. *Am J Cardiol.* 2022;163:98–103. doi:10.1016/j.amjcard.2021.10.013
- Butts R, Atz AM, BaezHernandez N, Sutcliffe D, Reisch J, Mahony L. Carvedilol does not improve exercise performance in Fontan patients: Results of a crossover trial. *Pediatr Cardiol.* 2021;42(4):934–941. doi:10.1007/s00246-021-02565-6
- Wang W, Hu X, Liao W, et al. The efficacy and safety of pulmonary vasodilators in patients with Fontan circulation: A meta-analysis of randomized controlled trials. *Pulm Circ.* 2019;9(1):2045894018790450. doi:10.1177/2045894018790450
- Neijenhuis RML, Nederend M, Jongbloed MRM, et al. The potential of sodium-glucose cotransporter 2 inhibitors for the treatment of systemic right ventricular failure in adults with congenital heart disease. *Front Cardiovasc Med.* 2023;10:1093201. doi:10.3389/fcvm.2023.1093201
- Packer M. Mechanisms of enhanced renal and hepatic erythropoietin synthesis by sodium–glucose cotransporter 2 inhibitors. *Eur Heart J.* 2023;44(48):5027–5035. doi:10.1093/eurheartj/ehad235
- Thiele K, Rau M, Hartmann NK, et al. Effects of empagliflozin on erythropoiesis in patients with type 2 diabetes: Data from a randomized, placebo-controlled study. *Diabetes Obes Metab.* 2021;23(12):2814–2818. doi:10.1111/dom.14517
- Mazer CD, Hare GMT, Connelly PW, et al. Effect of empagliflozin on erythropoietin levels, iron stores, and red blood cell morphology in patients with type 2 diabetes mellitus and coronary artery disease. *Circulation.* 2020;141(8):704–707. doi:10.1161/CIRCULATIONAHA.119.044235
- Skorek P, Skubera M, Natorka J, Ząbczyk M, Smaś-Suska M, Tomkiewicz-Pająk L. Role of red blood cells in hemostasis and whole blood clot contraction in adults after Fontan procedure. *Pol Arch Intern Med.* 2023;133(2):16412. doi:10.20452/pamw.16412
- Smaś M, Skubera M, Wilkosz T, et al. Noninvasive assessment of liver status in adult Fontan patients. *Pol Arch Intern Med.* 2019;129(3):181–188. doi:10.20452/pamw.4452
- Lan NSR, Fegan PG, Yeap BB, Dwivedi G. The effects of sodium-glucose cotransporter 2 inhibitors on left ventricular function: Current evidence and future directions. *ESC Heart Fail.* 2019;6(5):927–935. doi:10.1002/ehf2.12505
- Cai C, Guo Z, Chang X, et al. Empagliflozin attenuates cardiac microvascular ischemia/reperfusion through activating the AMPKα1/ULK1/FUNDC1/mitophagy pathway. *Redox Biol.* 2022;52:102288. doi:10.1016/j.redox.2022.102288
- Rau M, Thiele K, Hartmann NUK, et al. Empagliflozin does not change cardiac index nor systemic vascular resistance but rapidly improves left ventricular filling pressure in patients with type 2 diabetes: A randomized controlled study. *Cardiovasc Diabetol.* 2021;20(1):6. doi:10.1186/s12933-020-01175-5

Patient's characteristic included for treatment with individualized allogenic 3D bone block before or during/after orthodontic treatment: A 6-year observational study

Sebastian Dominiak^{A–F}, Marzena Dominiak^{A,D–F}, Paweł Kubasiewicz-Ross^{D–F}, Tomasz Gedrange^{A,D–F}

Department of Dental Surgery, Wrocław Medical University, Poland

A – research concept and design; B – collection and/or assembly of data; C – data analysis and interpretation;
D – writing the article; E – critical revision of the article; F – final approval of the article

Advances in Clinical and Experimental Medicine, ISSN 1899–5276 (print), ISSN 2451–2680 (online)

Adv Clin Exp Med. 2025;34(9):1501–1520

Address for correspondence

Sebastian Dominiak
E-mail: sebastian.dominiak95@wp.pl

Funding sources

None declared

Conflict of interest

None declared

Received on September 25, 2024

Revised on January 7, 2025

Accepted on January 10, 2025

Published online on March 11, 2025

Cite as

Dominiak S, Dominiak M, Kubasiewicz-Ross P, Gedrange T.
Patient's characteristic included for treatment with individualized allogenic 3D bone block before or during/after orthodontic treatment: A 6-year observational study.
Adv Clin Exp Med. 2025;34(9):1501–1520.
doi:10.17219/acem/199994

DOI

10.17219/acem/199994

Copyright

Copyright by Author(s)

This is an article distributed under the terms of the Creative Commons Attribution 3.0 Unported (CC BY 3.0) (<https://creativecommons.org/licenses/by/3.0/>)

Abstract

Background. The most important part of orthodontic treatment (OT) is the pre-orthodontic examination (PE). Only a precise evaluation of clinical and radiological features can reduce the risk of complications.

Objectives. To develop practical guidelines for advanced clinical-radiological pre-orthodontic examinations and for qualifying patients for alveolar bone reconstructions.

Materials and methods. A retrospective assessment was performed on 49 out of 145 patients (aged 22–55) referred for alveolar bone reconstructions over a 6-year observation period, with 77.6% of the patients being women. Patient examinations were conducted using the following parameters: clinical (e.g., gingival recession (GR), Miller and Angle classifications), radiological (using cone beam computed tomography (CBCT) to evaluate bone dehiscence, occlusal plane (OccP), atlanto-occipital joint position (O–C1), width of mentalis muscle (B:D), bone marrow steatosis (BMS), and various cephalometric parameters such as the position of the alveolar ridge (AR) relative to the mandible, labial width angle, and volumetry of AR, as well as vitamin D level. Statistical analyses were performed using Student's t-test, Shapiro–Wilk test and Pearson's χ^2 test.

Results. In the group of patients before orthodontic treatment (OT), the average bone marrow steatosis (BMS) was significantly lower compared to that in patients after treatment (–12 HU vs –137 Hounsfield units (HU)). In patients with class C dehiscence, the B:D measurement was significantly greater than in those with class A dehiscence (15.0 mm vs 12.5 mm). Additionally, a lateral shift of the atlanto-occipital joint (O–C1) had a significant negative impact on the angles describing lower teeth inclination. Overall, the odds of gingival recession (GR) were 6.5 times higher in women (OR = 6.55); GR odds increased by more than 3.5 times when B:D exceeded 14.1 mm, by 4 times when the occlusal plane (OccP) was flat, and by 8 times when bone density was 24.9 ng/mL.

Conclusions. Insufficient bone volume was observed in a similar proportion both before and during/after orthodontic treatment. The described pre-orthodontic examination allows for an accurate assessment of soft tissue and bone condition, thereby reducing the risk of further complications. CBCT should become a standard component of the pre-orthodontic examination.

Key words: orthodontics, early diagnosis, recession, cone-beam computed tomography, dehiscence

Highlights

- Modern orthodontic treatment faces problem of insufficient bone volume.
- Identifying possible complications before active treatment allows reducing chances of incomplete treatments.
- An analysis of patients conducted for augmentation of dehiscence in front of lower teeth demonstrate necessity of the CBCT examination
- Severe dehiscences might be congenital or iatrogenic as well.

Background

Dentition and dental arch sizes have progressed significantly in the last 100 years; however, orthodontic guidelines have not. Diet has been shown to have a major impact on the dentition, the orthodontic area of interest also had to change.^{1,2} As teeth and alveolar processes become smaller, consequently, a reduction in the width of the alveolar ridge is observed.

Therefore, during orthodontic treatment, a thorough pre-orthodontic examination must be performed, including evaluation of three-dimensional (3D) properties of the alveolar processes. For this purpose, cone beam computed tomography (CBCT) should be performed. Only this type of the X-ray examination allows to determine direction in which the orthodontic treatment should be carried out to avoid disturbing natural boundaries. Ignoring these principles is associated with a higher risk of complications such as gingival recessions, bone dehiscences, teeth mobility, or even teeth loss.^{3–5}

One of the most common complications are gingival recessions. They are described as a progressive loss of the gingiva and the underlying bone.^{6,7} According to the above information, when the tooth is translated through the vestibular cortical bone, bone dehiscence will occur. Taking into account the biological width, or supracrestal apparatus, which is the biologically determined distance between the alveolar crest and the top of the keratinized gingiva (typically around 2.04 mm), apical migration of the gingiva can occur.^{8,9} Considering that gingival recession is a common condition affecting much of the population, orthodontists face significant limitations in ridge expansion procedures to avoid violating the bony envelope and causing or exacerbating recession.¹⁰

Therefore, to avoid such complications, complete examination of the oral cavity should be carried out. Conditions which need to be taken into account are: the patient's gingival phenotype, palpable roots through the soft tissue, pre-existing recessions, or patient's pericervical restorations which may disturb biological width, and the depth of vestibule and frenula attachments. After (or even before) the intraoral examination, an extraoral examination should be done as well in which we should focus on the tension of the muscles surrounding the oral cavity, type of swallowing and breathing. Tension of the muscles around and inside the oral cavity is a crucial factor for the future success

of the planned treatment. Imbalance between internal and external muscles might be a reason for teeth inclination. However, strong tension of muscles, such as the mentalis or mylohyoid muscle, may reduce the volume of the dental arches. Additionally, if the lingual frenulum is stiff and short, it is called ankyloglossia. It is responsible for several problems inside the oral cavity. It might be a reason for malocclusions, anterior and posterior crossbite, open bite, mouth breathing, and enlarged space between teeth called diastema. However, the organism should be considered as a whole and not as individual parts, so if one part is not working properly, it will affect the others. The influence of ankyloglossia can also be seen in a bad posture. This is caused by the anterior fascia which interconnects the whole body, from head to toe. A shorter and/or stiffer tongue frenulum will misalign the temporomandibular joints, which may also affect the occlusal plane and back problem of muscular origin.^{11–13}

Leszczyszyn et al. reported a positive correlation between vitamin D₃ deficiency and problematic skeletal growth.¹⁴ As this vitamin controls bone metabolism, its levels should be checked prior to orthodontic treatment, with adequate supplementation. In general, the endogenous vitamin D₃ deficiency has been reported in the European population in several studies, so blood serum level should be assessed.¹⁵

However, vitamin D₃ deficiency is not just a general problem in dentistry, since it can lead to poorer bone architecture and volume. Worse bone quality, increased fragility and susceptibility to microdamage are the results of many autoimmune diseases as well. For instance, in the case of the diabetes type I, it is caused by microangiopathy, insulin resistance, and lack of insulin-like growth factor 1 (IGF-1). In case of type II diabetes, the drugs lowering sugar concentration in the blood serum might influence in bone fragility too.¹⁶ Celiac disease might affect bones through malabsorption of minerals and vitamin D from intestines.¹⁷ Even bleeding disorders, such as hemophilia, can reduce bone density, not to mention bone diseases such as Paget's disease.¹⁸ Another concerning issue is a growing problem of obesity and high-fat diet, common in a modern society. It weakens the bone by the T-lymphocytes which induce osteoclastogenesis through production of interleukin 6 (IL-6), osteoclastogenic cytokines such as RANKL, tumor necrosis factor alpha (TNF- α), IL-1 β , and interferon gamma (IFN- γ).¹⁹

Patients facing these challenges often seek treatment through individualized 3D allogeneic bone block grafting. This surgical method, described and patented by Dominiak and Gedrange, has shown promising results in resolving complications, completing problematic orthodontic treatments, and even initiating treatment in complex cases. The entire method and surgical procedure are described in previous publications.^{3–5,20}

Objectives

The aim of this study was twofold: first, to evaluate the characteristics of patients who require individualized 3D allogenic bone block grafting – either prior to orthodontic treatment or following complications – and second, to develop practical guidelines for advanced clinical-radiological pre-orthodontic assessments and patient qualification for alveolar bone reconstructions.

Materials and methods

The study was conducted in accordance with the guidelines of the Declaration of Helsinki. Data were collected and analyzed with the approval of the Bioethics Committee of Wrocław Medical University, Wrocław, Poland (approval No. KB-530/2021), and the study followed the Strengthening the Reporting of Observational Studies in Epidemiology (STROBE) checklist.²¹

Study group

Between 2018 and 2023, 145 patients were referred to a private dental clinic in Wrocław, Poland, for consultation regarding soft or hard tissue prior to (group 1) and during or after (group 2) orthodontic treatment. Group 1 consisted of 16 patients, of whom 10 were women (62.5%), with a mean age of 35 years. Group 2 comprised 33 patients, with 28 women (84.8%) and a mean age of 39 years. As a result, a group of 49 patients was identified. The analysis included adult Caucasian patients of both genders who were referred as follows:

- Patients with pre-existing abnormalities of the dental arches prior to orthodontic treatment, such as visible recessions, loss of keratinized gingiva, palpable roots through the soft tissue, and periodontitis.
- Prolonged or complicated orthodontic treatment.
- Patients after partially successful orthodontic treatment, for whom procedures were postponed due to insufficient tooth movement or discontinued by the orthodontist because of emerging soft and/or hard tissue issues.
- Patients with full examination including CBCT scans prior to the start of a treatment with severe loss of teeth support.

Additional inclusion criteria for the study were generally healthy patients, with bone defect located in the anterior part of alveolar process and symphysis with remaining dentition.

All patients with any past systemic diseases and drug treatments that could affect bone tissue (e.g., Paget's disease, osteoporosis, use of bisphosphonates, or denosumab), previous surgical or periodontal treatments in the anterior mandible, craniofacial anomalies, and previous trauma to the mandible were excluded from the study. All patients enrolled for study were qualified for the 3D allograft bone grafting procedure according to the method previously described.^{3,4}

Data collection

Data were gathered retrospectively from patients' records, which included complete examination notes, clinical intra- and extraoral photographs and radiological CBCT scans. This subchapter is structured to reflect the methodology of data collection. The assessment of extra- and intraoral soft and hard tissues, the relationship between the dento-alveolar arches to teeth, and the relationship between the position of the upper maxilla with dentition as a part of craniofacial part of the skull with and O-C1 joint (atlanto-occipital joint) position were made by 2 different doctors independently independently and merged into 1 dataset. These parameters were chosen because of their possible mutual influence of musculo-fascial system on the condition of craniofacial part of the cranium. The visual representation of data collection is shown in Fig. 1.

Radiological examination

The CBCT scans were acquired using the Pax Flex3D Vatech computed tomography radiography system (Vatech® Europe, Prague, Czech Republic). For the mandible center image, a field of view (FOV) of 80 mm in width and 50 mm in height was used, with a voxel size of 0.2 mm³. All images were analyzed using EzDent-i software (Vatech). Only CBCT scans that displayed the entire mandible and maxilla were included in the analysis.

Angle between the long axis of the tooth and the long axis of mandible

The angle between the long axis of the tooth and the long axis of the mandible (1:MI) was measured to assess tooth inclination; a larger angle indicated a more protruded tooth. This angle was measured on the sagittal plane of the CBCT using software tools, with a mean value ranging between 10° and 15°. The long axis of the tooth was defined as the line connecting the tip of the crown to the apical point of the most anterior mandibular central incisor (I1a). The long axis of the mandible was determined by identifying 2 points on the mandible and drawing a line between them: the 1st point was located at half the width

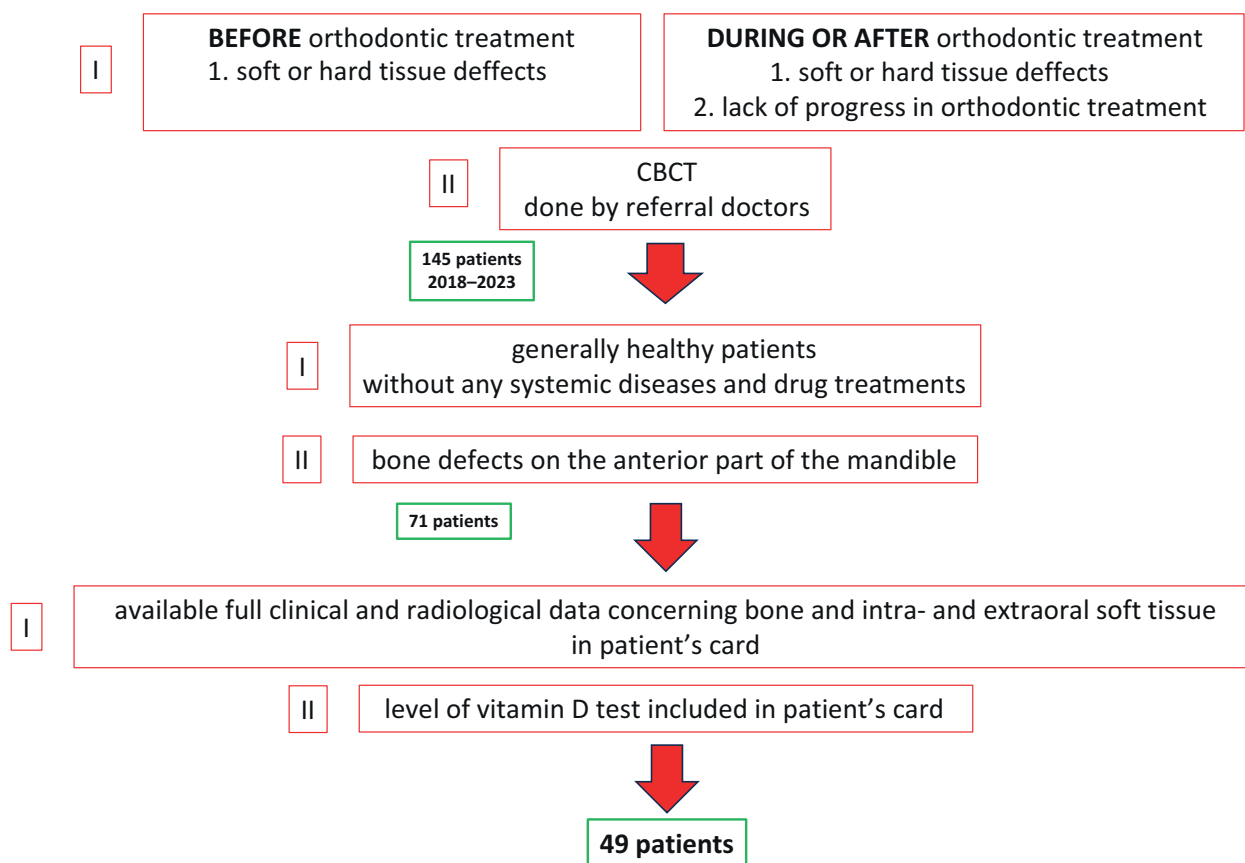


Fig. 1. Flowchart visualizing data collection

CBCT – cone beam computed tomography.

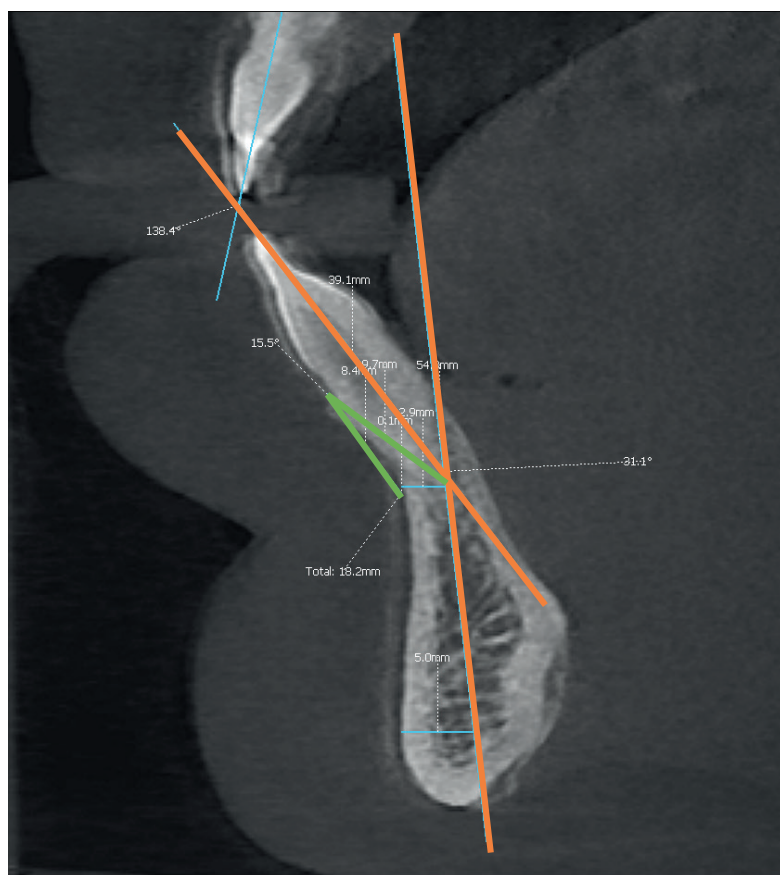


Fig. 2. Angle between long axis of the tooth and long axis of mandible (orange). Assessment of angle API-CEJ2-B (green)

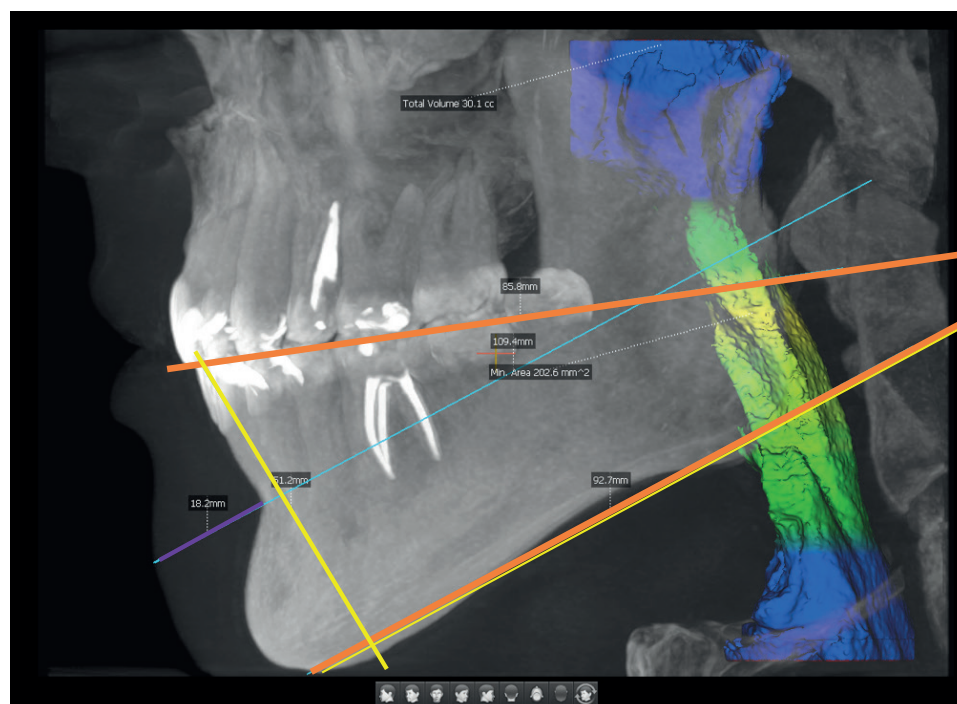


Fig. 3. Angle between the occlusal plane (OccP) and GoGn plane (orange). Angle set between lines set by Gnathion and Gonion points and long axis of the lower incisor (yellow). Assessment of the width of the mental muscle (purple)

in the tooth's apex region, and the 2nd was set 5 mm above the inferior border of the mandible (Gnathion (Gn)). The half-width point was also measured (Fig. 2).

API-CEJ2-B angle

The API-CEJ2-B angle was measured to assess the remaining labial bone in front of the teeth. Long lines were drawn connecting the following points: the deepest point on the anterior concavity of the mandibular symphysis (point B), the apical point of the most anterior mandibular central incisor (Iia), and the point located 2 mm apical to the cemento-enamel junction (CEJ) of the incisor (Fig. 2), which reflects the sulcus depth.²²

Classification of bone dehiscence

Examination of dehiscence was based on the sagittal plane of the CBCT, employing the classification system of Yang et al., as explained by Dominiak et al., to ensure accurate classification.^{5,23} The highest labial and lingual points of the alveolar wall were determined to select the appropriate class and then compared to the positions of the CEJ and the tooth apex. The classification stages were modified to provide a more detailed description of Class II, highlighting various stages of dehiscence on both sides of the dental arch. Additionally, a new class (Class X) was introduced to describe dehiscence occurring simultaneously on both the labial and lingual sides.

Interincisal angle (1:1 angle)

The interincisal angle is defined as the angle between the long axes of the lower and upper incisors. Its mean

value is approx. 122°, and it is used to assess the relationship between the lower and upper dental arches – particularly the protrusion of the incisors, which may indicate an insufficient bony base for the teeth. A decrease in this angle may suggest the need for tooth extraction as part of pre-orthodontic treatment.²⁴

1:GoGn angle

The GoGn angle is defined as the angle between the line connecting Gnathion (Gn) and Gonion (Go) and the long axis of the lower incisor. Its average value is approx. 90°. This angle provides information about the inclination of the alveolar process and teeth relative to the GoGn line.²⁵ It was measured on the sagittal plane of the entire area, which mimics a cephalometric X-ray. For optimal precision, the angle was measured using a protractor on a fixed screen image (Fig. 3).²⁶

OccP/GoGn angle

The angle between the occlusal plane (OccP) and the GoGn plane represents the inclination of the dental portion of the mandible relative to its base. Like the previous angle, it was measured using a protractor. For retrospective measurement on CBCT scans, a line was drawn from the tip of the lower incisor to the distal cusp of the lower first molar, and this line was compared to the GoGn line.

Anterior and lateral Stafne bone defects

The commonly known lateral or posterior Stafne bone defect is classified as a pseudocyst, with its origin attributed to either a salivary gland extension into the mandible

or calcification of Meckel's cartilage.²⁷ In contrast, the anterior Stafne bone defect is less documented in the literature. It is located in the anterior region of the mandible, below the teeth and above the mylohyoid muscle.²⁸ According to the 1993 classification, Stafne bone defects are divided into 4 types – the first 3 refer to posterior defects, while the 4th type represents the anterior Stafne bone defect (ASBD), which is explained as an insertion of the mylohyoid muscle.²⁹ This deviation from normal bone structure should be considered during pre-orthodontic examinations, as it may indicate high muscle tension that could be problematic due to the tongue's pushing pattern. Figure 4 illustrates both anterior and lateral Stafne bone defects.

Width of the mental muscle

The method for measuring the width of the mentalis muscle was proposed by Dominiak.²² Assessing this width helps estimate muscle tension and hyperactivity. In her method, a new landmark, point "D," is defined on the soft tissue. To locate point D, a "GoGn" line is drawn between the Gnathion and Gonion points. Additionally, point "B" is identified as the deepest point on the mandibular concavity. Next, a line parallel to the GoGn line is drawn through point B, and its intersection with the soft tissue border marks point D. The width of the mentalis muscle on the sagittal plane is then defined as the distance between points B and D (B:D) (Fig. 3).

Tongue position

Assessment of tongue position on CBCT scans was conducted on the midline sagittal plane. This approach allows for the visualization of the tongue, mylohyoid muscle, tongue frenulum, and the tongue's resting position, which may provide insights into the patient's breathing and swallowing patterns. Three classes have been established to categorize tongue positions: Class 0 – The tongue is positioned on the hard palate, with the entire dorsal surface in contact; Class 1 – The tongue is placed beneath the incisors; it may touch the palate, but not as extensively as in Class 0; Class 2 – The tongue rests at the bottom of the mouth.

Volume of the airways

Airway measurement has become accessible to dentists through the increased use of CBCT. Thanks to built-in software, airway assessment is now one of the options available during routine X-ray examinations. It is reported – and as shown in Fig. 5 below – that an airway capacity of approx. 200 mm² is considered satisfactory. To measure the airways, a CBCT scan with the full available field of view (80 mm in width and 50 mm in height) is required. Subsequently, the visible airway, extending

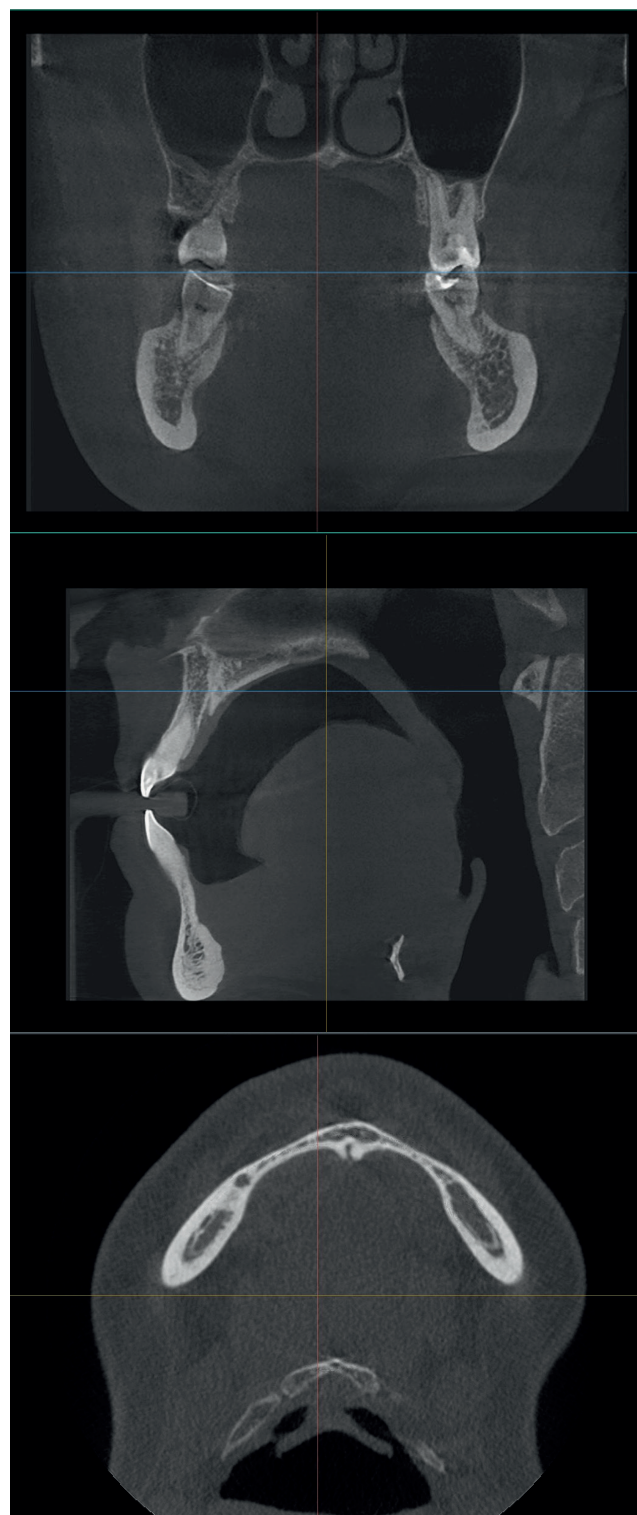


Fig. 4. Upper panel – anterior Stafne bone defect; middle panel – lateral Stafne bone defect; lower panel – anterior Stafne bone defect in occlusal view

from the nasopharynx to the sphincter, should be marked. It is known that airway narrowing is quite common in cases of malocclusion, especially in Class II malocclusion, where the retruded mandible reduces the space available for the tongue and decreases airway capacity.



Fig. 5. Measuring volume of airways and occlusal plane

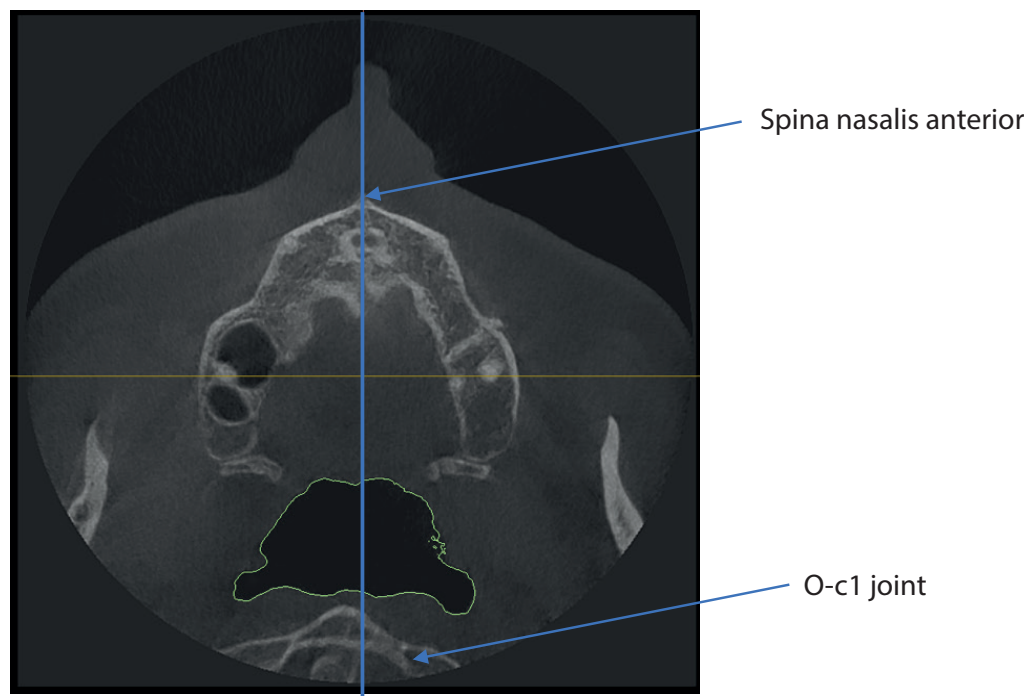


Fig. 6. Rotation of the O-c1 vs spina nasalis anterior

Abnormality in the position of the O-C1 joint

In addition to airway volume, the study investigated the correlation between lower airway capacity, dental abnormalities, and postural problems at a vertebral level. The deviation of the O-C1 (atlanto-occipital) joint was measured by automatically drawing a sagittal midline using the spina nasalis and the sutura palatina media as reference points. Any displacement of the O-C1 spinous

process relative to this midline was used to assess vertebral asymmetry. The methodology is illustrated in Fig. 6.

Occlusal plane

Abnormalities and changes in the occlusal plane are among the most common issues in dentistry. The occlusal plane (OccP) can be altered over time due to wear, excessive biting force, bruxism, iatrogenic factors from

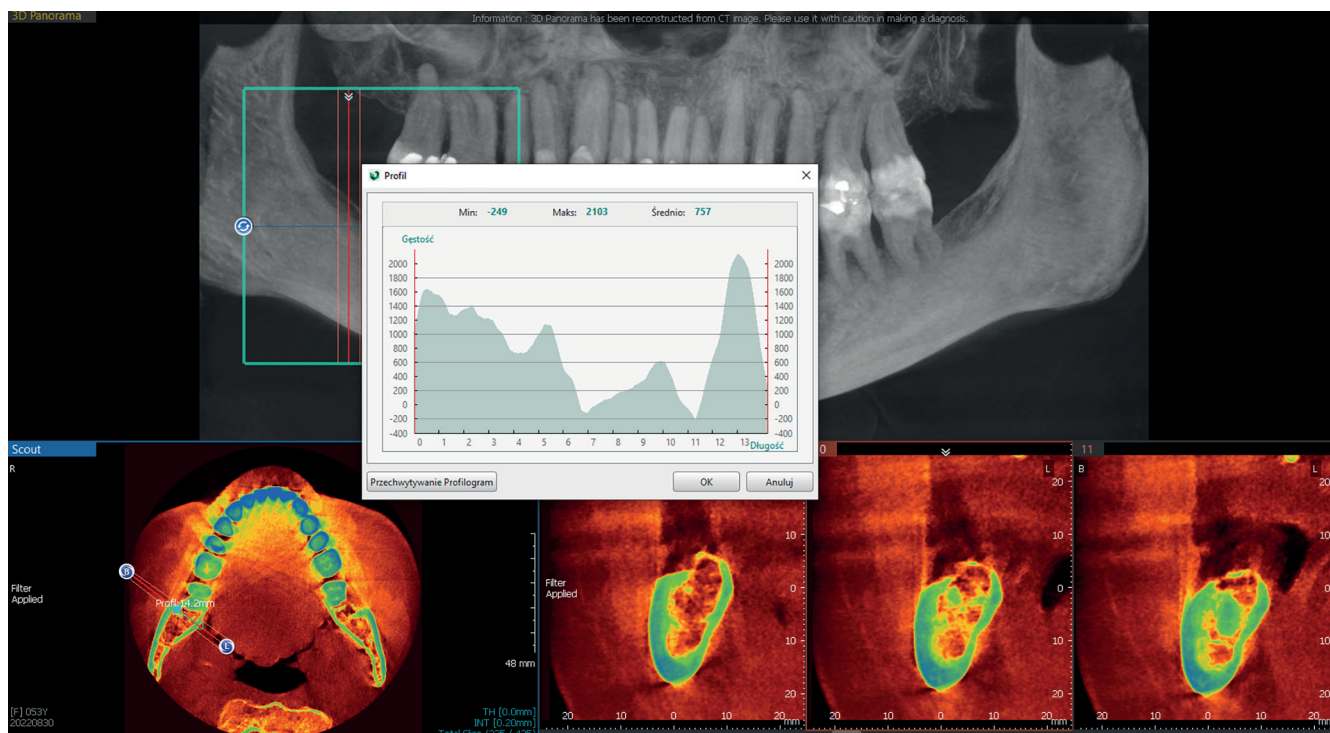


Fig. 7. Steatosis of bone marrow

dental procedures, or even congenital malocclusions. The occlusal plane is described in detail in point 6. If the cusps of the lower teeth align with the line following the curve of Spee, the occlusal plane is considered normal. If the curve of Spee is not maintained, the occlusal plane is classified as flat. If the curve of Spee is more pronounced, the occlusal plane is considered deepened. Finally, if the cusps of the premolars reach or extend above the line, the occlusal plane is referred to as a reverse occlusal plane (Fig. 3).

Bone marrow steatosis (BMS)

Measurement of this factor was enabled by the imaging software tools (Fig. 7). It was quantified in Hounsfield units (HU), which are based on a calibrated grey-level scale of X-ray images. Originally, HU measurements were used to assess tissue density on CT scans; however, several authors have reported that CBCT images yield similar values.^{30–32} Nevertheless, it should be noted that these measurements are approximations that indicate the general direction in which tissue characteristics are changing, and they cannot yet be used with the same precision as CT scans. For example, compact bone typically measures between 662 and 1988 HU, spongy bone between 148 and 661 HU and fat between –205 and –51 HU. Measurements were consistently taken at the end of the retromolar triangle, at the level of the beginning of the ascending ramus of the mandible, using a specialized sub-option of the Vatech software.

Clinical intra- and extraoral photographs

Non-carious lesions

These lesions occur without bacterial interference and are classified as a loss of hard tissue around the CEJ with various morphologies.³³ Their etiology is multifactorial; they can be caused by improper brushing techniques (particularly excessive force), erosive destruction or abfraction.³⁴ In any case, understanding their origin is essential, as these lesions may affect orthodontic treatment.

Gingival recession

Gingival recession is characterized by the progressive loss of soft tissue, along with bone loss in the anterior region of the teeth. This condition was verified through clinical and radiological examinations in a retrospective study, which utilized clinical photographs and CBCT scans. Miller's classification was employed to categorize the severity of the recession.⁶

Angle classification

To assess the presence of malocclusion, the classic Angle classification was used.³⁵ When the Angle classification was not applicable, e.g., when a tooth was missing, the canine classification was used instead. The position of the teeth was examined using clinical photographs.

Faces' profile type

To assess facial profile types, we distinguished between straight, oblique forward and oblique backward profiles. On clinical photographs, a vertical line was drawn from the Nasion, along with another line from the center of the iris, to create a biometric field. Two key points – Pogonion and Subnasale – were then evaluated in relation to this biometric field.

Examination notes

Orthodontic treatment

Patients were divided into 2 groups according to their treatment history: one group included patients before orthodontic treatment, and the other comprised those during or after orthodontic treatment.

Vitamin D₃

Vitamin D₃ levels and supplementation were assessed, as deficiency in vitamin D₃ has been implicated in the development of malocclusion. The vitamin D₃ level was determined using the VHC Vitamin-D-Test (Jungbrunnen–Fountain of Youth® GmbH, Rostock, Germany), a quantitative assay that employs immunochromatography to detect anti-25-OH-vitamin D monoclonal antibodies. Vitamin D₃ levels were measured from capillary blood samples obtained via a finger prick collection.³⁶

Statistical analyses

For quantitative variables, basic descriptive statistics were calculated, i.e., means (M), standard deviations (SD), minimum (Min), maximum (Max), medians (Me), and lower (Q1) and upper quartiles (Q3). In contingency tables, qualitative variables (nominal and ordinal) were presented as counts (n) and percentages (%). The Shapiro–Wilk test was used to confirm that the empirical distribution of quantitative variables fit the normal distribution. When quantitative data had a normal distribution, the t-test was used to check the statistical significance of differences in the mean values of quantitative variables between 2 independent groups, and when the data did not meet the assumptions of normality, the Mann–Whitney test was used. In the case of a larger number of groups, either analysis of variance and Tukey's test were used as a post hoc test, or the Kruskal–Wallis (K–W) test and Dunn's test were used as a post hoc test. The Pearson's χ^2 test with Yates's correction or Fisher's exact test were used to confirm the independence of 2 qualitative factors. Univariate and multivariate logistic regression analysis was used to estimate the probability of recession. Odds ratios (ORs) and their 95% confidence intervals (95% CIs) were estimated for statistically significant predictors of recession. For continuous variables, receiver operating characteristic (ROC) curve analysis and Youden index

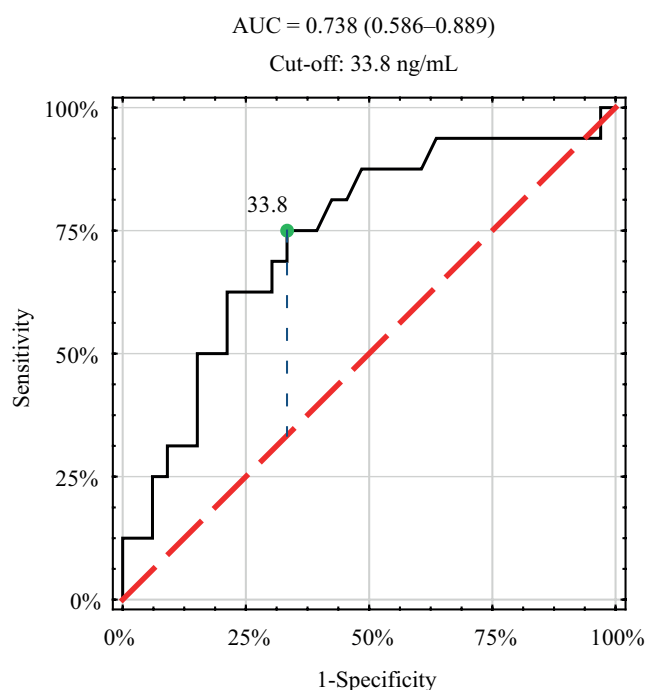


Fig. 8. Receiver operating characteristic (ROC) curve for estimating the probability of tongue position between incisors (group C) based on vitamin D₃ concentration, concentration threshold value (≥ 33.8 ng/mL) and area under the curve (AUC = 0.738)

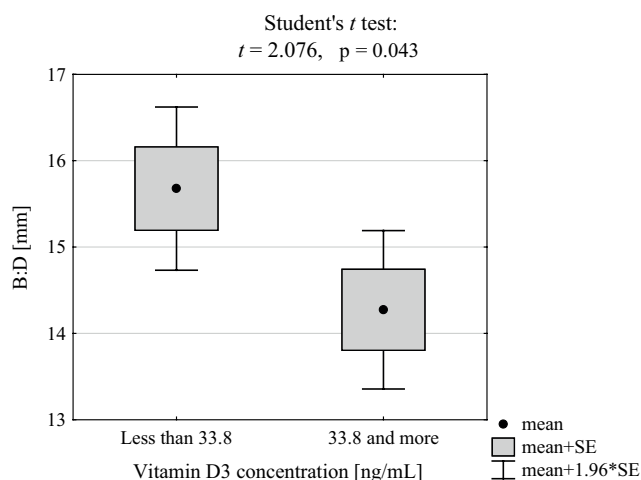


Fig. 9. Comparison of the width of the mentalis muscle (B:D) in groups of patients with different vitamin D₃ concentrations and the results of significance tests

values were used to establish cutoff values. The strength and significance of correlations between 2 quantitative variables were assessed by calculating the Pearson's r correlation coefficient or Spearman's rho-rank correlation coefficient. All statistical analyses were performed at the significance level of 0.05 and presented in graphs as M and standard error (SE) or Me and interquartile range [Q1; Q3]. All statistical analyses were performed using STATISTICA v. 13.3 (TIBCO Software Inc., Palo Alto, USA).

In the comparisons of “volume of respiratory tract”, “API-CEJ2- B angle” and “B-D” 3 groups of patients differing in “position of the tongue in the resting position”,

“vitamin D₃ deficiency” and “classification of dehiscence” were used. In the first 2 cases, the distributions of residuals (deviations) in all 3 groups did not deviate from the normal distribution (Shapiro–Wilk test), and the variances were similar (as verified by the Levene’s test). In the 3rd case, the assumption of normality was not met, so the K–W test was used for comparisons, and the Dunn’s test was used as a post hoc test.

The variationally independent were not closely correlated with each other, which was checked using the variance inflation factor (VIF) index. No outliers were observed on the quantile–quantile (Q–Q) plots and residual histograms. Checking whether the assumption of linearity in the logit function was met involved analyzing residual plots, performing the Box–Tidwell test, and checking whether additional coefficients taking into account interactions between variables were statistically significant.

For the K–W test, post hoc multiple comparisons were performed using the Dunn’s test with Bonferroni correction. Univariate and multivariate logistic regression analysis was used to estimate the probability of recession (binary variable). Model parameters were estimated using the maximum likelihood method. The goodness-of-fit of the model to the observed data was verified using the Hosmer–Lemeshow test, and the statistical significance of individual independent variables was checked using the Wald test. Cutoff values for continuous variables were determined using ROC curve analysis and Youden index values. Odds ratios and their 95% CIs were calculated for statistically significant predictors.

Results of statistical analyses

Patients characteristic

This study included 49 patients who qualified for bone reconstruction using an individualized allogeneic bone graft. The participants’ ages ranged from 22 to 55 years, with a median age of 36 years, and the majority were women (77.6%). All variables are presented in Table 1.

Influence of orthodontic treatment

In the group of patients before orthodontic treatment, the average bone marrow steatosis was significantly lower compared to patients after treatment (–12 HU vs –137 HU, $p = 0.010$). A statistically significant relationship was observed between the position of the tongue in the resting position and the patient’s status due to orthodontic treatment (K–W test: $p = 0.038$). The tongue in the resting position between the incisors was significantly more common in the group of patients before orthodontic treatment (56.2% vs 21.2%, $p = 0.014$). The tongue stuck to the palate behind the upper incisors was more common among patients after orthodontic treatment, but this difference was

borderline significant (36.4% vs 12.5%, $p = 0.082$). All interconnections are shown in Table 2.

Influence of vitamin D₃ concentration

No statistically significant differences were observed among patients with varying vitamin D₃ concentrations across the analyzed parameters ($p > 0.05$). All interconnections are detailed in Table 3.

In this study, a significant dependence of vitamin D₃ concentration on the position of the tongue in position 2 was observed. The ROC curve analysis (Fig. 8) showed that the threshold value for the vitamin D₃ concentration is 33.8 ng/mL, which means that when patients get this amount of the vitamin D₃, they will put their tongues between the incisors.

Group A and group B patients were combined, and for this dichotomous division (A + B vs C), the optimal vitamin D₃ concentration threshold was determined using ROC curve analysis (Fig. 8).

Table 4 contains calculations for the new division of patients according to vitamin D₃ concentration. As a result, it turned out that there is a statistically significant relationship between the level of vitamin D₃ concentration and gender, the width of the mentalis muscle and, of course, the position of the tongue in the resting position. Since there was a significant correlation between the width of the mentalis muscle and gender, a multivariate analysis was performed to determine independent predictors of the position of the tongue between the incisors (group C). It was found that the only independent factor differentiating patients according to the level of vitamin D₃ concentration was the width of the mentalis muscle “B:D”.

The average width of the mentalis muscle in women was smaller compared to men (14.6 mm vs 15.2 mm, $p = 0.164$), but the difference was borderline significant (Fig. 9).

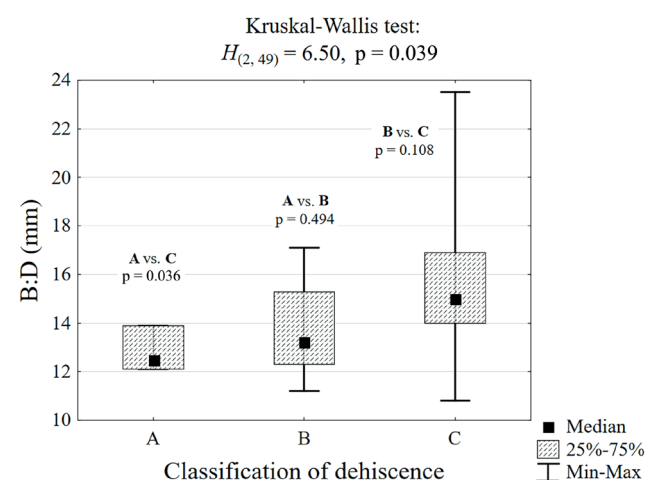


Fig. 10. Comparison of the width of the mentalis muscle (B:D) in groups of patients with different degrees of dehiscence and the results of the Kruskal–Wallis test and the post hoc test (Dunn)

Table 1. Demographic, cephalometric and clinical characteristics of 49 patients

Feature (variable)		Statistics
Sex	women, n (%)	38 (77.6)
	men, n (%)	11 (22.4)
Age [years]	M \pm SD	37.8 \pm 8.9
	Me [Q1; Q3]	36 [30; 47]
	Min–Max	22–55
1:MI angle between long axis of the tooth to the long axis of mandible [°]	M \pm SD	17.7 \pm 5.5
	Me [Q1; Q3]	17 [14; 22]
	Min–Max	10–49
API-CEJ2-B Angle [°]	M \pm SD	18.1 \pm 5.7
	Me [Q1; Q3]	18 [14; 22]
	Min–Max	9–33
Classification of dehiscence	A – dehiscence of the vestibular plate up to 2/3 of its height, n (%)	3 (6.1)
	B – complete loss of the vestibular lamina or with periapical defects and/or fenestrations, n (%)	7 (14.3)
	C – dehiscence on the lingual and vestibular sides, n (%)	39 (79.6)
Angle between long axis of upper and lower incisor: 1:1 Angle [°]	M \pm SD	124.2 \pm 15.1
	Me [Q1; Q3]	121 [114; 136]
	Min–Max	95–157
Angle between the long axis of the lower incisor and the base of the mandible 1:GoGn [°]	M \pm SD	95.2 \pm 10.2
	Me [Q1; Q3]	93 [88; 102]
	Min–Max	78–125
Angle between occlusal plane and bottom of mandible Occl:GoGn [°]	M \pm SD	19.6 \pm 5.6
	Me [Q1; Q3]	19 [15; 24]
	Min–Max	8–32
Stafne anterior bone defect, n (%)		11 (22.4)
Stafne lateral bone defect, n (%)		22 (44.9)

Correlation between width of mentalis muscle and dehiscence

A statistically significant relationship (Fig. 10) was observed between the width of the mentalis muscle and the dehiscence class. In patients with class C dehiscence, the mental width was significantly greater compared to class A patients (15.0 mm vs 12.5 mm, $p = 0.036$).

Correlation between tongue position and volume of respiratory tract

No statistically significant relationship was observed ($p > 0.05$). However, it was visible that around 2/3 of examined patients had some kind of an issue with muscular position of the tongue in the oral cavity (Table 5).

Feature (variable)		Statistics
Width of the mentalis muscle B:D [mm]	M \pm SD	15.0 \pm 2.4
	Me [Q1; Q3]	15 [14; 16]
	Min–Max	11–24
Position of the tongue in the resting position	glued to the palate behind the upper incisors, n (%)	14 (28.6)
	between the incisors, n (%)	16 (32.6)
	behind the lower incisors, it rests on the bottom, n (%)	19 (38.8)
Volume of respiratory tract [mm ²]	M \pm SD	226 \pm 93
	Me [Q1; Q3]	208 [176; 269]
	Min–Max	47–515
Spine O-c1	shift to the right, n (%)	18 (36.7)
	shift to the left, n (%)	13 (26.6)
	symmetry, n (%)	18 (36.7)
Flat, n (%)	normal, n (%)	20 (40.8)
	deepened, n (%)	9 (18.4)
	inverted (open bite), n (%)	1 (2.0)
Steatosis of bone marrow [HU]	flat, n (%)	19 (38.8)
	M \pm SD	–85 \pm 207
	Me [Q1; Q3]	–100 [–224; 31]
Vitamin D ₃ concentration [ng/mL]	Min–Max	–507 – 325
	M \pm SD	35.7 \pm 16.3
	Me [Q1; Q3]	32.2 [24.7; 42.2]
Min–Max		13.6–91.4
Orthodontic treatment, n (%)		33 (67.3)
Recessions, n (%)		47 (95.9)
Miller's recession class	I, n (%)	17 (34.7)
	II, n (%)	20 (40.8)
	III, n (%)	8 (16.3)
	IV, n (%)	4 (8.2)
Location of the recession	maxilla and mandible, n (%)	29 (59.2)
	maxilla, n (%)	1 (2.0)
	mandible, n (%)	19 (38.8)
Schwarz's patient profile	non-carries lesion, n (%)	10 (20.4)
	straight, n (%)	15 (30.6)
	oblique forward, n (%)	10 (20.4)
Angle class	oblique backward, n (%)	24 (49.0)
	I, n (%)	15 (30.6)
	II, n (%)	16 (32.7)
	III, n (%)	18 (36.7)

M – arithmetic mean; SD – standard deviation; Me – median (50%); Q1 – lower quartile (25%); Q3 – upper quartile (75%); Min – smallest value; Max – highest value; n – number; % – fraction; Occl – occlusal; GoGn – Gonion–Gnathion.

Table 2. Comparison of the analyzed parameters in the groups of patients treated and not treated orthodontically

Feature (variable)		Orthodontically treated		Test results
		no n = 16	yes n = 33	
Women, n (%)		10 (62.5)	28 (84.8)	p = 0.141 ^a
Age [years], Me [Q1; Q3]		35 [30; 47]	39 [30; 49]	p = 0.371 ^b
1:MI [°], M (SD)		25.8 (11.2)	28.5 (9.0)	p = 0.280 ^c
API-CEJ2B [°], M (SD)		16.5 (4.2)	18.4 (6.0)	p = 0.151 ^c
Dehiscence class	A, n (%)	2 (12.5)	1 (3.0)	$\chi^2 = 1.69$ df = 2 p = 0.429 ^d
	B, n (%)	2 (12.5)	5 (15.2)	
	C, n (%)	12 (75.0)	27 (81.8)	
1:1 Angle [°], M (SD)		127.9 (14.0)	124.4 (15.3)	p = 0.321 ^c
1:GoGn [°], M (SD)		93.8 (9.6)	94.3 (10.9)	p = 0.853 ^c
OccP: GoGn [°], M (SD)		19.8 (5.8)	19.2 (4.9)	p = 0.671 ^c
Stafne anterior bone defect, n (%)		4 (25.0)	7 (21.2)	p = 1.000 ^a
Stafne lateral bone defect, n (%)		8 (50.0)	14 (42.4)	p = 0.761 ^a
B:D [mm], M (SD)		14.9 (2.7)	15.4 (2.6)	p = 0.382 ^c
Volume of respiratory tract [mm ²], M (SD)		245 (107)	220 (99)	p = 0.320 ^c
Steatosis of bone marrow [HU], M (SD)		-12 (195)	-137 (190)	p = 0.010 ^c
Vitamin D ₃ ≥35 ng/mL, n (%)		6 (37.5)	16 (48.5)	p = 0.549 ^a
Position of the tongue in the resting position	glued to the palate behind the upper incisors, n (%)	2 (12.5)	12 (36.4)	$\chi^2 = 6.55$ df = 2 p = 0.038 ^d
	between the incisors, n (%)	9 (56.2)	7 (21.2)	
	behind the lower incisors, it rests on the bottom, n (%)	4 (31.3)	14 (42.4)	
O-c1 joint position	shift to the right, n (%)	5 (31.2)	13 (39.4)	$\chi^2 = 0.53$ df = 2 p = 0.766 ^d
	shift to the left, n (%)	4 (25.0)	9 (27.3)	
	symmetry, n (%)	7 (43.8)	11 (33.3)	
Occlusal plane	flat, n (%)	7 (43.8)	12 (36.4)	$\chi^2 = 1.74$ df = 3 p = 0.628 ^d
	normal, n (%)	5 (31.2)	15 (45.4)	
	deepened, n (%)	4 (25.0)	5 (15.2)	
	inverted (open bite), n (%)	0 (0.0)	1 (3.0)	
Recessions, n (%)		14 (87.5)	33 (100.0)	p = 0.102 ^a
Miller's recession class	I, n (%)	7 (43.8)	10 (30.3)	$\chi^2 = 2.20$ df = 3 p = 0.533 ^d
	II, n (%)	7 (43.8)	13 (39.4)	
	III, n (%)	1 (6.2)	7 (21.2)	
	IV, n (%)	1 (6.2)	3 (9.1)	
Location of the recession	maxilla and mandible, n (%)	12 (75.0)	17 (51.5)	$\chi^2 = 2.65$ df = 2 p = 0.266 ^d
	maxilla, n (%)	0 (0.0)	1 (3.0)	
	mandible, n (%)	4 (25.0)	15 (45.5)	

M – arithmetic mean; SD – standard deviation; Me – median (50%); Q1 – lower quartile (25%); Q3 – upper quartile (75%); df – degrees of freedom; n – number; % – fraction. Significant differences at the level of $p < 0.05$; 1:GoGn – angle between lines set by points Gnathion (Gn) and Gonion (Go) and long axis of the lower incisor; 1:MI – angle between long axis of the tooth to the long axis of mandible; API-CEJ2B – angle assessing remaining labial bone in front of the teeth; 1:1 angle- inter incisal angle; OccP: GoGn – angle between occlusal plane (OccP) and GoGn plane; B:D – width of the mental muscle; O-c1 joint- atlanto-occipital joint; ^a – Fisher's exact test, ^b – Mann-Whitney U test, ^c – t-test, ^d – Pearson χ^2 consistency test with Yates's correction.

Correlation between OC-1 joint position to malocclusion, bone parameters, volume of respiratory tract, and recessions

A statistically significant negative correlation was observed between the O-c1 joint shift and the 1:MI

(rho = -0.330), API-CEJ2-B (rho = -0.319) and 1:GoGn (rho = -0.455) angles. An increase in the OccP:GoGn angle by 1° is accompanied by a decrease in the 1:GoGn angle by an average of 0.97°. The correlation between OccP:GoGn and volume of respiratory tract (mm²) was statistically insignificant (rho = 0.135, p = 0.262) (Table 6).

Table 3. Comparison of the analyzed parameters in groups of patients differing in vitamin D₃ concentration

Feature (variable)		Vitamin D ₃ concentration		Test results
		<35 ng/mL n = 27	≥35 ng/mL n = 22	
Women, n (%)		18 (66.7)	20 (90.9)	p = 0.083 ^a
Age [year] Me [Q1; Q3]		33 [29; 42]	39 [32; 47]	p = 0.099 ^b
1:MI [°], M (SD)		28.3 (8.4)	29.1 (11.6)	p = 0.781 ^c
API-CEJ2B [°], M (SD)		18.8 (6.2)	17.2 (5.0)	p = 0.332 ^d
Dehiscence class	A, n (%)	1 (3.7)	2 (9.1)	χ ² = 1.24 df = 2 p = 0.539 ^d
	B, n (%)	3 (11.1)	4 (18.2)	
	C, n (%)	23 (85.2)	16 (72.7)	
1:1 Angle [°], M (SD)		125 (14)	124 (17)	p = 0.817 ^c
1:GoGn [°], M (SD)		94 (9)	97 (12)	p = 0.351 ^c
OccP: GoGn [°], M (SD)		19.7 (5.7)	19.5 (5.5)	p = 0.879 ^c
Stafne anterior bone defect, n (%)		8 (29.6)	3 (13.6)	p = 0.303 ^a
Stafne lateral bone defect, n (%)		13 (48.2)	9 (40.9)	p = 0.774 ^a
B:D [mm], M (SD)		15.6 (2.4)	14.3 (2.3)	p = 0.053 ^c
Volume of respiratory tract [mm ²], M (SD)		224 (106)	227 (77)	p = 0.898 ^c
Steatosis of bone marrow [HU], M (SD)		−95 (203)	−73 (216)	p = 0.716 ^c
Position of the tongue in the resting position	glued to the palate behind the upper incisors, n (%)	10 (37.1)	4 (18.2)	χ ² = 5.69 df = 2 p = 0.058
	between the incisors, n (%)	5 (18.5)	11 (50.0)	
	behind the lower incisors, it rests on the bottom, n (%)	12 (44.4)	7 (31.8)	
Spine O-c1	shift to the right, n (%)	12 (44.4)	6 (27.3)	χ ² = 3.10 df = 2 p = 0.212
	shift to the left, n (%)	8 (29.6)	5 (22.7)	
	symmetry, n (%)	7 (25.9)	11 (50.0)	
Occlusal plane	flat, n (%)	8 (29.6)	11 (50.0)	χ ² = 3.80 df = 3 p = 0.284
	normal, n (%)	13 (48.2)	7 (31.8)	
	deepened, n (%)	6 (22.2)	3 (13.6)	
	inverted (open bite), n (%)	0 (0.0)	1 (4.6)	
Orthodontic treatment, n (%)		17 (63.0)	16 (72.7)	p = 0.549
Recessions, n (%)		25 (92.6)	22 (100.0)	p = 0.495
Miller's recession class	I, n (%)	9 (33.3)	8 (36.4)	χ ² = 0.76 df = 3 p = 0.860
	II, n (%)	11 (40.8)	9 (40.9)	
	III, n (%)	4 (14.8)	4 (18.2)	
	IV, n (%)	3 (11.1)	1 (4.5)	
Location of the recession	maxilla and mandible, n (%)	17 (63.0)	12 (54.6)	χ ² = 1.42 df = 2 p = 0.492
	maxilla, n (%)	1 (3.7)	0 (0.0)	
	mandible, n (%)	9 (33.3)	10 (45.4)	
Non-carries lesion, n (%)		6 (22.2)	4 (18.2)	p = 1.000
Schwarz's patient profile	straight, n (%)	9 (33.3)	6 (27.3)	χ ² = 2.91 df = 2 p = 0.200
	oblique forward, n (%)	3 (11.1)	7 (31.8)	
	oblique backward, n (%)	15 (55.6)	9 (40.9)	
Angle class	I, n (%)	8 (29.6)	7 (31.8)	χ ² = 0.03 df = 2 p = 0.986
	II, n (%)	9 (33.3)	7 (31.8)	
	III, n (%)	10 (37.1)	8 (36.4)	

M – arithmetic mean; SD – standard deviation; Me – median (50%); Q1 – lower quartile (25%); Q3 – upper quartile (75%); Min – smallest value; df – degrees of freedom; n – number; % – fraction; 1:GoGn – angle between lines set by points Gnathion (Gn) and Gonion (Go) and long axis of the lower incisor; 1:MI – angle between long axis of the tooth to the long axis of mandible; API-CEJ2B – angle assessing remaining labial bone in front of the teeth; 1:1 Angle – interincisal angle; OccP: GoGn – angle between occlusal plane (OccP) and GoGn plane; B:D – width of the mental muscle; O-c1 joint – atlanto-occipital joint; ^a – Fisher's exact test; ^b – Mann-Whitney U test; ^c – t-test; ^d – Pearson χ² consistency test with Yates's correction.

Table 4. Comparison of the analyzed parameters in groups of patients differing in vitamin D₃ concentration

Feature (variable)		Vitamin D ₃ concentration		Test results
		<33.8 ng/mL n = 26	≥33.8 ng/mL n = 23	
Women, n (%)		17 (65.4)	21 (91.3)	p = 0.042 ^a
Age [years], M (SD)		36.4 (9.3)	39.3 (8.5)	p = 0.252 ^c
1:MI [°], M (SD)		28.4 (8.6)	29.0 (11.4)	p = 0.828 ^c
API-CEJ2B [°], M (SD)		19.1 (6.1)	16.9 (5.1)	p = 0.179 ^c
Dehiscence class	A, n (%)	1 (3.9)	2 (8.7)	χ ² = 0.94 df = 2 p = 0.626 ^d
	B, n (%)	3 (11.5)	4 (17.4)	
	C, n (%)	22 (84.6)	17 (73.9)	
1:1 Angle [°], M (SD)		125 (14)	124 (17)	p = 0.761 ^c
1:GoGn [°], M (SD)		94.3 (8.7)	96.3 (11.8)	p = 0.501 ^c
OccP: GoGn [°], M (SD)		19.6 (5.8)	19.6 (5.5)	p = 0.984 ^c
Stafne anterior bone defect, n (%)		7 (26.9)	4 (17.4)	p = 0.506 ^a
Stafne lateral bone defect, n (%)		12 (46.2)	10 (43.5)	p = 1.000 ^a
B:D [mm], M (SD)		15.7 (2.5)	14.3 (2.2)	p = 0.043 ^c
Volume of respiratory tract [mm ²], M (SD)		223 (108)	228 (75)	p = 0.843 ^c
Steatosis of bone marrow [HU], M (SD)		−92 (206)	−78 (212)	p = 0.814 ^c
Position of the tongue in the resting position	glued to the palate behind the upper incisors, n (%)	10 (38.5)	4 (17.4)	χ ² = 7.73 df = 2 p = 0.021 ^d
	between the incisors, n (%)	4 (15.4)	12 (52.2)	
	behind the lower incisors, it rests on the bottom, n (%)	12 (46.1)	7 (30.4)	
Spine O-c1	shift to the right, n (%)	11 (42.3)	7 (30.4)	χ ² = 2.30 df = 2 p = 0.317 ^d
	shift to the left, n (%)	8 (30.8)	5 (21.7)	
	symmetry, n (%)	7 (26.9)	11 (47.8)	
Occlusal plane	flat, n (%)	7 (26.9)	12 (52.2)	χ ² = 4.95 df = 3 p = 0.175 ^d
	normal, n (%)	13 (50.0)	7 (30.4)	
	deepened, n (%)	6 (23.1)	3 (13.0)	
	inverted (open bite), n (%)	0 (0.0)	1 (4.4)	
Orthodontic treatment, n (%)		16 (61.5)	17 (73.9)	p = 0.382 ^a
Recessions, n (%)		24 (92.3)	23 (100.0)	p = 0.492 ^a
Miller's recession class	I, n (%)	9 (34.6)	8 (34.8)	χ ² = 0.88 df = 3 p = 0.831 ^d
	II, n (%)	10 (38.5)	10 (43.5)	
	III, n (%)	4 (15.4)	4 (17.4)	
	IV, n (%)	3 (11.5)	1 (4.3)	
Location of the recession	maxilla and mandible, n (%)	16 (61.5)	13 (56.5)	χ ² = 1.18 df = 2 p = 0.553 ^d
	maxilla, n (%)	1 (3.9)	0 (0.0)	
	mandible, n (%)	9 (34.6)	10 (43.5)	
Non-carries lesion, n (%)		6 (23.1)	4 (17.4)	p = 0.731 ^a
Schwarz's patient profile	straight, n (%)	9 (34.6)	6 (26.1)	χ ² = 2.69 df = 2 p = 0.260 ^d
	oblique forward, n (%)	3 (11.5)	7 (30.4)	
	oblique backward, n (%)	14 (53.9)	10 (43.5)	
Angle class	I, n (%)	8 (30.8)	7 (30.4)	χ ² = 0.11 df = 2 p = 0.949 ^d
	II, n (%)	8 (30.8)	8 (34.8)	
	III, n (%)	10 (38.4)	8 (34.8)	
CBCT mouth closed, n (%)		8 (30.8)	10 (43.5)	p = 0.390

M – arithmetic mean; SD – standard deviation; Me – median (50%); Q1 – lower quartile (25%); Q3 – upper quartile (75%); df – degrees of freedom; CBCT – cone beam computed tomography; n – number; % – fraction; significant differences at the level of p < 0.05; 1:GoGn – angle between lines set by points Gnathion (Gn) and Gonion (Go) and long axis of the lower incisor; 1:MI – angle between long axis of the tooth to the long axis of mandible; API-CEJ2B – angle assessing remaining labial bone in front of the teeth; 1:1 angle – interincisal angle; OccP:GoGn – angle between occlusal plane (OccP) and GoGn plane; B:D – width of the mental muscle; O-c1 joint – atlanto-occipital joint; ^a – Fisher's exact test, ^b – Mann-Whitney U test, ^c – t-test, ^d – Pearson χ² consistency test with Yates's correction.

Table 5. Relationship between tongue position and airway volume – result of analysis of variance (ANOVA)

Variable	Position of tongue in the resting position			ANOVA
	A n = 14	B n = 16	C n = 19	
Volume of respiratory tract, [mm ²], mean (SD)	196 (88)	258 (104)	220 (82)	F = 1.79 df = 46 p = 0.178

A – glued to the palate behind the upper incisors; B – between the incisors; C – behind the lower incisors, it rests on the bottom; SD – standard deviation; F – test statistics; df – degree of freedom; p – test significance level.

Table 6. Values of the Spearman's rank correlation coefficient (rho) between O-c1 joint shift and skeletal parameters in 49 patients

OccP:GoGn	1:ML	API-CEJ2-B	1:1 Angle	1:GoGn	B:D
rho =	–0.330	–0.319	0.129	–0.455	0.127
t(N-2) =	–2.399	–2.310	0.894	–3.502	0.880
p-value	0.020	0.025	0.376	0.001	0.383

1:GoGn – angle between lines set by points Gnathion (Gn) and Gonion (Go) and long axis of the lower incisor; API-CEJ2-B – angle assessing remaining labial bone in front of the teeth; 1:1 angle – interincisal angle; OccP:GoGn – angle between occlusal plane (OccP) and GoGn plane; B:D – width of the mental muscle; O-c1 joint – atlanto-occipital joint; 1:ML – angle between long axis of the tooth to the long axis of mandible.

Correlation between the occlusal plane and malocclusion, mentalis muscle, angles and airway, tongue position, and Stafne defect

A statistically significant relationship was observed between the occlusal plane and the 1:ML angle ($p = 0.013$; Table 7).

Determining critical values when a recession occurs

Among the 49 patients qualified for jawbone reconstruction, gingival recession was observed in 46 individuals (93.6%). Specifically, 19 patients (38.8%) exhibited recession only in the mandible, while 27 patients (55.1%) exhibited recession in both the mandible and the maxilla.

Patients were divided into 2 groups: group 1, consisting of patients with no mandibular gingival recession (Miller classes 0 and I), and group 2, consisting of patients with mandibular gingival recession (Miller classes II and higher). Both groups had similar sample sizes. The frequency of occurrence of the analyzed recession predictors in both groups was evaluated using Fisher's exact test, and the results are presented in Table 8. Cutoff values for continuous quantitative variables were established based on ROC curve analysis.

In the univariate analysis, statistically significant predictors (stimulants) of recession were: female gender (90.0% vs 57.9%, $p = 0.014$), API-CEJ2-B angle $\leq 19.9^\circ$ (76.7% vs 47.4%, $p = 0.040$), width of mental muscle ≥ 14.1 mm (76.7% vs 47.4%, $p = 0.040$), dehiscence on the lingual and vestibular side (93.3% vs 57.9%, $p = 0.008$), flat occlusal plane (50.0% vs 21.1%, $p = 0.049$), steatosis of mandibular bone marrow score less than or equal to 139 HU (60.0% vs 15.8%, $p = 0.003$), and vitamin D₃ concentration ≥ 24.9 ng/mL (80.0% vs 52.6%, $p = 0.048$).

The odds of gingival recession are 6.5 greater in women (OR = 6.55), more than 3.5 times greater among patients with an API-CEJ2-B angle $\leq 19.9^\circ$ (OR = 3.65), also more than 3.5 times greater among patients with the width of the mentalis muscle ≥ 14.1 mm (OR = 3.65), more than 10 times greater among patients with bone dehiscence on the lingual and vestibular sides (OR = 10.2), almost 4 times greater among patients with a flat occlusal plane (OR = 3.75), 8 times higher among patients with steatosis of mandibular bone marrow score less than or equal to –139 HU (OR = 8.00), and 3.5 times higher among patients with vitamin D₃ concentration ≥ 24.9 ng/mL (OR = 3.60).

Due to the significant correlations between some recession risk factors (e.g., female gender and width of mentalis muscle), a multivariate logistic regression analysis was performed to determine independent predictors of recession.

In the logistic regression analysis, the recession variable was the dependent variable, where the value of 1 meant the occurrence of gingival recession at the level of at least Miller class II, and the value of 0 – no recession or class I recession. The remaining variables served as independent variables (predictors). The results are presented in Table 9, which highlights significant results at the $p < 0.05$ level.

Dichotomous independent variables were variables significant in univariate analysis at the $p < 0.1$ level.

In multivariate logistic regression analysis, independent predictors of gingival recession were: female gender, API-CEJ2-B angle $\leq 19.9^\circ$, dehiscence on both sides (DBS), flat occlusal plane, and steatosis of mandibular bone marrow score less than –139 HU.

The logistic regression equation used to predict the probability of gum recession takes the following logit form:

$$\text{logit Pr}\{\text{Recession} = 1|X\} = -6.96 + 2.62 \times (\text{Female}) + 3.34 \times (\text{DBS}) + 2.49 \times (\text{OPF}) + 2.06 \times (\text{API-CEJ2-B} \leq 19.9^\circ) + 2.00 \times (\text{SBM} \leq -139 \text{ HU})$$

Table 7. Influence of occlusal plane to variables

Variable		Occlusal plane				p-value
		flat n = 19	normal n = 20	deepened n = 9	inverted n = 1	
Angle class	I, n (%)	7 (36.8)	4 (20.0)	3 (33.3)	1 (100.0)	$\chi^2 = 3.84$ df = 6 0.678 ^d
	II, n (%)	6 (31.6)	7 (35.0)	3 (33.3)	0 (0.0)	
	III, n (%)	6 (31.6)	9 (45.0)	3 (33.3)	0 (0.0)	
B:D [mm], Me [Q1;Q3]		15 [13;16]	15 [14; 17]	14 [13; 16]	16	0.771 ^b
1:MI [°], Me [Q1;Q3]		38 [27; 42]	29 [24; 34]	23 [15; 25]	26	0.013 ^b
API-CEJ2-B [°], Me [Q1;Q3]		19 [16; 22]	17 [12; 24]	16 [11; 20]	18	0.695 ^b
Dehiscence class	A, n (%)	1 (5.3)	2 (10.0)	0 (0.0)	0 (0.0)	$\chi^2 = 2.01$ df = 6 0.919 ^d
	B, n (%)	3 (15.8)	2 (10.0)	2 (22.2)	0 (0.0)	
	C, n (%)	15 (78.9)	16 (80.0)	7 (77.8)	1 (100.0)	
1:1 Angle [°], Me [Q1;Q3]		118 [112; 133]	123 [115; 134]	136 [119; 142]	119	0.354 ^b
1:GoGn [°], Me [Q1;Q3]		95 [86; 109]	94 [91; 101]	89 [85; 93]	95	0.372 ^b
OccP: GoGn [°], Me [Q1;Q3]		15 [14; 23]	21 [18; 25]	22 [18; 24]	22	0.125 ^b
Stafne anterior bone defect, n (%)		3 (15.8)	6 (30.0)	2 (22.2)	0 (0.0)	0.699 ^d
Stafne lateral bone defect, n (%)		7 (36.8)	8 (40.0)	6 (66.7)	1 (100.0)	0.303 ^d
Volume of respiratory tract [mm ²], Me [Q1;Q3]		208 [176; 249]	204 [164; 272]	237 [203; 341]	50	0.295 ^b
Steatosis of bone marrow [HU], Me [Q1;Q3]		-105 [-225; 71]	-37 [-224; 36]	-108 [-186; -48]	-507	0.347 ^b
Position of the tongue in the resting position	behind the upper incisors, n (%)	2 (10.5)	8 (40.0)	3 (33.3)	1 (100.0)	$\chi^2 = 10.4$ df = 6 0.110 ^d
	between the incisors, n (%)	10 (52.6)	5 (25.0)	1 (11.1)	0 (0.0)	
	behind the lower incisors, n (%)	7 (36.9)	7 (35.0)	5 (55.6)	0 (0.0)	

M – arithmetic mean; SD – standard deviation; Me – median (50%); Q1 – lower quartile (25%); Q3 – upper quartile (75%); df – degrees of freedom; n – number; % – fraction; significant differences at the level of $p < 0.05$; 1:GoGn – angle between lines set by points Gnathion (Gn) and Gonion (Go) and long axis of the lower incisor; 1:MI – angle between long axis of the tooth to the long axis of mandible; API-CEJ2B – angle assessing remaining labial bone in front of the teeth; 1:1 angle – interincisal angle; OccP:GoGn – angle between occlusal plane (OccP) and GoGn plane; B:D – width of the mental muscle; O-c1 joint – atlanto-occipital joint; ^b – Kruskal–Wallis test, ^d – Pearson's χ^2 .

For the cutoff value of the logistic model: Pr = 0.61, the sensitivity is Sens. = 0.933, specificity Spec. = 0.842, accuracy Acc. = 0.900, PPV = 0.90, NPV = 0.89 and LR(+) = 5.91.

Discussion

Bone density is not only crucial in implantology, but it can be also a significant factor in oral surgery and orthodontics as well. Knowing patient's bone density, proper methodology might be implemented, which reduces chances of complications. Nowadays, the most common classification of bone density is the one presented by Misch, which evaluated ratio between trabecular and spongy bone.³⁷ More common usage of CT allows to assess density of tissues using HU. Patients with a history of an orthodontic treatment who were evaluated during our study usually presented some kind of complications, for example teeth excess mobility or gingival recessions and bone dehiscence. Most of orthodontic complications are somehow related to bone issues. In our study, the majority of the participants were women. In our opinion, it might be explained firstly with other studies' findings that periodontal phenotype

in women is generally thinner than in males, and consequently the buccal cortical plate is more exposed and predisposed to dehiscence in case of orthodontic treatment or malocclusion. Behavioral studies³⁸ indicate that women are more likely to seek dental services, adhere to medical instructions and pay for dental visits, and they are also more inclined to undergo expensive surgical treatments.³⁹ Comparing patients who visited the dental office before and after orthodontic treatment, the post-treatment group exhibited statistically lower bone density (measured in HU) than the pre-treatment group (-12 ± 195 to -137 ± 190). These results are similar to those obtained by other researchers.^{40–42} On the contrary, some studies have demonstrated that bone density may increase after orthodontic treatment due to the remodeling effects associated with tooth movement.^{43,44} However, only a limited number of factors have been shown to affect bone density, particularly in the lateral part of the mandible. One such factor is bone steatosis. In the literature, early stages of steatosis are described as nonbacterial osteomyelitis of the mandible, which should be differentiated from conditions such as sarcoma, Ewing sarcoma and Langerhans cell histiocytosis. The etiology is considered an autoinflammatory disorder characterized by the hyperactivation of the immune system.⁴⁵

Table 8. Number (percentage) of patients qualified for allogeneic bone block treatment in groups with different socio-demographic, clinical and radiological data and presence of gingival recession, results of Fisher exact test and values of ORs and their 95% CIs

Feature (variable)	Gingival recession				p-value	OR [95% CI]
	yes (n = 30)		no (n = 19)			
	n	%	n	%		
Sex, female	27	90.0	11	57.9	0.014	6.55 [1.46–29.4]
Age ≥36 years	9	30.0	4	21.1	0.741	1.61 [0.42–6.21]
1:MI ≥ 28.7°	18	60.0	7	36.8	0.148	2.57 [0.79–8.40]
API-CEJ2-B ≤ 19.9°	23	76.7	9	47.4	0.040	3.65 [1.06–12.6]
1:1 Angle ≥ 112.6°	27	90.0	13	68.4	0.072	4.15 [0.89–19.3]
1:GoGn ≤ 88°	11	36.7	2	10.5	0.053	4.92 [0.95–25.4]
OccP:GoGn ≥ 16.5°	22	73.3	11	57.9	0.351	2.00 [0.59–6.76]
B:D ≥ 14.1 mm	23	76.7	9	47.4	0.040	3.65 [1.06–12.6]
Dehiscence on both side	28	93.3	11	57.9	0.008	10.2 [1.86–55.7]
Stafne anterior bone defect	7	23.3	4	21.1	1.000	1.14 [0.28–4.58]
Stafne lateral bone defect	14	46.7	8	42.1	0.777	1.20 [0.38–3.84]
Occlusal plane flat	15	50.0	4	21.1	0.049	3.75 [1.01–14.0]
Orthodontic treatment	23	76.7	10	52.6	0.119	2.69 [0.86–10.2]
VRT ≥ 231.1 mm ²	16	53.3	5	26.3	0.081	3.20 [0.92–11.1]
BMS ≤ –139 HU	18	60.0	3	15.8	0.003	8.00 [1.91–33.5]
Vitamin D ₃ ≥ 24.9 ng/mL	24	80.0	10	52.6	0.048	3.60 [1.01–12.8]

Significant differences at the level of $p < 0.05$; 1:GoGn – angle between lines set by points Gnathion (Gn) and Gonion (Go) and long axis of the lower incisor; 1:MI – angle between long axis of the tooth to the long axis of mandible; API-CEJ2B – angle assessing remaining labial bone in front of the teeth; 1:1 angle – inter incisal angle; OccP:GoGn – angle between occlusal plane (OccP) and GoGn plane; B:D – width of the mental muscle; VRT – volume of respiratory tract; BMS – bone marrow steatosis; OR (95% CI) – odds ratio and 95% confidence interval.

Table 9. Results of univariate and multivariate logistic regression analysis of mandibular recession and values of ORs and their 95% CIs

Predictors	Univariate analysis			Multivariate analysis		
	β	p-value	OR [95% CI]	β	p-value	OR [95% CI]
Sex, female	1.879	0.014	6.55 [1.46; 29.4]	2.617	0.019	13.7 [1.52; 123]
API-CEJ2-B ≤ 19.9°	1.295	0.040	3.65 [1.06; 12.6]	2.058	0.037	7.83 [1.13; 54.2]
DBS	2.321	0.007	10.2 [1.86; 55.7]	3.343	0.016	28.3 [1.87; 429]
OccPF	1.322	0.049	3.75 [1.01; 14.0]	2.486	0.029	12.0 [1.28; 112]
BMS ≤ -139 HU	2.079	0.005	8.00 [1.91; 33.5]	1.998	0.043	7.38 [1.07; 50.9]

DBS – dehiscence on the lingual and vestibular sides; BMS – steatosis of bone marrow; OccPF – occlusal plane flat; β – regression coefficient in univariate analysis; β – regression coefficient in multivariate analysis; p – test significance level; OR (95% CI) – odds ratio and 95% confidence interval; significant differences at the level of $p < 0.05$.

Lower density is also visible in the course of hemorrhagic cyst and all types of dysplasia. Another factor is the level of vitamin D. More and more studies show or confirm correlation between its deficiency and tissue functioning. Vitamin D₃ influences bone remodeling and muscles activity, has an anti-inflammatory effect and influences autoimmune diseases. As vitamin D₃ receptors are present in muscle tissue, its higher amount will allow muscles to work with less contraction and more resilience. It is shown in our results as a better tongue position and slimmer mentalis muscle in people with vitamin D₃ concentration in serum over 33.8 ng/mL, which is similar level to the mean value – 30–100 ng/mL.^{46–48} However, we found the tendency to lowering of the API-CEJ2-B with lowering of vitamin D serum

concentration (without statistically important significance). This may lead to the conclusion that with lower concentration of vitamin D, the lesser thickness of labial bone will be present, as it is visible in the group C <20 ng/mL API-CEJ2-B reach only 17.5°. These findings are comparable to those of Leszczyszyn et al.¹⁴, who suggested that low concentrations of vitamin D₃ are associated with a significantly increased risk of recession. They also found that low vitamin D levels correlate with crowding in the upper jaw, crossbite and narrowing of the upper arch. Furthermore, in another publication, the constructed model of multiple regression for parameters which influence significantly gingival recession (API-CEJ2-B, CEJ2-ID, age) allowed to explain their potential recession-causing influence in 72% chance of the recession occurrence.⁴⁹

Atypical tongue position may be a problem by itself or it can be connected with malocclusion (e.g., open bite). It is known that during orthodontic therapy, tongue position is crucial for the long-term results, so during or even before the treatment, patients are referred to the specialist or trained by the orthodontist. It is therefore not surprising that better tongue position is observed after orthodontic treatment.^{50,51} There is no significant correlation between tongue position and the capacity of the airways. It is a similar result to the one obtained by the Chauhan et al.,⁵² who did not find such correlation as well.

Although the anterior Stafne defect may be attributed to hyperactivity of the mylohyoid muscle, our study did not find a statistically significant association between this defect and tongue position in the oral cavity. Therefore, it can be concluded that myofunctional disorders do not have a major impact on this poorly documented abnormality. However, the results of correlation between position shift of first cervical vertebrae and shape of the body of mandible with teeth inclination should be discussed in more detail. It is well known that increased tension of head and neck muscles might lead to orofacial pain and muscular rehabilitation may decrease patient's pain.⁵³ Therefore, it should be possible to interconnect the incorrect position of Oc-1 joint, which is caused most likely with abnormal head position, with increased tension of the muscle, larger teeth inclination and with larger posterioversion of the mandible (which might lead to temporomandibular joints disorders). Important results were obtained by Olchowy et al.,⁵⁴ who investigated masseter muscle stiffness and its rehabilitation by standard masticatory muscle therapy involving manual therapy and splint occlusal stabilization. The masseter stiffness has been measured by shear wave elastography. They stated that the above treatment has significant impact in pain reduction. Those promising results are similar to ours – that manual therapy might be a key factor in therapy of craniofacial area.

The etiological factors of gingival recession are well documented. Common factors include gender, toothbrushing techniques, improper tooth positioning, as well as systemic disorders and lifestyle habits. In contrast to other publications, in our study, women had gingival recession 6 times more often than men.^{55–57} Similar to the study by Cortellini and Bissada, tooth position and width of the buccal plate is important factor during genesis of the recession. API-CEJ2-B angle indicates remaining labial wall of alveolar part of mandible. With lower value of the angle, chances of the recession increase, and when the value is lower than 19.9°, chances of the recession are higher by 3.5 times.⁵⁸ An even more important aspect is the appearance of the bone dehiscence on both sides of the tooth, which induce chances of the gingival recession up to 10 times; this factor is not discussed enough in the literature. A high frenulum is one factor that increases the risk of gingival recession.⁵⁹ Our study confirms this association: a wider mental muscle, which is linked to the frenulum attachment position due to its effect on vestibular depth, transmits greater forces

to the gingiva, leading to pull syndrome. In another paper, it was stated as well that width of mentalis muscle significantly correlates with appearance of the dehiscences.²² Occlusal plane and occlusal trauma is another important factor of the gingival migration and flat occlusal plane indicates more pathological contacts between dentitions. Our results are similar to findings presented in other studies.^{60,61}

Systemic disorders are known to influence gingival recession, and their impact is increasingly being explored. It was presented by Jepsen et al. in the recent study.⁶² This association is also evident in our study. As steatosis of the bone marrow increases the chances for the recession by 8 times, it has to be seen as inflammatory process showing deeper problems with the system. In contrast to other researchers' results, in our study, data indicate 3.5 times higher chances of gingival recession as the concentration of the vitamin D is higher than 24.9 ng/mL⁶³; however, it concerns a specific group of patients, because these patients are prepared to the regenerative surgery with allogenic bone graft and supplementation of the vitamin D₃ is a part of preoperative pharmacology.

The numerous findings obtained from CBCT image assessments clearly demonstrate that a wealth of information – reflected in basic cephalometric measurements – should be analyzed before beginning orthodontic treatment. In today's increasingly digital world, we should embrace the benefits that digitalization offers in dental examinations. Other researchers have reached a similar conclusion, noting that digitalization allows for the collection of more comprehensive treatment-related information – even in the early stages of potential disorders – than traditional standalone X-ray imaging.⁶⁴

Limitations

One limitation of this study is that the retrospective selection process may have introduced selection bias. Additionally, no initial pre-orthodontic variables were analyzed; therefore, factors such as the amount, direction or speed of orthodontic tooth movement were not considered. Furthermore, assessing tongue position on a single CBCT scan may not accurately reflect its actual position. The study was conducted exclusively on a group of patients undergoing augmentation of the dentulous part of the mandible with an allogenic bone block, all of whom had a thin gingival biotype and existing recessions. There was no control group of "healthy patients," and in some cases, patients without orthodontic treatment might have genetically or functionally determined changes that influence the reduction of the mandibular bone base. Consequently, the obtained values may differ from those in the general population. Comparing these results with data from individuals with a thick or normal biotype might provide a better assessment of the predisposition to these changes. Moreover, there is a limited number of studies on 3D bone allograft procedures performed in the mandible, and to the best of our knowledge, none have specifically focused on patient characteristics, which hampers meaningful comparisons with other findings.

Conclusions

The main purpose of this article was to shed some light on the rather serious consequences that may result from ignorant orthodontic treatment or not starting the treatment in a difficult situation without proper pre-orthodontic treatment based on surgical grafting of soft and hard tissues. Patients referred for the regenerative treatment with allogenic bone block usually had already undergone long treatment, which could be much shorter if orthodontists would make full examination, with CBCT visualization as well. More thorough results give the most important feedback, especially for the patients, who usually ask if their complications are less likely to have happened if they had not had the orthodontic treatment. The answer is complex, but statistical analysis gives a hint that there is no significant difference between pre- and post-treatment patients. Their problem might be congenital or caused by interconnection between many internal and external factors. Sometimes, it is impossible to avoid these factors. However if they are diagnosed early, it will be easier to solve these problems. The way of conducting pre-orthodontic examination presented in Materials and Methods section, added to classical cephalometric and dental arches models measurements, might be treated as guideline for avoiding complications. Orthodontic treatment should be considered as a complex one that often needs long preparation, and should include oral surgeon, restorative dentist, physiotherapist, and neuro-speech therapist.

Data Availability Statement

The datasets supporting the findings of the current study are openly available in Zenodo at <https://doi.org/10.5281/zenodo.13869897>.

Consent for publication


Not applicable.


Use of AI and AI-assisted technologies


Not applicable.

ORCID iDs

Sebastian Dominiak  <https://orcid.org/0000-0001-7623-7811>

Marzena Dominiak  <https://orcid.org/0000-0001-8943-0549>

Paweł Kubasiewicz-Ross  <https://orcid.org/0000-0001-7305-7161>

Tomasz Gedrange  <https://orcid.org/0000-0002-3551-6467>

References

- Brace CL, Mahler PE. Post-Pleistocene changes in the human dentition. *Am J Phys Anthropol*. 1971;34(2):191–203. doi:10.1002/ajpa.1330340205
- Bernal V, Perez SI, Gonzalez PN, Diniz-Filho JAF. Ecological and evolutionary factors in dental morphological diversification among modern human populations from southern South America. *Proc Biol Sci*. 2010;277(1684):1107–1112. doi:10.1098/rspb.2009.1823
- Dominiak M, Dominiak S, Targonska S, Gedrange T. Three-dimensional bone block planning for mandibular sagittal bone defect reconstruction. *J Healthcare Eng*. 2020;2020:8829288. doi:10.1155/2020/8829288
- Dominiak M, Hnitecka S, Olchowcy C, Dominiak S, Gedrange T. Possible treatment of severe bone dehiscences based on 3D bone reconstruction: A description of treatment methodology. *Appl Sci*. 2021;11(21):10299. doi:10.3390/app112110299
- Dominiak M, Hnitecka S, Olchowcy C, Olchowcy A, Gedrange T. Analysis of alveolar ridge width in an area of central lower incisor using cone-beam computed tomography in vivo. *Ann Anat*. 2021;236:151699. doi:10.1016/j.aanat.2021.151699
- Miller PD. A classification of marginal tissue recession. *Int J Periodontics Restorative Dent*. 1985;5(2):8–13. PMID:3858267.
- Cairo F, Nieri M, Cincinelli S, Mervelt J, Pagliaro U. The interproximal clinical attachment level to classify gingival recessions and predict root coverage outcomes: An explorative and reliability study: Interproximal CAL for gingival recessions. *J Clin Periodontol*. 2011;38(7):661–666. doi:10.1111/j.1600-051X.2011.01732.x
- Smukler H, Chaibi M. Periodontal and dental considerations in clinical crown extension: A rational basis for treatment. *Int J Periodontics Restorative Dent*. 1997;17(5):464–477. PMID:9497735.
- Mulla SA, Patil A, Mali S, et al. Exploring the biological width in dentistry: A comprehensive narrative review. *Cureus*. 2023;15(7):e42080. doi:10.7759/cureus.42080
- Yadav VS, Gumber B, Makker K, et al. Global prevalence of gingival recession: A systematic review and meta-analysis. *Oral Dis*. 2023;29(8):2993–3002. doi:10.1111/odi.14289
- Olivi G, Signore A, Olivi M, Genovese MD. Lingual frenectomy: Functional evaluation and new therapeutical approach. *Eur J Paediatr Dent*. 2012;13(2):101–106. PMID:22762170.
- Arruda KEM, Valladares Neto J, Almeida GDA. Assessment of the mandibular symphysis of Caucasian Brazilian adults with well-balanced faces and normal occlusion: The influence of gender and facial type. *Dent Press J Orthod*. 2012;17(3):40–50. doi:10.1590/S2176-94512012003000012
- Kalecińska E, Dominiak M, Dominiak P, Anwajler J. Postural disturbances in the presence of the dysfunction of the masticatory system: Case report. *Dent Med Probl*. 2004;41(2):305–312. https://www.dbc.wroc.pl/Content/2265/DMP_2004412305_Kale.pdf. Accessed August 15, 2024.
- Leszczyszyn A, Hnitecka S, Dominiak M. Could vitamin D3 deficiency influence malocclusion development? *Nutrients*. 2021;13(6):2122. doi:10.3390/nu13062122
- Holick MF, Chen TC. Vitamin D deficiency: A worldwide problem with health consequences. *Am J Clin Nutr*. 2008;87(4):1080S–1086S. doi:10.1093/ajcn/87.4.1080S
- Pietschmann P, Patsch JM, Schernthaner G. Diabetes and bone. *Horm Metab Res*. 2010;42(11):763–768. doi:10.1055/s-0030-1262825
- Lungaro L, Manza F, Costanzini A, et al. Osteoporosis and celiac disease: Updates and hidden pitfalls. *Nutrients*. 2023;15(5):1089. doi:10.3390/nu15051089
- Nebot Valenzuela E, Pietschmann P. Epidemiology and pathology of Paget's disease of bone: A review. *Wien Med Wochenschr*. 2017;167(1–2):2–8. doi:10.1007/s10354-016-0496-4
- Graham LS, Tintut Y, Parhami F, et al. Bone density and hyperlipidemia: The T-lymphocyte connection. *J Bone Miner Res*. 2010;25(11):2460–2469. doi:10.1002/jbmr.148
- Hnitecka S, Dominiak M, Olchowcy C, Gedrange T. An innovative method for three-dimensional bone reconstruction of the anterior mandible with preserved dentition using an allogeneic bone block: A 6-month follow-up [published online as ahead of print on August 9, 2024]. *Adv Clin Exp Med*. 2024. doi:10.17219/acem/189840
- von Elm E, Altman DG, Egger M, et al. The Strengthening of Reporting of Observational Studies in Epidemiology (STROBE) statement: Guidelines for reporting observational studies. *Lancet*. 2007;370(9596):1453–1457. doi:10.1016/S0140-6736(07)61602-X
- Dominiak M. Własna metoda oceny prognozowania recesji przyzębia. Wrocław, Poland: Akademia Medyczna im. Piastów Śląskich we Wrocławiu; 2009. ISBN:978-83-7055-505-4.
- Yang Y, Yang H, Pan H, Xu J, Hu T. Evaluation and new classification of alveolar bone dehiscences using cone-beam computed tomography in vivo. *Int J Morphol*. 2015;33(1):361–368. doi:10.4067/S0717-95022015000100057

24. Nötzel F, Schultz C. *Leitfaden der kieferorthopädischen Diagnostik: Analysen und Tabellen für die Praxis*. 2nd ed. Cologne, Germany: Deutscher Zahnärzte Verlag; 2009. ISBN:978-3-7691-3369-1.
25. Chhibber A, Upadhyay M, Shetty VS, Mogra S. Cephalometric comparison of vertical changes between Begg and preadjusted edgewise appliances. *Eur J Orthod*. 2011;33(6):712–720. doi:10.1093/ejo/cjq176
26. Majewski S. *Współczesna protetyka stomatologiczna: podstawy teoretyczne i praktyka kliniczna*. Wrocław, Poland: Elsevier Urban & Partner; 2014. ISBN:978-83-7609-731-2.
27. Kramer IRH, Pindborg JJ, Shear M. *Histological Typing of Odontogenic Tumours*. Berlin–Heidelberg, Germany: Springer Berlin Heidelberg; 1992. doi:10.1007/978-3-662-02858-2
28. Richard EL, Ziskind J. Aberrant salivary gland tissue in mandible. *Oral Surg Oral Med Oral Pathol*. 1957;10(10):1086–1090. doi:10.1016/0030-4220(57)90059-2
29. Shigematsu H, Suzuki S, Osuga T, Okumura Y, Fujita K. A radiographical classification of Stafne's bone cavity. *Oral Radiol*. 1993;9(2):13–18. doi:10.1007/BF02351544
30. Parsa A, Ibrahim N, Hassan B, Van Der Stelt P, Wismeijer D. Bone quality evaluation at dental implant site using multislice CT, micro-CT and cone beam CT. *Clin Oral Implants Res*. 2015;26(1):e1–e7. doi:10.1111/clr.12315
31. Van Dessel J, Nicolielo LFP, Huang Y, et al. Accuracy and reliability of different cone beam computed tomography (CBCT) devices for structural analysis of alveolar bone in comparison with multislice CT and micro-CT. *Eur J Oral Implantol*. 2017;10(1):95–105. PMID:28327698.
32. Cano Martins LA, Sarna-Boś K, Kalinowski P, Różyło-Kalinowska I. Cone-beam computed tomography density measurement repeatability in Hounsfield units: A preliminary study. *J Stomatol*. 2023;76(3): 191–195. doi:10.5114/jos.2023.131318
33. Nguyen C, Ranjitkar S, Kaidonis J, Townsend G. A qualitative assessment of non-carious cervical lesions in extracted human teeth. *Aust Dent J*. 2008;53(1):46–51. doi:10.1111/j.1834-7819.2007.00009.x
34. Goodacre CJ, Eugene Roberts W, Munoz CA. Noncarious cervical lesions: Morphology and progression, prevalence, etiology, pathophysiology, and clinical guidelines for restoration. *J Prosthodont*. 2023;32(2):e1–e18. doi:10.1111/jopr.13585
35. Angle EH. *Treatment of Malocclusion of the Teeth: Angle's System*. 7th ed. Lakewood, USA: S.S. White Dental Manufacturing Company; 1907.
36. Vitality Health Check. VHC Vitamin-D Test Principle. Rostock, Germany: Jungbrunnen – Fountain of Youth GmbH; 2024. <https://vitality-health-check.com/vitality-health-check-vit-d/vitamin-d-testing>. Accessed August 15, 2024.
37. Resnik R. *Misch's Contemporary Implant Dentistry E-Book*. 4th ed. Philadelphia, USA: Mosby; 2020. ISBN:978-0-323-39155-9, 978-0-323-47826-7.
38. Kolte R, Kolte A, Mahajan A. Assessment of gingival thickness with regards to age, gender and arch location. *J Indian Soc Periodontol*. 2014;18(4):478. doi:10.4103/0972-124X.138699
39. Sfeatcu R, Balgiu BA, Mihai C, Petre A, Pantea M, Tribus L. Gender differences in oral health: Self-reported attitudes, values, behaviours and literacy among Romanian adults. *J Pers Med*. 2022;12(10):1603. doi:10.3390/jpm12101603
40. Yu JH, Huang HL, Liu CF, et al. Does orthodontic treatment affect the alveolar bone density? *Medicine (Baltimore)*. 2016;95(10):e3080. doi:10.1097/MD.00000000000003080
41. Ma ZG, Yang C, Fang B, Xia YH, Mao LX, Feng YM. Three-D imaging of dental alveolar bone change after fixed orthodontic treatment in patients with periodontitis. *Int J Clin Exp Med*. 2015;8(2):2385–2391. PMID:25932177. PMCID:PMC4402824.
42. Hsu JT, Chang HW, Huang HL, Yu JH, Li YF, Tu MG. Bone density changes around teeth during orthodontic treatment. *Clin Oral Invest*. 2011; 15(4):511–519. doi:10.1007/s00784-010-0410-1
43. Campos MJDS, De Albuquerque EG, Pinto BCH, et al. The role of orthodontic tooth movement in bone and root mineral density: A study of patients submitted and not submitted to orthodontic treatment. *Med Sci Monit*. 2012;18(12):CR752–CR757. doi:10.12659/MSM.883604
44. Zhuang L, Bai Y, Meng X. Three-dimensional morphology of root and alveolar trabecular bone during tooth movement using micro-computed tomography. *Angle Orthod*. 2011;81(3):420–425. doi:10.2319/071910-418.1
45. Kim Y, Choi J, Jung HI, Ku JK. A rare case of chronic nonbacterial osteomyelitis of the mandible in a young adult male. *Oral Biol Res*. 2020;44(1):51–60. doi:10.21851/obr.44.01.202003.51
46. Lips P. Vitamin D physiology. *Prog Biophys Mol Biol*. 2006;92(1):4–8. doi:10.1016/j.pbiomolbio.2006.02.016
47. Choukroun E, Parnot M, Surmenian J, et al. Bone formation and maintenance in oral surgery: The decisive role of the immune system. A narrative review of mechanisms and solutions. *Bioengineering*. 2024;11(2):191. doi:10.3390/bioengineering11020191
48. Rajaei E. The relationship between serum level of vitamin D₃ and the severity of new onset rheumatoid arthritis activity. *J Clin Diagn Res*. 2017;11(3):OC28–OC30. doi:10.7860/JCDR/2017/24014.9486
49. Warmuz J, Jagielak M, Botzenhart U, Seeliger J, Gedrange T, Dominiak M. Influence of morphological parameters on the development of gingival recession in class III malocclusion. *Ann Anat*. 2016;206:64–72. doi:10.1016/j.aanat.2015.04.008
50. Koletsis D, Makou M, Pandis N. Effect of orthodontic management and orofacial muscle training protocols on the correction of myofunctional and myoskeletal problems in developing dentition: A systematic review and meta-analysis. *Orthod Craniofac Res*. 2018;21(4):202–215. doi:10.1111/ocr.12240
51. Maspero C, Prevedello C, Giannini L, Galbiati G, Farronato G. Atypical swallowing: A review. *Minerva Stomatol*. 2014;63(6):217–227. PMID:25267151.
52. Chauhan A, Autar R, Pradhan K, Yadav V. Comparison of pharyngeal airway dimension, tongue and hyoid bone position based on ANB angle. *Natl J Maxillofac Surg*. 2015;6(1):42. doi:10.4103/0975-5950.168237
53. Calixtre LB, Oliveira AB, De Sena Rosa LR, Armijo-Olivo S, Visscher CM, Albuquerque-Sendin F. Effectiveness of mobilisation of the upper cervical region and craniocervical flexor training on orofacial pain, mandibular function and headache in women with TMD: A randomised, controlled trial. *J Oral Rehabil*. 2019;46(2):109–119. doi:10.1111/joor.12733
54. Olchoway A, Seweryn P, Olchoway C, Wieckiewicz M. Assessment of the masseter stiffness in patients during conservative therapy for masticatory muscle disorders with shear wave elastography. *BMC Musculoskelet Disord*. 2022;23(1):439. doi:10.1186/s12891-022-05392-9
55. Manchala SR, Vandana K, Mandalapu N, Mannem S, Dwarakanath C. Epidemiology of gingival recession and risk indicators in dental hospital population of Bhimavaram. *J Int Soc Prevent Communit Dent*. 2012;2(2):69. doi:10.4103/2231-0762.109374
56. Albandar JM, Kingman A. Gingival recession, gingival bleeding, and dental calculus in adults 30 years of age and older in the United States, 1988–1994. *J Periodontol*. 1999;70(1):30–43. doi:10.1902/jop.1999.70.1.30
57. Mythri S, Arunkumar S, Hegde S, Rajesh S, Munaz M, Ashwin D. Etiology and occurrence of gingival recession: An epidemiological study. *J Indian Soc Periodontol*. 2015;19(6):671. doi:10.4103/0972-124X.156881
58. Cortellini P, Bissada NF. Mucogingival conditions in the natural dentition: Narrative review, case definitions, and diagnostic considerations. *J Clin Periodontol*. 2018;45(Suppl 20):S190–S198. doi:10.1111/jcpe.12948
59. Mary AF, Govindaraju L. High frenal attachment and its prevalence among children: A retrospective study. *J Adv Pharm Tech Res*. 2022; 13(Suppl 2):S573–S577. doi:10.4103/japtr:japtr_155_22
60. Gürbüz S, Bakhishov H, Koçyiğit EG, Işık A, Tuncer BB, Özdemir B. Evaluation of mid-buccal gingival recessions and occlusal interferences. *J Oral Rehabil*. 2023;50(10):1058–1069. doi:10.1111/joor.13543
61. Krishna Prasad D, Sridhar Shetty N, Solomon EGR. The influence of occlusal trauma on gingival recession and gingival clefts. *J Indian Prosthodont Soc*. 2013;13(1):7–12. doi:10.1007/s13191-012-0158-1
62. Jepsen S, Caton JG, Albandar JM, et al. Periodontal manifestations of systemic diseases and developmental and acquired conditions: Consensus report of workgroup 3 of the 2017 World Workshop on the Classification of Periodontal and Peri-Implant Diseases and Conditions. *J Periodontol*. 2018;89(Suppl 1):S237–S248. doi:10.1002/JPER.17-0733
63. Liang F, Zhou Y, Zhang Z, Zhang Z, Shen J. Association of vitamin D in individuals with periodontitis: An updated systematic review and meta-analysis. *BMC Oral Health*. 2023;23(1):387. doi:10.1186/s12903-023-03120-w
64. Frąckiewicz W, Jankowska A, Machoy ME. CBCT and modern intra-oral scanners as tools for developing comprehensive, interdisciplinary treatment plans. *Adv Clin Exp Med*. 2024;33(11):1267–1276. doi:10.17219/acem/175817

MiRNA in archival serum samples derived from breast cancer patients treated with neoadjuvant chemotherapy vs freshly collected samples: Pilot study

Marcin Kubiczko^{A–F}, Patrycja Tudrej^{A–F}, Tomasz Tyszkiewicz^{A–F},
Aleksandra Krzywon^{C–F}, Małgorzata Oczko-Wojciechowska^{A,E,F}, Michał Jarzab^{A,B,E,F}

Maria Skłodowska-Curie National Research Institute of Oncology, Gliwice Branch, Poland

A – research concept and design; B – collection and/or assembly of data; C – data analysis and interpretation;
D – writing the article; E – critical revision of the article; F – final approval of the article

Advances in Clinical and Experimental Medicine, ISSN 1899–5276 (print), ISSN 2451–2680 (online)

Adv Clin Exp Med. 2025;34(9):1521–1530

Address for correspondence

Marcin Kubiczko

E-mail: marcin.kubiczko@gliwice.nio.gov.pl

Funding sources

National Science Centre, Poland (project No. 2021/05/X/NZ5/00971).

Conflict of interest

Marcin Kubiczko declares conference fees for Pfizer, Roche, Novartis, Teva, Amgen, Swixx Biopharma, and Gilead; clinical trials for Roche, MSD, Novartis, Seagen, and Gilead; speaker's honoraria from Novartis, Roche, Lilly, Teva, Amgen, Swixx Biopharma, and Gilead; advisory board for Novartis; all outside the submitted work. Michał Jarzab declares conference fees for Gilead and Roche; clinical trials for Roche, MSD, Novartis, Seagen, and Gilead; speaker's honoraria from Novartis, Roche, Lilly, Pfizer, Teva, Gilead, Exact Sciences, and Mamotome; advisory boards for Novartis and Pfizer; all outside submitted work. All other authors declare they have no competing interests.

Received on March 18, 2024

Reviewed on July 31, 2024

Accepted on September 13, 2024

Published online on December 16, 2024

Cite as

Kubiczko M, Tudrej P, Tyszkiewicz T, Krzywon A, Oczko-Wojciechowska M, Jarzab M. MiRNA in archival serum samples derived from breast cancer patients treated with neoadjuvant chemotherapy vs freshly collected samples Pilot study. *Adv Clin Exp Med.* 2025;34(9):1521–1530. doi:10.17219/acem/193265

DOI

10.17219/acem/193265

Copyright

Copyright by Author(s)

This article was originally published under a CC BY 3.0 license and is now available under a CC BY 4.0 license

Creative Commons Attribution 3.0 Unported (CC BY 4.0)

(https://creativecommons.org/licenses/by/4.0/)

Abstract

Background. Liquid biopsy, including miRNA profiling, is a promising approach to identify breast cancer (BC) resistance. However, the effect of long-term storage on the quality of miRNA assessment in archival serum has not been fully addressed.

Objectives. We aimed to determine whether miRNAs were recoverable from long-stored serum samples to subsequently evaluate prognostic and predictive miRNA value in the archival collection of samples from patients treated with neoadjuvant chemotherapy at Maria Skłodowska-Curie National Research Institute of Oncology, Gliwice, Poland.

Material and methods. We have evaluated miRNA quantity in serum samples stored for up to 12 years. Additionally, we compared miRNA expression in archival samples to freshly collected samples derived from advanced BC patients.

Results. Forty BC patients were included in the study. Archival samples were derived from 20 BC patients treated with radical intent between 2011 and 2015. Freshly collected samples were collected from 20 advanced BC patients in 2022. miRNA was present in archived serum samples frozen at -80°C for at least 12 years. Additionally, we found significantly different expressions between the 2 analyzed groups. Expression of circulating miR-16, -17, -18a, -20a, -21, -27a, -30b, -222, and -326 were significantly higher in archival samples, whereas expression of circulating miR-19a, -29b, -29c, -128, -145, -146a, -193b, -195, -200b, -210, -221, -424, and -451a were lower than in freshly collected samples. In 14 miRs, we observed expression in both groups; however, differences were statistically insignificant (miR-1, -7a, -10b, -19b, -34a, -99a, -106b, -122, -125b, -155, -200a, -205, -223, -340).

Conclusions. MiRNA can be identified from long-stored samples, making large prospectively collected serum repositories with long follow-up time an invaluable source for miRNA biomarker discovery.

Key words: breast cancer, biomarkers, liquid biopsy, miRNA, archival samples

Background

Breast cancer (BC) is the most commonly diagnosed cancer globally.¹ Early detection intensifies the effort toward discovering new biomarkers that can improve its prognosis and therapeutic outcomes. Numerous systemic treatment approaches for BC are still in their early phases of development; thus, it is essential to find precise biomarkers that may be used to guide therapeutic decisions regarding cytotoxic agents, targeted therapies and immunotherapy.²

Substantial advances in molecular signalling processes have lead to a discovery of a variability of biomarkers in tissues and blood (liquid biopsy) that may help predict the probability of cancer spread, treatment efficacy and tolerance.² Tumor cells are heterogeneous; therefore, a single biomarker is not precise enough to effectively diagnose cancer progression and metastasis, and a combination of biomarkers is preferred. Prognostic and predictive biomarkers are 2 categories of biomarkers that indicate likely clinical outcomes and treatment efficacy. MicroRNA (miRNA) can be utilized in both of these applications.³

The miRNAs are short non-coding RNA molecules containing about 22 nucleotides. To date, 48,860 have been identified, including 2,654 mature sequences in the human genome.⁴ More than half of human protein-coding genes are regulated by miRNAs.⁵ They act as tumor suppressors or oncogenes, and functional studies have proven that miRNA dysregulation is causal in numerous cancer cases.⁶ Expanded insights into the roles of miRNA dysregulation in development and cancer progression have made miRNAs attractive tools and targets for new treatment approaches.⁶ They can be found both in tissue and blood, allowing the utilization of liquid biopsy, which is a useful clinical technique.⁷

Neoadjuvant chemotherapy has an essential role in the prevention of BC recurrence. However, the primary obstacle is drug resistance. The miRNA profiling is the prominent approach to identifying BC resistance. Expression of several miRNAs was decreased in chemotherapy resistance. In cells derived from triple-negative breast cancer (TNBC) patients treated with neoadjuvant paclitaxel, elevated expression of miR-18a increased paclitaxel resistance.⁸ MiR-90b, -130a, -200b, and -452 may lead to chemoresistance by regulating drug-related cellular pathways.⁹ Responders to neoadjuvant chemotherapy had significantly lower levels of miR-21 and miR-195 than non-responders.¹⁰ Serum miR-125b also predicted poor chemotherapy outcomes and shorter disease-free survival (DFS).¹¹ MiR-34a has recently emerged as a tumor suppressor of significant interest. Liu et al. found that changes in serum miR34a expression were associated with treatment response and DFS.¹² In a small group of 27 patients, serum miR-451 was higher and showed a significant gradual decline during neoadjuvant chemotherapy, consisting of doxorubicin/cyclophosphamide and taxane, in the patients stratified as clinical responders.¹³ The increase of serum expressions of both miR-19a and miR-205 during neoadjuvant chemotherapy consisting of doxorubicin and paclitaxel in patients with luminal A BC was more pronounced in the resistant group compared with the sensitive group. Furthermore, both were independent predictive factors for chemotherapy response.¹⁴ The downregulation of serum miR-99a expression in BC patients has been closely associated with a poor prognosis.¹⁵ The expression of miR-10b, -21, -34a, -125b, -145, -155, and -373 in patients before the start of treatment was significantly higher, and miR-210 was lower than levels in healthy controls.¹⁶ A summary of studies on circulating miRs in BC patients is presented in Table 1.^{11–41}

Table 1. Summary of studies on circulating microRNAs in BC patients

miR	Level	Source	Role	Reference
miR-1	upregulation	plasma	cardiotoxicity – increasing circulating levels during CHT containing DOX and PXL associated with a decrease in LVEF	17
miR-7a	downregulation	plasma	in comparison to HC (before CHT); increase after treatment	18
	downregulation	serum	in comparison to HC and patients with benign lesions	19
	upregulation	serum	in HER2-pos vs HER2-neg subtype	20
miR-7c	downregulation	serum	in comparison to HC	21
	downregulation	serum	in comparison to HC; no difference between ER-pos and ER-neg BC	22
miR-9	upregulation	serum	in comparison to HC; in HER2-positive vs HER2-negative BC	23
miR-10b	upregulation	plasma	in comparison to HC (before CHT); decrease after Tx	18
miR-16	downregulation	serum	in comparison to HC	24
miR-17	downregulation	serum	pCR after neoadjuvant CT	25
miR-18b	upregulation	serum	predictive for tumor relapse and OS	26
miR-19a	upregulation	serum	resistance to neoadjuvant CT in LUM A	14
miR-19b	downregulation	serum	pCR after neoadjuvant CT	25
miR-21	upregulation	plasma	in comparison to HC (before CHT), decrease after Tx	18
	upregulation	serum	in comparison to HC (before CHT)	21
miR-27a	upregulation	serum	higher CS and histological grade, ER-neg, HER2-pos	27

Table 1. Summary of studies on circulating microRNAs in BC patients – cont.

miR	Level	Source	Role	Reference
miR-29b	downregulation	plasma	In comparison to HC	28
miR-30b	downregulation	serum	pCR after neoadjuvant CT	25
miR-34a	downregulation	serum	Response to neoadjuvant CT, longer DFS	12
miR-99a	downregulation	serum	Shorter OS, higher TNM stage	15
miR-106b	upregulation	plasma	In comparison with benign breast lesions; Shorter DFS and OS	29
miR-122	upregulation	plasma	In comparison to HC	30
miR-125b	upregulation	serum	Response to neoadjuvant CT, longer DFS	11
	upregulation	serum	Higher number of metastatic lymph nodes	20
	upregulation	serum	In comparison to HC	16,24
	upregulation	serum	Resistance to neoadjuvant CHT	31
miR-129	downregulation	serum	Shorter OS	32
miR-141	upregulation	plasma	Predictive for shorter PFS and OS	33
miR-145	upregulation	serum	In comparison to HC (before CHT)	16
miR-146a	downregulation	plasma	In patients with sentinel lymph nodes metastases vs N0	34
miR-155	upregulation	plasma	In comparison to HC (before CHT)	18
	upregulation	plasma	In comparison to HC; higher CS in BC (CS III vs II; II vs I)	18
	downregulation	serum	In comparison to healthy controls	21,24
	downregulation	serum	Response to Tx	35
	downregulation	plasma	Response to Tx	18
miR-195	upregulation	whole blood	In comparison to HC; larger breast tumors; BC-specific	36
	downregulation	serum	In comparison to HC and benign lesions	19
	downregulation	serum	In comparison to HC; increase with response to neoadjuvant CT	37
	downregulation	plasma	Metastatic LUM A BC in comparison to local BC	38
miR-200a	upregulation	serum	Higher number of metastatic lymph nodes	20
	upregulation	plasma	Predictive for shorter PFS and OS	33
miR-200b	upregulation	plasma	Predictive for shorter PFS and OS	33
miR-200c	upregulation	plasma	In metastatic BC vs locally advanced BC	39
	upregulation	plasma	Predictive for shorter PFS and OS	33
miR-205	upregulation	serum	Resistance to neoadjuvant CT in LUM A	14
miR-210	downregulation	serum	In comparison to HC (before CHT)	16
miR-222	upregulation	serum	Shorter DFS and OS; lower rates of pCR; trastuzumab-resistance	40
miR-326	downregulation	plasma	In patients with sentinel lymph nodes metastases vs N0	34
miR-373	upregulation	serum	In comparison to HC (before CHT)	16
miR-451	downregulation	serum	During neoadjuvant CT in responders	13
miR-455	downregulation	serum	In comparison with HC, In pts with LN metastases vs N0 Infiltrating carcinoma vs carcinoma in situ	41

miR – microRNA; CHT – chemotherapy; DOX – doxorubicin; PXL – paclitaxel; HC – healthy controls; pos – positive; neg – negative; ER – estrogen receptor; BC – breast cancer; HER2 – human epidermal growth factor receptor 2; Tx – treatment; pCR – pathologic complete response; OS – overall survival; LUM – luminal subtype; DFS – disease-free survival; CS – clinical stage; TNM – tumor-nodule-metastasis staging system; PFS – progression-free survival; pts – patients; LVEF – left ventricular ejection fraction; LN – lymph node; N0 – node negative.

Objectives

We aimed to determine whether miRNAs were recoverable from long-stored serum samples. To achieve this, we assessed serum samples from 20 BC patients, drawn at various time points. Additionally, we compared them to miRNA expression from freshly collected samples derived from the group of patients with advanced BC.

Materials and methods

Study population

Archival serum samples were taken from the patients with BC recruited into prospective observational clinical trial concerning neoadjuvant chemotherapy. All patients had serial blood collection before the beginning

of the treatment and during systemic treatment. For the purpose of this pilot study, only samples collected at the beginning of the treatment were used. These samples were taken between 2011 and 2015. A tumor biopsy at Maria Skłodowska-Curie National Research Institute of Oncology (Gliwice, Poland) was performed for histopathological verification and the possibility of further molecular assessment. Moreover, patients underwent multimodality treatment (systemic treatment including chemotherapy, endocrine therapy, targeted therapy, surgery, and radiation therapy) at our institution and remained in follow-up. Furthermore, extensive radiologic evaluation was performed, including baseline and serial breast magnetic resonance imaging (MRI) assessment, baseline ^{18}F -fluorodeoxyglucose positron emission tomography (^{18}F -FDG-PET/CT), and assessment of early metabolic response after the 1st cycle of chemotherapy. Freshly collected samples were taken from the group of patients with advanced BC.

Clinical samples

Blood processing and sample storage

All laboratory procedures were performed at Maria Skłodowska-Curie National Research Institute of Oncology in the Department of Clinical and Molecular Genetics. All clinical samples described here were obtained from subjects with informed consent. Freshly collected samples comprised plasma. Blood was processed for plasma isolation within 1 h of collection. Blood was centrifuged in cRNA collection tubes (RNA Complete BCT[®] CE; Streck LLC, La Vista, USA) at $1,800 \times g$ at room temperature in an Eppendorf 5810R (Eppendorf AG, Hamburg, Germany) for 15 min. Plasma was transferred to a fresh tube and centrifuged at $2,800 \times g$ for 15 min. Plasma was aliquoted, with inversion to mix between each aliquot, and stored at -80°C . Archival samples comprised serum samples. For serum collection, blood was collected into BD Vacutainer[®] serum tubes (BD Biosciences, Franklin Lakes, USA) and allowed to clot for 30–60 min at room temperature. Clot was removed by centrifugation at $1,300 \times g$ at room temperature for 10 min. Serum was aliquoted and stored at -80°C until miRNA isolation.

MiRNA isolation and measurement of miRNA expression

MiRNA isolation was performed with the TaqMan[®] miRNA ABC (Anti-miRNA Bead Capture) Purification Kit – Human Panel A (Thermo Fisher Scientific Inc., Waltham, USA). Complementary DNA (cDNA) template from miRNA was prepared with the TaqMan[®] Advanced miRNA cDNA Synthesis Kit (Thermo Fisher Scientific Inc.). Mature miRNAs from total RNA were modified by extending the 3' end of the mature transcript through poly(A) addition, and then the 5' end was lengthened

by the 5' end by adaptor ligation. The modified miRNAs were then subjected to universal reverse transcription followed by amplification to increase uniformly the amount of cDNA for all miRNAs (miR-Amp reaction). Analysis of miRNA expression was performed with TaqMan[®] Advanced miRNA Assays. The assays can detect and quantify the mature form of the miRNA from 2 μL of total RNA from serum or plasma. TaqMan[®] Fast Advanced Master Mix was used to prepare PCR Reaction Mix. Customizable TaqMan[®] Advanced MicroRNA Cards (ADV MIRNA CARD FRMT 48; Thermo Fisher Scientific Inc.) were used to measure expression. Quantitative real-time polymerase chain reaction (qPCR) was carried out on a QantStudio 12K FLEX (Thermo Fisher Scientific Inc.) with a TaqMan[®] Array Micro Fluidic Thermal Cycling Block. Nucleic acid-free pipette tips were used to handle all reagents. All procedures were performed following the manufacturer's protocol.

Based on published literature, 48 miRNAs were selected for expression measurement: miR-16, -17, -18a, -20a, -21, -27a, -30b, -222, and -326, -19a, -29b, -29c, 128, -145, -146a, -193b, -195, -200b, -210, -221, -424, -451a, -1, -7a, -10b, 19b, -34a, 99a, -106b, -122, -125b, -155, -200a, -205, -223, -340, -7c, -9, -18b, -33b, -124, -126, -129, -141, -196b, -200c, -373, and -455.

Response assessment

The early metabolic response to treatment in (^{18}F -FDG-PET/CT) was assessed based on the European Organisation for Research and Treatment of Cancer (EORTC) guidelines.⁴² Specifically, complete metabolic response was defined as a complete resolution of fluorodeoxyglucose (FDG) uptake in all sites, partial metabolic response referred to a reduction of at least 25% in maximum standardized uptake value (SUVmax), an increase or decrease of less than 25% in SUVmax indicated stable metabolic disease, whereas progressive metabolic disease was defined as either a $>25\%$ increase in SUVmax or the development of a new FDG-avid lesion.

Tumor response in MRI was assessed according to Response Evaluation Criteria in Solid Tumours (RECIST) v. 1.1, categorizing outcomes as a complete response, partial response, stable disease, or progressive disease.⁴³

Statistical analyses

Continuous data were summarized as median values and presented with an interquartile range (IQR; Q1–Q3). Wilcoxon rank sum test evaluated differences between the 2 groups. The Benjamini–Hochberg correction was used as an adjustment for multiple testing. To assess the normality of the data, the Shapiro–Wilk test was employed. A two-sided p-value <0.05 was considered statistically significant. All computational analyses were performed in the R environment for statistical

computing v. 4.0.1, “See Things Now,” released on June 6, 2020 (R Foundation for Statistical Computing, Vienna, Austria; <http://www.r-project.org>, accessed December 20, 2022).

Results

Archival samples were derived from BC patients treated with radical intent between 2011 and 2015, including 6 in 2011, 4 in 2012, 2 in 2014, and 8 in 2015. Half of the patients were premenopausal. Seventeen patients were diagnosed with early BC. In contrast, 3 patients were diagnosed with oligometastatic disease and were included in treatment with radical intent by the multidisciplinary team. Five patients received the AC-P regimen (AC – doxorubicin plus cyclophosphamide, followed by paclitaxel), 2 patients AC regimen, 7 patients TAC regimen (docetaxel, AC), 3 patients TEC regimen (docetaxel, epirubicin and cyclophosphamide), 2 patients FEC regimen (fluorouracil, AC), and 1 patient the AT regimen (doxorubicin plus docetaxel). All patients with archival samples underwent baseline positron emission tomography / computed tomography (PET/CT) scanning and MRI imaging. The majority of patients (13, 65%) had early metabolic assessment after the 1st chemotherapy cycle. For this subgroup, the median decrease in SUVmax following the 1st chemotherapy cycle was 28% (IQR: 13.0–60.5). Specifically, a partial metabolic response was observed in 69% of patients (9 of 13), while 31% had stable metabolic disease (4 of 13 patients). Serial MRI assessments were conducted for all patients except 1. Seventeen patients (89%) achieved partial remission on MRI. Stable disease was observed in 2 patients (11%). Sixteen patients underwent subsequent surgery. In 2 patients, complete histopathologic remission was observed (12.5%). All of the analyzed patients experienced disease recurrence. The median DFS was 31.2 months (5.8–72.3 months). Fresh samples were derived from advanced BC patients in 2022. Patients’ characteristics are presented in Table 2.

In all but 1 archival sample, miRNA expression was detected. The expression of circulating miR-16, -17, -18a, -20a, -21, -27a, -30b, -222, and -326 was significantly higher in archival samples than in freshly collected samples. The results are depicted in Fig. 1. Specifically, miR-17 exhibited higher expression in patients treated with radical intent. Among this group, the vast majority received taxane-containing chemotherapy regimens (16 patients, 80%), including 11 patients treated with docetaxel and 5 patients treated with paclitaxel.

The expression of circulating miR-19a, -29b, -29c, 128, -145, -146a, -193b, -195, -200b, -210, -221, -424, and -451a was lower in archival samples than in freshly collected samples. These results are depicted in Fig. 2.

In 14 miRs, we observed expression in archival samples and freshly collected samples; however, differences between the groups were statistically insignificant (miR-1,

Table 2. Patients characteristics

Patient characteristics		Patients with archival samples (n = 20)	Patients with freshly collected samples (n = 20)
Median age (Q1–Q3) [years]		41.2 [36.8–55.8]	58 [50.3–67.8]
Histologic subtype	NST	17	14
	ILC	3	6
	Grade 1	2	1
	Grade 2	15	14
	Grade 3	3	5
Biologic subtype	LUM A	2	6
	LUM B HER2-	18	14
Clinical stage	IIA/B	7	0
	IIIA/B/C	10	0
	IV	3	20
PET SUVmax – median (Q1–Q3)		7.0 [3.8–10.6]	8.1 [4.5–13.2]

IQR – interquartile range; NST – invasive cancer of no special type; ILC – invasive lobular cancer; LUM – luminal; PET – positron emission tomography; SUVmax – maximum standardized uptake value.

-7a, -10b, 19b, -34a, 99a, -106b, -122, -125b, -155, -200a, -205, -223, and -340). Finally, no expression of the remaining 12 miRs was observed (miR-7c, -9, -18b, -33b, -124, -126, -129, -141, -196b, -200c, -373, and -455). Results of the normality tests are presented in Supplementary Tables 1 and 2.

Discussion

Levels of specific circulating microRNAs in BC patients are associated with tumor development and progression and may be involved in chemotherapy resistance. Moreover, the dynamics of circulating microRNAs might serve as a novel biomarker of clinical response to neoadjuvant chemotherapy.

Our study’s archival samples were derived mostly from early BC, except for 3 patients with the oligometastatic disease treated with radical intent. Freshly collected samples included those obtained from BC patients. That would be the primary explanation for different expressions of miR-16, -17, -18a, -20a, -21, -27a, -30b, -222, -326, -19a, -29b, -29c, -128, -145, -146a, -193b, -195, -200b, -210, -221, -424, and -451a.

Serum miR-21 expression could predict response to neoadjuvant chemotherapy.¹¹ In our study, the expression of miR-21 was higher in archival samples, comprising mostly patients with early BC, compared to fresh samples collected from patients with advanced disease. However, it is worth pointing out that not only baseline expression is important, but also the dynamic changes during treatment. Lowering serum miR-21 expression could predict response to neoadjuvant chemotherapy as early as the end of the 2nd treatment cycle. Furthermore, patients with decreasing miR-21 expression during neoadjuvant

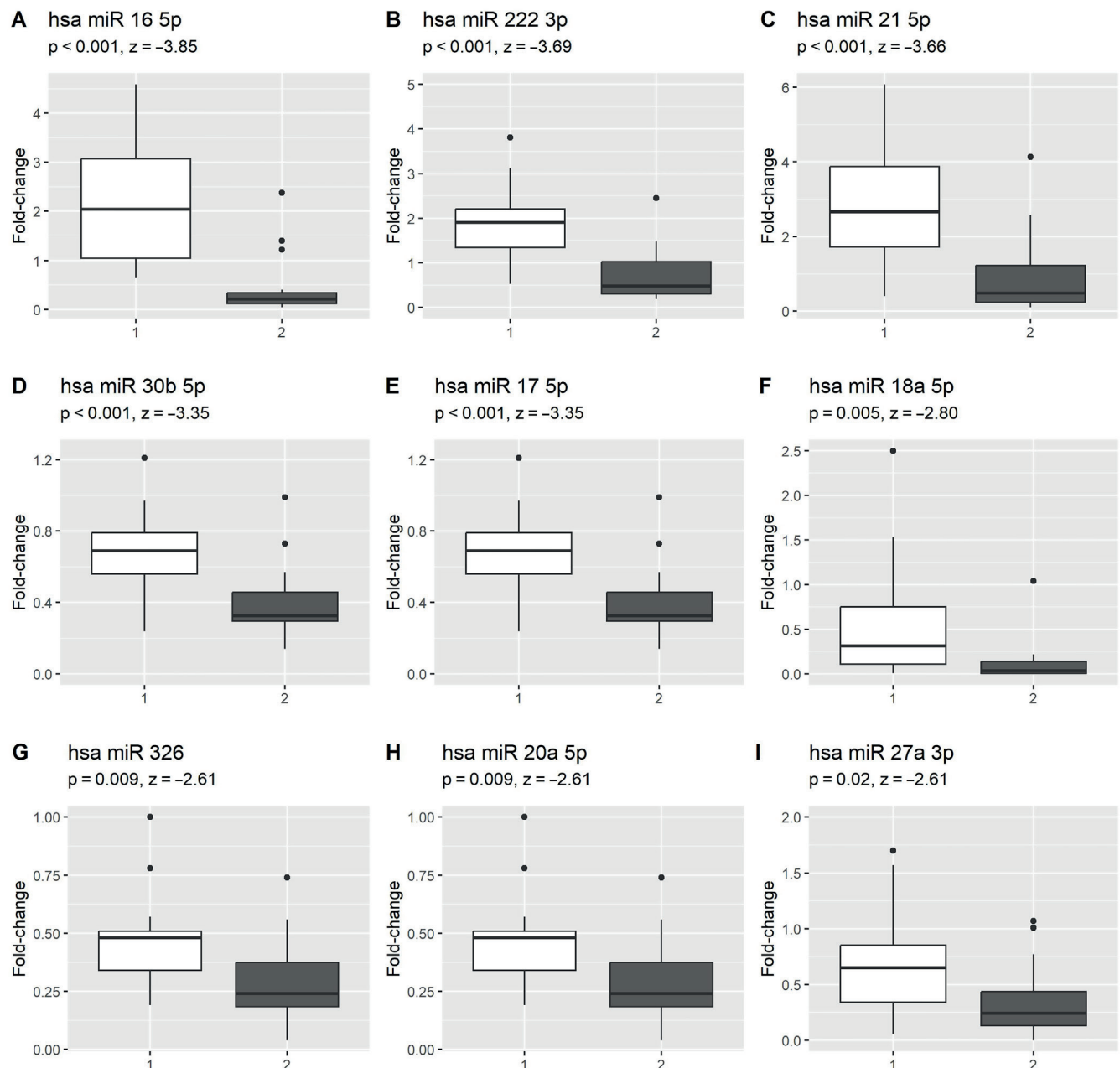


Fig. 1. MiRNAs with higher expression in archival samples (1) than freshly collected samples (2). In 1 archival sample, miRNA expression was not detected. All miRNA types were measurable in the remaining 39 samples (including 19 archival samples from patients treated with radical intent and 20 freshly collected samples from patients with advanced breast cancer)

z – Z-test statistic.

chemotherapy had better DFS than those showing increased ser-miR-21 expression. In another study, changes in ser-miR-21 levels during neoadjuvant chemotherapy were correlated with clinical response and survival; however, it was not associated with pathology response.¹⁶

In BC tissues and cells resistant to taxol, the increased expression of nuclear receptor co-activator 3 (NCOA3) results in downregulation of miR-17. Thus, NCOA3 and miR-17 may serve as a biomarkers and a therapeutic targets in BC resistance to taxol.⁴⁴ By directly targeting NCOA3, miR-17 enhanced the sensitivity of BC cells to taxol, implying a potential tumor-suppressor role for miR-17 in BC.⁴⁴

In our study, higher levels of miR-17 were observed in a population undergoing taxol-containing chemotherapy. Thus, further analysis of our group with miRNA assessment in serially collected samples would be interesting to verify this hypothesis on a liquid biopsy level. Moreover, blood-derived data suggested a potential association between miR-17, -19b and -30b expression levels and complete clinical response after neoadjuvant chemotherapy,²⁵ and miR-30b was another overexpressed miRNA in our study.

Elevated circulating levels of miR-195, in contrast to other miRs (such as let-7a, miR-10b and miR-155), were found

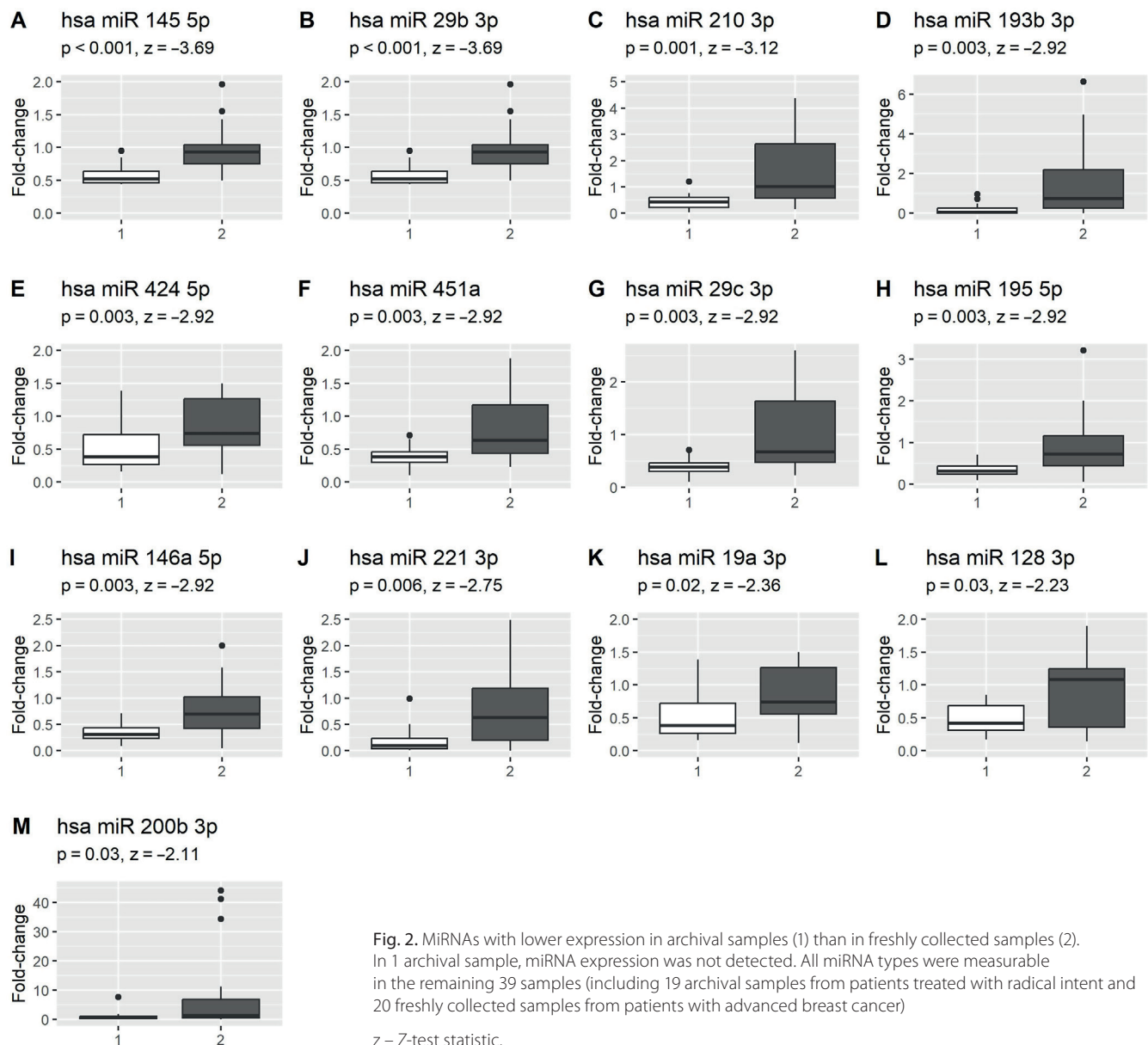


Fig. 2. MiRNAs with lower expression in archival samples (1) than in freshly collected samples (2). In 1 archival sample, miRNA expression was not detected. All miRNA types were measurable in the remaining 39 samples (including 19 archival samples from patients treated with radical intent and 20 freshly collected samples from patients with advanced breast cancer)
z – Z-test statistic.

to be specific for BC.³⁶ Furthermore, systemic miR-195 levels showed incremental increase with larger breast tumors.³⁶ In BC patients, circulating miR-195 was significantly higher compared to control patients.³⁶ In contrast, some studies showed lower levels of miR-195 in BC patients than in healthy control,³⁷ or no significant differences in blood serum expression values of miR-195 between these 2 groups.²⁰ Interestingly, in luminal A BC, miR-195 was found to be underexpressed in patients with metastatic disease compared to patients with local disease.³⁸ In our study, which predominantly included patients with luminal B BC, we observed higher miR-195 expression in patients with metastatic disease. To fully understand miR-195 dynamics, further evaluation involving a larger cohort of patients is necessary. This assessment should explore differences in miR-195 expression between subtypes and investigate its predictive value during neoadjuvant treatment.³⁷

Levels of circulating miR-373 were significantly higher in TNBC patients.⁴⁵ In our study, which was comprised of only luminal cases, we did not observe miR-373 expression in archival or freshly collected samples.

Serum miR-222 predicted both efficacy and trastuzumab-induced cardiotoxicity.⁴⁰ Furthermore, miR-222, -20a and -451 level changes were associated with chemosensitivity, whereas a chemo-induced decrease in plasma miR-34a in the insensitive patients was found.⁴⁶ We found higher levels of miR-222 and miR-20a in a population undergoing neoadjuvant chemotherapy; levels of miR-451 were lower, whereas miR-34a was comparable to those observed in advanced BC patients. Since we have toxicity data in our population, we would like to further evaluate the potential of miR-222 in cardiotoxicity prediction.

Few studies have been performed to verify the predictive potential of circulating miRNAs in BC. MiR-125b was

correlated with resistance to chemotherapy,³¹ whereas downregulation of miR-155 suggested treatment response.³⁵ Our study found similar serum expression of miR-125b and miR-155 in archival samples, derived mostly from early BC patients and freshly collected samples from advanced BC patients. The expression of plasma miR-122 was found to be significantly upregulated in BC patients compared to healthy controls.³⁰ In our study, no significant differences were found between patients with early-stage and advanced-stage BC. Nonetheless, miR-122 dysregulation may be involved in response to chemotherapy, radiotherapy and BC progression.⁴⁷

Despite the advantages associated with miRNA evaluation as potential blood-based biomarkers, reproducible and robust miRNA quantification is challenging, and attention must be paid to the numerous technological parts of the measurements. Recently published reviews have comprehensively discussed the challenges and difficulties in accurately quantifying miRNAs, comprising pre-analytical, analytical and methodological issues contributing to result heterogeneity.⁴⁸ During the preanalytical phase, meticulous attention to practical details is crucial. We emphasized the importance of collecting an adequate blood volume. This includes ensuring an appropriate ratio to anticoagulant. Ensuring timely processing of samples for subsequent steps was a priority. In order to minimize transport time, we prepared the sample for processing before blood sampling. During blood draw, we took great care to prevent hemolysis, which could affect sample integrity. Our stored materials adhered strictly to appropriate conditions, avoiding any individual deviations.

Moving on to the analytic phase, we maintained a meticulous approach. Two individuals independently verified probe identification numbers. We followed manufacturer guidelines meticulously throughout the process. Our methodology was tailored to meet the expectations and requirements of the source material, which comprised both plasma and serum.

Heterogeneity may result from various situations. For instance, adequate probe rotation within the center, from the moment of blood draw to the time of analysis, plays a crucial role. While this procedure is not always feasible for every center, we were fortunate to perform all procedures within 1 building. Additionally, using specialized probes and preparing experiments specifically for the material contributed positively to our study.

Remarkably stable form is an essential prerequisite for utility as a biomarker.⁴⁹ The miRNA molecules are robust and survive harsh treatment and storage conditions.⁴⁸ Incubation of plasma at room temperature for up to 24 h or subjecting it to 8 freeze–thaw cycles appears to have minimal impact on the levels of specific miRNAs.⁴⁹

Another issue is the type of blood derivative. Serum has less baseline platelet contamination than plasma, while the differential release of confounding miRNAs by blood cells may be associated with clot formation.⁵⁰ Measurements of selected miRNAs obtained from the matched

samples of plasma or serum collected from a given individual at the same blood draw were strongly correlated, showing that both plasma and serum samples are suitable for miRNAs investigation as blood-based biomarkers.⁴⁹ However, studies have yielded conflicting results as to which type of sample is superior to the other.⁵¹ MiRNA was found to be potentially recoverable from plasma samples stored for more than 12 years.⁵² It showed high stability and long frozen half-life in plasma samples stored for 14 years.⁵³ On the contrary, despite storage at -80°C , miRNA levels were significantly changed in whole blood samples in long-term storage, defined as 9 months.⁵⁴ Our repository, like many others, contains a greater number of clinical serum specimens than plasma samples. Thus, our results may enable further research of archival samples.

As we validated the identification of miRNAs from long-stored samples in our repository, we intend to assess miRNA expression in a large cohort of patient samples. This comprehensive evaluation will allow us to address the crucial question of miRNA utility as a prognostic and predictive biomarker.

Neoadjuvant treatment offers the chance to tailor therapy based on the tumor's observed response during therapy and allows for adjustments, such as escalating, de-escalating or switching to other systemic regimens. Biomarkers for predicting treatment response play a crucial role in all these scenarios. Combining both liquid biopsy and imaging represents a promising approach for predicting and optimizing neoadjuvant systemic treatment in BC.^{55,56}

Limitations

To our knowledge, there are no prior reports of recovery of miRNA from serum samples stored for this length of time compared to the expression of freshly collected samples. Nonetheless, we have to admit several drawbacks. MiRNA in archival samples was derived from serum, whereas in freshly collected samples from plasma. In addition, we acknowledged the difficulty of drawing conclusions from comparisons between early and advanced BC patients. However, in this pilot study, we primarily wanted to assess whether it is possible to measure miRNA levels in samples from our repository, and samples derived from advanced BC patients were chosen as anticipated to have measurable levels of most miRNAs. We have to emphasize that the utility of miRNA evaluation in long-stored samples was assessed specifically in samples derived from 20 patients. The potential correlation between the expression levels of different miRNA types and treatment response, particularly early metabolic response, is an intriguing issue. However, data on early response assessment using a combination of FDG-PET-CT and miRNA in BC patients undergoing neoadjuvant systemic therapy are lacking. Currently, due to the limited number of patients in this pilot study, drawing definitive conclusions is challenging. Further evaluation would be conducted after testing a larger sample size since the vast majority of patients

in our cohort underwent FDG-PET-CT scans with early metabolic assessment after the 1st chemotherapy cycle.

For now, circulating miRNAs were not compared to tissue expression. Nevertheless, due to the positive results of our study, our next step would be to proceed with genetic testing of tumor tissue and an extensive assessment of serum samples in our repository. The timing seems optimal: on the one hand, our dataset is mature; patients were treated around a decade ago, and we have complete results concerning DFS, overall survival and long-term treatment toxicity. On the other hand, patients were diagnosed and treated according to current guidelines with modern chemotherapy regimens and the addition of trastuzumab as needed.

Conclusions

MiRNA can be identified from long-stored samples, making large prospectively collected serum repositories with long follow-up time an invaluable source for miRNA biomarker discovery. Specifically, miR-16, -17, -18a, -20a, -21, -27a, -30b, -222, -326, -19a, -29b, -29c, 128, -145, -146a, -193b, -195, -200b, -210, -221, -424, -451a, -1, -7a, -10b, 19b, -34a, -99a, -106b, -122, -125b, -155, -200a, -205, -223, and -340 were identified.

Supplementary data

The Supplementary materials are available at <https://doi.org/10.5281/zenodo.13619558>. The package includes the following files:

Supplementary Table 1. Results of the normality test as presented in Fig. 1 (performed using the Shapiro–Wilk test).

Supplementary Table 2. Results of the normality test as presented in Fig. 2 (performed using the Shapiro–Wilk test).

Supplementary Table 3. Testing the assumption of normality for age and PET SUV variables in groups of patients with archival samples and patients with freshly collected samples.

Supplementary Table 4. Results of the Brown–Forsythe test for homogeneity of variance among different groups for miR-326, miR-20a and miR-128.

Data availability


The datasets generated and/or analyzed during the current study are available from the corresponding author on reasonable request.


Consent for publication


Not applicable.

ORCID iDs


Marcin Kubiczek - 0000-0003-1877-5691


Patrycja Tudrej  <https://orcid.org/0000-0003-0414-3853>

Tomasz Tyszkiewicz  <https://orcid.org/0000-0003-4863-0143>

Aleksandra Krzywón  <https://orcid.org/0000-0003-4796-5478>

Małgorzata Oczko-Wojciechowska

 <https://orcid.org/0000-0002-8989-0075>

Michał Jarzab  <https://orcid.org/0000-0002-2642-9724>

References

1. Wilkinson L, Gathani T. Understanding breast cancer as a global health concern. *Br J Radiol.* 2022;95(1130):20211033. doi:10.1259/bjr.20211033
2. Wu HJ, Chu PY. Recent discoveries of macromolecule- and cell-based biomarkers and therapeutic implications in breast cancer. *Int J Mol Sci.* 2021;22(2):636. doi:10.3390/ijms22020636
3. Janes H, Pepe MS, McShane LM, Sargent DJ, Heagerty PJ. The fundamental difficulty with evaluating the accuracy of biomarkers for guiding treatment. *J Nat Cancer Inst.* 2015;107(8):djv157. doi:10.1093/jnci/djv157
4. Kozomara A, Birgaoanu M, Griffiths-Jones S. miRBase: From microRNA sequences to function. *Nucl Acids Res.* 2019;47(D1):D155–D162. doi:10.1093/nar/gky1141
5. Friedman RC, Farh KKH, Burge CB, Bartel DP. Most mammalian mRNAs are conserved targets of microRNAs. *Genome Res.* 2009;19(1):92–105. doi:10.1101/gr.082701.108
6. Rupaimoole R, Slack FJ. MicroRNA therapeutics: Towards a new era for the management of cancer and other diseases. *Nat Rev Drug Discov.* 2017;16(3):203–222. doi:10.1038/nrd.2016.246
7. Voith Von Voithenberg L, Crocetti E, Martos C, et al. Cancer registries: Guardians of breast cancer biomarker information. A systematic review. *Int J Biol Markers.* 2019;34(2):194–199. doi:10.1177/1724600819836097
8. Sha LY, Zhang Y, Wang W, et al. MiR-18a upregulation decreases Dicer expression and confers paclitaxel resistance in triple negative breast cancer. *Eur Rev Med Pharmacol Sci.* 2016;20(11):2201–2208. PMID:27338043.
9. Jayaraj R, Madhav MR, Nayagam SG, et al. Clinical theragnostic relationship between drug-resistance specific miRNA expressions, chemotherapeutic resistance, and sensitivity in breast cancer: A systematic review and meta-analysis. *Cells.* 2019;8(10):1250. doi:10.3390/cells8101250
10. McGuire A, Casey MC, Waldron RM, et al. Prospective assessment of systemic microRNAs as markers of response to neoadjuvant chemotherapy in breast cancer. *Cancers (Basel).* 2020;12(7):1820. doi:10.3390/cancers12071820
11. Liu B, Su F, Chen M, et al. Serum miR-21 and miR-125b as markers predicting neoadjuvant chemotherapy response and prognosis in stage II/III breast cancer. *Hum Pathol.* 2017;64:44–52. doi:10.1016/j.humpath.2017.03.016
12. Liu B, Su F, Li Y, et al. Changes of serum miR34a expression during neoadjuvant chemotherapy predict the treatment response and prognosis in stage II/III breast cancer. *Biomed Pharmacother.* 2017;88:911–917. doi:10.1016/j.biopha.2017.01.133
13. Al-Khanbashi M, Caramuta S, Alajmi AM, et al. Tissue and serum miRNA profile in locally advanced breast cancer (LABC) in response to neo-adjuvant chemotherapy (NAC) treatment. *PLoS One.* 2016;11(4):e0152032. doi:10.1371/journal.pone.0152032
14. Li Q, Liu M, Ma F, et al. Circulating miR-19a and miR-205 in serum may predict the sensitivity of luminal A subtype of breast cancer patients to neoadjuvant chemotherapy with epirubicin plus paclitaxel. *PLoS One.* 2014;9(8):e104870. doi:10.1371/journal.pone.0104870
15. Li J, Song ZJ, Wang YY, Yin Y, Liu Y, Nan X. Low levels of serum miR-99a is a predictor of poor prognosis in breast cancer. *Genet Mol Res.* 2016;15(3). doi:10.4238/gmr.15038338
16. Liu B, Su F, Lv X, et al. Serum microRNA-21 predicted treatment outcome and survival in HER2-positive breast cancer patients receiving neoadjuvant chemotherapy combined with trastuzumab. *Cancer Chemother Pharmacol.* 2019;84(5):1039–1049. doi:10.1007/s00280-019-03937-9

17. Rigaud VOC, Ferreira LRP, Ayub-Ferreira SM, et al. Circulating miR-1 as a potential biomarker of doxorubicin-induced cardiotoxicity in breast cancer patients. *Oncotarget*. 2017;8(4):6994–7002. doi:10.18632/oncotarget.14355
18. Khalighfar S, Alizadeh AM, Irani S, Omranipour R. Plasma miR-21, miR-155, miR-10b, and Let-7a as the potential biomarkers for the monitoring of breast cancer patients. *Sci Rep*. 2018;8(1):17981. doi:10.1038/s41598-018-36321-3
19. Marques MM, Evangelista AF, Macedo T, et al. Expression of tumor suppressors miR-195 and let-7a as potential biomarkers of invasive breast cancer. *Clinics (Sao Paulo)*. 2018;73:e184. doi:10.6061/clinics/2018/e184
20. Turkoglu F, Calisir A, Ozturk B. Clinical importance of serum miRNA levels in breast cancer patients. *Discov Oncol*. 2024;15(1):19. doi:10.1007/s12672-024-00871-y
21. Aksan H, Kundaktepe BP, Sayili U, et al. Circulating miR-155, let-7c, miR-21, and PTEN levels in differential diagnosis and prognosis of idiopathic granulomatous mastitis and breast cancer. *BioFactors*. 2020;46(6):955–962. doi:10.1002/biof.1676
22. Li XX, Gao SY, Wang PY, et al. Reduced expression levels of let-7c in human breast cancer patients. *Oncol Lett*. 2015;9(3):1207–1212. doi:10.3892/ol.2015.2877
23. Li X, Tang X, Li K, Lu L. Evaluation of serum microRNAs (miR-9-5p, miR-17-5p, and miR-148a-3p) as potential biomarkers of breast cancer. *Biomed Res Int*. 2022;2022:9961412. doi:10.1155/2022/9961412
24. Feliciano A, González L, García-Mayea Y, et al. Five microRNAs in serum are able to differentiate breast cancer patients from healthy individuals. *Front Oncol*. 2020;10:586268. doi:10.3389/fonc.2020.586268
25. Ritter A, Hirschfeld M, Berner K, et al. Circulating non-coding RNA-biomarker potential in neoadjuvant chemotherapy of triple negative breast cancer? *Int J Oncol*. 2019;56(1):47–68. doi:10.3892/ijo.2019.4920
26. Kleivi Sahlberg K, Bottai G, Naume B, et al. A serum microRNA signature predicts tumor relapse and survival in triple-negative breast cancer patients. *Clin Cancer Res*. 2015;21(5):1207–1214. doi:10.1158/1078-0432.CCR-14-2011
27. Swellam M, Zahrn RFK, Ghonem SA, Abdel-Malak C. Serum MiRNA-27a as potential diagnostic nucleic marker for breast cancer. *Arch Physiol Biochem*. 2021;127(1):90–96. doi:10.1080/13813455.2019.1616765
28. Li X, Zou W, Wang Y, et al. Plasma-based microRNA signatures in early diagnosis of breast cancer. *Mol Genet Genomic Med*. 2020;8(5):e1092. doi:10.1002/mgg3.1092
29. Zheng R, Pan L, Gao J, et al. Prognostic value of miR-106b expression in breast cancer patients. *J Surg Res*. 2015;195(1):158–165. doi:10.1016/j.jss.2014.12.035
30. Li M, Zou X, Xia T, et al. A five-miRNA panel in plasma was identified for breast cancer diagnosis. *Cancer Med*. 2019;8(16):7006–7017. doi:10.1002/cam4.2572
31. Wang H, Tan G, Dong L, et al. Circulating MiR-125b as a marker predicting chemoresistance in breast cancer. *PLoS One*. 2012;7(4):e34210. doi:10.1371/journal.pone.0034210
32. Xue J, Zhu X, Huang P, et al. Expression of miR-129-5p and miR-433 in the serum of breast cancer patients and their relationship with clinicopathological features. *Oncol Lett*. 2020;20(3):2771–2778. doi:10.3892/ol.2020.11827
33. Fischer C, Deutsch TM, Feisst M, et al. Circulating miR-200 family as predictive markers during systemic therapy of metastatic breast cancer. *Arch Gynecol Obstet*. 2022;306(3):875–885. doi:10.1007/s00404-022-06442-2
34. Escuin D, López-Vilaró L, Mora J, et al. Circulating microRNAs in early breast cancer patients and its association with lymph node metastases. *Front Oncol*. 2021;11:627811. doi:10.3389/fonc.2021.627811
35. Sun Y, Wang M, Lin G, et al. Serum microRNA-155 as a potential biomarker to track disease in breast cancer. *PLoS One*. 2012;7(10):e47003. doi:10.1371/journal.pone.0047003
36. Heneghan HM, Miller N, Kelly R, Newell J, Kerin MJ. Systemic miRNA-195 differentiates breast cancer from other malignancies and is a potential biomarker for detecting noninvasive and early stage disease. *Oncologist*. 2010;15(7):673–682. doi:10.1634/theoncologist.2010-0103
37. Zhao FL, Dou YC, Wang XF, et al. Serum microRNA-195 is down-regulated in breast cancer: A potential marker for the diagnosis of breast cancer. *Mol Biol Rep*. 2014;41(9):5913–5922. doi:10.1007/s11033-014-3466-1
38. McAnena P, Tanriverdi K, Curran C, et al. Circulating microRNAs miR-331 and miR-195 differentiate local luminal a from metastatic breast cancer. *BMC Cancer*. 2019;19(1):436. doi:10.1186/s12885-019-5636-y
39. Navarro-Manzano E, Luengo-Gil G, González-Conejero R, et al. Prognostic and predictive effects of tumor and plasma miR-200c-3p in locally advanced and metastatic breast cancer. *Cancers (Basel)*. 2022;14(10):2390. doi:10.3390/cancers14102390
40. Zhang S, Wang Y, Wang Y, et al. Serum miR-222-3p as a double-edged sword in predicting efficacy and trastuzumab-induced cardiotoxicity for HER2-positive breast cancer patients receiving neoadjuvant target therapy. *Front Oncol*. 2020;10:631. doi:10.3389/fonc.2020.00631
41. Guo J, Liu C, Wang W, et al. Identification of serum miR-1915-3p and miR-455-3p as biomarkers for breast cancer. *PLoS One*. 2018;13(7):e0200716. doi:10.1371/journal.pone.0200716
42. Young H, Baum R, Cremerius U, et al. Measurement of clinical and subclinical tumour response using [18F]-fluorodeoxyglucose and positron emission tomography: Review and 1999 EORTC recommendations. *Eur J Cancer*. 1999;35(13):1773–1782. doi:10.1016/S0959-8049(99)00229-4
43. Eisenhauer EA, Therasse P, Bogaerts J, et al. New response evaluation criteria in solid tumours: Revised RECIST guideline (version 1.1). *Eur J Cancer*. 2009;45(2):228–247. doi:10.1016/j.ejca.2008.10.026
44. Ao X, Nie P, Wu B, et al. Decreased expression of microRNA-17 and microRNA-20b promotes breast cancer resistance to taxol therapy by upregulation of NCOA3. *Cell Death Dis*. 2016;7(11):e2463–e2463. doi:10.1038/cddis.2016.367
45. Eicheler C, Stückrath I, Müller V, et al. Increased serum levels of circulating exosomal microRNA-373 in receptor-negative breast cancer patients. *Oncotarget*. 2014;5(20):9650–9663. doi:10.18632/oncotarget.2520
46. Zhu W, Liu M, Fan Y, Ma F, Xu N, Xu B. Dynamics of circulating microRNAs as a novel indicator of clinical response to neoadjuvant chemotherapy in breast cancer. *Cancer Med*. 2018;7(9):4420–4433. doi:10.1002/cam4.1723
47. Faramin Lashkarian M, Hashemipour N, Niaraki N, et al. MicroRNA-122 in human cancers: From mechanistic to clinical perspectives. *Cancer Cell Int*. 2023;23(1):29. doi:10.1186/s12935-023-02868-z
48. Khan J, Lieberman JA, Lockwood CM. Variability in, variability out: Best practice recommendations to standardize pre-analytical variables in the detection of circulating and tissue microRNAs. *Clin Chem Lab Med*. 2017;55(5):608–621. doi:10.1515/cclm-2016-0471
49. Mitchell PS, Parkin RK, Kroh EM, et al. Circulating microRNAs as stable blood-based markers for cancer detection. *Proc Natl Acad Sci U S A*. 2008;105(30):10513–10518. doi:10.1073/pnas.0804549105
50. Tan GW, Khoo ASB, Tan LP. Evaluation of extraction kits and RT-qPCR systems adapted to high-throughput platform for circulating miRNAs. *Sci Rep*. 2015;5(1):9430. doi:10.1038/srep09430
51. Tiberio P, Callari M, Angeloni V, Daidone MG, Appierto V. Challenges in using circulating miRNAs as cancer biomarkers. *Biomed Res Int*. 2015;2015:731479. doi:10.1155/2015/731479
52. Page K, Guttery DS, Zahra N, et al. Influence of plasma processing on recovery and analysis of circulating nucleic acids. *PLoS One*. 2013;8(10):e77963. doi:10.1371/journal.pone.0077963
53. Balzano F, Deiana M, Dei Giudici S, et al. miRNA stability in frozen plasma samples. *Molecules*. 2015;20(10):19030–19040. doi:10.3390/molecules201019030
54. Glinge C, Clauss S, Boddum K, et al. Stability of circulating blood-based microRNAs: Pre-analytic methodological considerations. *PLoS One*. 2017;12(2):e0167969. doi:10.1371/journal.pone.0167969
55. Janssen LM, Suelmann BBM, Elias SG, et al. Improving prediction of response to neoadjuvant treatment in patients with breast cancer by combining liquid biopsies with multiparametric MRI: Protocol of the LIMA study. A multicentre prospective observational cohort study. *BMJ Open*. 2022;12(9):e061334. doi:10.1136/bmjopen-2022-061334
56. Janssen LM, Janse MHA, Penning De Vries BBL, et al. Predicting response to neoadjuvant chemotherapy with liquid biopsies and multiparametric MRI in patients with breast cancer. *NPJ Breast Cancer*. 2024;10(1):10. doi:10.1038/s41523-024-00611-z

Peptide pool instability of precancerous lesions in rats with chronic pancreatitis model and/or without type 1 diabetes mellitus

Sergii Sukhodolia^{1,B–F}, Olesia Kalmukova^{2,B–F}, Natalia Raksha^{2,B–F}, Anatoliy Sukhodolia^{1,A,C,E,F}, Olena Kuryk^{2,A–F}, Olexiy Savchuk^{2,A–C,E,F}

¹ National Pirogov Memorial Medical University, Vinnytsya, Ukraine

² Educational and Scientific Center (ESC) "Institute of Biology and Medicine", Taras Shevchenko National University of Kyiv, Ukraine

A – research concept and design; B – collection and/or assembly of data; C – data analysis and interpretation;

D – writing the article; E – critical revision of the article; F – final approval of the article

Advances in Clinical and Experimental Medicine, ISSN 1899–5276 (print), ISSN 2451–2680 (online)

Adv Clin Exp Med. 2025;34(9):1531–1540

Address for correspondence

Olesia Kalmukova

E-mail: olesiakalmukova@knu.ua

Funding sources

None declared

Conflict of interest

None declared

Received on March 28, 2024

Reviewed on August 23, 2024

Accepted on September 12, 2024

Published online on January 14, 2025

Abstract

Background. The search for early and minimally invasive diagnostic approaches to pancreatic cancer (PC) remains an important issue. One of the most promising directions is to find a sensitive key in the metabolic changes during widespread causes of PC, i.e., chronic pancreatitis (CP) and diabetes mellitus (DM).

Objectives. The main objective of this study was to analyze the peptide pools in the blood plasma and pancreas of rats with modeling of CP and/or without type 1 DM in association with pancreas histopathological grading features.

Materials and methods. The study was conducted on white non-linear male rats, divided into 3 groups: 1st group: control, 2nd group: rats with cerulein-stimulated CP, and 3rd group: rats with CP and streptozotocin-inducible type 1 DM. Total protein and peptide content were determined in the pancreas and blood plasma. The peptide pools were fractionated using size-exclusion chromatography.

Results. Rats with CP showed a high degree of fibrosis in the pancreas and grade 1 ductal pancreatic intraepithelial neoplasia (PanIN), associated with decreased total peptides in the pancreas. In rats with CP and DM, 2nd and 3rd grade PanIN with pronounced acinar metaplasia was observed in association with decreasing total pancreatic protein and peptide pools. While there was a decrease in total protein and an increase in total peptide in blood serum, the changes were more pronounced in rats with CP and DM. A study revealed both qualitative and quantitative differences in the distribution of peptide pools in 2 groups with pathologies. Qualitatively, plasma samples from pathological groups exhibited an increased number of peaks. Quantitatively, there was a higher proportion of peptides with molecular weights exceeding 700 Da observed in both plasma and pancreas.

Conclusions. The analysis of peptide pools obtained from plasma and PanIN development demonstrated that the peptide pool can serve as an early and complementary indicator of PC emergence.

Key words: adenocarcinoma, fibrosis, pancreatic neoplasms, metaplasia, metabolome

Cite as

Sukhodolia S, Kalmukova O, Raksha N, Sukhodolia A, Kuryk O, Savchuk O. Peptide pool instability of precancerous lesions in rats with chronic pancreatitis model and/or without type 1 diabetes mellitus. *Adv Clin Exp Med.* 2025;34(9):1531–1540. doi:10.17219/acem/193243

DOI

10.17219/acem/193243

Copyright

Copyright by Author(s)

This is an article distributed under the terms of the Creative Commons Attribution 3.0 Unported (CC BY 3.0) (<https://creativecommons.org/licenses/by/3.0/>)

Background

Pancreatic cancer (PC) is a very aggressive disease, with rising incidence and poor clinical outcomes, despite recent innovations in diagnosis and treatment.¹ Pancreatic cancer is one of the leading causes of cancer death worldwide, with an overall 5-year survival rate of less than 6–7%.² First of all, this is due to the difficulty of PC diagnosis in the early stages.³ The course of the disease in most patients is asymptomatic before the development of complications and decompensation with the appearance of distant metastases.⁴ Therefore, early detection or suspicion of the development of PC is of great importance for the treatment of patients.⁵ Chronic pancreatitis (CP),⁶ diabetes mellitus (DM),⁷ obesity, smoking, alcohol, and cancer in the anamnesis are all known risk factors for the development of PC.⁸ Coronavirus disease 2019 (COVID-19) is a global health threat, whose causative agent, severe acute respiratory syndrome coronavirus-2 (SARS-CoV-2), is an enveloped positive single-stranded RNA virus, responsible for a pulmonary and extrapulmonary infection, by simultaneously involving multiple organs, from the heart to the pancreas, as highlighted by recent histopathological evidence. Furthermore, during the SARS-COV-2 pandemic, healthcare systems were impacted by the inflow of infected patients, with significant consequences on the care trajectories of cancer patients worldwide.⁹

The latest data from the GLOBOCAN 2018 program, conducted by the International Agency for Research on Cancer (IARC), indicates an increase in the number of diagnosed patients with PC to 458,918 and an increase in the number of deaths due to PC to 432,242 during the year.¹⁰ According to GLOBOCAN 2020, the number of newly diagnosed PC patients continues to grow and is 495,773, and the number of deaths is 466,003.^{11,12}

In Ukraine in 2018, 6,246 new cases of PC were detected. At the same time, 5,923 people died from this pathology caused by complications of PC. This indicates a negative dynamic, because in 2012, 4,728 people of both sexes were registered and diagnosed with PC. In addition, 4,168 deaths caused by PC complications were registered.¹³ The findings corroborate the progression of this pathology, highlighting challenges in its diagnosis and therapeutic management.

Given that both diabetes mellitus (DM) and chronic pancreatitis (CP) are recognized risk factors for pancreatic ductal adenocarcinoma (PDAC), their co-presence may significantly increase the risk and raise increased concerns about disease progression.¹⁴ Today, pancreatic intraepithelial neoplasia (PanIN) and intraductal papillary mucinous neoplasm (IPMN) are the most necessary and prognostically important in suspected PC in patients with pancreatitis in the anamnesis.^{15,16} Pancreatic intraepithelial neoplasia is a noninvasive proliferation of the pancreatic epithelium, which, depending on the degree of its progression, is graded from PanIN-1 to PanIN-3, which in turn reflects the intensity of architectural and cyto-nuclear abnormalities.^{17,18}

Several authors have analyzed the stages of PanIN progression to carcinoma *in situ*; however, at this stage, it is still impossible to accurately predict the percentage of malignancy and the development of adenocarcinoma.^{19,20} Currently, it is difficult to detect PanIN and its degree of progression using minimally invasive methods.^{21,22} Considering the above, the search for additional markers or the improvement of existing approaches for the diagnosis of oncological and other diseases is crucial.²³ The tissue peptide pool consists of a set of molecules, in particular growth factors, hormones, cytokines, and molecules that are formed as a result of protein processing.²⁴ Consequently, peptide pools reflect the metabolic activity of an organ.²⁵ As the composition and amount of individual peptides in pools are not static values, but change dynamically depending on the physiological state or the development of a pathological process, the analysis of the tissue peptide pool can be an additional tool for assessing the severity of disease.²⁶

Therefore, we consider the experimental investigation of this topic to be highly relevant. It necessitates a comprehensive approach that integrates diverse methodologies, including molecular analysis. Specifically, this involves examining variations in the peptide pool and comparing their composition across different stages of complication development in these pathologies.

Objectives

The main objective of this study was to analyze the formation and accumulation of the peptide pools in blood serum and pancreas of rats with modeling of CP and/or without type 1 DM in association with pancreas histopathological grading features.

Materials and methods

Study design

Experiments were conducted on male white Wistar rats weighing 200 ± 10 g. When working with laboratory animals, we followed generally accepted international recommendations regarding the conduct of medical and biological research using animals by the European Convention for the Protection of Vertebrate Animals Used for Experimental and Other Scientific Purposes (Strasbourg, France, 1986). The work with animals has been regulated by the Rules for the Conduct of Experimental Work with Laboratory Animals, which have been approved by the Bioethics Committee of the Educational and Scientific Centre “Institute of Biology and Medicine” of Taras Shevchenko National University of Kyiv, Ukraine (protocol registration No. 4, issued May 25, 2020).

The following conditions were maintained in the room for keeping animals: temperature 20–24°C, humidity

43 ± 2%, 12-h/12-h day/night cycle. The animals were fed standard chow (VITA, Obukhiv, Ukraine). Rats had free access to water and food.

The CP was induced by intraperitoneal (ip.) injection of cerulein (Sigma-Aldrich GmbH, Steinheim, Germany) diluted in physiological solution ($5 \mu\text{g} \times \text{kg}^{-1}$ body weight), 5 times a day with an interval of 1 h.²⁷ Control rats received equal volumes of 0.9% NaCl administered ip. Injections were carried out for 5 consecutive days. There were 25 injections in total. After the last day of cerulein injection, the rats were kept under standard conditions, with free access to water, for the following 9 days. The development of pancreatitis was confirmed by a high level of amylase in the blood serum, as well as by the study of pathohistological changes in the parenchyma of the pancreas of experimental rats, which confirmed the above. On the 14th day from the start of the experiment, half of the animals from the CP group were randomly selected and used to model DM. Diabetes mellitus was induced in rats fasted for 16 h by a single ip. injection of streptozotocin (Sigma-Aldrich, St. Louis, USA) at a dose of $65 \text{ mg} \times \text{kg}^{-1}$ of body weight, dissolved in 0.5 mL of freshly prepared 0.01 M citrate buffer, pH 4.5. Other animals in the CP group and all control rats received an equal amount of placebo. The validity of DM was confirmed by the high blood glucose concentration (above $15 \text{ mM} \times \text{l}^{-1}$) and a high level of glycosylated hemoglobin. Blood glucose concentration was determined using a glucometer Hlyukofot II (Norma, Kyiv, Ukraine) according to the manufacturer's instructions. The glycosylated hemoglobin kit (Spectrum, El Ubour, Egypt) was used for the determination of glycosylated hemoglobin.

Finally, there were 3 experimental groups: 1) control ($n = 10$); 2) CP ($n = 20$); and 3) CP + DM ($n = 20$). On the last day of the experiment (44th day), the animals were killed by decapitation, and then blood samples and pancreatic tissue were collected.

Histopathological analysis

Histopathological examination was performed to characterize the morphology and functional status of the pancreas. Pancreatic fragments were fixed in 4% neutral buffered paraformaldehyde and embedded into the paraffin according to standard procedures. Slides were stained with Bemer's hematoxylin and eosin (H&E). Even though there are other methods of staining pancreatic sections, mainly for fibrosis, Bemer's method with H&E remains widespread, as evidenced in modern literature.^{28,29}

All microphotographs were obtained using a light microscope Axio Imager A2 (Carl Zeiss Microscopy GmbH, Jena, Germany) with a $\times 10$, $\times 20$ and $\times 40$ objective lens. Microphotographs were taken using the AxioCam 105 color (Carl Zeiss Microscopy GmbH) digital camera and the Zen2 (blue edition) software (Carl Zeiss Microscopy GmbH).

Obtaining peptide pools

The peptide pool was prepared according to the generally accepted methods.³⁰ Blood plasma or tissue homogenate (10% homogenate in 50 mM Tris-HCl buffer (pH 7.4) containing 130 mM NaCl) was mixed with 1.2 M HClO_4 at a 1:1 (v/v) ratio to precipitate the proteins. After centrifugation ($10,000 \times g$, 20 min, $+4^\circ\text{C}$), the supernatant was neutralized with 5 M potassium hydroxide (KOH) to pH 7.0, and the samples were centrifuged again. At the final stage, the oligopeptides were precipitated with ethyl alcohol at a final concentration of 67% and the supernatant was lyophilized. The peptide concentration was determined at 210 nm after dissolving of lyophilized samples in 50 mM Tris-HCl buffer (pH 7.4) containing 130 mM NaCl. Dipptide N-carboxy-glycyl-glycine was used to construct the calibration graph. The protein concentration was determined according to the method described by Bradford,³¹ using crystalline bovine serum albumin as a standard protein, and the absorbance was measured at 595 nm with a Smart SpecTMPlus spectrophotometer (BioRad Laboratories Inc., Hercules, USA).

Fractionation of peptide pools by size-exclusion chromatography

Size exclusion chromatography on Sephadex G 15 (BioRad Laboratories) was used to fractionate the peptide pool.³² To estimate the molecular weight of the peptides, the column was precalibrated with substances of known molecular weight – lysozyme (14.3 kDa); insulin (5.7 kDa); vitamin B12 (1.35 kDa).

Statistical analyses

The distribution of the data was assessed using the Shapiro–Wilk W-test for normality and the test for homogeneity of variance (Supplementary Table 1). Nonparametric tests (Kruskal–Wallis as overall test and post hoc Dunn's test with Bonferroni correction) were used to assess the significance of the observed changes. A statistically significant difference was evaluated at $p < 0.05$ using Origin 8 Pro (OriginLab, Northampton, USA). Histograms were created using Microsoft Excel 2010 software (Microsoft Corp., Redmond, USA) and Origin 8 Pro. The obtained results are presented as the median, 25% and 75% quartile and minimum and maximum.

Results

Histopathological analysis

Histopathological observation included both ductal and acinar parts of the pancreas. Changes in the ductal part were classified according to the PanIN grading system.³³

In the control group, the ductal part (Fig. 1) was characterized by the typical structure of a simple cuboidal epithelium. In the CP group (Fig. 1), most ducts were surrounded by developed connective tissue stromal elements, which in some samples could be classified as an early stage of fibrosis (also around the vascular part). The presence of immune cell infiltration (the most common cells are neutrophils and macrophages) in the expanded stromal part of the round ducts also indicated the intervention of a low degree of chronic inflammation. Ductal cells in the CP group (Fig. 2) in all samples changed their shape from cuboidal to prismatic; in some of them, active proliferation with a dysplastic process was observed, which led to the appearance of glandular epithelium in the thickened wall of the duct. These changes stimulated the epithelium for invagination. This type of pancreas lesion manifestation is classified as a PanIN-1A - PanIN-1B according to the established grading system.

In the CP + DM group, in some samples with pronounced dysplasia, the ductal part exhibited the previously described features (Fig. 1). The ductal epithelium was frequently transformed into a pseudostratified type (Fig. 3) and pseudopapillary structures were formed within the wall (Fig. 3B). Additionally, villous-like structures were observed in the duct lumen (Fig. 3C), indicating a high-grade PanIN-2 and PanIN-3.

The changes observed in the ductal part were accompanied by corresponding changes in the exocrine acinar part (Fig. 4). The CP group (Fig. 4B) exhibited significant morphological heterogeneity in the acini, including loss of polarization in some acini and a notable difference between the eosinophilic apical part and the basophilic basal part. Conversely, the CP + DM group demonstrated acinar-ductal metaplasia through intermediate mucinous cells (Fig. 4C).

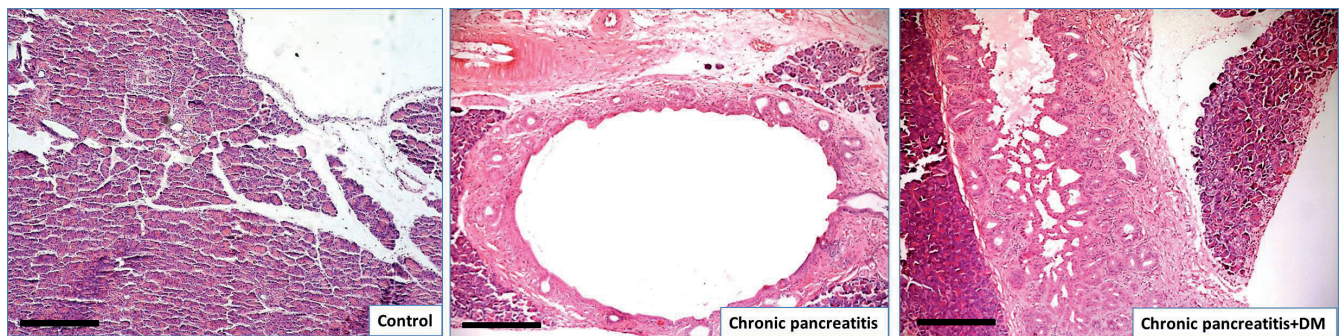


Fig. 1. Microphotographs of rat's pancreas of experimental groups: control, chronic pancreatitis (CP) and CP + diabetes mellitus (DM). In the CP and CP + DM groups, a ductal part with a degree of changes in PanIN-1 and PanIN-3 was demonstrated. Hematoxylin & eosin (H&E) staining, scale bar 100 μ m

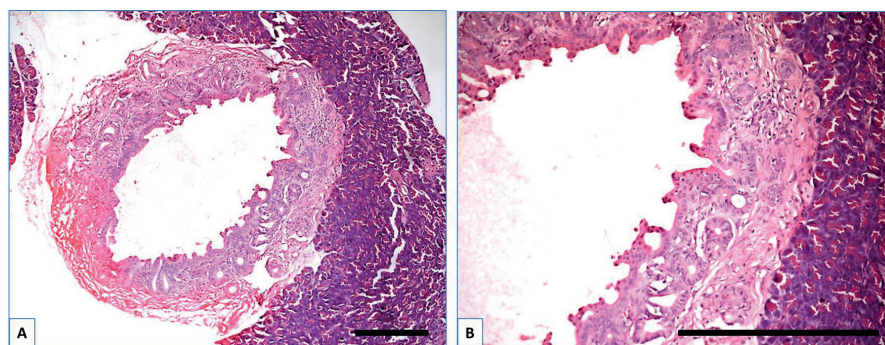


Fig. 2. Microphotographs of rat's pancreas of chronic pancreatitis (CP) group. Hematoxylin & eosin (H&E) staining, scale bar 100 μ m

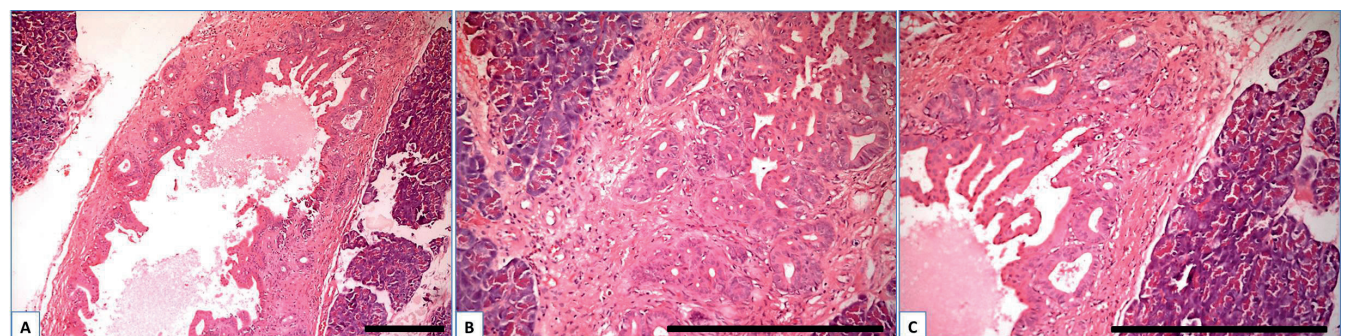


Fig. 3. Microphotographs of rat's pancreas of chronic pancreatitis (CP) + diabetes mellitus (DM) group. Hematoxylin & eosin (H&E) staining, scale bar 100 μ m

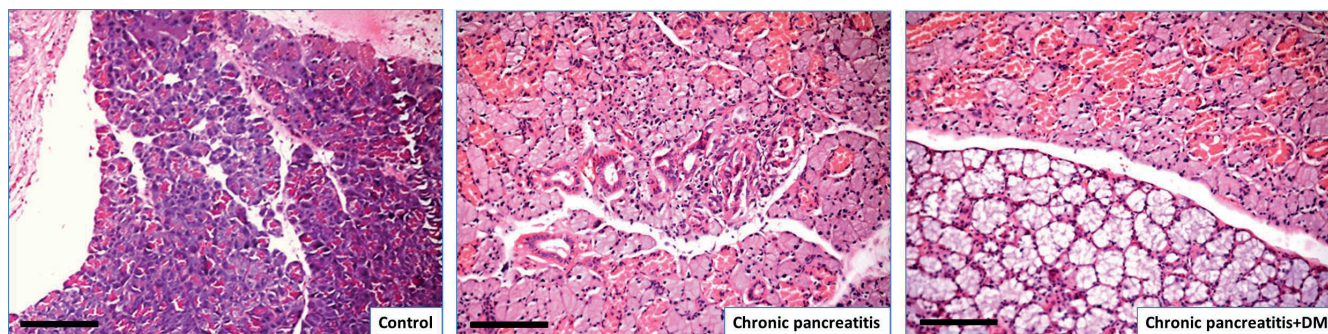


Fig. 4. Microphotographs of rat's pancreas of experimental groups: control, chronic pancreatitis (CP) and CP + diabetes mellitus (DM) groups. In the CP and CP + DM groups, acinar-ductal metaplasia is observed in the acini of the exocrine part. Hematoxylin & eosin (H&E) staining, scale bar 100 μ m

The total protein and peptide concentration in plasma and pancreas

Biochemical analysis showed a significant decrease in total plasma protein of 26% and 20% in the CP and CP + DM groups, respectively, compared to the control level (Fig. 5). In the pancreas, the level of total proteins exhibited a more pronounced decrease under conditions of CP in the context of diabetes (by 40% compared to the control and by 45% compared to the CP group). In addition, the CP + DM group

had a 30% increase in total peptides in blood plasma compared to the control group (any significant changes were not fixed in the CP group). The alterations in total protein and peptide levels in blood plasma observed in the CP + DM group may serve as an early indicator of proteolysis in metabolic processes. The total peptide level in the pancreas was reduced by 46% and 70% in the CP and CP + DM groups, respectively, compared to the control level. In addition, the CP + DM group showed a significant 46% decrease in this parameter compared to CP.

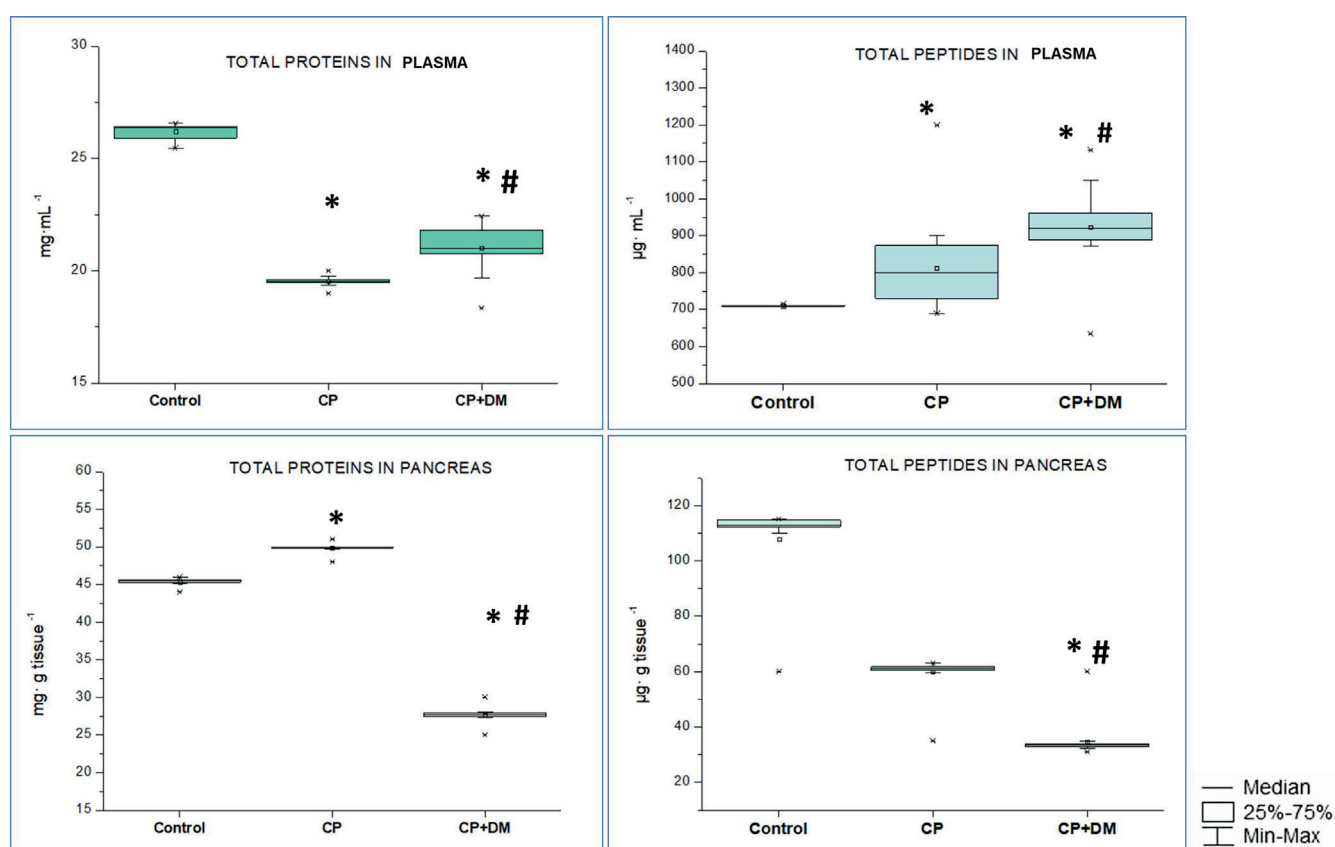


Fig. 5. Results of biochemical determination of total protein and peptides in plasma and pancreas of experimental groups: control, chronic pancreatitis (CP) and CP + diabetes mellitus (DM) groups. Data were analyzed using nonparametric tests (Kruskal–Wallis as the overall test and post hoc Dunn's test with Bonferroni correction) (see Supplementary Table 2). The obtained results are presented as the median, 25% and 75% quartile and minimum and maximum

* compared with control value; # compared with CP.

Fractionation of peptide pools using size-exclusion chromatography

Chromatographic analysis of the peptide pools of patients in the CP and CP + DM groups revealed deviations in the quantitative and qualitative composition of peptides when compared to the control group (Fig. 6). The appearance of peptides in a wider range of molecular weights, as well as changes in the concentration of some peptides in the blood plasma of patients were found. The peptide pool derived from the blood plasma of the study participants in the control group consisted of 4 main peptide fractions with a molecular weight of 1,017 Da, 689 Da, 545 Da, and 444 Da. At the same time, the number

of peptide fractions in both pathologies increased to 6 main peptide fractions.

The differences were noticeable in blood serum more prominently than in the pancreas, and for peptide pools with a molecular weight greater than 700 Da. Peptide pool peaks were detected in the blood plasma of CP and CP + DM, but not in the control samples.

Thus, it was shown that the degree of PanIN 1A–PanIN-1B histopathologic changes was accompanied by decreased total plasma proteins and total pancreatic peptides, while total pancreatic proteins and total plasma peptides (with increased part of peptides 1,100 Da) increased in CP group. In the CP + DM group, we observed another pattern of changes. Specifically, high-grade PanIN-2 and

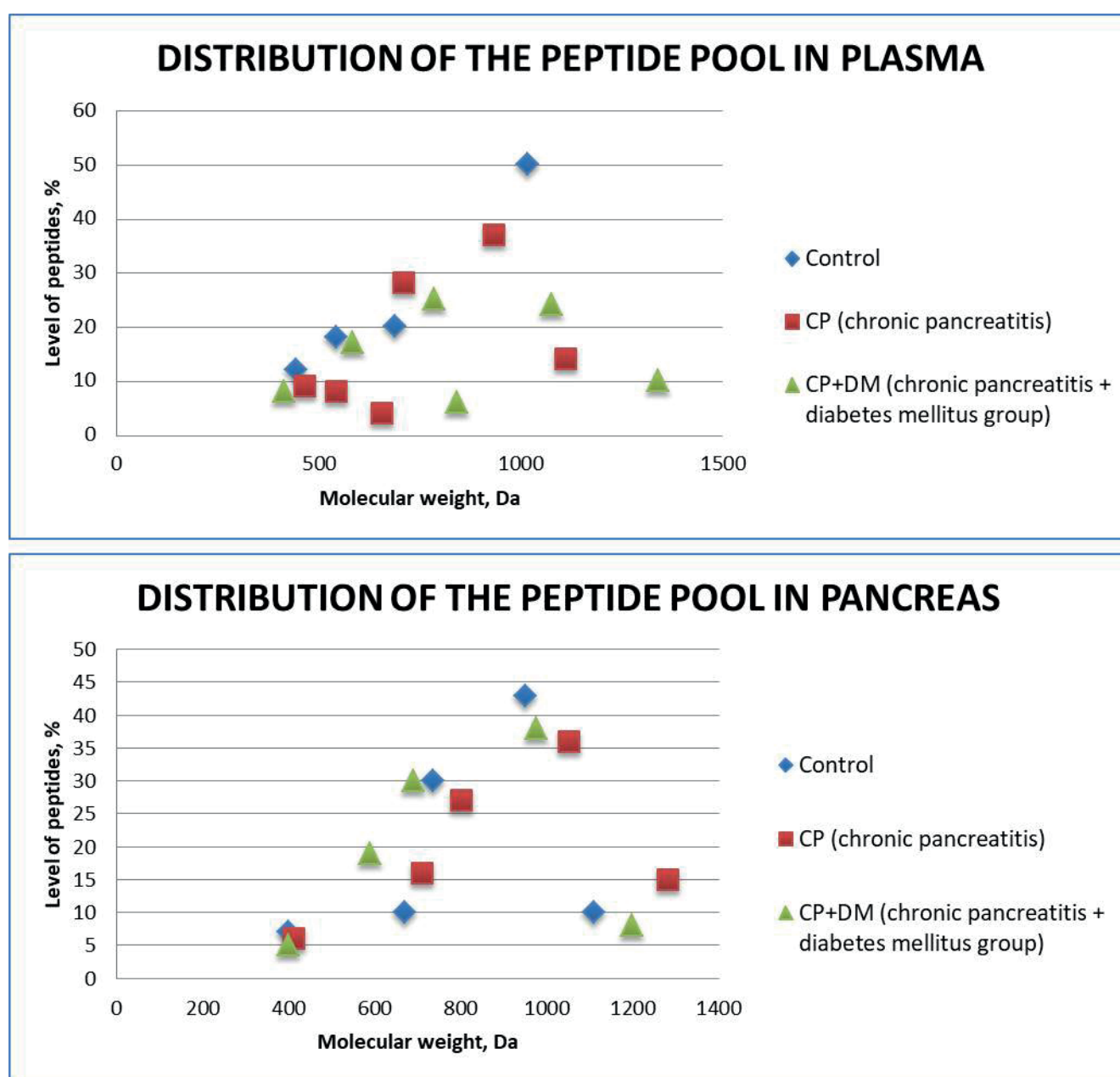


Fig. 6. Results of biochemical distribution of the peptide pool in plasma and pancreas of experimental groups: control, chronic pancreatitis (CP) and CP + diabetes mellitus (DM) groups

PanIN-3 histopathological changes were followed by decreased total proteins in plasma and pancreas, and total peptides in the pancreas. Conversely, only total peptides in plasma (with elevated levels of peptides increased from 1,100 Da to 1,300 Da). The total amount of proteins in the pancreas and the peak distribution of the peptides in the serum changed differently in the CP and CP + GM groups.

Discussion

It is now widely accepted that the structural and functional disorders of the pancreas that result in the development of pancreatitis are caused by a cascade of molecular events initiated by the uncontrolled activation of pancreatic enzymes.³⁴ Even though this factor is actively involved in the initial stages of the disease, the pathogenesis of CP is also closely associated with changes in the functioning of the proteolytic link,³⁵ which is a prerequisite for the development of several accompanying manifestations of pancreatitis. These manifestations are associated with clinical and pathophysiological characteristics.³⁶ One of the complications is the development of fibrosis and the subsequent exhaustion of the exocrine and endocrine functions of the pancreas, which leads to the further development of diabetes, as well as maldigestion and malabsorption syndrome in patients.^{37,38}

This study was the first to report the relationship between pancreatic histopathological features and peptide pool changes in a rat model of CP and CP combined with DM. The full mechanisms underlying and ensuring this connection remain unclear.³⁹ Our previous study showed a significant increase in the content of interleukin 6 (IL-6), tumor necrosis factor alpha (TNF- α) and matrix metalloproteinase (MMP)-2 and -9 in blood serum, liver and pancreas of animals with CP separately and under DM conditions.⁴⁰ We determined the levels of these factors in animals with CP and CP + DM because the main enzymes involved in maintaining the metabolism of extracellular matrix (ECM) proteins are MMPs, which contribute to the appearance of changes in peptide levels.⁴¹ Therefore, the difference in the distribution of peptides on criteria such as molecular weight and amounts of individual peptide fractions observed in the control and CP and CP + DM groups may represent the disorders of proteolytic homeostasis and deregulation of protease activity under the development of pathology. It is possible that these peptides may be among the first features involved in the development of different grades of dysplasia (including PanIN).⁴² On the other hand, changes in the peptide pools can be a signal of the severity of the disease, and in our study, a sign of pancreatic lesions. According to modern concepts, tissue peptide pools are quite stable under physiological conditions, based on criteria such as qualitative and quantitative composition, so they can be considered

an important indicator characterizing the functional state of organs. One of the explanations for the significant decrease in the level of peptides in the pancreas in patients with CP and CP + DM is their release into the bloodstream due to cell damage.⁴³ This assumption is partly confirmed by the increase in the concentration of blood plasma peptides. Changes in peptide concentrations were more pronounced in the CP + DM group, which may be a direct consequence of more severe cell metabolism disorders in patients suffering from both pathologies simultaneously. Additionally, increased plasma peptide levels may in part result from the proteolytic breakdown of plasma proteins mediated by enzymes that appear in the plasma as a result of disruption of proteolytic homeostasis. Our previous findings highlighted changes in proteolytic balance, namely a significant increase in the level of MMPs, particularly MMP-2 and MMP-9, in the serum of rats with CP.⁴⁰ Analysis of the peptide pools using chromatography confirmed the hypothesis that the accumulation of peptides of different molecular weights in the blood plasma of patients with CP and CP + DM may be associated with protein degradation due to the activation of proteolytic reactions.

The pool of plasma peptides has the potential to serve as a valuable source of diagnostic information, as it represents a comprehensive record of cellular and extracellular enzymatic events characteristic of the pathological process. Consequently, the pool of blood plasma peptides can be considered an integral indicator reflecting the general metabolic state of the body.⁴⁴ To some extent, an increase in plasma peptide concentration may be a consequence of a decrease in plasma detoxification potential. One mechanism for the elimination of low-molecular-weight substances involves their absorption into abundant blood proteins such as albumin and further excretion through the liver and kidneys. Therefore, a decrease in protein concentration in the blood of patients in both the CP and the CP + DM groups may be an additional factor leading to the accumulation of peptides. Moreover, given the ability of the glomeruli to effectively remove low molecular weight substances, thereby reducing the concentration of potentially toxic molecules, the accumulation of peptides that we detected in the plasma of patients may be an indirect evidence of renal dysfunction, especially in patients in the CP + DM group.

It should be noted that a violation of the composition of peptide pools, as well as an increase in the concentration of some peptides, not only indicates the severity of the pathological process, but may be an additional factor causing PC progression and provoking the development of a number of complications. It can be assumed that pathological peptide pools may contain molecules structurally similar to biologically active peptides, or molecules with activity atypical for “physiological” peptides. Such molecules can alter cellular metabolism by binding to the active and/or regulatory sites of enzymes. In addition, pathological

peptides can occupy cellular receptors, thereby disrupting intracellular signaling pathways and affecting intercellular communication.

As shown above, in the pancreas of rats of the CP + DM group, we observed the development of changes (ductal dysplasia, pronounced acinar metaplasia, formation of glands in the fibrotic tissue of the duct, proliferation of the epithelium of glands with severe dysplasia, appearance of papillary and cribriform structures) corresponding to high and moderate ductal dysplasia (PanIN-2 and PanIN-3). These changes are direct predictors of pancreas adenocarcinoma. The impairment of PanIN represents a pathway to the development of PC and directly to ductal adenocarcinoma. This conclusion has been corroborated in several studies.^{45,46}

Diabetes mellitus is another common comorbidity known to contribute to changes in the serum metabolome.⁴⁷ In ductal adenocarcinoma, DM may promote tumor progression through changes in the transcriptome and metabolome.⁴⁸ Its close association with chronic inflammation adds an additional risk for complicating and advancing PC.^{49,50}

Limitations

The design of the study lacks a group of animals with only 1 model of diabetes. The distribution of the peptide pool is a nonspecific parameter. In any case, it may vary with another type of pathology development. Therefore, an additional specific test for pathology identity should always be performed. The cerulein-induced model of pancreatitis demonstrated significant regenerative capacity in the rat organism. In some cases, only mild morphological alterations were observed in the pancreas. However, in the CP + DM group, lesions ranged from PanIN-1 to PanIN-3, indicating a wide spectrum of pancreatic intraepithelial neoplasia. Also, the exact direct mechanism of the reciprocal relationship between the histophysiological changes of the pancreas and its peptide pool remains unclear.

Conclusions

Blood collection for plasma peptide pool analysis, in comparison to pancreatic biopsy, provides a less invasive alternative for diagnostic evaluation. In the case of cerulein-induced CP, alterations in the ductal region of the pancreas classified as PanIN-1A to PanIN-1B were observed, accompanied by increased total protein in the pancreas and low prevalence of peptide pool molecular weight of 450–770 Da in plasma compared to controls. In the presence of comorbidities such as DM (streptozotocin-induced) changes in the ductal part of the pancreas were classified as PanIN-2 and PanIN-3 grade, accompanied by a decrease in total pancreatic protein and the appearance of 2 new fractions of the high molecular weight peptide pool (more than 1,000 Da) in plasma

compared to controls. Overall, chronic pancreatitis (CP) with diabetes mellitus (DM) is marked by significant histopathological alterations in the pancreas, characterized by pronounced neoplastic changes. These changes are accompanied by a reduction in total pancreatic protein levels and an increase in peptide fractions of 1,100 Da and 1,300 Da compared to CP lesions without diabetes mellitus. These results suggest that combined plasma and pancreatic peptide pool analysis has great diagnostic potential for assessing the severity of PC. It is a fundamental promise for finding possible associations, predicting the progression and early detection of the threat of PC development in patients with a difficult medical history, namely: surgery for CP, obesity, diabetes, coronavirus disease, alcohol consumption, and smoking.

Supplementary data

The Supplementary materials are available at <https://doi.org/10.5281/zenodo.13630059>. The package includes the following files:

Supplementary Table 1. Data of Shapiro–Wilk (W) normality test and homogeneity of variance test (Levene's F test).

Supplementary Table 2. Kruskal–Wallis as the overall test (H-values) and post hoc Dunn's test with Bonferroni correction. The corrected α using the Bonferroni correction method is 0.017.

Data availability

The datasets generated and/or analyzed during the current study are available from the corresponding author on reasonable request.


Consent for publication


Not applicable.


ORCID iDs


Sergii Sukhodolia  <https://orcid.org/0000-0002-5784-703X>

Olesia Kalmukova  <https://orcid.org/0000-0001-5025-0938>

Natalia Raksha  <https://orcid.org/0000-0001-6654-771X>

Anatolyi Sukhodolia  <https://orcid.org/0000-0002-8744-5584>

Olena Kuryk  <https://orcid.org/0000-0003-3093-4325>

Olexiy Savchuk  <https://orcid.org/0000-0003-3621-6981>

References

1. Sung H, Ferlay J, Siegel RL, et al. Global cancer statistics 2020: GLOBOCAN estimates of incidence and mortality worldwide for 36 cancers in 185 countries. *CA Cancer J Clin*. 2021;71(3):209–249. doi:10.3322/caac.21660
2. Xiao AY, Tan MLY, Wu LM, et al. Global incidence and mortality of pancreatic diseases: A systematic review, meta-analysis, and meta-regression of population-based cohort studies. *Lancet Gastroenterol Hepatol*. 2016;1(1):45–55. doi:10.1016/S2468-1253(16)30004-8
3. Zhang L, Sanagapalli S, Stoita A. Challenges in diagnosis of pancreatic cancer. *World J Gastroenterol*. 2018;24(19):2047–2060. doi:10.3748/wjg.v24.i19.2047

4. Ren B, Cui M, Yang G, et al. Tumor microenvironment participates in metastasis of pancreatic cancer. *Mol Cancer*. 2018;17(1):108. doi:10.1186/s12943-018-0858-1
5. Pereira SP, Oldfield L, Ney A, et al. Early detection of pancreatic cancer. *Lancet Gastroenterol Hepatol*. 2020;5(7):698–710. doi:10.1016/S2468-1253(19)30416-9
6. Gheorghe G, Ionescu VA, Moldovan H, Diaconu CC. Clinical and biological data in patients with pancreatic cancer vs. chronic pancreatitis: A single center comparative analysis. *Diagnostics (Basel)*. 2023;13(3):369. doi:10.3390/diagnostics13030369
7. Sukhodolia AI, Sukhodolia SA, Mosiychuk VP, Makohonskyi MV. Chronic pancreatitis and diabetes mellitus: Predictors of development of pancreatic cancer [in Ukrainian]. *Klinicheskaia Khirurgiia*. 2019;86(4):67–71. doi:10.26779/2522-1396.2019.04.67
8. Rawla P, Sunkara T, Gaduputi V. Epidemiology of pancreatic cancer: Global trends, etiology and risk factors. *World J Oncol*. 2019;10(1):10–27. doi:10.14740/wjon1166
9. Torge D, Bernardi S, Arcangeli M, Bianchi S. Histopathological features of SARS-CoV-2 in extrapulmonary organ infection: A systematic review of literature. *Pathogens*. 2022;11(8):867. doi:10.3390/pathogens11080867
10. WHO GLOBOCAN database. Estimated number of new cases from 2022 to 2045, Incidence, Both sexes, age [0–85+]: Pancreas. Geneva, Switzerland: World Health Organization (WHO); 2022. <https://gco.iarc.who.int/tomorrow/en/dataviz/tables?cancers=13>. Accessed July 6, 2023.
11. National Cancer Institute (NCI) Surveillance, Epidemiology and End Results (SEER) Program. Cancer Stat Facts: Pancreatic Cancer. Bethesda, USA: National Institutes of Health (NIH); 2024. <https://seer.cancer.gov/statfacts/html/pancreas.html>. Accessed July 6, 2023.
12. Siegel RL, Miller KD, Jemal A. Cancer statistics, 2020. *CA Cancer J Clin*. 2020;70(1):7–30. doi:10.3322/caac.21590
13. National Cancer Registry of Ukraine. Pancreas C25: Adjust 2018. Kyiv, Ukraine: National Cancer Registry of Ukraine; 2018. http://www.ncru.inf.ua/publications/BULL_21/PDF_E/30-31-podg.pdf. Accessed July 6, 2023.
14. Waleleng BJ, Adiwinata R, Wenas NT, et al. Screening of pancreatic cancer: Target population, optimal timing and how? *Ann Med Surg (Lond)*. 2022;84:104814. doi:10.1016/j.amsu.2022.104814
15. Distler M, Aust D, Weitz J, Pilarsky C, Grützmann R. Precursor lesions for sporadic pancreatic cancer: PanIN, IPMN, and MCN. *Biomed Res Int*. 2014;2014:474905. doi:10.1155/2014/474905
16. Søreide K, Ismail W, Roalsø M, Ghotbi J, Zaharia C. Early diagnosis of pancreatic cancer: Clinical premonitions, timely precursor detection and increased curative-intent surgery. *Cancer Control*. 2023;30:107327482311547. doi:10.1177/10732748231154711
17. Ledniczky G, Bognár G, Bereczky B, Barabás L, Ondrejka P. Precursors of pancreatic cancer: Intraepithelial neoplasia (PanIN) and intraductal papillary mucinous neoplasms (IPMN) [in Hungarian]. *MaSeb*. 2009;62(1):22–26. doi:10.1556/maseb.62.2009.1.6
18. Adsay N, Basturk O, Cheng J, Andea A. Ductal neoplasia of the pancreas: Nosologic, clinicopathologic, and biologic aspects. *Semin Radiat Oncol*. 2005;15(4):254–264. doi:10.1016/j.semradi.2005.04.001
19. Ledniczky L, Bognar G, Fiore N, Grosfeld JL, Ondrejka P. Pancreatic intraepithelial neoplasia (PanIN) and intraductal papillary mucinous neoplasms (IPMN) [in Hungarian]. *Magy Seb*. 2006;59(1):12–19. PMID:16637385.
20. Safadi S, Martin DR, Rustagi T. Pancreatic intraepithelial neoplasia in heterotopic pancreas: Incidentally diagnosed on endoscopic mucosal resection of a duodenal polyp. *BMJ Case Rep*. 2018;2018:bcr2018224414. doi:10.1136/bcr-2018-224414
21. Vujasinovic M, Dugic A, Maisonneuve P, et al. Risk of developing pancreatic cancer in patients with chronic pancreatitis. *J Clin Med*. 2020;9(11):3720. doi:10.3390/jcm9113720
22. Alhobayb T, Peravali R, Ashkar M. The relationship between acute and chronic pancreatitis with pancreatic adenocarcinoma: Review. *Diseases*. 2021;9(4):93. doi:10.3390/diseases9040093
23. Figueiredo D, Cruz RGB, Normando AGC, et al. Peptidomics strategies to evaluate cancer diagnosis, prognosis, and treatment. *Peptidomics*. 2024;2758:401–423. doi:10.1007/978-1-0716-3646-6_22
24. Pandey S, Malviya G, Chottova Dvorakova M. Role of peptides in diagnostics. *Int J Mol Sci*. 2021;22(16):8828. doi:10.3390/ijms22168828
25. Peng J, Zhang H, Niu H, Wu R. Peptidomic analyses: The progress in enrichment and identification of endogenous peptides. *Trends Anal Chem*. 2020;125:115835. doi:10.1016/j.trac.2020.115835
26. Zhu C, Yuan C, Wei F, Sun X, Zheng S. Characterising salivary peptidome across diurnal dynamics and variations induced by sampling procedures. *Clin Oral Invest*. 2022;27(1):285–298. doi:10.1007/s00784-022-04722-4
27. Aghdassi AA, Mayerle J, Christochowitz S, Weiss FU, Sendler M, Lerch MM. Animal models for investigating chronic pancreatitis. *Fibrogenesis Tissue Repair*. 2011;4(1):26. doi:10.1186/1755-1536-4-26
28. Chan JKC. The wonderful colors of the hematoxylin-eosin stain in diagnostic surgical pathology. *Int J Surg Pathol*. 2014;22(1):12–32. doi:10.1177/1066896913517939
29. Rao M, Pai SM, Khanagar SB, Siddeeqh S, Devang DD, Naik S. Micro of different thicknesses: A comparative study. *J Oral Maxillofac Pathol*. 2020;24(1):186. doi:10.4103/jomfp.JOMFP_290_19
30. Joyce JG, Cook JC, Przysiecki CT, Dale Lehman E. Chromatographic separation of low-molecular-mass recombinant proteins and peptides on Superdex 30 prep grade. *J Chromatogr B Biomed Sci Appl*. 1994;662(2):325–334. doi:10.1016/0378-4347(94)00206-1
31. Bradford MM. A rapid and sensitive method for the quantitation of microgram quantities of protein utilizing the principle of protein-dye binding. *Anal Biochem*. 1976;72:248–254. doi:10.1006/abio.1976.9999
32. Hong P, Koza S, Bouvier ESP. A review size-exclusion chromatography for the analysis of protein biotherapeutics and their aggregates. *J Liq Chromatogr Relat Technol*. 2012;35(20):2923–2950. doi:10.1080/10826076.2012.743724
33. Sipos B, Frank S, Gress T, Hahn S, Klöppel G. Pancreatic intraepithelial neoplasia revisited and updated. *Pancreatol*. 2009;9(1–2):45–54. doi:10.1159/000178874
34. Campello E, Ilich A, Simioni P, Key NS. The relationship between pancreatic cancer and hypercoagulability: A comprehensive review on epidemiological and biological issues. *Br J Cancer*. 2019;121(5):359–371. doi:10.1038/s41416-019-0510-x
35. Capurso G, Traini M, Piciucchi M, Signoretti M, Arcidiacono PG. Exocrine pancreatic insufficiency: Prevalence, diagnosis, and management. *Clin Exp Gastroenterol*. 2019;12:129–139. doi:10.2147/CEG.5168266
36. Mayerle J, Sendler M, Hegyi E, Beyer G, Lerch MM, Sahin-Tóth M. Genetics, cell biology, and pathophysiology of pancreatitis. *Gastroenterology*. 2019;156(7):1951–1968.e1. doi:10.1053/j.gastro.2018.11.081
37. Gál E, Dolensek J, Stožer A, Czakó L, Ébert A, Venglovecz V. Mechanisms of post-pancreatitis diabetes mellitus and cystic fibrosis-related diabetes: A review of preclinical studies. *Front Endocrinol (Lausanne)*. 2021;12:715043. doi:10.3389/fendo.2021.715043
38. Kunovský L, Dítě P, Jabandžiev P, et al. Causes of exocrine pancreatic insufficiency other than chronic pancreatitis. *J Clin Med*. 2021;10(24):5779. doi:10.3390/jcm10245779
39. Satyanarayan ST, Petrov MS, Phillips A, Windsor JA. Protease-related predictors of acute pancreatitis severity: A systematic review of the literature. *J Pancreas (Online)*. 2016;17(6):592–606. <https://www.primescholars.com/articles/protease-related-predictors-of-acute-pancreatitis-severity-a-systematic-review-of-the-literature.pdf>. Accessed August 15, 2023.
40. Raksha N, Halenova T, Vovk T, et al. Disturbances of extracellular protein metabolism in cerulein-induced pancreatitis. *Curr Issues Pharm Med Sci*. 2020;33(3):121–124. doi:10.2478/cipms-2020-0022
41. Van Doren SR. MMP-7 marks severe pancreatic cancer and alters tumor cell signaling by proteolytic release of ectodomains. *Biochemical Society Transactions*. 2022;50(2):839–851. doi:10.1042/BST20210640
42. Pan S, Brentnall TA, Chen R. Proteomics analysis of bodily fluids in pancreatic cancer. *Proteomics*. 2015;15(15):2705–2715. doi:10.1002/pmic.201400476
43. Görgülü K, Diakopoulos KN, Kaya-Aksoy E, et al. The role of autophagy in pancreatic cancer: From bench to the dark bedside. *Cells*. 2020;9(4):1063. doi:10.3390/cells9041063
44. Maus A, Fatica EM, Taylor R, et al. Identification, measurement, and assessment of the clinical utility of human pancreatic polypeptide by liquid chromatography–tandem mass spectrometry. *J Proteome Res*. 2023;22(4):1322–1330. doi:10.1021/acs.jproteome.2c00829

45. Marstrand-Daucé L, Lorenzo D, Chassac A, Nicole P, Couvelard A, Haumaitre C. Acinar-to-ductal metaplasia (ADM): On the road to pancreatic intraepithelial neoplasia (PanIN) and pancreatic cancer. *Int J Mol Sci.* 2023;24(12):9946. doi:10.3390/ijms24129946
46. Basturk O, Hong SM, Wood LD, et al. A revised classification system and recommendations from the Baltimore Consensus Meeting for Neoplastic Precursor Lesions in the Pancreas. *Am J Surg Pathol.* 2015;39(12):1730–1741. doi:10.1097/PAS.0000000000000533
47. Morze J, Wittenbecher C, Schwingshackl L, et al. Metabolomics and type 2 diabetes risk: An updated systematic review and meta-analysis of prospective cohort studies. *Diabetes Care.* 2022;45(4):1013–1024. doi:10.2337/dc21-1705
48. Roy A, Sahoo J, Kamalanathan S, Naik D, Mohan P, Kalayarasan R. Diabetes and pancreatic cancer: Exploring the two-way traffic. *World J Gastroenterol.* 2021;27(30):4939–4962. doi:10.3748/wjg.v27.i30.4939
49. Velazquez-Torres G, Fuentes-Mattei E, Choi HH, Yeung SCJ, Meng X, Lee MH. Diabetes mellitus type 2 drives metabolic reprogramming to promote pancreatic cancer growth. *Gastroenterol Rep (Oxf).* 2020;8(4):261–276. doi:10.1093/gastro/goaa018
50. Zechner D, Radecke T, Amme J, et al. Impact of diabetes type II and chronic inflammation on pancreatic cancer. *BMC Cancer.* 2015;15(1):51. doi:10.1186/s12885-015-1047-x

Chemopreventive role of β -caryophyllene in DMBA-induced skin cancer: Modulation of apoptotic pathways and PI3K/Akt signaling in Swiss albino mice

Ying Sun^{A–D}, Yingying Ma^{B–D}, Hailiang Wang^{A–C,F}

Department of Dermatology, The Affiliated Hospital to Changchun University of Chinese Medicine, China

A – research concept and design; B – collection and/or assembly of data; C – data analysis and interpretation;
D – writing the article; E – critical revision of the article; F – final approval of the article

Advances in Clinical and Experimental Medicine, ISSN 1899–5276 (print), ISSN 2451–2680 (online)

Adv Clin Exp Med. 2025;34(9):1541–1552

Address for correspondence

Hailiang Wang

E-mail: whldoctor@outlook.com

Funding sources

None declared

Conflict of interest

None declared

Received on March 3, 2024

Revised on September 2, 2024

Accepted on October 10, 2024

Published online on January 24, 2025

Cite as

Sun Y, Ma Y, Wang H. Effect of β -caryophyllene suppresses DMBA-induced skin cancer through apoptosis modulating PI3K/AKT signaling pathways in Swiss albino mice.

Adv Clin Exp Med. 2025;34(9):1541–1552.

doi:10.17219/acem/194482

DOI

10.17219/acem/194482

Copyright

Copyright by Author(s)

This is an article distributed under the terms of the Creative Commons Attribution 3.0 Unported (CC BY 3.0) (<https://creativecommons.org/licenses/by/3.0/>)

Abstract

Background. The skin, with its robust structural integrity and advanced immune defense system, serves as a critical protective barrier against environmental toxins and carcinogenic compounds. Despite this, it remains vulnerable to the harmful effects of certain hazardous agents.

Objectives. This study aimed to investigate the chemopreventive potential of β -caryophyllene (BCP) in mitigating 7,12-dimethylbenz[a]anthracene (DMBA)-induced skin carcinogenesis, focusing on the modulation of apoptosis and PI3K/AKT signaling pathways.

Materials and methods. Swiss albino mice were utilized to assess the preventive effects of BCP in DMBA-induced skin cancer. Skin carcinogenesis was initiated by topical DMBA application, followed by promotion using croton oil. To evaluate the chemopreventive efficacy of BCP, a 50 mg/kg oral dose was administered 3 times a week for 16 weeks.

Results. The BCP treatment in DMBA-induced skin cancer mice significantly reduced tumor incidence, tumor burden and the total number of papillomas compared to untreated DMBA-exposed mice. Notably, BCP administration ($p < 0.05$) resulted in a marked increase in body weight and improvement in antioxidant enzyme activity. Additionally, BCP treatment led to significant reductions in lipid peroxidation and enhanced detoxification enzyme function. Histological examination of DMBA-induced skin tissues revealed the presence of keratin pearls, well-differentiated tumor cells and neutrophil infiltration. In contrast, BCP-treated mice showed only mild hyperplasia, dysplasia and moderate keratosis, suggesting a lower degree of tissue damage. Furthermore, BCP demonstrated a protective effect on liver histology, counteracting the toxic effects of DMBA exposure. Gene expression analysis revealed that BCP treatment significantly ($p < 0.05$) upregulated the pro-apoptotic genes Bax, p53, caspase-3 and caspase-9, while downregulating the anti-apoptotic Bcl-2 expression. Additionally, BCP treatment led to a marked reduction in the expression of proliferating cell nuclear antigen (PCNA), cyclin D1 and PI3K/Akt signaling pathways, which are key regulators of cell proliferation and survival.

Conclusions. This study provides compelling evidence that the antioxidant and pro-apoptotic effects of β -caryophyllene contribute to its chemopreventive properties in DMBA-induced skin carcinogenesis in mice. The modulation of key apoptotic signaling pathways and the suppression of the PI3K/Akt pathway by BCP underscores its potential as a therapeutic agent for preventing skin cancer. These findings pave the way for further exploration of BCP as a promising candidate for skin cancer prevention and therapy.

Key words: chemoprevention, skin carcinogenesis, β -caryophyllene, oxidative stress, papilloma

Introduction

Skin cancer is thought to be the most common disease affecting people.¹ According to a literature review, 40% of all newly diagnosed cancer cases worldwide are skin cancer instances.² A survey conducted in India indicates that cutaneous neoplasms make up roughly 1–2% of all human cancers.³ The prevalence of skin cancer has increased due to changes in lifestyle and environmental risks. The skin's keratin layer and immune system provide an effective barrier against potentially hazardous exposures, including those that may be carcinogenic.⁴ The chemical pollutant 7,12-dimethylbenz[a]anthracene (DMBA) induces DNA damage and interferes with xenobiotic metabolism.^{5,6} It also breaks the bonds that bind proteins to DNA, leading to genomic instability and inflammation, which are 2 primary indicators of cancer.⁷ DMBA, a polycyclic aromatic hydrocarbon, is frequently used in animal models to induce cancer.⁸

Humans are often exposed to a variety of chemical mutagens and carcinogens, either through unintended contact, occupational hazards or lifestyle choices. The skin, due to its direct exposure to a wide range of xenobiotics, is particularly vulnerable to cancer development.⁹ Polycyclic aromatic hydrocarbons (PAHs), such as benzo(a)pyrene, 3-methylcholanthrene (MCA) and DMBA, are well-documented for their ability to induce skin cancer in animal models, particularly when used in one-step or two-step carcinogenic protocols (initiation and promotion).¹⁰ Recent findings from our research group have also pointed to aflatoxin B1 (AFB1) as a precursor to skin cancer formation.⁷ These discoveries have prompted an increased focus on identifying compounds that can inhibit the enzymes responsible for activating xenobiotic metabolism, as such inhibitors could potentially lower cancer risk and offer a safer alternative in cancer prevention.

Uncontrolled cell proliferation and the evasion of apoptosis are key factors that drive tumor growth.¹¹ Extensive research has shown that many natural chemopreventive agents exert their effects by promoting apoptosis.^{12–14} The protein p53, recognized as a transcriptional activator for pro-apoptotic genes, is a crucial tumor suppressor. Mutations or inactivation of the *p53* gene, which governs processes such as apoptosis, senescence and cell cycle regulation, are common in nearly all human cancers, including skin cancer.^{15,16} Additionally, alterations in the Bcl-2 family of proteins, which play a vital role in regulating apoptosis, have been implicated in various cancers. Studies have demonstrated that in several human cancers, including skin cancer, Bcl-2 is overexpressed while Bax, a pro-apoptotic protein, is downregulated.^{17,18} The interaction between Bcl-2 and Bax prevents Bax from dimerizing with Bad, thus impeding the apoptotic process.¹⁹ Upon Bax/Bad dimer formation, caspases-9 and -3 are activated, leading to mitochondrial membrane disruption, which allows cytochrome-c to leak from the mitochondria into the cytoplasm, triggering further apoptotic events.^{20–22}

β -caryophyllene (BCP) is a prominent constituent of essential oils derived from various food and spice plants.²³ Research in Wistar rats has highlighted the anti-inflammatory properties of BCP, particularly in the essential oil of *Erymanthus erythropappus*, which is rich in this compound. Moreover, BCP has been found to inhibit the expression of pro-inflammatory markers such as inducible nitric oxide synthase (iNOS), interleukin (IL)-1, IL-6, and cyclooxygenase-2 (COX-2) in C6 microglia cells when administered at a dose of 10 mg/kg.²⁴ Additionally, BCP was shown to mitigate the neuroinflammatory response triggered by hypoxia by blocking nuclear factor kappa-light-chain-enhancer of activated B cells (NF- κ B) activation, and by reducing nitric oxide and PGE2 production in the BV2 mouse cell line.

Objectives

The current study aimed to explore the potential chemopreventive mechanisms of BCP against DMBA-induced skin carcinogenesis, focusing on identifying possible pathways through which BCP may exert its protective effects. We performed a comprehensive histological analysis along with assessments of lipid peroxidation, antioxidant levels and detoxification enzyme activity. We also evaluated tumor incidence, volume and burden. To investigate the molecular mechanisms, we utilized quantitative reverse transcription polymerase chain reaction (RT-qPCR), proliferating cell nuclear antigen (PCNA) and analysis of the PI3K/Akt signaling pathway to measure the mRNA expression of p53 and several key apoptotic proteins, including Bcl-2, Bax, caspase-3, and caspase-9.

Materials and methods

Chemicals

Dimethylsulfoxide (DMSO), DMBA (95% purity, Chemical Abstracts Service (CAS) No. 57-97-6, soluble in mineral oil) and β -caryophyllene (BCP, 90% purity, CAS No. 87-44-5) were purchased from Sigma-Aldrich Chemical Pvt. Ltd. (St. Louis, USA). Antibodies were obtained from BioGenex (Freemont, USA). All other analytical-grade chemicals used in the study were also supplied by Sigma-Aldrich.

Animals

Male Swiss albino mice, aged 5 to 6 weeks and weighing between 15 and 20 g, were randomly selected, transported and housed for the study. The animals were acclimated and maintained in accordance with the ethical guidelines set forth by the Animal Care Committee of Changchun University of Chinese Medicine, China. The experimental protocol was approved by the Institutional Animal Ethics

Committee of Changchun University of Chinese Medicine (registration No. 2023551).

Experimental design

Six experimental groups, each consisting of 6 animals, were established from the animal population. Group 1 served as the normal control, while group 2 received a single dose of 25 mg/kg DMBA dissolved in 100 μ L of acetone. In group 3, animals were administered a 1% DMSO solution containing both 50 mg/kg of BCP and 50 mg/kg of DMBA. Group 4 animals received a 50 mg/kg body weight dose of BCP, administered orally 3 times per week, starting 1 week prior to DMBA application and continuing through the 25th week. The study concluded after 25 weeks, at which point all animals were euthanized. The skin and liver tissues were promptly harvested, cleaned and weighed for further analysis.

Tumor induction and assessment

Over the course of 8 weeks, DMBA was applied topically, and tumor progression was closely monitored. Throughout the study, body weight of all animals was recorded weekly across all experimental groups. To prepare for treatment, the dorsal area of each mouse was shaved using a depilatory cream, and the skin was left undisturbed for 2 days. Mice with no hair regrowth during this period were selected for inclusion in the study. At the conclusion of the experiment, all animals were euthanized by cervical dislocation. Tumor burden was calculated by multiplying the number of tumors by the tumor volume per animal. Tumor volume was determined using the formula $v = (4/3) [D1/2] [D2/2] [D3/2]$, where D1, D2 and D3 represent the 3 tumor diameters (in mm³).

Histopathological examinations

Skin and liver tissues containing tumors were promptly excised from the animals after the rats were sacrificed, and washed with saline solution. Following this, all animals were humanely euthanized by cervical dislocation. Tissue specimens, sectioned at 3–5 μ m thickness using a rotating microtome, were stained with hematoxylin and eosin (H&E). The stained slides were then examined under a light microscope (Nikon Eclipse TS100; Nikon Corp., Tokyo, Japan), and photomicrographs were captured from both the experimental and control groups.

Biochemical analysis

The liver tissues of the same animals were further analyzed to assess the expression of xenobiotic-metabolizing enzymes (XMEs) involved in both phase I and phase II detoxification pathways. The skin and liver tissues were homogenized using an all-glass homogenizer equipped with a Teflon pestle (DuPont, Wilmington, USA) along

with the appropriate buffer solution, following a rinse with ice-cold saline.²⁵ Protein content was quantified using the established method. To evaluate the enzymatic activities of cytochrome P450 (Cyt-P450), cytochrome b5 (Cyt-b5), glutathione S-transferase (GST), and glutathione reductase (GR) in the liver, we applied the procedure described by Esteves et al.²⁶ The same methodology was used to measure the concentrations of thiobarbituric acid reactive substances (TBARS) in the skin tissue samples. Enzymatic activities for superoxide dismutase (SOD), glutathione peroxidase (GPx), catalase (CAT), and glutathione peroxidase (GPx) were determined according to standard protocols.²⁷ Additionally, the levels of glutathione (GSH), as well as oxidized GSH, were assessed in the skin tissues.²⁷

mRNA expressions detected with quantitative reverse transcription polymerase chain reaction (RT-qPCR)

Total RNA was extracted from skin tissues using TRIzol reagent (Thermo Fisher Scientific, Waltham, USA) according to the manufacturer's protocol. The isolated RNA was subsequently converted into complementary DNA (cDNA) using the cDNA Reverse Transcription Kit. For gene expression analysis, the cDNAs were evaluated using the Faststart SYBR Green Master Mix (Thermo Fisher Scientific), following the manufacturer's instructions. Electrophoresis was performed on 1.5% agarose gels to visualize the RNA bands, and the band intensity was quantified using ImageJ v. 1.48 software (National Institutes of Health (NIH), Bethesda, USA).

Western blotting

To prepare cell lysates for western blot analysis, lysis buffer was stored at freezing temperatures. Protein concentration was determined using the BCA Protein Assay Kit (Thermo Fisher Scientific). The proteins were then separated by electrophoresis and transferred onto a polyvinylidene difluoride (PVDF) membrane. The membrane was blocked with bovine serum albumin (BSA) for approx. 1 h at room temperature. Next, primary antibodies were applied at a 1:1,000 dilution, and the membrane was incubated overnight at 4°C. Following this, secondary antibodies were applied for 2 h. Enhanced chemiluminescence was used to visualize the protein bands. Quantification of the bands was performed through densitometric analysis using ImageJ software.

Statistical analyses

The data from each group were statistically analyzed using GraphPad Prism v. 8.0.2 (GraphPad Software, San Diego, USA) and IBM SPSS software v. 25 (IBM Corp., Armonk, USA). The results are presented as the median with the interquartile range (Q1 and Q3). The normality

Table 1. Comparison of the studied groups

Variables	Group 1 (n = 6)	Group 2 (n = 6)	Group 3 (n = 6)	Group 4 (n = 6)	Test value (H)***	p-value**
Body weight	37.92 (34.77–41.02)	26.06 (23.90–28.24)	33.28 (30.50–36.01)	35.63 (32.67–38.54)	15.62	<0.001*, #
TBARS	71.83 (65.88–77.72)	137.08 (125.70–148.51)	89.34 (81.93–96.66)	73.75 (67.63–79.80)	19.68	<0.001*, #
SOD	8.60 (7.89–9.31)	4.71 (4.32–5.10)	7.11 (6.52–7.69)	8.31 (7.62–8.99)	18.52	<0.001*, #
CAT	51.82 (47.53–56.07)	40.04 (36.72–43.38)	44.27 (40.60–47.90)	49.98 (45.83–54.08)	16.05	<0.001*, #
GPx	38.03 (34.87–41.14)	15.47 (14.18–16.76)	29.31 (26.88–31.71)	37.01 (33.93–40.04)	19.68	<0.001*, #
GSH	55.83 (51.20–60.40)	35.28 (32.35–38.22)	41.78 (38.31–45.20)	50.66 (46.46–54.81)	20.08	<0.001*, #
Cyt-p450	0.58 (0.53–0.63)	1.46 (1.33–1.58)	0.85 (0.77–0.92)	0.56 (0.51–0.60)	19.73	<0.001*, #
Cyt-b5	1.21 (1.10–1.31)	2.99 (2.74–3.24)	1.75 (1.60–1.89)	1.10 (1.00–1.19)	20.62	<0.001*, #
GR	32.76 (30.04–54.45)	13.30 (12.20–14.41)	28.06 (25.74–30.37)	30.97 (28.40–33.51)	17.12	<0.001*, #
GST	96.35 (88.35–104.24)	25.75 (23.61–27.90)	76.17 (69.85–82.41)	94.86 (86.99–102.64)	19.68	<0.001*, #
p53	1.00 (0.91–1.08)	2.57 (2.35–2.78)	1.70 (1.56–1.84)	1.25 (1.14–1.35)	21.62	<0.001*, #
Bcl-2	1.00 (0.91–1.08)	2.34 (2.14–2.53)	1.53 (1.40–1.65)	1.09 (0.99–1.18)	20.22	<0.001*, #
Bax	1.00 (0.91–1.08)	0.66 (0.60–0.71)	0.75 (0.68–0.81)	0.94 (0.86–1.02)	18.87	<0.001*, #
Caspase-3	1.00 (0.91 to 1.08)	0.29 (0.26–0.31)	0.73 (0.66–0.79)	0.91 (0.83–0.98)	20.62	<0.001*, #
Caspase-9	1.00 (0.91–1.08)	0.42 (0.38–0.45)	0.65 (0.59–0.70)	0.81 (0.74–0.87)	21.63	<0.001*, #
PCNA	1.00 (0.91–1.08)	2.50 (2.29–2.71)	1.48 (1.35–1.60)	1.19 (1.08–1.29)	21.20	<0.001*, #
Cyclin-D1	1.00 (0.91–1.08)	2.19 (2.01–2.37)	1.50 (1.37–1.62)	1.09 (0.99–1.18)	20.18	<0.001*, #
PI3K	1.00 (0.91–1.08)	2.26 (2.07–2.45)	1.42 (1.30–1.53)	1.10 (1.00–1.19)	20.62	<0.001*, #

Data were presented as median (Q1 and Q3); **p-value generated from Kruskal–Wallis test with Dunn's post hoc test (significance value adjusted by the Bonferroni correction for multiple tests); ***degrees of freedom (df) = 3; *p < 0.001 vs the DMBA + BCP; #p < 0.001 vs the control model. BCP – β -caryophyllene; DMBA – 7,12-dimethylbenz[*a*]anthracene; TBARS – thiobarbituric acid reactive substances; SOD – superoxide dismutase; CAT – catalase; GPx – glutathione peroxidase; GSH – glutathione; Cyt-P450 – cytochrome P450; Cyt-b5 – cytochrome b5; GST – glutathione S-transferase; GR – glutathione reductase; Bcl-2 – B-cell lymphoma 2; Bax – BCL2-associated agonist of cell death; PCNA – proliferating cell nuclear antigen; PI3K – phosphoinositide 3-kinase.

Table 2. Effect of BCP on tumor incidence, tumor volume and tumor burden of experimental mice

Groups/ treatments	Number of mice	Tumor incidence	Tumor number	Tumor volume	Tumor burden
Group I	6	–	–	–	–
Group II	6	100%	14.70 \pm 1.14	505.10 \pm 39.48	7424.97 \pm 505.10
Group III	6	–	–	–	–
Group IV	6	–	–	–	–

Values are expressed as mean \pm SD of 6 mice. Values not sharing a common superscript letter differ significantly at p < 0.05. BCP – β -caryophyllene; SD – standard deviation.

of the data distributions was assessed using the Kolmogorov–Smirnov test. Since all distributions were normal, the Brown–Forsythe test was employed to assess the equality of variances. Significant differences between multiple groups were determined using the Kruskal–Wallis test, followed by Dunn's post hoc test for pairwise comparisons. A p-value of less than 0.05 was considered statistically significant. All statistical tests were two-tailed.

Results

The results of the Kruskal–Wallis test and Dunn's post hoc test are presented in Table 1

Effect of BCP on body weight changes

To evaluate the chemopreventive potential of BCP, a DMBA-induced mouse skin carcinogenesis model was first established in vivo (Fig. 1A). The body weight of the mice in the DMBA group showed a significantly lower gain compared to the BCP-only group (p > 0.02). However, the DMBA group exhibited a marked reduction in body weight compared to the control group (p > 0.001). Experimental groups treated with DMBA + BCP showed a significantly greater reduction in body weight compared to the BCP-only group (p < 1.000). Moreover, the body weight of the DMBA + BCP group was significantly lower than the control group (p < 0.615). Kruskal–Wallis

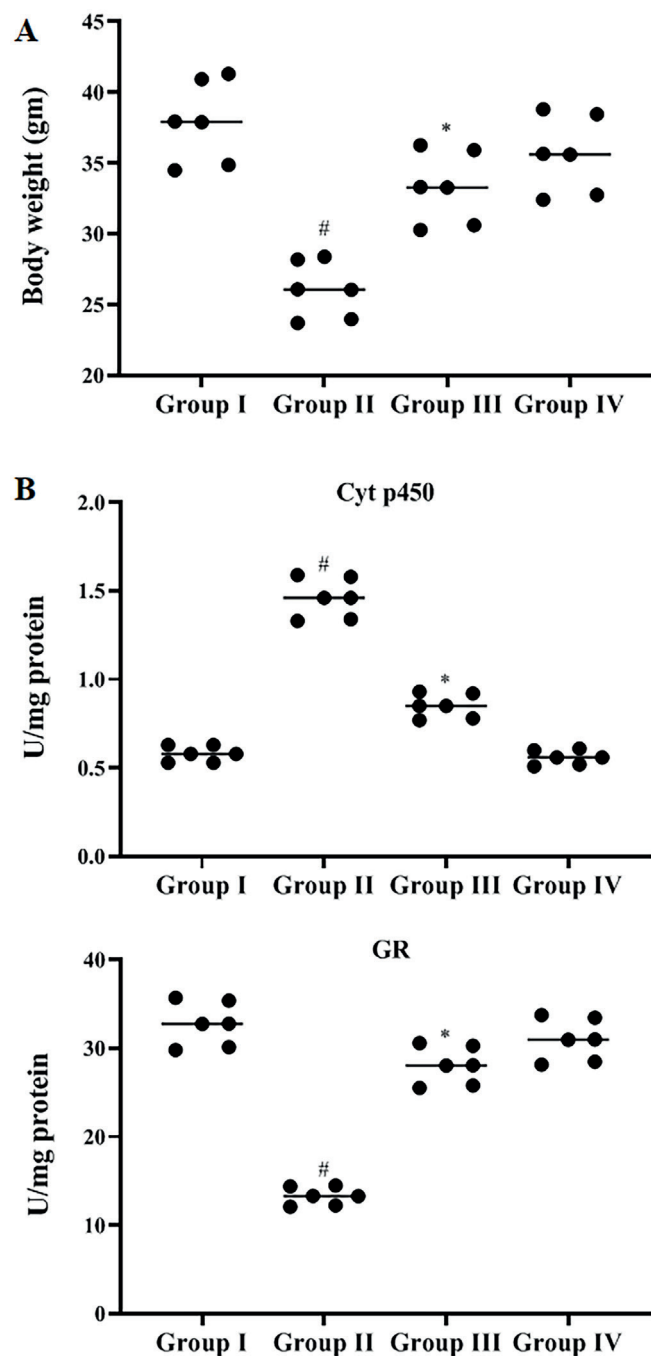


Fig. 1. A. The body weight changes of control and experimental rats; B. Effect of BCP on levels of non-enzymatic antioxidants in the skin tissues of the experimental rats. Results were presented as median (min and max) of 6 observations and the significance was considered as * $p < 0.001$ vs the DMBA + BCP, # $p < 0.001$ vs the control model; ** p -value generated from Kruskal–Wallis test with Dunn’s post hoc test (significance value adjusted with the Bonferroni correction for multiple tests)

BCP – β -caryophyllene; DMBA – 7,12-dimethylbenz[a]anthracene.

statistical analysis revealed significant differences across the experimental groups ($H = 15.62$; degrees of freedom (df) = 3; $p > 0.001$) as shown in Table 1.

Effect of BCP on tumor incidence

DMBA-induced mice exhibited a significantly higher incidence of papillomas, which was notably reduced in the BCP-treated group. Additionally, DMBA exposure resulted in a greater number of skin papillomas, which was significantly suppressed ($p < 0.001$) in the mice receiving BCP treatment, reflecting a reduction in the number of tumors per mouse. The suppressive effect of BCP

on tumorigenesis was further corroborated by the size distribution of the papillomas. Notably, while DMBA treatment increased tumor area, BCP administration significantly reduced the tumor area as the treatment progressed over time (Table 2)

Levels of phase I and II detoxification enzymes

The levels of phase I detoxification enzymes, Cyt-P450 and Cyt-b5, were significantly higher in the livers of mice treated with BCP alone compared to those exposed to DMBA alone (Cyt-P450: $p < 0.001$; Cyt-b5: $p = 0.000$).

In contrast, the phase I enzymes were significantly lower in the livers of control mice than in the DMBA group (Cyt-P450: $p < 0.004$; Cyt-b5: $p < 0.01$). The Kruskal–Wallis statistical test provided the following significance values: Cyt-P450 ($H = 19.731$, $df = 3$, $p = 0.000$) and Cyt-b5 ($H = 20.629$, $df = 3$, $p = 0.000$), indicating significant differences among the experimental groups. Regarding phase II detoxifying enzymes, GSH, GST, and GR, their levels were significantly reduced in the DMBA group compared to both the control group (GSH: $p < 0.000$; GST: $p < 0.001$; GR: $p < 0.001$) and the BCP alone group (GSH: $p < 0.017$; GST: $p < 0.004$; GR: $p < 0.007$).

The Kruskal–Wallis test for these enzymes revealed the following significance values: GSH ($H = 20.087$, $df = 3$, $p = 0.000$), GST ($H = 19.680$, $df = 3$, $p = 0.000$) and GR ($H = 17.120$, $df = 3$, $p = 0.001$), highlighting substantial differences among the groups. The administration of BCP at 50 mg/kg bw in DMBA-treated animals effectively restored phase I and phase II detoxifying agents to near normal levels. However, no significant changes were observed when 50 mg/kg of BCP was given alone. The BCP alone treatment resulted in reduced levels of GSH, with no notable effect on phase II enzyme activities (Table 1, Fig. 1B).

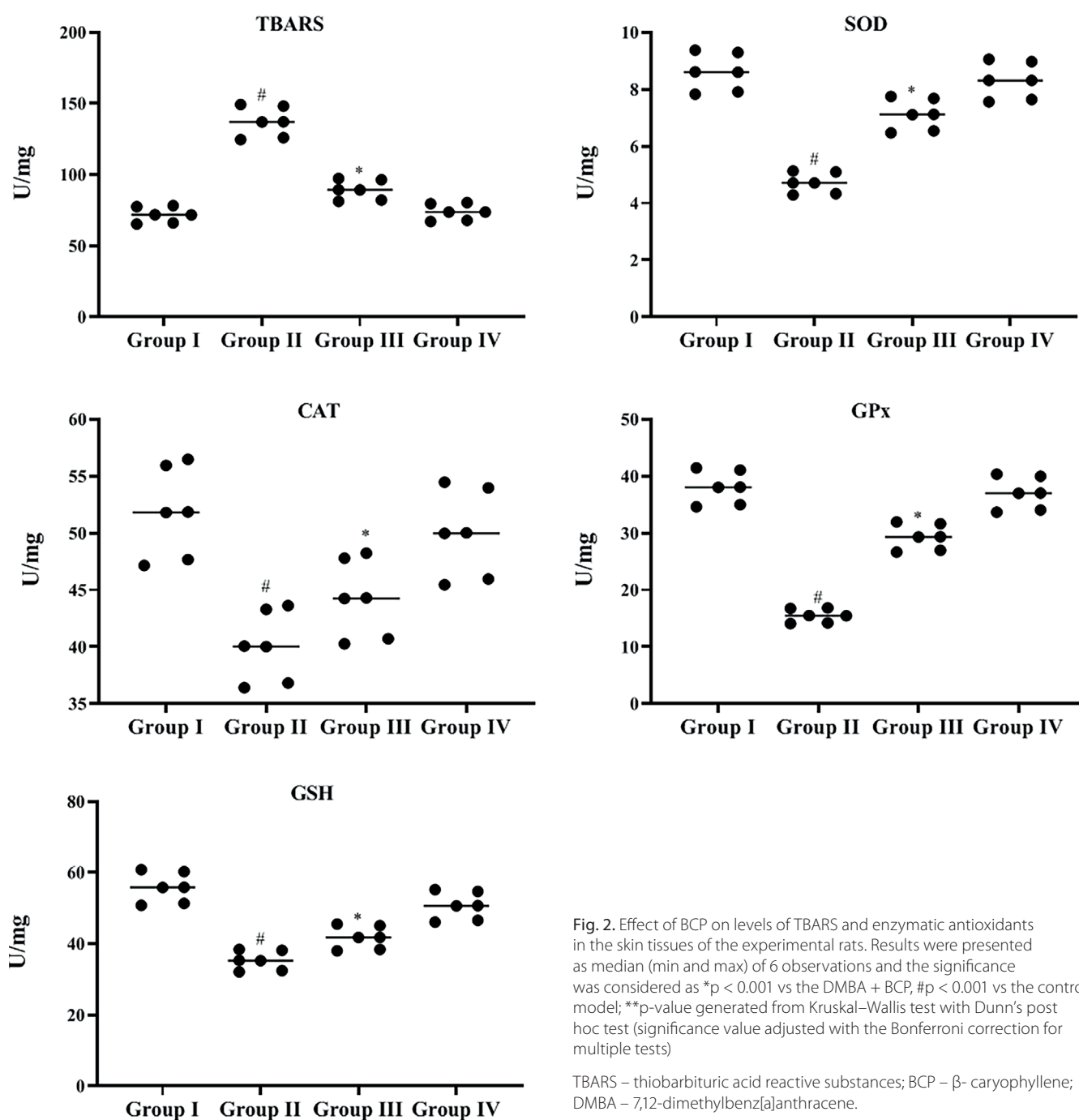


Fig. 2. Effect of BCP on levels of TBARS and enzymatic antioxidants in the skin tissues of the experimental rats. Results were presented as median (min and max) of 6 observations and the significance was considered as * $p < 0.001$ vs the DMBA + BCP, # $p < 0.001$ vs the control model; ** p -value generated from Kruskal–Wallis test with Dunn's post hoc test (significance value adjusted with the Bonferroni correction for multiple tests)

TBARS – thiobarbituric acid reactive substances; BCP – β -caryophyllene; DMBA – 7,12-dimethylbenz[a]anthracene.

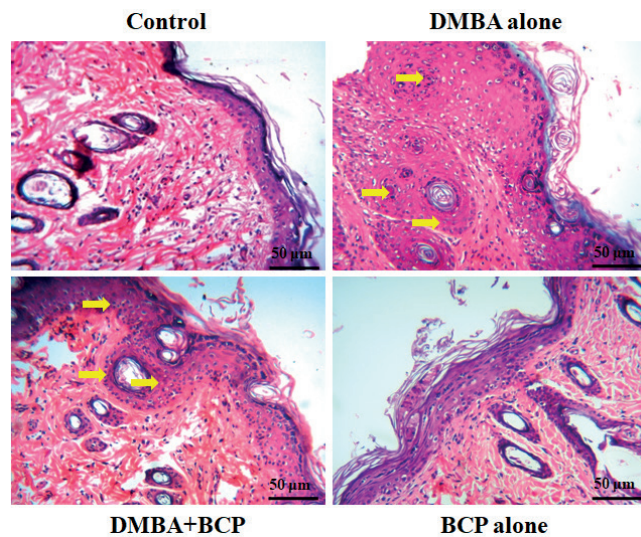


Fig. 3. Anti-tumor effects of BCP on DMBA-induced skin cancer rats. Histopathological profiles of representative skin tissues control and experimental rats (hematoxylin and eosin (H&E) staining). Scale bar = 50 µm

BCP – β -caryophyllene; DMBA – 7,12-dimethylbenz[a]anthracene.

Estimation of lipid peroxidation and antioxidants

The levels of antioxidant indicators — SOD, CAT and GPx — in the skin tissue of experimental and control rats are summarized in Table 1 and Fig. 2. In the skin tissues, the enzymatic antioxidant content was significantly lower in the rats treated with DMBA alone compared to those in the BCP alone group (SOD: $p < 0.007$; CAT: $p < 0.012$; GPx: $p < 0.004$) and the control group (SOD: $p < 0.001$; CAT: $p < 0.002$; GPx: $p < 0.001$). In contrast, administration of BCP (50 mg/kg bw) alongside DMBA notably improved antioxidant levels ($p < 0.001$), outperforming both the DMBA group (SOD: $p < 0.133$; CAT: $p < 0.203$; GPx: $p < 0.086$) and the BCP alone group (SOD: $p < 0.614$; CAT: $p < 0.615$; GPx: $p < 0.300$). Moreover, the levels of lipid peroxidation (LPO) indicators, specifically TBARS, were significantly lower in the skin tissue of control rats compared to the DMBA-only group ($p < 0.001$). Rats treated with BCP alone exhibited significantly higher LPO by-products ($p < 0.004$) compared to controls. However, the oral administration of BCP at 50 mg/kg bw significantly reduced the LPO by-product levels in the skin tissue ($p < 0.086$) when compared to the DMBA-only group. No significant differences were observed between the rats in the control group (group 1) and the BCP-alone group (group 4). The statistical analysis, using the Kruskal–Wallis test, revealed the following significance values among the experimental groups: TBARS ($H = 19.680$, $df = 3$, $p = 0.000$), SOD ($H = 18.523$, $df = 3$, $p = 0.000$), CAT ($H = 16.053$, $df = 3$, $p < 0.001$), and GPx ($H = 19.680$, $df = 3$, $p = 0.000$).

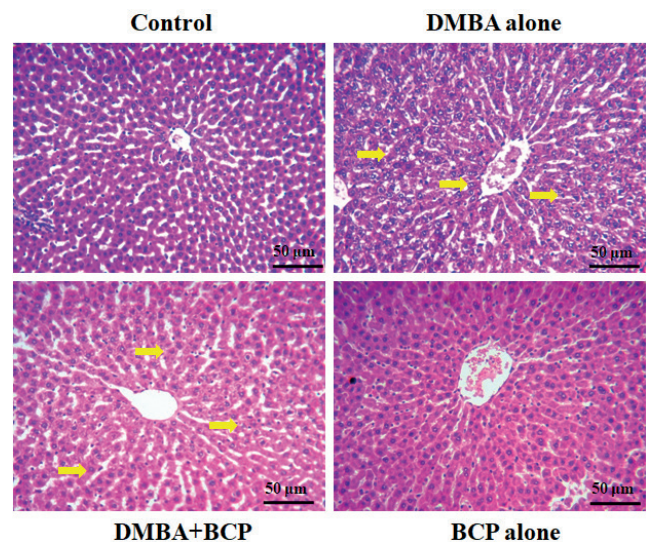


Fig. 4. Histopathological changes in the liver tissue of the control and experimental rats (hematoxylin and eosin (H&E) staining). Scale bar = 50 µm

BCP impact on the DMBA-induced in skin tissues

Hematoxylin and eosin (H&E) staining of skin tissue illustrates the progression of squamous cell carcinoma (SCC) in mice. In the normal control (NC) group, skin tissues exhibited a typical, intact epithelial layer. In contrast, the DMBA-treated mice showed significant epidermal thickening, hyperplasia and the development of well-formed SCC with characteristic keratin pearls. Notably, oral administration of BCP at 50 mg/kg bw effectively suppressed these DMBA-induced skin alterations, including hyperplasia, hyperkeratosis and the progression of SCC, in a dose-dependent manner. These findings collectively demonstrate the potent inhibitory effect of BCP on DMBA-induced skin carcinogenesis in mice (Fig. 3).

BCP impact on the DMBA-induced in liver tissues

In the DMBA-induced model mice, hepatic tissue sections exhibited pronounced signs of inflammation, including neutrophil infiltration, lymphocyte presence and liver cell damage. Liver cell injury was evident through necrotic changes, such as membrane collapse, cytoplasmic damage, alterations in nuclear pyknosis, and dilation of Bowman's capsule. Remarkably, these pathological alterations were significantly alleviated with the administration of BCP at 50 mg/kg bw, in a dose-dependent manner (Fig. 4).

Analysis of apoptotic mRNA expressions in skin region tissue using RT-qPCR

Table 1 and Fig. 5 illustrate the analysis of apoptotic markers including p53, Bcl-2, Bax, caspase-3, and caspase-9 in skin tissue samples from both experimental and control

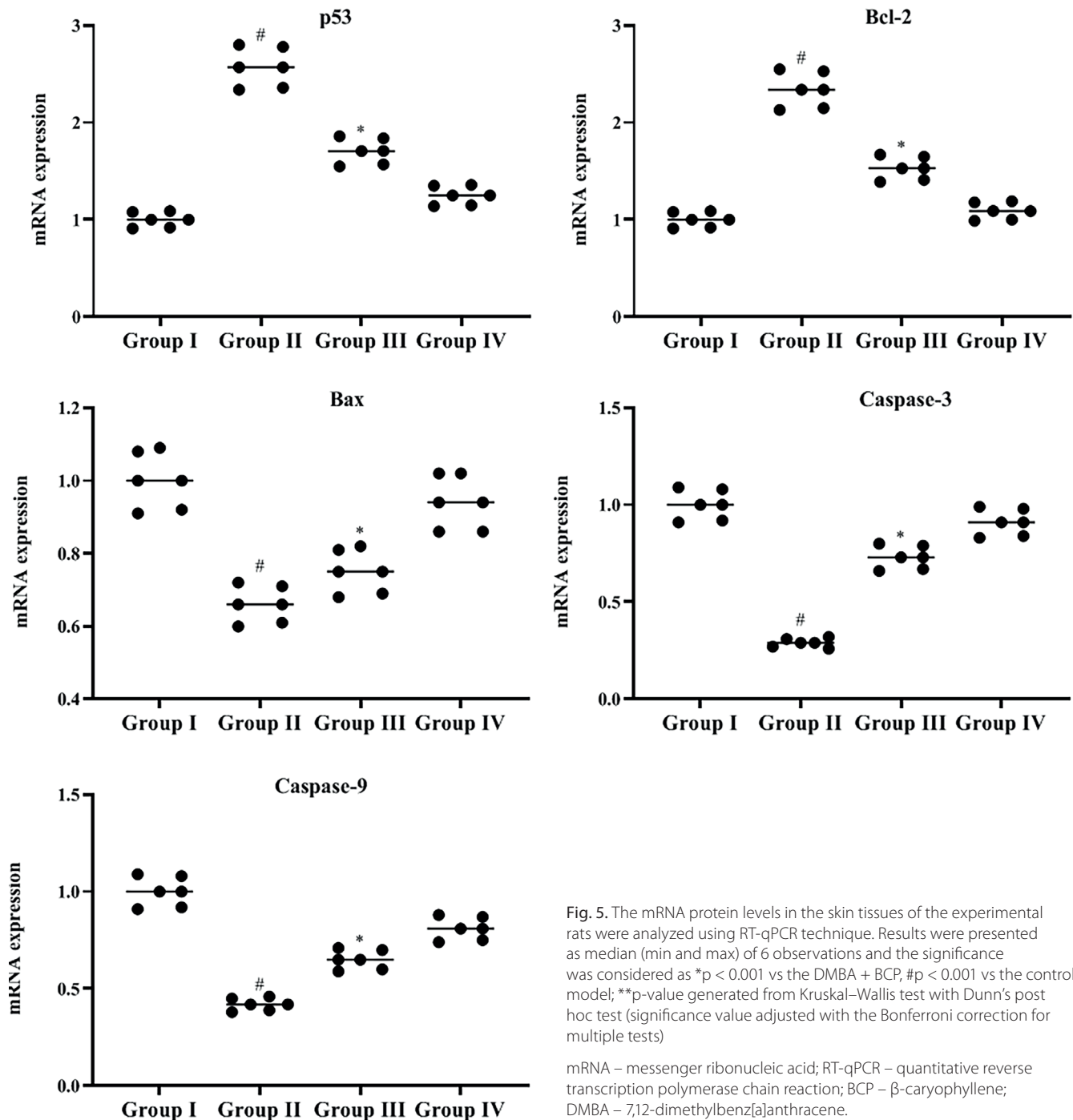


Fig. 5. The mRNA protein levels in the skin tissues of the experimental rats were analyzed using RT-qPCR technique. Results were presented as median (min and max) of 6 observations and the significance was considered as * $p < 0.001$ vs the DMBA + BCP, # $p < 0.001$ vs the control model; ** p -value generated from Kruskal–Wallis test with Dunn's post hoc test (significance value adjusted with the Bonferroni correction for multiple tests)

mRNA – messenger ribonucleic acid; RT-qPCR – quantitative reverse transcription polymerase chain reaction; BCP – β -caryophyllene; DMBA – 7,12-dimethylbenz[a]anthracene.

groups. In mice from group 2 (tumor-bearing), the levels of Bax, caspase-3 and caspase-9 were significantly reduced compared to both the control (Bax: $p > 0.001$; caspase-3: $p = 0.000$; caspase-9: $p = 0.000$) and BCP-alone groups (Bax: $p > 0.006$; caspase-3: $p > 0.010$; caspase-9: $p > 0.020$). Treatment with BCP in group 3 (DMBA-painted) effectively restored these markers to near-normal levels, significantly differing from group 1 (Bax: $p > 0.053$; caspase-3: $p > 0.037$; caspase-9: $p > 0.020$). There was no notable difference in the expression of these markers between mice treated with BCP (group 3) and those in groups 1 and 4. Statistical significance was confirmed with the Kruskal–Wallis

test, with the following results: Bax: $H = 18.876$, $df = 3$, $p = 0.000$; caspase-3: $H = 20.629$, $df = 3$, $p = 0.000$; caspase-9: $H = 21.638$, $df = 3$, $p = 0.000$.

In contrast, p53 and Bcl-2 expressions were notably lower in group 1 than in both the DMBA-only group (p53: $p = 0.000$; Bcl-2: $p = 0.000$) and the DMBA + BCP group (p53: $p > 0.020$; Bcl-2: $p > 0.005$). When BCP was administered alone, its effect was also significant in reducing these markers compared to group 2 (p53: $p > 0.020$; Bcl-2: $p > 0.007$). There were no significant differences in p53 and Bcl-2 levels between the group 3 (BCP) and groups 1 and 4. Kruskal–Wallis analysis revealed strong statistical

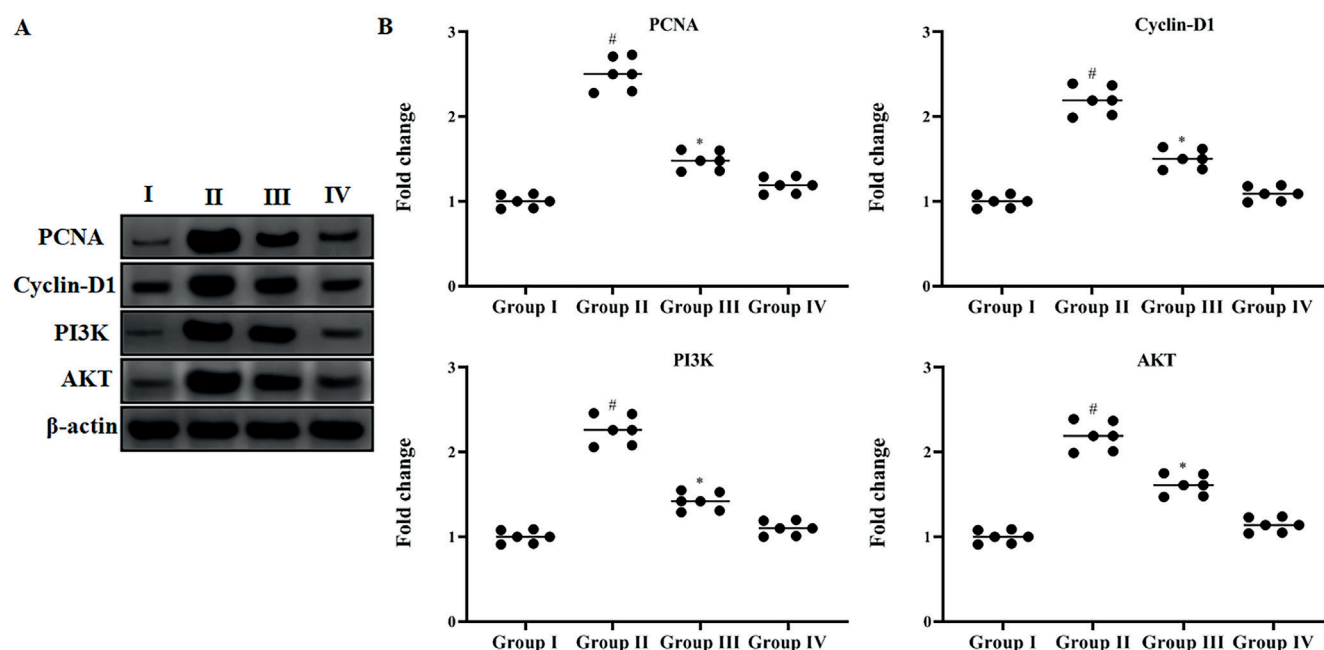


Fig. 6. A. Effect of BCP on levels of signaling molecules and cell markers in the skin tissues of the experimental rats using western blot; B. Results were presented as median (min and max) of 6 observations and the significance was considered as * $p < 0.001$ vs the DMBA + BCP, # $p < 0.001$ vs the control model; ** p -value generated from Kruskal–Wallis test with Dunn's post hoc test (significance value adjusted with the Bonferroni correction for multiple tests)

BCP – β -caryophyllene; DMBA – 7,12-dimethylbenz[a]anthracene.

significance: p53: $H = 21.628$, $df = 3$, $p = 0.000$; Bcl-2: $H = 20.228$, $df = 3$, $p = 0.000$.

Influence of BCP on P13K/Akt pathway

One of the key factors influencing cell proliferation pathways in skin cancer development is the expression of proteins such as PCNA, cyclin-D1 and PI3K/Akt (Table 1, Fig. 6). In the normal control group, the expression of cyclin-D1, PI3K and Akt was significantly lower compared to the DMBA-only group (PCNA: $p = 0.000$; cyclin-D1: $p = 0.000$; PI3K: $p = 0.000$) and the DMBA + BCP group (PCNA: $p > 0.025$; cyclin-D1: $p > 0.053$; PI3K: $p > 0.037$). Mice treated with BCP alone showed expression levels of PCNA, cyclin-D1 and PI3K/Akt similar to normal, with minimal differences compared to the control group (PCNA: $p > 0.015$; cyclin-D1: $p > 0.006$; PI3K: $p > 0.010$). Based on these results, it is suggested that BCP may effectively inhibit tumor growth by modulating these key cell proliferation proteins. Statistical significance was confirmed through Kruskal–Wallis testing, with the following results: PCNA: $H = 21.202$, $df = 3$, $p = 0.000$; cyclin-D1: $H = 20.186$, $df = 3$, $p = 0.000$; PI3K: $H = 20.629$, $df = 3$, $p = 0.000$.

Discussion

Skin cancer is widely regarded as one of the most prevalent diseases affecting humans. According to estimates, cutaneous neoplasms account for approx. 1–2% of all

human malignancies in India, based on a 2014 survey.^{1,3} The increasing incidence of skin cancer has been associated with changes in lifestyle and environmental factors. The oral cavity, due to its direct exposure to phytochemicals, presents a unique opportunity for studying the chemopreventive potential of diet.²⁸ One of the key constituents of essential oils from culinary and spice plants is BCP, which has garnered attention for its potential anticancer properties.²³ Animal models of cancer, particularly those induced by the polycyclic aromatic hydrocarbon DMBA, are commonly used to explore the disease's development.⁷ The most effective pharmaceutical strategies against carcinogenesis are thought to involve a combination of both natural and synthetic agents.²⁹ In our study, oral administration of BCP (50 mg/kg/bw) in DMBA-induced rats effectively inhibited tumor growth. No significant differences in cancer incidence or other metrics were observed between the 2 doses tested. Based on these findings, we proceeded with further research using a BCP dose of 50 mg/kg/bw. Similarly, oral supplementation with 10 mg/kg bw of sanggenol L in DMBA-painted hamsters effectively prevented tumor development, enhanced biochemical markers, suppressed inflammatory markers, and promoted apoptosis.³⁰

Dietary antioxidants play a crucial role in regulating the activity of cytochrome P450 enzymes, which are essential for the metabolic breakdown of xenobiotics (including carcinogens), while phase I enzymes initiate the activation of these substances. To assess the chemopreventive potential of test compounds, it is important to understand the levels of both phase I and phase II enzymes.^{31,32} In this

study, the administration of BCP (50 mg/kg/bw) to DMBA-induced rats effectively reversed the marked alterations in phase I enzyme activities. This suggests that BCP inhibits the metabolic activation of DMBA, thus offering potential protective effects against carcinogenesis. Furthermore, BCP has been found to exert cardioprotective benefits against doxorubicin-induced injury, attributed to its anti-inflammatory and antioxidant properties. Sesquiterpenes, such as BCP, have demonstrated the ability to scavenge reactive oxygen species (ROS), including superoxide anions and hydroxyl radicals. Additionally, BCP significantly reduces the levels of pro-inflammatory cytokines, COX-2 and iNOS. Therefore, BCP is proposed as a potent chain-breaking antioxidant, offering protection against oxidative stress-related damage.³³

Glutathione reductase plays a crucial role in maintaining stable GSH levels by facilitating the NADPH-dependent reduction of glutathione disulfide (GSSG). Glutathione, a non-enzymatic tripeptide antioxidant containing a cysteine residue, is vital for protecting cells against ROS and free radicals. In this study, we observed that DMBA-induced liver damage in mice led to reduced levels of GST, GR and GSH. However, administration of BCP (50 mg/kg/bw) effectively restored these levels to near-normal values, highlighting its potent antioxidant activity. The chemopreventive effects of BCP (50 mg/kg/bw) in counteracting DMBA-induced skin carcinogenesis were further confirmed by histopathological analysis. β -caryophyllene has also demonstrated its ability to mitigate toxicity from various harmful agents, including carbon tetrachloride, glutamate, 1-methyl-4-phenylpyridinium, and d-galactose, in both in vitro and in vivo models.³⁴ Additionally, Chang et al. demonstrated that BCP exhibits a stronger cytoprotective effect than the epoxide metabolite, reinforcing its potential therapeutic value.³⁵

Mutant p53 accumulates in cells as a result of stress and DNA damage, disrupting normal cellular processes.³⁶ In fact, the inactivation of wild-type p53 is a hallmark of several cancers, often leading to poor clinical outcomes.³⁷ Alterations in the Bax/Bcl-2 ratio have been reported in various malignancies, including skin cancer. In this study, we observed that DMBA-induced rats exhibited elevated levels of mutant p53 and Bcl-2, coupled with reduced levels of Bax. However, oral administration of BCP (50 mg/kg/bw) effectively induced apoptosis, as evidenced by an increase in Bax expression and a reduction in both mutant p53 and Bcl-2 levels.

Apoptotic caspases are generally classified into 2 categories: caspase-9, which acts as an upstream initiator, and caspase-3, a downstream effector. However, mitochondria can contribute to the activation of both caspases. Notably, significant oxidative stress is often linked to the activation of death receptors or the mitochondrial pathway. Bcl-2, a pro-apoptotic B-cell lymphoma protein, has been shown to mediate mitochondrial-driven apoptosis. Furthermore, when cellular stress becomes severe or prolonged, disruptions in the endoplasmic reticulum

(ER) trigger the unfolded protein response (UPR), which can culminate in an apoptotic response.³⁸ In the DMBA-induced skin cancer model, downregulation of caspase-3 and caspase-9 was observed.³⁹ In this study, DMBA-induced mice exhibited a compromised apoptotic response, but oral administration of BCP (50 mg/kg/bw) restored the expression of caspase-3 and -9, effectively preventing the development of skin cancer.

The expression levels of PCNA mRNA, cyclin-D1 protein, and other key markers can serve as valuable indicators for predicting malignant transformation. In the present study, we observed that DMBA-induced mice exhibited elevated levels of PI3K, Akt, PCNA, and cyclin-D1 in their skin tissues.³⁹ Notably, the overexpression of PCNA has been associated with enhanced tumorigenesis and increased aggressiveness of tumors, especially during the progression from hyperplasia to dysplasia, and eventually to skin cancer. Assessing the tissue distribution of cyclin-D1 may prove instrumental in evaluating the extent of cancer progression, particularly in oral tumors. Furthermore, cyclin-D1 plays a critical role as a sensor of extracellular signals, especially during the early to mid-G1 phase of cell division.⁴⁰ These findings are consistent with our research, which demonstrates that BCP effectively inhibits cell proliferation and division by downregulating the expression of PI3K, Akt, cyclin-D1, and PCNA.

Limitations

Our study suggests that the BCP major role in preventing skin cancer, but the molecular mechanism of inflammatory markers and molecular modeling will be studied in future research. Detailed mechanisms of action still need to be clarified.

Conclusions

Altogether, the study suggested that BCP has garnered considerable pharmacological attention for its potential therapeutic benefits. When administered to mice, BCP effectively controls tumor progression by inducing apoptotic signaling, as evidenced by the upregulation of Bax, Bcl-2 and caspase-3 and -9. Additionally, BCP inhibits cell proliferation by downregulating PCNA, cyclin-D1, p53, and the PI3K/Akt signaling pathway. These findings highlight the potential of BCP and similar natural compounds as promising chemopreventive agents, warranting further pharmacological and pharmaceutical studies to fully explore their therapeutic applications.

Supplementary data

The supplementary materials are available at <https://doi.org/10.5281/zenodo.13836654>. The package includes the following files:

Supplementary Fig. 1. Results of Kruskal–Wallis test as presented in Fig. 1.

Supplementary Fig. 2. Results of Kruskal–Wallis test as presented in Fig. 2.

Supplementary Fig. 3. Results of Kruskal–Wallis test as presented in Fig. 5.

Supplementary Fig. 4. Results of Kruskal–Wallis test as presented in Fig. 6.

Data availability


The datasets generated and/or analyzed during the current study are available from the corresponding author on reasonable request.


Consent for publication

Not applicable.

ORCID iDs

Ying Sun  <https://orcid.org/0009-0007-7912-2359>

Yingying Ma  <https://orcid.org/0009-0001-5010-8699>

Hailiang Wang  <https://orcid.org/0009-0008-2827-8684>

References

- Ramos S. Cancer chemoprevention and chemotherapy: Dietary polyphenols and signalling pathways. *Mol Nutr Food Res*. 2008;52(5):507–526. doi:10.1002/mnfr.200700326
- Jemal A, Siegel R, Ward E, Murray T, Xu J, Thun MJ. Cancer statistics, 2007. *CA Cancer J Clin*. 2007;57(1):43–66. doi:10.3322/canjclin.57.1.43
- Khullar G, Saikia U, De D, Radotra B. Nonmelanoma skin cancers: An Indian perspective. *Indian J Dermatopathol Diagn Dermatol*. 2014;1(2):55. doi:10.4103/2349-6029.147282
- Neagu M, Caruntu C, Constantin C, et al. Chemically induced skin carcinogenesis: Updates in experimental models (Review). *Oncol Rep*. 2016;35(5):2516–2528. doi:10.3892/or.2016.4683
- Balmain A, Brown K. Oncogene activation in chemical carcinogenesis. *Adv Cancer Res*. 1988;51:147–182. doi:10.1016/S0065-230X(08)60222-5
- Fujiki H, Suganuma M, Yoshizawa S, et al. Codon 61 mutations in the c-Harvey-ras gene in mouse skin tumors induced by 7,12-dimethylbenz[a]anthracene plus okadaic acid class tumor promoters. *Mol Carcinog*. 1989;2(4):184–187. doi:10.1002/mc.2940020403
- Rastogi S, Shukla Y, Paul B, Chowdhuri D, Khanna S, Das M. Protective effect of *Ocimum sanctum* on 3-methylcholanthrene, 7,12-dimethylbenz(a)anthracene and aflatoxin B1 induced skin tumorigenesis in mice. *Toxicol Appl Pharmacol*. 2007;224(3):228–240. doi:10.1016/j.taap.2007.05.020
- Mestas J, Hughes CCW. Of Mice and Not Men: Differences between mouse and human immunology. *J Immunol*. 2004;172(5):2731–2738. doi:10.4049/jimmunol.172.5.2731
- Scotto J, Fears TM. Skin cancer epidemiology: Research needs. *Natl Cancer Inst Monogr*. 1978;(50):169–177. PMID:753973.
- Didona D, Paolino G, Bottoni U, Cantisani C. Non melanoma skin cancer pathogenesis overview. *Biomedicines*. 2018;6(1):6. doi:10.3390/biomedicines6010006
- Kulms D, Schwarz T. Molecular mechanisms of UV-induced apoptosis. *Photoderm Photobiomed Photomed*. 2000;16(5):195–201. doi:10.1034/j.1600-0781.2000.160501.x
- Steele VE. Current mechanistic approaches to the chemoprevention of cancer. *BMB Rep*. 2003;36(1):78–81. doi:10.5483/BMBRep.2003.36.1.078
- Sulaiman H, Hamid R, Ting Y, Othman F. Anti-tumor effect of *Ardisia crispa* hexane fraction on 7, 12-dimethylbenz[a]anthracene-induced mouse skin papillomagenesis. *J Can Res Ther*. 2012;8(3):404. doi:10.4103/0973-1482.103521
- Roy AM, Baliga MS, Katiyar SK. Epigallocatechin-3-gallate induces apoptosis in estrogen receptor-negative human breast carcinoma cells via modulation in protein expression of p53 and Bax and caspase-3 activation. *Mol Cancer Ther*. 2005;4(1):81–90. PMID:15657356.
- Houben R, Hesbacher S, Schmid CP, et al. High-level expression of wild-type p53 in melanoma cells is frequently associated with inactivity in p53 reporter gene assays. *PLoS One*. 2011;6(7):e22096. doi:10.1371/journal.pone.0022096
- Alikhah H, Khodaeiani E, Fakhrjou A, et al. Immunohistochemical evaluation of p53 and Ki67 expression in skin epithelial tumors. *Indian J Dermatol*. 2013;58(3):181. doi:10.4103/0019-5154.110824
- Llambi F, Green DR. Apoptosis and oncogenesis: Give and take in the BCL-2 family. *Curr Opin Genet Dev*. 2011;21(1):12–20. doi:10.1016/j.gde.2010.12.001
- Loro LL, Vintermyr OK, Johannessen AC. Cell death regulation in oral squamous cell carcinoma: Methodological considerations and clinical significance. *J Oral Pathol Med*. 2003;32(3):125–138. doi:10.1034/j.1600-0714.2003.00052.x
- Youle RJ, Strasser A. The BCL-2 protein family: Opposing activities that mediate cell death. *Nat Rev Mol Cell Biol*. 2008;9(1):47–59. doi:10.1038/nrm2308
- Devarajan E, Sahin AA, Chen JS, et al. Down-regulation of caspase 3 in breast cancer: A possible mechanism for chemoresistance. *Oncogene*. 2002;21(57):8843–8851. doi:10.1038/sj.onc.1206044
- Cheng T, Yang I, Irby R, et al. Regulation of caspase expression and apoptosis by *Adenomatous polyposis coli*. *Cancer Res*. 2003;63(15):4368–4374. PMID:12907606.
- Manoharan S, Sindhu G, Nirmal MR, Vetrivel V, Balakrishn S. Protective effect of berberine on expression pattern of apoptotic, cell proliferative, inflammatory and angiogenic markers during 7,12-dimethylbenz(a)anthracene induced hamster buccal pouch carcinogenesis. *Pak J Biol Sci*. 2011;14(20):918–932. doi:10.3923/pjbs.2011.918.932
- Fidyk K, Fiedorowicz A, Strzdała L, Szumny A. β-caryophyllene and β-caryophyllene oxide: Natural compounds of anticancer and analgesic properties. *Cancer Med*. 2016;5(10):3007–3017. doi:10.1002/cam4.816
- Francomano F, Caruso A, Barbarossa A, et al. β-caryophyllene: A sesquiterpene with countless biological properties. *Appl Sci*. 2019;9(24):5420. doi:10.3390/app9245420
- Vidjaya Letchoumy P, Chandra Mohan KVP, Stegeman JJ, Gelboin HV, Hara Y, Nagini S. Pretreatment with black tea polyphenols modulates xenobiotic-metabolizing enzymes in an experimental oral carcinogenesis model. *Oncol Res*. 2008;17(2):75–85. doi:10.3727/096504008784523649
- Esteves F, Rueff J, Kranendonk M. The central role of cytochrome P450 in xenobiotic metabolism: A brief review on a fascinating enzyme family. *J Xenobiot*. 2021;11(3):94–114. doi:10.3390/jox11030007
- Rasik AM, Shukla A. Antioxidant status in delayed healing type of wounds. *Int J Exp Pathol*. 2000;81(4):257–263. doi:10.1046/j.1365-2613.2000.00158.x
- Teegarden MD, Knobloch TJ, Weghorst CM, Cooperstone JL, Peterson DG. Storage conditions modulate the metabolomic profile of a black raspberry nectar with minimal impact on bioactivity. *Food Funct*. 2018;9(9):4593–4601. doi:10.1039/C8FO00639C
- Tiwari P, Sahay S, Pandey M, Qadri SSYH, Gupta KP. Combinatorial chemopreventive effect of butyric acid, nicotinamide and calcium gluconate against the 7,12-dimethylbenz(a)anthracene induced mouse skin tumorigenesis attained by enhancing the induction of intrinsic apoptotic events. *Chem Biol Interact*. 2015;226:1–11. doi:10.1016/j.cbi.2014.11.018
- Fu Q, Zhang F, Vijayalakshmi A. The protective effect of sanggenol L against DMBA-induced hamster buccal pouch carcinogenesis induces apoptosis and inhibits cell proliferative signalling pathway. *Comb Chem High Throughput Screen*. 2024;27(6):885–893. doi:10.2174/1386207326666230726140706
- Kaur R, Arora S. Interactions of betulonic acid with xenobiotic metabolizing and antioxidative enzymes in DMBA-treated Sprague Dawley female rats. *Free Radic Biol Med*. 2013;65:131–142. doi:10.1016/j.freeradbiomed.2013.06.016
- Vijayalakshmi A, Sindhu G. Dose responsive efficacy of umbelliferone on lipid peroxidation, anti-oxidant, and xenobiotic metabolism in DMBA-induced oral carcinogenesis. *Biomed Pharmacother*. 2017;88:852–862. doi:10.1016/j.biopha.2017.01.064

33. Horváth B, Mukhopadhyay P, Kechrid M, et al. β -caryophyllene ameliorates cisplatin-induced nephrotoxicity in a cannabinoid 2 receptor-dependent manner. *Free Radic Biol Med*. 2012;52(8):1325–1333. doi:10.1016/j.freeradbiomed.2012.01.014
34. Tambe Y, Tsujiuchi H, Honda G, Ikeshiro Y, Tanaka S. Gastric cytoprotection of the non-steroidal anti-inflammatory sesquiterpene, β -caryophyllene. *Planta Med*. 1996;62(5):469–470. doi:10.1055/s-2006-957942
35. Chang HJ, Kim HJ, Chun HS. Quantitative structure–activity relationship (QSAR) for neuroprotective activity of terpenoids. *Life Sci*. 2007;80(9):835–841. doi:10.1016/j.lfs.2006.11.009
36. Pfeffer C, Singh A. Apoptosis: A target for anticancer therapy. *Int J Mol Sci*. 2018;19(2):448. doi:10.3390/ijms19020448
37. Williams AB, Schumacher B. p53 in the DNA-damage-repair process. *Cold Spring Harb Perspect Med*. 2016;6(5):a026070. doi:10.1101/cshperspect.a026070
38. Zakariah M, Molele Reneilwe A, Mahdy MAA, Ibrahim MIA, McGaw Lyndy J. Regulation of spermatogenic cell apoptosis by the pro-apoptotic proteins in the testicular tissues of mammalian and avian species. *Animal Reprod Sci*. 2022;247:107158. doi:10.1016/j.anireprosci.2022.107158
39. McIlwain DR, Berger T, Mak TW. Caspase functions in cell death and disease. *Cold Spring Harb Perspect Biol*. 2013;5(4):a008656. doi:10.1101/cshperspect.a008656
40. Surguchov A, Bernal L, Surguchev AA. Phytochemicals as regulators of genes involved in synucleinopathies. *Biomolecules*. 2021;11(5):624. doi:10.3390/biom11050624

Anticancer potential of nerolidol on acute lymphoblastic leukemia cells through the interactions with the NF- κ B/STAT-3 and PI3K/Akt signaling pathways

Xuejiao Wang^{1,A,B,D}, Ke Wang^{2,A-C}, Hengfei Du^{1,A,B,F}

¹ Department of Hematology, Rheumatology and Immunology, The First People's Hospital of Xianyang, China

² Department of Respiratory and Critical Care Medicine, Xidian Group Hospital, Xi'an, China

A – research concept and design; B – collection and/or assembly of data; C – data analysis and interpretation; D – writing the article; E – critical revision of the article; F – final approval of the article

Advances in Clinical and Experimental Medicine, ISSN 1899–5276 (print), ISSN 2451–2680 (online)

Adv Clin Exp Med. 2025;34(9):1553–1564

Address for correspondence

Hengfei Du

E-mail: ll309321560@sina.com

Funding sources

None declared

Conflict of interest

None declared

Received on April 13, 2024

Reviewed on June 5, 2024

Accepted on August 28, 2024

Published online on January 16, 2025

Abstract

Background. Leukemia may form at any age, from newborns to the elderly, and accounts for considerable mortality worldwide.

Objectives. Nerolidol (NRD) is isolated from the aromatic florae oils and was found to have anticancer activities. However, the role of NRD in antiproliferative and apoptosis actions in acute lymphoblastic leukemia (ALL) is unclear.

Materials and methods. Human ALL cell lines, MOLT-4, were used to examine the potential anticancer mechanisms of NRD on cellular proliferation, reactive oxygen species (ROS)-mediated apoptosis, oxidative stress markers, caspases, PI3K/AKT, nuclear factor kappa B (NF- κ B), and STAT-3/VEGF/Bcl-2 signaling pathways.

Results. The MTT (3-(4,5-dimethylthiazolyl)-2,5-diphenyltetrazolium bromide) assay demonstrated that NRD inhibited MOLT-4 cell proliferation in a concentration-dependent manner, with an IC₅₀ value of 30 μ M. It was found that NRD (20 and 30 μ M/mL) resulted in accumulated intracellular ROS, reduced oxidative stress and loss of mitochondrial membrane potential (MMP) in MOLT-4 cells in a concentration-related way. Nerolidol was able to induce apoptosis, as evidenced by dual acridine orange/ethidium bromide (AO/EB) staining. The levels of antioxidants, caspases-3, -8 and -9 were enhanced by NRD. This research proves that NRD instantaneously triggers ROS-mediated pro-apoptotic signaling and caspases and attenuates PI3K/Akt/NF- κ B and STAT3/VEGF/Bcl-2 anti-apoptotic signaling.

Conclusions. Our results suggest that NRD treatment stimulates apoptosis in MOLT-4 cells by causing the accumulation of intracellular ROS through PI3K/AKT/STAT-3 signaling pathways.

Key words: proliferation, apoptosis, blood cancer, nerolidol, PI3K/AKT/NF- κ B signaling

Cite as

Wang X, Wang K, Du H. Anticancer potential of nerolidol on acute lymphoblastic leukemia cells through the interactions with the NF- κ B/STAT-3 and PI3K/Akt signaling pathways. *Adv Clin Exp Med.* 2025;34(9):1553–1564. doi:10.17219/acem/192695

DOI

10.17219/acem/192695

Copyright

Copyright by Author(s)

This is an article distributed under the terms of the Creative Commons Attribution 3.0 Unported (CC BY 3.0) (<https://creativecommons.org/licenses/by/3.0/>)

Background

Leukemia is the heterogeneous assembly of hematopoietic cells that transform to form a malignant neoplasm,¹ which is the principal source of tumor-related death in patients under 20 years of age.² According to the GLOBOCAN 2018 statistics, 437,033 new leukemia cases and 309,006 leukemia deaths were recorded.³ Contact with environmental radiation and exposure to extreme radiation levels are recognized as leukemia risk factors.⁴ Leukemia can develop at any age, from newborns to the elderly, and accounts for considerable mortality worldwide. Among these, acute lymphoblastic leukemia (ALL) commonly affects infants.⁵ In the USA, nearly 6,000 newly diagnosed cases of ALL subtypes are detected annually,¹ while the curative rate is almost $\geq 80\%$.⁶ Despite the high remedial rate, disease resistance and degeneration remain the foremost cause of tumor-related deaths in progenies. Additionally, the ALL cure ratio in adults is $\sim 50\%$, which is relatively poor.⁷ Although current treatments such as stem cell transplantation and chemotherapy are emerging quickly, deterioration and medicine-associated obstacles are still endured by patients.^{8,9} Another major difficulty is the progression of multi-drug resistance in these patients.¹⁰ Thus, innovative anti-leukemic medications and optimizing dominant chemotherapeutic usages are essential to rapid the diagnosis and enhancing patients' quality of life in ALL.¹¹ Hence, new therapeutic strategies are urgently required.

Epigenetics refers to the heritable changes in gene function with no alterations in DNA sequences, consisting of DNA methylation, histone modification and nucleosome remodeling, among others. Epigenetic modifications play a key role in regulating DNA-based processes. During the past few decades, epigenetic modifications were found to play a significant role in the occurrence and development of leukemia and were considered a promising target for treating different types of leukemia and other hematological malignancies, and sound clinical effects have been achieved.¹²

Several naturally occurring phytochemicals have been identified due to evidence of their anticancer properties, and they are considered possible therapeutics for regulating various malignant cells by inhibiting multiplication, incursion and metastasis.¹³ Nerolidol (NRD) is isolated from the aromatic florae as essential oil and identified as a sesquiterpene alcohol.¹⁴ It has numerous pharmacological properties, including anticancer, apoptotic, anti-oxidative, and anti-inflammatory effects.¹⁵ Recently, NRD has been revealed to alleviate inflammation, oxidative stress and apoptosis in cyclophosphamide-induced cardiotoxicity.¹⁶ It has also been documented that NRD blocked the inflammatory reaction in lipopolysaccharide (LPS)-stimulated acute lung injury by the elevation of antioxidants and AMPK/Nrf-2/(HO)-1 signaling.¹⁷ Furthermore, NRD has been demonstrated to be valuable as an anticancer complex, owing to its efficiency in suppressing proliferation

and targeting cell survival¹⁸; it acts as a chemosensitizer in many malignancies.^{19,20} Nerolidol was shown to improve the efficacy of doxorubicin (DOX) in breast carcinogenesis¹⁹ and enhance its effectiveness in lymphoblast and ovarian carcinoma cells.²¹ Nevertheless, to the best of our knowledge, the anticancer and apoptotic activities of NRD in ALL cells MOLT-4 have not yet been reported.

Apoptosis is an active cell death program that occurs in normal physiological and pathological environments. It has been established that triggering apoptotic cell death is a highly beneficial approach by which anti-tumor compounds can target malignant cells.²² Chemotherapeutic mediators may stimulate apoptotic signaling via 2 crucial pathways: an intrinsic mitochondrial-facilitated pathway and a death receptor-facilitated extrinsic pathway. An intrinsic cascade is activated by specific molecules, ultimately inducing downstream caspase-3 stimulation, which is one of the vital apoptotic mediators.²³ Caspases are a series of cysteine proteases that play a critical part in the molecular pathways of cell death.²⁴ A set of oxygen-containing chemicals comprise reactive oxygen species (ROS), generally produced from the mitochondria.^{25,26} Tumor cells usually accumulate more ROS than typical cells.²⁷ Reactive oxygen species-stimulated apoptosis is greatly dependent on the triggering of pro-apoptotic signaling pathways such as PI3K/AKT, STAT-3, NF- κ B, and MAPKs. The NF- κ B is a well-known chemo-resistance-related anti-apoptotic factor.²⁸ Acute lymphoblastic leukemia cells' elevated constitutive NF- κ B activity caused anti-apoptosis and inflammation.²⁹ Therefore, regulation of NF- κ B is a strong molecular target for therapeutics. Trials have revealed cellular communications relating to ROS and NF- κ B.²⁸ While ROS might activate the tumor cell apoptosis, the ROS-prompted anti-apoptotic component, NF- κ B, can reduce the apoptotic activity of ROS. PI3K/Akt is the most activated network, observed in 70–85% of ALL patients.³⁰ Dysregulation of PI3K/Akt signaling is a major event occurring in both T-cell and B-cell ALL, resulting in increased proliferation, survival and drug resistance.³¹ Due to the significant physiological communication between STAT-3, Bcl-2 and PI3K/Akt networks in acute leukemia, these signaling networks are strong targets for collective inhibition.^{32,33} The vascular endothelial growth factor (VEGF) protein family has been implicated in vascular angiogenesis regulation.³⁴ More importantly, increasing evidence has established that aberrant regulation of VEGF signaling triggering stimulation of the PI3K/Akt pathway is connected to the poor prognosis in ALL.³⁵ Hence, identifying medications that can concurrently trigger persistent ROS-facilitated pro-apoptotic signaling and inhibit PI3K/Akt/NF- κ B and STAT3/VEGF/Bcl-2 activities may advance cancer chemotherapy.

Even though NRD has been described as having anti-tumorigenesis activities in numerous human malignant cell lines, its anticancer benefits on blood cancer have barely been researched. However, the possible use of NRD

in anti-tumor therapy in ALL cells is relatively unexplored, especially in MOLT-4 cells. Therefore, the current work is focused on assessing NRD for inhibiting cell multiplication and stimulating apoptosis in the ALL cell line, MOLT-4.

Objectives

This research aimed to demonstrate that NRD instantaneously triggers ROS-mediated pro-apoptotic signaling and caspases and attenuates PI3K/Akt/NF- κ B and STAT3/VEGF/Bcl-2 anti-apoptotic signaling.

Materials and methods

Reagents and chemicals

Nerolidol (NRD), Dulbecco's modified Eagle's medium (DMEM), antibiotics, fetal bovine serum (FBS), phosphate-buffered saline (PBS), 3-(4,5-dimethylthiazol-2-yl)-2,5-diphenyltetrazolium bromide (MTT), dimethyl sulfoxide (DMSO), Rhodamine-123 (Rh-123), sodium dodecyl sulfate (SDS), acridine orange/ethidium bromide (AO/EB), and 2'-7'-dichlorodihydrofluorescein diacetate (DCFH-DA) were obtained from Ruicong Ltd (Shanghai, China). The primary and secondary antibodies were acquired from Elabscience Biotechnology (Wuhan, China).

Culturing of MOLT-4 cells

Human blood cancer MOLT-4 cells were procured from the German Collection of Microorganisms and Cell Cultures ((DSMZ); Braunschweig, Germany). They were matured and maintained in DMEM, with the addition of antibiotics (100 U/mL) and FBS (10%), at 37°C, 5% CO₂ atmosphere and less than 95% humidified air.

Cell cytotoxicity assay

Using the MTT test, the effect of NRD on MOLT-4 cells was measured³⁶ and was used to determine cell proliferation. MOLT-4 cells were sown at 6×10^3 cells/well in 96-well plates kept overnight in DMEM media. Treated cells were given various doses of NRD (5–50 μ M/mL) at 37°C. A volume of 20 μ L of MTT was administered to an individual well and kept at 37°C for 4 h to permit the MTT conversion into formazan insoluble crystals through mitochondrial dehydrogenase. The subsequent formazan crystals were softened by adding 150 μ L DMSO to the culture media. Each experiment was repeated thrice, and cells grown in a culture medium containing DMSO were used as a control. To assess cell proliferation, the optical density (OD) was determined at 570 nm employing a microplate reader (Pope Scientific, Inc, Saukville, USA). Cell proliferation was determined as the ratio of cell viability against

untreated MOLT-4 cells (100%). The IC₅₀ (drug concentration that caused a 50% reduction in MTT assay) was determined.

Measurement of intracellular level ROS

The level of ROS was determined with the DCFH-DA staining method.³⁷ Blood cancer cells, MOLT-4, were seeded in 6 culture dishes each and maintained for 24 h, and various concentrations of NRD (control and 20 and 30 μ M/mL) were administered. Following this, all groups were stained with DCFH-DA (10 μ M) and subsequently kept at 37°C. Treated cells were gathered and then cleaned twice with ice-cold PBS to remove extra dye. The fluorescence was measured by excitation at 485 ± 10 and emission at 530 ± 12.50 nm, compatible with a multimode reader (PerkinElmer EnVision; PerkinElmer, Waltham, USA).

Analysis of mitochondrial membrane potential

The mitochondrial membrane potential (MMP) was estimated to understand early apoptotic phases by conducting Rh-123 staining.³⁷ Human ALL adult cells, MOLT-4, were seeded in 6 wells and sustained with CO₂ (5%) at 37°C in a humidified CO₂ incubator for 24 h. Subsequently, MOLT-4 cells were exposed to a control solution and 20 and 30 μ M of NRD for 1 day, wet twice with cold PBS, fixed with paraformaldehyde (4%) for 20 min and swabbed. Successively, all groups were stained with Rh-123 (10 μ g/mL) in darkness at 37°C for 30 min. Following this, they were washed twice with washing buffer to remove any extra stain, and the MMP difference was determined using fluorescent microscopy (Nikon Eclipse TS100; Nikon Corp., Tokyo, Japan). The intensity of fluorescence in the captured images was examined using ImageJ v. 1.48 software (National Institutes of Health (NIH), Bethesda, USA).

Evaluation of apoptosis demonstrated by AO/EB staining

Morphological and nuclear changes were assessed in MOLT-4 human ALL cells, to which NRD was added, and were distinguished by staining with AO/EB.³⁷ MOLT-4 cells were supplemented with control and NRD (20 and 30 μ M/mL) conditions and sustained for 24 h. All groups were administered the dye mixture of AO/EB (100 μ g/mL per each). Treated cells were maintained in the dark for 20 min, ensuring unbound dye was eliminated by washing with PBS and viewing through a fluorescence microscope (Nikon Eclipse TS100; Nikon Corp.).

Analysis of oxidative stress markers

The oxidative stress markers assessed were glutathione (GSH), catalase (CAT), superoxide dismutase (SOD), and

thiobarbituric acid reactive substances (TBARS), using assay kits provided by Biomed (Badr City, Egypt).

Measurement of caspase -3, -9 and -8

The activity of the caspases caspase-3 (cat. No. 32203), caspase-9 (cat. No. 13915) and caspase-8 (cat. No. 13913) was determined with an enzyme-linked immunosorbent assay (ELISA) kit procured from Cayman Chemical (Ann Arbor, USA). These experiments were conducted according to the manufacturer's protocol, and 3 independent replicates were carried out.

Estimation of mRNA levels using quantitative reverse transcription polymerase chain reaction

Total RNA was isolated from human ALL cells, MOLT-4, according to the procedures indicated for TRIzol® reagent (Bio-Rad, Hercules, USA). The isolated RNA was reverse transcribed into cDNA using the High-Capacity cDNA Reverse Transcription kit (Thermo Fisher Scientific, Waltham, USA) following the kit protocols. Next, the Fast Start SYBR Green master mix (Bio-Rad) was used to investigate the cDNAs according to the company's protocols. The samples were subjected to electrophoresis, and the resulting band intensities were measured using ImageJ v. 1.48 software (National Institutes of Health (NIH), Bethesda, USA). Fold conversions for the individual gene expressions were determined using a comparative threshold cycle (Ct) method, according to the formula $2^{-(\Delta\Delta Ct)}$. The series of primers for using quantitative reverse transcription polymerase chain reaction (RT-qPCR) were as follows:

TNF- α F: 5'-CTTCTGCCTGCTG CACTTTGGA-3'
R: 5'-TCCCAAAGTAGACCTGCCAG-3'
NF- κ B F: 5'-GCAAAGGGAACATTCCGATAT-3'
R: 5'-GCGACATCACATGGAAATCTA-3'
COX-2 F: 5'-CCGGGTACAATCGCACTTAT-3'
R: 5'-GGCGCTCAGCCATACAG-3'
IL-6 F: 5'-GACTGATGTTGTTGACAGCCACTGC-3'
R: 5'-TAGCCACTCCTTCTGTGACTCTAACT-3'
GAPDH F: 5'-CTTCTTTTTCGTC GCCAGCCGA-3'
R: 5'-ACCAGGCGCCCAATACGACCAA-3'

Western blot study

The human blood cancer cells, MOLT-4, were given NRD (control and 20 and 30 μ M/mL) and grown for

1 day. The cell lysates were prepared with ice-cold lysis buffer, including protease inhibitors, and a western blot experiment was carried out. The measurement of protein was performed using a Protein BCA Assay Kit (Pierce Chemical Co, Rockford, USA). Briefly, the proteins were electrophoretically dispersed and relocated to a polyvinylidene difluoride (PVDF) film. Then, the film was blocked using a probe overnight at 4°C, and primary antibodies were administered in 1:1,000 dilutions, preserved overnight at 4°C; secondary antibodies (1:5,000) were subsequently added. Beta-actin was employed as an internal control. After introducing the specific antibodies, the proteins were visualized with an LI-COR Odyssey imaging system (LI-COR, Belfast, UK).

Statistical analyses

The statistical analysis of data from each group was conducted using GraphPad Prism v. 8.0.2 (GraphPad Software, San Diego, USA) and IBM SPSS software v. 25 (IBM Corp., Armonk, USA). Data are presented as the median (min–max). As the sample size was too small to verify normal data distribution, the differences between the groups were analyzed using the nonparametric Kruskal–Wallis test with Dunn's post hoc test. Subsequently, significant differences among multiple groups were examined using the Kruskal–Wallis test, and Dunn's post hoc test was employed for multiple comparisons. Dunn's post hoc test was employed for multiple comparisons to control for the false positive rate due to multiple testing. Dunn's test adjusts the significance levels to account for multiple comparisons, ensuring the control of type I error rates across the 16 comparisons. A statistically notable data divergence was considered when $p < 0.05$. All tests in this study were bilateral.

Results

The results of the Kruskal–Wallis test and Dunn's post hoc test are presented in Table 1–3.

Cytotoxicity effect of NRD on human ALL cells

The MTT test estimated human MOLT-4 cell proliferation at various quantities (control, 5, 10, 20, 30, 40, and 50 μ M/mL) of NRD (Table 1, Fig. 1A). It was revealed that NRD had antiproliferative effects on MOLT-4 cells

Table 1. Comparison of the study groups

Variables	Control	5 μ M	10 μ M	20 μ M	30 μ M	40 μ M	50 μ M	test value (H)**	p-value*
MTT	98.95 (90.00–107.80)	89.99 (81.85–98.05)	76.84 (69.89–83.71)	63.75 (57.99–69.45)	51.65 (46.98–56.28)	38.42 (34.94–41.86)	25.31 (23.02–27.58)	39.51	<0.001

Data was presented as median (min–max); *p-value was generated using the Kruskal–Wallis test; **degrees of freedom (df) is equal to 5.

Table 2. Comparison of the study groups

Variables	Control (n = 6)	20 μ M (n = 6)	25 μ M (n = 6)	test value (H)**	p-value*
SOD	29.54 (26.87–32.19)	15.92 (14.48–17.34)	11.07 (10.07–12.07)	13.66	0.001
CAT	23.16 (21.07–25.23)	14.90 (13.56–16.24)	7.12 (6.48–7.76)	15.15	0.001
GSH	21.65 (19.69–23.59)	12.75 (11.60–13.90)	0.93 (0.85–1.01)	13.66	0.001
TBARS	6.10 (5.55–6.65)	29.38 (26.73–32.01)	45.12 (41.04–49.16)	15.20	<0.001
Caspase-9	100.05 (91.00–109.00)	135.79 (123.51–147.93)	152.87 (139.05–166.55)	15.26	<0.001
Caspase-8	100.05 (91.00–109.00)	141.32 (128.54–153.96)	169.45 (154.13–184.61)	15.20	<0.001
Caspase-3	100.05 (91.00–109.00)	150.17 (136.59–163.61)	175.30 (159.44–190.98)	15.20	<0.001
TNF- α	100.05 (91.00–109.00)	0.63 (0.57–0.69)	0.42 (0.38–0.46)	15.15	0.001
NF- κ B	100.05 (91.00–109.00)	0.70 (0.64–0.76)	0.48 (0.44–0.52)	15.15	0.001
COX-2	100.05 (91.00–109.00)	0.68 (0.62–0.74)	0.39 (0.35–0.43)	15.17	0.001
IL-6	100.05 (91.00–109.00)	0.75 (0.68–0.82)	0.53 (0.48–0.58)	15.15	0.001
p-PI3K/PI3K	1.00 (0.91–1.09)	0.73 (0.66–0.80)	0.45 (0.41–0.49)	15.23	<0.001
p-AKT/AKT	1.00 (0.91–1.09)	0.80 (0.73–0.87)	0.52 (0.47–0.57)	15.22	<0.001
p-STAT3/STAT3	1.00 (0.91–1.09)	0.69 (0.63–0.75)	0.44 (0.40–0.48)	15.26	<0.001
VEGF	1.00 (0.91–1.09)	0.58 (0.53–0.63)	0.39 (0.35–0.43)	15.23	<0.001
Bcl-2	1.00 (0.91–1.09)	0.74 (0.67–0.81)	0.53 (0.48–0.58)	15.20	<0.001

Data were presented as median (min–max); *The p-value was generated using the Kruskal–Wallis test; **Degrees of freedom (df) is equal to 2. Dunn's post hoc test was employed for multiple comparisons to control for the false-positive rate due to multiple testing. Dunn's test adjusts the significance levels to account for multiple comparisons, ensuring the control of type I error rates across the 16 comparisons made.

SOD – superoxide dismutase; CAT – catalase; GPx – glutathione peroxidase; TBARS – thiobarbituric acid reactive substances; TNF- α – tumor necrosis factor alpha; NF- κ B – necrosis factor kappa B; COX-2 – cyclooxygenase; IL-6 – interleukin 6; PI3K – phosphoinositide 3-kinase; Akt – protein kinase B; VEGF – vascular endothelial growth factor; Bcl-2 – B-cell lymphoma 2.

Table 3. The results of the Dunn's post hoc test

Explained variable	C vs 20 μ M	C vs 25 μ M	20 μ M vs 25 μ M
SOD	0.155	p < 0.001	0.155
CAT	0.155	p < 0.001	0.155
GSH	0.154	p < 0.001	0.154
TBARS	0.155	p < 0.001	0.155
Caspase-9	0.092	p = 0.001	0.390
Caspase-8	0.155	p < 0.001	0.155
Caspase-3	0.092	p = 0.001	0.390
TNF- α	0.154	p < 0.001	0.154
NF- κ B	0.152	p < 0.001	0.152
COX-2	0.154	p < 0.001	0.154
IL-6	0.154	p < 0.001	0.154
p-PI3K/PI3K	0.153	p < 0.001	0.153
p-AKT/AKT	0.153	p < 0.001	0.153
p-STAT3/STAT3	0.152	p < 0.001	0.152
VEGF	0.153	p < 0.001	0.153
Bcl-2	0.154	p < 0.001	0.154

SOD – superoxide dismutase; CAT – catalase; GPx – glutathione peroxidase; TBARS – thiobarbituric acid reactive substances; TNF- α – tumor necrosis factor alpha; NF- κ B – necrosis factor kappa B; COX-2 – cyclooxygenase; IL-6 – interleukin 6; PI3K – phosphoinositide 3-kinase; Akt – protein kinase B; VEGF – vascular endothelial growth factor; Bcl-2 – B-cell lymphoma 2.

in a concentration-dependent manner. Untreated control cells did not exhibit altered MOLT-4 cell proliferation and showed 100% viability. However, NRD at dosages of 10, 20

and 30 μ M/mL considerably (p < 0.05) inhibited the viability of MOLT-4 cells compared to control. Viability was extremely inhibited by the administration of a high dosage of NRD (40 and 50 μ M/mL). From the MTT test, the IC₅₀ value was determined to be 30 μ M for MOLT-4 cells. To avoid the destruction caused by high dosages of NRD in ALL cells, we added various dosages of NRD to the MOLT-4 cells, assessing their sensitivity to NRD administration. Based on data from the IC₅₀ value of NRD (20 and 30 μ M/mL), we opted for further experiments. The MOLT-4 human ALL cells' morphological variations were detected with a phase-contrast microscope (Nikon Eclipse TS100; Nikon Corp.) in the bright field. Administration of 20 μ M NRD resulted in a substantial loss of cell viability and morphological modifications, and augmented morphological changes were observed with higher amounts of NRD. The IC₅₀ value of 30 μ M NRD reduced cell proliferation and additional morphological modifications of MOLT-4 cells (Fig. 1B).

Influence of NRD-induced intracellular ROS generation in MOLT-4 cells

The formation of ROS in cells is related to different stimuli and can induce apoptosis and block the cell cycle (Fig. 2A). To assess ROS accumulation, DCFH-DA-labeled MOLT-4 cells were examined with a fluorescence microscope (Nikon Eclipse TS100). High-intensity green fluorescence correlated with the level of ROS. Administration of NRD (20 μ M/mL) in MOLT-4 cells resulted in a weak

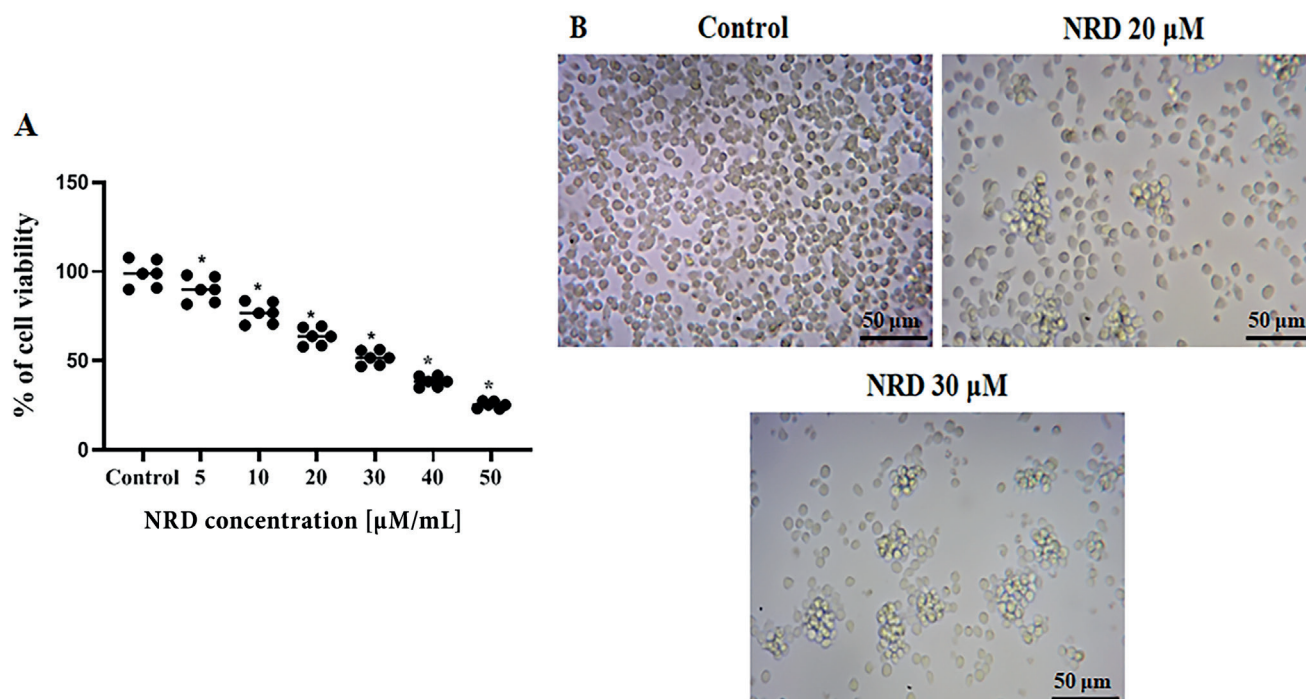


Fig. 1. Nerolidol inhibits human ALL cell proliferation. A. MOLT-4 human ALL cells were added with various quantities (5–50 $\mu\text{M/mL}$) of NRD for 24 h. An MTT experiment measured cell viability. Results are presented as median (min–max) for triplicate assays. The significance is reflected as * $p < 0.05$ against control; B. Effect of NRD on MOLT-4 cell morphological variations analyzed using phase-contrast microscopy

ALL – acute lymphoblastic leukemia; NRD – nerolidol; MTT – 3-(4,5-dimethylthiazol-2-yl)-2,5-diphenyltetrazolium bromide.

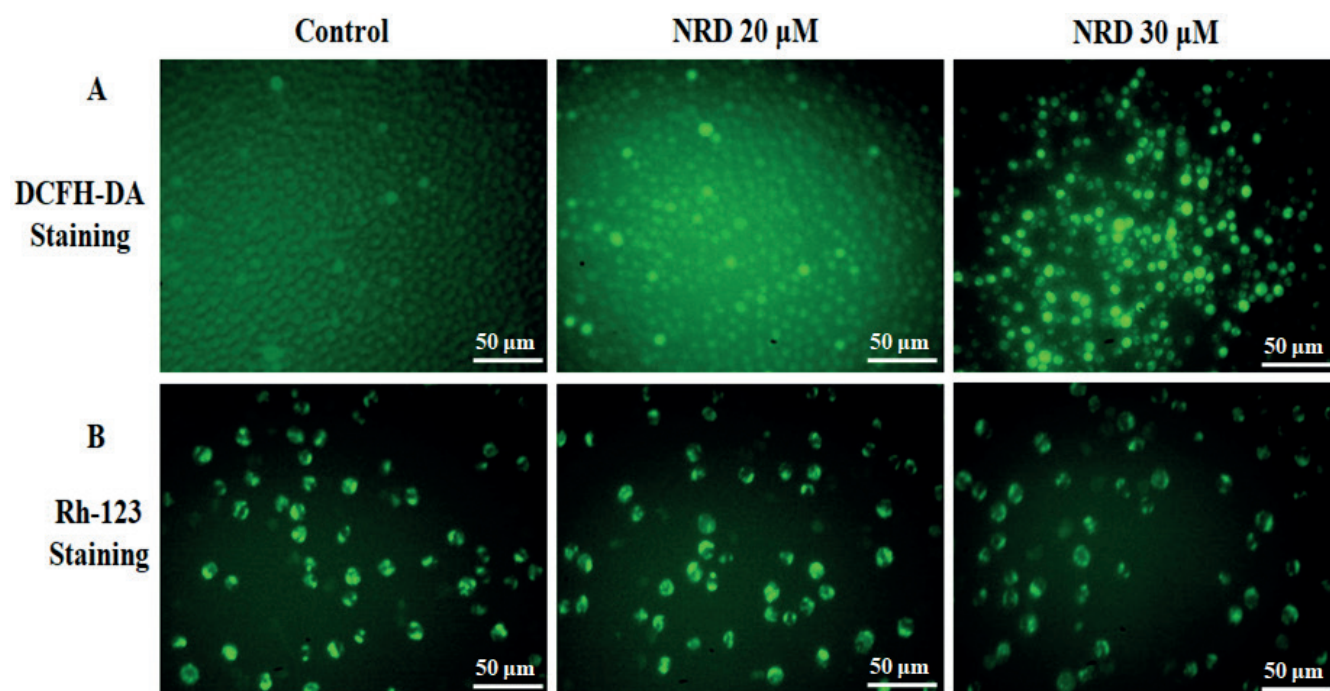


Fig. 2. Nerolidol increases the accumulation of reactive oxygen species (ROS) and depolarization of mitochondrial membrane potential (MMP) in MOLT-4 cells. Human acute lymphoblastic leukemia (ALL) cells were administered nerolidol (NRD) (20 and 30 $\mu\text{M/mL}$) for 24 h. A. The accumulation of 2'-7'-dichlorodihydrofluorescein diacetate (DCFH-DA) fluorescence is depicted using an inverted fluorescence microscope; B. Apoptotic action of NRD was assessed as MMP deviation using fluorescent microscopy employing a 485–530 nm blue filter

fluorescent background, whereas NRD (30 $\mu\text{M/mL}$) treatment resulted in bright green fluorescence, which signified an elevated ROS level. The formation of ROS

in the MOLT-4 human ALL cells was very low, while the level of ROS increased in the NRD-supplemented (20 and 30 $\mu\text{M/mL}$) groups in a concentration-dependent

manner. Treatment with 30 μ M NRD significantly ($p < 0.05$) enhanced ROS generation in MOLT-4 cells compared to control and 20 μ M NRD.

Nerolidol stimulated the loss of MMP in human ALL cells

The MMP depolarization was assessed measuring the cell's ability to take up Rh-123 dye (Fig. 2B). MOLT-4 human acute lymphoblastic leukemia control cells presented high Rh-123 intensity, depicted as green fluorescence and almost 99% MMP. Rh-123 fluorescence accumulation was reduced to a weak green fluorescence signal in NRD-treated (20 and 30 μ M/mL) MOLT-4 cells in a dosage-related manner. Nerolidol (30 μ M) supplemented with MOLT-4 cells resulted in an extensive increase ($p < 0.05$) in MMP loss due to strengthened mitochondrial depolarization.

Nerolidol-triggered apoptosis in human ALL cells as demonstrated with AO/EB staining

Apoptotic cells were revealed due to the unique morphological changes identified using AO/EB dual staining (Fig. 3). Human MOLT-4 cells were visible as homogeneously dyed green live cells. Nerolidol (20 and 30 μ M/mL) supplementation increased cell apoptosis dose-dependently. When intercalated into dsDNA, AO is collected by both viable and non-viable cells and exhibits green fluorescence, whereas EB only accumulates in non-viable cells, where it intercalates into DNA to produce red fluorescence. Therefore, early apoptotic cells have green-fluorescent nucleus with dense green spots where chromatin is condensing, in contrast with the shorter or fragmented orange chromatin. Early apoptotic cells showed abridged chromatin and membrane blebbing with 20 μ M NRD administration, which appeared as pale greenish-yellow marks. Late apoptotic cells exhibited an orange

color, indicating a decrease in their membrane integrity owing to the ethidium bromide co-stain in 30 μ M NRD-administered MOLT-4 cells.

Nerolidol enhances antioxidant status and reduces lipid peroxidation

To observe the influence of NRD on oxidative stress, we analyzed the antioxidant status and lipid peroxidation levels in MOLT-4 cells. Human MOLT-4 cells showed elevated levels of TBARS with decreased SOD, CAT and GSH compared to NRD-treated cells. However, the antioxidant status and lipid peroxidation levels were reversed by the administration of NRD. Treatment with NRD (20 and 30 μ M/mL) significantly reduced ($p < 0.05$) the intensity of TBARS, whereas SOD, CAT and GSH increased compared to control dose-dependently (Table 2,3 and Fig. 4).

Measurement of caspase -3, -8 and -9 activities with ELISA

MOLT-4 cells administered NRD showed elevated activity of caspase-3, -8 and -9 when compared to untreated control cells (Table 2,3 and Fig. 5). Nerolidol (30 μ M) significantly ($p < 0.05$) enhanced the caspase protein levels compared to 20 μ M NRD-treated MOLT-4 cells. These results reveal that NRD stimulated the pro-apoptotic markers, such as caspase proteins, in MOLT-4 cells.

Influence of NRD on the mRNA expression of anti-apoptotic inflammatory cytokines

Figure 6 depicts the influence of NRD on the mRNA level of anti-apoptotic pro-inflammatory mediators in human ALL cells (Table 2,3). MOLT-4 cells exhibited upregulated tumor necrosis factor alpha (TNF- α), nuclear factor kappa B (NF- κ B), interleukin 6 (IL-6), and cyclooxygenase-2 (COX-2) mRNA levels. Nerolidol (20 and 30 μ M/mL)

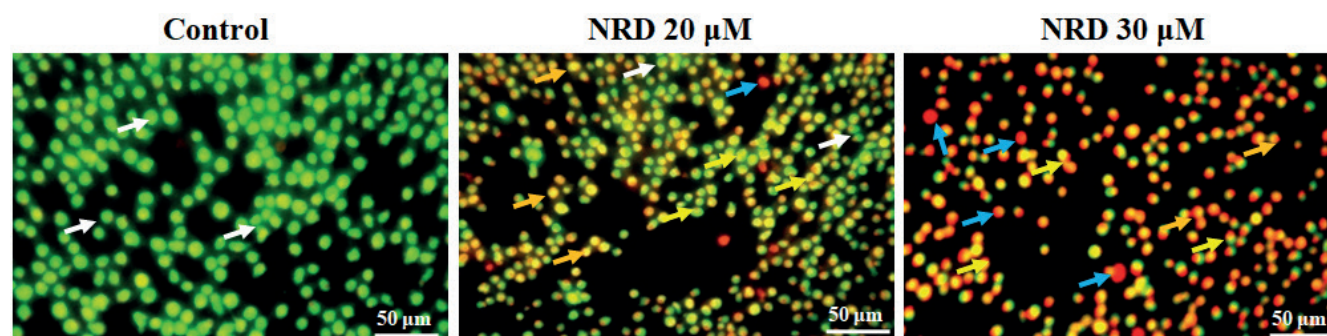


Fig. 3. Nerolidol triggered apoptosis in MOLT-4 cells demonstrated using AO/EB staining. MOLT-4 cells are shown treated under control and with NRD conditions at different concentrations (20–30 μ M/mL) at 24 h, stained with AO/EB. The white arrow indicates green fluorescence, the orange arrow indicates apoptotic bodies, the blue arrow indicates apoptotic cells, and the yellow arrow indicates necrotic cells. Nerolidol induced apoptosis by generating ROS and disrupting MMP

AO/EB – acridine orange/ethidium bromide; NRD – nerolidol; MMP – mitochondrial membrane potential; ROS – reactive oxygen species.

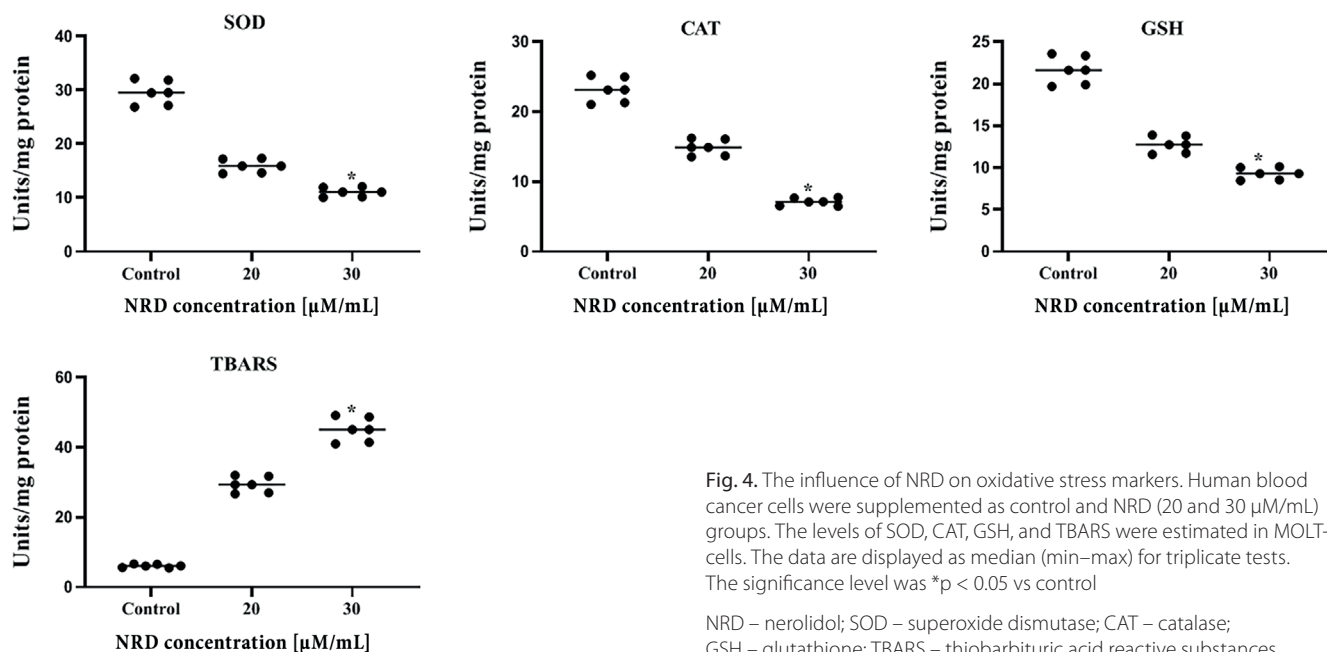


Fig. 4. The influence of NRD on oxidative stress markers. Human blood cancer cells were supplemented as control and NRD (20 and 30 μM/mL) groups. The levels of SOD, CAT, GSH, and TBARS were estimated in MOLT-4 cells. The data are displayed as median (min–max) for triplicate tests. The significance level was * $p < 0.05$ vs control

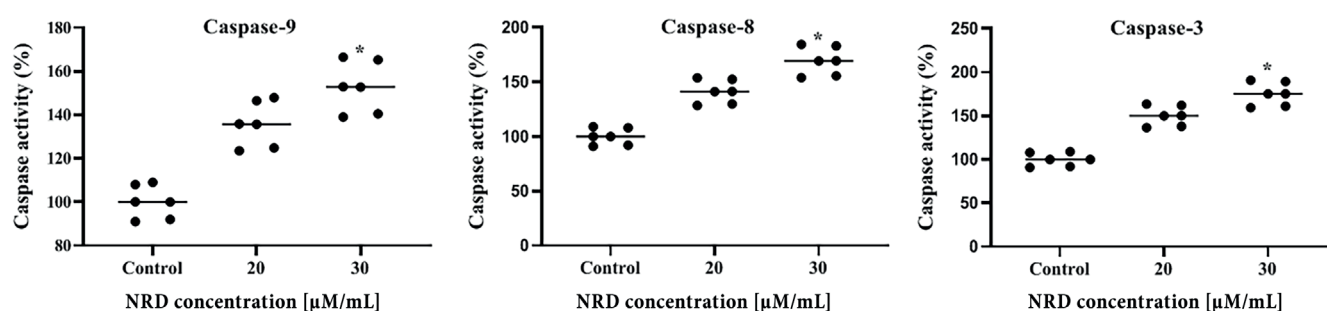


Fig. 5. The influence of NRD on caspase-3, -8 and -9 levels. Human blood cancer cells were supplemented as control and NRD (20 and 30 μM/mL) groups. The levels of caspase-3, -8 and -9 were assessed using ELISA. The data are displayed as median (min–max) for triplicate tests. The significance is shown as * $p < 0.05$ vs control

NRD – nerolidol; ELISA – enzyme-linked immunosorbent assay.

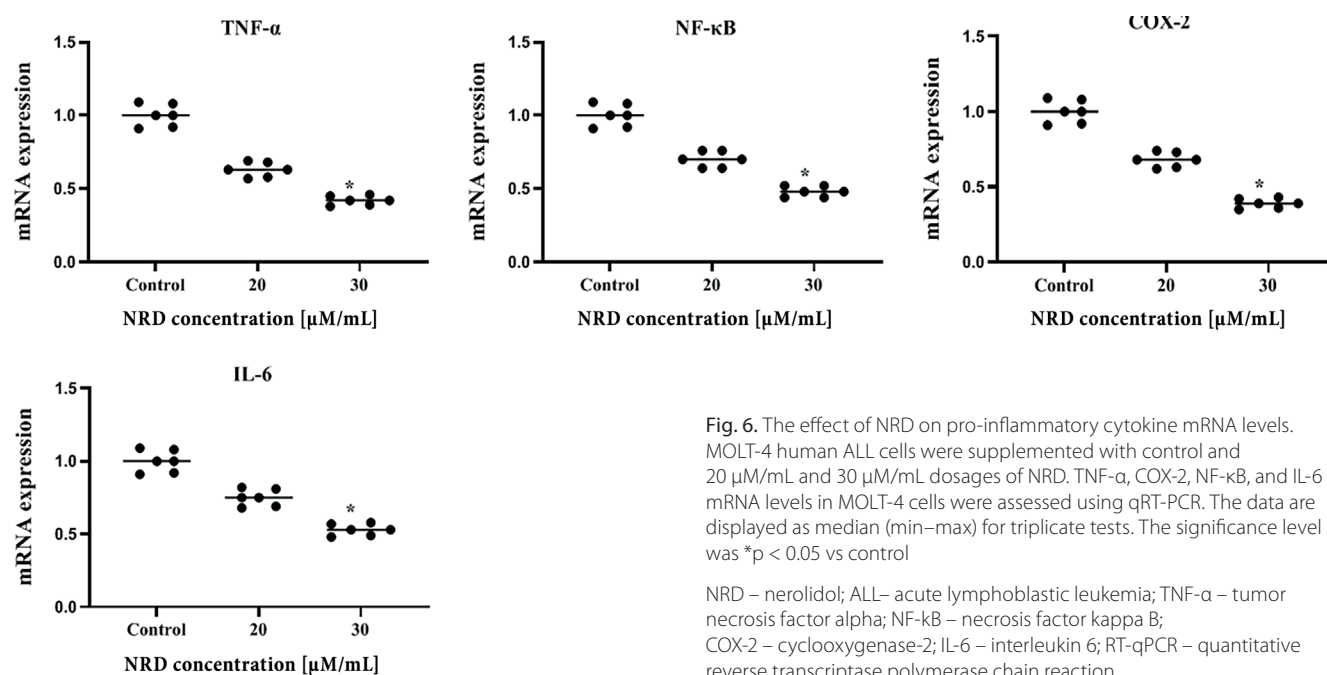


Fig. 6. The effect of NRD on pro-inflammatory cytokine mRNA levels. MOLT-4 human ALL cells were supplemented with control and 20 μM/mL and 30 μM/mL dosages of NRD. TNF-α, COX-2, NF-κB, and IL-6 mRNA levels in MOLT-4 cells were assessed using qRT-PCR. The data are displayed as median (min–max) for triplicate tests. The significance level was * $p < 0.05$ vs control

NRD – nerolidol; ALL – acute lymphoblastic leukemia; TNF-α – tumor necrosis factor alpha; NF-κB – necrosis factor kappa B; COX-2 – cyclooxygenase-2; IL-6 – interleukin 6; RT-qPCR – quantitative reverse transcriptase polymerase chain reaction.

treated-MOLT-4 cells significantly ($p < 0.05$) attenuated the levels of these cytokines dose-dependently. These results suggest that NF- κ B inhibition is involved in NRD-triggered MOLT-4 cell growth inhibition.

Effect of NRD on the PI3K/AKT pathway

Administration of NRD (20 and 30 μ M/mL) resulted in dose-dependent downregulation of phosphorylated PI3K and AKT protein expression compared to untreated controls (Table 2,3 and Fig. 7). MOLT-4 human ALL cells treated with NRD showed reduced p-PI3K, PI3K, p-AKT, and AKT protein expression; thus, NRD induced apoptosis in MOLT-4 cells through inhibition of PI3K/AKT signaling.

Influence of NRD on STAT-3/VEGF/Bcl-2 protein levels

Administration of NRD (20 and 30 μ M/mL) resulted in dose-dependent downregulation of phosphorylated STAT-3 as well as VEGF and Bcl-2 protein expression levels compared to untreated controls (Table 2,3 and Fig. 8). MOLT-4 human ALL cells treated with NRD attenuated p-STAT-3, VEGF and Bcl-2 protein expression, showing that NRD induced apoptosis and inhibited proliferation and angiogenesis in MOLT-4 cells through the suppression of STAT-3/VEGF/Bcl-2 signaling.

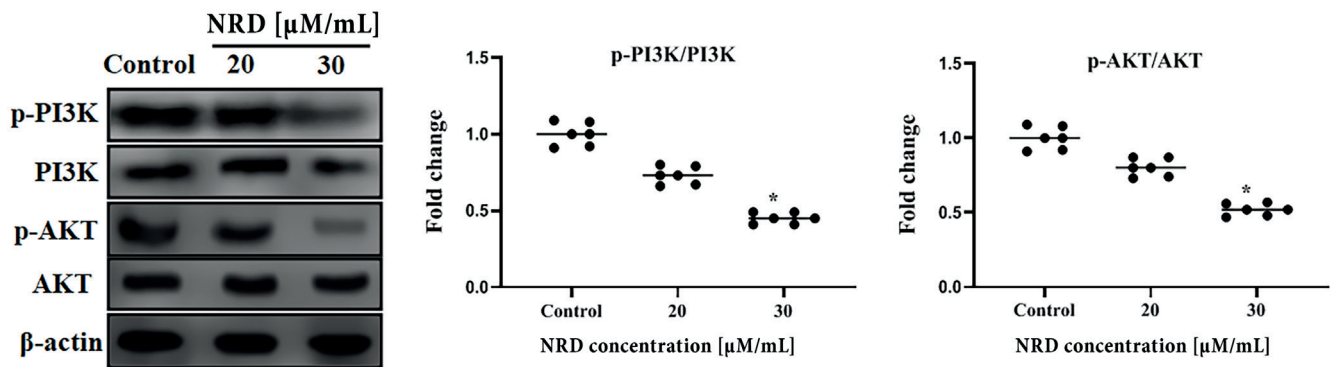


Fig. 7. The influence of NRD on PI3K/AKT pathway. MOLT-4 human ALL cells were administered NRD (20 and 30 μ M/mL) for 24 h. p-PI3K, PI3K, p-AKT, and AKT protein expression levels were examined using western blot. The data are presented as median (min–max) for triplicate tests. The significance is shown as * $p < 0.05$ vs control

NRD – nerolidol; PI3K – phosphoinositide 3 kinase; Akt – protein kinase B.

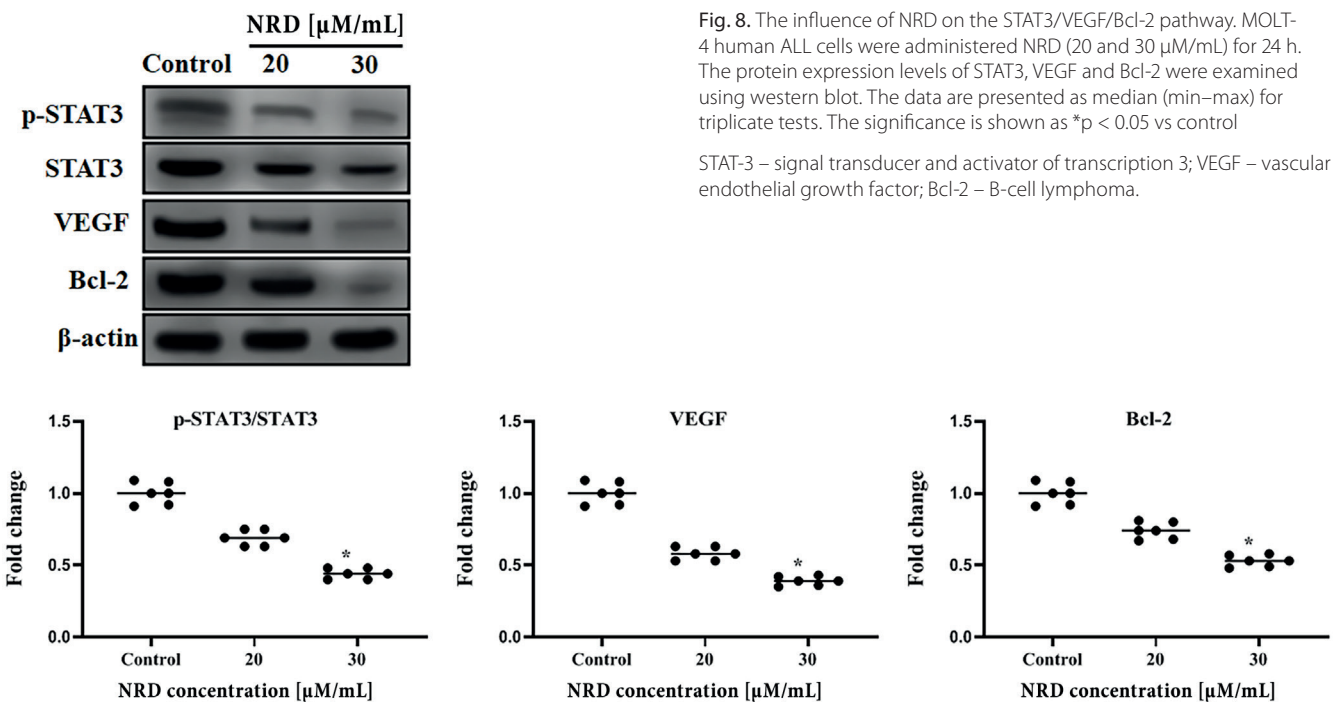


Fig. 8. The influence of NRD on the STAT3/VEGF/Bcl-2 pathway. MOLT-4 human ALL cells were administered NRD (20 and 30 μ M/mL) for 24 h. The protein expression levels of STAT3, VEGF and Bcl-2 were examined using western blot. The data are presented as median (min–max) for triplicate tests. The significance is shown as * $p < 0.05$ vs control

STAT-3 – signal transducer and activator of transcription 3; VEGF – vascular endothelial growth factor; Bcl-2 – B-cell lymphoma.

Discussion

While there are several remedies available for ALL, there is a need for more effective and less toxic treatments due to harmful effects and drug resistance. This objective has resulted in an increased focus on investigating and improving natural agents used for chemoprevention or in cases of tumor relapses. Recently, NRD has sparked interest due to its immense array of pharmacological actions, including anti-tumor and apoptotic activities.¹⁵ The anticancer efficacy of NRD has been widely examined in various types of cancer cells, including oral cancer,^{38,39} ovarian cancer,²¹ osteosarcomas,⁴⁰ breast cancer,¹⁹ and hepatocellular carcinomas,⁴¹ among others. There are no previous reports on the induction of apoptosis in MOLT-4 cells by NRD. The current study demonstrates that NRD exhibited an antiproliferative and apoptotic effect on human ALL cell lines MOLT-4. Our results revealed that NRD (20 and 30 $\mu\text{M/mL}$) efficiently inhibited MOLT-4 cellular proliferation, elevated intracellular ROS accumulation, reduced MMP, and induced apoptosis dose-dependently. In this study, we have shown for the first time that NRD dose-dependently induces significant cytotoxicity in MOLT-4 human ALL cells. Nerolidol reduced cell viability chiefly due to the induction of apoptosis. Numerous anti-tumor medications have been shown to cause death of susceptible cells by stimulating apoptosis. This type of cell death is regarded as a significant reaction to the best chemotherapeutic drugs for leukemia.^{22,23} According to the data, this current research is the first description of the antiproliferative and apoptotic actions of NRD on MOLT-4 human ALL cells.

Apoptosis is a highly controlled kind of cell death, through which cells with substantial damage are eradicated.²² Apoptotic cell death can be induced by either an intrinsic mitochondria-facilitated or an extrinsic death receptor-facilitated pathway.²³ Hence, medicines are needed that selectively prompt apoptosis in tumor cells by inducing tumor-specific upstream activity. Tumors have recurrently utilized these pathways, and it may be promising to selectively stimulate apoptosis in malignant cells or sensitize them to well-known cytotoxic agents.²² Our experiments prove that NRD stimulated apoptosis in ALL cells through the mitochondria-mediated intrinsic pathway and suggest it may translate as a potential drug candidate for a leukemia remedy. We noticed that NRD effectively induced ROS generation and subsequently reduced MMP, along with high levels of caspase-3, -8 and -9 in ALL cells in a quantity-reliant mode. Reactive oxygen species are intermediaries of several intracellular signaling cascades; however, upon hyperproduction, they may promote MMP collapse, which activates a series of mitochondria-related events comprising apoptosis.^{25,26} Related findings were previously reported that NRD exerts antiproliferative and apoptotic activities in osteosarcoma⁴⁰ and hepatoprotective activities.¹⁶ Our study

demonstrated that NRD supplementation enhanced ROS generation and MMP loss, correlating with high caspase activity in mitochondrial-mediated ALL cell apoptosis. Thus, NRD triggered ROS-mediated mitochondrial apoptosis in MOLT-4 cells.

Apart from inducing apoptotic features, ROS can also prompt anti-apoptotic elements. The influence of ROS on tumor cells depends on the balance between ROS-promoted pro- and anti-apoptotic factors. Human ALL cells constitutively express enhanced levels of a vital anti-apoptotic factor, nuclear factor kappa-light-chain-enhancer of activated B cells (NF- κ B).²⁹ However, Nakano et al. established that NF- κ B-controlled genes exhibit a crucial action in the accumulation of ROS in the cells.²⁸ It has been shown that ROS have diverse stimulatory or inhibitory actions in the NF- κ B pathway.^{28,29} Our results point out that NRD significantly suppressed the mRNA expression of COX-2, TNF- α , NF- κ B, and IL-6 in a concentration-dependent manner. Therefore, NRD can inhibit NF- κ B activation and may stimulate apoptosis in ALL cells. Prior research has established that NRD constrains the intensities of TNF- α and IL-1 β in rats with LPS-prompted acute kidney injury and peritoneal macrophages.^{41,42} Another study revealed that NRD inhibited rotenone-promoted IL-6, COX-2, IL-1 β , and TNF- α expression in rat brain.⁴³ Prior research reported that NRD sequestered from *Lindera erythrocarpa* essential oil alleviated I κ B kinase (I κ B) disintegration and NF- κ B phosphorylation by MAPK phosphorylation in LPS-triggered macrophages.⁴² These studies showed that the protective actions of NRD were involved in the attenuation of pro-inflammatory mediators. Our current research found that NRD was able to suppress tumor growth and anti-proliferation by the induction of apoptosis through the inhibition of inflammatory mediators in MOLT-4 cells.

NF- κ B, PI3K/AKT and STAT3/VEGF/Bcl-2 signaling pathways are involved in cell proliferation, differentiation, angiogenesis, metastasis, and apoptosis signal transduction, along with their regulatory role in human ALL.^{28,32,33} Aberrant PI3K/AKT and STAT 3 protein expression leads to various aspects of malignant cell growth, differentiation, survival, transformation, metabolism, and cell cycle regulation.^{32,33} In this study, NRD (20 and 30 $\mu\text{M/mL}$) was able to alter PI3K/AKT and STAT3/VEGF/Bcl-2 protein expression dose-dependently. Previously, similar results were reported that NRD induced apoptosis and cell cycle arrest in MG-63 osteosarcoma cells via PI3K/AKT/JNK regulation.⁴⁰ Several molecular pathways are involved in malignant metastasis, including the VEGF signaling pathway.³⁴ VEGF signaling regulates trans-endothelial leukemia cell migration, contributes to extramedullary infiltration of ALL cells, and is implicated in vascular angiogenesis regulation.³⁴ More importantly, increasing evidence has established that aberrant regulation of VEGF signaling triggering the stimulation through the PI3K/Akt pathway is connected to a poor prognosis in ALL.³⁵ Based

on the physiological communication between the STAT-3, BCL-2 and PI3K/Akt signaling networks, which are significant to acute leukemias, these pathways comprise strong targets for collective inhibition.^{32,33} Our current findings showed that NRD inhibited PI3K/AKT/NF- κ B and STAT-3/VEGF/Bcl-2 signaling and induced apoptotic, anti-inflammatory, anti-oxidative, anti-angiogenic, and antiproliferative actions in MOLT-4 cells. This may be the first report that NRD inhibits the PI3K/AKT/NF- κ B and STAT3/VEGF/Bcl-2 signaling pathways in MOLT-4 human ALL cells and provides additional proof of the underlying anticancer mechanisms of NRD. Important to this study, the development of microscopic techniques has revolutionized the morphological sciences, progressively providing new levels of magnification and resolution for exploring biological and non-biological samples. Microscopy, in fact, provides an understanding of the structure and ultrastructure and of the organization of the main cellular components.⁴⁴

Limitations

In vivo method could not be conducted in this study; however, it will be utilized in future research. PI3K, AKT, STAT3, VEGF, Bcl-2, caspase-3, caspase-9, and caspase-8 were analyzed in protein levels, but need to be analyzed also in RNA levels in future research. Moreover, detailed mechanisms of action still need to be clarified.

Conclusions

Nerolidol was shown to effectively suppress the viability and inflammation and dose-dependently induce apoptosis in MOLT-4 human ALL cells. By increasing the antioxidant status, NRD demonstrated its lethal effects by forming intracellular ROS, which may be caused by MMP collapse, caspase activation or the reduction of NF- κ B-associated inflammatory mediators. By blocking the PI3K/AKT/NF- κ B pathways, NRD caused ROS-mediated mitochondrial death. Moreover, by blocking STAT-3/VEGF/Bcl-2 signaling, NRD decreased the viability of MOLT-4 cells and angiogenesis. These results suggest that NRD may be developed as a potential preventative therapeutic for ALL in humans. Additional investigations should confirm the anticancer activity using in vivo animal models.

Supplementary data

The supplementary materials are available at <https://doi.org/10.5281/zenodo.13268443>. The package includes the following files:

Supplementary Fig. 1. Results of Kruskal–Wallis test as presented in Fig. 1.

Supplementary Fig. 2. Results of Kruskal–Wallis test as presented in Fig. 4.

Supplementary Fig. 3. Results of Kruskal–Wallis test as presented in Fig. 5.

Supplementary Fig. 4. Results of Kruskal–Wallis test as presented in Fig. 6.

Supplementary Fig. 5. Results of Kruskal–Wallis test as presented in Fig. 7.

Supplementary Fig. 6. Results of Kruskal–Wallis test as presented in Fig. 8.

Data availability


The datasets generated and/or analyzed during the current study are available from the corresponding author on reasonable request.


Consent for publication

Not applicable.

ORCID iDs

Xuejiao Wang  <https://orcid.org/0009-0007-0777-1018>

Ke Wang  <https://orcid.org/0009-0004-7752-4950>

Hengfei Du  <https://orcid.org/0009-0006-2914-1036>

References

- Ghosh S, Bandyopadhyay S, Pal S, Das B, Bhattacharya DK, Mandal C. Increased interferon gamma production by peripheral blood mononuclear cells in response to stimulation of overexpressed disease-specific 9-O-acetylated sialoglycoconjugates in children suffering from acute lymphoblastic leukaemia. *Br J Haematol*. 2005;128(1):35–41. doi:10.1111/j.1365-2141.2004.05256.x
- Siegel R, Ma J, Zou Z, Jemal A. Cancer statistics, 2014. *CA Cancer J Clin*. 2014;64(1):9–29. doi:10.3322/caac.21208
- Bray F, Ferlay J, Soerjomataram I, Siegel RL, Torre LA, Jemal A. Global cancer statistics 2018: GLOBOCAN estimates of incidence and mortality worldwide for 36 cancers in 185 countries. *CA Cancer J Clin*. 2018;68(6):394–424. doi:10.3322/caac.21492
- Belson M, Kingsley B, Holmes A. Risk factors for acute leukemia in children: A review. *Environ Health Perspect*. 2007;115(1):138–145. doi:10.1289/ehp.9023
- Juliusson G, Hough R. Leukemia. *Prog Tumor Res*. 2016;43:87–100. doi:10.1159/000447076
- Gregers J, Gr  en H, Christensen IJ, et al. Polymorphisms in the *ABCB1* gene and effect on outcome and toxicity in childhood acute lymphoblastic leukemia. *Pharmacogenomics J*. 2015;15(4):372–379. doi:10.1038/tpj.2014.81
- Neumann M, Vosberg S, Schlee C, et al. Mutational spectrum of adult T-ALL. *Oncotarget*. 2015;6(5):2754–2766. doi:10.18632/oncotarget.2218
- Chowdhury S, Bandyopadhyay S, Mandal C, Chandra S, Mandal C. Flow-cytometric monitoring of disease-associated expression of 9-O-acetylated sialoglycoproteins in combination with known CD antigens, as an index for MRD in children with acute lymphoblastic leukaemia: A two-year longitudinal follow-up study. *BMC Cancer*. 2008;8(1):40. doi:10.1186/1471-2407-8-40
- Pal S, Ghosh S, Mandal C, et al. Purification and characterization of 9-O-acetylated sialoglycoproteins from leukemic cells and their potential as immunological tool for monitoring childhood acute lymphoblastic leukemia. *Glycobiology*. 2004;14(10):859–870. doi:10.1093/glycob/cwh111
- Pui CH, Robison LL, Look AT. Acute lymphoblastic leukaemia. *Lancet*. 2008;371(9617):1030–1043. doi:10.1016/S0140-6736(08)60457-2
- Pui CH, Evans WE. Acute lymphoblastic leukemia. *N Engl J Med*. 1998;339(9):605–615. doi:10.1056/NEJM199808273390907
- Zhang X, Wang H, Zhang Y, Wang X. Advances in epigenetic alterations of chronic lymphocytic leukemia: From pathogenesis to treatment. *Clin Exp Med*. 2024;24(1):54. doi:10.1007/s10238-023-01268-x

13. Kumar M, Kaur V, Kumar S, Kaur S. Phytoconstituents as apoptosis inducing agents: Strategy to combat cancer. *Cytotechnology*. 2016; 68(4):531–563. doi:10.1007/s10616-015-9897-2
14. Azzi J, Auezova L, Danjou PE, Fourmentin S, Greige-Gerges H. First evaluation of drug-in-cyclodextrin-in-liposomes as an encapsulating system for nerolidol. *Food Chem*. 2018;255:399–404. doi:10.1016/j.foodchem.2018.02.055
15. Chan WK, Tan L, Chan KG, Lee LH, Goh BH. Nerolidol: A sesquiterpene alcohol with multi-faceted pharmacological and biological activities. *Molecules*. 2016;21(5):529. doi:10.3390/molecules21050529
16. Iqbal A, Sharma S, Ansari MA, et al. Nerolidol attenuates cyclophosphamide-induced cardiac inflammation, apoptosis and fibrosis in Swiss Albino mice. *Eur J Pharmacol*. 2019;863:172666. doi:10.1016/j.ejphar.2019.172666
17. Ni YL, Shen HT, Su CH, et al. Nerolidol suppresses the inflammatory response during lipopolysaccharide-induced acute lung injury via the modulation of antioxidant enzymes and the AMPK/Nrf-2/HO-1 pathway. *Oxid Med Cell Longev*. 2019;2019:9605980. doi:10.1155/2019/9605980
18. Biazzi BI, Zanetti TA, Baranoski A, Corveloni AC, Mantovani MS. Cis-nerolidol induces endoplasmic reticulum stress and cell death in human hepatocellular carcinoma cells through extensive CYP2C19 and CYP1A2 oxidation. *Basic Clin Pharmacol Toxicol*. 2017;121(4):334–341. doi:10.1111/bcpt.12772
19. Hanušová V, Caltová K, Svobodová H, et al. The effects of β -caryophyllene oxide and trans-nerolidol on the efficacy of doxorubicin in breast cancer cells and breast tumor-bearing mice. *Biomed Pharmacother*. 2017;95:828–836. doi:10.1016/j.biopha.2017.09.008
20. Ambrož M, Boušková I, Skarka A, et al. The influence of sesquiterpenes from *Myrica rubra* on the antiproliferative and pro-oxidative effects of doxorubicin and its accumulation in cancer cells. *Molecules*. 2015;20(8):15343–15358. doi:10.3390/molecules200815343
21. Ambrož M, Matoušková P, Skarka A, Zajdlová M, Žáková K, Skálová L. The effects of selected sesquiterpenes from *Myrica rubra* essential oil on the efficacy of doxorubicin in sensitive and resistant cancer cell lines. *Molecules*. 2017;22(6):1021. doi:10.3390/molecules22061021
22. Kaufmann SH, Earnshaw WC. Induction of apoptosis by cancer chemotherapy. *Exp Cell Res*. 2000;256(1):42–49. doi:10.1006/excr.2000.4838
23. Hengartner MO. The biochemistry of apoptosis. *Nature*. 2000;407(6805):770–776. doi:10.1038/35037710
24. Lindsten T, Ross AJ, King A, et al. The combined functions of proapoptotic Bcl-2 family members Bak and Bax are essential for normal development of multiple tissues. *Mol Cell*. 2000;6(6):1389–1399. doi:10.1016/S1097-2765(00)00136-2
25. Konishi A, Shimizu S, Hirota J, et al. Involvement of histone H1.2 in apoptosis induced by DNA double-strand breaks. *Cell*. 2003;114(6):673–688. doi:10.1016/S0092-8674(03)00719-0
26. Gupte A, Mumper RJ. Elevated copper and oxidative stress in cancer cells as a target for cancer treatment. *Cancer Treat Rev*. 2009;35(1):32–46. doi:10.1016/j.ctrv.2008.07.004
27. Sporn MB, Liby KT. NRF2 and cancer: The good, the bad and the importance of context. *Nat Rev Cancer*. 2012;12(8):564–571. doi:10.1038/nrc3278
28. Nakano H, Nakajima A, Sakon-Komazawa S, Piao JH, Xue X, Okumura K. Reactive oxygen species mediate crosstalk between NF- κ B and JNK. *Cell Death Differ*. 2006;13(5):730–737. doi:10.1038/sj.cdd.4401830
29. Jung HJ, Chen Z, Fayad L, et al. Bortezomib-resistant nuclear factor κ B expression in stem-like cells in mantle cell lymphoma. *Exp Hematol*. 2012;40(2):107–118.e2. doi:10.1016/j.exphem.2011.10.004
30. Silva A, Yunes JA, Cardoso BA, et al. PTEN posttranslational inactivation and hyperactivation of the PI3K/Akt pathway sustain primary T cell leukemia viability. *J Clin Invest*. 2008;118(11):3762–3774. doi:10.1172/JCI34616
31. Gomes AM, Soares MVD, Ribeiro P, et al. Adult B-cell acute lymphoblastic leukemia cells display decreased PTEN activity and constitutive hyperactivation of PI3K/Akt pathway despite high PTEN protein levels. *Haematologica*. 2014;99(6):1062–1068. doi:10.3324/haematol.2013.096438
32. Fruman DA, Rommel C. PI3K and cancer: Lessons, challenges and opportunities. *Nat Rev Drug Discov*. 2014;13(2):140–156. doi:10.1038/nrd4204
33. Neri LM, Cani A, Martelli AM, et al. Targeting the PI3K/Akt/mTOR signaling pathway in B-precursor acute lymphoblastic leukemia and its therapeutic potential. *Leukemia*. 2014;28(4):739–748. doi:10.1038/leu.2013.226
34. Lee CY, Tien HF, Hu CY, Chou WC, Lin LI. Marrow angiogenesis-associated factors as prognostic biomarkers in patients with acute myelogenous leukaemia. *Br J Cancer*. 2007;97(7):877–882. doi:10.1038/sj.bjc.6603966
35. Gong B, Li Z, Xiao W, et al. Sec143 potentiates VEGFR2 signaling to regulate zebrafish vasculogenesis. *Nat Commun*. 2019;10(1):1606. doi:10.1038/s41467-019-09604-0
36. Mosmann T. Rapid colorimetric assay for cellular growth and survival: Application to proliferation and cytotoxicity assays. *J Immunol Methods*. 1983;65(1–2):55–63. doi:10.1016/0022-1759(83)90303-4
37. Annamalai V, Kotakonda M, Periyannan V. JAK1/STAT3 regulatory effect of β -caryophyllene on MG-63 osteosarcoma cells via ROS-induced apoptotic mitochondrial pathway by DNA fragmentation. *J Biochem Mol Toxicol*. 2020;34(8):e22514. doi:10.1002/jbt.22514
38. Kasibhatla S, Amarante-Mendes GP, Finucane D, Brunner T, Bossy-Wetzel E, Green DR. Acridine orange/ethidium bromide (AO/EB) staining to detect apoptosis. *Cold Spring Harb Protoc*. 2006;2006(3):pdb.prot4493. doi:10.1101/pdb.prot4493
39. Balakrishnan V, Ganapathy S, Veerasamy V, et al. Anticancer and antioxidant profiling effects of nerolidol against DMBA induced oral experimental carcinogenesis. *J Biochem Mol Toxicol*. 2022;36(6):e23029. doi:10.1002/jbt.23029
40. Yu Y, Velu P, Ma Y, Vijayalakshmi A. Nerolidol induced apoptosis via PI3K/JNK regulation through cell cycle arrest in MG-63 osteosarcoma cells. *Environ Toxicol*. 2022;37(7):1750–1758. doi:10.1002/tox.23522
41. Fonsêca DV, Salgado PRR, De Carvalho FL, et al. Nerolidol exhibits anti-nociceptive and anti-inflammatory activity: Involvement of the GABAergic system and proinflammatory cytokines. *Fundam Clin Pharmacol*. 2016;30(1):14–22. doi:10.1111/fcp.12166
42. Zhang L, Sun D, Bao Y, Shi Y, Cui Y, Guo M. Nerolidol protects against LPS-induced acute kidney injury via inhibiting TLR4/NF- κ B signaling. *Phytother Res*. 2017;31(3):459–465. doi:10.1002/ptr.5770
43. Javed H, Azimullah S, Abul Khair SB, Ojha S, Haque ME. Neuroprotective effect of nerolidol against neuroinflammation and oxidative stress induced by rotenone. *BMC Neurosci*. 2016;17(1):58. doi:10.1186/s12868-016-0293-4
44. Torge D, Bernardi S, Ciciarelli G, Macchiarelli G, Bianchi S. Dedicated protocol for ultrastructural analysis of farmed rainbow trout (*Oncorhynchus mykiss*) tissues with red mark syndrome: The skin (part one). *Methods Protoc*. 2024;7(3):37. doi:10.3390/mps7030037

Polish validation of the LGBTQ+ Healthcare Experiences Scale (LGBTQ+ HCES)

Michał Czapla^{1,2,A–F}, Bartłomiej Stańczykiewicz^{3,C–F}, Donata Kurpas^{4,B,D–F},
Izabella Uchmanowicz^{4,5,B,D–F}, Bartosz Uchmanowicz^{4,D–F}, Raúl Juárez-Vela^{2,A–F}, Piotr Karniej^{6,A–F}

¹ Department of Emergency Medical Service, Faculty of Nursing and Midwifery, Wrocław Medical University, Poland

² Group of Research in Care (GRUPAC), Faculty of Health Sciences, University of La Rioja, Logroño, Spain

³ Division of Consultation Psychiatry and Neuroscience, Department of Psychiatry, Wrocław Medical University, Poland

⁴ Department of Nursing, Faculty of Nursing and Midwifery, Wrocław Medical University, Poland

⁵ Centre for Cardiovascular Health, Edinburgh Napier University, Sighthill Campus, UK

⁶ WSB MERITO University, Wrocław, Poland

A – research concept and design; B – collection and/or assembly of data; C – data analysis and interpretation;

D – writing the article; E – critical revision of the article; F – final approval of the article

Advances in Clinical and Experimental Medicine, ISSN 1899–5276 (print), ISSN 2451–2680 (online)

Adv Clin Exp Med. 2025;34(9):1565–1574

Address for correspondence

Michał Czapla

E-mail: michal.czapla@umw.edu.pl

Funding sources

None declared

Conflict of interest

None declared

Acknowledgements

We want to express our sincere gratitude to all expert panel members who contributed to the content validation of the LGBTQ+ HCES with their knowledge, insights, and time. In particular, we thank Dr. Łukasz Jacheć, psychiatrist, for his exceptional contribution and support throughout the validation process.

Received on July 25, 2025

Reviewed on August 14, 2025

Accepted on August 20, 2025

Published online on September 15, 2025

Cite as

Czapla M, Stańczykiewicz B, Kurpas D, et al. Polish validation of the LGBTQ+ Healthcare Experiences Scale (LGBTQ+ HCES). *Adv Clin Exp Med.* 2025;34(9):1565–1574. doi:10.17219/acem/209762

DOI

10.17219/acem/209762

Copyright

Copyright by Author(s)

This is an article distributed under the terms of the Creative Commons Attribution 3.0 Unported (CC BY 3.0) (<https://creativecommons.org/licenses/by/3.0/>)

Abstract

Background. The Lesbian, Gay, Bisexual, Transgender, and Queer individuals frequently encounter disparities in healthcare access, quality and inclusivity. Despite growing awareness of these challenges, Poland has lacked a psychometrically validated tool to assess the experiences of sexual and gender minorities in clinical settings.

Objectives. This study aimed to develop and validate the LGBTQ+ Healthcare Experiences Scale (LGBTQ+ HCES) tailored to the Polish context.

Materials and methods. A multi-phase cross-sectional study was conducted in 2025. The initial pool of items was developed through a narrative literature review and refined by 4 researchers with clinical and academic experience in LGBTQ+ health. Content validity was assessed using a 2-round Delphi process involving a multidisciplinary panel of experts (n = 12), who rated item clarity and relevance using Aiken's V. A pilot test with 30 LGBTQ+ participants confirmed comprehension and technical usability. The final 15-item instrument, comprising 3 subscales (Respect and Inclusivity, Discrimination and Microaggressions, Trust and Comfort), was administered to 172 LGBTQ+ individuals recruited via social media. Psychometric evaluation included descriptive analysis, confirmatory factor analysis (CFA) and reliability testing (Cronbach's α , McDonald's ω).

Results. Confirmatory factor analysis supported a 3-factor model comprising Respect and Inclusivity, Discrimination and Microaggressions, and Trust and Comfort. Model fit indices met recommended thresholds (root mean square error of approximation = 0.041, standardized root mean square residual = 0.057, comparative fit index = 0.998). All subscales demonstrated acceptable to strong internal consistency (α = 0.745–0.778; ω = 0.92). No significant floor or ceiling effects were found to compromise the scale's performance. All items showed positive item-total correlations and contributed meaningfully to their respective subscales.

Conclusions. The LGBTQ+ HCES is a valid, reliable and culturally grounded instrument for assessing healthcare experiences among LGBTQ+ populations in Poland. It holds promise for research, public health surveillance and health system quality improvement efforts to promote inclusive and equitable care.

Key words: health equity, LGBTQ+ health, healthcare experiences, inclusivity in healthcare

Highlights

- LGBTQ+ Healthcare Experiences Scale (LGBTQ+ HCES) validated in Poland, filling a critical gap in assessing LGBTQ+ patient experiences within healthcare.
- Three-factor model established – Respect and Inclusivity, Discrimination and Microaggressions, Trust and Comfort – with excellent fit indices (comparative fit index [CFI] = 0.998, root mean square error of approximation (RMSEA) = 0.041).
- Strong reliability across subscales (Cronbach's α = 0.745–0.778; McDonald's ω = 0.92) and no floor/ceiling effects confirm measurement robustness.
- LGBTQ+ HCES provides a reliable tool for research and health system improvement, enabling progress toward inclusive, equitable healthcare delivery in Poland.

Background

Sexual and gender minorities (SGM) – including lesbian, gay, bisexual, transgender, queer, and other non-heteronormative identities (LGBTQ+) – face disproportionate barriers to accessing equitable, culturally competent and respectful healthcare globally.¹ These disparities are not isolated incidents, but rather the result of entrenched systemic discrimination, institutional neglect and a lack of clinician preparedness to deliver inclusive care.^{1,2} Across health systems, LGBTQ+ individuals are more likely to report experiences of microaggressions, heteronormative assumptions, diagnostic overshadowing, and outright mistreatment.^{3,4} These interactions contribute to widespread healthcare avoidance, psychological distress, and worse outcomes in both mental and physical health domains.^{5,6}

In Central and Eastern Europe, and Poland in particular, these disparities are amplified by hostile sociopolitical climates that institutionalize stigma and marginalization.⁷ International Lesbian, Gay, Bisexual, Trans and Intersex Association (ILGA)-Europe's 2025 Rainbow Europe Index ranked Poland last among 49 countries regarding LGBTQ+ equality, highlighting a stark regression in legal protection, public policy and social acceptance.⁸ Over the past decade, Polish authorities have promoted exclusionary rhetoric, established so-called “LGBT-free zones,” and restricted public expressions of LGBTQ+ identity, including pride marches and education campaigns.^{7,9} These structural conditions cultivate fear, social invisibility and medical mistrust, particularly in healthcare settings that are often perceived as unsafe or overtly discriminatory.¹⁰

Evidence from high-income countries suggests that LGBTQ+ patients often internalize prior negative experiences with clinicians, leading to chronic underutilization of services, delays in diagnosis and a reluctance to disclose identity in clinical contexts.^{11–13} In Poland, however, these patterns remain under-researched. Despite increasing international recognition of LGBTQ+ health disparities, few tools exist to systematically assess the lived healthcare experiences of LGBTQ+ individuals in culturally specific, non-English-speaking settings. This gap limits the development

of local data-driven interventions and the ability to monitor progress toward equity-based health system reform.

While several instruments assessing healthcare professionals' competence in working with LGBTQ+ populations have been developed and validated in Poland, there remains a critical gap in tools that capture the patient perspective.¹⁴ Specifically, no validated instrument currently exists to assess how LGBTQ+ individuals themselves perceive respect, discrimination and emotional safety during clinical encounters. Internationally, only a few patient-centered instruments have been developed to assess LGBTQ+ individuals' experiences in healthcare. For example, the Sexual Stigma in Health-Care Services Scale, recently validated in Taiwan, focuses on the experiences of gay and bisexual men.¹⁵ However, this tool remains population-specific and does not provide a comprehensive measure of healthcare experiences across the broader LGBTQ+ community. This patient-centered perspective is essential for understanding the full scope of healthcare (in)equity and informing interventions aimed at system-level change in the Polish context.

Objectives

This study aimed to develop and validate the Lesbian, Gay, Bisexual, Transgender, and Queer+ Healthcare Experiences Scale (LGBTQ+ HCES), a self-report instrument designed to assess the quality, inclusivity, and safety of healthcare experiences among LGBTQ+ individuals in Poland.

Materials and methods

Design

This study employed an instrumental design, as described by Montero and León,¹⁶ which focuses on developing measurement tools – including item construction and psychometric validation. The research aimed to create and validate a novel self-report instrument to assess the healthcare experiences of LGBTQ+ individuals in Poland.

Item development

The initial development of the LGBTQ+ HCES took place between January and February 2024. A narrative literature review was conducted to identify existing instruments and conceptual frameworks related to LGBTQ+ patient experiences. Although several tools exist to assess healthcare providers' cultural competence, no validated, patient-centered instruments were available in the Polish context at the time of the study. The preliminary pool of items was generated through collaborative discussions among 4 researchers with expertise in LGBTQ+ health, health psychology and public health. These items were grounded in existing theoretical models, including the minority stress framework, structural stigma theory and prior empirical studies focusing on LGBTQ+ individuals' interactions with healthcare systems. Each author contributed to conceptualizing the scale domains, item drafting and the review process. A total of 15 items were developed to capture key dimensions such as respect and inclusivity, experiences of discrimination and microaggressions, and emotional safety and trust in clinical encounters. Items were designed to be brief, culturally relevant and linguistically appropriate for Polish-speaking respondents.

Selection of experts

A panel of 12 multidisciplinary experts was recruited to evaluate the content validity of the LGBTQ+ HCES. Experts were defined as professionals with a minimum of 5 years of clinical or academic experience in health-related fields and documented engagement in LGBTQ+ health, human rights or public health practice. The panel included: a psychiatrist, psychologist, family physician, psychotherapist, paramedic, dietitian, nurse, public health specialist, pharmacist, physiotherapist, laboratory diagnostician, and a patient representative from the LGBTQ+ community.

Experts were invited via email, and the invitation included a cover letter outlining the study's goals, the rationale for developing the scale, the selection criteria for participation, and ethical assurances concerning confidentiality, data protection and voluntary participation. Each expert received an information sheet describing the questionnaire structure and participation instructions.

The expert evaluation process was conducted through an online form hosted on Webankieta.pl, a secure Polish data collection platform. Before beginning their review, all participants provided informed consent electronically, which was in line with national data protection regulations. Participation was anonymous, confidential and voluntary.

Delphi method

A conventional Delphi method was employed to evaluate the content validity of the LGBTQ+ HCES, involving 2 structured rounds of expert consultation.¹⁷ This approach,

widely used in instrument development, facilitates consensus-building among experts while allowing for iterative refinement of questionnaire items. Following the recommendations of Linstone and Turoff,¹⁸ 2 rounds were deemed sufficient to ensure informed agreement among participants. The Delphi process was conducted in March 2024, during the 1st month of the study. In Round 1, experts were asked to assess each item for content relevance and linguistic clarity using a 5-point Likert scale (1 = not at all; 5 = completely). Additionally, qualitative feedback was collected through open-ended comment boxes, where panelists could suggest modifying item structure, language or conceptual scope. This feedback was reviewed in detail, and items requiring revision were adjusted accordingly. In Round 2, experts re-evaluated the modified items using the same procedure. This round confirmed whether the revisions enhanced clarity and relevance, and whether consensus had improved. All items in the final version met the predefined inclusion thresholds (Aiken's $V \geq 0.75$), and no further changes were deemed necessary. Initially, invitations were sent to 16 experts, covering all predefined disciplines. Four invitees either did not return the survey or provided incomplete responses, and were therefore excluded from the Delphi process. The final expert panel consisted of 12 members. All 12 completed both Delphi rounds, yielding a 100% response rate in the qualified panel. Communication with the panel was conducted via email, and both Delphi rounds were administered using a secure online survey platform (<https://www.webankieta.pl/>). No experts were lost between rounds; full participation was retained throughout the process.

Content validity analysis

The content validity of the questionnaire was assessed using Aiken's V coefficient, a widely used index for evaluating the relevance and clarity of individual items based on expert ratings. Each expert rated every item using a 5-point Likert scale (1 = not at all relevant/clear; 5 = completely relevant/clear). Aiken's V was calculated for each item using the standard formula:

$$V = (X - l)/k,$$

where X is the mean of expert ratings, l is the lowest possible rating (1), and k is the range of the scale (4, for a 1–5 scale). A threshold of Aiken's $V \geq 0.75$ was used to indicate acceptable content validity. Items scoring below this value in the first round were revised before re-evaluation. All calculations were conducted in Microsoft Excel 2013 (Microsoft Corp., Redmond, USA).

Comprehensibility analysis and linguistic validation

In both rounds of expert review, participants were asked to assess the content relevance and the linguistic clarity

of each item. Ratings were provided on a 5-point Likert scale (1 = unclear, 5 = completely clear). Items receiving lower clarity scores in the 1st round – particularly those with Aiken's $V < 0.75$ – were revised for improved wording. In the 2nd round, experts re-evaluated the revised items.^{19,20} This 2-step process allowed for refinement of item phrasing based on expert feedback to ensure that all items were linguistically clear and culturally appropriate for the Polish context. No items required further revision after the 2nd round, as all reached acceptable clarity levels.

Instrument description

The LGBTQ+ HCES is a 15-item self-report questionnaire developed to assess the healthcare experiences of LGBTQ+ individuals within the Polish healthcare system. The tool was designed to evaluate how affirming, respectful and safe these interactions were, particularly in terms of inclusivity, perceived discrimination and emotional comfort when disclosing one's sexual orientation and/or gender identity.

The items reflect 3 key dimensions: 1) Respect and Inclusivity, which addresses whether patients felt acknowledged and valued regardless of their identity; 2) Discrimination and Microaggressions, which captures instances of subtle or overt exclusion, bias or inappropriate language from healthcare providers; and 3) Trust and Comfort, which assesses the extent to which respondents felt emotionally safe and supported in clinical encounters. Responses are rated on a 7-point Likert scale ranging from 1 ("strongly disagree") to 7 ("strongly agree"), with 5 negatively worded items reverse-coded to ensure higher scores consistently represent more positive healthcare experiences. Subscale scores are computed by averaging the relevant items, and an overall mean score is derived to reflect general experiences across domains.

The instrument used gender-inclusive and non-binary-affirming language to promote psychological safety and accommodate diverse gender identities. Respondents are invited to reflect on direct and perceived experiences, regardless of whether their LGBTQ+ identity was disclosed to medical personnel.

For transparency, all 15 questionnaire items are shown in their English translation in the Results section. The original Polish version of the LGBTQ+ HCES is provided in the raw data to support further validation and implementation efforts. The finalized version of the LGBTQ+ HCES was pilot-tested among 30 participants using an online survey (<https://www.webankieta.pl/>). The aim was to evaluate the clarity of item wording and the technical functionality of the questionnaire. No comprehension issues or technical difficulties were reported. The platform's built-in IP filtering system was used to identify potential duplicate entries; none were detected. To further minimize the risk of duplicate or invalid responses, the platform also applied completeness checks and time monitoring.

Additionally, all responses were screened for internal consistency, and no irregular patterns were detected.

Main study design and participants

A cross-sectional study was conducted between April and May 2024 using convenience sampling via social media platforms, including Instagram and a closed Facebook group for the LGBTQ+ community. Participants were eligible if they were aged 18 years or older, self-identified as LGBTQ+ and had accessed healthcare services in Poland within the past 24 months (including primary care, emergency departments, hospitalizations, diagnostic testing, ambulance services, or private healthcare).

All participants provided informed consent before participation. The survey was fully anonymous and voluntary, and participants were informed that they could withdraw anytime without giving a reason.

A total of 172 participants were enrolled. Sample size determination followed recommendations suggesting 5–10 participants per item for psychometric validation. Given the 18-item structure, a minimum of 90–180 respondents was targeted, which aligns with Argimon-Pallàs's guidelines.²¹ The study was conducted by the Declaration of Helsinki and approved by the Bioethics Committee of Wrocław Medical University, Poland (approval No. KB 976/2022). This research is part of the Health Exclusion Research in Europe2 (HERE2) project.

Statistical analyses

Internal consistency of the questionnaire was checked with confirmatory factor analysis (CFA). Standardized root mean square residual (SRMR), root mean square error of approximation (RMSEA), comparative fit index (CFI), and Tucker–Lewis index (TLI) were used within the Hu–Bentler 2-index strategy to assess the goodness of fit of the CFA model (criteria: SRMR < 0.09 plus at least 1 of the following: CFI > 0.96, TLI > 0.96, or RMSEA < 0.06). Cronbach's α and discriminative power index were internal consistency measures. The following thresholds for internal consistency were used: $0.9 \leq \alpha$ – excellent; $0.8 \leq \alpha < 0.9$ – good; $0.7 \leq \alpha < 0.8$ – acceptable; $0.6 \leq \alpha < 0.7$ – questionable; $0.5 \leq \alpha < 0.6$ – poor; and $\alpha < 0.5$ – unacceptable. R 4.4.1 (R Foundation for Statistical Computing, Vienna, Austria) and RStudio (<https://posit.co/products/open-source/rstudio/?sid=1>) GUI and psy,²² lavaan,²³ psych,²⁴ and diagram packages²⁵ were used.

Results

Sociodemographic characteristics

A total of 172 individuals participated in the study. The mean age was 30.95 years (standard deviation

(SD) = 8.69). Nearly half of the sample identified as cisgender men (47.67%) and almost 1/3 as cisgender women (29.65%), with a notable proportion identifying as non-binary (11.63%). The majority reported a homosexual orientation (69.77%). Most participants lived in large urban areas (>500,000 inhabitants) and held at least a secondary education, with over 30% having a master's degree. Detailed sociodemographic characteristics are presented in Table 1.

Instrument outcomes

Mean scores across the LGBTQ+ HCES and its 3 subscales suggest moderately positive healthcare experiences within the sample, though with considerable variability (Table 2). The highest mean was observed for Respect and Inclusiveness (mean (M) = 25.56, SD = 5.93), while Discrimination and Microaggressions showed the lowest (M = 16.41, SD = 7.24), indicating unequal exposure to negative experiences.

Analysis of the individual questionnaire item

Descriptive item-level analysis revealed high ceiling effects for items 2 and 5, with 57.6% and 50.0% of respondents selecting the maximum response (Table 3). This suggests these items may have limited discriminative capacity in this sample. While this could indicate redundancy, it is also possible that these items tap into universally positive experiences that are crucial to the construct and were designed to function as intentional “anchor” or “booster” items. In contrast, item 15 showed the highest floor effect (31.4%), potentially pointing to problematic or poorly experienced care domains.

Confirmatory factor analysis

The HCES items are measured on an ordinal scale, and the Diagonally Weighted Least Squares (DWLS) estimator was used for CFA. The initial 3-factor model (Model I) showed suboptimal fit indices. Correlations between selected item pairs within the same factor were added to improve model fit based on modification indices. The revised model (Model II) showed improved fit and met recommended thresholds (SRMR < 0.08, RMSEA < 0.06, CFI > 0.95). These adjustments preserved the original factor structure of the HCES. Detailed results are presented in Table 4.

Internal consistency analysis of the LGBTQ+ HCES

All item loadings were statistically significant ($p < 0.001$), ranging from 0.329 to 0.863, indicating adequate association with their respective subscales. Cronbach's α coefficients

Table 1. Sociodemographic characteristics of the sample

Parameter		Total (n = 172)
Age	mean (SD)	30.95 (8.69)
	median (IQR)	29 (23.75–37)
	range	18.5–56
	n	172
Gender	cisgender woman	51 (29.65%)
	transgender woman	7 (4.07%)
	cisgender man	82 (47.67%)
	transgender man	8 (4.65%)
	non-binary person	20 (11.63%)
	other	4 (2.33%)
Sexual orientation	heterosexual	5 (2.91%)
	homosexual	120 (69.77%)
	bisexual	25 (14.53%)
	pansexual	10 (5.81%)
	asexual	10 (5.81%)
	queer	14 (8.14%)
Current relationship status	yes, monogamous relationship	95 (55.23%)
	yes, polyamorous relationship	11 (6.40%)
	no	62 (36.05%)
	other	4 (2.33%)
Place of residence	rural area	15 (8.72%)
	city <100,000 inhabitants	23 (13.37%)
	city 100,000–500,000 inhabitants	38 (22.09%)
Education level	city >500,000 inhabitants	96 (55.81%)
	primary/elementary	2 (1.16%)
	vocational	3 (1.74%)
	secondary	61 (35.47%)
	bachelor's or engineering degree	40 (23.26%)
	master's degree	52 (30.23%)
	doctoral or higher	14 (8.14%)

SD – standard deviation; IQR – interquartile range.

showed acceptable internal consistency across the 3 subscales: Respect and Inclusiveness ($\alpha = 0.770$), Discrimination and Microaggressions ($\alpha = 0.745$) and Trust and Comfort ($\alpha = 0.778$). McDonald's ω index ($\omega = 0.92$) further confirmed the strong internal consistency of the scale.

Item-level reliability analysis revealed no substantial gains in α values upon removal of any item. Although minor increases were observed for Item 5 and Item 15 within their respective subscales, these changes were insufficient to justify item deletion. All items demonstrated positive item-total correlations, supporting their contribution to internal consistency. Detailed results for item loadings and internal consistency are presented in Table 5, with additional reliability metrics shown in Table 6. The path diagram for the CFA of the LGBTQ+ HCES is illustrated in Fig. 1.

Table 2. Descriptive statistics for the LGBTQ+ HCES and its subscales

LGBTQ+ HCES	Score (range)	N	Mean	SD	Median	Min	Max	Q1	Q3
Total LGBTQ+ HCES Score	15–105	172	62.70	9.40	63	39	90	55.75	69
Respect and Inclusiveness	5–35	172	25.56	5.93	26	6	35	21.00	30
Discrimination and Microaggressions	5–35	172	16.41	7.24	16	5	35	11.00	21
Trust and Comfort	5–35	172	20.72	6.93	20	5	35	15.00	26

LGBTQ+ HCES – LGBTQ+ Healthcare Experiences Scale.

Table 3. Floor and ceiling effects per item of the LGBTQ+ HCES

Item*	Floor effect	Ceiling effect
1. My health needs as an LGBTQ+ person were taken seriously.	2.9%	27.9%
2. I have avoided seeking medical care at some point due to fear of how my gender identity and/or sexual orientation might be received.	8.1%	57.6%
3. I have encountered stereotypical or offensive language from healthcare staff directed at me or at the LGBTQ+ community.	13.4%	43.0%
4. I trust healthcare providers to provide appropriate care for LGBTQ+ people.	9.3%	11.0%
5. Healthcare staff respected my gender identity (e.g., by using my correct name or pronouns), regardless of whether I had to explain it.	8.7%	50.0%
6. I felt safe discussing my gender identity and/or sexual orientation with healthcare professionals.	7.6%	20.3%
7. I have avoided disclosing my gender identity and/or sexual orientation due to fear of negative reactions from healthcare providers (e.g., bias, denial of care, or mistreatment).	29.7%	18.6%
8. I was treated with respect by healthcare staff.	1.7%	29.7%
9. I experienced prejudice or discrimination based on my gender identity and/or sexual orientation.	9.3%	30.8%
10. Healthcare staff demonstrated awareness and understanding of LGBTQ+ health needs.	8.1%	14.5%
11. I felt welcomed as an LGBTQ+ person in the healthcare setting.	9.3%	15.7%
12. I felt I was treated equally to other patients, regardless of my gender identity and/or sexual orientation.	4.1%	28.5%
13. I felt that my experiences as an LGBTQ+ person were acknowledged and taken into account in the care I received.	5.8%	18.6%
14. I felt judged or stereotyped by healthcare staff (e.g., through tone of voice, eye contact, or body language) due to my gender identity and/or sexual orientation.	5.8%	27.9%
15. I know where to find an LGBTQ+-affirming healthcare provider or facility.	31.4%	22.7%

*Items are shown in English translation for presentation purposes only. The original validation was conducted using the Polish version of the LGBTQ+ HCES.

Table 4. Results of fit indices

Model	χ^2/df	p-value	RMSEA	CFI	SRMR
Model I	1.876	p < 0.001	0.072	0.992	0.069
Model II	1.284	p = 0.047	0.041	0.998	0.057

RMSEA – root mean square error of approximation; CFI – comparative fit index; SRMR – standardized root mean square residual; df – degrees of freedom.

Discussion

To our knowledge, this study presents the first validated, patient-centered instrument in Poland explicitly designed to capture the healthcare experiences of LGBTQ+ individuals. The LGBTQ+ HCES demonstrated strong psychometric properties, including acceptable internal consistency across all subscales and excellent model fit indices, supporting its use as a reliable tool in research and applied settings.

The final version of the scale, encompassing 3 dimensions – Respect and Inclusivity, Discrimination and Microaggressions, and Trust and Comfort – closely reflects conceptual

frameworks rooted in the minority stress model and structural stigma theory. These dimensions have also been identified in previous studies as key determinants of healthcare quality and access for SGM populations.^{2,26–28} Importantly, our findings indicate that even within a relatively young, urban and highly educated LGBTQ+ cohort, negative clinical experiences remain common, with notably lower scores in perceived discrimination and provider competence.

The high internal consistency and robust factor structure suggest that the LGBTQ+ HCES successfully captures distinct but interrelated aspects of the patient experience. The Discrimination and Microaggressions subscale, which

Table 5. Standardized factor loadings and internal consistency of the LGBTQ+ HCES subscales

Scale	Item	Loading	p-value	Cronbach's α	McDonald's ω index
Respect and Inclusiveness	HCES 1	0.700	p < 0.001	0.770	0.92
	HCES 5	0.426	p < 0.001		
	HCES 8	0.724	p < 0.001		
	HCES 12	0.845	p < 0.001		
	HCES 13	0.863	p < 0.001		
Discrimination and Microaggressions	HCES 2	0.673	p < 0.001	0.745	
	HCES 3	0.601	p < 0.001		
	HCES 7	0.787	p < 0.001		
	HCES 9	0.691	p < 0.001		
	HCES 14	0.685	p < 0.001		
Trust and Comfort	HCES 4	0.723	p < 0.001	0.778	
	HCES 6	0.829	p < 0.001		
	HCES 10	0.809	p < 0.001		
	HCES 11	0.834	p < 0.001		
	HCES 15	0.329	p < 0.001		

LGBTQ+ HCES – LGBTQ+ Healthcare Experiences Scale.

Table 6. Item-level reliability analysis for the LGBTQ+ HCES subscales

Scale	Item	Alpha when item omitted	Item-total correlation
Respect and Inclusiveness	HCES 1	0.712	0.590
	HCES 5	0.806	0.354
	HCES 8	0.706	0.631
	HCES 12	0.679	0.678
	HCES 13	0.732	0.531
Discrimination and Microaggressions	HCES 2	0.720	0.453
	HCES 3	0.693	0.529
	HCES 7	0.697	0.518
	HCES 9	0.704	0.496
	HCES 14	0.685	0.561
Trust and Comfort	HCES 4	0.729	0.582
	HCES 6	0.696	0.672
	HCES 10	0.691	0.698
	HCES 11	0.704	0.662
	HCES 15	0.854	0.273

LGBTQ+ HCES – LGBTQ+ Healthcare Experiences Scale.

yielded the lowest mean score, underscores the persistence of subtle and overt biases in Polish healthcare settings. This finding aligns with international literature demonstrating the pervasiveness of microaggressions – often invisible to cisgender and heterosexual providers – such as inappropriate assumptions, invalidation of identity or reluctance to use inclusive language.^{29,30}

Conversely, the Respect and Inclusivity subscale had the highest score, suggesting that some interpersonal aspects of care – particularly overt disrespect or denial of identity – may be less prevalent. However, the relatively high ceiling effects on items related to being treated

respectfully may also reflect limited item sensitivity or social desirability bias.

The Trust and Comfort subscale revealed moderate scores, consistent with studies showing that even when overt discrimination is absent, LGBTQ+ patients frequently report discomfort disclosing their identities or anticipating poor treatment.^{2,12,15,26} This has critical implications for clinical care: nondisclosure is associated with reduced diagnostic accuracy, inappropriate treatment plans and poor health outcomes, particularly in mental health, sexual health and chronic disease management.^{31–33} Item 15 within this subscale demonstrated the highest

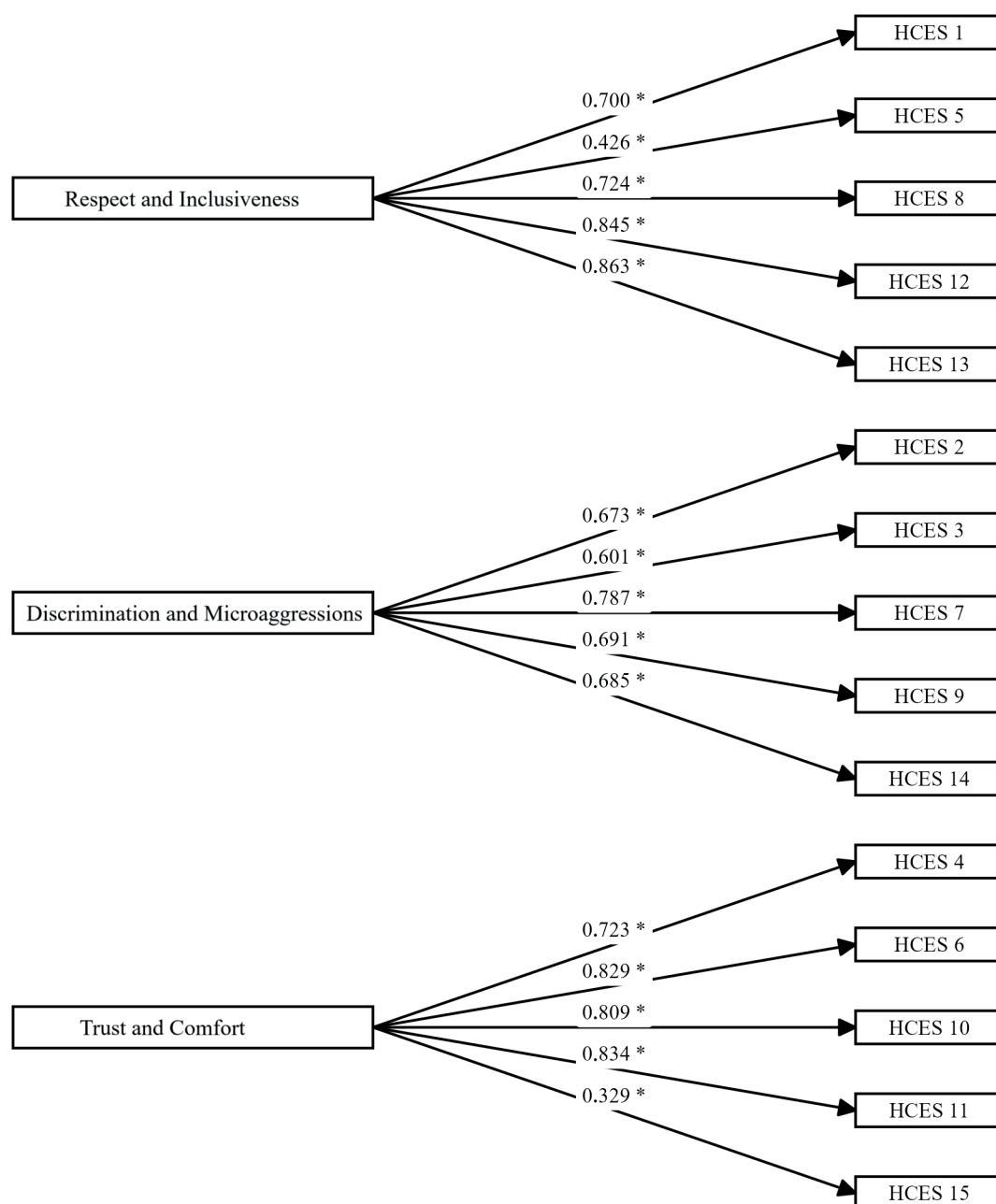


Fig. 1. Path diagram for confirmatory factor analysis (CFA) of the LGBTQ+ Healthcare Experiences Scale (HCES)

floor effect (31.4%). This finding likely reflects structural barriers in the Polish healthcare system, where information about LGBTQ+-affirmative providers remains scarce and often inaccessible. Although the item showed lower factor loading and item–total correlation compared to other items, it was retained due to its conceptual relevance: knowing where to find inclusive services is a critical dimension of comfort and trust in healthcare. Importantly, the overall reliability of the subscale remained acceptable, indicating that inclusion of this item did not compromise the psychometric integrity of the instrument.

While several instruments assess healthcare provider competencies toward LGBTQ+ patients (e.g., the LGBT-DOCSS, the GAP), these tools do not capture the patients' perspectives.^{2,34} The LGBTQ+ HCES fills this gap

in Poland, where widespread institutional hostility and sociopolitical marginalization exacerbate mistrust toward healthcare services.^{7,8,35}

Practical implications

The validated LGBTQ+ HCES provides a robust, culturally relevant instrument for assessing the healthcare experiences of sexual and gender minorities in Poland. Its practical applications span clinical, administrative and policy levels. The scale enables routine monitoring of inclusivity and patient-centeredness in clinical settings, offering insight into perceived respect, safety and discrimination. Facilities may use subscale scores to identify specific domains – such as fear of disclosure or lack of cultural competence – that

require targeted interventions. At the healthcare system level, the tool can facilitate equity-focused audits and inform continuous quality improvement initiatives. Integration into national health reporting frameworks would allow for standardized benchmarking and longitudinal tracking of LGBTQ+ patient experiences across regions and care settings. The LGBTQ+ HCES may also serve as an outcome measure in intervention studies, evaluating the impact of inclusivity training or structural reforms (e.g., removal of binary intake forms). Finally, it offers a means of amplifying community voice, enabling LGBTQ+ individuals to report health system performance based on lived experience. By translating subjective experiences into measurable data, the LGBTQ+ HCES provides the empirical foundation needed to guide responsive, equity-driven health system reforms in settings where LGBTQ+ health remains politically contested and structurally neglected. Beyond Poland, the LGBTQ+ HCES also holds potential for cross-cultural adaptation. Applying the scale in other healthcare systems would allow for standardized international comparisons of LGBTQ+ patients' experiences, facilitating both the identification of universal barriers and the recognition of context-specific challenges. Such comparative research could strengthen the global evidence base needed to inform inclusive and equity-driven healthcare reforms. This makes the LGBTQ+ HCES particularly valuable for use in countries with sociopolitical contexts comparable to Poland, where LGBTQ+ health remains under-researched and marginalized.

Limitations

This study has several limitations. First, participants were recruited through convenience sampling on social media platforms, which may limit representativeness to LGBTQ+ individuals who are active online and engaged in digital communities. As a result, the findings may not fully reflect the experiences of those with limited internet access or those less connected to LGBTQ+ networks. Second, self-report questionnaires introduce the potential for social desirability or recall bias. Lastly, while the scale demonstrated strong psychometric properties in the Polish context, future studies may explore its test–retest reliability and sensitivity to change over time in intervention-based research.

Conclusions

The LGBTQ+ HCES demonstrated strong psychometric properties, including robust content validity, high internal consistency, and good model fit. The tool captures 3 core dimensions of LGBTQ+ individuals' experiences in the healthcare system: Respect and Inclusivity, Discrimination and Microaggressions, and Trust and Comfort in clinical settings.

The LGBTQ+ HCES provides a reliable and practical measure for evaluating healthcare experiences among sexual and gender minorities in Poland. It is suitable for academic research and public health applications, health system evaluation and equity-focused service improvement. The scale is intended to inform efforts to identify and address healthcare inequities affecting LGBTQ+ populations and support interventions to enhance inclusivity and responsiveness in clinical practice. Its adoption in health systems and research settings may contribute to more inclusive policy development and patient-centered care for LGBTQ+ populations.

Data Availability Statement

The datasets generated and/or analyzed during the current study are available in Zenodo at <https://doi.org/10.5281/zenodo.17026585>.

Consent for publication

Not applicable.

Use of AI and AI-assisted technologies

OpenAI's ChatGPT was used for language editing and proofreading to ensure the final manuscript's clarity, coherence, and linguistic accuracy.

ORCID iDs

Michał Czapla  <https://orcid.org/0000-0002-4245-5420>
 Bartłomiej Stańczykiewicz  <https://orcid.org/0000-0001-9221-3502>
 Donata Kurpas  <https://orcid.org/0000-0002-6996-8920>
 Izabella Uchmanowicz  <https://orcid.org/0000-0001-5452-0210>
 Bartosz Uchmanowicz  <https://orcid.org/0000-0002-9387-4158>
 Raúl Juárez-Vela  <https://orcid.org/0000-0003-3597-2048>
 Piotr Karniej  <https://orcid.org/0000-0002-6489-2525>

References

1. Lund EM, Burgess CM. Sexual and gender minority health care disparities. *Primary Care Clin Office Pract.* 2021;48(2):179–189. doi:10.1016/j.pop.2021.02.007
2. Bidell MP. The Lesbian, Gay, Bisexual, and Transgender Development of Clinical Skills Scale (LGBT-DOCSS): Establishing a new interdisciplinary self-assessment for health providers. *J Homosex.* 2017;64(10):1432–1460. doi:10.1080/00918369.2017.1321389
3. Sileo KM, Baldwin A, Huynh TA, et al. Assessing LGBTQ+ stigma among healthcare professionals: An application of the health stigma and discrimination framework in a qualitative, community-based participatory research study. *J Health Psychol.* 2022;27(9):2181–2196. doi:10.1177/13591053211027652
4. Tran NM, Gonzales G, Fry CE, Dusetzina SB, McKay T. Patterns of lesbian, gay, bisexual, transgender, and queer patient experiences and receipt of preventive services [published online as ahead of print on May 4, 2025]. *Health Serv Res.* 2025. doi:10.1111/1475-6773.14632
5. Nair JM, Waad A, Byam S, Maher M. Barriers to care and root cause analysis of LGBTQ+ patients' experiences: A qualitative study. *Nurs Res.* 2021;70(6):417–424. doi:10.1097/NNR.0000000000000541
6. Nowaskie DZ, Menez O. Healthcare experiences of LGBTQ+ people: Non-binary people remain unaffirmed. *Front Sociol.* 2024;9:1448821. doi:10.3389/fsoc.2024.1448821

7. Kubal A. Queer coalition? The crisis of justice in Poland and LGBTQ+ rights before the Polish courts. *Europe-Asia Studies*. 2024;76(9): 1347–1370. doi:10.1080/09668136.2024.2402342
8. Jesus S. Annual Review 2025. Geneva, Switzerland: International Lesbian, Gay, Bisexual, Trans and Intersex Association (ILGA); 2025. <https://www.ilga-europe.org/report/annual-review-2025>. Accessed July 27, 2025.
9. Baiocco R, Pezzella A, Pistella J, et al. LGBTQ+ training needs for health and social care professionals: A cross-cultural comparison among seven European countries. *Sex Res Soc Policy*. 2022;19(1):22–36. doi:10.1007/s13178-020-00521-2
10. Donisi V, Amadeo F, Zakrzewska K, et al. Training healthcare professionals in LGBTI cultural competencies: Exploratory findings from the Health4LGBTI pilot project. *Patient Educ Couns*. 2020;103(5):978–987. doi:10.1016/j.pec.2019.12.007
11. Casey LS, Reisner SL, Findling MG, et al. Discrimination in the United States: Experiences of lesbian, gay, bisexual, transgender, and queer Americans. *Health Serv Res*. 2019;54(Suppl 2):1454–1466. doi:10.1111/1475-6773.13229
12. Hatzenbuehler ML, Lattanner MR, McKetta S, Pachankis JE. Structural stigma and LGBTQ+ health: A narrative review of quantitative studies. *Lancet Public Health*. 2024;9(2):e109–e127. doi:10.1016/S2468-2667(23)00312-2
13. Hash KM, Rogers A. Clinical practice with older LGBT clients: Overcoming lifelong stigma through strength and resilience. *Clin Soc Work J*. 2013;41(3):249–257. doi:10.1007/s10615-013-0437-2
14. Karniej P, Pietrzykowski Ł, Dissen A, Juárez-Vela R, Kulińska J, Czapla M. Lesbian, gay, bisexual, and transgender (LGBT) clinical competence of medical professionals in Poland [published online as ahead of print on March 10, 2025]. *Sex Res Soc Policy*. 2025. doi:10.1007/s13178-025-01081-z
15. Huang MF, Chang YP, Lin CY, Yen CF. A newly developed scale for assessing experienced and anticipated sexual stigma in health-care services for gay and bisexual men. *Int J Environ Res Public Health*. 2022;19(21):13877. doi:10.3390/ijerph192113877
16. Montero I, León OG. A classification system for method within research reports in psychology [in Spanish]. *Int J Clin Health Psychol*. 2005;5(1):115–127.
17. Hasson F, Keeney S, McKenna H. Research guidelines for the Delphi survey technique. *J Adv Nurs*. 2000;32(4):1008–1015. doi:10.1046/j.1365-2648.2000.t01-1-01567.x
18. Linstone HA, ed. *The Delphi Method: Techniques and Applications*. 3rd ed. Reading, USA: Addison-Wesley; 1979. ISBN: 978-0-201-04294-8, 978-0-201-04293-1.
19. Aiken LR. Three coefficients for analyzing the reliability and validity of ratings. *Educ Psychol Meas*. 1985;45(1):131–142. doi:10.1177/0013164485451012
20. Zamanzadeh V, Ghahramanian A, Rassouli M, Abbaszadeh A, Alavi-Majd H, Nikanfar AR. Design and Implementation Content Validity Study: Development of an instrument for measuring patient-centered communication. *J Caring Sci*. 2015;4(2):165–178. doi:10.15171/jcs.2015.017
21. Argimon Pallàs JM, Jiménez Villa J. *Métodos de investigación clínica y epidemiológica*. Madrid, Spain: Elsevier España, S.L; 2019. ISBN:978-84-9113-007-9.
22. Falissard R. psy: Various Procedures Used in Psychometrics. The Comprehensive R Archive Network (CRAN); 2022. <https://cran.r-project.org/web/packages/psy/index.html>. Accessed April 1, 2024.
23. Rosseel Y. lavaan: An R package for structural equation modeling. *J Stat Soft*. 2012;48(2):1–36. doi:10.18637/jss.v048.i02
24. Revelle W. psych: Procedures for Psychological, Psychometric, and Personality Research. The Comprehensive R Archive Network (CRAN); 2024. <https://cran.r-project.org/web/packages/psych/index.html>. Accessed April 1, 2024.
25. Soetaert K. diagram: Functions for Visualising Simple Graphs (Networks), Plotting Flow Diagrams. The Comprehensive R Archive Network (CRAN); 2020. <https://cran.r-project.org/web/packages/diagram/index.html>. Accessed April 1, 2024.
26. Karniej P, Dissen A, Juárez-Vela R, Gea-Caballero V, Echániz-Serrano E, Czapla M. Psychometric properties and cultural adaptation of the Polish version of the Lesbian, Gay, Bisexual, and Transgender Development of Clinical Skills Scale (LGBT-DOCSS-PL). *J Homosex*. 2025;72(1):45–59. doi:10.1080/00918369.2024.2302970
27. Yu H, Flores DD, Bonett S, Bauermeister JA. LGBTQ+ cultural competency training for health professionals: A systematic review. *BMC Med Educ*. 2023;23(1):558. doi:10.1186/s12909-023-04373-3
28. Bonvicini KA. LGBT healthcare disparities: What progress have we made? *Patient Educ Couns*. 2017;100(12):2357–2361. doi:10.1016/j.pec.2017.06.003
29. Beaton DE, Bombardier C, Guillemin F, Ferraz MB. Guidelines for the Process of Cross-Cultural Adaptation of Self-Report Measures. *Spine (Phila Pa 1976)*. 2000;25(24):3186–3191. doi:10.1097/00007632-200012150-00014
30. European Union Agency for Fundamental Rights. *A Long Way To Go for LGBTI Equality*. Luxembourg, Luxembourg: Publications Office; 2020. <https://data.europa.eu/doi/10.2811/348583>. Accessed August 21, 2025.
31. Morris M, Cooper RL, Ramesh A, et al. Training to reduce LGBTQ-related bias among medical, nursing, and dental students and providers: A systematic review. *BMC Med Educ*. 2019;19(1):325. doi:10.1186/s12909-019-1727-3
32. Brooks H, Llewellyn CD, Nadarzynski T, et al. Sexual orientation disclosure in health care: A systematic review. *Br J Gen Pract*. 2018;68(668): e187–e196. doi:10.3399/bjgp18X694841
33. Makadon HJ. Ending LGBT invisibility in health care: The first step in ensuring equitable care. *Cleve Clin J Med*. 2011;78(4):220–224. doi:10.3949/ccjm.78gr.10006
34. Crisp C. The Gay Affirmative Practice Scale (GAP): A new measure for assessing cultural competence with gay and lesbian clients. *Soc Work*. 2006;51(2):115–126. doi:10.1093/sw/51.2.115
35. Nakielska J. Polityka polskich władz dewastuje sytuację życiową osób LGBTQ+: publikujemy raport o Sytuacji społecznej osób LGbTA w Polsce. Warsaw, Poland: Kampania Przeciw Homofobii; 2021. <https://kph.org.pl/polityka-polskich-wladz-dewastuje-sytuacje-zyciowa-osob-lgbt-publikujemy-raport-o-sytuacji-spoecznej-osob-lgbta-w-polsce>. Accessed August 25, 2024.

The role of *p16* gene and P16INK4a protein in hematologic malignancies and therapeutic implications: A systematic review

Paula Jabłowska-Babij^{1,A–F}, Maciej Majcherek^{1,A–F}, Anna Kłopot^{2,B–F}, Agnieszka Szeremet^{1,B–F}, Tomasz Wróbel^{1,A,E,F}, Anna Czyż^{1,A–F}

¹ Department and Clinic of Hematology, Blood Neoplasms and Bone Marrow Transplantation, Wrocław Medical University, Poland

² Department of Medical Biochemistry, Wrocław Medical University, Poland

A – research concept and design; B – collection and/or assembly of data; C – data analysis and interpretation;

D – writing the article; E – critical revision of the article; F – final approval of the article

Advances in Clinical and Experimental Medicine, ISSN 1899–5276 (print), ISSN 2451–2680 (online)

Adv Clin Exp Med. 2025;34(9):1575–1587

Address for correspondence

Paula Jabłowska-Babij

E-mail: paula.jablowska@student.umw.edu.pl

Funding sources

None declared

Conflict of interest

None declared

Received on May 7, 2024

Reviewed on August 26, 2024

Accepted on September 3, 2024

Published online on December 4, 2024

Abstract

Hematological malignancies encompass a diverse group of cancers affecting the blood, bone marrow and lymph nodes. The *p16* gene, encoding the P16INK4A protein, plays a pivotal role in cell cycle regulation and tumor suppression. Understanding the involvement of *p16* in the development and progression of hematological malignancies is crucial for advancing therapeutic strategies.

This systematic review aims to elucidate the multifaceted roles of the *p16* gene and P16INK4A protein in hematological malignancies, focusing on their impact on disease pathogenesis, prognostic significance and therapeutic implications. A comprehensive search was conducted across electronic databases, including PubMed, Scopus and Google Scholar, using predefined search terms related to *p16*, P16INK4A, hematological malignancies, and therapy. Studies published up to 2023 were included, encompassing clinical trials, observational studies, meta-analyses, and preclinical research.

The review synthesizes evidence highlighting the dysregulation of the *p16* pathway in various hematological cancers. Alterations in *p16* expression levels, genetic mutations and epigenetic modifications contribute to disease initiation and progression. Moreover, the prognostic significance of *p16* status in predicting therapeutic outcomes and patient survival is explored. The *p16* gene and P16INK4A protein emerge as promising biomarkers and therapeutic targets in hematological malignancies. Integrating knowledge of *p16* dysregulation into clinical practice holds the potential to optimize treatment strategies, enhance patient outcomes and pave the way for personalized medicine approaches in the management of these challenging diseases.

Key words: prognostic factor, hematological malignancies, *p16*, therapeutic implications, P16INK4A

Cite as

Jabłowska-Babij P, Majcherek M, Kłopot A, et al.

The role of *p16* gene and P16INK4a protein in hematologic malignancies and therapeutic implications: A systematic review. *Adv Clin Exp Med.* 2025;34(9):1575–1587.

doi:10.17219/acem/192903

DOI

10.17219/acem/192903

Copyright

Copyright by Author(s)

This is an article distributed under the terms of the Creative Commons Attribution 3.0 Unported (CC BY 3.0) (<https://creativecommons.org/licenses/by/3.0/>)

Introduction

Hematological malignancies account for 9.7% of all cancers, ranking them the 4th most common in the human population.¹ The huge number of cases poses a significant obstacle for the healthcare system. It is believed that a comprehensive understanding of cancer pathophysiology can serve as a basis for the discovery of new medications to optimize and maximize the outcomes of patients with hematological malignancies. Moreover, gaining further knowledge of the systems responsible for cancer formation and progression could potentially enable the early detection of susceptible patients and the implementation of preventive measures. Identification of predictive and prognostic indicators is crucial for tailoring preventive strategies, improving clinical practice and allocating research resources.²

P16^{INK4a} is a protein classified as a tumor suppressor, mostly due to the widespread genetic inactivation of the *p16^{INK4a}* (or *CDKN2A*) gene in almost all forms of human malignancies. P16^{INK4a} is a component in regulating the cell cycle and working in conjunction with the P53 protein; research has demonstrated that an increased amount of P16^{INK4a} expression (upregulation) has a role in cellular senescence, aging and the advancement of cancer. This suggests that the control of P16^{INK4a} is significant for its proper functioning.³

The systematic review used PubMed, Scopus and Google Scholar search engines. The following key words were used: “*p16^{INK4a}*”, “INK4a, P16^{INK4a}”, “hematologic malignancies”, “acute myeloid leukemia”, “acute lymphoblastic leukemia”, “myelodysplastic syndromes”, “chronic myeloid leukemia”, “mastocytosis”, “chronic lymphocytic leukemia”, “Hodgkin’s lymphoma”, “Hodgkin’s disease”, “non-Hodgkin’s lymphoma”, “plasma cell myeloma”, “multiple myeloma”, and “prognostic factors”, “*p16^{INK4a}* expression”, “DNA methylation”, “chromosomal deletions”. The search was limited to the period from 1993 to 2023. Articles published more than 10 years ago were used only when necessary. The sources were last searched on July 24, 2024.

Objectives

The primary objective of this systematic review was to present an overview of the existing knowledge on the function of the *p16^{INK4a}* gene and P16^{INK4a} protein in the development of hematological malignancies. Additionally, the review aimed to investigate the *p16* gene and P16^{INK4a} protein potential roles as prognostic factors, and the therapeutic implications of targeting the *p16* gene and P16^{INK4a} protein in anticancer treatment. Furthermore, the review attempted to familiarize the reader with the structure of these elements and the mechanisms of their interaction with the cell cycle.

Structure and function of the *p16* gene and P16INK4a protein

Serrano et al. identified P16^{INK4a} as a protein that binds to CDK4 and inhibits the catalytic activity of the CDK4/cyclin D enzymes in 1993.⁴ The protein is also known as P16 or MTS1 (multiple tumor suppressor 1) and is encoded by the *CDKN2A* gene located at the INK4b/ARF/INK4a locus on chromosome 9p21.3 (Fig. 1).^{5,6} *CDKN2A* also encodes for P14^{ARF} (P19^{ARF} in mice), while *CDKN2B* encodes for P15^{INK4b}, *CDKN2C* for P18^{INK4d} and *CDKN2D* for P19^{INK4d}.⁷ Additionally, the INK4b/ARF/INK4a locus encodes antisense non-coding RNA in the INK4/ARF locus (ANRIL).⁸

P16^{INK4a} and P15^{INK4b} bind and inhibit CDK4 and CDK6, which in turn are significant to relieve the cell cycle inhibitory activity of the retinoblastoma (Rb) tumor suppressor, whereas P14^{ARF} is an activator of tumor suppressor p53 (Fig. 2).^{7,9,10}

P16^{INK4a} and P15^{INK4b}, as well as P18 and P19, belong to the INK4 protein family.⁹ The common feature of these 4 proteins is that they are built of ankyrin repeat (AR) motifs, each of which is composed of 31–34 amino acids.¹¹ Ankyrin repeat motifs are found in many proteins and are responsible for protein–protein interactions. The studies have shown that P16^{INK4a} and P15^{INK4b} proteins are composed of 4 ankyrin repeat (AR) motifs, whereas P18 and P19 contain 5 AR motifs.¹² In addition to their similar structure, all INK4 proteins bind to CDK4/6 and inhibit its activity. Unlike P16^{INK4a} and P15^{INK4b}, which are encoded by the same locus and most likely resulted from gene duplication,¹³ genes encoding P18 and P19 proteins are located within chromosomes 1p32 and 19p13.2, respectively.¹⁴

The studies on interactions between P16^{INK4a} and CDK4/6 have shown that residues of P16^{INK4a} that interact with CDK4/6 are located in the 2nd and 3rd AR motif. Crystallographic studies revealed that AR motifs present in the P16^{INK4a} protein form a helix bundle with a concave surface in which clusters of charged groups are present for target binding.¹⁵

P16^{INK4a} inhibits CDK4/CDK6 proteins in 2 ways. First, the concave surface of the P16^{INK4a} protein interacts with a catalytic site of CDK4/6 proteins, leading to a decrease in the kinase activity of CDK4/6 proteins. Second, the interaction between P16^{INK4a} and CDK4/6 induces changes in the tertiary structure of CDK4/6, which affects the binding between CDK4/6 and its activator, cyclin D.¹⁶

The studies conducted until now have revealed that the primary function of the P16^{INK4a} protein is regulation of the cell cycle. P16^{INK4a} involvement in the regulation of cell cycle progression occurs through at least 2 mechanisms. The best description is the contribution of P16^{INK4a} to the pRb/E2F pathway. P16^{INK4a} binds and inhibits the activity of CDK4 and CDK6 proteins, whose role is to phosphorylate Rb proteins. When P16^{INK4a} inhibits the activity of the CDK4/6 protein, it results in hypophosphorylation of the Rb protein. Hypophosphorylated Rb protein inhibits

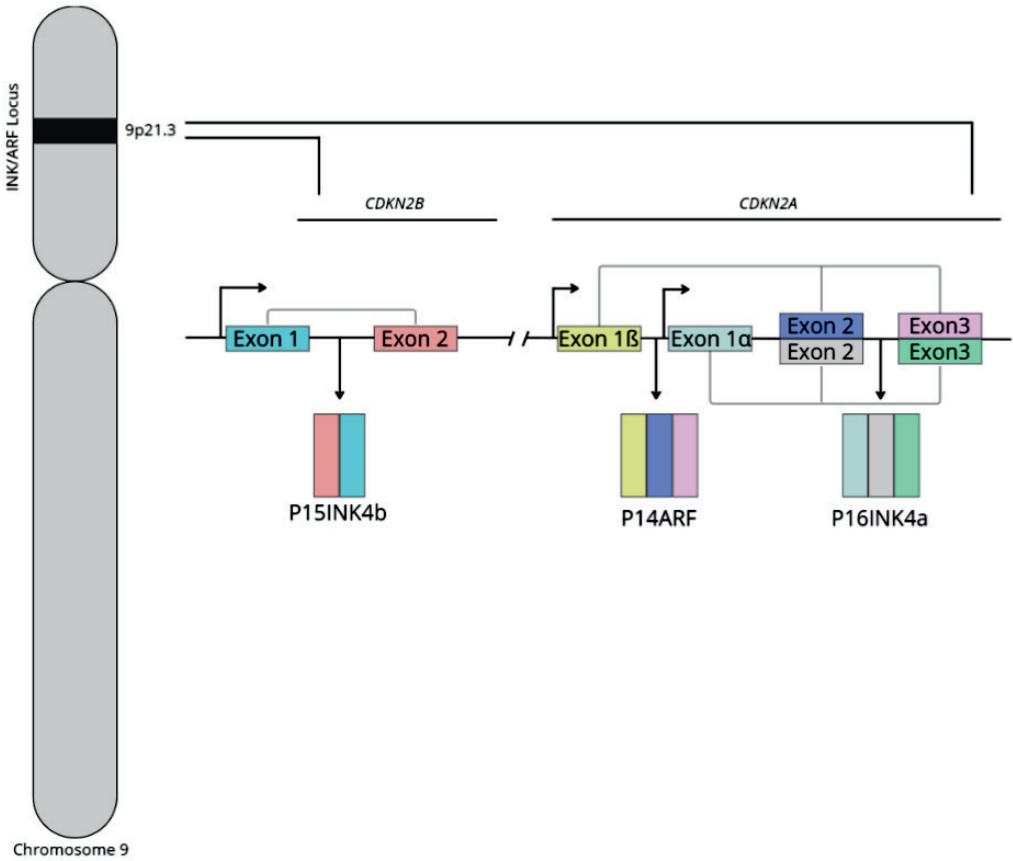


Fig. 1. Schematic structure of the INK4a/ARF locus

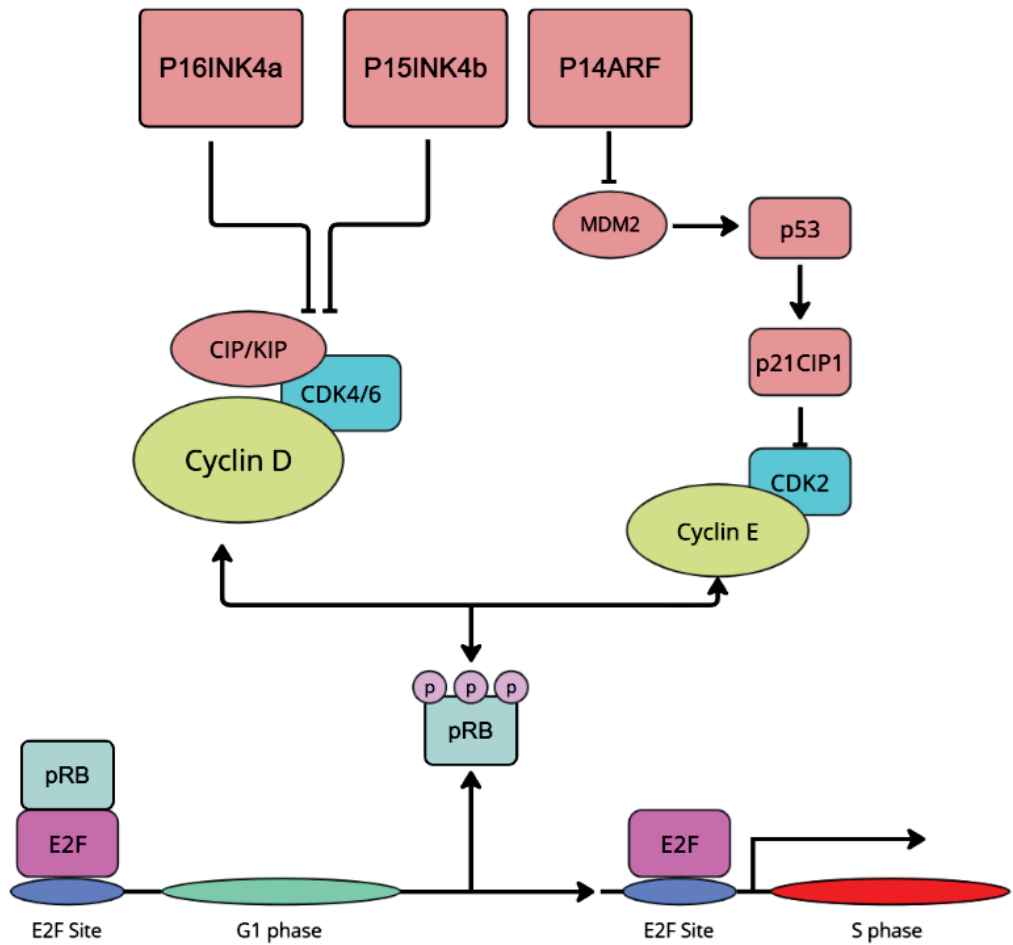


Fig. 2. The mechanism of cell cycle regulation

association of E2F protein with promoters of proliferation-associated genes (e.g., cyclin B1, dihydrofolate reductase, thymidine kinase, and JunB proto-oncogene), thus preventing the entrance of cells into the S phase and proliferation. On the other hand, cell commitment to proliferation results in pRb hyperphosphorylation by CDK6/4 in late G1, resulting in the entry of the cell into the S phase (Fig. 2). The 2nd mechanism involves the interaction of P16^{INK4a} with TFIIH in the pre-initiation complex, which prevents the CDK7 subunit of this transcription factor from phosphorylating the carboxy-terminal domain of the large subunit of RNA polymerase II, a step required for the transcription of RNAII polymerase-dependent genes.^{17,18}

Regulation of P16^{INK4a} expression

Traversing the G1/S cell cycle checkpoint is one of the critical events in cell life and is therefore tightly regulated by multiple pathways. In general, the main outcome of this regulation should be to allow only fit and unstressed cells to proliferate and to inhibit the proliferation of cells exposed to stress and oncogenic stimuli. In general – because of the importance of the *p16^{INK4a}* gene for cell cycle control – this gene is maintained in a repressed state in normal cells so they can proliferate. Expression of this gene requires: 1) a permissive state of chromatin surrounding the *p16^{INK4a}* gene; and 2) stimulation of transcription by activator proteins. The induction of *p16^{INK4a}* gene expression is usually observed during cellular senescence, a state of the cell during which the cell is metabolically active but cannot proliferate.¹² The cellular senescence might be induced by a number of factors, including UV light, reactive oxygen species (ROS) and oncogenes.¹⁹

Epigenetic regulation

It has been reported that the *p16^{INK4a}* gene undergoes in cells silencing by evolutionary conserved multiprotein complexes polycomb repressive complex 1 (PRC1) and polycomb repressive complex 2 (PRC2).⁵ The studies have shown that long non-coding (lnc) RNAs such as ANRIL and MOV10 are responsible for the recruitment of the PRC2 complex to the *p16^{INK4a}* gene.²⁰ According to the well-established model, the enzymatic subunits of this complex, Ezh1 and Ezh2, are responsible for the trimethylation of lysine 27 of histone H3 (H3K27me2/3),²¹ which is next recognized by the subunit of the PRC1 complex, the CBX protein, and the entire PRC1 complex is recruited to target locus.²² A part of the PRC1 complex E3 ubiquitin ligase RING1A/B is responsible for the monoubiquitination of histone H2A at lysine 119 (H2AK119ub1), which, along with local chromatin compaction, leads to gene silencing. The studies also showed that histone deacetylases (HDAC) are involved in *INK4* genes silencing. One mechanism by which HDACs contribute to this phenomenon is that they promote dissociation of E2F1 from Rb, and

the former induces transcription of C-MYC, which in turn is a positive regulator of BMI-1 expression. BMI-1 is a part of the PRC1 complex.²³ Similarly, Ezh protein levels are increased as a result of E2F dependent transcription, leading to increased activity of the PRC2 complex.⁵ This altogether results in long-term reversible suppression of the *INK4* genes: *p19^{ARF}* and *p16^{INK4a}*. The mechanism responsible for the removal of repressive histone marks from the *p16^{INK4a}* gene is less understood; however, the analyzed studies point to several possible mechanisms. First, they suggest the involvement of histone demethylases. In particular, levels of H3K27me3 demethylase Jmjd3 were shown to be increased by oncogenic stressors, leading to the removal of repressive histone marks from the *p16^{INK4a}* gene promoter,²⁴ resulting in dissociation of the PRC1 complex, and decondensation of *p16^{INK4a}* gene promoter. Second, Jun dimerization protein 2 (JDP2) may bind and sequester H3K27 away from PRC2.¹⁹

In addition to this reversible repression of the *p16^{INK4a}* gene locus, PRC1 and PRC2 complexes are responsible for irreversible *p16^{INK4a}* gene silencing that occurs in many forms of cancer. Irreversible repression of the *p16^{INK4a}* locus is characterized by trimethylation of H3 at lysine 9 by the PRC2 complex, binding of the HP-1 adaptor molecule, and irreversible binding of the PRC1 complex.²⁵

Regulation of *p16^{INK4a}* gene transcription

The expression of the *p16^{INK4a}* gene can be regulated by several transcription factors.²³ It should be noted that there is complex interplay between positive and negative regulators of *p16^{INK4a}* gene transcription that allows to fine-tune *p16^{INK4a}* gene expression in response to multiple signals to which cells are exposed – e.g., oncogenic signaling leads to the activation of Ras/MEK/MAP kinase. This pathway may lead to increased activity of at least 3 transcription factors that stimulate *p16^{INK4a}* gene expression. One of them is an HMG box containing protein 1 (HBP1). It was shown that HBP1-induced expression of the *p16^{INK4a}* gene may lead to cellular senescence.²⁶

It is also well established that this signal stimulates increased activity of Ets1 or Ets2 transcription factors. These proteins recognize the E-box element located in the *p16^{INK4a}* gene and stimulate its transcription. It is worth noting that other signaling pathways may modulate Ets1/2 transcriptional activity. For example, inhibitor of DNA binding 1 (ID1) prevents the binding of Ets1/2 to the *p16^{INK4a}* gene promoter.²⁷

Another example of fine-tuning *p16^{INK4a}* gene expression is the interaction of AP1 transcription factors with the *p16^{INK4a}* gene promoter. AP-1 transcription factors are known to regulate gene expression in response to a variety of signals, including cytokines, growth factors, stress signals, bacterial and viral infections, and oncogenic stimuli.²⁸ The overexpression of certain proteins, e.g., Jun-B in cells, leads to increased P16^{INK4a} levels

and the premature senescence in primary mouse fibroblast.²⁶ In contrast, another AP1 protein, c-Jun, reduces the expression of *p16^{INK4a}*, promoting cell proliferation.²⁹ It is worth noting that the P16^{INK4a} protein inhibits c-Jun kinase, which is necessary for c-Jun activation and oncogenic transformation induced by ultraviolet (UV) light.³⁰

The role of the *P16* gene and P16^{INK4a} protein in hematological malignancies

In many human cancers, the INK4b/ARF/INK4a locus on chromosome 9p21 is completely deleted. Additionally, inactivation of *p16* at the gene level is observed and may include homozygous deletion, promoter hypermethylation, loss of heterozygosity (LOH), or point mutation. For example, 48% of pancreatic cancer samples contain homozygous deletions of the *p16^{INK4a}* gene, and approx. 73% of hepatocellular carcinoma samples have hypermethylation of the *p16* promoter. While deletions of the *p16* gene and promoter hypermethylation lead to complete loss of the P16 protein, mutations can have variable effects on the activity and function of this protein.³

It has been hypothesized that *p16^{INK4a}* serves as a backup tumor suppressor gene for *p53*. In normal cells where *p53* signaling is unaltered, oncogenic Ras stimulation triggers DNA damage, which in turn leads to activation of *p53*, induction of *p21*, and inhibition of cell proliferation. In numerous cancerous cells, *p53* is rendered nonfunctional, potentially resulting in DNA damage due to hyperproliferation. In such cells, DNA damage may trigger the expression of the *p16^{INK4a}* gene and the onset of cellular senescence. However, when both the *p53* and *p16^{INK4a}* genes are inoperative, this condition facilitates the unchecked proliferation of cancer cells.³¹

Given the prevalence and mortality of hematological malignancies, especially among older individuals with multiple comorbidities, investigators continuously seek new predictive and prognostic markers. A thorough evaluation of a patient's health condition and prognosis before treatment can assist physicians in optimizing and tailoring therapy, ultimately leading to favorable treatment outcomes.³²

In the following sections, we will examine existing data on the significance of the *p16^{INK4a}* gene and the P16^{INK4a} protein as prognostic factors in hematological malignancies. We will explore their involvement in tailoring treatments to individualize and personalize anticancer therapy. Additionally, we will assess the potential influence of deletions, mutations and other alterations of the *p16* gene and P16^{INK4a} protein on the prognosis of patients with hematological malignancies.

Acute myeloid leukemia

Acute myeloid leukemia (AML) is characterized by distinct biological and clinical pathways in patients of different age groups, with older patients often exhibiting altered

gene expression and karyotype abnormalities. The highest incidence of AML is observed in older individuals, which may be related to the expression of *p16^{INK4a}* mRNA in bone marrow stromal cells.³³ Although AML patients often experience remissions following therapy, overall survival (OS) rates remain unsatisfactory.³⁴ The reduced long-term survival rate is primarily due to weaker cytostatic tolerance and therapy resistance in older patients.³³

Abdul-Aziz et al. showed that high levels of the *p16^{INK4a}* gene in bone marrow stem cells are linked to the presence of pro-tumor factors related to senescence-associated secretory phenotype (SASP) and the promotion of the survival of AML cancer cells. Removing *p16^{INK4a}* mRNA stops its effect and slows the growth of the tumor.³⁴

Tschan et al. quantitatively assessed the level of *p16^{INK4a}* and *p14^{ARF}* mRNA expression. Higher amounts of *p16^{INK4a}* and *p14^{ARF}* were found in myeloblasts compared to normal monocytes and granulocytes, according to their study. The obtained results may suggest that increased expression levels of both of these genes participate in the pathogenesis of AML.³⁵ De Jonge et al. conducted a study of *p16^{INK4a}* mRNA expression to identify molecular differences between older and younger AML patients. They concluded that the expression of *p16^{INK4a}* mRNA in older individuals, belonging to the intermediate- and high-risk groups, is much lower than in the group of young patients, and the *p16^{INK4a}* gene may be an independent prognostic factor.³³

Faderl et al. analyzed the deletion of *p16^{INK4a}*, *p14^{ARF}* and *p15^{INK4b}* in 74 patients with AML. Additionally, to determine the phosphorylation of Rb protein in patients with deletions of *p16^{INK4a}*, *p14^{ARF}* and *p15^{INK4b}*, the western blot method was utilized. Deletions of *p16^{INK4a}*, *p14^{ARF}* and *p15^{INK4b}* occurred in 5% of the patients in the studied group, indicating that such chromosomal aberrations occur at a low frequency in patients with AML. The study also compared the complete response (CR) rate of the disease, duration of CR and OS of patients without deletions of *p16^{INK4a}*, *p14^{ARF}* and *p15^{INK4b}* with those with the aforementioned abnormalities. The results suggest that patients with deletions of *p16^{INK4a}*, *p14^{ARF}* and *p15^{INK4b}* have significantly shorter duration of CR and OS rates compared to patients without deletions.³⁶

Acute lymphoblastic leukemia

Radiotherapy, allogeneic hematopoietic stem cell transplantation (allo-HSCT), multidrug treatment, and a better understanding of chromosomal translocations and somatic mutations have improved OS in acute lymphoblastic leukemia (ALL) patients.^{37,38} Young patients and children show significant progress. Prognosis for older patients is still unsatisfactory. This is because chromosomal, clinical and biochemical issues are more frequent. The poor prognosis of older patients is also due to treatment-related mortality and/or less toxic but less effective treatment regimens.³⁹

Prognostic variables for adult ALL patients include age, leukocyte count and cytogenetic abnormalities. Disease risk assessment must be enhanced due to high treatment failures.⁴⁰

Stock et al. examined lymphoblasts for abnormalities of the *p16^{INK4a}*, *Rb* and *p53* genes. Disorders of the *p16^{INK4a}* gene were found in 17 patients. The mutation occurred in 7 patients: 6 with the *Rb* mutation and 3 with the *p53* mutation. All 3 changes occurred in 1 patient. Then, in 5 patients with a detected *p16* gene mutation, CD34⁺ Lin⁻ cells were isolated and immunohistochemical examination was performed. In 3 patients, there was a complete lack of *p16^{INK4a}* expression; in the remaining 2 patients, the expression was reduced. This may indicate that mutations leading to the loss of *p16* expression may be a step in the leukemogenesis of ALL.⁴⁰

Omura-Minamisawa et al. proposed that knocking down the *p16^{INK4a}* gene at the RNA or protein level causes T-cell acute lymphoblastic leukemia (T-ALL). Previous investigations showed DNA loss, mutation or hypermethylation inactivating *p16^{INK4a}*. Authors observed that 93% of T-ALL patients had *p16^{INK4a}* switched off at the DNA, RNA and protein levels. This shows that T-ALL pathogenesis requires *p16^{INK4a}* inactivation.⁴¹

Fizzotti et al. examined DNA samples from patients with hematological malignancies to determine the frequency of homozygous *p16* gene deletion. In 10 of 58 samples (17%) of B-ALL and T-ALL patients, *p16* homozygous deletions were found. Homozygous *p16* deletion patients had more leukocytes and leukemic cells than those with the normal gene. The authors also examined 2 cases of ALL in which DNA samples were available, collected before the start of treatment and after disease progression. In both cases, the occurrence of the *p16* deletion was confirmed during relapse. Therefore, the authors concluded that deletion of the *p16* gene may help identify patients with features of aggressive disease and may be a negative prognostic factor.⁴²

Soenena et al. studied adult ALL patients' P16^{INK4a} protein expression. Patients with negative immunocytochemical tests had significantly worse OS and event-free survival (EFS). This was only found in standard-risk karyotype patients.⁴³

Wang et al. researched the prognostic and clinical effects of *p16* gene deletion in ALL patients. *P16* deletions were found in 33 of 86 cases. Higher leukocyte and decreased platelet counts were associated with the *p16* deletion. Treatment results for EFS and OS were significantly poorer with the *p16* deletion. Allo-HSCT was performed on 22 of 33 *p16* deletion patients. Patients with deletion had prolonged EFS and OS following allo-HSCT. The authors concluded that *p16* deletion is a significant, negative prognostic factor in adult ALL, while performing allo-HSCT in this group of patients markedly improves the prognosis.⁴⁴

Myelodysplastic syndromes

Myelodysplastic syndromes (MDS) is a group of hematopoietic stem cell disorders characterized by inefficient hematopoiesis and frequent transformation to AML.⁴⁵ This disease occurs mainly in older individuals.⁴⁶ Accelerated cell aging, oxidative stress and aberrant DNA methylation may induce MDS.⁴⁷ Currently, many different therapies are used in MDS. However, the only option that guarantees a complete cure is allo-HSCT. Unfortunately, many patients cannot undergo this procedure due to advanced age or concomitant diseases. Therefore, the main goal in the treatment of patients with MDS who cannot undergo allo-HSCT is to prolong and improve quality of life. This is possible thanks to the use of optimized treatment adapted to the patient's opportunities and prognosis.⁴⁸

Wang. et al. conducted a study aimed at determining the impact of cell aging on the development and prognosis of patients with MDS. The results showed increased expression of *p16^{INK4a}* mRNA and P16^{INK4a} protein in cells collected from MDS patients compared to the control group. Interestingly, AML patients showed lower *p16^{INK4a}* mRNA expression compared to samples collected from healthy volunteers and MDS patients. This may suggest that the increased expression of *p16^{INK4a}* mRNA in the cells of MDS patients is associated with the occurrence of this disease.⁴⁹

Other conclusions were presented by Papageorgiou et al., who examined *p16* and *p27* gene alterations in 51 untreated MDS patients. The Southern blot showed no homozygous *p16* deletions. Except for 2 allelic polymorphisms, polymerase chain reaction-single-strand conformation polymorphism (PCR-SSCP) analysis and Sanger sequencing could not find *p16* point mutations. The foregoing data imply that the *p16* gene is not mutated during MDS pathogenesis and that other mechanisms boost expression.⁵⁰

Nakamaki et al. studied *CDK* genes in MDS to see if genetic alterations in these genes affect MDS development and progression. The results showed no alterations in the *p16* gene coding areas, suggesting that genetic anomalies of the gene are rare in MDS and cannot be used as a prognostic factor.⁵¹

Chronic myeloid leukemia

Chronic myeloid leukemia (CML) originates from stem cells. A characteristic genetic abnormality in this disease entity is the chimeric fusion gene *BCR/ABL1*, which arises from the rearrangement of the Philadelphia chromosome t(9;22)(q34;q11). The introduction of molecularly targeted medicines, tyrosine kinase inhibitors (TKIs), has drastically changed the method of treatment and risk assessment in CML. Currently, the most important prognostic factor in CML is the early response to treatment with TKIs.⁵² Every study on the *p16* gene and P16^{INK4a} protein

as a predictive factor was published before TKIs were extensively used.

Lee et al. tested samples collected from healthy donors and patients with granulocytic reactions, and found barely detectable expression of *p16^{INK4a}* mRNA. However, *p16^{INK4a}* mRNA expression was abnormally increased in CML patient samples. *P16^{INK4a}* overexpression in CML patients occurred much more often (80%) than in the control group.⁵³

While studying CML patients' *p16^{INK4a}* suppressor gene expression, Cividin et al. noted other observations. In 11 untreated chronic CML patients, *p16^{INK4a}* mRNA levels were low. Interferon alpha (IFN- α)-treated individuals, especially resistant ones, had significantly higher *p16^{INK4a}* levels. This may show the *p16^{INK4a}* gene's predictive relevance in CML therapy.⁵⁴ Güran et al. examined *p53*, *p16^{INK4a}*, *p15^{INK4b}*, and *p57^{KIP2}* gene mutations and homo/hemizygous deletions in interferon alpha (IFN- α)-treated CML patients. The study examined molecular changes linked to disease progression. Blast crisis occurred in 4 of the 12 study participants during therapy. All 4 instances had *p53*, *p16^{INK4a}* and *p15^{INK4b}* mutations. In the conclusions, the authors observed a correlation between the progression of CML and somatic mutations in *p53*, *p16^{INK4a}* and *p15^{INK4b}*, and suggested that detecting alterations in the genes *p16^{INK4b}* and *p15^{INK4b}*, as well as mutations in *p53*, may serve as prognostic markers in patients with CML.⁵⁵

Xu et al. examined CML blast crises and homozygous *p16* gene deletions. After conducting the analyses, no homozygous deletion of the *p16* gene was found in the chronic phase. Deletion was found in samples collected from patients in myeloid blast crisis, in lymphoid blast crisis and in mixed blast crisis. The results suggest that there is a strong correlation between homozygous deletions of the *p16* gene in lymphoid blast crisis, and conducting PCR testing may help in the early detection of CML patients at risk of blast crisis occurrence.⁵⁶

Mastocytosis

Mastocytosis refers to a number of diseases defined by clonal mast cell proliferation in various organs. It can emerge at any age and take many forms. The somatic KIT D816V mutation affects 90% of adult patients.⁵⁷

Tsujita et al. examined mastocytosis P16^{INK4a} protein expression immunohistochemically. All 4 mastocytosis samples had P16^{INK4a} protein overexpression. The scientists also reported decreased Ki-67 expression in cancer cells. The scientists found that overexpression of the P16^{INK4a} protein ages cancer mast cells and suppresses their growth, reducing mastocytosis.⁵⁸

A review of the currently available literature revealed that the role of the *p16* gene and P16^{INK4a} protein in the prognosis of mastocytosis has not been sufficiently investigated and described.

Chronic lymphocytic leukemia

In Western countries, the most common type of leukemia is chronic lymphocytic leukemia (CLL).⁵⁹ The pathogenic molecular pathways of the disease are unknown.⁶⁰ Patients with active, symptomatic disease or advanced stages of the disease require therapy. When treatment is necessary, there are several options, including targeted therapies. Clinical staging systems provide prognostic information based on physical examination results and blood counts. Early identification of patients who are likely to relapse appears to be the most effective way to avoid progression-related adverse events.⁶¹

According to Tsirigotis et al., CLL patients seldom have *p16* gene mutations. In this study, a total of 34 samples from CLL patients were analyzed. The Southern blot analysis showed non-rearranged bands in 33 out of 34 cases. No homozygous deletions were detected in any of the cases.

The PCR-SSCP analysis of exons 1 and 3 showed a normal migration pattern in all examined cases.

In contrast, the analysis of exon 2 identified an abnormal migration pattern in 2 out of 34 cases.

The methylation analysis of the *p16* gene promoter revealed hypermethylation of CpG islands in 6 out of 34 cases.⁶⁰

Forsterová et al. examined 5 tumor suppressor gene promoter methylations. Abnormal *p16* methylation was observed in 31% of patients. It suggests that the *p16* gene is not important for determining the stage and prognosis of patients with CLL.⁶²

Given the foregoing findings, *p16* gene promoter methylation's significance in CLL's etiology requires conducting a larger number of studies.

Non-Hodgkin lymphoma

Non-Hodgkin lymphomas (NHLs) are lymphoid malignancies with distinct biochemical and clinical characteristics.⁶³ Despite significant advances in therapeutic modalities, the lack of etiological data continues to impede the development of optimal treatment strategies for NHL. Several variables that may coexist in the incidence of these disorders have been explored, but the results were unclear.⁶⁴

Pinyol et al. studied how *p16^{INK4a}* gene alterations cause NHLs. The Southern blot was used to examine the *p16* gene in 95 genomically available lymphomas, including 55 indolent and 40 aggressive cases. *P16* homozygous deletions were found in 10 tumors. In 1 blastoid mantle cell lymphoma (MCL) without DNA, cytogenetic analysis found a 9p21 locus hemizygous deletion. Ultimately, the results suggest that *p16* gene mutations are not common in NHLs.⁶⁵

Fresh tissues from patients with untreated NHLs were tested for homozygous deletions and point mutations

in the *p16* coding areas by Gombart et al. One diffuse large B-cell lymphoma (DLBCL) cell line and 2 uncultured lymphomas: 1 large B-cell and 1 mixed T-cell lymphoma showed homozygous deletions of either the *p16* gene or both the *p15* and *p16* genes. On the other hand, no point mutations were found in the lymphomas or cell lines. These results suggest that the rate of *p15* and *p16* gene alterations in lymphomas is low, but some lymphomas may develop as a result of *p16* and/or *p15* loss.⁶⁶

Liu et al. analyzed NHL patient's tumor samples collected before treatment. The samples were examined for *p16* gene and P16^{INK4a} protein expression abnormalities. Thirty-four of 64 samples had P16^{INK4a} protein, while 45 had *p16* mRNA. Results suggest that post-transcriptional abnormalities may contribute to NHL etiology in some cases.⁶⁷

Villuendas et al. analyzed the expression of P16^{INK4a} in various types of NHLs. Loss of P16^{INK4a} expression was observed in 41 of the 112 samples tested. The loss of P16^{INK4a} expression was observed in all samples that exhibited a high degree of malignancy. Loss of P16^{INK4a} was found more frequently in cases progressing from low-grade lymphomas (e.g., follicular lymphoma) compared to high-grade lymphomas (e.g. DLBCL). The authors suggested that the loss of P16^{INK4a} protein expression contributes to the progression of lymphomas, and gene expression level (assessed before starting treatment) may be a prognostic factor.⁶⁸

Martinez-Delgado et al. examined lymphoid nodes and bone marrow samples for *p16*^{INK4a} and *p15*^{INK4b} methylation. All patients were tested for monoclonal immunoglobulin and T-cell receptor gene rearrangements. Six patients were diagnosed with gene methylation. Two patients showed methylation during therapy. Five instances were never methylated. Disease signs revealed methylation. This suggests that *p16*^{INK4a} methylation may be a valuable disease marker and help detect recurrence.⁶⁹

Hodgkin's lymphoma

Hodgkin's lymphoma (HL) is one of the most common lymphomas.⁷⁰ A characteristic feature of HL and a factor necessary to make the diagnosis is the presence of Reed–Sternberg cells. These cells have a large cell morphology, and cell enlargement is one of the hallmarks of aging.⁷¹ Hodgkin's lymphoma is considered a highly curable disease with first-line chemotherapy and/or radiotherapy. Unfortunately, some patients resist treatment or progress during or after the end of therapy. Numerous HL patients die prematurely due to the late toxic effects of intensive treatment.⁷⁰

Although the same chemotherapy regimen (doxorubicin, bleomycin, vinblastine, and dacarbazine) has been the mainstay of treatment over the past 30 years, risk-adapted approaches have helped to de-escalate therapy in low-risk patients while intensifying treatment in high-risk patients.⁷²

Garcia et al. conducted a study involving immunohistochemical staining of 40 samples collected from patients with HL to elucidate whether *p16* inactivation is involved in the development of this disease entity. Polymerase chain reaction was also utilized to assess exon 1 methylation of the *p16*^{INK4a} gene. Thirty of 37 instances showed a *p16*^{INK4a} loss. Only 7 samples had tumor cell nuclear expression. The PCR analysis found gene hypermethylation in 14 of 23 instances. The *p16*^{INK4a} gene was hypermethylated in 25% of pre-treatment samples and 83% of relapse samples. Methylation may be relevant for HL recurrence. The data also demonstrate that Reed–Sternberg cells lose *p16*^{INK4a} gene expression, which may support the hypothesis that *p16* is involved in HL.⁷³

Calio et. al. examined 147 patients to investigate if the expression of the protein P16^{INK4a} in HL may help clinicians predict EFS. Samples were tested for P16^{INK4a} and P21^{CIP1/WAF} protein levels. The findings revealed that both compounds may be independent EFS prognostic factors. The objective response rate (ORR) was 45% for patients with low P16^{INK4a} expression and 89% for those with high expression.⁷⁴

Plasma cell myeloma

Plasma cell myeloma (PCM) is characterized by infiltration of the bone marrow by malignant plasma cells, which synthesize and secrete monoclonal immunoglobulins (Ig) or their fragments⁷⁵ Plasma cell myeloma mostly affects the elderly population.⁷⁶ In the plasma cells of PCM, cytogenetic abnormalities are frequently detected, which serve as the basis for classifying patients into risk groups.⁷⁷ It is known that abnormalities in genes controlling the cell cycle, including *p16*, contribute to the carcinogenesis of PCM.⁷⁸ The ever-increasing number of medications used to treat PCM has improved the response and OS rates in patients with PCM. However, biomarkers for intensifying, de-escalating or completely changing treatment have not yet been established.⁷⁹

According to Ng et al., up to 2/3 of studied PCM cells have hypermethylation that causes *p16* gene function loss at diagnosis. Patients with plasmablastic transformation have 100% hypermethylated cells that silence the *p16* gene. The results of the studies conducted using cell lines and primary PCM confirm that hypermethylation of *p16* plays a significant role in PCM carcinogenesis.⁸⁰

Wang et al. published a meta-analysis aiming to comprehensively assess the potential role of *p16*^{INK4a} in the pathogenesis of PCM. The research results showed that the frequency of *p16*^{INK4a} methylation was significantly higher in patients with PCM compared to healthy individuals.⁸¹

Chen et al. examined how often the *p16* and *p15* genes are methylated in PCM. In 10 of 22 instances, the *p16* and *p15* genes were methylated. According to the investigators, patients with *p16* and *p15* gene methylation experienced delayed cell apoptosis, an insufficient therapeutic

response and a short OS. This suggests that methylation of the *p16* and *p15* genes is important for PCM apoptosis and prognosis.⁸²

Mateos et al. examined the methylation status of the *p16* gene in samples collected from patients with PCM. Forty-one samples showed methylation. Moreover, the percentage of S-phase plasma cells in these patients was almost 3 times higher than in patients with unmethylated *p16* genes. The authors observed a correlation between the presence of *p16* methylation, an increased level of B2-microglobulin and high values of C-reactive protein (CRP). Patients with the methylated *p16* gene also had shorter OS and progression-free survival (PFS) rates. In results, the authors suggested that methylation of the *p16* gene is a common event in PCM patients at the time of diagnosis and is associated with an increased rate of plasma cell proliferation and a worse prognosis.⁸³

The potential therapeutic implications of targeting *p16* gene and P16^{INK4a} protein in hematological malignancies

The therapeutic potential of targeting the *p16* gene and the P16^{INK4a} protein in various cancers is highly significant.^{84,85}

Based on the data presented in the preceding sections of this review, it is plausible to hypothesize that therapies employed in the treatment of hematological malignancies (often characterized by disruptions in cell cycle regulation) that focus on reactivating or enhancing the expression of the *p16* gene may restore proper cell cycle control and thereby contribute to the inhibition of cancer progression.⁸⁶

The analyzed studies suggest that reactivating or increasing the expression of the *p16* gene can be achieved through gene therapy or epigenetic modifications, such as reducing DNA methylation.⁸⁷ For example, the use of demethylating agents or histone deacetylase (HDAC) inhibitors has shown promise in reactivating the expression of tumor suppressor genes, including those involved in key regulatory pathways disrupted in tumorigenesis.^{88–91}

Li and Seto have shown that HDAC inhibitors, such as suberoylanilide hydroxamic acid (SAHA), can induce the re-expression of silenced genes, including *p16*, thereby promoting cell cycle arrest and apoptosis in cancer cells.⁹²

Furthermore, the combination of these epigenetic therapies with other treatment modalities has been explored. For instance, the integration of demethylating agents with traditional chemotherapy has shown enhanced efficacy in preclinical models of hematological malignancies.^{93,94} Such combination therapies may potentiate the reactivation of P16^{INK4a}, leading to improved therapeutic outcomes and offering a promising avenue for personalized cancer treatment strategies. Li et al. suggested that demethylation of the *p16* gene may enhance the sensitivity of cancer cells

to anti-cancer treatments, making cancer cells more susceptible to traditional chemotherapy and thereby rendering it a more effective treatment method.⁹⁵

The P16^{INK4a} protein plays a crucial role in cellular senescence, a state characterized by the irreversible cessation of cell division in previously proliferative cells. This process acts as a critical barrier to tumor progression by limiting the replicative potential of cancer cells. Employing therapeutic strategies to increase P16^{INK4a} levels could, therefore, promote cellular senescence in cancer cells, effectively halting their proliferation and inducing a state resistant to further malignant transformation.^{7,96}

The potential of P16^{INK4a} to induce senescence has been substantiated by several studies. For example, Alcorta et al. suggested that overexpression of P16^{INK4a} in human fibroblasts leads to premature senescence, underscoring its role in cell cycle regulation and tumor suppression.⁹⁷ Similarly, Collado et al., found that oncogene-induced senescence is often mediated by the upregulation of P16^{INK4a}, highlighting its significance in tumor biology.⁹⁸

Integrating therapies targeting the P16^{INK4a} protein with other molecularly targeted drugs, such as TKIs or immune checkpoint inhibitors (CPIs), holds significant potential for achieving synergistic effects and thereby improving overall treatment efficacy. The P16^{INK4a} protein, a critical tumor suppressor, inhibits cyclin-dependent kinases 4 and 6 (CDK4/6), which play a pivotal role in regulating the cell cycle. By targeting these mechanisms, combination therapies can simultaneously disrupt multiple pathways essential for cancer cell survival, enhancing therapeutic outcomes. Preclinical and clinical studies have demonstrated that CDK4/6 inhibitors, such as palbociclib, ribociclib and abemaciclib, show promising results in treating various cancers, particularly those characterized by dysfunction of the tumor suppressor P16^{INK4a}. These inhibitors work by halting cell cycle progression, which is particularly effective in cancers with disrupted cell cycle regulation. Such cancers include not only solid tumors like breast cancer but also hematological malignancies, where aberrations in cell cycle regulators are common.^{99,100–103}

For instance, the combination of the CDK4/6 inhibitor palbociclib with endocrine therapy has shown improved outcomes in hormone receptor-positive breast cancer. In a study by Finn et al., patients receiving palbociclib in combination with letrozole exhibited significantly prolonged PFS compared to those receiving letrozole alone. This combination therapy exemplifies how targeting the cell cycle machinery can enhance therapeutic efficacy.¹⁰⁴ This finding is supported by multiple studies, including the PALOMA-2 and PALOMA-3 trials, which demonstrated that palbociclib combined with letrozole or fulvestrant significantly improved median PFS in hormone receptor-positive, HER2-negative advanced breast cancer.^{105,106}

Furthermore, CPIs such as pembrolizumab and nivolumab, which target PD-1/PD-L1 pathways, have

revolutionized cancer therapy by enhancing the immune system's ability to target tumors. Combining these CPIs with CDK4/6 inhibitors has shown potential in preclinical models to improve antitumor responses by modulating the tumor microenvironment and enhancing immune-mediated tumor cell killing.¹⁰⁷

Finally, analyzed studies have demonstrated that various cytogenetic and molecular genetic abnormalities in cancer cells contribute to resistance against standard anti-cancer treatments. The data previously discussed suggest that evaluating the status of the *p16* gene and P16^{INK4a} protein offers valuable prognostic information. This assessment can be instrumental in personalizing or targeting therapy plans, thereby improving treatment outcomes.

Limitations

This systematic review faces one main limitation. The key issue is study heterogeneity. The inclusion of studies with differences in population demographics, intervention methods, study designs, and methodological quality presents a challenge to the consistency of the synthesized findings. This variation across the included studies makes it more difficult to combine and interpret the results.

Conclusions

The literature review elucidates the intricate interplay between the physiological functions and altered expression patterns of the *p16* gene and its corresponding P16^{INK4a} protein, discernibly linked to the etiology of select hematological malignancies. Noteworthy is the recognition by select authors, whose work is surveyed within the review, of the *p16*^{INK4a} gene and its protein product as discerning prognostic markers, underscored by their prognostic relevance concerning key clinical endpoints such as OS and EFS.

Furthermore, scholarly discourse extends to deliberations on the potential role of the *p16* gene and P16^{INK4a} protein in facilitating the customization and refinement of anticancer therapeutic regimens, thereby accentuating the burgeoning scope for prospective inquiry and scholarly elucidation.


Nevertheless, it is incumbent upon researchers to acknowledge that our current comprehension of the involvement of the *p16* gene and P16^{INK4a} protein in the pathogenic cascade of numerous cancers remains only partially elucidated. This caveat is particularly salient within the context of hematological malignancies, a notably diverse and expansive spectrum. Consequently, there exists a manifold of disease entities yet to be scrutinized for putative correlations with the *p16* gene and its protein counterpart. Moreover, the presence of incongruences in findings across select investigations underscores the exigency for sustained scholarly engagement and methodological

refinement, thereby underscoring the imperative for a meticulous and iterative exploration of this intricate domain to furnish the scientific community with the most cogent and comprehensive insights.


ORCID iDs

Paula Jabłonowska-Babij  <https://orcid.org/0000-0001-6984-2116>

Maciej Majcherek  <https://orcid.org/0000-0001-6064-296X>

Anna Kłopot  <https://orcid.org/0000-0002-0556-3414>

Agnieszka Szeremet  <https://orcid.org/0000-0002-1897-3180>

Tomasz Wróbel  <https://orcid.org/0000-0002-6612-3535>

Anna Czyż  <https://orcid.org/0000-0001-6641-0182>

References

1. Frenkel M, Sapire K. Complementary and integrative medicine in hematologic malignancies: Questions and challenges. *Curr Oncol Rep.* 2017;19(12):79. doi:10.1007/s11912-017-0635-0
2. Zhang N, Wu J, Wang Q, et al. Global burden of hematologic malignancies and evolution patterns over the past 30 years. *Blood Cancer J.* 2023;13(1):82. doi:10.1038/s41408-023-00853-3
3. Li J, Poi MJ, Tsai MD. Regulatory mechanisms of tumor suppressor P16^{INK4a} and their relevance to cancer. *Biochemistry (Moscow).* 2011; 50(25):5566–5582. doi:10.1021/bi200642e
4. Serrano M, Hannon GJ, Beach D. A new regulatory motif in cell-cycle control causing specific inhibition of cyclin D/CDK4. *Nature.* 1993; 366(6456):704–707. doi:10.1038/366704a0
5. LaPak KM, Burd CE. The molecular balancing act of p16^{INK4a} in cancer and aging. *Mol Cancer Res.* 2014;12(2):167–183. doi:10.1158/1541-7786.MCR-13-0350
6. Farooq U, Notani D. Transcriptional regulation of INK4/ARF locus by cis and trans mechanisms. *Front Cell Dev Biol.* 2022;10:948351. doi:10.3389/fcell.2022.948351
7. Safwan-Zaiter H, Wagner N, Wagner KD. P16^{INK4a}: More than a senescence marker. *Life.* 2022;12(9):1332. doi:10.3390/life12091332
8. Pasmant E, Laurendeau I, Héron D, Vidaud M, Vidaud D, Bièche I. Characterization of a germ-line deletion, including the entire *INK4/ARF* locus, in a melanoma-neural system tumor family: Identification of *ANRIL*, an antisense noncoding RNA whose expression coclusters with *ARF*. *Cancer Res.* 2007;67(8):3963–3969. doi:10.1158/0008-5472.CAN-06-2004
9. Kim WY, Sharpless NE. The regulation of INK4/ARF in cancer and aging. *Cell.* 2006;127(2):265–275. doi:10.1016/j.cell.2006.10.003
10. Zhang Y, Xiong Y, Yarbrough WG. ARF promotes MDM2 degradation and stabilizes p53: ARF-INK4a locus deletion impairs both the Rb and p53 tumor suppression pathways. *Cell.* 1998;92(6):725–734. doi:10.1016/S0092-8674(00)81401-4
11. Li J, Mahajan A, Tsai MD. Ankyrin repeat: A unique motif mediating protein–protein interactions. *Biochemistry (Moscow).* 2006;45(51): 15168–15178. doi:10.1021/bi062188q
12. Hirai H, Roussel MF, Kato JY, Ashmun RA, Sherr CJ. Novel INK4 proteins, p19 and p18, are specific inhibitors of the cyclin D-dependent kinases CDK4 and CDK6. *Mol Cell Biol.* 1995;15(5):2672–2681. doi:10.1128/MCB.15.5.2672
13. Gil J, Peters G. Regulation of the INK4b–ARF–INK4a tumour suppressor locus: All for one or one for all. *Nat Rev Mol Cell Biol.* 2006;7(9): 667–677. doi:10.1038/nrm1987
14. Carnero A, Hannon GJ. The INK4 family of CDK inhibitors. *Curr Top Microbiol Immunol.* 1998;227:43–55. doi:10.1007/978-3-642-71941-7_3
15. Byeon IJL, Li J, Ericson K, et al. Tumor suppressor p16^{INK4a}: Determination of solution structure and analyses of its interaction with cyclin-dependent kinase 4. *Mol Cell.* 1998;1(3):421–431. doi:10.1016/S1097-2765(00)80042-8
16. Russo AA, Tong L, Lee JO, Jeffrey PD, Pavletich NP. Structural basis for inhibition of the cyclin-dependent kinase Cdk6 by the tumour suppressor p16^{INK4a}. *Nature.* 1998;395(6699):237–243. doi:10.1038/26155
17. Nishiwaki E, Turner SL, Harju S, et al. Regulation of CDK7–carboxyl-terminal domain kinase activity by the tumor suppressor p16^{INK4a} contributes to cell cycle regulation. *Mol Cell Biol.* 2000;20(20):7726–7734. doi:10.1128/MCB.20.20.7726-7734.2000

18. Serizawa H. Cyclin-dependent kinase inhibitor p16^{INK4A} inhibits phosphorylation of RNA polymerase II by general transcription factor TFIIF. *J Biol Chem*. 1998;273(10):5427–5430. doi:10.1074/jbc.273.10.5427
19. Nakade K, Wasylyk B, Yokoyama KK. Epigenetic regulation of p16^{INK4a} and Arf by JDP2 in cellular senescence. *Biomol Concepts*. 2010;1(1):49–58. doi:10.1515/bmc.2010.008
20. Aguilo F, Zhou MM, Walsh MJ. Long noncoding RNA, polycomb, and the ghosts haunting *INK4b-Arf-INK4a* expression. *Cancer Res*. 2011;71(16):5365–5369. doi:10.1158/0008-5472.CAN-10-4379
21. Margueron R, Reinberg D. The Polycomb complex PRC2 and its mark in life. *Nature*. 2011;469(7330):343–349. doi:10.1038/nature09784
22. Geng Z, Gao Z. Mammalian PRC1 complexes: Compositional complexity and diverse molecular mechanisms. *Int J Mol Sci*. 2020;21(22):8594. doi:10.3390/ijms21228594
23. Rayess H, Wang MB, Srivatsan ES. Cellular senescence and tumor suppressor gene *p16*. *Int J Cancer*. 2012;130(8):1715–1725. doi:10.1002/ijc.27316
24. Agger K, Cloos PAC, Rudkjær L, et al. The H3K27me3 demethylase JMJD3 contributes to the activation of the *INK4A-Arf* locus in response to oncogene- and stress-induced senescence. *Genes Dev*. 2009;23(10):1171–1176. doi:10.1101/gad.510809
25. Bannister AJ, Zegerman P, Partridge JF, et al. Selective recognition of methylated lysine 9 on histone H3 by the HP1 chromo domain. *Nature*. 2001;410(6824):120–124. doi:10.1038/35065138
26. Li H, Wang W, Liu X, Paulson KE, Yee AS, Zhang X. Transcriptional factor HBP1 targets P16^{INK4A}, upregulating its expression and consequently is involved in Ras-induced premature senescence. *Oncogene*. 2010;29(36):5083–5094. doi:10.1038/ncr.2010.252
27. Ohtani N, Zebedee Z, Huot TJG, et al. Opposing effects of Ets and Id proteins on p16^{INK4a} expression during cellular senescence. *Nature*. 2001;409(6823):1067–1070. doi:10.1038/35059131
28. Hess J, Angel P, Schorpp-Kistner M. AP-1 subunits: Quarrel and harmony among siblings. *J Cell Sci*. 2004;117(25):5965–5973. doi:10.1242/jcs.01589
29. Ke H, Harris R, Colloff JL, et al. The c-Jun NH2-terminal kinase 2 plays a dominant role in human epidermal neoplasia. *Cancer Res*. 2010;70(8):3080–3088. doi:10.1158/0008-5472.CAN-09-2923
30. Choi BY, Choi HS, Ko K, et al. The tumor suppressor p16^{INK4a} prevents cell transformation through inhibition of c-Jun phosphorylation and AP-1 activity. *Nat Struct Mol Biol*. 2005;12(8):699–707. doi:10.1038/nsmb960
31. Yamakoshi K, Takahashi A, Hirota F, et al. Real-time in vivo imaging of p16^{INK4a} reveals cross talk with p53. *J Cell Biol*. 2009;186(3):393–407. doi:10.1083/jcb.200904105
32. Pasqui DM, Latorraca CDOC, Pacheco RL, Riera R. CAR-T cell therapy for patients with hematological malignancies: A systematic review. *Eur J Haematol*. 2022;109(6):601–618. doi:10.1111/ejh.13851
33. De Jonge HJM, De Bont ESJM, Valk PJM, et al. AML at older age: Age-related gene expression profiles reveal a paradoxical down-regulation of p16^{INK4A} mRNA with prognostic significance. *Blood*. 2009;114(14):2869–2877. doi:10.1182/blood-2009-03-212688
34. Abdul-Aziz AM, Sun Y, Hellmich C, et al. Acute myeloid leukemia induces protumoral p16^{INK4a}-driven senescence in the bone marrow microenvironment. *Blood*. 2019;133(5):446–456. doi:10.1182/blood-2018-04-845420
35. Tschan MP, Vonlanthen S, Cajot JF, et al. Different p16^{INK4a} and p14^{ARF} expression patterns in acute myeloid leukaemia and normal blood leukocytes. *Leuk Lymphoma*. 2001;42(5):1077–1087. doi:10.3109/10428190109097728
36. Faderl S, Kantarjian HM, Estey E, et al. The prognostic significance of *p16^{INK4a}/p14^{ARF}* locus deletion and MDM-2 protein expression in adult acute myelogenous leukemia. *Cancer*. 2000;89(9):1976–1982. PMID:11064355.
37. Chang JH, Poppe MM, Hua C, Marcus KJ, Esiashvili N. Acute lymphoblastic leukemia. *Pediatr Blood Cancer*. 2021;68(Suppl 2):e28371. doi:10.1002/pbc.28371
38. DeAngelo DJ, Jabbour E, Advani A. Recent advances in managing acute lymphoblastic leukemia. *Am Soc Clin Oncol Educ Book*. 2020;40:330–342. doi:10.1200/EDBK_280175
39. Rousselot P, Delannoy A. Optimal pharmacotherapeutic management of acute lymphoblastic leukaemia in the elderly. *Drugs Aging*. 2011;28(9):749–764. doi:10.2165/11592850-000000000-00000
40. Stock W, Tsai T, Golden C, et al. Cell cycle regulatory gene abnormalities are important determinants of leukemogenesis and disease biology in adult acute lymphoblastic leukemia. *Blood*. 2000;95(7):2364–2371. PMID:10733508.
41. Omura-Minamisawa M, Diccianni MB, Batova A, et al. Universal inactivation of both p16 and p15 but not downstream components is an essential event in the pathogenesis of T-cell acute lymphoblastic leukemia. *Clin Cancer Res*. 2000;6(4):1219–1228. PMID:10778944.
42. Fizzotti M, Cimino G, Pisegna S, et al. Detection of homozygous deletions of the cyclin-dependent kinase 4 inhibitor (*p16*) gene in acute lymphoblastic leukemia and association with adverse prognostic features. *Blood*. 1995;85(10):2685–2690. PMID:7742527.
43. Soenen V, Lepelletier P, Gyan E, et al. Prognostic significance of p16^{INK4a} immunocytochemistry in adult ALL with standard risk karyotype. *Leukemia*. 2001;15(7):1054–1059. doi:10.1038/sj.leu.2402153
44. Wang Y, Chen G, Cao R, et al. Allogeneic hematopoietic stem cell transplantation improves the prognosis of p16-deleted adult patients with acute lymphoblastic leukemia. *Pharmacogenomics*. 2017;18(1):77–84. doi:10.2217/pgs-2016-0075
45. Lee P, Yim R, Yung Y, Chu HT, Yip PK, Gill H. Molecular targeted therapy and immunotherapy for myelodysplastic syndrome. *Int J Mol Sci*. 2021;22(19):10232. doi:10.3390/ijms221910232
46. Wells RA, Buckstein R, Reznovitz J. Myelodysplastic syndrome. *Can Med Assoc J*. 2016;188(10):751. doi:10.1503/cmaj.151077
47. Gonçalves AC, Cortesão E, Oliveiros B, et al. Oxidative stress levels are correlated with P15 and P16 gene promoter methylation in myelodysplastic syndrome patients. *Clin Exp Med*. 2016;16(3):333–343. doi:10.1007/s10238-015-0357-2
48. Sanchez JF. Treatment of myelodysplastic syndromes in elderly patients. *Adv Ther*. 2011;28(Suppl 2):1–9. doi:10.1007/s12325-011-0001-9
49. Wang YY, Cen JN, He J, et al. Accelerated cellular senescence in myelodysplastic syndrome. *Exp Hematol*. 2009;37(11):1310–1317. doi:10.1016/j.exphem.2009.09.002
50. Papageorgiou SG, Pappa V, Papageorgiou E, et al. Absence of p16 and p27 gene rearrangements and mutations in de novo myelodysplastic syndromes. *Eur J Haematol*. 2005;75(3):193–198. doi:10.1111/j.1600-0609.2005.00475.x
51. Nakamaki T, Bartram C, Seriu T, et al. Molecular analysis of the cyclin-dependent kinase inhibitor genes, *p15*, *p16*, *p18* and *p19*, in the myelodysplastic syndromes. *Leuk Res*. 1997;21(3):235–240. doi:10.1016/S0145-2126(96)00115-4
52. Uehara E, Takeuchi S, Yang Y, et al. Aberrant methylation in promoter-associated CpG islands of multiple genes in chronic myelogenous leukemia blast crisis. *Oncol Lett*. 2012;3(1):190–192. doi:10.3892/ol.2011.419
53. Lee YK, Park JY, Kang HJ, Cho HC. Overexpression of p16^{INK4A} and p14^{ARF} in haematological malignancies. *Clin Lab Haematol*. 2003;25(4):233–237. doi:10.1046/j.1365-2257.2003.00520.x
54. Cividin M, Ayrault O, Sorel N, et al. Expression of the cell cycle regulators p14^{ARF} and p16^{INK4a} in chronic myeloid leukemia. *Leuk Res*. 2006;30(10):1273–1278. doi:10.1016/j.leukres.2006.02.002
55. Güran S, Başçe M, Beyan C, Korkmaz K, Yalçın A. P53, p15INK4B, p16INK4A and p57KIP2 mutations during the progression of chronic myeloid leukemia. *Haematologia (Budap)*. 1998;29(3):181–193. PMID:10069444.
56. Xu D, Hong W, Wang S. Relationship between blast crisis of chronic myeloid leukemias and abnormality of p16 and calcitonin genes [in Chinese]. *Zhonghua Zhong Liu Za Zhi*. 2000;22(2):151–153. PMID:11776646.
57. Broesby-Olsen S, Kristensen TK, Agertoft L, et al. Mastocytosis [in Danish]. *Ugeskr Laeger*. 2016;178(7):V10150854. PMID:27063008.
58. Tsujita J, Doi K, Nakahara M, et al. Overexpression of p16^{INK4a} in mastocytosis (urticarial pigmentosa). *Fukuoka Igaku Zasshi*. 2016;107(1):12–17. PMID:27333655.
59. Hallek M, Shanafelt TD, Eichhorst B. Chronic lymphocytic leukaemia. *Lancet*. 2018;391(10129):1524–1537. doi:10.1016/S0140-6736(18)30422-7
60. Tsigotitis P, Pappa V, Labropoulos S, et al. Mutational and methylation analysis of the cyclin-dependent kinase 4 inhibitor (*p16^{INK4A}*) gene in chronic lymphocytic leukemia. *Eur J Haematol*. 2006;76(3):230–236. doi:10.1111/j.1600-0609.2005.00604.x
61. Hallek M, Al-Sawaf O. Chronic lymphocytic leukemia: 2022 update on diagnostic and therapeutic procedures. *Am J Hematol*. 2021;96(12):1679–1705. doi:10.1002/ajh.26367

62. Forsterová K, Votavová H, Schwarz J, Karban J, Stuka C, Trněný M. Advanced RAI stage in patients with chronic lymphocytic leukaemia correlates with simultaneous hypermethylation of plural tumour suppressor genes. *Folia Biol (Praha)*. 2010;56(4):158–164. PMID:20974048.
63. Ansell SM. Non-hodgkin lymphoma: Diagnosis and treatment. *Mayo Clin Proc*. 2015;90(8):1152–1163. doi:10.1016/j.mayocp.2015.04.025
64. Carli PM, Maynadié M. Epidemiology and etiology of non-Hodgkin's lymphoma [in French]. *Rev Prat*. 2002;52(9):945–950. PMID:12063759.
65. Pinyol M, Cobo F, Bea S, et al. *p16^{INK4a}* gene inactivation by deletions, mutations, and hypermethylation is associated with transformed and aggressive variants of non-Hodgkin's lymphomas. *Blood*. 1998; 91(8):2977–2984. PMID:9531609.
66. Gombart AF, Morosetti R, Miller CW, Said JW, Koeffler HP. Deletions of the cyclin-dependent kinase inhibitor genes *p16^{INK4A}* and *p15^{INK4B}* in non-Hodgkin's lymphomas. *Blood*. 1995;86(4):1534–1539. PMID:7632961.
67. Liu M, Lou F, Ding H. Expression of *p16* gene in malignant lymphoma detected by immunohistochemical and in situ hybridization techniques [in Chinese]. *Zhonghua Bing Li Xue Za Zhi*. 1998;27(5):366–369. PMID:11245014.
68. Villuendas R, Sánchez-Beato M, Martínez JC, et al. Loss of *p16^{INK4A}* protein expression in non-Hodgkin's lymphomas is a frequent finding associated with tumor progression. *Am J Pathol*. 1998;153(3):887–897. doi:10.1016/S0002-9440(10)65630-1
69. Martínez-Delgado B, Richart A, García MJ, et al. Hypermethylation of *P16^{INK4a}* and *P15^{INK4b}* genes as a marker of disease in the follow-up of non-Hodgkin's lymphomas. *Br J Haematol*. 2000;109(1):97–103. doi:10.1046/j.1365-2141.2000.01991.x
70. Brice P, De Kerviler E, Friedberg JW. Classical Hodgkin lymphoma. *Lancet*. 2021;398(10310):1518–1527. doi:10.1016/S0140-6736(20)32207-8
71. Gopas J, Stern E, Zurgil U, et al. Reed–Sternberg cells in Hodgkin's lymphoma present features of cellular senescence. *Cell Death Dis*. 2016;7(11):e2457. doi:10.1038/cddis.2016.185
72. Shanbhag S, Ambinder RF. Hodgkin lymphoma: A review and update on recent progress. *CA Cancer J Clin*. 2018;68(2):116–132. doi:10.3322/caac.21438
73. García JF, Villuendas R, Algara P, et al. Loss of *p16* protein expression associated with methylation of the *p16^{INK4A}* gene is a frequent finding in Hodgkin's disease. *Lab Invest*. 1999;79(12):1453–1459. PMID:10616196.
74. Calì A, Zamò A, Ponzoni M, et al. Cellular senescence markers *p16^{INK4a}* and *p21^{CIP1/WAF}* are predictors of Hodgkin lymphoma outcome. *Clin Cancer Res*. 2015;21(22):5164–5172. doi:10.1158/1078-0432.CCR-15-0508
75. Kastrinakis NG, Gorgoulis VG, Foukas PG, Dimopoulos MA, Kittas C. Molecular aspects of multiple myeloma. *Ann Oncol*. 2000;11(10):1217–1228. doi:10.1023/A:1008331714186
76. Zweegman S, Engelhardt M, Larocca A. Elderly patients with multiple myeloma: Towards a frailty approach? *Curr Opin Oncol*. 2017; 29(5):315–321. doi:10.1097/CCO.0000000000000395
77. Fonseca R, Barlogie B, Bataille R, et al. Genetics and cytogenetics of multiple myeloma. *Cancer Res*. 2004;64(4):1546–1558. doi:10.1158/0008-5472.CAN-03-2876
78. Park G, Kang SH, Lee JH, et al. Concurrent *p16* methylation pattern as an adverse prognostic factor in multiple myeloma: A methylation-specific polymerase chain reaction study using two different primer sets. *Ann Hematol*. 2011;90(1):73–79. doi:10.1007/s00277-010-1043-9
79. Wallington-Beddoe CT, Mynott RL. Prognostic and predictive biomarker developments in multiple myeloma. *J Hematol Oncol*. 2021; 14(1):151. doi:10.1186/s13045-021-01162-7
80. Ng M, Wong M, Lo K. DNA methylation changes and multiple myeloma. *Leuk Lymphoma*. 1999;34(5–6):463–472. doi:10.3109/10428199909058473
81. Wang X, Zhu YB, Cui HP, Yu TT. Aberrant promoter methylation of *p15^{INK4b}* and *p16^{INK4a}* genes may contribute to the pathogenesis of multiple myeloma: A meta-analysis. *Tumor Biol*. 2014;35(9):9035–9043. doi:10.1007/s13277-014-2054-2
82. Chen W, Wu Y, Zhu J, Liu J, Tan S, Xia C. Methylation of *p16* and *p15* genes in multiple myeloma. *Chin Med Sci J*. 2002;17(2):101–105. PMID:12906163.
83. Mateos MV, García-Sanz R, López-Pérez R, et al. Methylation is an inactivating mechanism of the *p16* gene in multiple myeloma associated with high plasma cell proliferation and short survival. *Br J Haematol*. 2002;118(4):1034–1040. doi:10.1046/j.1365-2141.2002.03749.x
84. Witkiewicz AK, Knudsen KE, Dicker AP, Knudsen ES. The meaning of *p16^{INK4a}* expression in tumors: Functional significance, clinical associations and future developments. *Cell Cycle*. 2011;10(15):2497–2503. doi:10.4161/cc.10.15.16776
85. Zhao R, Choi BY, Lee MH, Bode AM, Dong Z. Implications of genetic and epigenetic alterations of CDKN2A (*p16* *INK4a*) in cancer. *EBioMedicine*. 2016;8:30–39. doi:10.1016/j.ebiom.2016.04.017
86. Gonzalez-Paz N, Chng WJ, McClure RF, et al. Tumor suppressor *p16* methylation in multiple myeloma: Biological and clinical implications. *Blood*. 2007;109(3):1228–1232. doi:10.1182/blood-2006-05-024661
87. Nandakumar V, Vaid M, Katiyar SK. (–)-Epigallocatechin-3-gallate reactivates silenced tumor suppressor genes, *Cip1/p21* and *p16INK4a*, by reducing DNA methylation and increasing histones acetylation in human skin cancer cells. *Carcinogenesis*. 2011;32(4):537–544. doi:10.1093/carcin/bgq285
88. Ruzic D, Djoković N, Srdić-Rajić T, Echeverria C, Nikolic K, Santibanez JF. Targeting histone deacetylases: Opportunities for cancer treatment and chemoprevention. *Pharmaceutics*. 2022;14(1):209. doi:10.3390/pharmaceutics14010209
89. Roche J, Bertrand P. Inside HDACs with more selective HDAC inhibitors. *Eur J Med Chem*. 2016;121:451–483. doi:10.1016/j.ejmech.2016.05.047
90. Jung M, Brosch G, Kölle D, Scherf H, Gerhäuser C, Loidl P. Amide analogues of trichostatin A as inhibitors of histone deacetylase and inducers of terminal cell differentiation. *J Med Chem*. 1999;42(22):4669–4679. doi:10.1021/jm991091h
91. Kim JK, Noh JH, Eun JW, et al. Targeted inactivation of HDAC2 restores *p16INK4a* activity and exerts antitumor effects on human gastric cancer. *Mol Cancer Res*. 2013;11(1):62–73. doi:10.1158/1541-7786.MCR-12-0332
92. Li Y, Seto E. HDACs and HDAC inhibitors in cancer development and therapy. *Cold Spring Harb Perspect Med*. 2016;6(10):a026831. doi:10.1101/cshperspect.a026831
93. Howell PM, Liu Z, Khong HT. Demethylating agents in the treatment of cancer. *Pharmaceutics*. 2010;3(7):2022–2044. doi:10.3390/ph3072022
94. Xia Y, Sun M, Huang H, Jin WL. Drug repurposing for cancer therapy. *Sig Transduct Target Ther*. 2024;9(1):92. doi:10.1038/s41392-024-01808-1
95. Li P, Zhang X, Gu L, Zhou J, Deng D. *P16* methylation increases the sensitivity of cancer cells to the CDK4/6 inhibitor palbociclib. *PLoS One*. 2019;14(10):e0223084. doi:10.1371/journal.pone.0223084
96. He S, Sharpless NE. Senescence in health and disease. *Cell*. 2017; 169(6):1000–1011. doi:10.1016/j.cell.2017.05.015
97. Alcorta AD, Xiong Y, Phelps D, Hannon G, Beach D, Barrett JC. Involvement of the cyclin-dependent kinase inhibitor *p16* (*INK4a*) in replicative senescence of normal human fibroblasts. *Proc Natl Acad Sci U S A*. 1996;93(24):13742–13747. doi:10.1073/pnas.93.24.13742
98. Collado M, Gil J, Efeyan A, et al. Senescence in premalignant tumours. *Nature*. 2005;436(7051):642. doi:10.1038/436642a
99. Yang J, Friedman R. Combination strategies to overcome drug resistance in FLT⁺ acute myeloid leukaemia. *Cancer Cell Int*. 2023;23(1):161. doi:10.1186/s12935-023-03000-x
100. Dubey R, Makhija R, Sharma A, Sahu A, Asati V. Unveiling the promise of pyrimidine-modified CDK inhibitors in cancer treatment. *Bioorg Chem*. 2024;149:107508. doi:10.1016/j.bioorg.2024.107508
101. Maylina L, Kambayashi S, Baba K, Igase M, Mizuno T, Okuda M. Decreased sensitivity of cyclin-dependent kinase 4/6 inhibitors, palbociclib and abemaciclib to canine lymphoma cells with high *p16* protein expression and low retinoblastoma protein phosphorylation. *J Vet Med Sci*. 2023;85(1):99–104. doi:10.1292/jvms.22-0498
102. Tanaka Y, Momose S, Tabayashi T, et al. Abemaciclib, a CDK4/6 inhibitor, exerts preclinical activity against aggressive germinal center-derived B-cell lymphomas. *Cancer Sci*. 2020;111(2):749–759. doi:10.1111/cas.14286

103. Wu Y, Shrestha P, Heape NM, Yarchoan R. CDK4/6 inhibitors sensitize gammaherpesvirus-infected tumor cells to T-cell killing by enhancing expression of immune surface molecules. *J Transl Med.* 2022;20(1):217. doi:10.1186/s12967-022-03400-z
104. Finn RS, Martin M, Rugo HS, et al. Palbociclib and letrozole in advanced breast cancer. *N Engl J Med.* 2016;375(20):1925–1936. doi:10.1056/NEJMoa1607303
105. Finn RS, Rugo HS, Gelmon KA, et al. Long-term pooled safety analysis of palbociclib in combination with endocrine therapy for hormone receptor-positive/human epidermal growth factor receptor 2-negative advanced breast cancer: Updated analysis with up to 5 years of follow-up. *Oncologist.* 2021;26(5):e749–e755. doi:10.1002/onco.13684
106. DeMichele A, Cristofanilli M, Brufsky A, et al. Comparative effectiveness of first-line palbociclib plus letrozole versus letrozole alone for HR⁺/HER2⁻ metastatic breast cancer in US real-world clinical practice. *Breast Cancer Res.* 2021;23(1):37. doi:10.1186/s13058-021-01409-8
107. Goel S, DeCristo MJ, Watt AC, et al. CDK4/6 inhibition triggers anti-tumour immunity. *Nature.* 2017;548(7668):471–475. doi:10.1038/nature23465

Best practice approaches to social prescribing in European Primary Care: A Delphi protocol focused on link workers

*Ferdinando Petrazzuoli^{1,2,A–F}, *Josep Vidal-Alaball^{3,4,A–F}, Joyce Kenkre^{5,4,A,D–F}, Thomas Kloppe^{6,4,A–F}, Sinah Evers^{4,A,D–F}, Hendrik Napierala^{7,4,A,D–F}, Jean-Pierre Jacquet^{8,4,A–F}, Wolfram J. Herrmann^{7,4,A,D–F}, Natasa Mrduljaš-Đujić^{9,2,A,D–F}, Andrea Neculau^{10,2,D–F}, Katerina Javorska^{11,2,A,D–F}, David Halata^{11,4,A,B,E,F}, Miriam Dolan^{12,4,A,D–F}, Joanne Robins^{4,A,D–F}, Patrick Ouvrard^{4,A,D–F}, Juan Manuel Mendive^{13,4,A,D–F}, Carmen López Fando^{4,A,D–F}, Jane Randall-Smith^{4,A,D–F}, Erwin Rebhander^{14,4,A,D–F}, Sara Paternoster^{15,A,B,D–F}, Hans Thulesius^{1,2,A,D–F}, Sian Brand^{16,A,D–F}, Gindrovel Dumitra^{17,4,A,B,E,F}, Donata Kurpas^{18,2,A,D–F}

¹ Department of Clinical Sciences in Malmö, Centre for Primary Health Care Research, Lund University, Sweden

² European General Practice Research Network (EGPRN)

³ Research and Innovation Unit in Primary Care of Central Catalonia, Catalan Health Institute/Jordi Gol Institute for Primary Care Research (IDIAPJGol)/Fundació Institut Universitari per a la Recerca a l'Atenció Primària de Salut Jordi Gol i Gurina, Manresa, Spain

⁴ World Organization for Colleges, Academies and Associations for General Practitioners (WONCA) Europe Social Prescribing and Community Orientation Special Interest Group, Paris, France

⁵ Life Sciences and Education, University of South Wales, Cardiff, UK

⁶ Department of General Practice and Primary Care, University Medical Center Hamburg-Eppendorf, Germany

⁷ Institute of General Practice and Family Medicine, Charité – Universitätsmedizin, Corporate Member of Freie Universität Berlin and Humboldt-Universität zu Berlin, Germany

⁸ French College of General Practice, Paris, France

⁹ Department of Family Medicine, University of Split, Specialist's Family Medicine Office Postira, Croatia

¹⁰ Department of Fundamental, Clinical and Prophylactic Sciences, Transylvania University of Braşov, Romania

¹¹ Department of Preventive Medicine, Faculty of Medicine in Hradec Kralove, Charles University, Czech Republic

¹² Department of General Practice, Medical School Queen's University Belfast, UK

¹³ La Mina Primary Care Academic Centre, Catalan Health Institute and Institute for Primary Health Care Research IDIAP Jordi Gol, Barcelona, Spain

¹⁴ Institute of General Practice, Johannes Kepler University Linz, Austria

¹⁵ Healthcare Trust of the Autonomous Province of Trento, Italy

¹⁶ Department of Sport and Health, Writtle University College, Chelmsford, UK

¹⁷ Department of Family Medicine, University of Medicine and Pharmacy, Craiova, Romania

¹⁸ Division of Research Methodology, Department of Nursing, Faculty of Nursing and Midwifery, Wrocław Medical University, Poland

A – research concept and design; B – collection and/or assembly of data; C – data analysis and interpretation;

D – writing the article; E – critical revision of the article; F – final approval of the article

Advances in Clinical and Experimental Medicine, ISSN 1899–5276 (print), ISSN 2451–2680 (online)

Adv Clin Exp Med. 2025;34(9):1589–1595

Address for correspondence

Ferdinando Petrazzuoli

E-mail: ferdinando.petrazzuoli@gmail.com

Funding sources

This work was supported by the European General Practice Research Network (EGPRN) under grant No. 2024/59 (www.egprn.org).

Cite as

Petrazzuoli F, Vidal-Alaball J, Kenkre J, et al. Best practice approaches to social prescribing in European Primary Care: A Delphi protocol focused on link workers. *Adv Clin Exp Med*. 2025;34(9):1589–1595. doi:10.17219/acem/208216

Conflict of interest

None declared

* Ferdinando Petrazzuoli and Josep Vidal-Alaball contributed equally to this work.

DOI

10.17219/acem/208216

Received on May 2, 2025

Reviewed on May 30, 2025

Accepted on July 13, 2025

Published online on August 1, 2025

Copyright

Copyright by Author(s)

This is an article distributed under the terms of the Creative Commons Attribution 3.0 Unported (CC BY 3.0) (<https://creativecommons.org/licenses/by/3.0/>)

Abstract

Introduction. Social prescribing (SP) is an innovative model that connects individuals to non-clinical community resources. However, its uptake and evaluation have been hindered by inconsistent role definitions for key stakeholders. Although recent studies have refined SP definitions, outside the UK, the responsibilities, educational backgrounds and training requirements of social prescribing link workers (SPLWs) remain poorly defined. Additionally, it is essential to identify which patient populations will benefit most from SP, establish specific methodologies, and standardize assessment tools and referral pathways.

Materials and methods. We will employ a 3-round Delphi protocol with an international expert panel to establish consensus on SP definitions. Approximately 60 participants from diverse disciplines and regions will be recruited to complete multiple survey rounds, providing insights into the roles of SPLWs, beneficiary populations, methodologies, and assessment tools. Consensus will be defined as at least 80% agreement on a 5-point Likert scale. Data collection and analysis will follow rigorous protocols to ensure validity, reliability and transparency, in accordance with the Guidance on Conducting and REporting DELphi Studies (CREDES) guidelines.

Objectives. The aim of this research is to unify the fragmented understanding of SP and the role of SPLWs, thereby establishing a foundation for integrating SPLWs into healthcare systems where appropriate. The Delphi technique offers key strengths – namely, participant anonymity and structured iterative feedback – to enable robust consensus building. While we acknowledge limitations such as potential participant attrition and the resource-intensive nature of the methodology, these will be mitigated through targeted engagement strategies and strict adherence to established best practices.

Conclusions. This study addresses critical gaps in SP engagement, conceptual understanding and implementation. The anticipated outcomes will reinforce SP's role in community-based, integrated care to reduce health inequalities and foster social cohesion across Europe and beyond. Ultimately, this work aims to enhance the uptake and adoption of SP in primary care.

Key words: primary health care, integrated care, social prescribing, link workers, community health services

Highlights

- Social prescribing (SP) connects patients to community resources – an innovative non-clinical approach that boosts health outcomes and wellbeing.
- Variation in SP definitions and roles across Europe – the absence of standardized personnel guidelines impedes consistent implementation within European healthcare systems.
- It is crucial to clarify the social prescribing link worker (SPLW) role and training – defining educational requirements and competencies is essential for professionalizing SP delivery.
- Targeted SP strategies require clear patient selection, methodologies and assessment tools – identifying who benefits most and how to measure outcomes will maximize SP effectiveness.

Introduction

Social prescribing (SP) represents an integrative approach within healthcare systems aimed at addressing social determinants of health through non-clinical interventions. Primarily delivered through referrals in primary care, SP addresses social determinants of health that are often beyond the scope of traditional biomedical interventions. This is by integrating health and social care with community activities. Social prescribing facilitates patient engagement in health-related decision-making and self-management.^{1–5}

Social prescribing involves directing individuals to activities that align with their social, emotional and physical needs as well as providing social counseling to address social problems. These include, e.g., walking, gardening, cooking, crafting, fieldwork, beekeeping, group learning, and/or sports.⁶ While these activities have historically been integral to European community life, their health benefits are not always formally recognized. However, as SP gains traction across Europe, implementation varies

significantly, shaped by country-specific healthcare systems and infrastructure.

England has pioneered SP, embedding it into its UK National Health Service (NHS) Long Term Plan as a central component of personalized care.⁷ This model emphasizes the role of link workers,⁸ who collaborate with patients to co-design individualized plans connecting them to local initiatives.^{9–18} Similarly, Wales has integrated SP into its Well-being of Future Generations Act, promoting a holistic approach to health.¹⁹

Despite its potential, SP faces challenges across Europe. Variability in program design and funding, limited integration with healthcare systems and uneven European awareness hinder its widespread adaptation. Countries like Italy and Croatia, where SP remains underdeveloped, show the need for systemic support and standardized frameworks.²⁰ Moreover, while SP demonstrates potential in improving mental health, reducing healthcare utilization and advancing community engagement, robust evidence on its long-term efficacy remains scarce.²¹ This lack of evidence

complicates efforts to quantify SP's impact and optimize its implementation.

Many countries struggle to establish systematic connections between healthcare and social systems. In Romania, although governmental and non-governmental organizations provide support to vulnerable populations, a formal referral system, such as SP, has not yet been established.²²

In Spain, Catalonia's SP framework, rooted in primary care and the Health Assets model, has demonstrated the potential to adapt SP to diverse healthcare contexts.²³ In Germany, Herrmann et al.²⁴ have identified significant barriers to implementing SP within the German healthcare system.

The need to tackle these challenges has become more urgent due to the growing prevalence of chronic diseases, mental health issues and social isolation across Europe. The COVID-19 pandemic further highlighted the importance of community-centered approaches, as it worsened loneliness and disconnection. Social prescribing offers a structured approach to linking medical care with social and community-based services that prioritize comprehensive, patient-centered solutions addressing the full spectrum of health determinants.²⁵

The World Organization for Colleges, Academies and Associations for General Practitioners (WONCA) Europe Social Prescribing and Community Orientation Special Interest Group (SPCO SIG) recognizes the potential of SP in advancing integrated care.²⁶ Leveraging their expertise in rural health and community engagement, the group seeks to clarify the SP concept and the role of social prescribing link workers (SPLWs), map existing SP programs and identify best practices for implementation across diverse healthcare systems.

This study seeks to advance the understanding of SP by identifying key elements that support its development and integration into contemporary healthcare systems. By addressing health inequalities, improving patient outcomes and strengthening community cohesion, SP has the potential to significantly contribute to the implementation of integrated and equitable models of primary care across Europe.^{26,27} The project is led by members of the SPCO SIG under the auspices of WONCA Europe, with support from colleagues in the European General Practice Research Network (EGPRN). The initiative has been awarded a research grant from the EGPRN.

Objectives

This study aims to reach expert consensus on 3 key areas: 1) the target populations most likely to benefit from SP; 2) the methodologies and assessment tools used to evaluate SP outcomes; and 3) the role, qualifications and training requirements of SPLWs.

Materials and methods

Study design

A 3-round Delphi study will be conducted to identify the key elements contributing to the success of SP programs within European primary care settings, as recognized by European experts.

The Delphi technique will be used as a structured method of achieving consensus among experts. This method involves multiple rounds of surveys, where experts respond to questions anonymously. After each round, participants receive feedback summarizing the group responses, allowing them to refine their input in subsequent rounds. This iterative process facilitates the convergence of opinions, enabling the development of agreed-upon definitions and frameworks.

Widely regarded as a robust approach in health science research, the Delphi method is particularly suited to addressing complex topics, such as SP, where diverse perspectives must be synthesized to establish consensus. This study design ensures systematic and comprehensive exploration of the critical factors underlying successful SP implementation in Europe.

This study will be conducted between April 2025 and August 2025. Given the importance of the online survey platform's quality to this study's success, we carefully reviewed and tested several different options before selection. We will use Welphi (www.welphi.com), which is an online survey platform that is designed explicitly for Delphi studies. The Welphi team will make coding changes when necessary to ensure that the online survey platform meets the needs of this study.

Before the start of each round, we will complete the survey development and perform pilot testing. Participants will receive a notification email 10 days before the launch of each round. At the start of each round, participants will receive an email with a link to the survey and a link to a calendar with the details of the round.

Participants will have 2 weeks to complete each round. Each survey will begin with a welcome page, which provides an overview of the survey, describes the data analysis procedures, explains what kind of feedback will be provided at the start of the next round, highlights the aim of the study, and outlines essential information about conceptual and operational definitions to ensure that there will be a common understanding of these terms. Participants will be able to return to the survey as often as they like until the round's closure – their progress will be saved if they leave the study and return later. Even after completing the survey, they can change their submission until the round closes. Each survey will take approx. 15 min to complete. Non-responders will be removed from the study.

Participants

Delphi studies have no universally agreed-upon definition of what constitutes an expert, making participant selection a critical aspect of the research.^{28–31} For this study, experts will be identified based on the following criteria: Individuals involved in the SP and Community Orientation Network, the Global Social Prescribing Alliance or the National Academies for Social Prescribing; authors of academic or grey literature related to SP, even if not explicitly labeled as such; researchers or healthcare providers engaged in SP activities; link workers facilitating SP, regardless of the terminology used to describe their role; patients with experience in SP; or healthcare administrators or managers overseeing the implementation of SP initiatives. The study will be conducted in English. Regarding the panel size, the literature on Delphi studies in health sciences suggests an average of approx. 40 participants, with typical ranges spanning 20–60 experts.^{28–31} This study will recruit approx. 60 participants, ensuring adequate representation from across European countries to achieve a meaningful consensus.

Recruitment

The recruitment process for the study will commence in November 2024 with the opening of the registration survey for members of the SPCO SIG under WONCA Europe. The steering group will develop a comprehensive list of experts from each country based on their expertise in SP, and invitations will be sent to these individuals via email. Publicly available sources will be used to gather contact information.

An international, multidisciplinary panel of experts will be prioritized, ensuring diversity in country, job title, SP expertise, and years of experience. A monitoring system will track recruitment to identify and address underrepresented groups. To this end, targeted invitations will be extended through relevant communication channels, including the Social Prescribing Network newsletter, the Social Interventions Research and Evaluation Network listserv, and the Canadian Social Prescribing Community of Practice listserv. Invitations will also be advertised on social media platforms like X (Twitter) and LinkedIn. Following the principles of snowball sampling, experts will be encouraged to share the recruitment call with their contacts.

Experts invited to participate will receive an email containing a link to the registration survey. The survey's first page will feature an information letter outlining the study's objectives and emphasizing that participation is voluntary. By proceeding beyond this page, experts will provide their informed consent. Consent will be ongoing and voluntary.

The registration survey will collect sociodemographic data, including the participant's name, email address, country, job title, organization, expertise in SP, and years of experience in the field. Once sufficient experts have

registered, participants will be notified about the start of the study's first round. The recruitment process will ensure a robust and representative panel of experts to achieve meaningful consensus on the topics of this study in European primary care settings.

Consensus

Without standardized guidelines for defining consensus in Delphi studies, this study will adopt a widely accepted threshold of $\geq 80\%$ agreement as the criterion for consensus. Participants will indicate their level of agreement on a 5-point Likert scale: 1 = "Strongly disagree", 2 = "Disagree", 3 = "Neutral", 4 = "Agree", and 5 = "Strongly agree". An item will achieve consensus if at least 80% of participants select "Agree" (4) or "Strongly agree" (5). This rigorous threshold aligns with best practices in health science research, where consensus is typically defined at levels of $\geq 70\%$, $\geq 75\%$ or $\geq 80\%$, with the latter representing the most stringent level of agreement.^{28–33}

Rounds

The study will include 3 rounds, reflecting the structure commonly employed in Delphi studies. This format is based on prior research demonstrating that most Delphi studies to establish agreed definitions are conducted in 3–5 rounds.^{34–37} Each round will refine and build upon the findings of the previous one, progressively working towards consensus among participants.

Data collection

The Delphi surveys will span 7 months. To ensure confidentiality and impartiality, participants will be assigned randomly generated participant codes by the online survey platform. These codes will not be shared with participants, nor will the research team have a key to link participants to their codes. This anonymization safeguards the integrity of responses and mitigates potential bias.

The study's online survey platform has been carefully selected to facilitate seamless data collection and management while ensuring participant anonymity throughout the study. The anonymized approach will foster an environment conducive to candid and unbiased input, supporting the study's objective of achieving robust expert consensus on SP in European primary care settings.

Round 1 will be conducted in April 2025, involving an open-ended survey designed to gather foundational insights from participants. They will be prompted to clarify 2 main aspects: identify the target populations of SP (i.e., those who are expected to benefit more from SP), the specific methodologies used and tools to assess their effectiveness, and the role, qualifications, skills, and training required of SPLW. Participants will have 2 weeks to complete the survey, with an additional 3-day extension provided for non-responders.

Data collected during this round will be synthesized and used to structure the content of the subsequent round.

The research team leaders will conduct a qualitative content analysis to analyze participants' responses. Two senior researchers, F.P. and D.K., will independently review and categorize the qualitative data to identify key themes. The analysis will be performed manually, following a systematic approach to ensure rigor and reliability.

The findings from this round will be used to develop a structured survey for the next round of the Delphi process. At the start of the next round, participants will receive an anonymized summary of the responses from this round, ensuring transparency and allowing for informed consensus-building in the subsequent phase.

Round 2 will take place between May and June 2025. Participants will evaluate the synthesized items from Round 1 through a structured survey. Each item will be rated using a 5-point Likert scale ranging from "Strongly disagree" to "Strongly agree". Items achieving 80% or greater agreement will be accepted as consensus. A free-text box will allow participants to provide additional comments or suggest refinements to the proposed items.

Round 3 is scheduled for July to August 2025 and will focus on finalizing the definitions of the role of SPLW, their education and training as well as the target population who is expected to benefit more from SP and the tools used to assess the effectiveness. Participants will rate their agreement using the same 5-point Likert scale. A consensus threshold of 80% agreement will be applied. Participants who rate definitions below the threshold will be encouraged to provide detailed feedback to inform potential refinement. Otherwise, if consensus is achieved, no further rounds will be necessary.

Data analysis

The data collected from the registration survey will be analyzed with IBM SPSS Statistics for Windows v. 29 (IBM Corp., Armonk, USA). Qualitative data will be presented for each survey item and analyzed through qualitative content analysis.³⁸

Quality and transparency

This study will be conducted and reported by the Conducting and REporting DElphi Studies (CREDES) guidelines.³⁹

Ethics

At all time, the ethical principles of the Declaration of Helsinki of 1964, revised by the World Medical Association (WMA) in 2013 in Fortaleza (Brazil), will be followed. Compliance with the European Data Protection Regulation 2016/679 of the European Parliament and of the Council,

dated April 27, 2016, regarding the protection of individuals concerning the processing of personal data and the free movement of such data, will be always ensured.

All data included in the study will be anonymized and treated confidentially. In the database, participants will be identified only by a code, without including any information that could allow for their identification.

The data obtained in the study will not be transferred to 3rd parties outside the members of the research team of this study at any time. All implemented security measures will be ensured to be sufficient to prevent any breaches of data confidentiality and privacy. Under no circumstances will the research team members have access to participant identification, either directly or indirectly.

Once the study is complete, the research team reserves the right to use the anonymized database solely for scientific purposes (journal articles, scientific papers, book chapters, etc.). The research team will not be permitted to access, use, transfer, or publish the project's database under any circumstances.

This study has been reviewed and approved for ethical compliance to the Research Ethics Committee of the ID-IAP Jordi Gol Primary Care Research Institute in Catalonia, Spain: V2, 08/03/2025 – 01/04/2025.

Data protection

The Principal Investigator, Ferdinando Petrazzuoli, will be responsible for the data storage and handling (ferdinando.petrazzuoli@gmail.com). The anonymized raw data that will support the findings of this study will be available from the corresponding author, upon reasonable request.

Discussion

By engaging diverse stakeholders and utilizing a structured consensus methodology, this study addresses the variability and lack of clarity surrounding the SPLW role, education, skills, and training across Europe, providing a unified framework that can inform research, policy and practice. Clarification and agreement on the target populations of SP (i.e., those who are expected to benefit more from SP), along with the methods and tools used for outcome evaluation, are also among the intended outcomes.

The findings of this Delphi study are expected to extend beyond conceptual clarification. By establishing consensus on the role, education and training of SPLWs, as well as the target populations and assessment tools, the results will inform the development of practical guidelines for health policy, educational curricula and clinical protocols. Specifically, they may inform national and regional policies on workforce development, serve as the basis for designing standardized educational curricula for SPLWs,^{4,7} and support clinicians in making more targeted referrals.⁸

Moreover, the recommendations developed through this process will be adaptable across diverse European health-care systems^{24–26} – whether centralized, decentralized or in developmental stages – facilitating context-sensitive adoption. Finally, the consensus definitions and frameworks may facilitate the design of future comparative and interventional studies evaluating the effectiveness of SP,^{2,3} thereby strengthening its evidence base and promoting integration into holistic models of care.

The Delphi method has distinct strengths make it particularly suited for this endeavor.⁴⁰ Its core features – participant anonymity, iterative rounds of questioning and structured feedback between rounds – help minimize bias and encourage independent and thoughtful contributions from experts. The flexibility of this approach allows for the integration of diverse perspectives on complex topics, such as SP, where consensus must be built across varied healthcare systems and cultural context.^{29,34} Furthermore, using an online platform ensures geographic inclusivity and logistical feasibility, allowing experts from across Europe and beyond to participate without the constraints of physical meetings.

Limitations

Despite its strengths, the Delphi technique is not without limitations. It is known to be resource-intensive and time-consuming, requiring careful management to ensure the process remains efficient and that panel attrition is minimized. This study employs regular reminder emails, clearly defined timelines and engaging communication strategies to sustain participant engagement over all 3 rounds. Another challenge is the lack of standardized guidelines in literature regarding the Delphi process, particularly in determining what constitutes expert status and consensus thresholds. This protocol has addressed these concerns through adherence to the CREDES guidelines, which provide a structured approach to mitigate variability and ensure methodological rigor.³⁹ We also acknowledge other potential limitations, which are common to all Delphi studies, such as the risk of participants dropping out in later rounds or the overrepresentation of certain occupational groups or countries.

Conclusions

This Delphi study constitutes an important step toward establishing a shared conceptual and operational framework for SP in European primary care. By achieving expert consensus on the role, qualifications and training of SPLWs, as well as identifying appropriate target populations and tools for outcome assessment, the study will generate practical recommendations applicable across diverse healthcare systems. The findings are expected to support the systematic integration of SP into patient-centered and community-oriented

models of care, enhance the coherence of future research, and inform educational and policy development. In doing so, this work addresses key gaps in the standardization and implementation of SP across Europe.

Use of AI and AI-assisted technologies

Not applicable.

ORCID iDs

Ferdinando Petrazzuoli  <https://orcid.org/0000-0003-1058-492X>
 Josep Vidal-Alaball  <https://orcid.org/0000-0002-3527-4242>
 Joyce Kenkre  <https://orcid.org/0000-0002-2067-9001>
 Thomas Kloppe  <https://orcid.org/0000-0002-2368-8333>
 Sinah Evers  <https://orcid.org/0000-0002-5399-3355>
 Hendrik Napierala  <https://orcid.org/0000-0002-1542-2877>
 Jean-Pierre Jacquet  <https://orcid.org/0000-0002-6377-7728>
 Wolfram J. Herrmann  <https://orcid.org/0000-0002-9505-4911>
 Natasa Mrduljaš-Dujić  <https://orcid.org/0000-0002-0339-4354>
 Andrea Neculau  <https://orcid.org/0000-0002-4031-5694>
 Katerina Javorska  <https://orcid.org/0000-0002-1810-2668>
 David Halata  <https://orcid.org/0000-0003-4629-2232>
 Miriam Dolan  <https://orcid.org/0000-0002-0922-7290>
 Joanne Robins  <https://orcid.org/0000-0002-5786-9108>
 Patrick Ouvrard  <https://orcid.org/0000-0002-7148-3922>
 Juan Manuel Mendive  <https://orcid.org/0000-0001-8095-7707>
 Carmen López Fando  <https://orcid.org/0009-0001-2989-5106>
 Jane Randall-Smith  <https://orcid.org/0000-0002-5627-0726>
 Erwin Rebhandl  <https://orcid.org/0009-0005-2851-1974>
 Sara Paternoster  <https://orcid.org/0009-0002-7273-3898>
 Hans Thulesius  <https://orcid.org/0000-0002-3785-5630>
 Sian Brand  <https://orcid.org/0009-0007-2118-9534>
 Gindrovel Dumitra  <https://orcid.org/0000-0002-8982-9645>
 Donata Kurpas  <https://orcid.org/0000-0002-6996-8920>

References

1. Vidovic D, Reinhardt GY, Hammerton C. Can social prescribing foster individual and community well-being? A systematic review of the evidence. *Int J Environ Res Public Health*. 2021;18(10):5276. doi:10.3390/ijerph18105276
2. Napierala H, Krüger K, Kuschick D, Heintze C, Herrmann WJ, Holzinger F. Social prescribing: Systematic review of the effectiveness of psychosocial community referral interventions in primary care. *Int J Integr Care*. 2022;22(3):11. doi:10.5334/ijic.6472
3. Cooper M, Avery L, Scott J, et al. Effectiveness and active ingredients of social prescribing interventions targeting mental health: A systematic review. *BMJ Open*. 2022;12(7):e060214. doi:10.1136/bmjopen-2021-060214
4. Brown RCH, Mahtani K, Turk A, Tierney S. Social prescribing in National Health Service primary care: What are the ethical considerations? *Milbank Q*. 2021;99(3):610–628. doi:10.1111/1468-0009.12516
5. Husk K, Blockley K, Lovell R, et al. What approaches to social prescribing work, for whom, and in what circumstances? A realist review. *Health Soc Care Community*. 2020;28(2):309–324. doi:10.1111/hsc.12839
6. Kim JE, Lee YL, Chung MA, et al. Effects of social prescribing pilot project for the elderly in rural area of South Korea during COVID-19 pandemic. *Health Sci Rep*. 2021;4(3):e320. doi:10.1002/hsr2.320
7. National Health Service (NHS). NHS long term workforce plan. London, UK: National Health Service (NHS); 2023. <https://www.england.nhs.uk/publication/nhs-long-term-workforce-plan>. Accessed April 22, 2025.
8. Kiely B, Croke A, O'Shea M, et al. Effect of social prescribing link workers on health outcomes and costs for adults in primary care and community settings: A systematic review. *BMJ Open*. 2022;12(10):e062951. doi:10.1136/bmjopen-2022-062951
9. Wildman JM, Moffatt S, Steer M, Laing K, Penn L, O'Brien N. Service-users' perspectives of link worker social prescribing: A qualitative follow-up study. *BMC Public Health*. 2019;19(1):98. doi:10.1186/s12889-018-6349-x

10. Sandhu S, Lian T, Drake C, Moffatt S, Wildman J, Wildman J. Intervention components of link worker social prescribing programmes: A scoping review. *Health Social Care Community*. 2022;30(6):e3761–e3774. doi:10.1111/hsc.14056
11. Frostick C, Bertotti M. The frontline of social prescribing: How do we ensure link workers can work safely and effectively within primary care? *Chronic Illn*. 2021;17(4):404–415. doi:10.1177/1742395319882068
12. Hayes S, Sharman L, McNamara N, Dingle G. Link workers' and clients' perspectives on how social prescribing offers a social cure for loneliness. *J Health Psychol*. 2025;30(7):1624–1637. doi:10.1177/13591053241274090
13. Hazeldine E, Gowan G, Wigglesworth R, Pollard J, Asthana S, Husk K. Link worker perspectives of early implementation of social prescribing: A 'Researcher-in-Residence' study. *Health Soc Care Community*. 2021;29(6):1844–1851. doi:10.1111/hsc.13295
14. Moore C, Unwin P, Evans N, Howie F. "Winging it": An exploration of the self-perceived professional identity of social prescribing link workers. *Health Soc Care Community*. 2023;2023:488615. doi:10.1155/2023/8488615
15. Mulholland J, Galway K, O'Hare L, Bertotti M, Gildea A. The Social Prescribing Link Worker: Clarifying the role to harness potential. A scoping review. *Health Soc Care Community*. 2025;2025(1):394123. doi:10.1155/hsc/4394123
16. Rhodes J, Bell S. "It sounded a lot simpler on the job description": A qualitative study exploring the role of social prescribing link workers and their training and support needs (2020). *Health Soc Care Community*. 2021;29(6):e338–e347. doi:10.1111/hsc.13358
17. Spencer LH, Lynch M, Makanjuola A. Qualifications and training needs of social prescribing link workers: An explorative study. *Lancet*. 2022;400(Suppl 1):S79. doi:10.1016/s0140-6736(22)02289-9
18. Turk A, Tierney S, Hogan B, Mahtani KR, Pope C. A meta-ethnography of the factors that shape link workers' experiences of social prescribing. *BMC Med*. 2024;22(1):280. doi:10.1186/s12916-024-03478-w
19. Welsh Government. National framework for social prescribing. Cardiff, UK: Welsh Government; 2023. <https://www.gov.wales/sites/default/files/pdf-versions/2024/1/2/1705399866/national-framework-social-prescribing.pdf>. Accessed April 22, 2025.
20. Linari A. Social prescribing: A means for combining social and health care? [doctoral thesis]. Milan, Italy: Polytechnic University of Milan; 2021. <https://www.politesi.polimi.it/handle/10589/179454>. Accessed April 22, 2025.
21. Husk K, Elston J, Gradinger F, Callaghan L, Asthana S. Social prescribing: Where is the evidence? *Br J Gen Pract*. 2019;69(678):6–7. doi:10.3399/bjgp19x700325
22. Surugiu R, Iancu MA, Lăcătuș AM, et al. Unveiling the presence of social prescribing in Romania in the context of sustainable healthcare: A scoping review. *Sustainability*. 2023;15(15):11652. doi:10.3390/su15111652
23. González JC, Braddick F, Schwartz Fields H, Segura Garcia L, Colom Farran J. Los retos de la prescripción social en la Atención Primaria de Catalunya: la percepción de los profesionales. *Comunidad*. 2016;2(18):7. https://comunidad.semfyc.es/wp-content/uploads/Comunidad_-_Los-retos-de-la-prescripci%C3%B3n-social-en-la-Atenci%C3%B3n-Primaria-de-Catalunya_la-percepci%C3%B3n-de-los-profesionales.pdf. Accessed April 22, 2025.
24. Herrmann JW, Laker K, Napierala H. Challenges and opportunities for social prescribing in Germany: Policy and methodological perspectives. In: Bertotti M, ed. *Social Prescribing Policy, Research and Practice*. Cham, Switzerland: Springer International Publishing; 2024:101–113. doi:10.1007/978-3-031-52106-5_7
25. Morse DF, Sandhu S, Mulligan K, et al. Global developments in social prescribing. *BMJ Glob Health*. 2022;7(5):e008524. doi:10.1136/bmjgh-2022-008524
26. Kurpas D, Mendive JM, Vidal-Alaball J, et al. European perspective on how social prescribing can facilitate health and social integrated care in the community. *Int J Integr Care*. 2023;23(2):13. doi:10.5334/ijic.7636
27. Baska A, Kurpas D, Kenkre J, et al. Social prescribing and lifestyle medicine: A remedy to chronic health problems? *Int J Environ Res Public Health*. 2021;18(19):10096. doi:10.3390/ijerph181910096
28. Chalmers J, Armour M. The Delphi technique. In: Liampittong P, ed. *Handbook of Research Methods in Health Social Sciences*. Singapore: Springer Singapore; 2019:715–735. doi:10.1007/978-981-10-5251-4_99
29. Niederberger M, Spranger J. Delphi technique in health sciences: A map. *Front Public Health*. 2020;8:457. doi:10.3389/fpubh.2020.00457
30. Muhl C, Mulligan K, Bayoumi I, Ashcroft R, Godfrey C. Establishing internationally accepted conceptual and operational definitions of social prescribing through expert consensus: A Delphi study. *BMJ Open*. 2023;13(7):e070184. doi:10.1136/bmjopen-2022-070184
31. Muhl C, Mulligan K, Bayoumi I, Ashcroft R, Godfrey C. Establishing internationally accepted conceptual and operational definitions of social prescribing through expert consensus: A Delphi study protocol. *Int J Integr Care*. 2023;23:3. doi:10.5334/ijic.6984
32. Frey BB, ed. *The SAGE Encyclopedia of Educational Research, Measurement, and Evaluation*. Thousand Oaks, USA: SAGE Publications; 2018. doi:10.4135/9781506326139
33. Barrett D, Heale R. What are Delphi studies? *Evid Based Nurs*. 2020;23(3):68–69. doi:10.1136/ebnurs-2020-103303
34. Puig A, Adams C. Delphi technique. In: Frey BB, ed. *The SAGE Encyclopedia of Educational Research, Measurement, and Evaluation*. Thousand Oaks, USA: SAGE Publications; 2018. doi:10.4135/9781506326139.n190
35. Metzelthin SF, Rostgaard T, Parsons M, Burton E. Development of an internationally accepted definition of reablement: A Delphi study. *Ageing Soc*. 2022;42(3):703–718. doi:10.1017/s0144686x20000999
36. Campbell KA, Wood JN, Lindberg DM, Berger RP. A standardized definition of near-fatal child maltreatment: Results of a multidisciplinary Delphi process. *Child Abuse Negl*. 2021;112:104893. doi:10.1016/j.chiabu.2020.104893
37. Esfandiari E, Chudyk AM, Grover S, et al. Social Prescribing Outcomes for Trials (SPOT): Protocol for a modified Delphi study on core outcomes. *PLoS One*. 2023;18(5):e0285182. doi:10.1371/journal.pone.0285182
38. Mayring P. *Qualitative Content Analysis: A Step-by-Step Guide*. Thousand Oaks, USA: SAGE Publications; 2021. ISBN: 978-1-5297-0197-5, 978-1-5297-0198-2.
39. Jünger S, Payne SA, Brine J, Radbruch L, Brearley SG. Guidance on Conducting and REporting DELphi Studies (CREDES) in palliative care: Recommendations based on a methodological systematic review. *Palliat Med*. 2017;31(8):684–706. doi:10.1177/0269216317690685
40. Savic LC, Smith AF. How to conduct a Delphi consensus process. *Anaesthesia*. 2023;78(2):247–250. doi:10.1111/anae.15808

